



906

Department of Energy  
Washington, D.C. 20545

Docket No. 50-537  
HQ:S:82:110

October 29, 1982

Mr. Paul S. Check, Director  
CRBR Program Office  
Office of Nuclear Reactor Regulation  
U.S. Nuclear Regulatory Commission  
Washington, D.C. 20555

Dear Mr. Check:

AMENDMENT NO. 72 TO THE PRELIMINARY SAFETY ANALYSIS REPORT (PSAR) FOR CLINCH RIVER BREEDER REACTOR PLANT (CRBRP)

The application for a Construction Permit and Class 104(b) Operating License for the CRBRP, docketed April 10, 1975, in NRC Docket No. 50-537, is hereby amended by the submission of Amendment No. 72 to the PSAR pursuant to 50.34(a) of 10 CFR, Part 50.

This Amendment No. 72 includes: Responses to U.S. Nuclear Regulatory Commission requests for additional information contained in letters dated April 19 and 30, May 14, June 9 and 21, and July 16, 1982; Revisions to Section 11.4, "Process and Effluent Radiological Monitoring System;" Chapter 12, "Radiation Protection;" and other updates and revisions.

A Certificate of Service, confirming service of Amendment No. 72 to the PSAR upon designated local public officials and representatives of the Environmental Protection Agency, will be filed with your office after service has been made. Three signed originals of this letter and 97 copies of this amendment, each with a copy of the submittal letter, are hereby submitted.

Sincerely,

John R. Longenecker  
Acting Director, Office of the  
Clinch River Breeder Reactor  
Plant Project  
Office of Nuclear Energy

Enclosure

cc: Service List  
Standard Distribution  
Licensing Distribution

SUBSCRIBED AND SWORN to before me  
this 22 day of October 1982

  
NOTARY PUBLIC

SERVICE LIST

Atomic Safety & Licensing Board  
U. S. Nuclear Regulatory Commission  
Washington, D. C. 20555

Atomic Safety & Licensing Board Panel  
U. S. Nuclear Regulatory Commission  
Washington, D. C. 20555

Mr. Gerald Largen  
Office of the County Executive  
Roane County Courthouse  
Kingston, TN 37763

Dr. Thomas Cochran  
Natural Resources Defense Council, Inc.  
1725 I Street, NW  
Suite 600  
Washington, DC 20006

Docketing & Service Station  
Office of the Secretary  
U. S. Nuclear Regulatory Commission  
Washington, DC 20555

Counsel for NRC Staff  
U. S. Nuclear Regulatory Commission  
Washington, DC 20555

William B. Hubbard, Esq.  
Assistant Attorney General  
State of Tennessee  
Office of the Attorney General  
422 Supreme Court Building  
Nashville, TN 37219

Mr. Gustave A. Linenberger  
Atomic Safety & Licensing Board  
U. S. Nuclear Regulatory Commission  
Washington, DC 20555

Marshall E. Miller, Esq.  
Chairman  
Atomic Safety & Licensing Board  
U. S. Nuclear Regulatory Commission  
Washington, DC 20555

William E. Lantrip, Esq.  
Attorney for the City of Oak Ridge  
725 Main Street, East  
Oak Ridge, TN 37830

Dr. Cadet H. Hand, Jr., **Director**  
Bodega Marine Laboratory  
University of California  
P. O. Box 247  
Bodega Bay, CA 94923

Lewis E. Wallace, Esq.  
Division of Law  
Tennessee Valley Authority  
Knoxville, TN 37902

STANDARD DISTRIBUTION

Mr. R. J. Beeley (2)  
Program Manager, CRBRP  
Atomics International Division  
Rockwell International  
P. O. Box 309  
Canoga Park, CA 91304

Mr. Michael C. Ascher (2)  
Project Manager, CRBRP  
Burns and Roe, Inc.  
700 Kinderkamack Road  
Oradell, NJ 07649

Mr. Percy Brewington, Jr. (2)  
Acting Director  
Clinch River Breeder Reactor Plant  
P. O. Box U  
Oak Ridge, TN 37830

Mr. Dean Armstrong (2)  
Acting Project Manager, CRBRP  
Stone & Webster Engineering Corp.  
P. O. Box 811  
Oak Ridge, TN 37830

Mr. William J. Purcell (2)  
Project Manager, CRBRP  
Westinghouse Electric Corporation  
Advanced Reactors Division  
P. O. Box W  
Oak Ridge, TN 37830

Mr. W. W. Dewald, Project Manager (2)  
CRBRP Reactor Plant  
Westinghouse Electric Corporation  
Advanced Reactors Division  
P. O. Box 158  
Madison, PA 15663

Mr. H. R. Lane (1)  
Resident Manager, CRBRP  
Burns and Roe, Inc.  
P. O. Box T  
Oak Ridge, TN 37830

Mr. George G. Glenn, Manager (2)  
Clinch River Project  
General Electric Company  
P. O. Box 508  
Sunnyvale, CA 94086

Number of copies in parentheses.

1/11/82

LICENSING DISTRIBUTION

Mr. Hugh Parris  
Manager of Power  
Tennessee Valley Authority  
500A CST 2  
Chattanooga, TN 37401

Dr. Jeffrey H. Broido, Manager  
Analysis and Safety Department  
Gas Cooled Fast Reactor Program  
General Atomics Company  
P. O. Box 81608  
San Diego, CA 92138

Mr. George Edgar  
Morgan, Lewis, and Bockius  
1800 M Street  
Suite 700  
Washington, DC 20036

2/17/82

PAGE REPLACEMENT GUIDE FOR  
AMENDMENT 72  
CLINCH RIVER BREEDER REACTOR PLANT  
PRELIMINARY SAFETY ANALYSIS REPORT

(DOCKET NO. 50-537)

Transmitted herein is Amendment 72 to Clinch River Breeder Reactor Plant Preliminary Safety Analysis Report, Docket 50-537. Amendment 72 consists of new and replacement pages for the PSAR text and Responses to NRC Questions.

Vertical margin lines on the right hand side of the page are used to identify changes resulting from NRC Questions and margin lines on the left hand side are used to identify new or changed design information.

The following attached sheets list Amendment 72 pages and instructions for their incorporation into the Preliminary Safety Analysis Report.

AMENDMENT 72  
PAGE REPLACEMENT GUIDE

REMOVE THESE PAGES

INSERT THESE PAGES

Chapter 1

1.3-21, 22

1.3-21, 22

Chapter 2

2.5-23b, 24  
2.5-61, 62

2.5-23b, 24  
2.5-61, 62

Chapter 3

3.1-19, 20  
3A.8-4, 5  
3A.8-9a, 9b

3.1-19, 20  
3A.8-4, 4a, 5  
3A.8-9a, 9b

Chapter 4

4.2-230, 231  
4.2-278 thru 281  
4.2-304, 305  
4.2-410, 411  
4.2-614 thru 617  
4.2-620, 621

4.2-230, 231  
4.2-278, 278a, 279, 280, 281  
4.2-304, 305  
4.2-410, 411  
4.2-614, 615, 615a, 616, 617  
4.2-620, 621

Chapter 5

5.2-4c, 4d  
5.2-6b, 7, 7a, 8  
5.2-10b, 10c, 10d, 11  
5.2-12, 12a, 13  
5.3-21, 21a  
5.5-12, 12a  
5.5-24, 24a  
5.5-35, 35a, 35b  
5.5-53a  
5.6-5, 6, 6a, 7  
5.6-42  
5.7-3, 3a, 4 thru 8  
-

5.2-4c, 4d  
5.2-6b, 7, 7a, 8  
5.2-10b, 10c, 10d, 11  
5.2-12, 12a, 13  
5.3-21, 21a  
5.5-12, 12a  
5.5-24, 24a  
5.5-35, 35a, 35b  
5.5-53a thru 53e  
5.6-5, 6, 6a, 6b, 7  
5.6-42 thru 47  
5.7-3, 3a, 4 thru 8  
5.7-14a thru 14k

REMOVE THESE PAGES

INSERT THESE PAGES

Chapter 6

6-i thru v  
6.2-14 thru 17

6-i, ii, iia, iii, iv, v  
6.2-14, 15, 15a, 16, 16a, 17

Chapter 7

7-i thru v, va, vi, via,  
vii thru xii  
7.1-1, 2  
7.1-7 thru 10  
7.2-1, 1a  
7.2-11 thru 14, 14a, 15, 16  
7.2-22, 23  
7.3-3, 4, 4a, 5, 6  
7.4-1, 2  
7.4-5 thru 8, 8a thru 8e  
  
7.4-10c  
7.5-7, 8, 8a, 9, 10  
7.5-18a, 18b, 19, 19a, 20 thru 25  
  
7.5-33f, 33g  
7.5-33j  
-  
7.6-1, 2, 2a, 2b  
7.6-2e  
7.6-8, 9  
7.6-16 thru 19  
7.6-26, 27  
7.7-9, 9a  
7.9-5, 6, 6a thru 6d

7-i thru v, va, vi, via, vii,  
viii, ix, ixa, x thru xv  
7.1-1, 2, 2a  
7.1-7 thru 10  
7.2-1, 1a  
7.2-11 thru 15, 15a, 16  
7.2-22, 23, 23a  
7.3-3, 4, 5, 5a, 6  
7.4-1, 2  
7.4-5, 5a, 5b, 6, 7, 8,  
8a thru 8f  
7.4-10c, 10d  
7.5-7 thru 10  
7.5-18a, 18b, 19, 20, 21, 21a,  
22 thru 25  
7.5-33f, 33g  
7.5-33j  
7.5-54, 55  
7.6-1, 2, 2a, 2b  
7.6-2e  
7.6-8, 9, 9a  
7.6-16, 17, 18, 18a, 18b, 19  
7.6-26, 27  
7.7-9  
7.9-5, 6, 6a thru 6d

Chapter 9

9.1-60, 61  
9.6-45, 45a  
9.6-47, 48  
9.7-3, 4  
9.7-7, 8

9.1-60, 61  
9.6-45, 45a  
9.6-47, 47a, 48  
9.7-3, 4  
9.7-7, 8

Chapter 11

11.2-20, 20a  
11.4-1, 2, 3, 3a, 4 thru 13

11.2-20, 20a  
11.4-1, 2, 3, 3a, 4 thru 15

REMOVE THESE PAGES

INSERT THESE PAGES

Chapter 12

12.1-22b, 23, 23a, 24  
12.1-28, 29  
12.1-78, 79, 80, 80a  
12.1-81, 82  
12.1-85  
12.1-87  
12.1-89 thru 94  
12.1-96  
12.1-99, 99a, 99b  
12.1-101  
12.2-3, 3a, 4, 4a, 4b, 4c, 5, 6  
12.2-9 thru 13  
12.3-13, 14

12.1-22b, 23, 23a, 23b, 24  
12.1-28, 29  
12.1-78, 79  
12.1-81, 82  
12.1-85  
12.1-87  
12.1-89 thru 94  
12.1-96  
12.1-99, 99a, 99b  
12.1-101  
12.2-3, 3a, 4, 4a, 4b, 4c, 5, 6  
12.2-9, 10, 10a, 11, 12, 13  
12.3-13, 14, 14a, 14b

Chapter 15

15.1-105, 106  
15.3-6, 7  
15.3-28  
15.3-34, 35  
15.3-49

15.1-105, 106  
15.3-6, 7  
15.3-28, 28a, 28b  
15.3-34, 35  
15.3-49



AMENDMENT 72

QUESTION/RESPONSE SUPPLEMENT

This Question/Response Supplement contains an Amendment 72 tab sheet to be inserted following Qi page Amendment 71, September 1982. Page Qi Amendment 72 is to be inserted following the Amendment 72 tab sheet.

This Amendment 72 provides both new and revised Question/Response pages for NRC QUESTIONS RECEIVED SINCE THE FALL OF 1981.

The following Question/Response pages are to be inserted in numerical order behind the appropriate numbered tabs in PSAR Volume 25 or 26 as appropriate. The parenthesis beside Question/Response shown indicates the number of pages associated with each Question/Response.

*QCS220.25 (84)	QCS421.37 (1)	QCS760.105 (1)
(1st page is a replacement)	QCS421.42 (2)	QCS760.110 (2)
*QCS421.9 (1)	QCS421.47 (1)	QCS760.116 (1)
*QCS421.17 (1)	QCS421.48 (5)	QCS760.131 (1)
QCS421.22 (3)	QCS421.58 (1)	QCS760.166 (6)
QCS421.27 (1)	QCS721.1 (10)	QCS760.172 (4)
QCS421.30 (1)	*QCS760.13(1)	QCS760.175 (1)
QCS421.31 (2)	QCS760.28 (28)	QCS760.176 (29)
QCS421.34 (1)	QCS760.30 (1)	QCS760.177 (1)
*QCS421.36 (1)	QCS760.36 (7)	QCS760.178 (120)

\*These are replacement pages.

CRBRP - 975 Mwt

FFTF - 400 Mwt

MONJU\*-714 Mwt

steam drum to atmosphere. Removes up to ~180 Mwt (18% rated power)

heat rejection capability is ~12% of rated power. (50 Mwt).

- Long term rejection of decay heat accomplished by condensing of steam in an air cooled condenser. Removes up to 4.5% rated power (45 Mwt). When these systems are unavailable, decay/residual heat is removed by cooling of the reactor overflow sodium by a Na/NaK heat exchanger. NaK heat load rejected to atmosphere by a NaK/air heat exchanger. Removes between 10-11 Mwt.

1.3-21

41

No. Loops

3

3

3

9. Plant Protection System

7.2

8

Reactor Trip Action

- |   |  |
|---|--|
| (1) Release Rods                        | (1) Release Rods                             |
| (2) Trip Primary and Intermediate Pumps | (2) Trip Primary and Intermediate Pumps      |
| (3) Provides Turbine Trip Signal        | (3) Programs Dump Heat Exchanger Guide Vanes |

Amend. 41  
Oct. 1977

	CFBRP 975 Mwt	FFTF 400 Mwt	MONJU* 714 Mwt	PSAR Section
Reactor Trip Circuits				
No. Circuits Monitored For Trip Actuation	24-Pri. System 16-Sec. System	23-Pri. System 19-Sec. System	--	
Basic Signal and Trip Output Signal Logic	Pri.-2/3 Local Coincidence Logic	Pri.-2/3 Local Coincidence Logic	--	
	Sec.-2/3 General Coincidence Logic	Sec.-1/4 2/3 Hybrid General Local Coincidence Logic	--	
No. External Flux Monitors	3	3	--	
Max. RSS Logic Response Time (From time RSS senses condition requiring trip to time when rods are released.) (Sec.)	0.200	0.200	--	

10. Containment

3.8

Type/Shape

Single steel vessel, cylindrical shell with flat bottom and hemi-ellipsoidal top. Concrete shielding inside, below operating floor. Steel containment surrounded by concrete confinement building. An annulus space between containment and confinement maintained at negative pressure with respect to outside atmosphere.

Single steel vessel, cylindrical shell with hemi-ellipsoidal top and bottom heads. Concrete shielding below operating floor.

Single steel vessel, cylindrical shell with hemi-spherical top and hemi-ellipsoidal bottom. Concrete cylinder surrounds entire containment.

1.3-22

Amendment  
72  
Oct. 1982

Figure 2.5-18, sheet 3 of 4 includes all historical earthquakes within 50 miles of the site. Maximum Modified Mercalli Intensity is shown by open circles. Unfelt events and events with unreported intensity are shown by the X's.

Figure 2.5-18, sheet 4 of 4 also includes all historical earthquakes within 50 miles of the site. Magnitude is shown by the square symbols. Events with unreported magnitude are shown by the X's.

The largest earthquakes ever recorded in the southeastern United States are the New Madrid earthquakes of December 16, 1811, January 23, 1812, and February 7, 1812, and the Charleston, South Carolina earthquake of August 31, 1886. The epicentral intensity at New Madrid, 300 miles west-northwest of the site, is estimated to be XII MM and the epicentral intensity of the Charleston earthquake 315 miles southeast of the site is estimated to be X MM (Ref. 120).

The observed surface intensity in the vicinity of the site from the New Madrid earthquakes is estimated to be VI-VII MM (Refs. 121 and 126). Topographic changes reportedly resulted from these earthquakes over an area of 30,000 to 50,000 square miles. At least a two million square-mile area was shaken (Ref. 129). Only a very small amount of damage was reported, mainly due to lack of inhabitants. The New Madrid earthquake produced the greatest ground motion at the site of any earthquake in historic time. As previously stated, these earthquakes have been assigned an intensity XII which is described by "total destruction" at the epicenter.

The observed surface intensity in the vicinity of the site from the Charleston earthquake is estimated to be VI MM (Ref. 111). This earthquake is reported to have been felt over an area of two million square miles. For its reported epicentral intensity, the Charleston earthquake was felt over a large area.

A moderately large earthquake within the southeastern region which was felt at the site was the Giles County, Virginia, earthquake of May 31, 1897, with a reported epicentral intensity of VII-VIII MM (Ref. 117). The Giles County earthquake, whose epicenter is about 220 miles northeast, is estimated to have been felt at the site at about intensity V MM (Ref. 112).

As stated in Section 2.5.2.3, the greatest historic ground motion of the site is estimated to have been intensity VI-VII MM and was produced by the New Madrid earthquake which occurred about 300 miles from the site.

#### 2.5.2.6 Correlation of Epicenters with Geologic Structures

The tectonic structures which occur in the CRBRP site area and region have been previously described. The tectonic structures or thrust faults within the Valley and Ridge Province are considered in the literature and by recognized geologic experts as ancient and inactive. Results of the recently completed Law Engineering site investigation substantiate this.

- (119) Meade, B. K. 1971 Report of the Sub-Commission on recent Crustal Movements In North America, N.O.A.A., U.S. Dept of Commerce. (SET)
- (120) 1982 Report by Law Engineering Testing Company, Inc., on CRBRP Earthquake Update, dated May 12, 1982. (SET)
- (121) Nuttall, O. W. Professor at Saint Louis University, Personal Communication to Law Engineering Testing Company. (SET)
- (122) Seed, H. B. 1968 (and Idriss, I. M.; Kelfer, F. W.) Characteristics of Rock Motion During Earthquakes, Earthquake Engineering Research Center, Report No. EE-5C G8-5, College of Engineering University of California, Berkeley, California.
- (123) Taber, S. 1914 Seismic Activity in the Atlantic Coastal Plain Near Charleston, South Carolina; Bulletin, Seismological Society of America, Vol. 4, No. 3.
- (124) Technical Information Division, U.S. Atomic Energy Commission 1967 Summary of Current Seismic Design Practice for Nuclear Reactor Facilities; John A. Blume and Associates, Engineers, San Francisco, California, TID-25021.
- (125) 1969 Tectonic Map of North America; U.S.G.S. and the American Association of Petroleum Geologists.
- (126) Tennessee Valley Authority Relationships of Earthquakes and Geology in West Tennessee and Adjacent Areas.
- (127) 1972 Preliminary Information on Clinch River Site for LMFBR Demonstration Plant.
- (128) U.S. Coast and Geodetic Survey United States Earthquakes, 1928 - 1970.
- (130) U.S. Coast and Geodetic Survey 1956 Earthquake History of the United States.
- (131) Gutenberg, B. (and Richter, C. F.) Earthquake Magnitude, 1956 Intensity, Energy, and Acceleration (second paper), Bulletin Seismological Society of America, Vol. 46.

- (132) Weston Geophysical Engineers, Inc., Weston, Massachusetts, "Seismic Velocity and Elastic Moduli Measurements", 1974.
- (133) Weston Geophysical Engineers, Weston Massachusetts, "Seismic Refraction Survey", Clinch River Breeder Reactor Plant, Oak Ridge, Tennessee, 1974.
- (134) Deere, D.U. 1967 (and Hendron, A. J.; Patton, F. D.; Cording E. J.) "Design of Surface and Near-Surface Construction in Rock", Failure and Breakage of Rock, Proceedings of the Eighth Symposium on Rock Mechanics, September 15-17, 1966, at the University of Minnesota, The American Institute of Mining, Metallurgical and Petroleum Engineers, Inc., New York.
- (135) Leonards, G.A. 1962 Foundation Engineering, McGraw-Hill, Inc., New York.
- (136) Stagg, K.G. 1968 (and Zienkiewicz, O. C.) Rock Mechanics in Engineering Practice, John Wiley and Sons, New York.
- (137) Law Engineering Testing Company in conjunction with Burns & Roe Inc. November, 1975, "Report on Evaluation of Intensity of Giles County Virginia Earthquake of May 31, 1897.
- (138) Neumann, Frank 1954 Earthquake Intensity and Related Ground Motion, University of Washington Press, Seattle.
- (139) Trifunac, M.D. 1954 (and Brady, A.G.) On the Correlation of Seismic Intensity Scales with the Peaks of Recorded Strong Ground Motion, Bulletin of the Seismological Society of America, Volume 65, No. 1, pp. 139-162.
- (140) Seed, H. Bolton 1972 (and Silver, Marshall L.) Settlement of Dry Sands during Earthquakes, Journal of the Soil Mechanics and Foundation Division, ASCE,
- (141) Pyke, Robert 1975 (Seed, H. Bolton, and Chan, Clarence K.) Settlement of Sands under Multidirectional Shaking Journal of the Geotechnical Division, ASCE.
- (142) Wong, Robert T. 1975 (Seed, H. Bolton, and Chan, Clarence K.) Cyclic Loading Liquefaction of Gravelly Soils, Journal of the Geotechnical Division, ASCE

## Criterion 10 Suppression of Reactor Power Oscillations

The reactor and associated coolant, control, and protection systems shall be designed to assure that power oscillations which can result in conditions exceeding specified acceptable fuel design limits are not possible or can be reliably and readily detected and suppressed.

### RESPONSE

42 | The CRBRP is neutronicly tightly coupled, preventing any possibility  
42 | of spatial instability. The main stabilizing feedback is due to Doppler and  
42 | the CRBRP is inherently stable in response to reactivity perturbations.

42 | The neutronic stability of the CRBRP has been analyzed with point-  
kinetics techniques (See Section 4.3). The reactor was modelled by a set of  
coupled linearized first-order differential equations with constant coef-  
ficient describing the neutronics and temperature behavior of the system.  
The temperature dependent reactivity feedback effects used in this model  
include Doppler and fuel axial expansion which are fuel temperature dependent  
and the sodium density effect which is coolant temperature dependent.

42 | These analyses have shown that CRBRP is a stable, well-behaved system  
in terms of the response of the reactor to reactivity perturbations about full  
power. The principal stabilizing feedback mechanism is the Doppler (fuel  
temperature) effect. The reactor remains a stable system even when the  
Doppler coefficient is halved and employed in any combination with the  
32 | other reactivity feedback coefficients.

42 | For worst case positive bowing reactivity characteristics, which  
can occur only in the startup range (0+ to 40% power), a net positive feed-  
back is possible. With this condition, present control system analyses  
predict a worst-case (maximum) limit cycle oscillation of +2.2% of full power,  
comprised of a + 2% dead band plus a 0.2% response turn around on both ends of  
the dead band. The smallest period associated with the worst-case condition  
is 500 seconds in that less bowing reactivity would result in a longer  
oscillation period. Recompensation of the flux control system for the final  
design may result in a reduction in amplitude of the limit cycle oscillation  
as well as a reduction in the frequency. Above 40% power and under all per-  
mitted conditions, where bowing reactivity is always negative, limit cycle  
oscillation due to this feedback component will not occur. Assurance that  
the specified acceptable fuel design limits will not be reached is provided  
throughout the 0 to 100% power operating range by the reactor trip functions.

Amend. 42  
Nov. 1977



## Criterion 11 - Instrumentation and Control

Instrumentation shall be provided to monitor variables and systems over their anticipated ranges for normal operation, for anticipated operational occurrences, and for postulated accident conditions as appropriate to assure adequate safety, including those variables and systems that can affect the fission process, the integrity of the reactor core, the reactor-coolant boundary, and the containment and its associated systems. Appropriate controls shall be provided to maintain these variables and systems within prescribed operating ranges.

### RESPONSE

Instrumentation and controls are provided to monitor and control neutron flux, control rod position, temperatures, pressures, flows, and levels as necessary to assure that adequate plant safety can be maintained. Instrumentation is provided in the Reactor System, Heat Transport System, Steam and Power Conversion System, the Engineered Safety Features Systems, Radwaste Systems and other auxiliaries. Parameters that must be provided for operator use under normal operating and accident conditions are indicated, in proximity with the controls for maintaining the indicated parameter in the proper range. The control room is provided as the focal point from which the plant can be operated safely during normal operation, anticipated operational occurrences, and for postulated accident conditions. The basic criteria for including instrumentation readout and control in the control room is as follows:

- o The displays or controls necessary to support all normal plant operating conditions;
- o The displays and controls necessary to respond to anticipated operational occurrences and accident conditions which impact on power operations capability;
- o The displays or controls necessary to prevent potential radiological hazards to offsite personnel;
- o The displays necessary to the operator for detection of fire hazards; or
- o The display and controls necessary to prevent potential damage to the plant.

### 3A.8.3.3 Liner Analysis

#### .1 General

The liner system is described in Section 3A.8.2. The Design Requirements, Load Categories, Load Combinations, Stress and Strain allowables and Design Analysis procedures are given in paragraphs 3.1 through 3.5 of PSAR Appendix 3.8-B. Attachment D to Appendix 3.8-B gives the bases for the strain criteria and strain limits adopted for the Postulated Large Liquid Metal Spill (PLLMS) Loads.

The spacing and size of the Nelson stud anchors in the wall and ceiling panels and of the floor anchors are designed such that the stresses and strains fall within the limits specified in Table 3.8-B-1 of Appendix 3.8-B.

The anchors will resist the shear forces induced when unbalanced forces exist between sections of the liner and axial forces caused by the maximum specified pressure (5 psig) acting on the backside of the liner under the PLLMS loads. Since there is a 1/4 inch gap between the cell liner and the insulating concrete, some axial loads in the anchors will be caused by the cell's internal pressure.

The insulating concrete does not act integrally with the structural concrete and a bond breaker will be provided on the surface separating the two materials to reduce shear transfer. The insulating concrete is not considered a main structural element; its main function is to provide a thermal shield to prevent degradation of the structural concrete under the elevated temperatures of the PLLMS conditions. The adequacy of the insulation thickness has been demonstrated by a preliminary finite element thermal analysis using the computer program ANSYS. The temperatures calculated at the face of the structural concrete did not exceed the limits established in Section 3.1.7 of Appendix 3.8-B. Local hotspots due to heat transfer into the structural concrete through the studs may occur. These effects will be evaluated by both analytical and testing methods.

Spalling or degradation of the insulating concrete under the PLLMS Loads will not cause a failure of the liners or liner anchor system. The anchors will be embedded in the structural concrete to ensure adequate restraint and the design is such that even if no lateral support to the anchors is provided by the insulating concrete, the specified anchor strain limits will not be exceeded.

Liner failure due to behind the liner steam pressure is prevented by the provision of a venting system on the backside of the liner where necessary, to reduce steam pressure generated from heatup of the insulating material and structural concrete during a sodium spill. The 5 psig cell liner vent system pressure developed behind the cell liner plate is addressed in the analysis of the liner system. Two cases of pressure differential across the liner are considered. The first case considers the 5 psig vent pressure behind the liner combined with the peak internal cell accident pressure; the second case a 0 psig vent pressure combined with the peak internal cell accident pressure. These two cases provide conservative bounding conditions for the pressure differential across the cell liner under Design Basis Accident conditions.

Specific vent paths behind the liner will be provided where analysis and/or testing indicates they are required. Steam produced would be vented to the non-inerted areas

59 |

within the RCB or RSB consistent with the location of the sodium spill. Preliminary analysis under Postulated Large Liquid Metal Spill (PLLMS) conditions indicates that this venting scheme will not require the containment to be purged. A more detailed analysis will be performed to verify these preliminary indications. Since any steam produced during a sodium spill would be vented to the non-inerted areas, hydrogen evolution due to sodium/water reactions would occur only following a liner failure. Failed liner testing is planned and the amount of hydrogen evolved during these tests will be monitored. Even in the unlikely event of the liner failure, purging of containment is not expected to be required. The liner system will be designed to withstand a backside pressure of 5 psig.

59 |

Due to the magnitude of the compressive thermal forces caused by the restraining actions of the concrete structure, buckling of the liner plates is anticipated. Buckling in itself will not produce failure since the thermal deformations are self limiting. However, due to the reduced load carrying capacity of a buckled panel, unbalanced lateral forces can be induced at the anchor. The liner-anchor system will be designed such that under the unbalanced lateral forces due to panel buckling, the strains will not exceed the allowable limits. Buckling of panels will improve the stress-strain conditions at the corner anchors since the unbalanced lateral forces will be reduced.

The dead and live loads, seismic loads, operating pressure and thermal loads, etc., will affect the cell liners through the interaction of the liner-anchor system with the structural concrete. Since the structural concrete is by far more rigid than the liner, the deformations of the concrete under these loads and the restraint it provides to the liner will determine the stress-strain condition of the liner-anchor system for these loads. For these conditions other than sodium spills, the stress levels in the cell liners are expected to be below the yield strength of the material. The maximum normal operating temperature (peak) will not exceed 180°F and no significant stresses and strains will be imposed on the liners under these conditions.

The cyclic temperature variation in the cells during the lifetime of the plant (10 cycles from 70°F to 140°F, 100 cycles from 100°F to 140°F and 100 cycles from 140°F to 180°F) are within the ASME Code limitations such that the cyclic fatigue should not be a problem. Based on Section NE-3222. 4d of Section III, Division 1 of the ASME B&PV Code, for the specified temperature ranges and number of cycles, no fatigue analysis is required.

.2 Analysis

45 | 37 |

Calculations have been conducted to investigate the adequacy of the liner-anchor system under the PLLMS Condition. They consist of elasto-plastic analyses using the computer program ANSYS. The strain values obtained from the finite element analyses under sodium spill conditions are compared against the allowable strains at the exposure temperature. The allowable PLLMS strains are determined using Table 3.8-B-1 and the materials test data presented in 3A.8.4. Table 3A.8-1 summarize the allowable strains under load combination D (PLLMS spill).

59 |

Following selections of the prime sealant material, prototypic electrical cable penetration assembly performance testing were conducted. The results of this testing program were published in Reference (4).

Base Material Tests for Liner Steels

59|           The objective of this completed testing program was to determine  
the response of the cell liner plate material (SA-516 Grade 55) and its  
associated weldment material to elevated temperatures up to 1700<sup>o</sup>F.  
The base liner steel will be tested for residual tensile strength (in-  
59| cluding stress-strain response), stress-rupture (Creep) and thermal expansion.  
The weldment material was tested for residual tensile strength (including  
59| stress-strain response) and stress-rupture (Creep). Both longitudinal  
and transverse welds were investigated. The results of the base liner  
45| steel and weldment material tests have been published in Reference 6.

59|           The material properties information at elevated temperatures  
which was obtained in this program has been used in the design and analysis  
of the cell liner system.

References:

1. McAfee, W.J., Sartory, W.K., "Evaluation of the Structural Integrity of LMFBR cell liners - Results of Preliminary Investigations", ORNL-TM-5145, January, 1976.
2. Chapman, R.H., ORNL-TM-4714, "A State of the Art Review of Equipment Cell Liners for LMFBR's", February, 1975.
3. Sartory, W.K., McAfee, W.J., ORNL-TM-5145, "Evaluation of the Structural Integrity of LMFBR Equipment Cell Liner - Results of Preliminary Investigation", February, 1976.
4. Humphrey, L.H., Horton, P.H., AI-DOE-13227 "Selection of a Sodium and Radiation Resistant Sealant for LMFBR Equipment Cell Penetrations", January 31, 1978.
5. Wireman, R., Simmons, L., Muhlestein, I., HEDL TME 79-35, "Large Scale Liner Sodium Spill Test (LT-1)", December, 1980.
6. Cowgill, M.G., WARD-D-0252, "Base Material Tests for Cell Liner Steels", February, 1980.

#### 4.2.3.1 Design Basis

##### 4.2.3.1.1 General Safety Design Criteria

The General Safety Design Criteria are discussed in detail in Section 3.1.3, subsection III, Protection and Reactivity Control Systems, and are outlined here for completeness. Specific criteria which are a part of the design basis for the reactivity control systems mechanical components are:

1. Criterion 20 - Protection System Independence
2. Criterion 21 - Protection System Failure Modes
3. Criterion 23 - Protection System Requirements for Reactivity Control Malfunctions
4. Criterion 24 - Reactivity Control System Redundancy and Capability
5. Criterion 25 - Combined Reactivity Control Systems Capability

These criteria are augmented by the following requirements:

1. The speed of response of the control rod system, acting as part of the Plant Protection System, shall be sufficient to assure that the Damage Severity Limits of Table 4.2-35 are not exceeded. Specific requirements for speed of response are presented in Section 4.2.3.1.3.

The allowable damage limits are related to the frequency of the transient condition so that anticipated events do not lead to a reduction in the effective fuel lifetime. RDT Standard C16-1T, Dec. 1969, is used as the basis for the primary control rod system damage severity limits, without a stuck rod. (See Table 4.2-35.) To provide conservative plant protection, the same primary system damage limits are required to be satisfied under the assumption of a stuck rod. The primary system has the function of limiting fuel damage to design limits for anticipated events. Failure of the primary system is an extremely unlikely event. Consequently, the secondary system, which is needed for shutdown only if the primary system fails, need only limit damage to the major incident limit of an extremely unlikely fault. For additional conservatism in limiting plant damage for an anticipated event, the limits of Table 4.2-35 require only minor incident damage for the secondary system. The combined probability of an extremely unlikely fault event concurrent with failure of the primary system is exceedingly low and is not applied as a design basis.

- 51 | 2. For an Operational Basis Earthquake (OBE), an anticipated fault, both control rod systems shall be capable of functioning, including reactor scram, both during and after the earthquake. Reactor shutdown shall be achieved assuming loss of offsite power and/or a step reactivity insertion (maximum of 30¢) coincident with the earthquake (concurrent events defined as an unlikely fault) without exceeding the damage severity limits of a minor incident for primary system shutdown and of a major incident for secondary system shutdown.

51 | For a Safe Shutdown Earthquake (SSE) (extremely unlikely fault), either control rod system shall be capable of shutting down the reactor during the earthquake but is not required to function after the earthquake other than passively assuring that shutdown is maintained. Reactor shutdown shall be achieved assuming concurrent loss of offsite power and a step reactivity insertion (maximum of 60¢) coincident with the earthquake without exceeding the damage severity limits of a major incident for both systems.

The requirement for functioning of the secondary system in an SSE provides an additional protective margin beyond that of Table 4.2-35.

3. No electric or other external (to the mechanical control rod system) power shall be required for a scram of any control rod.

#### 4.2.3.1.2 Control Rod System Clearances

The specific goal in establishing control rod system clearances is to ensure safe and reliable shutdown and control capability for the reactor. To this end, the basis for establishing clearances fall into the following general categories:

Limit scram retarding forces resulting from misalignment of components.

Limit scram retarding forces resulting from material effects from thermal, radiation, and other environmental characteristics.

Assure normal operation of the control rod systems under misaligned and environmental conditions.

Control Systems clearance requirements and their bases are summarized in Table 4.2-36.

#### 4.2.3.1.3 Mechanical Insertion Requirements

This section describes mechanical insertion requirements with regard to scram speed of response, alignment requirements, scram arrest, normal insertion and withdrawal speeds, and coefficient of friction considerations.



#### 4.2.3.3.1.3 Scram Analysis

This section describes the scram analyses performed for the primary control rod system to demonstrate the expected rates of reactivity insertion during a reactor scram. Considered in this section are available shutdown reactivities, typical rod positions, control rod scram speeds and scram reactivity insertion rates.

##### Typical Rod Withdrawal Positions

Rod positions at the time of the scram may vary significantly due to: withdrawal over the fuel cycle, potential variations in rod bank positions, uncertainties in rod worths and variations in the fuel cycle length between the first and later cores. This time to insert the first dollar of shutdown reactivity in the reactor scram is typically of greatest importance as this first dollar is sufficient to turn around the power peak or fuel temperature increase for most transients. Table 4.2-44 shows typical rod withdrawal positions over the first five operating cycles. BOC-5 has been shown to be the worst case for the slowest first dollar insertion and is therefore the basis for the scram insertion analysis.

##### Control Rod Scram Speed

Control rod insertion speeds are calculated by the CRAB-II computer code which solves the equations of motion considering all the forces acting on the PCRS translating assembly, both scram assisting and scram retarding. Section 4.2.3.3.1.1 presents the analysis of the scram retarding forces, and Table 4.2-43 gives the total drag force as a function of withdrawal.

Validation of the CRAB-II code for predicting speed of insertion was done using test data from the PCRS system tests. Figure 4.2-112 shows insertion profiles from various withdrawal positions based on the drag forces given in Table 4.2-43. Figure 4.2-113 demonstrates the ability of CRAB-II to predict actual test data using conditions expected to occur in the core. Also shown in Figure 4.2-113 is the CRAB-II predicted speed of insertion using the conservative design conditions described in Section 4.2.3.3.1.1. The difference between the two curves represents the conservative margin for speed of insertion used in the scram analysis. Figure 4.2-113a demonstrates the ability of CRAB-II to predict test data over a range of flow rates and insertion times.

##### Scram Reactivity Insertion Rates

Scram reactivity insertion rates have been calculated based on the displacement/time profiles given in Figure 4.2-112, the cycle dependent rod positions of Table 4.2-44 and the minimum and expected bank worths appropriate to each cycle with the single most reactive rod stuck. The results of these calculations are shown in Figure 4.2-114. Although BOC-5 procedures the minimum shutdown, BOC-4 has been included to show the change in scram insertion from BOC-5 to BOC-4. All other cases insert reactivity faster due to higher worths or farther initial rod withdrawal.

An evaluation of the inherent shutdown margin can be obtained by comparing the minimum reactivity insertion with the expected reactivity insertion. The

minimum reactivity insertion represents a  $3\sigma$  worst case evaluation of maximum excess reactivity and minimum control rod worth, while the reactivity insertion represents nominal core conditions. Additional margin on reactivity insertion for both minimum and expected conditions is included in these curves by using speed of insertion calculated with the conservative design conditions of drag shown in Figure 4.2-113.

End of cycle reactivity insertions are significantly greater due to increased shutdown margins and faster rod speeds due to greater scram assist forces at these positions.

All curves in Figure 4.2-114 have assumed a delay of 0.1 seconds from the advent of a scram signal to the start of rod motion. Actual test data from the PCRS system tests has shown this unlatch time to be  $0.0486 \pm 0.0002$  seconds. Thus, on a  $3\sigma$  basis, the scram insertion curves in Figure 4.2-114 could be moved to the left by 0.05 seconds.

It is therefore concluded that the primary control rod system satisfies the speed of response requirements given in Section 4.2.3.1.3 for all conditions.

#### 4.2.3.3.1.4 Seismic Scram Analysis\*

An analysis was performed to determine the effect of a safe shutdown earthquake (SSE) on the CRBRP Primary Control System's scram capability. Lateral contact forces on the translating assembly were determined for a severe three second segment of the SSE which was then used in evaluation of scram performance under seismic conditions.

The worst time to initiate a scram in this 3 sec. time interval was identified by determining the time required to scram 9 inches. This criterion was used because it represents the required rod travel of the rods to insert approximately one dollar of reactivity. A 1.2 second load time history whose initial point is the worst scram initiation time was then used repetitively until the rods were fully inserted. A dynamic impact coefficient of friction of 0.5 was used since this value is conservative relative to the coefficient of friction averaged over the length of the PCRS (see paragraph 4.2.3.1.3).

The ANSYS computer program was used to perform the seismic analysis, using the semi-linear transient dynamic (time history) option of the program. An overall reactor system model was first used to determine the motions of the important components. The gross motions of the system components were then used as input functions in a decoupled primary control rod system model to determine the response of the leadscrew, driveline and control assembly within the PCRD, shroud tube and control assembly duct.

The nonlinear primary control rod system model and its use in the seismic impact analysis are discussed in Section 3.7.3.15.3. The results of this analysis used in the scram calculations are the contact forces (vs. time) during the seismic event.

---

\*See footnote to Section 3.7.3.15.

The scram analysis was performed using the CRAB computer code (See App. A) incorporating the dashpot model and time variant scram retarding force capability. The results of the SSE scram insertion predictions are compared with the seismic scram requirements in Figure 4.2-119. BOC-5 was determined to be the time in life which produced the minimum reactivity insertion due to bank position and available worth. An evaluation of the inherent shutdown margin can be obtained by comparing the minimum reactivity insertion with the expected reactivity insertion. The minimum reactivity insertion represents a 3 $\sigma$  worst case evaluation of maximum excess reactivity and minimum control rod worth, while the expected reactivity insertion represents nominal core conditions.

It is concluded that the primary control system satisfies the SSE scram insertion requirement of Figure 4.2-93. The reactivity effects of the slightly increased scram time are evaluated in Section 15.2.3.3.

The seismic scram analysis is a conservative evaluation of scram capability under SSE environment in that a conservative calculation of loads and scram initiation time was employed.

#### 4.2.3.3.1.5 Control Assembly Analyses

##### Absorber Pin

The primary control assembly utilizes enriched B<sub>4</sub>C (approximately 92 atom percent <sup>10</sup>B in Boron). Data on helium release, thermal conductivity and pellet swelling, required for absorber design, are available in References 44 and 44a.

Currently committed B<sub>4</sub>C tests providing EBR-II irradiation data in support of CRBRP control assembly design are given in Table 4.2-46A. The table summarizes each test using the HEDL name for the test. Typical test parameters for pellet temperature, pellet diameter and B-10 captures completion dates for the EBR-II irradiations.

The tests of Table 4.2-46A will extend the irradiation data well above the pellet temperature and pellet sizes anticipated for the primary control assembly. The BICM-1 test has provided data to 80X10<sup>20</sup> B-10 captures/cc, which is comparable of first core burnups for CRBRP. The BV-2 test for vented pins will provide data on pellet swelling for burnups typical of 275 FPD cycle operation. The tests of Table 4.2-46A cover the operating range for the primary control assembly over its required lifetime.

The planned EBR-II B<sub>4</sub>C irradiation tests do not include in-reactor transient cycling of absorber rods. Out-of-pile testing of irradiated pellets has been performed under the HEDL development program to determine gas release under transient thermal conditions. Preliminary results indicate that helium release upon temperature increases occurs over a relatively long time (on the order of 15 minutes) characteristic of a Primary Control Assembly thermal transient. Since B<sub>4</sub>C temperature increases during transients are small (<100°F) the incremental gas increase from a transient is a small effect. Incremental gas release

during transients based on the thermal transient tests are included in the pin lifetime analyses. Since the absorber pins are designed to preclude pellet to clad interactions or  $B_4C$  melting under worst case transient conditions, gas release is the only  $B_4C$  variable required to be assessed in transient analyses.

53 | Further performance data for the PCA will be obtained from the  
PCA Irradiation Test (see Section 4.2.3.4.1.1) which will provide integrated  
51 | lifetime performance data for near prototypic environments and operating  
parameters.

51 | Table 4.2-46 summarizes performance parameters for the absorber  
pins. The thermal-hydraulic parameters are discussed in Section 4.4.  
For the current design, the plenum lengths have been established by  
the maximum available pin length, and the clad stresses at the end of  
one operating cycle are less than 5,000 psi as shown in Table 4.2-46.

51 | Preliminary strain analyses of the pin have indicated that there  
is only minimal accumulated strain at the end of the lifetime requirements.  
Additional analysis utilizing the cumulative damage function approach  
has been performed which also verifies the lifetime capability of the  
pins. Use of the CDF for the absorber cladding requires that the duty  
cycle be separated into various stress state/time segments superimposed  
on the steady state operating conditions. This introduces conservatism  
in the analysis since conservative estimates of stress and time form  
the basis for the analysis. Effects such as sodium interaction with the  
cladding and pin-duct interactions are included in the lifetime evaluation.  
 $B_4C$  swelling is calculated to assure that no force contact occurs  
between the pellets and the cladding (see Table 4.2-36) thus reducing  
the margin for error in the calculations. Figure 4.2-111a shows pellet  
swelling and associated pellet to clad gap for rod in the Row 7 corner  
location. Figure 4.2-111b shows axial B-10 burnup profiles for each  
rod position in the equilibrium cycle.

54 | 53 | 51 | Based on the results of the preliminary analyses performed, it  
is concluded that the pellet/clad gap clearance requirements are satisfied  
for the required 328 FPD lifetime with an initial gap of 0.028 inches  
(Figure 4.2-111a). The initial gap must be increased to allow for  
additional pellet swelling over the goal lifetime of 550 FPD.

#### Structural Evaluation

51 | A preliminary elastic analysis was performed to evaluate the  
structural adequacy of the control assembly outer ducts. Design stress  
limits were derived using the criteria defined in Table 4.2-37B. Both

#### 4.2.3.4.1 Performance Test Program

Extensive testing programs are planned for evaluation of the reliability and design of both reactivity control systems. These tests will include individual component tests and complete prototype systems tests.

##### 4.2.3.4.1.1 Primary Control Rod System

The PCRS testing program consists of the following major testing activities:

A) Component Tests: The following component design test and/or analysis program was established to provide design verification of the PCRS components.

##### 1. Dynamic Seismic Friction Test

This test was performed to evaluate the effective coefficient of friction between a rod and its guide bushings under impact loading conditions. Data obtained are used to provide friction coefficients for seismic scram insertion analyses.

##### 2. Control Assembly Hydraulic (Flow) Test

Test results will be used to verify the pressure drops, flow and vibration characteristics of the primary control assembly design under prototypic flow conditions.

##### 3. Control Assembly Pin Compaction Test

Test has provided data to determine inter-pin and pin-to-duct loads for the primary control assembly analyses.

##### 4. Control Assembly Rotational Joint Test

Test has provided performance data on the rotational joint which confirmed the reduction in control assembly wear and reliable operation of the joint.

##### 5. B<sub>4</sub>C Data Test

The base technology irradiation test program being conducted by HEDL includes acquisition of data required for design verification of CRBR control assemblies (see Table 4.2-46A).

##### 6. Friction and Wear Tests

The base technology materials test program being conducted at ETEC and ARD provides data for the material couples selected for fabrication of the primary control rod system.

## 7. Control Assembly Analytical Methods

Provides an analytical model calibrated with test results for predicting primary control assembly thermal-hydraulics performance, lifetime characteristics and scram dynamics behavior.

- B) System Level Tests: A series of Primary Control Rod System Prototype Tests have been performed to verify that the Primary Control Rod System performance is consistent with its design requirements under design basis operating conditions. The Control Rod Drive Mechanism was evaluated in a CRDM Accelerated Unlatching Life Test. This test program verified the unlatch performance characteristics of a prototype primary control rod drive mechanism over twice the design lifetime travel and scrams. The Accelerated Life Test involved testing of a full size prototype primary control rod system in sodium, sodium vapor, and argon gas environments that simulate operations in the Clinch River Breeder Reactor Plant. Phase I testing in this series completed 1/2 of the PCRS lifetime scrams, 1/3 of the leadscrew travel requirement, and about 5 times the PCA travel requirements. Phase II of this series will extend total test scrams and travel beyond CRBRP lifetime requirements.

During System Level Tests of the Primary Control Rod System, each subsystem was also tested, including the position indication system and the dash pot. Four prototype systems were tested and the results show PCRS performance including position indicator accuracy and dash pot performance were within this design requirements.

- C) PCA Irradiation Test: A PCA irradiation test is scheduled to be inserted in the FFTF for 600 FPD. The intent of this test is to provide near-prototypic irradiation performance data on the PCA absorber assembly to support the PCA lifetime evaluations. The test assembly will contain 37 pins of enriched B<sub>4</sub>C and will function as an integral part of the FFTF Secondary Control Assembly Bank. The parameters of the test assembly have been selected to provide data prototypic of the PCA for burnup, fluence, B<sub>4</sub>C and cladding temperatures and cladding strain. Data from this test are expected to be available in 1986.
- D) Other Tests: See Appendix C for Reliability Test Program.

### 4.2.3.4.1.2 Secondary Control Rod System

The SCRS testing program consists of the following major testing activities:

- A) Latch Tests: Component development tests of the scram latch configuration for the secondary control rod system verified the design of this component.
- B) Damper Tests: Component development tests of the damper configuration for the secondary control rod system verified the design of this component.

TABLE 4.2-44

PCRS CYCLE DEPENDENT WITHDRAWAL POSITIONS  
(IN INCHES)

CYCLE	ROW 4		ROW 7			
	BOC & EOC		Minimum		Expected	
			BOC	EOC	BOC	EOC
1	36		16.0	20.9	18.9	24.2
2	36		15.1	22.4	18.1	26.9
3	36		12.9	23.3	16.2	27.7
4	36		12.5	21.1	16.6	26.9
5	36		12.6		15.9	



51 |

TABLE 4.2-45 DELETED

4.2-411

Amend. 51  
Sept. 1979

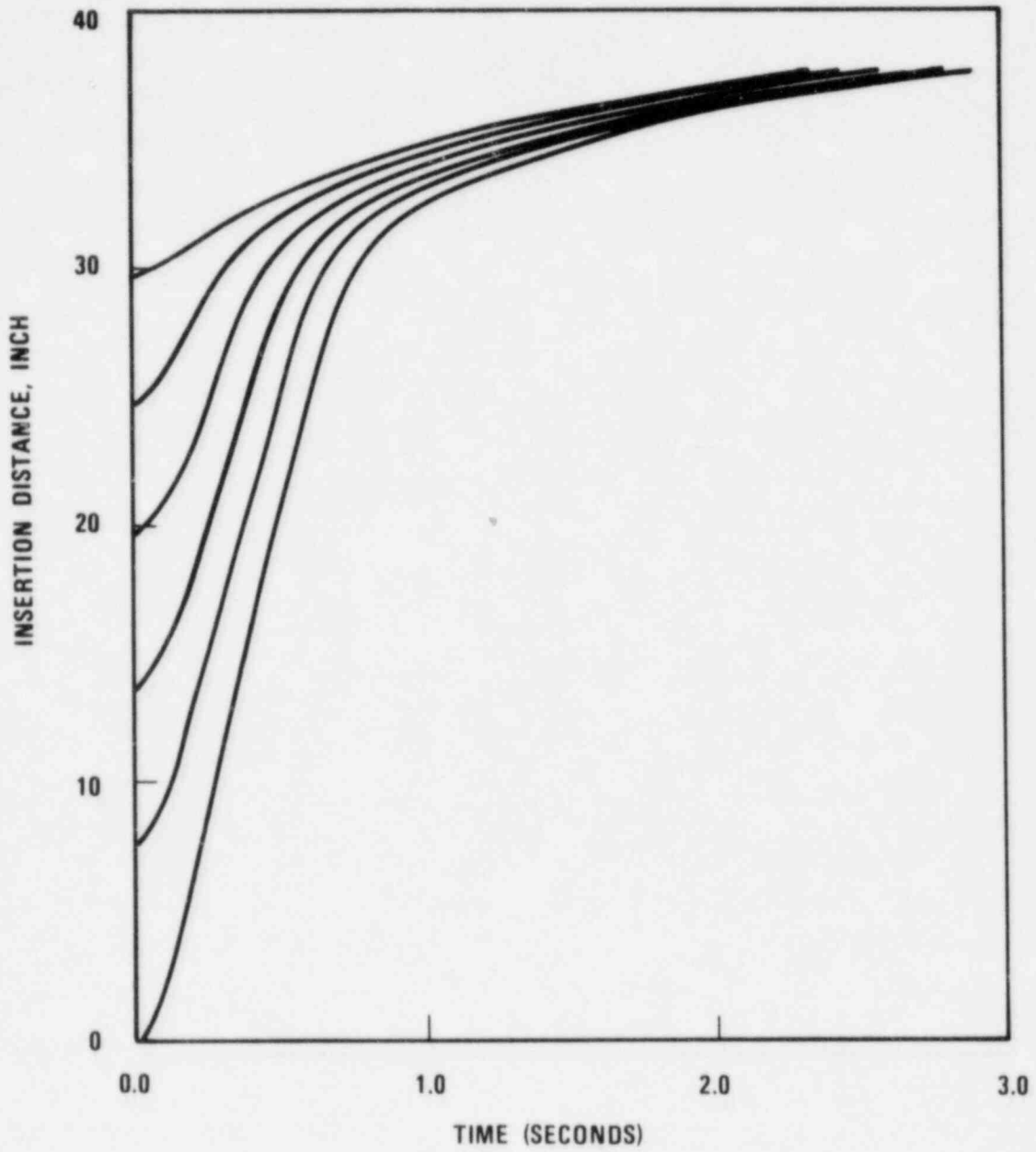


Figure 4.2-112 Primary Control Rod System Scram Insertion Distance vs Time

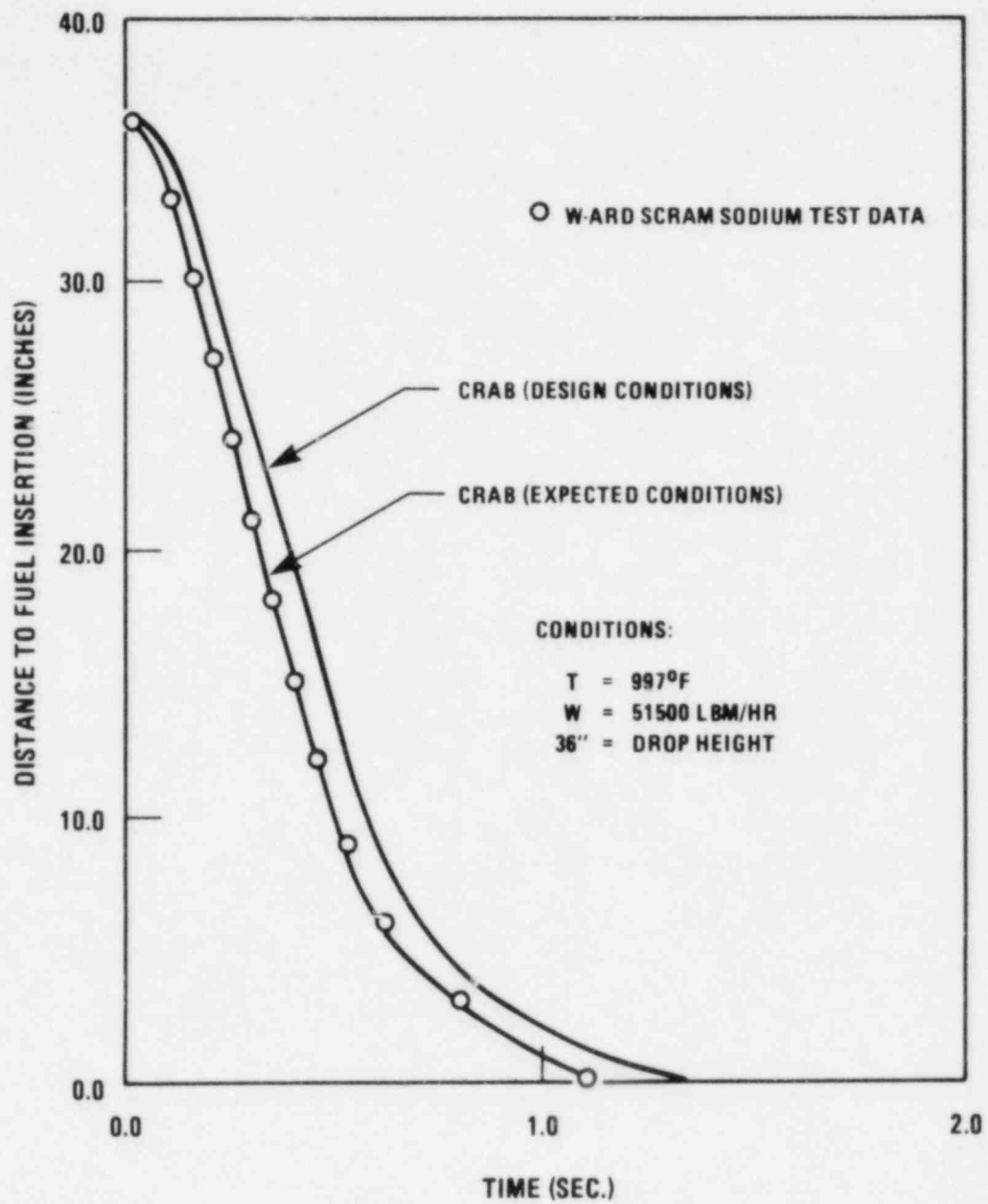


Figure 4.2-113. A Comparison Between Scram Predictions by CRAB-II and ARD Sodium Test Data

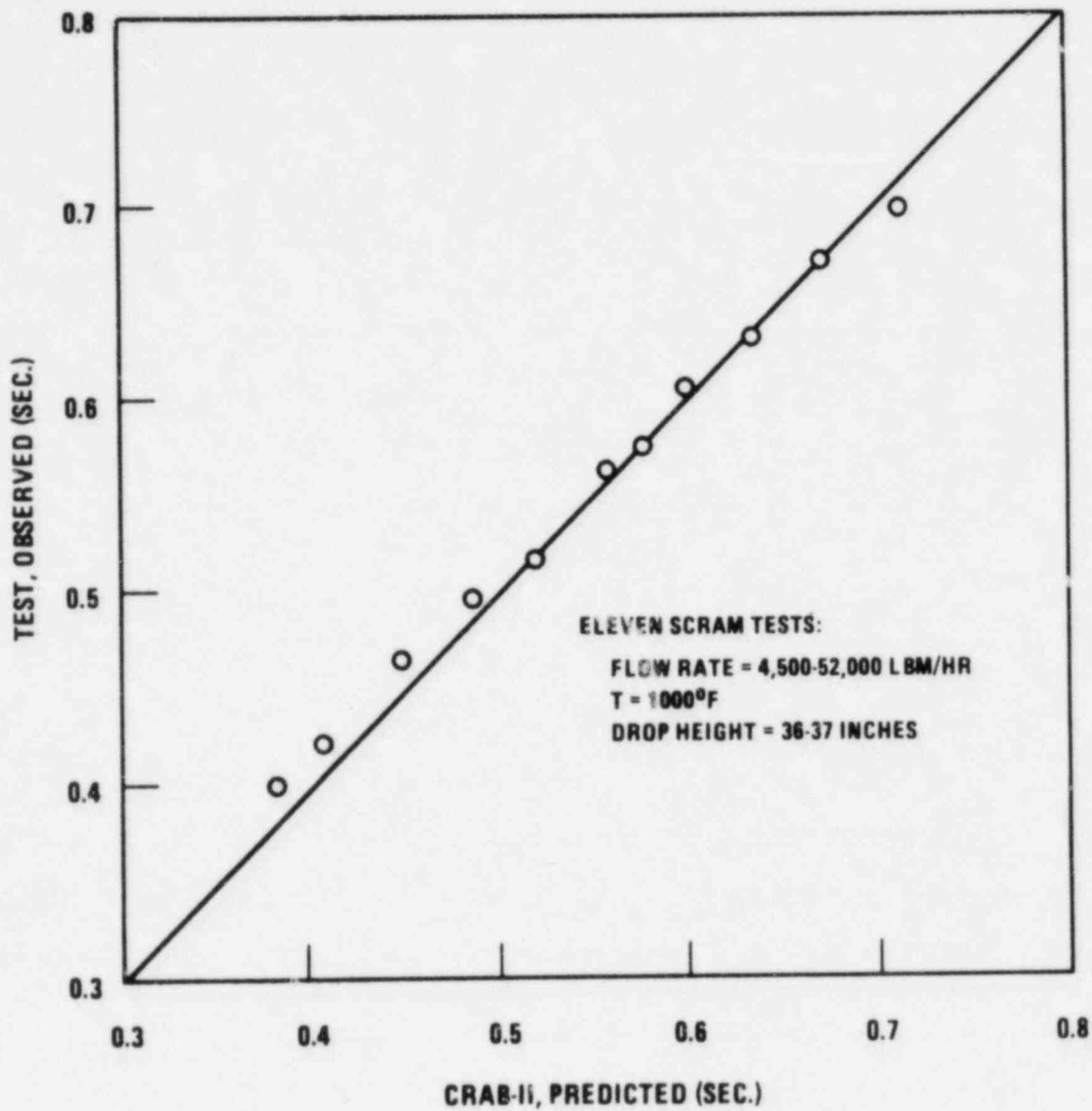
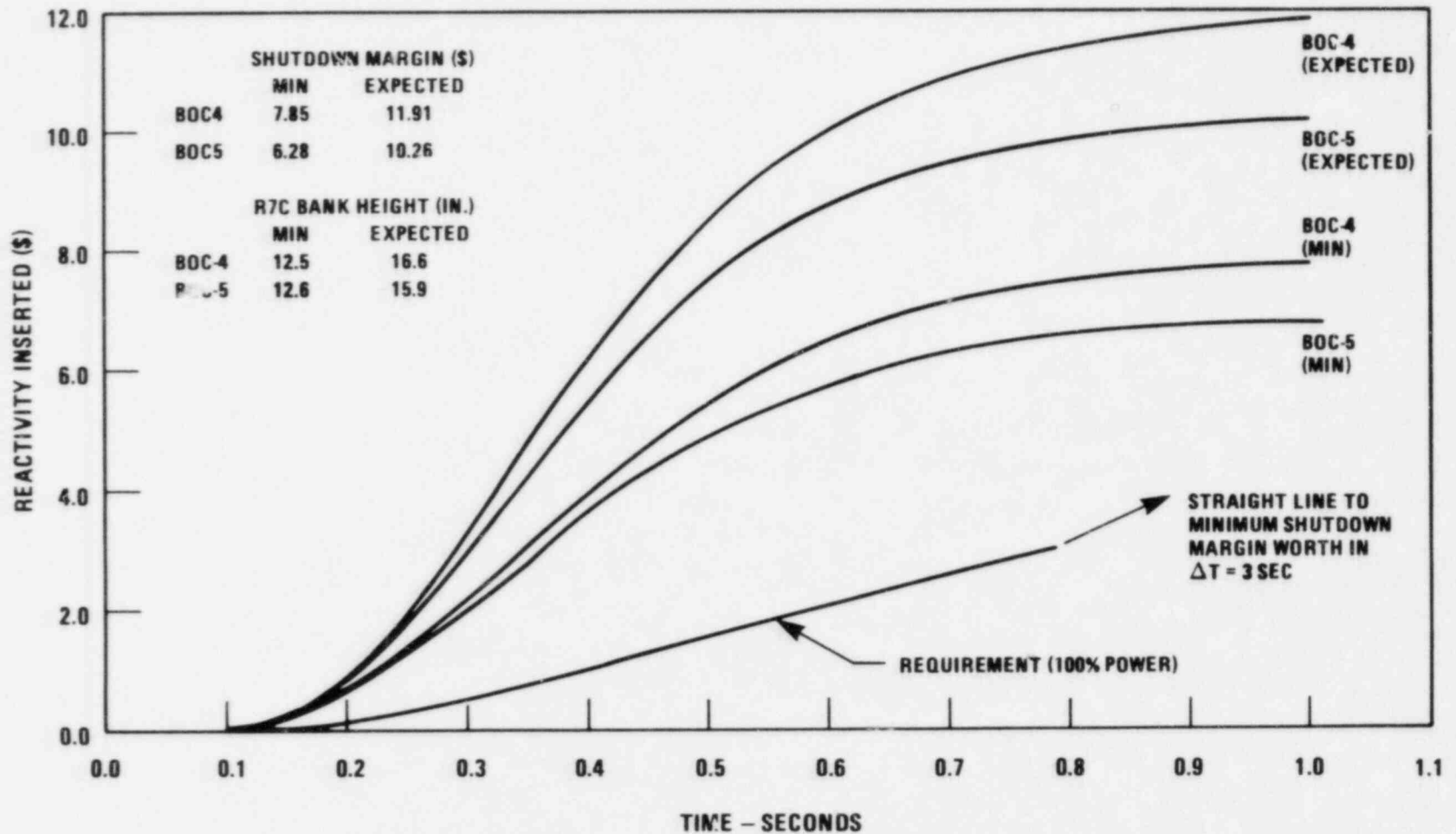


Figure 4.2-113a. Summary Comparison of the CRAB-II Predicted Versus Test Observed Scram Time to Reach the Dashpot

7081-2

4.2-615a

Amend. 72  
 Oct. 1982



4.2-616

Amend. 72  
Oct. 1982

Figure 4.2-114. PCS Scram Insertion Performance (Non-Seismic)

FIGURE 4.2-115 through 4.2-117 DELETED

4.2-617  
(next page is 4.2-620)

Amend. 53  
Jan. 1980

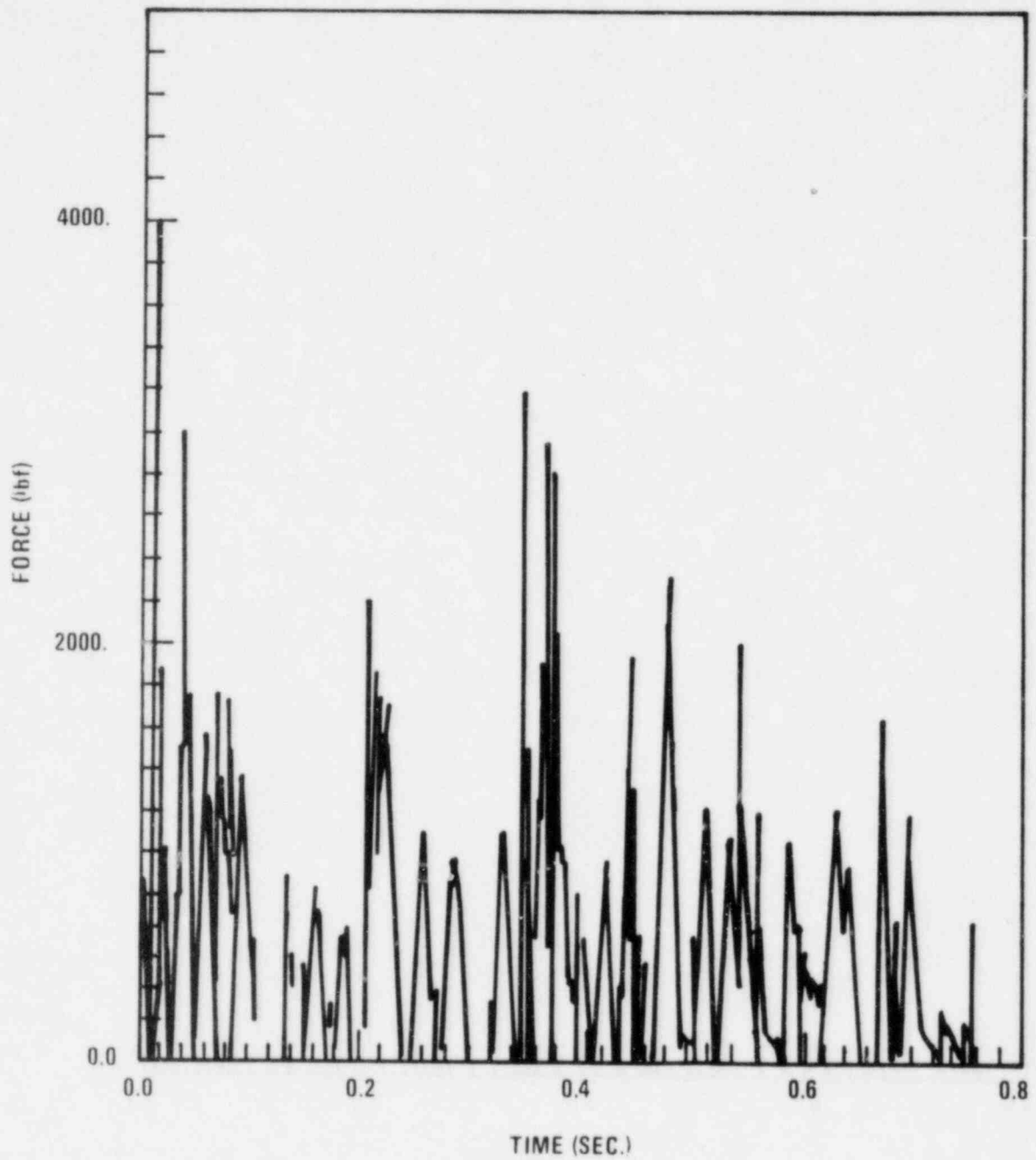


Figure 4.2-118. Typical PCRS Total Contact Force vs Time During SSE

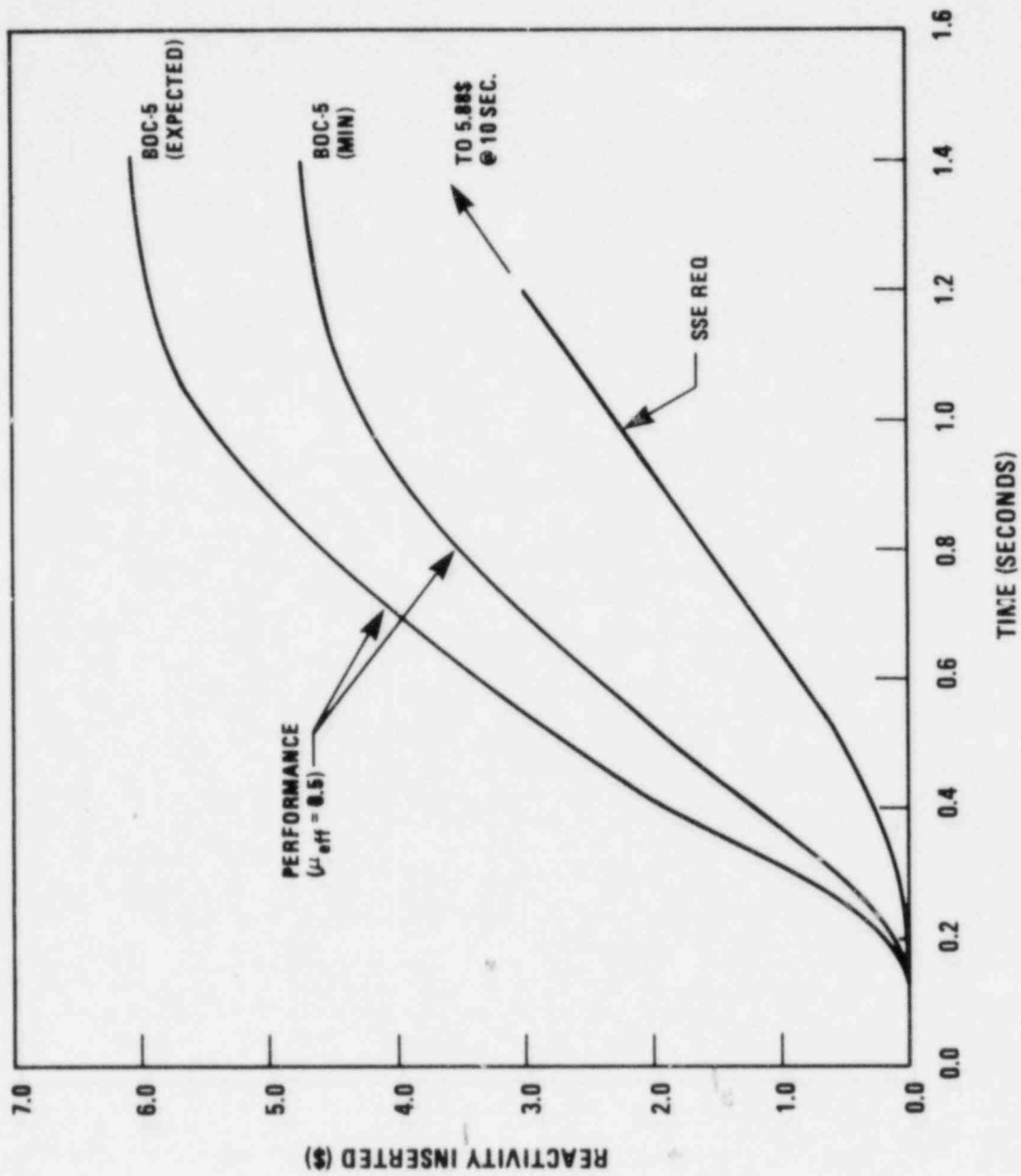


Figure 4.2-119. PCRS Seismic Scram Insertion Performance



#### 5.2.1.5 Reactor Vessel Preheat

The Reactor Vessel Preheat System will control the dry heat-up and cool down of the Guard Vessel, Reactor Vessel and Internals between ambient (70°F) and 400°F and if required will provide make-up heat for that lost to the Reactor Cavity during prolonged shutdowns.

The heat will be provided by tubular electrical heaters mounted between the Guard Vessel and insulation. These heaters will be arranged circumferentially around the Guard Vessel and will be grouped and controlled in zones of uniform heat output. Temperature sensing devices will monitor the Guard Vessel temperature in each of these zones and provide the necessary feedback for power level adjustments in the heaters.

The heaters will be mounted to the same framework which supports the Guard Vessel insulation. Attachment clips will offset the heaters from the Guard Vessel surface. Convective barriers, reflective sheaths and Guard Vessel insulation will be used to optimize heat input to the Guard Vessel and minimize losses to the Reactor Cavity.

Preliminary preheat, startup, shutdown analyses have been performed on the Reactor Vessel and Guard Vessel to determine the temperature differences which will result in opening and/or closure of the annular gap between the two vessels. By necessity the preheat analysis is very preliminary since no firm preheat procedure has yet been developed. Figures 5.2-4 through 5.2-6 show the temperature differences between the Reactor Vessel and Guard Vessel in the inlet and outlet plenum regions for the three transients in question. As shown the largest positive temperature difference between the Reactor Vessel and the Guard Vessel occurs in the outlet plenum region during startup (335°F) while the largest negative temperature difference occurs in the outlet plenum region during shutdown (-214°F). The nominal radial gap between the reactor vessel and guard vessel is 8 inches at assembly and at the end of preheat. This gap decreases to approximately 7.6 inches minimum during start-up and increases to approximately 8.3 inches maximum during shutdown. During preheat the gap also increases but to a lesser value than during shutdown due to the smaller maximum temperature difference.

Variations in the axial gap between the bottom of the reactor vessel and the inner surface of the guard vessel are noted between the states shown in the table. Thus the largest axial gap is 11.0 inches at the dry cold condition and the smallest gap is 6.2 inches at the end of the heating phase of preheat.

#### 5.2.2 Design Parameters

Overall schematic views of the reactor vessel, closure head assembly, inlet and outlet piping, and guard vessel are shown in Figures 5.2-1, 1A and 1B. The top view is given in Figure 5.2-2.

### 5.2.2.1 Reactor Vessel and Support

The reactor vessel and support will be constructed mainly of austenitic stainless and low alloy steels, and consists of six basic sections: the support ring, the vessel flange, the barrel, the core support forging and cone, the inlet plenum, and the vessel thermal liner.

17 | 59 | The support ring is an SA 508 Class 2 steel forging welded to the vessel flange. A box ring type of reactor vessel support interfaces with the vessel support ring and the reactor cavity support ledge. Holddown bolts pass through holes in the vessel support ring, the reactor vessel support and the support ledge clamping the three together. The vessel support is a ring structure with a box type cross section. The vertical sides of the box are Inconel 600 to limit the heat flow from the reactor vessel. The top and bottom plates of the box cross-section are 59 | 58 | SA 543 Class 2. The bolts are SA 193 Type B7 with 3.50-8UN threads. The ring supports the reactor vessel and internals and closure head. The vessel flange is a second SA 508 Class 2 steel ring forging welded to an Inconel 600 transition section. The latter is, in turn, welded to the barrel. Radiation shielding in the form of a boron carbide collar surrounding the vessel near the flange is provided in the annulus between the reactor vessel and the vessel support ledge. The barrel comprises the upper cylindrical portion of the vessel and has an inside diameter of 243 in. with a minimum wall thickness of 2.38 in. The lower end of the barrel is joined to the core support forging and cone, which provide support for the core support structure. The overall height of the reactor vessel and support is nominally 704 in. (58 ft. 8 in.). The inlet plenum is designed for 200 psig at 775<sup>o</sup>F and -15 psig at 600<sup>o</sup>F, the stainless steel portion of the outlet plenum is designed for 15 psig plus head of sodium 17 | at 900<sup>o</sup>F and -15 psig at 600<sup>o</sup>F.

Coolant enters the reactor vessel through three 24-inch nozzles located 120<sup>o</sup> apart in the inlet plenum below the core support structure. Core effluent and bypass flow are mixed in the outlet plenum region above the core, and the

The riser has been designed to maintain a maximum temperature of 125°F in the region of the elastomer seals. Thermal analysis has been completed for this design which shows that this temperature (125°F) is maintained by the head access area cooling system.

#### 5.2.2.3 Guard Vessel

The guard vessel is a bottom-supported, right circular cylindrical vessel surrounding the reactor vessel. It was fabricated from SA240 Type 304 stainless steel. The purpose of the guard vessel is to assure outlet nozzle submergence in the event of a leak in the reactor vessel nozzles, piping, or

pipng connections. To fulfill this requirement the guard vessel extends to approximately 6 ft. above the minimum safe sodium level providing for sodium shrinkage and pumping head differential. Also, the guard vessel permits inservice inspection of the reactor vessel by providing a nominal clearance of 8 in. between the two. The guard vessel is insulated on the outer surface to limit the heat load into the reactor cavity cell and to reduce heat loads to the Reactor Cavity Heating and Ventilating System. A trace heating system is mounted on the outside surface of the vessel for pre-heating and heating during prolonged plant shutdown.

Flux monitors for low, intermediate and full power operation are provided in the annulus between the guard vessel and reactor cavity cell walls. This annulus will be filled with nitrogen gas ( $\leq 2\%$  oxygen by volume). A discussion of the reactor cavity cell is found in Section 3.8 and 3.A.1.

Continuity detectors and aerosol sampling lines are mounted inside the guard vessel to detect potential leaks in the reactor vessel or inlet or outlet piping. See Section 7.5.5.1.

### 5.2.3 Special Processes for Fabrication and Inspection

#### 5.2.3.1 Nondestructive Examination

Nondestructive examination of materials and welds will be performed in accordance with the ASME Boiler and Pressure Vessel Code and RDT Standards. The techniques employed, as appropriate for the respective product forms, materials, and weld configurations comprising the reactor vessel, closure head, and guard vessel, are liquid penetrant, magnetic particle, ultrasonics, and radiography. Surface finish and cleanliness will also meet all requirements of the ASME Code and the other contract documents. Periodic swab tests of stainless steel surfaces during fabrication in the shop will be performed to assure that potentially harmful substances such as chlorides do not contact the components in concentrations greater than specified in applicable codes and standards.

#### 5.2.3.2 Controlled Welding to Maintain Alignments

Specified alignments must be maintained between the core support structure and the upper end of the reactor vessel. Where welds such as girth seams in the vessel and the weld attaching the core support structure to the vessel influence these alignments, special welding procedures and processes utilizing proven technology will be used to control the relative alignments of the parts being joined by welding.

Prior to any welding, the core support structure will be aligned by equalizing the gap between the core barrel and thermal liner support ring at four points located  $90^\circ$  apart. Also, the weld preps on the core support structure and core support cone will be aligned vertically and radially using the respective weld lands as the reference surface. Four wedges, which have been contour machined to match half the weld geometry, are placed in the top of the joint. Their purpose is to prevent movement during initial welding.

Welding will be accomplished by using four welders positioned  $90^\circ$  apart. Movement of the core support structure during welding will be monitored by

measuring the distances between the core barrel and the thermal liner support ring at four equally spaced locations. If 1/16 inch or more distortion occurs, welding will stop on one side and continue on the opposite side until re-alignment occurs. Continuous monitoring will be performed until 1/2 inch of weld has been deposited. At that point, the wedges will be removed and periodic monitoring will be performed during the remainder of the welding.

After welding is complete, the weld prep for the top portion of the vessel at the top of the thermal liner support ring will be machined concentric to the centerline of the core support structure. The top portion of the vessel is fabricated so that the bottom weld prep is concentric to the vessel flange. The top portion of the vessel is then assembled to the lower assembly using a ship-lap joint (sometimes known as a spigot fit). With this joint, no special welding techniques are required to maintain alignment, it is purely manual metal-arc welding. By having precise alignment within the two sub-assemblies, that is, centerline to weld prep and by using a precision fit-up of these sub-assemblies, the core support structure is located to vessel flange within the required tolerance.

The weld circumference was divided into four quadrants, each of which was divided further into 12-inch increments. The first weld pass was made using four welders working simultaneously, one welder per quadrant. The position of the core support structure then was measured. If a significant movement was found to occur, it was corrected by welding 12-inch increments which were selected by the welding engineer. The subsequent passes were welded and corrections made as necessary. This was repeated until movement of the core support structure ceased.

The selective placement of weld passes to control distortion during welding does not result in localization of overlaps or start-stops. The weld overlaps or start stops are no different from those encountered in normal arc welding. Sensitization is controlled, as it is in other shop fabrication and field welds, by limiting the interpass temperature to 350°F maximum per RDT Standard E15-2-NB, which is imposed by appropriate equipment specifications.

#### 5.2.3.3 Dimensional Checks

All dimensions of the reactor vessel, closure head, and guard vessel will be measured and checked against the dimensions and tolerances specified on the manufacturing drawings. Any deviations will be documented by Supplier

Nonconformance Reports. Approval of dimensions not in accordance with the drawings will be granted only after determining that safety and operability of the plant will not be affected adversely. Deviations which do not meet the requirements of the ASME Code will not be permitted.

#### 5.2.3.4 ASME Code Pressure Tests

Pressure tests will be performed on the completed reactor vessel and on the completed closure head as required by the ASME Code.

The high-pressure inlet plenum portion of the reactor vessel has been pressure tested to a pressure of 250 psig. This pressure test took place after the installation of the core support structure. The pressure test also provided structural verification of the core support structure, although not required by the ASME Code. Following the pressure test of the inlet plenum, the entire vessel was pneumatically tested; during this test, the upper end of the vessel was sealed by a test head.

The closure head was pneumatically tested to a pressure of 18 psig. A suitable test fixture was used to retain the head and apply the test pressure to it.

#### 5.2.4 Features for Improved Reliability

##### 5.2.4.1 Reactor Vessel Thermal Liner and Nozzle Liners

In order to protect the pressure boundary of the vessel in the outlet plenum region from high temperatures and severe temperature gradients during steady-state and transient conditions, the reactor vessel is provided with a thermal liner that extends downward from above the sodium pool level to an elevation below the core support horizontal baffle. Nozzle liners for this purpose also are provided for the three outlet nozzles and for the makeup nozzle.

##### 5.2.4.2 Internal Elbows in Reactor Vessel Inlet Plenum

In order to promote mixing of the three inlet streams in the reactor vessel inlet plenum and minimize thermal gradients in the pressure boundary of the inlet plenum, each inlet nozzle is provided with an internal pipe elbow that deflects the flow downward and away from the wall. In this manner, the mixing of the entering sodium occurs in the interior of the plenum, providing coolant uniform temperature to core components.

The method of obtaining data representative of irradiated permanent component materials consist of 1) selection of coupons of component materials used at locations where it is predicted that detectable change will occur, 2) fabrication of test specimens from the coupons, 3) irradiation of the specimens in the reactor in environments which will provide advanced data and 4) withdrawal of the specimens at planned intervals during the plant life and testing of the specimens at component anticipated service temperature. Details of the coupon/specimen selection, irradiation and testing requirements are as follows:

19

#### Coupon Selection Requirements

1. The materials of the permanent Reactor System components, which are designed for the full life of the plant, shall be considered for representation by surveillance coupons.
2. Materials surveillance coupons, to monitor radiation effects in the materials of permanent reactor system components, shall be required if the predicted fluence is greater than  $1 \times 10^{21}$  n/cm<sup>2</sup>, E > 0.0, in the component material.
3. Subject to requirements 1 and 2, base metal and weld metal coupons shall be required.
4. For each location defined by the application of requirements 1 through 3, sufficient material shall be obtained, during fabrication, to produce coupons from which 15 test specimens shall be fabricated.
5. The test specimens shall be sub-size tension specimens as indicated in ASTM E-8, having a gage diameter of 1/4 inch and a gage length of 1 inch and an overall length of 2 5/8 inch.

#### Test Specimen Irradiation Requirements

1. Surveillance test specimens shall be irradiated in the Removable Radial Shields and/or the Fuel Transfer and Storage Assembly as required to obtain environmental conditions as noted below.
2. Three test specimens of each component material, defined by the coupon selection requirements, shall be placed in a capsule set. (A capsule set shall be one or more individual capsules as required to obtain environmental conditions as noted below). Four capsule sets shall be assembled.

19

3. The four capsule sets shall be in place in the reactor at startup. One set shall be withdrawn at each of 1/4, 1/2 and 3/4 of plant life (to the nearest normal refueling interval). The fourth set shall remain in the reactor as a contingency set.
4. Positioning of the capsule sets and the distribution of test specimens within the capsules shall be such that the minimum anticipated fluence on the test specimens shall be as follows:
  - o Test Specimen to be withdrawn at 1/4 of plant life shall have anticipated total fluence at least equal to the anticipated total fluence on the component material at 1/2 plant life.
  - o Test Specimens to be withdrawn at 1/2 of plant life shall have anticipated total fluence at least equal to the anticipated total fluence on the component material at 3/4 plant life.
  - o Test Specimens to be withdrawn at 3/4 of plant life shall have anticipated total fluence at least equal to the anticipated total fluence on the component material at full plant life.
  - o Irradiation of the contingency test specimens shall essentially duplicate irradiation of the test specimens scheduled for withdrawal at 3/4 of plant life.
5. The test specimens shall be positioned so the anticipated total flux shall not exceed three times the anticipated total flux on the component material.
6. The test specimens shall be positioned to best simulate other component material service conditions after fluence criteria are met.

#### Test Specimen Testing Requirements

1. Three test specimens of each component material, defined by the coupon selection requirements, shall be tested in the unirradiated condition to provide reference data.
2. Irradiated specimens shall be tested after removal from the reactor according to the schedule defined by the irradiation requirements.
3. Specimens shall be tested at a strain rate of  $3 \times 10^{-5}$  in/in/ sec and at the anticipated service temperature of the component material.
4. Testing procedures shall include the use of extensometers and other devices to produce a record of load and elongation data.

#### 5.2.4.5.2 In-Service Inspection

In-service inspection (ISI) equipment is provided to perform a visual examination of the outer surface of the welds on the reactor vessel and



nozzles, and the inner surface of the welds of the reactor guard vessel. These examinations are to be performed during those periods when reactor coolant temperature is approximately 400°F. The ISI equipment for the reactor vessel/guard vessel annulus consists of a TV camera, transporter, and cabling to provide for cooling and appropriate electrical interfaces.

The overall sensitivity of the TV camera will be such that accumulations of liquids, liquid streams, liquid drops and smoke are discernible. The TV examination will also be capable of determining the presence of loose parts and debris.

The reactor vessel, guard vessel, guard vessel extension, and support ledge insulation form an assembly designed to provide transporter access to all reactor vessel welds, excepting portions of three reactor vessel longitudinal welds masked by the reactor cavity radiological shield and the reactor guard vessel longitudinal welds covered by the leak detector tubes mounted to the guard vessel. The transporter will be similar to the transporter design employed on FFTF.

#### 5.2.5 Quality Assurance Surveillance

Quality assurance surveillance for the reactor vessel and reactor vessel guard vessel has been performed by quality assurance personnel who were present at the fabricator's facility during all important phases. Quality assurance personnel have monitored all important phases of fabrication for the closure head. The interfaces between the various QA organizations are given in Chapter 17.0.

### 5.2.6 Materials and Inspections

The materials used in fabricating the reactor vessel, closure head and guard vessel are summarized in Table 5.2-3. In general these materials (for the reactor vessel and closure head) conform to ASME Boiler and Pressure Vessel Code, Section III, and the supplemental requirements of RDT Standard E15-2NB-T. The materials for the guard vessel conform to ASME Boiler and Pressure Vessel Code, Section III, requirements for Class I Vessel.

Requirements for delta ferrite content are given in the ASME Code, Section III, ASME Code Case 1592, RDT Standards M1-1T and M1-2T, and the reactor vessel specification. In all cases, the determination of delta ferrite content will be made from chemical analyses of welding materials as applied to the Shaeffler Diagram in the ASME Code. There is no requirement that delta ferrite determinations be made from production welds.

The service environment and temperature will not result in material degradation effects in the combination of dissimilar metals and weldments utilized between the Type 304 stainless steel vessel and the SA 508 class 2 ferrite vessel flange.

The transition region of the vessel is located in a position which has a total fluence of less than  $10^{15}$  n/cm<sup>2</sup> (E>0.0 MeV). This low fluence level is considered to be below the threshold level for mechanical property degradation of the materials involved (Ref. 1).

The service temperature for the SA 508 to Inconel 600 weld is approximately 465°F and that for the weldment between the Inconel 600 and Type 304 stainless steel is about 650°F. At these operating temperatures, the three base metals involved together with the Inconel 82 weld filler metal are metallurgically stable. (Ref. 2 and 3).

Both the internal and external environment are considered benign with regard to degradation of the various materials in the transition region. The internal environment will be argon gas and sodium vapor and essentially no sodium mass transfer or interstitial transfer effects occur at temperatures below 700°F, especially when the sodium is present as a vapor or thin condensed layer (Ref. 4 and 5). The external environment is reactor cavity gas, nitrogen plus approximately 2% oxygen, and the interaction of the materials involved with this reactor cavity gas are negligible at the low service temperatures.

Selection of the materials for this transition joint was made based on the above considerations coupled with the requirement to minimize thermal expansion differences which could cause high stresses to be built up during thermal cycling. In addition, the use of the nickel base alloy filler metal, Inconel 82, minimizes the depletion of carbon from the fusion zone of the SA 508 during welding and subsequent high temperature stress relief.

TABLE 5.2-1

SUMMARY OF CODE, CODE CASES AND RDT  
STANDARDS APPLICABLE TO DESIGN AND MANUFACTURE  
OF REACTOR VESSEL, CLOSURE HEAD AND GUARD VESSEL

Component/Criteria	Reactor Vessel	Closure Head*		Guard Vessel
		Pressure Boundary	Internals (as appropriate)	
Section III ASME Code, 1974 Edition	Addenda thru Winter '74  Class 1	Addenda thru Winter '74  Class 1	Addenda thru Winter '74  Class 1	Addenda thru Summer '75  Class 2**
ASME Code Cases	1521-1, 1592-2, 1593-0, 1594-1, 1595-1, 1596-1 (1682, 1690 Optional)	1682, 1690	1521-1 1592-4, 1593-1	1592-4, 1593-1, 1594-1 If elected by supplier 1521-1 & 1682
RDT Standards Mandatory	E8-18T, 2/75 E15-2NB-T, 11/74 Amend thru 1/75  F2-2, 8/73 Amend thru 7/75  F3-6T, 12/74  F6-5T, 8/74 Amend thru 2/75  F7-3T, 11/74  F9-4T, 9/74	E15-2NB-T, 11/74 Amend thru 6/75  F2-2, 8/73 Amend thru 7/75  F3-6T, 12/74***  F6-5T, 8/74 Amend thru 2/75  F7-3T, 6/75  M1-1T, 3/75 M1-2, 3/75 Amend thru 7/75	E15-NB-T, 11/74 Amend thru 6/75  F2-2, 8/73 Amend thru 7/75  F9-4, 9/74  F6-5T, 8/74 Amend thru 11/75  F7-3T, 6/75  F9-4, 9/74	E15-NB-T, 11/74 Amend thru 6/76  F2-2, 8/73 Amend thru 7/75  F3-6T, 10/75 With Amend. 1/75  F6-5T, 8/74 Amend thru 11/75  F7-3T, 6/75  F9-4, 9/74

\*For those reactor vessel and closure head components internal to the pressure boundary special purpose high cycle fatigue curves and creep damage rules have been developed as discussed in Appendix 5.2A.

5.2-12

Amend. 72  
Oct. 1982

TABLE 5.2-1 (Continued)

Component/Criteria	Reactor Vessel	Closure Head		Guard Vessel
		Pressure Boundary	Internals (as appropriate)	
RDT Standards	M1-1T, 3/75			
	M1-2T, 4/75	M1-4T, 3/75		
	Amend. 6/75			
	M1-4T, 3/75	M1-6T, 4/75		
		Amend 1-7/75		
	M1-6T, 4/75	M1-10T, 3/75		
	Amend. 6/75			
	M1-10T, 3/75	M1-11T, 3/75		
		Amend 1-7/75		
	M1-11T, 3/75	M1-17T, 3/75		
	Amend. 6/75			
	M1-17T, 3/75	M2-2T, 12/74		
	M2-2T, 12/74	M2-7T, 3/75***		
	M2-5T, 1/75	M3-10T, 7/75		
	Amend 1-2/75			
	M2-7T, 2/75	M7-4T, 3/75		
	M2-18T, 4/76			
	M2-21T, 12/77			
	M3-6T, 3/75			
	M3-7T, 4/75			
	M5-1T, 11/74			
	M5-2T, 5/73			
	M5-3T, 12/74			
	M5-4T, 1/75			
	M6-3T, 2/75			
	M6-4T, 2/75			
	M7-3T, 11/74			
M7-4T, 4/76				
Non-Mandatory	F9-5T, 9/74	F9-5T, 9/74	F9-5T, 9/74	

\*\*Functionally designated Class 2, and constructed to rules for Class 1, but not hydrostatically tested or code stamped.

\*\*\*Except for the three rotating plugs, for which the applicable issues are: F3-6T, 3/69 for LRP & SRP; F3-6T, 5/74 for IRP.  
M2-7T, 2/69 for LRP & SRP; M2-7T, 2/74 for IRP.

TABLE 5.2-2  
OBJECTIVES FOR IN-SERVICE INSPECTION

Components	Surface <sup>a</sup>	Type of Inspection			On-line Monitoring	
		ISI Transporter & TV Camera	Penetrant, Ultrasonic Magnetic Particle, Visual	Temperature	Leak Detection	
Reactor Vessel	o	X		X		
Guard Vessel	I	X				
Closure Head	o		X	X		
Closure Head	I			X		
Vessel Nozzles <sup>b</sup>	I, o	X		X		
Between Reactor Vessel and Guard Vessel					X	
Head Access Area					X	

<sup>a</sup> I - Inside, o - outside

<sup>b</sup> nozzle to vessel and nozzle to extension joint; reactor vessel-outside, guard vessel nozzle to vessel-Inside

Both PHTS and IHTS pumps require a shaft seal to effect a zero leak seal from cover gas to atmosphere. This shaft seal, shown schematically in Figure 5.3-14A, is an oil lubricated, double rubbing face seal. The seal has a shaft driven internal oil circulator and an integral air to oil heat exchanger, with oil supply to make up for oil leakage past the rubbing faces. Oil leakage from the seal assembly into the sodium coolant is prevented by two barriers. The first barrier is an oil dam approximately 1.2 inches above the lower face seal. The normal leakage from the lower face seal is diverted by this oil dam into the oil leakage drain passage into the lower seal leakage collection reservoir. A second barrier is the collar above the drop down seal located just above the purge labyrinth. This collar extends beyond and over the labyrinth, thereby shunting any oil to a drain plenum. For oil to penetrate into the sodium, three things must happen:

- o Failure of the oil dam
- o Failure of the collar to divert oil
- o Overflow of the plenum drainage over the drop down seal lip

A positive pressure is maintained in the shaft seal oil at all times by means of an oil supply tank which will be pressurized above the loop operating pressure. The oil feed line to the seal will be oriented to preclude seal drainage in the event of a line break. The seal is capable of many hours of operation on the self contained fluid.

The oil system supporting the shaft seal contains three tanks, each of which will have a level probe, thereby permitting monitoring of total oil inventory, its location, and permitting calculation of seal leak rate. The lower seal leakage collection tank is sized to hold the entire system's oil inventory of approximately 41 gallons.

Oil vapors which may potentially be drawn from the lower seal leakage collection tank into the tank ullage during draw down (pump speed up) are retarded from such passage by means of a split flow purge gas feed of recycled argon into the purge labyrinth. This gas feed splits and flows up and down the shaft from the feedpoint. This gas input is flow controlled at the inlet, and flow controlled at the discharge from the lower seal leakage collection tank. If feed pressure into the tank is detected to be low (by the gas feed system) the discharge of gas from the tank will be closed. In event of gas line rupture at the oil tank discharge, the orificing by the line will retard loss of cover gas pressure.

Radioactive vapors from the tank ullage are prevented from escape to the atmosphere by the two barriers consisting of the gas downflow at the purge labyrinth and the oil lubricated double shaft seal. Radioactive purging is continuous by means of the bubbling in the standpipe, which is connected to RAPS.

Functionally, the drum receives a saturated water/steam mixture from the evaporators and subcooled feedwater and produces saturated steam of low moisture content for the superheater and subcooled water of low steam content for the recirculation pump. The water/steam mixture from the evaporators enters the drum through the water/steam nozzles and flows into an annular volume along the sides of the inner drum wall created by a girth baffle extending along the side of the drum for the length of the cylinder. Centrifugal steam separators mounted along the length of the drum draw from this annular volume, separate the mixture into phases, and direct the steam upward and the water downward into the inner volume of the drum. The main feedwater enters the drum through a single nozzle which feeds two distribution pipes through a "Y" connection inside the drum. The feedwater is distributed along the length of the drum by rows of orifice holes in the two pipes which are located along each side of the drum beneath the steam separators. The auxiliary feedwater enters through a separate nozzle and is distributed along the length of the drum by two rows of spray nozzles in a single distribution pipe located above the water level in the drum. To preclude waterhammer due to injection of highly subcooled water interfacing with saturated steam within a closed volume, the spray line is vented by the nozzles plus 18 7/32" OD holes. These vents ensure that the feed line will remain full of water at the temperature of the steam drum inventory. Feedwater mixes with the water from the separators and is drawn downward and out through the water outlet nozzles by the recirculation pump. The steam passes upward through chevron type dryers in the upper portion of the drum and out through the steam outlet nozzles to the superheater. The dryers remove all but the last fractional percent of the moisture from the steam and drain this moisture back to mix with the resident drum water. Drum drain piping, located along either side of the drum in the region where the water from the separators enters the drum inner volume, draws water of high impurity concentration from the drum.

#### 5.5.2.4 Overpressure Protection

##### Location of Pressure Relief Devices

Safety/power relief valves are located in the steam generation system to:

1. Prevent a sustained pressure rise of more than 10 percent above system design pressure at the design temperature within the pressure boundary of the system protected by the valve under any pressure transients anticipated; and
2. Provide steam generator module blowdown capability.

Installation of the valves will comply with the requirements as specified in Section 3.9.2.5. Safety/power relief valves are installed on the outlet lines from each evaporator to provide venting capability and a portion of the required safety/relief capability. Safety valves are installed on the steam



drum to provide the remainder of the safety capability for the recirculation loop. Additional safety/power relief valves are installed on the steam exit line from the superheater because the steam lines to and from the superheater have isolation valves. The P&ID for the Steam Generation System, Figure 5.1-4 shows the locations of these safety/power relief valves. Additional details of sizes and pressure rating are given in Table 5.5-8.

### Pressure Relief Devices

#### Water/Steam Side

Each safety relief valve on the evaporator outlet piping provides a saturated steam (100% quality) relief capacity of 430,000 lb/hr, or 39% of the rated steam generating capacity of the recirculation loop. Each safety relief valve on the steam drum provides a saturated steam relief capacity of 410,000 lb/hr, or 37% of the rated steam generating capacity of the recirculation loop. The difference in rated capacity of these valves is due to the difference in the valve set pressure. The combined relief capacity of the six valves for the recirculation loop is therefore 230% of the rated steam generation capacity. This generous margin is provided for two reasons: (1) the capacity required to relieve most of the overpressure transients in the recirculation loop can be satisfied by opening one or both of the steam drum valves, relieving the system with dry steam rather than wet steam; (2) the capacity of the evaporator relief valves is based on the capacity required to achieve rapid blowdown of the evaporator modules following a water to sodium leak.

Three safety/power relief valves installed on the exit line from the superheater provide a relief capacity of 75% of rated superheater steam flow at a pressure of approximately 1800 psig and temperature of 900<sup>o</sup>F. The remaining 25% of rated flow is relieved by the steam drum valves.

Settings for the safety/power relief valves are in accordance with Code requirements. Setting presently selected are shown in Table 5.5-8.

### Tests and Inspections

In-service inspection of the steam generator modules is discussed under In-Service Inspection Program, Section 5.5.2.1.3.

### Part Load Operation

Part load operation curves over the range of steam flows from 40 to 100 percent are presented in Section 5.7.2.

Design module heat transfer length were used with nominal values of sodium, water or steam, and tube heat transfer correlations for purposes of this analysis. This implied excess area, therefore, results in sodium operating temperatures in the evaporator lower than those used for design. Design heat transfer areas are determined by adding sufficient margin to the module length to permit operation with fouled tubes at 100% power for nominal sodium conditions. The margin calculated is 10% and is arrived at considering the error-band in heat transfer coefficients and tube wall thickness. Also, included in the 10% margin is a 5% surface allowance made for tube plugging.

The steam flow rate is defined by turbine conditions, power level, and feedwater temperature.

The water or steam side temperature and flow rate are essentially the same for both clean operation and fouled operation. However, the presence of fouling will cause an increase in the required sodium operating temperatures and flow compared to clean operation.

For power levels below about 40 percent a good portion of the inlet sodium end of the superheater and the outlet sodium end of the evaporator will operate close to isothermal temperatures with small sodium to water temperature differences. This is because most of the heat transfer takes place in other portions of the modules.

### 5.5.3.6 Evaluation of Steam Generator Leaks

A primary design objective for the steam generators is that they be of sufficiently high quality that leaks in the sodium/water boundary will not occur. Careful design and close quality control of materials and manufacturing processes are expected to yield units which are free of common defects, and the probability of a leak in a steam generator tube is expected to be quite small. A Steam Generator Leak Detection System, described in Section 7.5.5, has been provided to allow operator action to limit the consequences of a leak. The leak detection system will alert the operator to the existence of a leak rate as low as  $2 \times 10^{-5}$  lb water/sec, which will allow sufficient time for operator action to prevent a significant increase in the leak rate for a broad spectrum of leak rates.

59

As a final level of protection against tube leaks in a steam generator, the steam generators and the IHTS are being designed to withstand the effects of a large sodium water reaction (SWR). The ASME Code categories being applied in the design of the steam generators and IHTS piping and components for the large SWR event are given in Table 5.5-10.

The design basis leak (DBL) for the CRBRP was selected based upon examination of the physical processes which exist for leak initiation and growth. Two types of tests have been reported which provide information on the leak growth mechanism - small scale tests which model effects of a SWR on materials, and large scale tests which model a large water leak in a model of a steam generator. Smaller scale sodium-water reaction tests have been done to develop an understanding of the effect of a SWR on neighboring tubes in a steam generator. Three mechanisms have been identified for leak growth: self-wastage, impingement, and overheating (mechanical damage from pipe whip, although extremely unlikely, could be considered another mechanism, as discussed later in this section). Self-wastage has been shown to occur for very small leaks in the range of  $10^{-6}$  to  $10^{-5}$  lb/sec (Ref. 13). The process is depicted in Figure 15.3.3.3-1. The result of this process is a leak size of the order of  $10^{-5}$  to  $10^{-2}$  lb/sec. which can produce wastage on another tube in the vicinity of the leaking tube.

Wastage can occur on the outside of a steam generator tube from a leak in another tube in the vicinity. Tests of this mechanism have typically been done by using a water jet directed through sodium to a target material sample. Water Injection rates of approximately  $10^{-4}$  lb/sec to 1 lb/sec have been tested. The wastage mechanism results in erosion of the target material at maximum rates of 0.001 to 0.007 inches per second (Ref. 14, 29). The wastage rate is found to be a function of the water injection rate, tube spacing, sodium temperature and leak geometry. Wastage occurring on the surface of a CRBRP steam generator tube at these rates could cause a secondary water leak from tube penetration. However, this would require at least 20 seconds to penetrate the 0.109 inch thick tube wall assuming an initiating leak of the proper characteristics to produce maximum wastage.

The size of a secondary water leak resulting from wastage is difficult to quantify since wastage tests are typically done on materials samples rather than pressurized tubes. The wastage areas observed in tests have ranged from  $0.1 \text{ in}^2$  to  $1.5 \text{ in}^2$ . Failure areas corresponding to the highest observed wastage areas would result in water leak rates corresponding to that of a double-ended guillotine tube failure. However, the entire wastage area would not be expected to blow out. The wasted areas are typically pit-shaped with the area of the pit decreasing with depth. It would be expected that the small area at the bottom of the pit would fail, yielding a return water leak which halts the wastage. Therefore, while the size of a secondary failure caused by wastage is difficult to predict, it is expected to be smaller than the leak rate corresponding to a double-ended guillotine failure.

References to Section 5.5

- \* 1. W.H. Yunker, "Standard FFTF Values for the Physical and Thermophysical Properties of Sodium" WHAM-D-3, July 6, 1970.
- \* 2. J.A. Bray, "Some Notes on Sodium/Water Reaction Work," CONF-710548, pp. 187-205, July 1972.
- \* 3. Nuclear System Materials Handbook, Hanford Engineering Development Laboratory, TID-26666, Volume 1, Section 2-2 1/4 Cr-Mo, pp. 1.0-1.2, Rev. 0, August 14, 1974.
- \* 4. R.B. Harty, "Modular Steam Generator Final Project Report," Atomic International, TR-097-330-010, September 1974.
- \* 5. Nuclear Systems Materials Handbook TID 26666, 1974.
- \* 6. V.L. Streeter and E.B. Wylie, Hydraulic Transients, McGraw-Hill, New York, 1967, Ch. 2 and 3.
- \* 7. John Pickford, Analysis of Surge, MacMillan, London, 1969, pp. 32-37.
- \* 8. D.J. Cagliostro, S.J. Wiersman, A.L. Florence, Stanford Research Institute Final Report P.O. 190-C1H88GX, "Pressure Pulse Propagation in a Simple Model of the Intermediate Heat Transport System of a Liquid Metal Fast Breeder Reactor," June 1975.
- \* 9. "RELAP4/MOD5 a Computer Program for Transient Thermal-Hydraulic Analysis of Nuclear Reactors and Related Systems," prepared by Aerojet Nuclear Company for U.S. Nuclear Regulatory Commission and Energy Research and Development Administration under Contract E (10-1) - 1375, ANCR-NUREG-1335, September 1976.
- \* 10. J.N. Fox, R. Salvatori, H.J. Thailar (W NES), "Experimental Bending Tests on Pressurized Piping Under Static and Simulated Accident Conditions" TRANSACTIONS, ANS Power Division Conference on Power Reactor Systems and Components, September 1-3, 1970.
- 11. "Draft Design Basis for Protection Against Pipe Whip," ANSI N176, June, 1974.
- 12. Deleted
- \* 13. Gudahl, J.A. and Magee, P.M., "Microleak Wastage Test Results," GEFR-00352, March 1978.

\* References annotated with an asterisk support conclusions in the Section. Other references are provided as background information.

- \* 14. Greene, D.A., Gudahl, J.A., Hunsicker, J.C., "Experimental Investigation of the Wastage of Steam Generator Materials by Sodium/Water Reactions," GEAP-14094, January 1976.
- \* 15. Dumm, K. et.al., Experimental and Theoretical Investigations on Safety of the SNR Straight-Tube Design Steam Generator with Sodium-Water Reactions, INTAT72.12 (ERDA-TR-27), INTERATOM, April 1972.
- 16. J.A. Bray, "Some Notes on Sodium/Water Reaction Work," Paper presented at the Specialists Meeting on Sodium Water Reactions, CONF-710548, held May 18-21, 1971, Melekess, USSR.
- \* 17. B.V. Kuplin, et.al., "Study of Na and H<sub>2</sub>O Interactions in a One Megawatt Modular Steam Generator," Paper presented at the Specialists Meeting on Sodium-Water Reactions, CONF-710548, Held May 18-21, 1971, Melekess, USSR.
- 18. Liquid Metal Engineering Center - Failure Data Handbook, LMEC Memo - 69-7, Volume 1, Atomics International, AI-RAR-096-13-00, August 15, 1969.
- 19. Reactor Primary Coolant System Rupture Study, Quarterly Report No. 23, October-December 1970, GEAP 10207-23, January 1971.
- 20. J.A. Bray, et al., "Sodium/Water Reaction Experiments on Model P.F.R. Heat Exchangers- The NOAH Rig Tests," TRG-Reports-1519, 1967.
- 21. J.A. Bray, "A Review of Some Sodium/Water Reaction Experiments," British Nuclear Energy Society Journal, Vol. 10, No. 2, April 1971.
- \* 22. P.B. Stephens, D.N. Rodgers, et.al., "DNB Effects Test Program Final Report," GEFR-00100(L), June 1977.
- \* 23. J.C. Whipple, et.al., "U.S. Program for Large Sodium/Water Reaction Tests," GEFR-SP-039, November 1977.
- 24. R.L. Eichelberger, "Sodium-Water Reaction Tests in LLTR Series I, Final Report," ETEC-78-10, July 15, 1978.
- 25. J.O. Sane, et. al., "Evaluation of Sodium-Water Reaction Tests No. 1 Through 6 Data and Comparison with TRANSWRAP Analysis Series I Large Leak Test Program, Volumes I and II," GEFR-00420, June 1980.
- 26. J.C. Whipple, et.al. "Evaluation of LLTR Series II Test A-2 Results," General Electric Advanced Reactor Systems Department, July 1980, Prepared for U.S. Department of Energy under Contract No. De-ATc3-76SF70030, Work Package AF 15 10 05, WPT No. SG037.

27. J. C. Amos, et.al, "Evaluation of LLTR Series II Test A-3 Results, Revision 1," General Electric Advanced Reactor Systems Department, May 1982, Prepared for U.S. Department of Energy under Contract No. DE-ATc3-76SF70030, Work Package AF 15 10 05, WPT No. SG037.
28. J. O. Sterns, "Metallurgical Evaluation of the Modular Steam Generator (MSG) after LLTR Testing," ETEC-78-12, Sept. 1978.
29. D. A. Greene, J. A. Gudahl and P. M. Magee, "Recent Experimental Results on Small Leak Behavior and Interpretation for Leak Detection," CONF-780201, Vol. 1, paper No. 12 (First Joint U.S./ Japan LMFBR Steam Generator Seminar), February 1978.
30. J. C. Amos, et al, "Evaluation of LLTR Series II Test A6 Results," prepared for U. S. DOE under Contract DE-AT03-76SF0030, June 1981.
31. D. E. Knittle, et al, "Evaluation of LLTR Series II Test A7 Results," prepared for U. S. DOE under Contract DE-AT03-76SF70030, September 1981.
32. J. J. Regimbal, et al, "Evaluation of LLTR Series II Test A-8 Results," prepared for U. S. DOE under contract DE-AT03-76SF70030, February 1982.

\*References annotated with an asterisk support conclusions in the Section. Other references are provided as background information.

TABLE 5.5.12 MAXIMUM ALLOWABLE STEAM GENERATOR SYSTEM PRESSURE BOUNDARY

VALVE LEAK RATES

VALVE	LEAK RATE, LB/HR
Evaporator Inlet Isolation	4.7
Evaporator Inlet Water Dump Isolation	.02
Evaporator Outlet Relief	1.0
Steam Drum Relief	1.0
Superheater Inlet Isolation	4.7
Superheater Relief	1.0
Superheater Outlet Isolation	4.7
Superheater Bypass	1.2
Main Feedwater Isolation	4.7
Steam Drum Drain Isolation	4.7
Nitrogen Supply (per Conn.)	1.0

TABLE 5.5-13 SUMMARY OF U.S. LARGE SODIUM/WATER REACTION TESTS

COUNTRY	TEST DESIGNATION/ OBJECTIVE	TEST VESSEL	TEST BUNDLE	INITIAL PRESS./TEMP. SODIUM WATER PSIG OF PSIG OF	METHOD	WATER INJECTION DURATION SEC	WEIGHT LB	SIGNIFICANT RESULTS
U.S.	LLTR Series 1, SWR-1/One Double ended Gullotine (DEG) Failure near lower nozzle, sub- cooled H <sub>2</sub> O	Al-MSG 16- Inch ID Vessel Proto- typic Height	158 tubes of prototypic material and dimensions, prototypic- ally spaced	122 600 1900 543	Rapid DEG of pre-weakened tube	10	80	No Secondary failures. Maxi- mum wastage on one tube near leak site = 0.16 Inches. Only significant wastage in all 6 Series 1 tests.
	LLTR Series 1, SWR-2/Same as SWR-1 @ mid-span	Same as SWR-1	Same as SWR-1	81 628 1900 543	Same as SWR-1	10	60	No secondary failures
	LLTR Series 1, SWR-3 One DEG @ 1.75 In from upper tube sheet, Two-Phase H <sub>2</sub> O	Same as SWR-1	Same as SWR-1	116 800 1900 700	Same as SWR-1	5	40	No secondary failures
	LLTR Series 1, SWR-4 Same as SWR-3 with superheated steam	Same as SWR-1	Same as SWR-1	80 800 1900 700	Same as SWR-1	3	8	No secondary failures
	LLTP Series 1, SWR-5 Same as SWR-4 with 700-F Nitrogen Injected	Same as SWR-1	Same as SWR-1	90 800 1900 700	Same as SWR-1	3	zero	Served to calli- brate RELAP code
	LLTR Series 1, SWR-5 Same as SWR-4 with Three Equivalent DEG	Same as SWR-1	Same as SWR-1	90 800 1900 700	Same as SWR-1	3	8	No secondary failures. Series 1 served to validate the TRANSTRAP Code.



TABLE 5.5-13 SUMMARY OF U.S. LARGE SODIUM/WATER REACTION TESTS

COUNTRY	TEST DESIGNATION/ OBJECTIVE	TEST VESSEL	TEST BUNDLE	INITIAL PRESS/TEMP.		WATER INJECTION			SIGNIFICANT RESULTS		
				SODIUM PSIG OF	WATER PSIG OF	METHOD	DURATION SEC	WEIGHT LB			
U.S.	LLTR Series II, Test Same as A2 A1a, One DEG @ Lower Midspan, Injected Nitrogen, Prototypic Rupture Disk Assembly used on all Series II Tests		Prototypic	125	580	2000	580	Same as SWR-1	30	0	Prototypic rup- ture disk assembly used on all Series II tests. Served to verify RELAP calibration
	LLTR Series II, Test Same as A2 A1b, Same as A1a ex- cept A1b used double disk and minor difference in leak location.		Same as A2	125	580	2000	580	Same as SWR-1	43	0	Served to verify RELAP calibra- tion
	LLTR Series II, Test A2, One DEG @ Lower Midspan, sub- cooled H <sub>2</sub> O	Prototypic Cross-Section 1/2 Length	Prototypic	125	580	1700	580	Same as SWR-1	40	200	No secondary failures. Max- imum measured secondary wastage equals 4 mils. Prototypic double disc assembly served to calibrate TRANSWRAP rup- ture disc model

5.5-53C

TABLE 5.5-13 SUMMARY OF U.S. LARGE SODIUM/WATER REACTION TESTS

COUNTRY	TEST DESIGNATION/ OBJECTIVE	TEST VESSEL	TEST BUNDLE	INITIAL PRESS/TEMP.		WATER INJECTION			SIGNIFICANT RESULTS		
				SODIUM PSIG OF	WATER PSIG OF	METHOD	DURATION SEC	WEIGHT LB			
U.S.	LLTR Series II, Test A-3, One self- Wastage Leak Simulation @ sub- cooled H <sub>2</sub> O @ 0.1 lbm/sec @imed for maximum secondary damage.	Same as A2	Same as A2	145	580	1700	580	Rapid pull- apart of prenotched tube to expose 0.040" dia. hole.	145	144 plus	Secondary failures (less than an EDEG) after long de- lays (one minute and longer).
	LLTR Series II, Test A6, One DEG @ Lower Midspan Peri- phery, subcooled H <sub>2</sub> O.	Same as A2	Same as A2	125	580	1700	580	Same as SWR-1	36	200	No secondary failures.

System modified  
as gas-free  
Actual test con-  
tained large gas  
space to S.G.  
TRANSWRAP over-  
predicted  
measured  
pressures where  
comparable.

5.5-53D

Amend. 72  
Oct. 1982

TABLE 5.5-13 SUMMARY OF U.S. LARGE SODIUM/WATER REACTION TESTS

COUNTRY	TEST DESIGNATION/ OBJECTIVE	TEST VESSEL	TEST BUNDLE	INITIAL PRESS/TEMP.		WATER INJECTION			SIGNIFICANT RESULTS		
				SODIUM PSIG °F	WATER PSIG °F	METHOD	DURATION SEC	WEIGHT LB			
U.S.	LLTR Series II, Test A7, One DEG @ Lower Midspan, sub- cooled H <sub>2</sub> O higher initial sodium pressure.	Same as A2	Same as A2	255	580	2000	580	Same as SWR-1	2	15	Secondary tubes filled with nitrogen @ 400 PSIG.
	LLTR Series II, Test A8, Intermed- iate-sized super- heated steam injection.	Same as A2	Same as A2	180	900	1550	700	Rapid pull- apart of prenotched tube to ex- pose 0.054" dia. hole.	40		No secondary failures deduced from instrum- entation and post test helium leak checks. Final confirm- ation awaits post test destructive examination.
	LLTR Series II, Test A5, Inter- mediate-sized superheat in- jection	Same as A2	Same as A2	50	625	1450	625	Rapid pull apart of tube to ex- pose 0.25" dia. hole	58	TBD	Test Report not available. Examination of of test article in progress.

5.5-53e

Amend. 72  
Oct. 1982

44 |  
17 |  
58 |

#### 5.6.1.2.1.3 Surveillance and In-service Inspection

The SGAHRS system will be inspected in accordance with the intent of Section XI Division 1 of the ASME Code.

#### 5.6.1.2.1.4 Protection Against Accelerated Corrosion and Material Degradation

In water and/or steam, carbon steels are susceptible to pitting in the presence of chloride and oxygen. Furthermore, below 550°F, these materials are susceptible to caustic gouging and, perhaps, caustic stress corrosion cracking. Maintaining the water purity consistent with the requirements for chlorides, caustics and oxygen for short term operation will prevent these forms of localized attack.

Carbon steel is also susceptible to hydrogen embrittlement under SGAHRS operating conditions. However, maintaining the specified water purity will prevent this occurrence. Administrative procedures will be established to assure that water purity will be maintained.

#### 5.6.1.2.1.5 Material Inspection Program

58 | The SGAHRS material inspection program will be based on the requirements of the ASME Code, Section III, for carbon steel and 2% Cr 1mo. steel.

#### 5.6.1.2.2 Material Properties

58 | The materials used in the SGAHRS are described and discussed in Section 5.6.1.1.4.

#### 5.6.1.2.3 Component Descriptions

The major SGAHRS components have been designed with sufficient margin to assure that they will provide adequate cooling after a plant shutdown from power operation up to 115% of rated power. The decay heat levels shown in Figure 5.6-6 were used for component sizing and system response calculations for SGAHRS.

### 5.6.1.2.3.1 Protected Air Cooled Condensers (PACC)

#### Component Description

The PACC is a tube-type steam condenser constructed of carbon steel. Heat is rejected to the atmosphere by condensing the saturated steam from the steam drums by forced circulation of air over the tube bundles.

Each unit is sized to reject 15 MWt under conditions of forced convection on the air side and natural circulation flow on the steam/water side. Each PACC has two half-size tube bundles, two variable blade pitch fans and two sets of variable position louvers to control airflow and, therefore, heat rejection. The electrical power supplies and instrument and control circuits for the PACCs are Class 1E. Refer to PSAR Section 7.4 for information on the power sources and I&C.

The arrangement of PACC is illustrated in Figures 5.6-8 and 5.6-9. Air is delivered from axial fans (one for each tube bundle) into the insulated plenum surrounding each tube bundle. Air flows circumferentially around the tube bundle, then radially inward through the fin tube bundle into a central core. Air then flows upward through the central core and exhausts through louvers to an exhaust stack.

Each tube bundle consists of 50 finned tubes connected in parallel between vertical pipe headers. Each tube is approximately 100 ft. long and, of the 100 ft. length, 95 ft. is finned. The individual finned tubes are formed in a conical spiral of approximately four concentric turns with a slope toward the center. The tubes are connected in parallel between vertical pipe headers. The inlet header is on the outside and outlet header is in the center of spiraled coils. The finned tubes are made of 2 inch O.D. tubes with 0.156 inch minimum wall as shown on Figure 5.6-10. The O.D. of the fin is 3.28 inches. The fins are serrated into 0.156 inch segments from continuous strip 0.050 inch thick x 0.75 inch wide. The strip is first formed into the shape of an "L". The strip is then wound around the tube O.D. to complete the footed fin attachment to the tube. There are two separate tube bundles in each PACC.

#### Design Data

##### Design Conditions:

Pressure	2200 psig
Temperature	650°F

##### Thermal Hydraulic Performance:

Heat Removal	15 MWt (7.5 MWt per tube bundle)
Steam Pressure	1450 psig
Steam Temperature	592°F
Moisture	0%
Condensate Temperature	592°F
Air Temperature	100°F
Air Pressure	14.3 psia

## Design Criteria

The power supplies to the PACC fans, instrumentation and controls are Class 1E. The Instrumentation and Control System is a safety related system and as such will meet the requirements of the regulatory guides and standards as listed in Tables 7.1-2 and 7.1-3 of the PSAR. The means of compliance are described in Section 7.1.2.

Three PACC units are provided, one for each heat transport loop, each capable of removing the total decay heat approximately 1 hour after shutdown. Each unit is single active failure proof in that no single active failure will result in the loss of more than 50% of heat removal capability. This is provided by utilizing two tube bundles, two fans, etc., such that at least half capacity is retained following the failure. The PACC unit is a Seismic Category 1 design, hardened against tornado missiles and designed to withstand the pressure loads from tornados. The PACC tube bundle design is based upon standard techniques for steam-to-air heat exchangers.

## Operation and Control

The airflow is regulated by the use of variable position inlet louvers and fans with variable blade pitch. There are separate controls for the air side of each PACC for each of the two fans and for each of the two sets of louvers. The inlet louvers and fan blade pitch are positioned by controllers which compare steam drum pressure to the setpoint and generate position demand signals to the louvers and fan blade pitch drives as required to maintain pressure at the setpoint value. In order for the PACC to effect heat rejection control over the range of operation there are two modes of air side operation:

- (1) Forced convection with the louvers open and airflow varied by changing the fan blade pitch.
- (2) Natural circulation with airflow varied by changing the position of the inlet louvers.

The range of automatic operation is from 15% to 100% heat rejection. From 100% down to approximately 30% (4.5 MWt) the unit is operating in the first mode, and from 30% to 15% in the second mode. Control is accomplished by sensing and maintaining the steam pressure at the desired set point.

#### 5.6.1.2.3.2 Auxiliary Feedwater Pumps (AFWP)

The AFWP will be a multi-stage, centrifugal pump selected from a commercial vendor's equipment line. No special requirements should be necessary since these pumps have been proven to be reliable in commercial applications. The turbine driven pump will be sized to deliver a 1432 GPM flow rate at 3927 feet developed head, and the two motor driven pumps will be sized to deliver one-half of this flow rate each at the same head. The predicted constant speed head/flow curves for the turbine driven and motor driven AFW pumps are shown on figures 5.6-11 and 5.6-12 respectively.

##### AFWP Motor Drives

These motor drives will be synchronous speed squirrel cage induction motors of 980 horsepower. These motors will be selected from a vendor's standard line and no special requirements are anticipated.

##### AFWP Turbine Drive

This component will be obtained from an experienced vendor and will be sized to produce 1960 horsepower. The turbine will be constructed with sufficient quality assurance coverage to assure its reliability during service.

The auxiliary feedpump turbine is not kept hot for quick start operation. The drive turbine concept selected for the Auxiliary Feed Pump is based on the capability of this turbine to withstand severe service conditions. This is accomplished by constructing the turbine wheel from a single forging with buckets milled into the forging. The start-up procedure is similar to that for the RCIC turbine in a BWR in that it will occur without pre-warming.

##### Pump Integrity

The auxiliary feed pumps will be designed to the requirements of ASME B&PV Code, Section III, Class 3. In addition, the pumps and their supports will be designed to Seismic Category 1 requirements. Allowable stress limits are specified in Table 3.9-3 and pressure limits are specified in Table 3.9-4.

#### 5.6.1.2.3.3 Protected Water Storage Tank (PWST)

The PWST holds the protected water to be supplied to the steam drums in the event of loss of normal feedwater or normal heat sink. The size is determined by detailed analysis of the heat removal conditions during the first several hours after shutdown and by anticipated component leakage rates. The tank will be constructed to the requirements for an ASME Section III/Class 2 vessel and it will operate at low temperature (<200°F) and low pressure (<15 psig).

#### 5.6.1.2.3.4 SGAHRs Piping and Support

The SGAHRs piping is described below and is shown in Figure 5.1-5. The SGAHRs piping will be designed in accordance with the ASME Code Section III as specified in Section 5.6.1.1.2. The material specifications are discussed in Section 5.6.1.1.4.

The SGAHRs piping runs can be categorized as follows:

a. PWST Fill Line

This 3 inch low pressure, low temperature, Class 3 carbon steel line runs from the 10 inch alternate water supply line through the motor-driven, normally closed PWST fill valve to the PWST inlet.

b. Protected Water Storage Tank (PWST) to Auxiliary Feedwater Pump (AFP) Inlet

There are three low pressure, low temperature, uninsulated carbon steel lines from the PWST to the three auxiliary feedwater pump inlets. Two of the lines, each of which leads to a half size, motor-driven pump are 6 inches in diameter and the third line to the full size turbine-driven pump is 8 inches. All three lines contain a manually operated, locked open valve and an electrically operated, normally open isolation valve. These lines are Class 2 from the PWST to the electrically-operated isolation valve and then Class 3 to the pump inlet.

c. Alternate Supply Line to AFWP Inlet

The alternate supply line provides the capability for the AFW pumps to take suction from the condensate storage tank. A 10 inch carbon steel line runs from the feedwater and condensate system junction to the first branch line. An 8 inch branch line passes through an electrically-operated, normally closed isolation valve and tees into the 8 inch turbine pump inlet piping. Two 6-inch branch lines each pass through electrically-operated, normally closed isolation valves and then tee into the 6 inch motor-driven pump inlet piping. The total run of piping is Class 3.

d. Auxiliary Feedwater Pump Discharge to Discharge Header (Inclusive)

The 6 inch carbon steel turbine pump discharge line leads to a 6 inch discharge header. This header in turn has three discharge points, one to each steam drum feedwater supply loop. a 6 inch carbon steel line from each motor driven pump feeds into a 6 inch header which also has three discharge points, one to each drum.

Amend. 58  
Nov. 1980

49 |

58 |

49 |

58 |

49 |

49 |

43 |

17 |



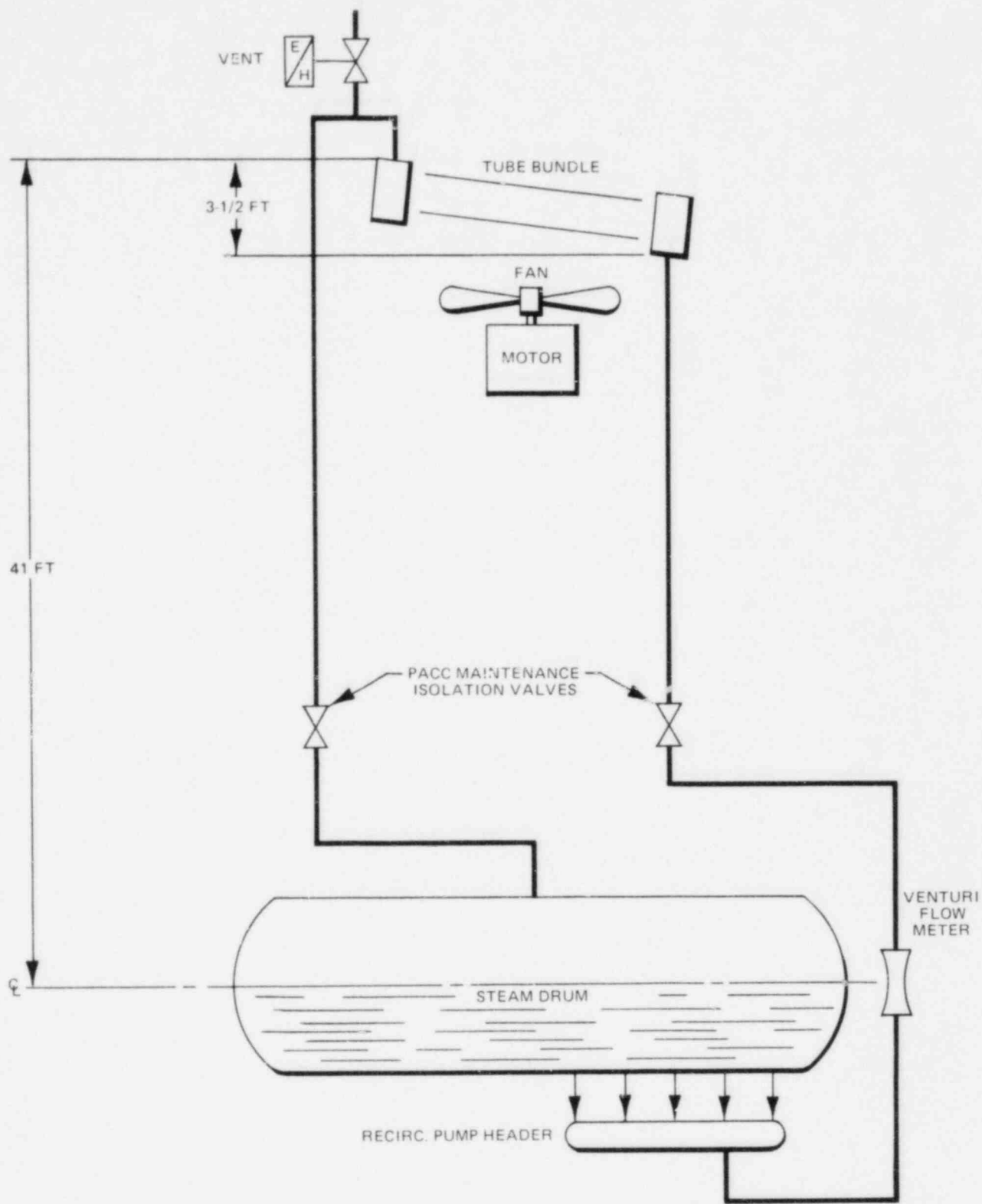
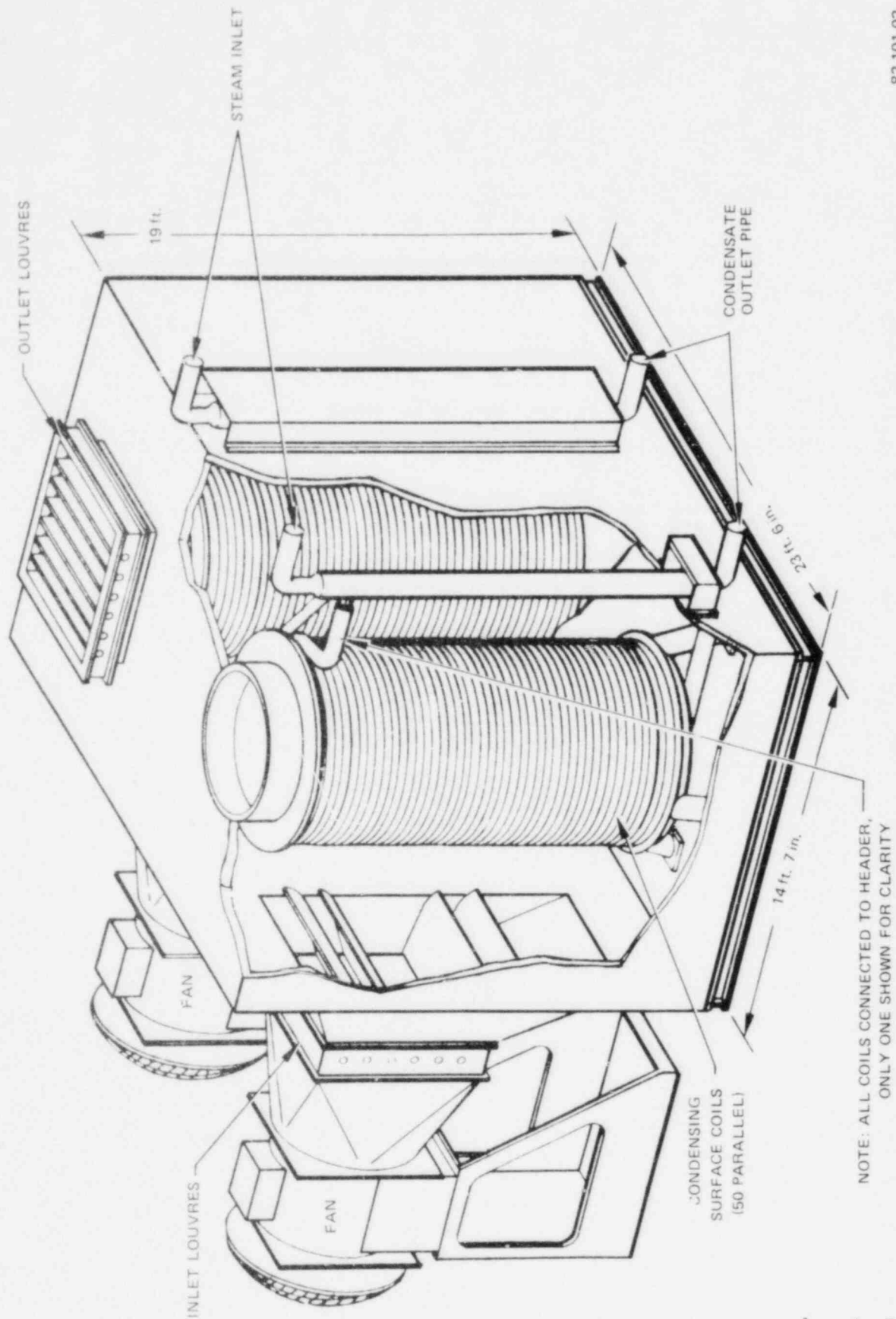


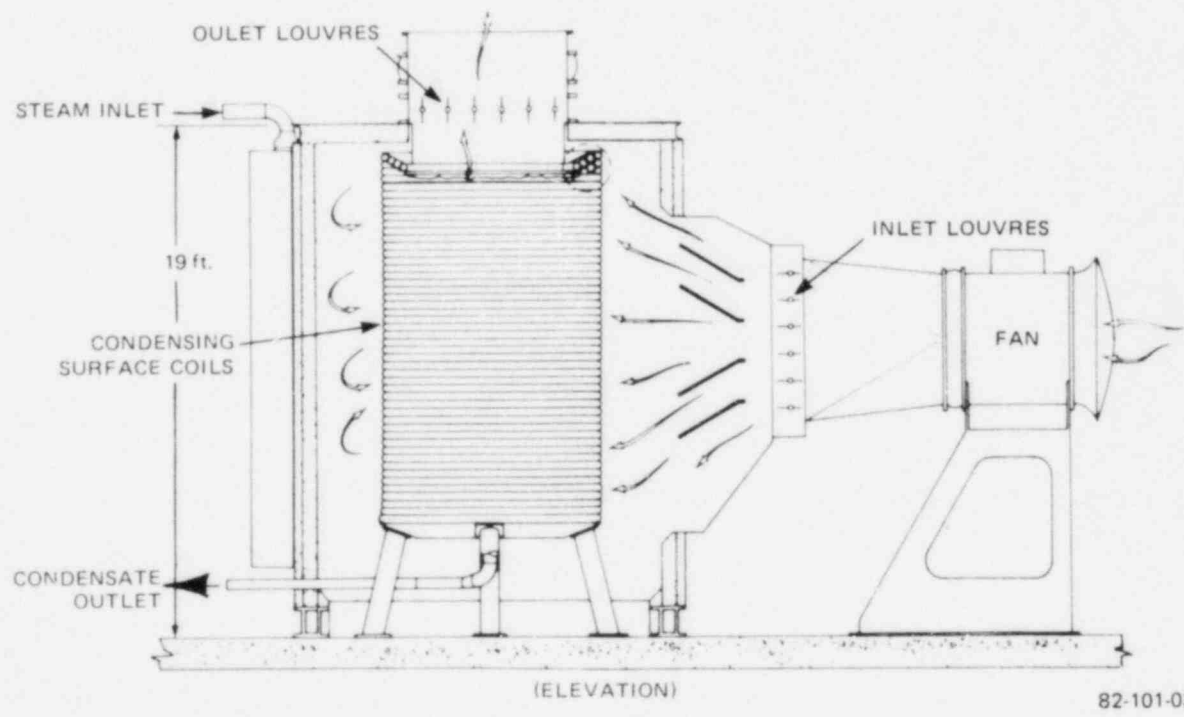
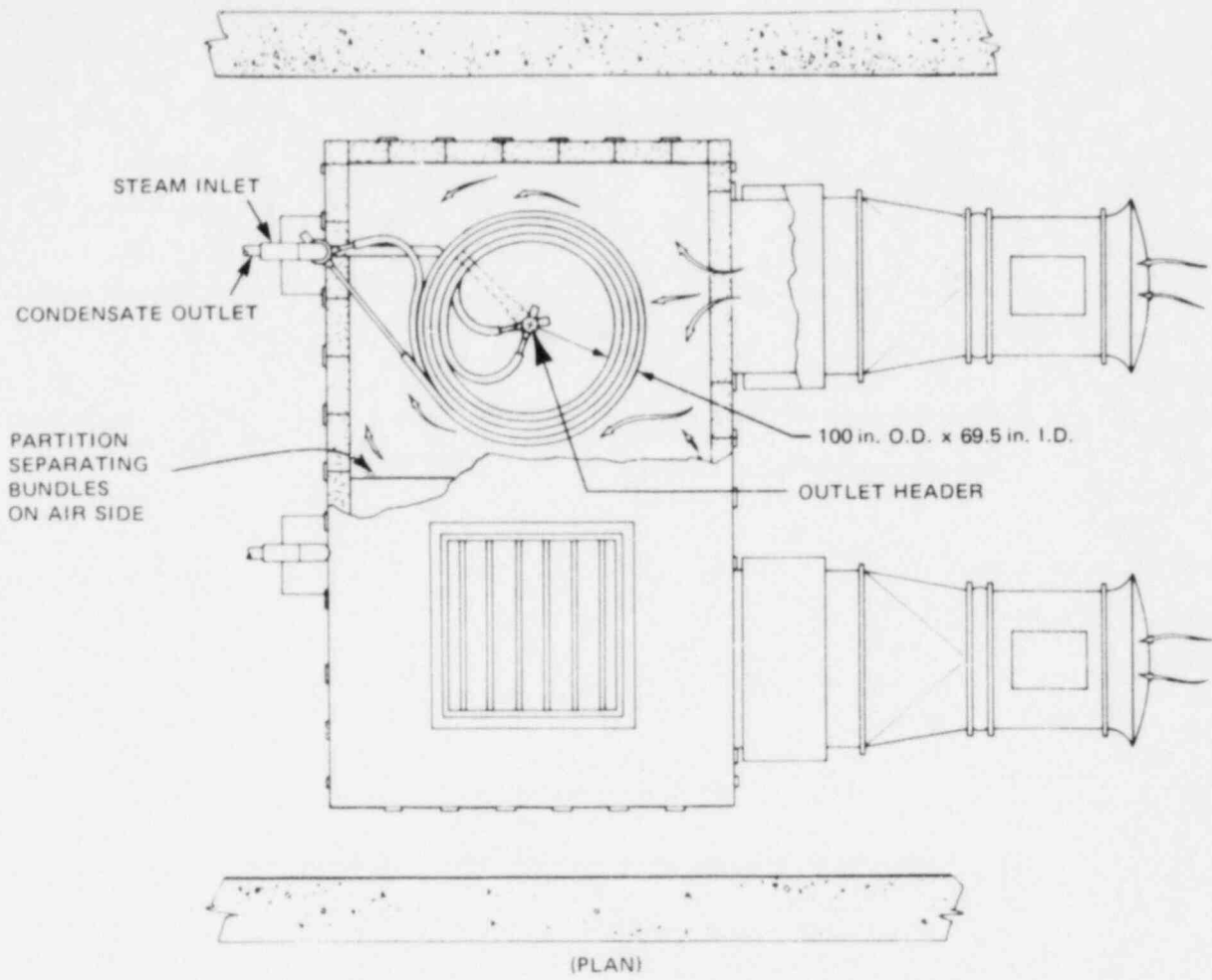
FIGURE 5.6-7 PACC Closed Loop Schematic (Shown During Normal Plant Operation - PACC Hot Standby)



82-101-02

Figure 5.6-8 PROTECTED AIR-COOLED CONDENSER

NOTE: ALL COILS CONNECTED TO HEADER,  
ONLY ONE SHOWN FOR CLARITY



82-101-03

Figure 5.6-9 PROTECTED AIR COOLED CONDENSER

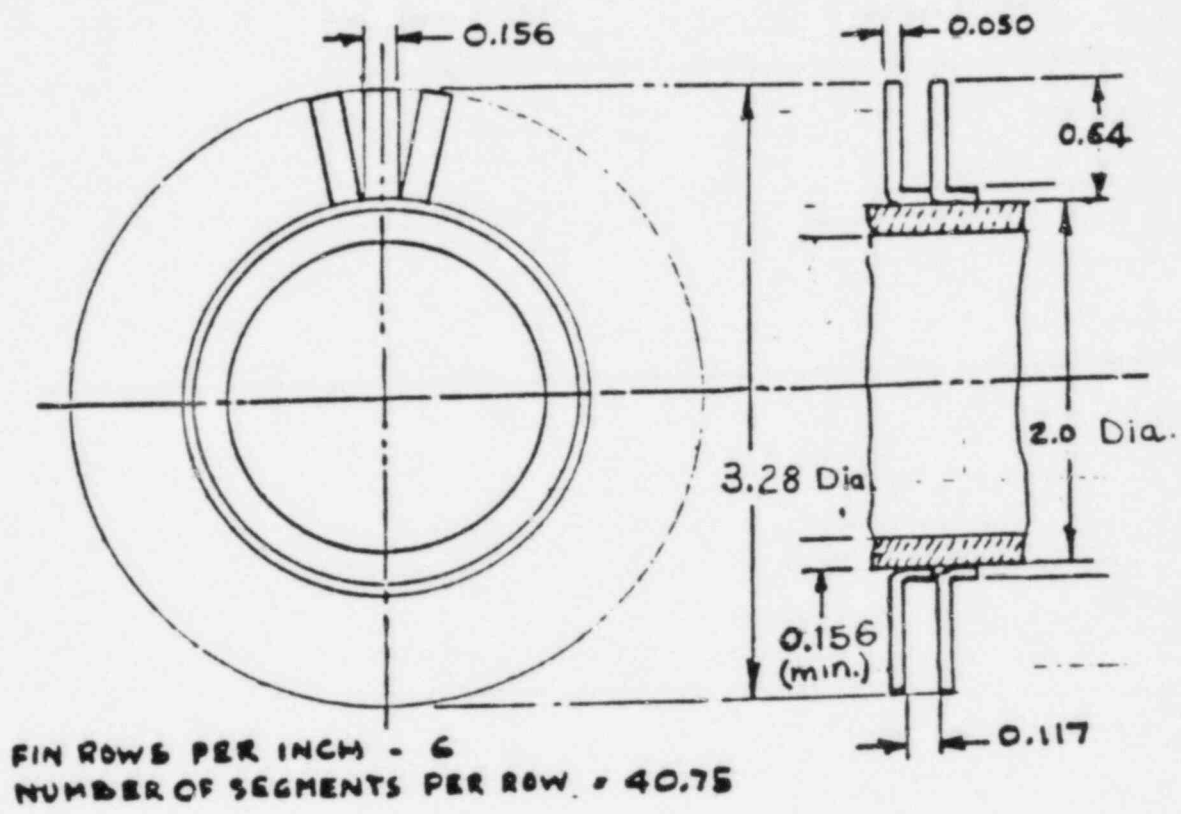


Figure 5.6-10 Nominal PACC Tube and Fin Geometry

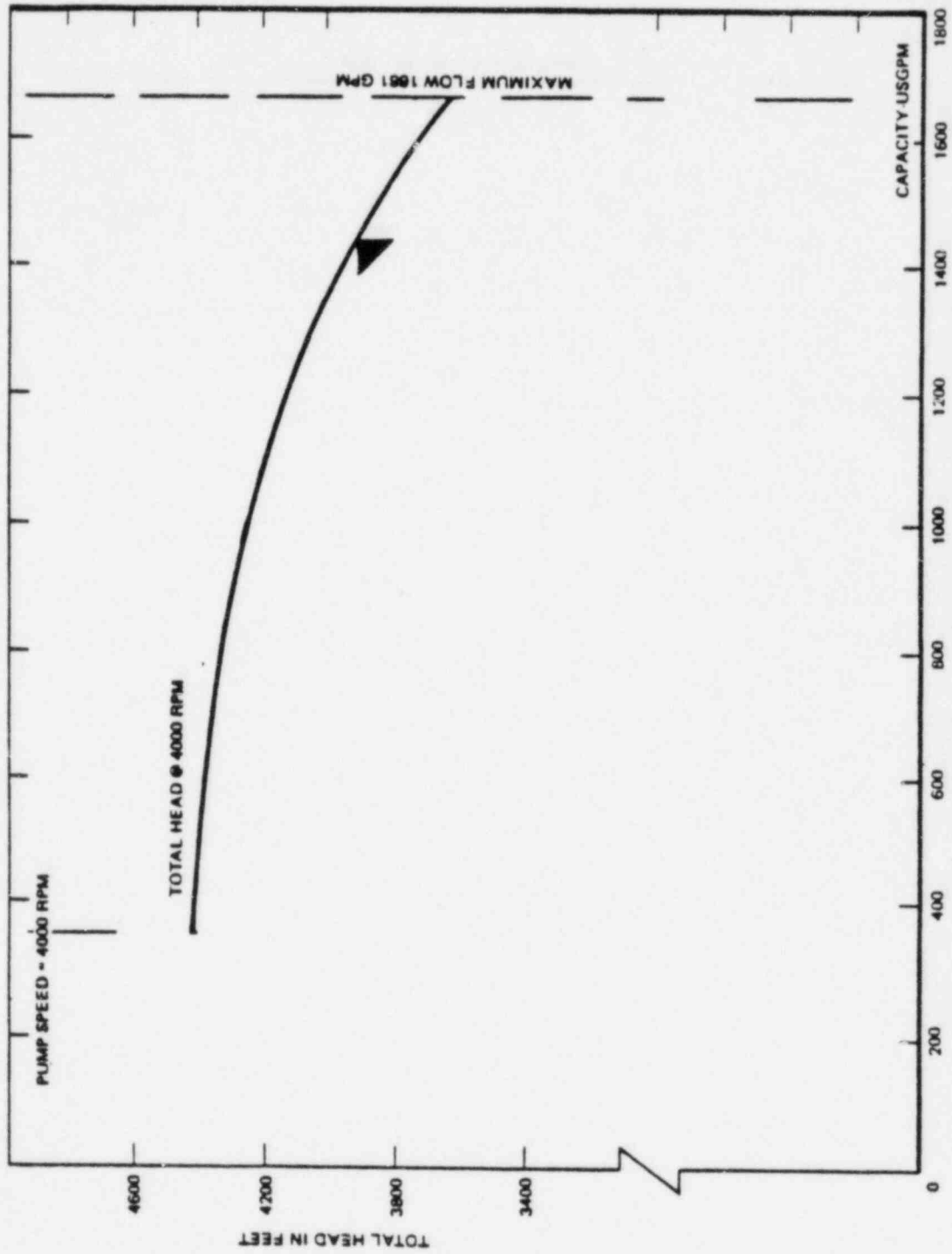
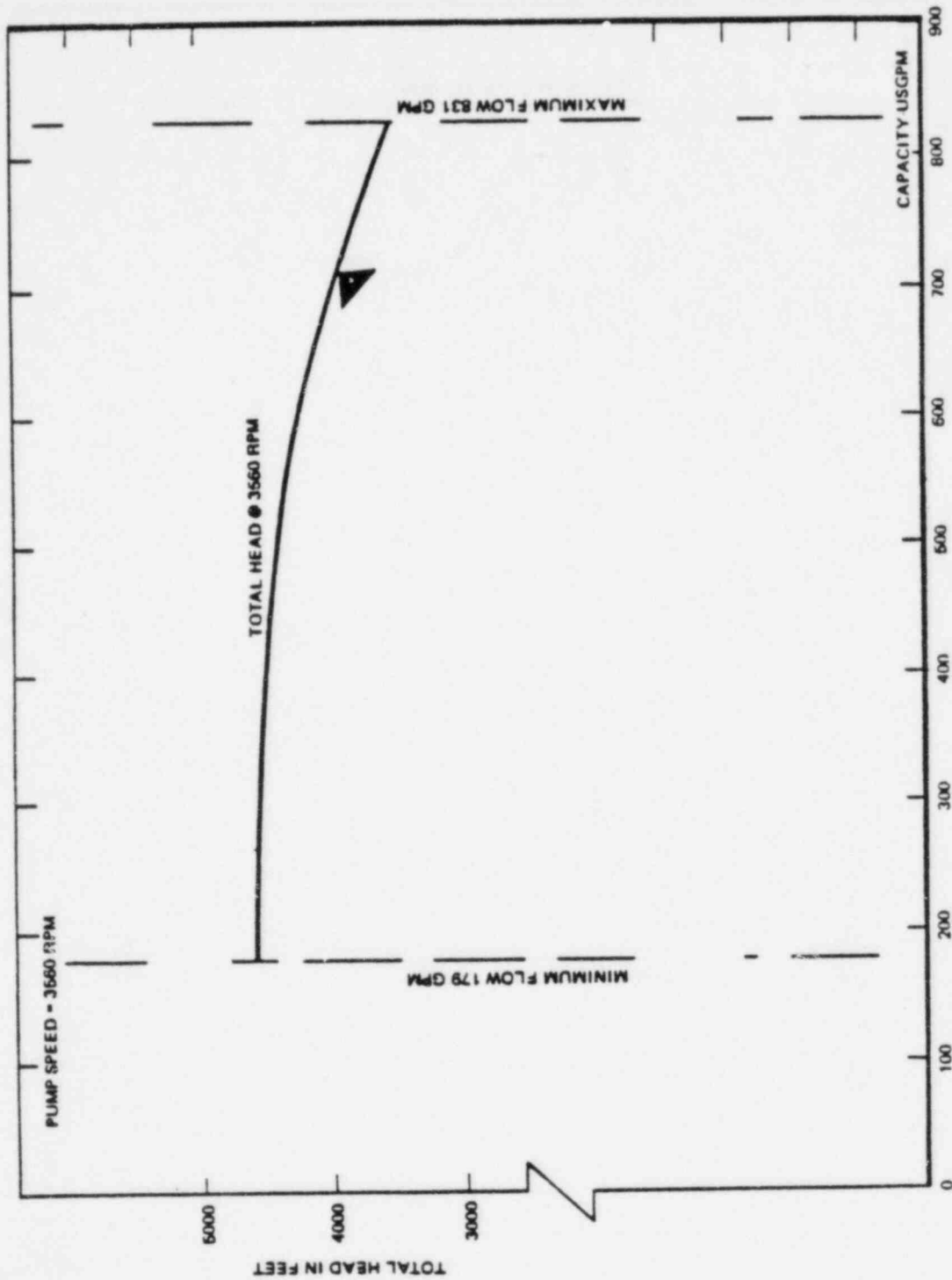


Figure 5.6-11 Turbine-Driven AFW Pump Characteristics

80-632-02



5.6-47

Amend. 72  
Oct. 1982

Figure 5.6-12 Motor-Driven AFW Pump Characteristics

80-632-03

occur during plant operation and are sufficiently severe or frequent to be of possible significance to component cyclic behavior. The transients selected may be regarded as a conservative representation of transients which, used as a basis for component structural evaluation, provide confidence that the component is appropriate for its application over the design life of the plant. Appendix B describes the events which result in transients on heat transport system components. Table 5.7-1 presents a summary of a preliminary selection of those transients.

Several events and examples of their affects on the components of the heat transport system are discussed and provided below to illustrate the transient behavior of the Heat Transport System. (More detailed discussions, including plots of temperature, flow, and pressure as a function of time, are included in Chapter 15):

a. Reactor Trip from Full Power

A reactor trip from full power results in the release of safety and/or control rods. Sodium pumps coast to pony motor speed. The continued transfer of heat results in rapid temperature reductions at the reactor vessel outlet, primary pump, IHX primary inlet, superheater sodium inlet and outlet, and evaporator sodium inlet. The primary hot leg temperatures drop about 300°F in 200 seconds while the superheater inlet sodium temperature drops about 200°F in the same time. Superheater outlet and evaporator inlet sodium temperatures fall about 170°F and then increase the same amount in a total of 100 seconds. The latter affect results from controlled dumping of steam to the condenser through the turbine bypass to maintain pressure at the turbine admission valve at 1450 psig to avoid lifting of safety or power relief valves. The transient is most severe when it occurs with minimum plant decay heat conditions since decay heat tends to slow the rate of temperature reduction. Figure 5.7-3 depicts the transient at the reactor vessel outlet where the rate of temperature change is the highest.

Substantial flow oscillations do not occur following reactor scram as discussed below.

The free surfaces in the reactor coolant system are 1) the free surface in the reactor vessel, 2) the free surfaces in each of the three primary pump tanks and 3) possibly a free surface at the high point of the primary side of the IHX in the annulus between the outer shell and the tube bundle support cylinder.

The only gas which would be under any significant pressure would be that which may accumulate in the IHX. The volume of this gas will deliberately be kept as small as possible by locating the vent line between the IHX and the pump tank as high as possible. The position of the vent line from the IHX is shown in Fig. 5.3-15 and shows the possible trapped gas volume to be extremely small. When the pump is tripped and the pressure in this gas space drops off rapidly from about 165 psia to approximately 15 psia, there will be an expansion of this gas and a lowering of the free surface. The volume of this gas when expanded will be small compared to the gas volume in the reactor vessel and pump tanks and as such, will not significantly affect sodium levels in either the pumps or reactor vessel.

The pump tank cover gas pressure during full flow conditions will be equal to or only slightly higher than the reactor vessel cover gas pressure (which is equalized with the overflow tank gas pressure through an equalization line). When the pumps are tripped, the level in the pump tanks will rise and submerge the stand pipe bubbler nozzle thereby cutting off communication of the pump cover gas with the rest of the cover gas in the primary system. The level rise in the tank is limited by the compression of the trapped gas. The increase in pump tank level is at the expense of the level in the reactor vessel but any oscillation in free surfaces in the pump and reactor vessel is precluded by providing a flow restriction between the pump hydraulics region and the pump tank which will critically damp any potential oscillation.

b. Uncontrolled Rod Movement

Control system malfunctions may cause uncontrolled control rod movement resulting in undesired insertion or withdrawal of one or more control rods. Uncontrolled insertion of a control rod, which could occur without a compensating reduction in sodium flows, results in rapid plant temperature reductions similar to those which occur from a reactor trip from full power.

Uncontrolled withdrawal of a control rod may occur under various initial conditions. If uncontrolled rod withdrawal occurs from 100% power, reactor vessel outlets, IHX primary inlets, and primary sodium pump temperatures will increase to values higher than normal and higher than from any other event. When power reaches 115%, a reactor trip occurs. Since temperatures just prior to reactor trip are higher than just prior to reactor trip from full power, a more severe transient will occur. Although the rate of temperature change is about the same as that for a reactor trip from full power, the extent of the transient is greater since it starts from a temperature about 60°F higher than that observed at 100% power. Figure 5.7-4 illustrates the nature of this transient.



Uncontrolled rod withdrawal during startup also results in an up temperature transient at the reactor vessel outlet although the transient occurs at a lower temperature than when the rod withdrawal starts from 100% power. Figure 5.7-5 depicts the transient initiated during startup.

c. Operating Basis Earthquake (OBE)

The operating basis earthquake results in reactive forces acting on the plant components as described in the Seismic Criteria Document. Five OBEs, each with 10 maximum peak response cycles, are assumed to occur over the design life of the plant. Four of these OBE's are assumed to occur during the most adverse Normal Operating Conditions determined on a component and design limit basis. The other one OBE is assumed to occur during the most adverse upset event determined on a component and design limit basis, and at the most adverse time in the upset event. Thus, the plant components are simultaneously exposed to the thermal effects of the thermal transients as well as the stresses of the OBE.

d. Loss of Steam Generator Load

Isolation and dumping of the water/steam sides of both evaporators and the superheater removes the load from that loop. This results in up temperature transients on the steam generator modules, the intermediate cold leg, the IHX intermediate inlet, the IHX primary outlet, and the reactor vessel inlet. The ensuing reactor trip then causes down temperature transients on these components. The intermediate cold leg temperature increases approximately 350°F in 400 seconds; then decreases approximately 220°F in 300 seconds. This transient is then transported to the IHX primary outlet and reactor vessel inlet. Figures 5.7-6 a-k presents the resulting transient at the intermediate sodium pump, core & steam generators.

e. Inadvertent Opening of Superheater Outlet Power or Safety Relief Valve

This event results in a large increase in load without an accompanying increase in reactor power or sodium flows. It occurs when a super-heater relief valve inadvertently opens to increase steam flow from 40% to 100%. The event results in a reactor trip but overcooling occurs due to the open relief valve. The steam generators, inter-mediate cold leg, IHX intermediate inlet, primary cold leg and reactor vessel inlet drop in temperature about 150°F in 100 seconds. The reactor vessel outlet, primary hot leg, and IHX primary inlet drop in temperature about 200°F in 75 seconds. Figure 5.7-7 depicts the transient at the intermediate pump.

f. Primary Pump Mechanical Failure

Primary pump mechanical failure involves the instantaneous stoppage of the impeller of one primary pump due to such reasons as seizure or breakage of the shaft or impeller. Flow in the affected loop rapidly goes to zero and a reactor trip occurs almost immediately after seizure based on primary to intermediate flow ratio. The event is characterized by a down transient in the intermediate hot leg and a check valve slam in the primary cold leg of the affected loop. The down-temperature transient in the intermediate hot leg results from the sudden loss of primary sodium flow while intermediate sodium flow continues. The intermediate hot leg temperature drops 300°F in about 200 seconds. The check valve slam, which results from the check valve being forced shut by reverse flow from the reactor vessel, results in significant pressure fluctuations at the reactor vessel inlet, the check valve, and the IHX primary outlet. Figure 5.7-8 presents the temperature transient at the superheater inlet while Figure 5.7-9 depicts the pressure effects of the check valve slam at the check valve inlet and outlet.

g. Saturated Steam Line Rupture

A rupture of the saturated steam line between the steam drum and the superheater inlet isolation valve results in immediate cessation of superheater steam flow in that loop and initiation of a reactor trip. The superheater rapidly becomes isothermal at the sodium inlet temperature due to the loss of cooling. Sodium leaving the evaporators of the affected loop initially drops in temperature due to over cooling as the water flow increases and flashes to atmospheric pressure through the steam drum. Then, as the loop blows dry through the rupture, evaporator sodium temperature rapidly increases to the superheater inlet temperature. This transient is the most severe that the evaporator and intermediate pump experience. The transient is propagated through the intermediate cold leg and results in similar severe transients on the intermediate pump, the IHX intermediate inlet, the IHX primary outlet, the primary cold leg and check valve, and the reactor vessel inlet nozzle. Subsequently, these components experience down temperature transients as a result of the reactor trip. Intermediate cold leg temperature drops 200°F in about 60 seconds and then increases 500°F in about 100 seconds. Figure 5.7-10 illustrates the transient at the intermediate pump.

h. Loss of One Primary Pump Pony Motor with Failure of the Check Valve in that Loop to Shut

This event occurs subsequent to a shut down or reactor trip and results in reverse flow in the affected primary loop as a result of the head developed by the two operating pumps. The reverse flow of primary sodium at reactor vessel inlet temperatures results in rapid down temperature transients at the IHX primary inlet, the primary pump, and the reactor vessel outlet nozzle of the affected loop. A core temperature increase occurs as a result of the bypassed flow. Primary hot leg temperature drops 425°F in about 150 seconds. Figure 5.7-11 depicts a typical transient.

5.7.4 Evaluation of Thermal Hydraulic Characteristics and Plant Design

Heat Transport System Design Transient Summary

The heat transport system design transients for the individual heat transport system components are described in Appendix B. Table 5.7-1 presents a preliminary summary listing of design transient events as well as the frequency of each event assigned to the reactor vessel, IHX, primary pump, intermediate pump, primary check valve, evaporator and super-heater.

It should be noted that the assigned frequency for a particular event varies among the components in some cases. This is the result of the method used in establishing the design transients. The events listed in Appendix B are the result of grouping less severe events under more severe events and applying the total frequency of all events in the group to the most severe event in the group. This approach was applied separately to each component so that the most transients discussed in Appendix B (where a particular transient applies to more than one component) do not have the same frequency applied to each component. This approach was required because each event does not result in the same transient effect on each component.

PRELIMINARY SUMMARY OF HEAT TRANSPORT SYSTEM DESIGN TRANSIENTS

DUTY CYCLE / EVENT NUMBER	Event Title	Reactor Vessel	IMX	Frequency (1/cycle)				Superheater
				Primary Pump	Inter. Pump	Check Valve	Evap.	
N-1	Dry system heatup and cooldown, sodium drain and fill	5	13	13	30	13	30	30
N-2a	Startup	140	140	140	140	140	214	214
N-2b	1. From refueling 2. From hot standby	886	728	728	728	728	638	638
N-3a	Normal shutdown	140	60	60	60	60	60	60
N-3b	1. To refueling 2. To hot standby	329	260	260	260	260	210	210
N-4a, N-4b <sup>2</sup>	Load follow	57,426	57,114	57,124	57,128	57,122	57,139	57,139
N-4a, N-4b <sup>4</sup>	1. Loading (total of 40-100% range and 60-100% range)	56,480	56,610	56,610	56,610	56,610	55,550	56,550
N-5	2. Unloading (total of 40-100% range and 80-100% range)	30 x 10 <sup>6</sup>	30 x 10 <sup>6</sup>	30 x 10 <sup>6</sup>	30 x 10 <sup>6</sup>	30 x 10 <sup>6</sup>	30 x 10 <sup>6</sup>	30 x 10 <sup>6</sup>
N-6	Steady state temperature fluctuations	1010	1010	1010	1010	1010	1010	1010
N-7	Steady state pressure fluctuations	180	268	258	258	258	315	315
U-1a	Reactor trip from full power	97	144	193	454	450	315	315
U-1b	1. Normal decay heat 2. Minimum decay heat	--	10	10	--	--	10	10
U-2a	Uncontrolled control rod movement	22	18	14	--	32	10	10
U-2b	1. Rod insertion from 100% power	20	20	20	--	--	20	20
U-2c	2. Rod withdrawal from 100% power	10	10	10	10	10	10	10
U-2d	3. Rod withdrawal from startup	--	7	--	6	41	--	15
U-2e	4. Plant loading at maximum rod withdrawal rate	153	15	--	--	--	--	--
U-3a	Intermediate pump control failure	--	5	5	5	--	--	--
U-11a	Turbine bypass valve fails open following reactor trip	35	9	11	19	21	84	84
U-20b	Loss of offsite power supplies	--	--	--	--	--	3	3
U-18	Evaporator outlet relief valves open	--	--	--	--	--	116	116
U-21a	Unaffected loops for water side isolation and blowdown-Superheater and (2) Evaporators	--	--	--	--	--	--	--
U-11a <sup>3</sup>								

Notes: 1. Event number and description are as found in Appendix B.  
 2. Event N-4a describes loadings and unloadings over the range of 40-100% power. Event N-4b describes loadings and unloadings (referred to in the duty cycle as load fluctuations) over the range of 80-100% power.  
 3. Refers to transient effects in the two unaffected loops when this event occurs in one loop.

TABLE 5.7-1 (continued)

## PRELIMINARY SUMMARY OF HEAT TRANSPORT SYSTEM DESIGN TRANSIENTS

DUTY CYCLE EVENT NUMBER <sup>1</sup>	Event Title	Reactor Vessel	IHX	Frequency (Lifetime)				
				Primary Pump	Inter. Pump	Check Valve	Evap.	Super- heater
U-11b	Water side isolation & blowdown of evaporator module	--	--	--	--	--	7	7
U-11b	Adjacent evaporator during water side isolation and blowdown of evaporator	--	--	--	--	--	9	9
U-21a	Adjacent evaporator outlet relief valves open	--	--	--	--	--	3	3
E-9a	Superheater isolation & blowdown-outlet valve open	--	--	--	--	--	Note 4	Note 4
E-14	Inadvertent dump of intermediate sodium	--	--	--	--	--	Note 4	Note 4
OBE <sup>5</sup>	Operating basis earthquake	5	5	5	5	5	5	5
E-16	Three loop natural circulation	Note 4						
U-21b	Inadvertent opening of superheater outlet power or safety relief valve	42	19	24	14	26	13	13
U-23	Inadvertent opening of evaporator inlet dump valve	--	33	--	37	--	--	--
U-8	Primary pump pony motor failure	*15	5	--	--	--	5	5
E-1	Primary pump mechanical failure	Note 4	Note 4	--	--	Note 4	--	--
E-5	Loss of one primary pump pony motor with failure of check valve in that loop to shut	Note 4	Note 4	Note 4	--	--	Note 4	Note 4
E-6	Design basis steam generator sodium/water reaction	--	Note 4	--	Note 4	--	Note 4	Note 4
E-7	One loop natural circulation (from initial two loop operation)	Note 4	Note 4	--	--	--	Note 4	Note 4
E-15	DHRS Activation 24 Hours After Scram	2	2	--	2	2	2	2
E-16	Three loop natural circulation	Note 4	Note 4	Note 4	--	--	Note 4	Note 4

Notes: 4. Each component, or part of a component, must accommodate 5 occurrences of the most severe emergency transient for that component or part of a component (one every 6 years) and two consecutive occurrences of the most severe event (or of unlike events if consecutive occurrences of unlike events provide a more severe effect than two occurrences of the most severe event).

5. See Paragraph 5.7.3(c)

5.7-8

Amend. 72  
Oct. 1982

Figure 5.7-6a Average Channel Sodium Exit Temperature Top of Active Core vs. Time for Loss of Steam Generator Load (Dumping of Water/Steam Sides of Both Evaporators and the Superheater)

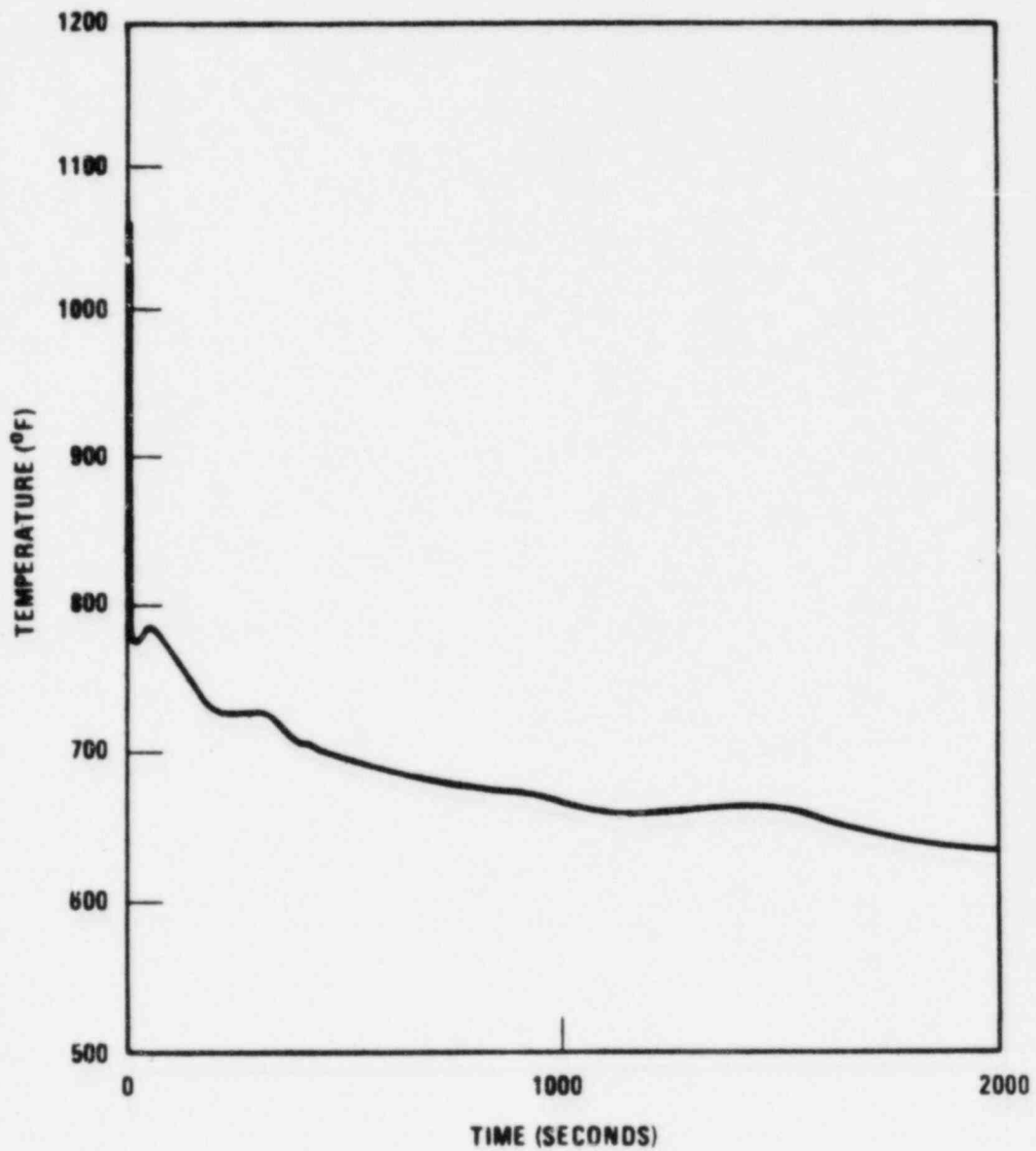


Figure 5.7-6b Maximum Channel Sodium Exit Temperature, Top of Active Core for Loss of Steam Generator Load (Dumping of Water/Steam Sides of Both Evaporators and the Superheater).

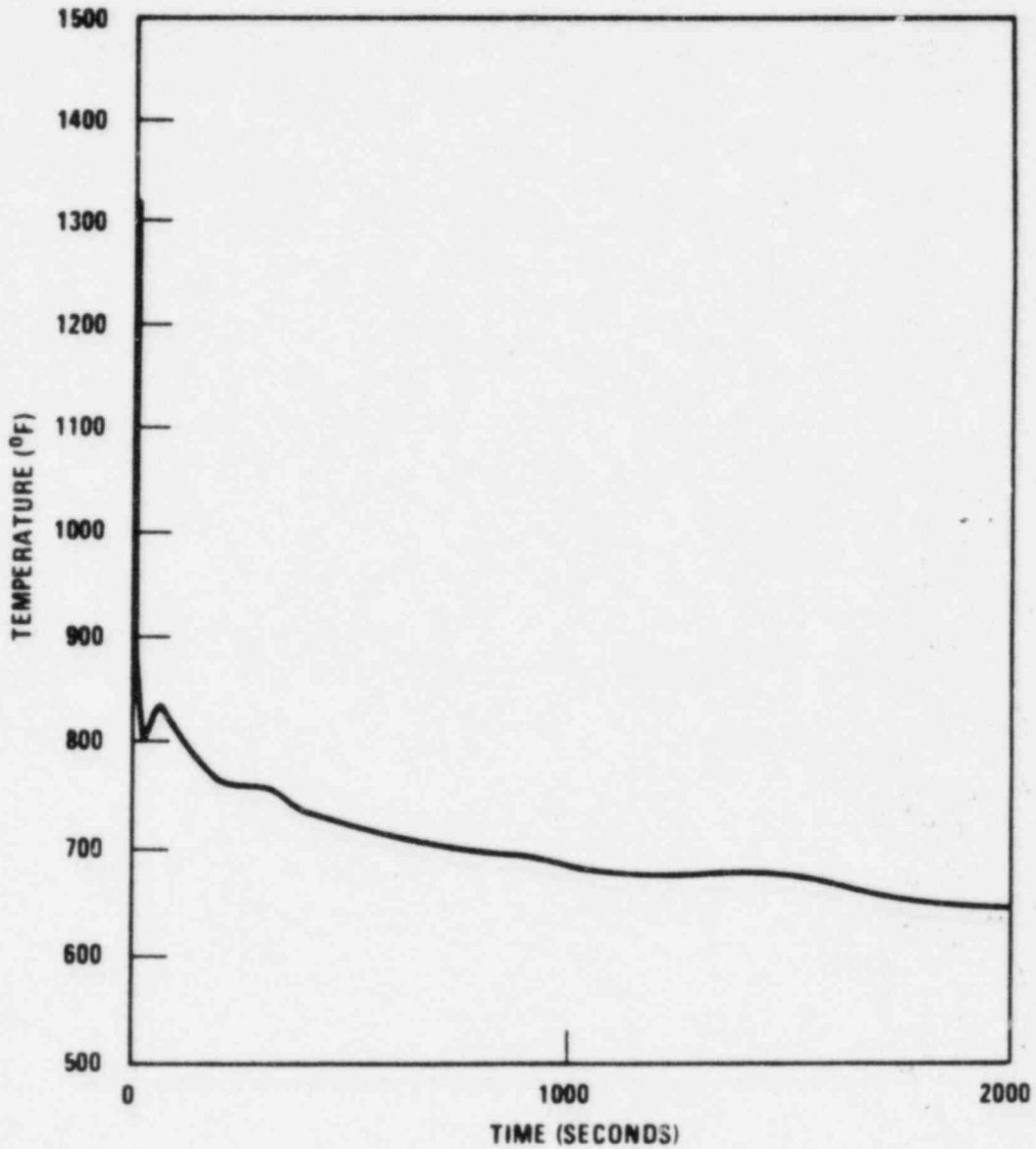


Figure 5.7-6C Blanket Hot Channel Sodium Outlet Temperature for Loss of Steam Generator Load (Dumping of Water/Steam Sides of Both Evaporators and the Superheater).

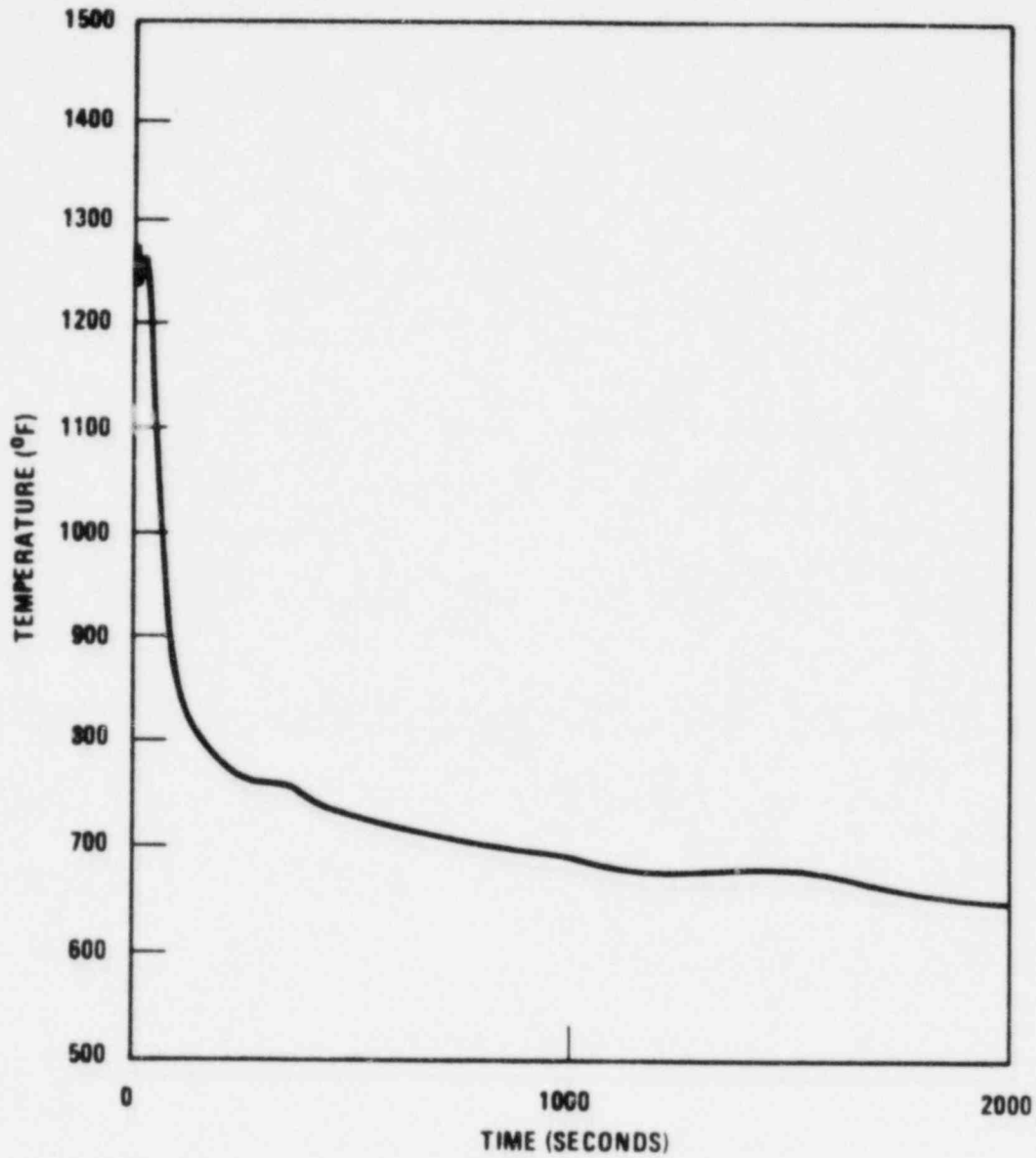




Figure 5.7-6D Reactor Vessel Exit Temperature for Loss of Steam Generator Load (Dumping of Water/Steam Sides of Both Evaporators and the Superheater).

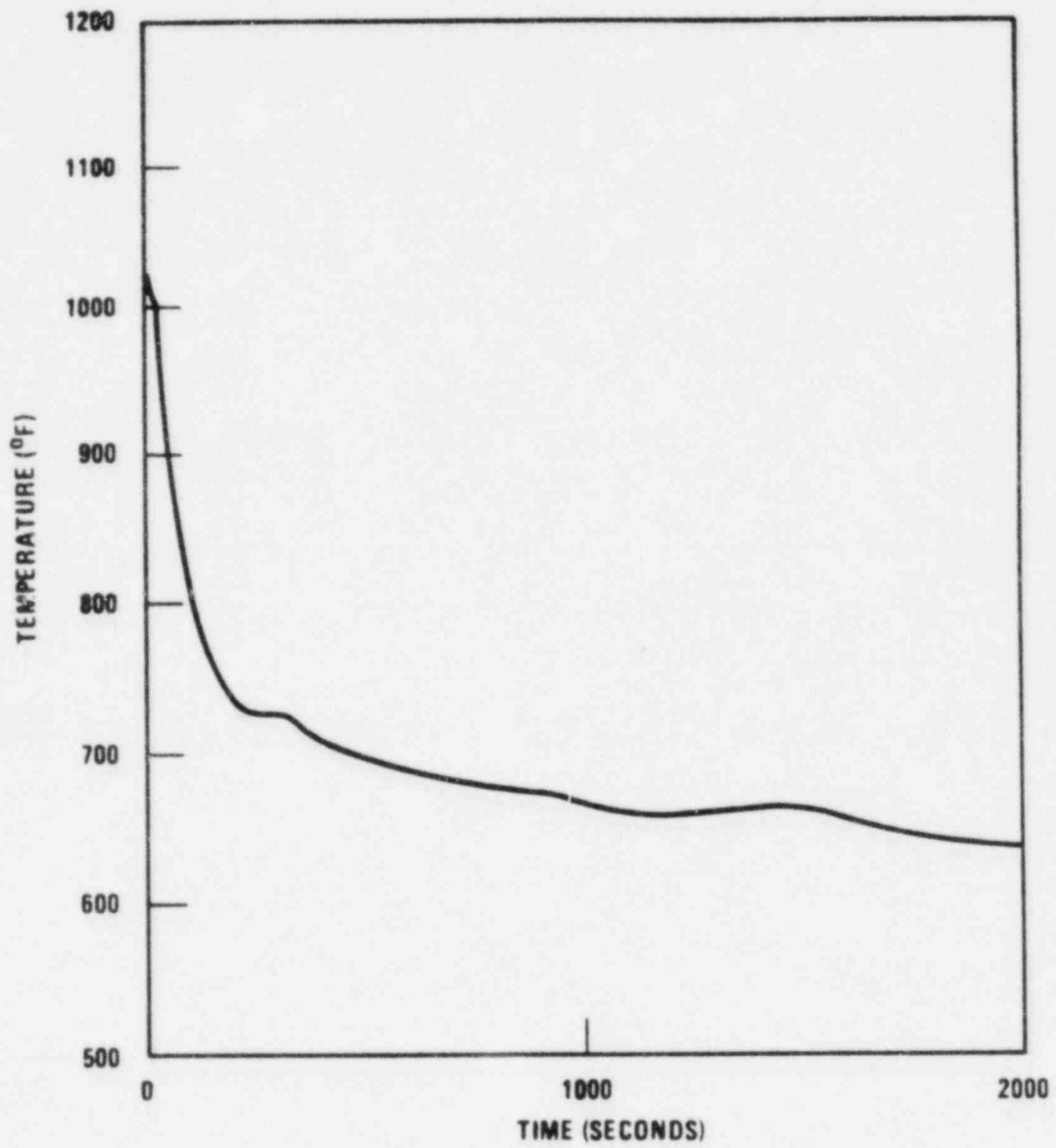


Figure 5.7-6E Affected Loop Superheater Sodium Inlet Temperature for Loss of Steam Generator Load (Dumping of Water/Steam Sides of Both Evaporators and the Superheater).

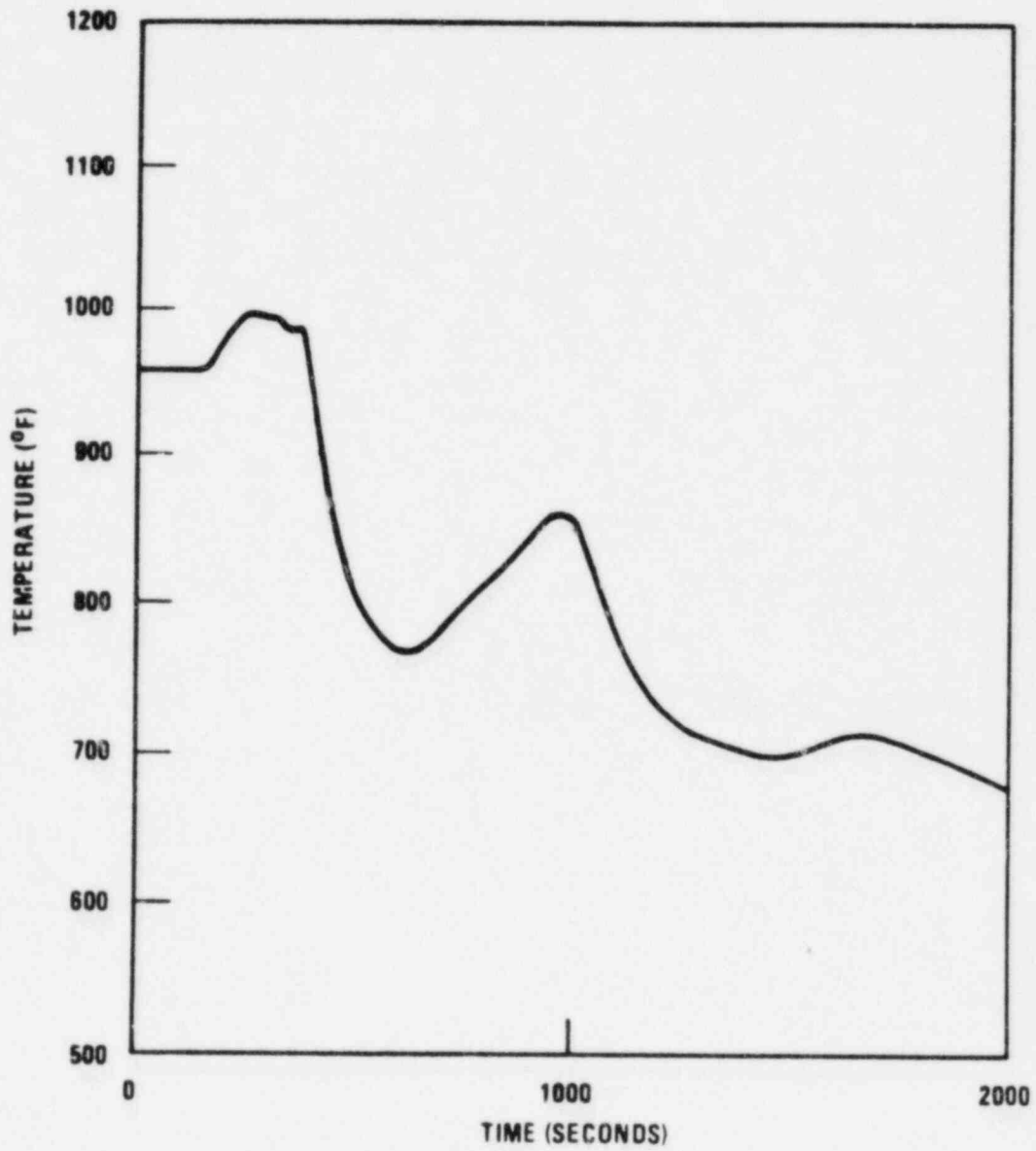


Figure 5.7-6F Affected Loop Evaporator Sodium Inlet Temperature for Loss of Steam Generator Load (Dumping of Water/Steam Sides of Both Evaporators and the Superheater).

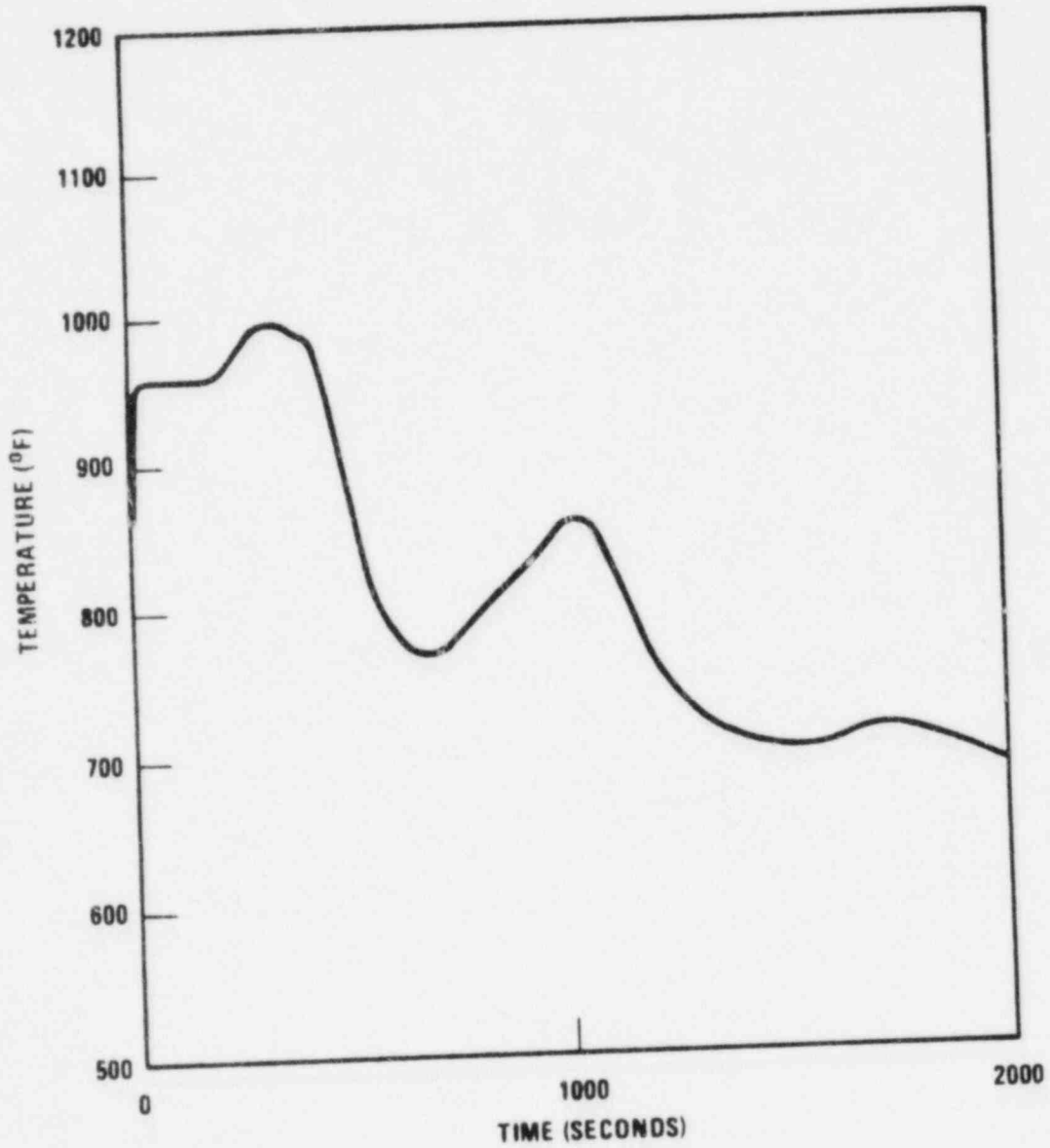


Figure 5.7-6G Affected Loop Evaporator Sodium Exit Temperature for Loss of Steam Generator Load (Dumping of Water/Steam Sides of Both Evaporators and the Superheater).

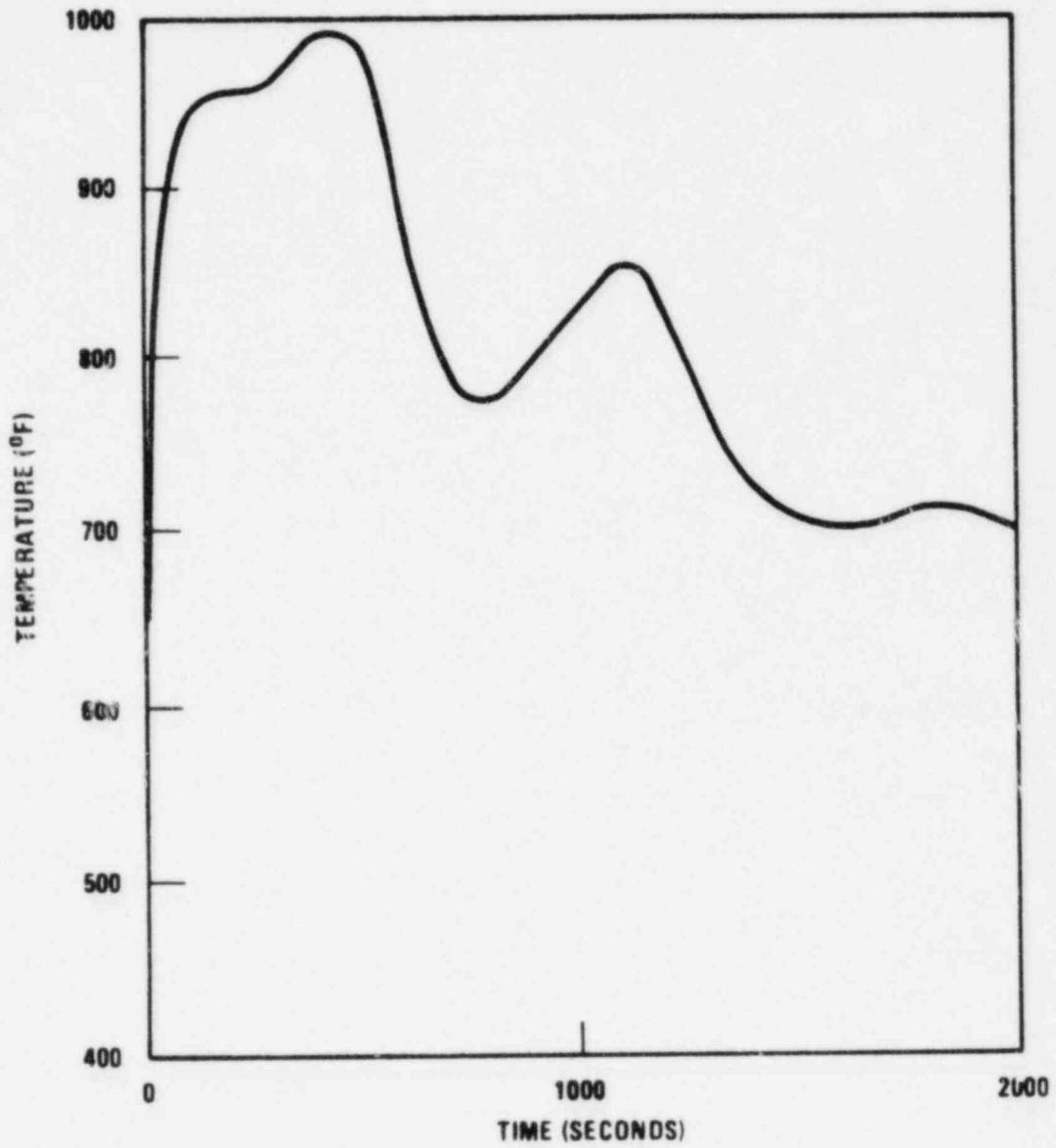


Figure 5.7-6H Intermediate Pump Sodium Temperature Vs. Time for Loss of Steam Generator Load (Dumping of Water/Steam Sides of Both Evaporators and the Superheater).

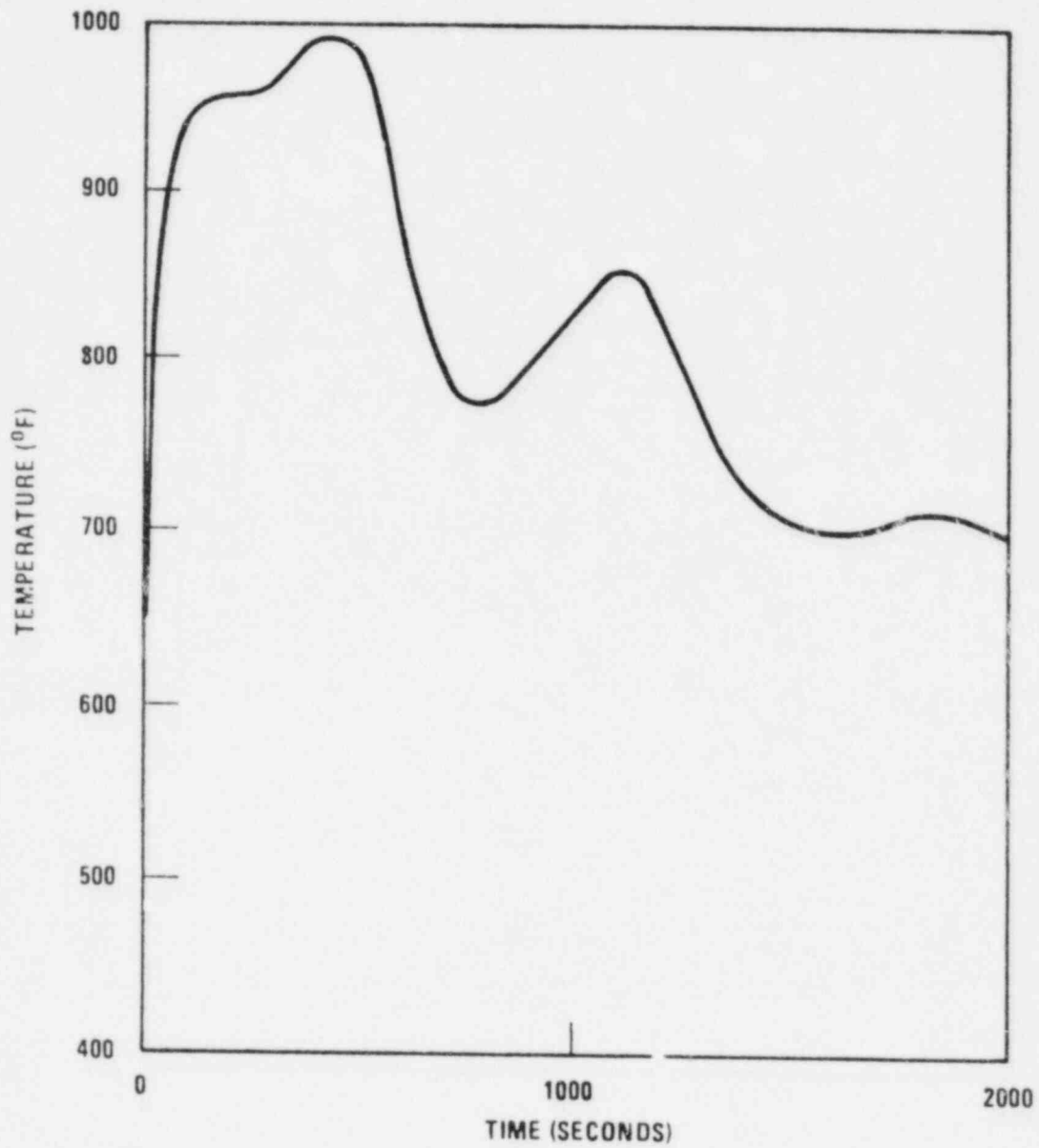


Figure 5.7-61 Affected Loop Drum Steam Temperature vs. Loss of Steam Generator Load (Dumping of Water/Steam Sides of Both Evaporators and the Superheater).

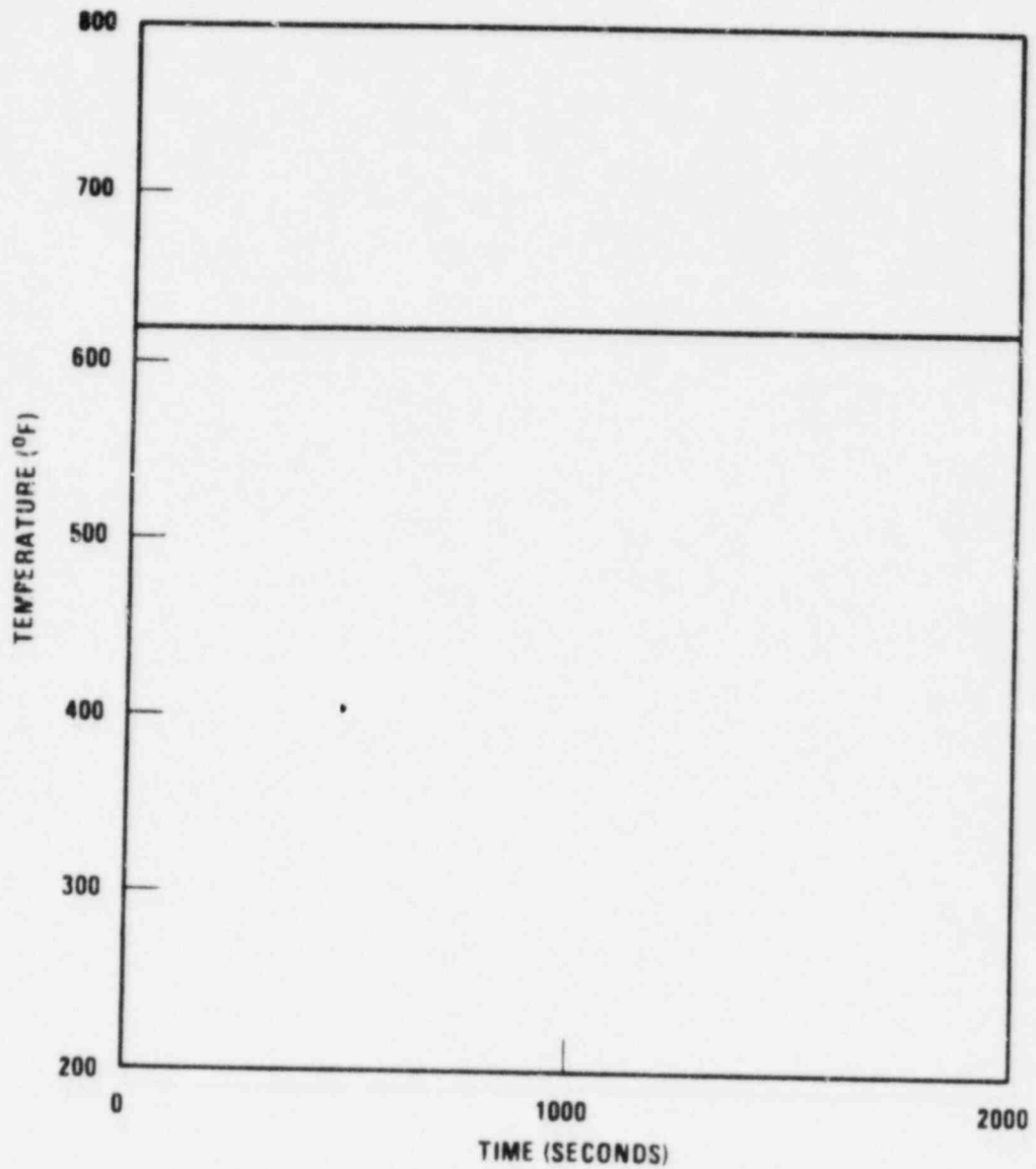


Figure 5.7-6J Affected Loop Evaporator Inlet Water Temperature for Loss of Steam Generator Load (Dumping of Water/Steam Sides of Both Evaporators and the Superheater).

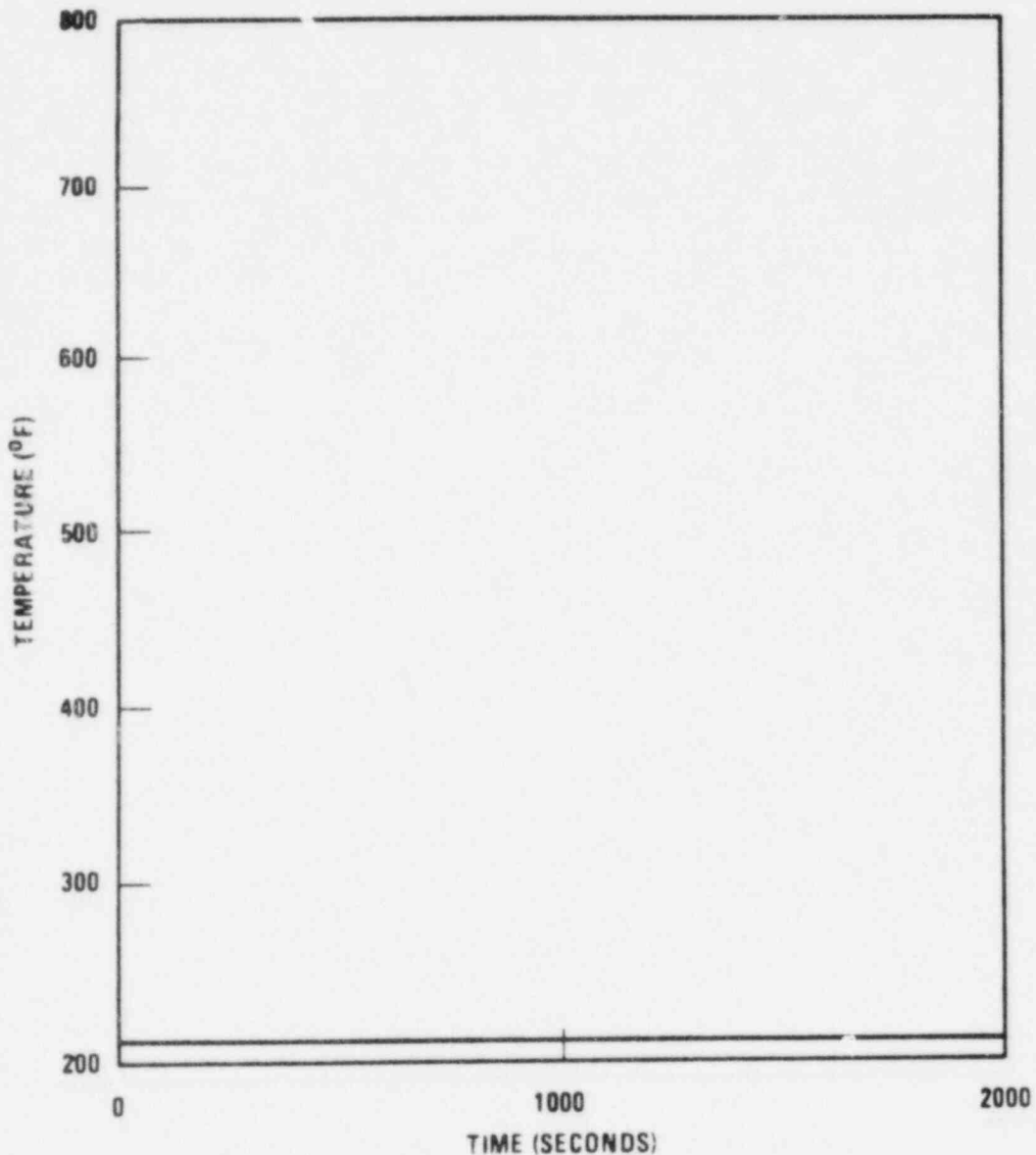
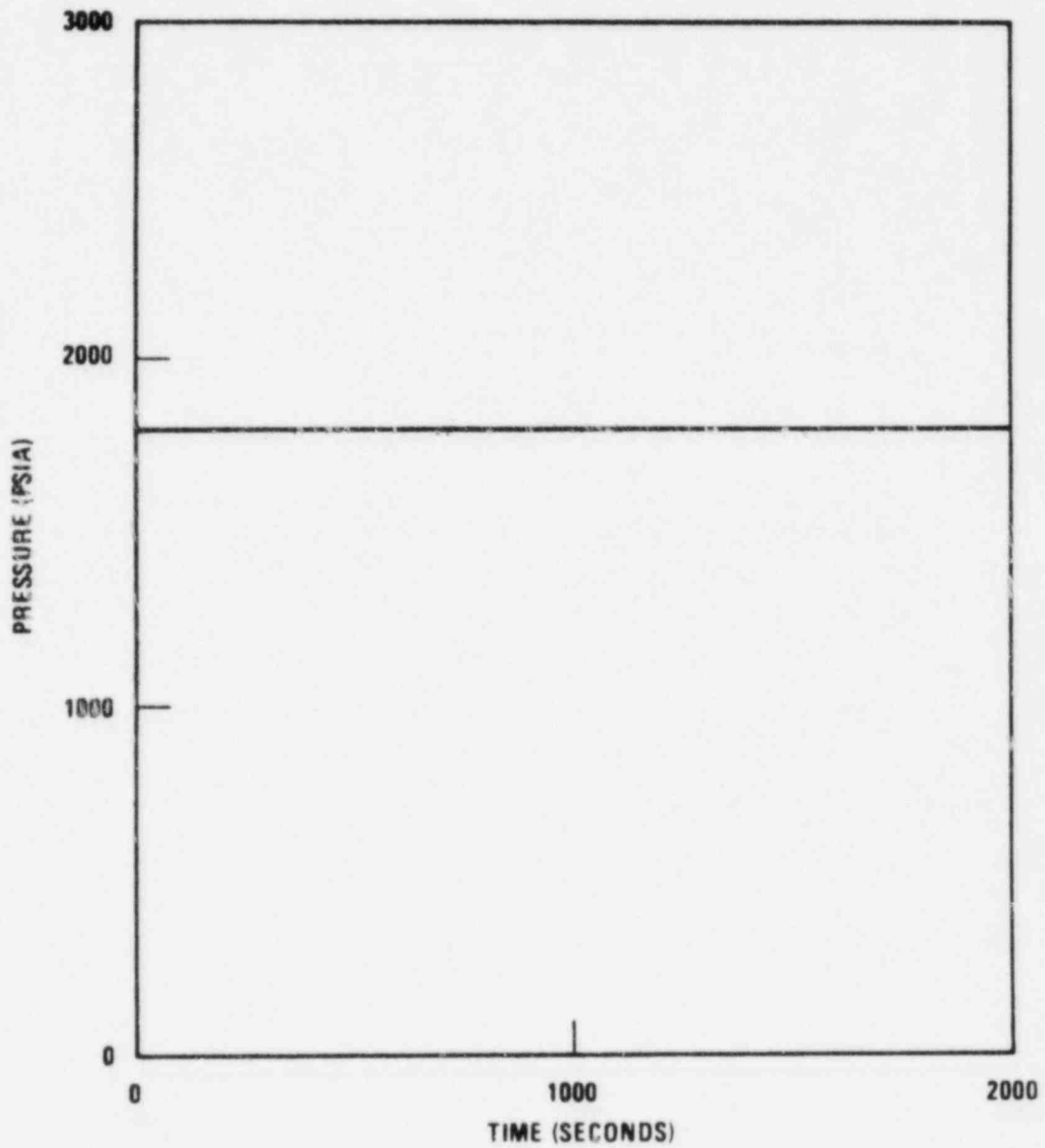


Figure 5.7-6K Affected Loop Drum Pressure for Loss of Steam Generator Load (Dumping of Water/Steam Sides of Both Evaporators and the Superheater).





CHAPTER 6.0 - ENGINEERED SAFETY FEATURES

TABLE OF CONTENTS

		<u>PAGE NO.</u>
6.0	<u>ENGINEERED SAFETY FEATURES</u>	6.1-1
6.1	<u>GENERAL</u>	6.1-1
6.2	<u>CONTAINMENT SYSTEMS</u>	6.2-1
6.2.1	Confinement/Containment Functional Design	6.2-1
6.2.1.1	Design Bases	6.2-1
6.2.1.2	System Design	6.2-2
6.2.1.3	Design Evaluation	6.2-3a
6.2.1.4	Testing and Inspection	6.2-7
6.2.1.5	Instrumentation Requirements	6.2-9
6.2.1.6	Materials	6.2-9
6.2.2	Containment Heat Removal	6.2-9
6.2.3	Containment Air Purification and Cleanup	6.2-9
6.2.4	Containment Isolation Systems	6.2-10
6.2.4.1	Design Bases	6.2-10
6.2.4.2	Systems Design	6.2-12
6.2.4.3	Design Evaluation	6.2-13
6.2.4.4	Tests and Inspections	6.2-14
6.2.5	Annulus Filtration System	6.2-14
6.2.5.1	Design Bases	6.2-14
6.2.5.2	System Design	6.2-14
6.2.5.3	Design Evaluation	6.2-15
6.2.5.4	Tests and Inspections	6.2-15

TABLE OF CONTENTS (CONT.)

		<u>PAGE NO.</u>
6.2.6	Reactor Service Building (RSB) Filtration System	6.2-16
6.2.6.1	Design Basis	6.2-16
6.2.6.2	System Design	6.2-16
6.2.6.3	Design Evaluation	6.2-16
6.2.6.4	Test and Inspection	6.2-17
6.2.7	Steam Generator Building Aerosol Release Mitigation System Functional Design	6.2-17
6.2.7.1	Design Bases	6.2-17
6.2.7.2	System Design	6.2-17
6.2.7.3	Design Evaluation	6.2-18
6.2.7.4	Testing	6.2-19
6.2.7.5	Instrumentation Requirements	6.2-19
6.3	<u>HABITABILITY SYSTEM</u>	6.3-1
6.3.1	Habitability System Functional Design	6.3-1
6.3.1.1	Design Bases	6.3-1
6.3.1.2	System Design	6.3-2a
6.3.1.3	Design Evaluation	6.3-4
6.3.1.4	Testing and Inspection	6.3-5
6.3.1.5	Instrumentation Requirement	6.3-7
6.3.1.6	Effects of Sodium Combustion Products or Other Toxic Gases on the Habitability System	6.3-7
6.3.1.6.1	Sodium Combustion Products	6.3-7
6.3.1.6.2	Toxic Gases	6.3-7a

TABLE OF CONTENTS (CONT.)

		<u>PAGE NO.</u>
6.4	<u>CELL LINER SYSTEM</u>	6.4-1
6.4.1	Design Base	6.4-1
6.4.2	System Design	6.4-1
6.4.3	Design Evaluation	6.4-1
6.4.4	Tests and Inspections	6.4-1
6.4.5	Instrumentation Requirements	6.4-1
6.5	<u>CATCH PAN</u>	6.5-1
6.5.1	Design Base	6.5-1
6.5.2	System Design Description and Evaluation	6.5-1
6.5.3	Tests and Inspections	6.5-1
6.5.4	Instrumentation Requirements	6.5-1

LIST OF TABLES

<u>TABLE NO.</u>		<u>PAGE NO.</u>
6.1-1	List of Engineered Safety Features in CRBRP	6.1-2
6.2-1	Reactor Containment Design Basis Sodium Pool Accident	6.2-21
6.2-2	Reactor Containment Design Basis Accident	6.2-22
6.2-3	Constituents of Containment Aerosol Following Failure of In-Containment Primary Sodium Storage Tank During Maintenance	6.2-23
6.2-4	Summary Description of Heat Sinks Used for Containment Pressure/Temperature Analysis	6.2-24
6.2-5	Lines Penetrating Containment	6.2-25
6.2-5A	Summary of Containment Isolation Valving Categories and Applicable GDC	6.2-34
6.2-6	Table of Bypass Leak Paths	6.2-35
6.3-1	Conformance of the Control Room Filtration System With Respect to Each Position of U.S. NRC Regulatory Guide 1.52	6.3-8
6.3-2	Free Air Space Volume Serviced by The Control Room Emergency Ventilation System	6.3-17
6.3-3	On Site Toxic Material Storage	6.3-18

## LIST OF FIGURES

<u>FIGURE NO.</u>		<u>Page No.</u>
6.2-1	Sodium Burning Rate-Primary Sodium In-Containment Storage Tank Failure During Maintenance	6.2-28
6.2-2	Containment Gas Pressure-Primary Sodium In-Containment Storage Tank Failure During Maintenance	6.2-39
6.2-3	Containment Gas Temperature-Primary Sodium In-Containment Storage Tank Failure During Maintenance	6.2-40
6.2-4	Containment Wall Temperature-Primary Sodium In-Containment Storage Tank Failure During Maintenance	6.2-41
6.2-5	Containment Aerosol Concentration-Primary Sodium In-Containment Storage Tank Failure During Maintenance	6.2-42
6.2-6	Gas Pressure in Storage Tank Cell Following Primary Sodium Storage Tank Failure in Containment During Maintenance	6.2-43
6.2-7	Gas Temperature in Storage Tank Cell Following Primary Sodium Storage Tank Failure in Containment During Maintenance	6.2-44
6.2-8	Cell Liner (Wall) Temperature in Storage Tank Cell Following Primary Sodium Storage Tank Failure in Containment During Maintenance	6.2-45
6.2-9	Cell Liner (Floor Surface) Temperature Following Primary Sodium Storage Tank Failure in Containment During Maintenance	6.2-46
6.2-10	Containment Isolation Valve Configurations	6.2-47

LIST OF REFERENCES

PAGE NO.

References to Section 6.2

6.2-20

The argon and nitrogen supply line valves provide a double barrier which is automatically activated on loss of the ex-containment boundary. The valves and associated actuators are located in protected areas and are testable. Remote and local manual initiations are provided. The nitrogen exhaust line to CAPS has two automatically initiated valves. The valves provide two barriers following closure. The valves and associated actuators are located in protected areas and are testable.

For the remainder of the penetrations, two valves are provided as barriers to release. Manual initiation will be adequate to prevent releases exceeding the guideline values.

For lines of closed systems penetrating containment, one isolation valve located outside of containment as close as practical to containment is provided. A single valve meets Criteria 48 and provides the necessary capability to limit the release of activity. For lines which do not contain radioactive fluids, the closed system provides the first boundary while the isolation valve provides the second boundary to release of activity. Therefore, in all cases, there are two boundaries which effectively limit the release of activity from a postulated event. The valves and associated actuators are located in protected areas and are testable. Manual initiation of isolation is provided.

#### 6.2.4.4 Tests and Inspections

The periodic test capability is described in Section 7.3.

#### 6.2.5 Annulus Filtration System

##### 6.2.5.1 Design Bases

The Annulus Filtration System is designed to ensure that an acceptable upper limit of leakage of radioactive material is not exceeded under the site suitability source term conditions.

The functional design and evaluation of the Annulus Filtration System is based upon the site suitability source term, as identified in Section 15.A. The design capability of the annulus filtration system as described in the following section will provide a large margin of safety over the containment design basis accident identified in Table 6.2-1.

##### 6.2.5.2 System Design

The RCB annulus filter system design shall satisfy the following criteria:

- (1) The containment/confinement annulus space shall be maintained under 1/4 inch W. G. negative pressure during normal plant operation and accident conditions.
- (2) Capability shall be provided to filter the containment/confinement annulus exhaust during normal operation.

Amend. 64  
Jan. 1982

- (3) Capability shall be provided to filter the RCB ventilation exhaust air through the annulus filter system during refueling operations, when the RCB/RSB refueling hatch is open.
- (4) Capability shall be provided to filter and recirculate the annulus air during accident conditions. For every 1000 CFM filtered exhaust air (required for the maintenance of 1/4 In. W. G. negative pressure) not less than 3500 CFM air shall be recirculated through the filters.
- (5) The recirculating duct system shall be designed to accomplish proper mixing in the annulus in accordance with USNRC Standard Review Plan Section 6.5.3.
- (6) The Annulus Filtration System shall fully comply with USNRC Regulatory Guide 1.52.
- (7) The filter system shall be designed to achieve a minimum of 99% particulate and 95% adsorbent efficiency.

Radiation monitoring equipment associated with the annulus filtration system is described in Section 12.2. By maintaining the annulus at a minimum of 1/4" water gauge negative pressure with respect to the outside atmosphere, the bypass leakage (that fraction of annulus radioactivity which leaks from the confinement building without being filtered) can be maintained at less than 1%.

#### 6.2.5.3 Design Evaluation

The Annulus Filtration System features of the design provide the necessary assurance that the radioactivity released as a result of the site suitability source term will not exceed the guidelines of 10CFR100.

The annulus pressure maintenance fans have been sized at 3000 CFM, which has conservatively been determined to be greater than the total leakage into the annulus from all sources, including the dampers (vents and cap) provided at the top of the Confinement Building and the dampers provided at the 816' - 0" elevation for the Annulus Cooling System (leakage based on a negative 1/4" w.g. pressure).

Analysis will be conducted to substantiate that the annulus space will remain under a 1/4" W.G. negative pressure considering the effects of heat transfer, barometric pressure change, inleakage and wind loads. The results of this analysis will be provided in the FSAR.

Two 100% redundant filter-fan units consisting of a demister, heating coil, prefilter bank, HEPA filter bank, adsorber bank, pressure maintenance and exhaust fan, annulus recirculation fan, with associated ductwork and accessories, are provided for the annulus exhaust, recirculation and filtering. This insures that no single active failure will prevent 100% operation of the annulus filtration system. The Annulus Filtration System is described in Section 9.6.2.2.4.



#### 6.2.5.4 Tests and Inspections

The annulus filtration system shall be tested per the requirements of Regulatory Guide 1.52. Containment penetrations shall be tested per Appendix J to 10CFR50 in order to verify bypass leakage assumptions used for radiological accident analyses.

## 6.2.6 Reactor Service Building (RSB) Filtration System

### 6.2.6.1 Design Basis

The RSB filtration system is designed as an Engineered Safety Feature (ESF) to filter the RSB exhaust air in order to mitigate the consequences of the Site Suitability Source Term (SSST) event.

The system is designed to function continuously.

### 6.2.6.2 System Design

The RSB is maintained at a minimum 1/4" negative water gauge pressure as described in Section 9.6.3.1.1.

The RSB Filtration System is used and designed to maintain the RSB at a minimum of 1/4" negative water gauge pressure and filter the RSB exhaust under all conditions except when the railroad door is open. A network of ducting is utilized in supplying and exhausting air to various floor elevations and/or cells in the RSB. This mode of operation exhausts 18,000 CFM of air through the missile protected exhaust on the Reactor Service Building (RSB).

During accident conditions the RSB Filtration System will automatically shift to an air recirculation mode of operation exhausting that amount of air (1700 CFM) required to maintain a minimum of 1/4" negative water gauge pressure.

The filter system will be designed as a Safety Class 3 system and will meet the requirements of Regulatory Guide 1.52. The filter system will be designed to achieve a minimum of 99% particulate and 95% adsorbent efficiencies.

### 6.2.6.3 Design Evaluation

The RSB filter system is designed to filter 18,000 CFM of air of which 1700 CFM of air is exhausted while 16,300 CFM of air is recirculated during accident conditions. The exhausted air is designed to offset building in leakage air while maintaining 1/4" negative water gauge pressure.

Analysis will be conducted to substantiate that the RSB will remain under a 1/4" W.G. negative pressure considering the effects of heat transfer, barometric pressure change, inleakage and wind loads. The results of this analysis will be provided in the FSAR.

Two (2) 100% redundant filter fan units consisting of a demister, heating coil, pre-filter bank, adsorber bank, HEPA filter bank, cleanup filter fan, with associated ductwork and accessories, are provided for the RSB exhaust, recirculation, and filtering. This insures that no single active failure will prevent 100% operation of the RSB filtration system. The RSB filtration system is described in Section 9.6.3.1.1.

The system ducting is designed to exhaust air from all potentially radioactive areas. Capability exists to isolate the supply and exhaust air flow to the areas where an accident has occurred and to maintain these areas at a greater negative pressure than other areas.

This capability is designed to prevent the spread of airborne radioactivity from contaminated to clean areas within the building.

#### 6.2.6.4 Test and Inspection

The RSB filtration system will be tested per the requirements of Regulatory Guide 1.52. Visual Inspection will be conducted on Installation.

#### 6.2.7 STEAM GENERATOR BUILDING AEROSOL RELEASE MITIGATION SYSTEM FUNCTIONAL DESIGN

##### 6.2.7.1 Design Bases

The Steam Generator Building Aerosol Release Mitigation System is designed to assure that release of a maximum of 630 lbs of sodium aerosols from the Steam Generator Building is not exceeded in the event of a design basis leak in one of the three loops in IHTS piping. This limit is obtained by releasing through a controlled vent area a maximum of 440 lbs of aerosols during the first five minutes of the accident. Between 5 minutes and 5000 seconds, 90 lbs of aerosols may be released through building cracks. Beyond 5000 seconds, an additional 100 lbs of aerosols could be released through building cracks.

A release of aerosols through the controlled vent area stack is required to maintain building overpressures below the 0.7 psig setpoint for opening of the large (360 Ft<sup>2</sup>) steam vent louvers.

The functional design and evaluation of the SGB Aerosol Release Mitigation Features are based upon the design basis accident described in Section 15.6.1.5 of the PSAR.

##### 6.2.7.2 System Design

Controlled release of aerosols from the Steam Generator Building (SGB) is accomplished by closure of SGB HVAC outlets and venting through a controlled area vent stack, both actions being initiated from either of a redundant set of safety-related aerosol smoke detectors located in the SGB HVAC exhaust stack. Aerosols are released from the controlled area vent stack for five minutes to assure until peak pressures in the SGB are within acceptable limits, at which time the vent path is closed to the external atmosphere.

The SGB Aerosol Release Mitigation Features consist of redundant sets of safety-related aerosol detectors (see Section 9.13.2) located in each SGB loop HVAC exhaust duct, redundant relief dampers to each loop controlled area vent stack, and redundant closure dampers in each controlled area vent stack.

Each aerosol detector set consists of three detectors provided power by three 1E uninterruptible power sources. These detectors trip when the sodium aerosol concentration in the SGB HVAC exhaust is  $10^{-7}$  gm/cc. When two of the three detectors in either set sense an aerosol concentration of  $10^{-7}$  gm/cc, a signal is provided to activate the I&C logic for the SGB aerosol release mitigation features. Within 10 seconds of receipt of an aerosol detection signal, the SGB building HVAC system will be closed to the outside atmosphere, the relief dampers to the controlled vent area will open, the controlled vent area closure devices will remain in their normally open position, and the remaining nuclear island building (RCB & RSB) HVAC systems will be closed to the outside atmosphere. The controlled vent area closure devices close five minutes after receipt of the trip signal from the aerosol detectors, with a

## CHAPTER 7.0 INSTRUMENTATION AND CONTROLS

### TABLE OF CONTENTS

		<u>PAGE NO.</u>
7.1	<u>INTRODUCTION</u>	7.1-1
7.1.1	Identification of Safety Related Instrumentation and Control Systems	7.1-1
7.1.2	Identification of Safety Criteria	7.1-1
7.1.2.1	Design Basis	7.1-2
7.1.2.2	Independence of Redundant Safety Related Systems	7.1-3
7.1.2.3	Physical Identification of Safety Related Equipment	7.1-4
7.1.2.4	Conformance to Regulatory Guides 1.11 "Instrument Lines Penetrating Primary Reactor Containment" and 1.63, "Electric Penetration Assemblies in Containment Structures for Water-Cooled Nuclear Power Plants"	7.1-4
7.1.2.5	Conformance to IEEE No. 323 "IEEE Standard for Qualifying Class 1E Equipment for Nuclear Power Generating Stations"	7.1-4
7.1.2.6	Conformance to IEEE No. 336 "Installation, Inspection and Testing Requirements for Instrumentation and Electric Equipment During the Construction of Nuclear Power Generating Stations"	7.1-4
7.1.2.7	Conformance to IEEE No. 338-1971 "Periodic Testing of Nuclear Power Generating Station Protection System"	7.1-5
7.1.2.8	Conformance to Regulatory Guide 1.22 "Periodic Testing of Protection System Actuation Functions"	7.1-5
7.1.2.9	Conformance to Regulatory Guide 1.47 "Bypassed and Inoperable Status Indication for Nuclear Power Plant Safety Systems"	7.1-6
7.1.2.10	Conformance to Regulatory Guide 1.53 "Application of the Single Failure Criterion to Nuclear Power Plant Protection Systems"	7.1-6

TABLE OF CONTENTS (CONT.)

		<u>PAGE NO.</u>
7.1.2.11	Conformance to Regulatory Guide 1.62 "Manual Initiation of Protective Functions"	7.1-6
7.1.2.12	Regulatory Guide 1.89 "Qualification of Class IE Equipment for Nuclear Power Plants"	7.1-6a
7.1.2.13	I & E Information Notice 79-22 "Qualification of Control Systems"	7.6-6a
7.2	<u>REACTOR SHUTDOWN SYSTEM</u>	7.2-1
7.2.1	Description	7.2-1
7.2.1.1	Reactor Shutdown System Description	7.2-1
7.2.1.2	Design Basis Information	7.2-6
7.2.1.2.1	Primary Reactor Shutdown System Subsystems	7.2-7
7.2.1.2.2	Secondary Reactor Shutdown System Subsystems	7.2-9
7.2.1.2.3	Essential Performance Requirements	7.2-11
7.2.2	Analysis	7.2-13
7.3	<u>ENGINEERED SAFETY FEATURE INSTRUMENTATION AND CONTROL</u>	7.3-1
7.3.1	Containment Isolation System	7.3-1
7.3.1.1	System Description	7.3-1
7.3.1.2	Design Basis Information	7.3-2
7.3.1.2.1	Containment Isolation System Subsystems	7.3-2
7.3.1.2.2	Essential Performance Requirements	7.3-3
7.3.2	Analysis	7.3-3
7.3.2.1	Functional Performance	7.3-3
7.3.2.2	Design Features	7.3-3
7.4	<u>INSTRUMENTATION AND CONTROL SYSTEMS REQUIRED FOR SAFE SHUTDOWN</u>	7.4-1
7.4.1	Steam Generator Auxiliary Heat Removal Instrumentation and Control System	7.4-1

TABLE OF CONTENTS (Cont.)

	<u>PAGE NO.</u>
7.4.1.1 Design Description	7.4-1
7.4.1.1.1 Function	7.4-1
7.4.1.1.2 Equipment Design	7.4-1
7.4.1.1.3 Initiating Circuits	7.4-3
7.4.1.1.4 Bypasses and Interlocks	7.4-3
7.4.1.1.5 Redundancy/Diversity	7.4-4
7.4.1.1.6 Actuated Devices	7.4-4
7.4.1.1.7 Testability	7.4-4
7.4.1.1.8 Separation	7.4-4
7.4.1.1.9 Operator Information	7.4-5
7.4.1.2 Design Analysis	7.4-6
7.4.2 Outlet Steam Isolation Instrumentation and Control System	7.4-6
7.4.2.1 Design Description	7.4-6
7.4.2.1.1 Function	7.4-6
7.4.2.1.2 Equipment Design	7.4-7
7.4.2.1.3 Initiating Circuits	7.4-7
7.4.2.1.4 Bypasses and Interlocks	7.4-7
7.4.2.1.5 Redundancy and Diversity	7.4-7
7.4.2.1.6 Actuated Device	7.4-8
7.4.2.1.7 Separation	7.4-8
7.4.2.1.8 Operator Information	7.4-8
7.4.2.2 Design Analysis	7.4-8
7.4.3 Pony Motors and Controls	7.4-8
7.4.3.1 Design Description	7.4-8a

TABLE OF CONTENTS (Cont.)

	<u>PAGE NO.</u>
7.4.3.2 Initiating Circuits	7.4-8a
7.4.3.3 Bypasses and Interlocks	7.4-8a
7.4.3.4 Analyses	7.4-8a
7.4.4 Remote Shutdown System	7.4-8b
7.4.4.1 Design Description	7.4-8b
7.4.4.1.1 Function	7.4-8b
7.4.4.1.2 Design Basis	7.4-8b
7.4.4.1.3 Remote Shutdown Operations	7.4-8c
7.4.4.1.4 Equipment Design	7.4-8d
7.4.4.2 Design Analysis	7.4-8f
7.5 <u>INSTRUMENTATION AND MONITORING SYSTEM</u>	7.5-1
7.5.1 Flux Monitoring System	7.5-1
7.5.1.1 Design Description	7.5-1
7.5.1.1.1 Source Range	7.5-2
7.5.1.1.2 Wide Range	7.5-3b
7.5.1.1.3 Power Range	7.5-3b
7.5.1.2 Design Analysis	7.5-4
7.5.2 Heat Transport Instrumentation System	7.5-5
7.5.2.1 Description	7.5-5
7.5.2.1.1 Primary and Intermediate Sodium Loops	7.5-5
7.5.2.1.2 Sodium Pumps	7.5-8
7.5.2.1.3 Steam Generator	7.5-9
7.5.2.2 Analysis	7.5-12
7.5.3 Reactor and Vessel Instrumentation	7.5-13
7.5.3.1 Description	7.5-13



TABLE OF CONTENTS (Cont.)

	<u>PAGE NO.</u>
7.5.3.1.1 Sodium Level	7.5-13
7.5.3.1.2 Temperature	7.5-13
7.5.3.1.3 Non-Replaceable Instruments	7.5-13
7.5.3.2 Analysis	7.5-14
7.5.4 Fuel Failure Monitoring System	7.5-14
7.5.4.1 Design Description	7.5-15
7.5.4.1.1 Cover Gas Monitoring Subsystem	7.5-15
7.5.4.1.2 Reactor Delayed Neutron Monitoring Subsystem	7.5-16
7.5.4.1.3 Failed Fuel Location Subsystem	7.5-17
7.5.4.1.4 Tests and Inspection	7.5-17
7.5.4.2 Design Analysis	7.5-18
7.5.5 Leak Detection Systems	7.5-18
7.5.5.1 Sodium to Gas Leak Detection System	7.5-18
7.5.5.1.1 Design Bases and Design Criteria for the Liquid Metal - to - Gas Leak Detection Systems	7.5-18a
7.5.5.1.1.1 Design Description	7.5-19
7.5.5.1.2 Design Analysis	7.5-22
7.5.5.2 Intermediate to Primary Heat Transport System Leak Detection	7.5-24
7.5.5.2.1 Design Description	7.5-24
7.5.5.2.2 Design Analysis	7.5-25
7.5.5.3 Steam Generator Leak Detection System	7.5-25
7.5.5.3.1 Design Description	7.5-26
7.5.5.3.2 Design Analysis	7.5-27a
7.5.6 Sodium-Water Reaction Pressure Relief System (SWRPRS) Instrumentation and Control	7.5-30
7.5.6.1 Design Description	7.5-30

TABLE OF CONTENTS (Cont.)

	<u>PAGE NO.</u>
7.5.6.1.1 Function	7.5-30a
7.5.6.1.2 SWRPRS Trip Logic	7.5-30a
7.5.6.1.3 Bypasses and Interlocks	7.5-32
7.5.6.1.4 Sodium Dump	7.5-32
7.5.6.1.5 Monitoring Instrumentation	7.5-32
7.5.6.1.6 Sodium Dump Tank Instrumentation	7.5-33
7.5.6.1.7 Water Dump Tank Instrumentation	7.5-33
7.5.6.2 Design Analysis	7.5-33a
7.5.7 Containment Hydrogen Monitoring	7.5-33b
7.5.7.1 Design Description	7.5-33b
7.5.8 Containment Vessel Temperature Monitoring	7.5-33b
7.5.8.1 Design Description	7.5-33b
7.5.9 Containment Pressure Monitoring	7.5-33b
7.5.9.1 Design Description	7.5-33b
7.5.10 Containment Atmosphere Temperature	7.5-33c
7.5.10.1 Design Description	7.5-33c
7.5.11 Post Accident Monitoring	7.5-33c
7.5.11.1 Description	7.5-33c
7.5.11.2 Instrumentation Design and Qualification	7.5-33d
7.5.11.2.1 Category 1	7.5-33d
7.5.11.2.2 Category 2	7.5-33f
7.5.11.2.3 Category 3	7.5-33g
7.5.11.2.4 General Requirements to Category 1,2, and 3	7.5-33g
7.5.11.3 Instrument Identification	7.5-33h
7.5.12 Inoperable Status Monitoring System	7.5-33i

	<u>PAGE NO.</u>
7.5.12.1 Design Description	7.5-33 i
7.5.12.2 Design Analysis	7.5-33 i
7.6 <u>OTHER INSTRUMENTATION AND CONTROL SYSTEMS REQUIRED FOR SAFETY</u>	7.6-1
7.6.1 Emergency Plant Service Water Instrumentation and Control Systems	7.6-1
7.6.1.1 Emergency Plant Service Water system (EPSW)	7.6-1
7.6.1.2 Design Criteria	7.6-1
7.6.1.3 Design	7.6-2
7.6.1.3.1 Control System	7.6-2
7.6.1.3.2 Monitoring Instrumentation	7.6-2
7.6.1.3.3 Inputs to PDH & DS	7.6-2a
7.6.1.3.4 Design Analysis	7.6-2a
7.6.2 Emergency Chilled Water (ECW) System	7.6-2b
7.6.2.1 Design Criteria	7.6-2b
7.6.2.2 Design	7.6-2c
7.6.2.2.1 Control System	7.6-2c
7.6.2.2.2 Monitoring Instrumentation	7.6-2c
7.6.2.2.3 Inputs to PDH & DS	7.6-2e
7.6.2.2.4 Design Analysis	7.6-2e
7.6.3 Direct Heat Removal Service Instrumentation and Control	7.6-3
7.6.3.1 Design Description	7.6-3
7.6.3.1.1 Function	7.6-3
7.6.3.1.2 Design Criteria	7.6-3
7.6.3.1.3 Equipment Design	7.6-3a
7.6.3.1.4 Initiating Circuits	7.6-3c
7.6.3.1.5 Bypass and Interlocks	7.6-3c

		<u>PAGE NO.</u>
7.6.3.2	Design Analysis	7.6-3d
7.6.4	Heating, Ventilating, and Air Conditioning Instrumentation and Control System	7.6-4
7.6.4.1	Design Criteria	7.6-4
7.6.4.2	Design Description	7.6-5
7.6.4.2.1	Control System	7.6-5
7.6.4.2.2	Monitoring Instrumentation	7.6-7
7.6.4.3	Design Analysis	7.6-8
7.6.5	SGB Flooding Protection System	7.6-9
7.6.5.1	Design Basis	7.6-9
7.6.5.2	Design Requirements	7.6-9
7.6.5.3	Design Requirements	7.6-9
7.6.5.3.1	Instrumentation	7.6-9
7.6.5.3.2	Controls	7.6-9
7.6.6	Recirculating Gas Cooling (RGC) Instrumentation and Coltron System	7.6-10
7.6.6.1	Design Criteria	7.6-10
7.6.6.2	Design	7.6-11
7.6.6.2.1	Control System	7.6-11
7.6.6.2.1.1	Safety-Related Subsystem Operation	7.6-11
7.6.6.2.1.1.1	Fan Operation	7.6-11
7.6.6.2.1.1.2	Automatic Isolation Valve Operation	7.6-13
7.6.6.2.1.1.3	Drain Valve Operation	7.6-13
7.6.6.2.1.1.4	Chilled Water Valve Operation	7.6-13
7.6.6.2.1.2	Safety-Related Subsystem EB	7.6-14
7.6.6.2.2	Monitoring Instrumentation	7.6-14
7.6.6.2.3	Inputs to PDH & DS	7.6-15

	<u>PAGE NO.</u>
7.6.6.2.4 Design Analysis	7.6-16
7.7 <u>INSTRUMENTATION AND CONTROL SYSTEMS NOT REQUIRED FOR SAFETY</u>	7.7-1
7.7.1 Plant Control System Description	7.7-1
7.7.1.1 Supervisory Control System	7.7-2
7.7.1.2 Reactor Control System	7.7-3
7.7.1.3 Primary and Secondary CRDM (Control Rod Drive Mechanism) Controller and Rod Position Indication	7.7-4
7.7.1.3.1 Primary CRDM Control	7.7-4
7.7.1.3.2 Rod Position Indication System	7.7-6
7.7.1.4 Sodium Flow Control System	7.7-7
7.7.1.5 Steam Generator Steam Drum Level Control System	7.7-8
7.7.1.5.1 Feedwater Flow Control Valve Control	7.7-8
7.7.1.5.2 Main Feedwater Isolation	7.7-9
7.7.1.5.3 Operational Considerations	7.7-9
7.7.1.6 Recirculation Flow Control System	7.7-10
7.7.1.7 Sodium Dump Tank Pressure Control System	7.7-10
7.7.1.8 Steam Dump and Bypass Control System	7.7-11
7.7.1.9 Fuel Handling and Storage Control System	7.7-12
7.7.1.10 Nuclear Island Auxiliary Instrumentation and Control Systems	7.7-15
7.7.1.11 Balance of Plant Instrumentation and Control	7.7-15a
7.7.1.11.1 Treated Water Instrumentation and Control System	7.7-15a
7.7.1.11.2 Waste Water Treatment Instrumentation and Control System	7.7-16
7.7.1.11.3 Remaining Systems	7.7-16
7.7.2 Design Analysis	7.7-16
7.7.2.1 Supervisory Control System	7.7-17

	<u>PAGE NO.</u>	
7.7.2.2	Reactor Control System	7.7-18
7.7.2.3	Sodium Flow Control System	7.7-18
7.7.2.4	Steam Generator Feedwater Flow Control System	7.7-19
7.7.2.5	Balance of Plant Instrumentation and Control	7.7-19
7.8	<u>PLANT DATA HANDLING AND DISPLAY SYSTEM</u>	7.8-1
7.8.1	Design Description	7.8-1
7.8.2	Design Analysis	7.8-2
7.9	<u>OPERATING CONTROL STATIONS</u>	7.9-1
7.9.1	Design Basis	7.9-1
7.9.2	Control Room	7.9-1
7.9.2.1	General Description	7.9-1
7.9.2.2	Control Room Arrangement	7.9-2
7.9.2.3	Main Control Board Arrangement	7.9-2
7.9.2.4	Main Control Board Design	7.9-5
7.9.3	Local Control Stations	7.9-6
7.9.4	Communications	7.9-6
7.9.5	Design Evaluation	7.9-6
7.9.5.1	Planning Phase	7.9-6
7.9.5.2	Review Phase	7.9-6a
7.9.5.3	Assessment and Implementation Phase	7.9-6b
7.9.5.4	Conclusions	7.9-6c

LIST OF TABLES

<u>TABLE NO.</u>		<u>PAGE NO.</u>
7.1-1	Safety Related Instrumentation and Control Systems	7.1-7
7.1-2	List of Regulatory Guides Applicable to Safety Related Instrumentation and Control Systems	7.1-8
7.1-3	List of IEEE Standards Applicable to Safety Related Instrumentation and Control Systems	7.1-9
7.1-4	Deleted	
7.1-5	Deleted	
7.1-6	Deleted	
7.2-1	Plant Protection System Protective Functions	7.2-18
7.2-2	PPS Design Basis Fault Events	7.2-19
7.2-3	Essential Performance Requirements for PPS Instrumentation	7.2-23
7.2-4	List of IEEE Standards Applicable to the Reactor Shutdown System Logic	7.2-23a
7.3-1	Containment Isolation System Design Basis	7.3-5
7.3-2	List of IEEE Standards Applicable to the Containment Isolation System Logic	7.3-5a
7.4-1	Sequence of Decay Heat Removal Events	7.4-9
7.4-2	SGAHRs Nominal Set Points	7.4-10a
7.4-3	List of IEEE Standards Applicable to SGAHRs and OSIS Instrumentation and Control Systems	7.4-10d
7.5-1	Instrumentation System Functions and Summary	7.5-34
7.5-2	Reactor and Vessel Instrumentation	7.5-39
7.5-3	Summation of Sodium/Gas Leak Detection Methods	7.5-40
7.5-4	Safety Functions and Primary Systems Monitored by ISMS	7.5-42

LIST OF TABLES (Cont.)

<u>TABLE NO.</u>		<u>PAGE NO.</u>
7.6-1	Symbols	7.6-17
7.6-2	List of IEEE Standards Applicable to Emergency Plant Service Water, Emergency Chilled Water, HVAC, and Recirculating Gas Instrumentation and Control Systems	7.6-18a
7.6-3	List of IEEE Standards Applicable to SGB Flooding Protection Subsystem	7.9-18b
7.7-1	Use of Refueling Interlocks	7.7-19a
7.9-1	Control Room Arrangements	7.9-8



## LIST OF FIGURES

<u>FIGURE NO.</u>		<u>PAGE NO.</u>
7.2-1	Reactor Shutdown System	7.2-24
7.2-2	HTS Pump Breaker Logic Diagram	7.2-25
7.2-2A	Typical Primary PPS Instrument Channel Logic Diagram	7.2-26
7.2-2AA	RSS Bypass Function Block Diagram	7.2-27
7.2-2B	Primary PPS Logic Diagram	7.2-28
7.2-2C	Typical Secondary PPS Instrument Channel Logic Diagram	7.2-29
7.2-2D	Secondary PPS Logic Diagram	7.2-30
7.2-3	Typical Primary Subsystem	7.2-31
7.2-4	Typical Secondary Subsystem	7.2-32
7.2-5	Functional Block Diagrams of the Flux-Delayed Flux, High Flux, Flux-Pressure, and Reactor Vessel Level Protective Subsystems	7.2-33
7.2-6	Functional Block Diagrams of the HTS Pump Frequency and Pump Speed Mismatch Protective Systems	7.2-34
7.2-7	Functional Block Diagrams of the IHX Primary Outlet Temperature and Steam to Feedwater Flow Mismatch Protective Subsystems	7.2-35
7.2-8	Functional Block Diagrams of the Flux-Total Flow, Startup Nuclear, Modified Nuclear Rate, and Primary to Intermediate Flow Rate Protective Subsystems	7.2-36
7.2-9	Functional Block Diagrams of the Steam Drum Level and HTS Pump Voltage Subsystems	7.2-37
7.2-10	Functional Block Diagrams of the Evaporator Outlet Sodium Temperature and Sodium Water Reaction Protective Subsystems	7.2-38
7.3-1	Containment Isolation System Block Diagram	7.3-6

LIST OF FIGURES (Cont.)

<u>FIGURE NO.</u>		<u>PAGE NO.</u>
7.3-2	Containment Selection System Logic Diagram	7.3-7
7.4-1	SGAHRs Initiation Logic	7.4-11
7.5-1	CRBRP Flux Monitoring System Block Diagram	7.5-43
7.5-2	CRBRP Flux Monitoring System Instrument Range Coverage	7.5-44
7.5-3	Fuel Failure Monitoring System	7.5-45
7.5-4	Main Sodium Stream First Pass Hydrogen Concentration Change vs. Leak Rate	7.5-46
7.5-4a	Main Sodium Stream First Pass Oxygen Concentration vs. Leak Rate	7.5-46a
7.5-5	Hydrogen Concentration vs. Time for Various Water Leak Rates	7.5-47
7.5-6	SWRPRS Trip & SWRPRS Controlled Isolation Valves Control Logic Diagram	7.5-48
7.6-1	Emergency cooling Tower Fan	7.6-19
7.6-2	Emergency Plant Service Water Makeup Pump	7.6-20
7.6-3	Emergency Plant Service Water Pump Start	7.6-21
7.6-4	Emergency Plant Service Water Pump Stop	7.6-22
7.6-5	Emergency Chilled Water Pumps Logic	7.6-23
7.6-6	Emergency Chilled Water Chiller Start	7.6-24
7.6-7	Emergency Chilled Water Chillers Stop	7.6-25
7.6-8	Emergency Chilled Water Isolation Valves to Secondary Coolant Loop	7.6-26
7.6-9	Emergency Chilled Water System NCW to ECW Isolation Valves	7.6-27
7.6-10	Emergency Chilled Water System Loop A & Loop B AOV's Normal & Emergency Operation	7.6-28
7.6-11	Safety Class Equipment: Vital Bus Hookup	7.6-29
7.6-12	Functional Control Diagram Typical HVAC Exhaust Fan	7.6-30

LIST OF FIGURES (Cont.)

<u>FIGURE NO.</u>		<u>PAGE NO.</u>
7.6-13	Functional Control Diagram Typical HVAC Unit Return Fan	7.6-31
7.6-14	Functional Control Diagram Typical Filter Unit Supply Fan	7.6-32
7.6-15	Functional Control Diagram Annulus Cooling Fan	7.6-33
7.6-16	Functional Control Diagram Containment Cleanup Scrubber Exhaust Fan	7.6-34
7.6-17	Functional Control Diagram Control Room HVAC Unit Supply Fan	7.6-35
7.6-18	Functional Control Diagram Diesel Room Emergency Supply Fan	7.6-36
7.6-19	Functional control Diagram 1 of 2 Redundant Supply Fans for SGB-IB Air Handling Unit	7.6-37
7.6-20	Functional Control Diagram Typical Unit Cooler Serving Cell Containing Safety Related Equipment	7.6-38
7.6-21	Functional Control Diagram Typical Unit Cooler Fan Serving Cell Containing Safety-Related Equipment Where Redundant Coolers are Required	7.6-39
7.6-22	Functional Control Diagram Typical Unit Cooler Fan Serving Cell Containing Containment Cleanup Equipment	7.6-40
7.6-23	Functional Control Diagram Containment Purge and Vent Valves	7.6-41
7.6-24	Functional control Diagram Containment Cleanup Scrubber Fan Discharge & Bypass Valves	7.6-42
7.6-25	Functional Control Diagram Control Room Outside Air Exhaust & HVAC Unit Outside Air Intake Valves	7.6-43
7.6-26	Functional Control Diagram Control Room Filter Unit Air Intake Valves	7.6-44
7.6-27	Functional Control Diagram Control Room Main Air Intake Isolation Valves	7.6-45
7.6-28	Functional Control Diagram Control Room Remote Air Intake Isolation Valves	7.6-46

LIST OF FIGURES (Cont.)

<u>FIGURE NO.</u>		<u>PAGE NO.</u>
7.6-29	Functional Control Diagram RCB Supply & Exhaust Containment Isolation Valves	7.6-47
7.6-30	Functional Control Diagram Annulus Cooling Exhaust & Fan Discharge Dampers	7.6-48
7.6-31	Functional Control Diagram Annulus Filtration Recirculation Dampers	7.6-49
7.6-32	Functional Control Diagram Annulus Filtration Exhaust Dampers	7.6-50
7.6-33	Functional Control Diagram RSB Cleanup Discharge, Exhaust, Decirculation & Cell Isolation Dampers	7.6-51
7.6-34	Functional Control Diagram Typical Process Parameter Control of Damper	7.6-52
7.6-35	Functional Control Diagram Diesel Generator Emergency Supply Fan Temperature Modulated Dampers	7.6-53
7.6-36	Functional Control Diagram Annulus Pressure Maintenance Fan Pressure Modulated Damper	7.6-54
7.6-37	Functional Control Diagram Typical Flow Modulated Vortex Damper	7.6-55
7.6-38	Loop Diagram Recirculating Gas Cooling Sys. Subsystem MA	7.6-56
7.6-39	Logic Diagram Subsystem MA Supply & Return Isolation Valves	7.6-57
7.6-40	Logic Diagram Subsystem MA Supply & Return Isolation Valves	7.6-58
7.6-41	Logic Diagram Subsystem MA Fan	7.6-59
7.6-42	Logic Diagram Subsystem MA Supply & Return Isolation Valves	7.6-60
7.6-43	Logic Diagram Subsystem MA Cooler Drain Valves	7.6-61
7.6-44	Logic Diagram Subsystem MA Emergency Chilled Water (to Cooler) Isolation Valve	7.6-62
7.6-45	Logic Diagram Subsystem MA Malfunction Alarm	7.6-63
7.6-46	Logic Diagram RGCS Safety-Related Subsystem Malfunction Common Alarm	7.6-64

LIST OF FIGURES (Cont.)

<u>FIGURE NO.</u>		<u>PAGE NO.</u>
7.7-1	Plant Control System	7.7-20
7.7-2	Supervisory Control System	7.7-21
7.7-3	Reactor Control	7.7-22
7.7-4	ORDM Controller and Power Train for Primary Rods	7.7-23
7.7-5	Block Diagram of Primary Rod Group Control	7.7-24
7.7-6	General Block Diagram for the Rod Misalignemnt Rod Block System	7.7-25
7.7-7	Sodium Flow Control System Flow/Speed Control	7.7-26
7.7-8	Fuel Handling and Storage Control System	7.7-27
7.8-1	Plant Data Handling and Display System Schematic	7.8-3
7.8-2	Plant data Handling and Display System Arrangement	7.8-4
7.9-1	Control Room Layout	7.9-11
7.9-2	Typical Control Panel (Side View)	7.9-12
7.9-3	Main Control Panel Plan View	7.9-13
7.9-4	Typical Control Panel Wiring Layout	7.9-14

LIST OF REFERENCES

Section 7.5

7.5-33j

Section 7.9

7.9-6d

## 7.0 INSTRUMENTATION AND CONTROLS

### 7.1 INTRODUCTION

This chapter includes a description of the Instrumentation and Control Systems provided for the CRBRP. Particular emphasis is placed on the description of safety-related systems, which include the Plant Protection System and the safety-related display instrumentation required to maintain the plant in a safe shutdown condition. The Plant Protection System includes all equipment to initiate and carry to completion reactor heat transport and balance of plant shutdown, decay heat removal and containment isolation. Safety-related display instrumentation assures that the operator has sufficient information to perform required manual safety functions and monitor the safety status of the plant. Major control systems not required for safety are described and analysis is included to demonstrate that even gross failure of those systems does not prevent Plant Protection System action. Analysis is also included to demonstrate that the requirements of the NRC General Design Criteria, IEEE Standard 279-1971, applicable NRC Regulatory Guides and other appropriate criteria and standards are satisfied.

#### 7.1.1 Identification of Safety-Related Instrumentation and Control Systems

Table 7.1-1 lists the Safety-Related Instrumentation and Control Systems and includes the definition of Safety-Related Equipment from Section 3.2.1. The entire Plant Protection System, including the Reactor Shutdown System, the Containment Isolation System and the Shutdown Heat Removal System is safety-related. The Reactor Shutdown System input variables are described in Section 7.2. The Containment Isolation Instrumentation and Control System is described in Section 7.4 and Section 7.6. The instrumentation which provides signal input to the Plant Protection System is also safety-related and is described in Section 7.5. Safety-Related Display Instrumentation, which assures that the operator has sufficient information to monitor the safety status of the plant and maintain it in a safe shutdown condition, is discussed in Sections 7.5 and 7.9. Other safety-related instrumentation and control systems including Emergency Chilled Water System, Emergency Plant Service Water System, and Fuel Handling and Storage Interlocks are described in Section 7.6.

#### 7.1.2 Identification of Safety Criteria

In addition to meeting the requirements of the CRBRP General Design Criteria (refer to Section 3.1), the safety-related I&C systems will be designed to meet the applicable requirements of the Regulatory Guides and IEEE Standards listed in Tables 7.1-2 and 7.1-3. The means of compliance with the guides and standards applicable to all safety-related instrumentation and control equipment are described in paragraphs 7.1.2.2 through 7.1.2.11. Compliance with guides or standards applicable to specific I&C systems or equipment are described in the paragraphs related to those systems. The instrument error and other performance consideration are addressed in the description of individual subsystems.

with guides or standards applicable to specific I&C systems or equipment are described in the paragraphs related to those systems. The instrument error and other performance considerations are addressed in the description of individual subsystems.

#### 7.1.2.1 Design Basis

The Plant Protection System (PPS) includes the Reactor Shutdown System (RSS), the Containment Isolation System and the Shutdown Heat Removal Systems.

The Reactor Shutdown System consists of a Primary and a Secondary System either of which is designed to initiate and carry to completion trip of the control rods and sodium coolant pumps to prevent the results of postulated fault conditions from exceeding the allowable limits. Table 4.2-35 shows the basis for Primary and Secondary RSS performance for the defined fault categories. The performance limits for the fuel and cladding are identified in Section 4. The Reactor Shutdown Systems are described in Section 7.2.

Two diverse Reactor Shutdown Systems have been provided for CRBRP to ensure that the reactor is protected from the consequences of all anticipated and unlikely events even if one of the Reactor Shutdown Systems fails. The two Reactor Shutdown Systems have been made diverse in order to reduce the probability that a common mode failure will prevent a reactor shutdown from taking place. This diversity extends from the sensors used as input to the two systems, through the logic utilized, to the actuation devices required to trip the two different control rod designs.

Table 7.1-4 lists the principal diverse design features present in the two systems. These different design features are discussed in more detail in Section 7.2.1.1. When combined with the separation, qualification and other design requirements arising from the Regulatory Guides listed in Tables 7.1-2 and 7.1-3, these designs provide protection against degradation of performance arising from common mode initiators.

The Containment Isolation System (CIS) is designed to react automatically to prevent or limit the release of radioactive material to the outside environment. The system acts to isolate the interior of the containment by closing the containment isolation valves in the event that radioactive material is released within the containment. Radiation monitors within the containment boundary are used to activate the CIS. A description of this system is given in Section 7.3.

The Shutdown Heat Removal Instrumentation and Control System is designed to provide assurance against exceeding acceptable fuel and reactor coolant system damage limits following normal and emergency shutdowns. The description of this instrumentation and control is given in Section 7.4 for the removal through the auxiliary steam/water system (Steam Generator Auxiliary Heat Removal System (SGAHS) and Outlet Steam Isolation System (OSIS) and Section 7.6 for removal through the NaK to air system (Direct Heat Removal System (DHRS)).

Sufficient instrumentation and associated display equipment will be provided to permit effective determination of the status of the reactor at any time. Section 7.5 provides a description of the instrumentation provided. The



above design bases have been applied to the PPS instrumentation listed in Table 7.5-1 and described in Section 7.5. In Section 7.9, a description of the control room, control room layout, operator-control panel interface, instrument and display groupings and habitability are given.

In the areas where the rupture of the steam or feedwater lines can occur, the field instrumentation and control shall be qualified to survive the resulting higher temperature and pressure transient.

TABLE 7.1-1

SAFETY RELATED INSTRUMENTATION AND CONTROL SYSTEMS\*

Reactor Shutdown Systems

Includes all RSS sensors, signal conditioning calculation units, comparators, buffers, 2/3 logic, scram actuators, scram breakers, control rods, back contacts on scram breakers, HTS shutdown logic, coolant pump breakers, and mechanical mounting hardware (equipment racks).

Containment Isolation System

Includes radiation monitoring sensors, signal conditioning, comparators, 2/3 logic, containment isolation valve actuators and valves.

Decay Heat Removal System Instrumentation and Control System

Includes initiating sensors, signal conditioning, calculation units, comparators, logic, auxiliary feedwater pump actuators and controls including feedwater turbine pump, PACC DHX actuators and controls, steam relief valve actuators and valves; sensors, signal conditioning, logic and actuators related to decay heat removal functions of DHRS including control of sodium and NaK pumps and air blast heat exchangers; and sensors, signal conditioning, logic and actuators related to removal of heat from the EVST.

Other Safety Related Instrumentation and Control

Includes Instrumentation and Controls for portions of the following functions to assure the plant is maintained in a safe shutdown condition:

- o Emergency Chilled Water System
- o Emergency Plant Service Water System
- o Instrumentation necessary to assure plant is maintained in safe shutdown status (See Table 7.5-4)
- o Fuel Handling and Storage Safety Interlocks
- o Heating, Ventilating, and Air Conditioning System
- o Recirculating Gas Cooling System

\*The Clinch River Breeder Reactor Plant (CRBRP) safety-related structures, systems, and components are designed to remain functional in the event of a Safe Shutdown Earthquake (SSE). These include, but are not limited to, those structures, systems and components which are necessary:

To assure the integrity of the Reactor Coolant Boundary;  
To shut down the reactor and maintain it in a safe shutdown condition;  
To prevent or mitigate the consequences of accidents which could result in potential off-site exposures comparable to the guideline exposures of 10CFR100.

NOTE: Class IE equipment loads are identified in Chapter 8.

TABLE 7.1-2

LIST OF REGULATORY GUIDES APPLICABLE TO SAFETY  
RELATED INSTRUMENTATION AND CONTROL SYSTEMS

- 1.6 Independence Between Redundant Power Sources and their Distribution Systems (as discussed in Sections 8.3.1.2 and 8.3.2.2)
- 1.12 Instrumentation for Earthquakes
- 1.17 Protection of Nuclear Power Plants Against Industrial Sabotage
- 1.22 Periodic Testing of Protection System Actuation Functions
- 1.28 Quality Assurance Program Requirements (Design and Construction)
- 1.29 Seismic Design Classification
- 1.30 Quality Assurance Program Requirements for the Installation, Inspection, and Testing of Instrumentation and Electric Equipment
- 1.32 Use of IEEE Std 308-1971 "Criteria for Class 1E Electric Systems for Nuclear Power Generating Stations"
- 1.40 Qualification Tests of Continuous Duty Motors Installed Inside the Containment of Water Cooled Nuclear Power Plants
- 1.47 Bypassed and Inoperable Status Indication for Nuclear Power Plant Safety Systems
- 1.53 Application of the Single Failure Criterion to Nuclear Power Plant Protection Systems
- 1.62 Manual Initiation of Protective Actions
- 1.63 Electric Penetration Assemblies in Containment Structures for Water-Cooled Nuclear Power Plants
- 1.64 Quality Assurance Program Requirements for the Design of Nuclear Power Plants
- 1.73 Qualification Tests of Electric Valve Operators Installed Inside the Containment of Nuclear Power Plants
- 1.75 Physical Independence of Electric System
- 1.79 Control Room Habitability During Chemical Release (as discussed in Section 6.3).
- 1.89 Qualification of Class 1E Equipment for Nuclear Power Plants (as discussed in Section 7.1.2.5).

22

22

22

TABLE 7.1-3

LIST OF IEEE STANDARDS APPLICABLE TO  
SAFETY RELATED INSTRUMENTATION AND CONTROL SYSTEMS

IEEE-279-1971	IEEE Standard: Criteria for Protection Systems for Nuclear Power Generating Stations
IEEE-308-1974	Criteria for Class 1E Power Systems for Nuclear Power Generating Stations
IEEE-317-1976	Electric Penetration Assemblies in Containment Structures for Nuclear Power Generating Stations
IEEE-323-1974	Qualifying Class 1E Electric Equipment for Nuclear Power Generating Stations
IEEE-323-A-1975	Supplement to the Foreword of IEEE 323-1974
IEEE-336-1971	IEEE Standard: Installation, Inspection, and Testing Requirements for Instrumentation and Electric Equipment During Construction of Nuclear Power Generating Stations
IEEE-338-1977	Criteria for the Periodic Testing of Nuclear Power Generating Station Safety Systems
IEEE-344-1975	IEEE Std. 344-1975, IEEE Recommended Practices for Seismic Qualification of Class 1 Equipment for Nuclear Power Generating Stations
IEEE-352-1975	General Principles for Reliability Analysis of Nuclear Power Generating Station Protection Systems
IEEE-379-1972	IEEE Trial-Use Guide for the Application of the Single-Failure Criterion to Nuclear Power Generating Station Protection Systems
IEEE-383-1974	Standard for Type Test of Class 1E Electric Cables, Field Splices, and Connections for Nuclear Power Generating Station.
IEEE-384-1974	IEEE Trial Use Standard Criteria for Separation of Class 1E Equipment and Circuits
IEEE-420-1973	Trial-Use Guide for Class 1E Control Switchboards for Nuclear Power Generating Stations
IEEE-494-1974	IEEE Standard Method for Identification of Documents Related to Class 1E Equipment and Systems for Nuclear Power Generating Station

TABLE 7.1-4  
RSS DIVERSITY

	<u>Primary</u>	<u>Secondary</u>
Logic:	Local Coincidence	General Coincidence
Sensors:	Inlet Plenum Pressure	Primary Loop Flow
	Primary Pump Speed	Primary Loop Flow
	Intermediate Pump Speed	Intermediate Loop Flow
	HTS Bus Frequency	HTS Bus Voltage
	Steam Flow	Steam Drum Level
	Feedwater Flow	Reaction Products Flow
	IHX Primary Outlet	Evaporator Outlet
	Temperature	Sodium Temperature
Logic Isolation:	Light Coupling	Direct Coupled
Equipment:		
o Circuitry	Integrated Circuits	Discrete Components
o Power Supplies	Separate vendors utilized	
o Potentiometers	Separate vendors utilized	
o Buffers	Light Coupling	Magnetic Coupling
o Control Rod Release	Circuit Breakers in 2/3 Logic Arrangement	Solenoid Operated Pneumatic Valve in a 2/3 Logic Arrangement

## 7.2 REACTOR SHUTDOWN SYSTEM

### 7.2.1 Description

#### 7.2.1.1 Reactor Shutdown System Description

The Reactor Shutdown System (RSS) consists of two independent and diverse systems, the Primary and Secondary Reactor Shutdown Systems, either of which is capable of Reactor and Heat Transport System Shutdown. All anticipated and unlikely events can be terminated without exceeding the specified limits by either system even if the most reactive control rod in the system cannot be inserted. In addition, the Primary RSS acting alone can terminate all extremely unlikely events without exceeding specified limits even if the most reactive control rod in the system cannot be inserted. To assure adequate independence of the shutdown systems, mechanical and electrical isolation of redundant components is provided. Functional or equipment diversity is included in the design of instrumentation and electronic equipment. The Primary RSS uses a local coincidence logic configuration while the Secondary RSS uses a general coincidence. Sufficient redundancy is included in each system to prevent single random failure degradation of either the Primary or Secondary RSS.

As shown in the block diagram of the Reactor Shutdown System, Figure 7.2-1, the Primary RSS is composed of 24 subsystems and the Secondary RSS is composed of 16 subsystems. Figure 7.2-2A is a typical Primary RSS instrument channel logic diagram. Each protective subsystem has 3 redundant sensors to monitor a physical parameter. The output signal from each sensor is amplified and converted for transmission to the trip comparator in the control room. Three physically separate redundant instrument channels are used. When necessary, calculational units derive additional variables from the sensed parameters, with the calculational units inserted in front of the comparators as needed. The comparator in each instrument channel determines if that instrument channel signal exceeds a specified limit and outputs 3 redundant signals corresponding to either the reset or trip state. The 3 outputs of each comparator are isolated and recombined with the isolated outputs of the redundant instrument channels as inputs to three redundant logic trains. The recombination of outputs is in a 2 out of 3 local coincidence logic arrangement.

Operating bypasses are necessary to allow RSS functions to be bypassed during main sodium coolant pump startup, ascent to power, and two loop operation. Operating bypasses are accomplished in the instrument channels. For bypasses associated with normal three loop operation, the bypass cannot be instated unless certain permissive conditions exist which assure that adequate protection will be maintained while these protective functions are bypassed. Permissive comparators are used to determine when bypass conditions are satisfied. When permissive conditions are within the allowable range, the operator may manually instate the bypass. If the permissive condition goes

out of the allowable range, the protective function is automatically reinstated. The trip function will remain reinstated until the permissive conditions are again satisfied and the operator again manually initiates the bypass. Operator manual bypass control is not effective unless the bypass comparator indicates that permissive conditions are satisfied. A functional diagram of the Primary and Secondary bypass permissive logic is shown in Figure 7.2-2AA.

Two loop bypasses are established under administrative control by changing the hardware configuration within the locked comparator cabinets. These bypasses are also under permissive control such that the plant must be shutdown to establish two loop operation and if the shutdown loop is activated the bypass is automatically removed.

Bypass features included within the Primary and Secondary RSS hardware for two loop operation will be deactivated during all three loop operating modes so that the three loop operating configuration can not be affected by these bypass features either by operator action or by two loop hardware failure.

Bypass permissives are part of the Plant Protection System (PPS), and are designed according to the PPS requirements detailed elsewhere in this section of the PSAR.

Continuous local and remote indication of bypassed instrument channels will be provided in conformance with Regulatory Guide 1.47, "Bypassed and Inoperable Status Indication for Nuclear Power Plant Safety Systems".

## Evaporator Outlet Sodium Temperature

The Evaporator Outlet Sodium Temperature subsystems (Figure 7.2-10) compare the sodium temperature at the outlet of the evaporator in each HTS loop to a fixed set point. If this temperature exceeds the set point, a reactor trip is initiated. There are three of these subsystems, one per loop. These subsystems detect a large class of events which impair the heat removal capability of the steam generators. These subsystems are never bypassed.

## Sodium Water Reaction

The Sodium Water Reaction subsystems (Figure 7.2-10) detect the occurrence of a sodium water reaction within a superheater or evaporator module. There are three of these subsystems, one per loop. Each subsystem 57| receives nine signals from the sensors in the reaction products vent lines of a steam generator. These subsystems are never bypassed.

### 7.2.1.2.3 Essential Performance Requirements

In order to implement the required protective functions within the appropriate limits, PPS equipment must meet several essential performance requirements. These essential performance requirements and the PPS equipment to which they apply are summarized below.

The PPS instrumentation will meet the essential performance require- 57| ments of Table 7.2-3. This table defines the minimum accuracy and time constants which will result in acceptable performance of the PPS.

Analysis of worst case PPS functional performance is based on the values given in Table 7.2-3.

The maximum delay between the time a protective subsystem indicates the need for a trip and the time the rods are released is 0.200 second. 41| This time includes the delays due to the calculational units, comparators, logic, scram breakers, and control rod release.

The maximum delay between the time a protective subsystem indicates the need for a trip and the time the HTS sodium pumps are tripped is 0.500 second. This time also includes the delays due to the logic and HTS scram breakers.

The PPS is designed to meet these essential performance requirements over a wide range of environmental conditions and credible single events to assure that environmental effects do not degrade the performance



o Environmental Changes

All electrical equipment is subject to performance degradation due to major changes in the operating environment. Where practical, PPS equipment is designed to minimize the effects of environmental changes; if not, the performance at the environmental extremes is used in the analysis.

Measures have been taken to assure that the RSS electronics are capable of performing according to their essential performance requirements under variations of temperature. The range of temperature environment specified for all the electronic equipment considered here is greater than is expected to occur during normal or abnormal conditions. Electronics do not fail catastrophically when these limits are exceeded even though this is the assumed failure mode. The detailed design of the circuit boards, board mounting and racks includes free ventilation to minimize hot spots. Ventilation is a result of natural convection air flow.

The RSS is designed to operate under or be protected from a wider range of relative humidity than that produced by normal or postulated accident conditions.

Vibration and shock are potential causes of failure in electronic components. Design measures, including the prudent location of equipment, minimize the vibration and shock experienced by RSS electronics. The equipment is qualified to shock and vibration specifications which exceed all normal and off-normal occurrences.

The RSS comparators and protective logic are designed to operate over a power source voltage range of 108 to 132 VAC and a power source frequency range of 57 to 63 Hz. The maximum variation of the source voltage is expected to be  $\pm 10\%$ . More extreme variations in the power source may result in the affected channel comparator or logic train outputting a trip signal. In addition, testing and monitoring of RSS equipment is used, where appropriate, to warn of impending equipment degradation. Therefore, it is not expected that changes in the environment will cause total failure of an instrument channel or logic train, much less the simultaneous failure of all instrument channels or logic trains.

The majority of the RSS electronics is located in the control building, and is not subjected to a radioactive environment. Any PPS equipment located in the radioactive areas (such as the head access area) will be designed to withstand the level of activity to which it will be subjected, if its function is required.

- o Tornado

The RSS is protected from the effects of the design basis tornado by locating the equipment within tornado hardened structures.

- o Local Fires

All RSS equipment, including sensors, actuators, signal conditioning equipment, wiring, scram breakers, and cabinets housing this equipment is redundant and separated. These characteristics make any credible fire of no consequence to the safety of the plant. The separation of the redundant components increases the time required for fire to cause extensive damage and also allows time for the fire to be brought to the attention of the operator such that corrective action may be initiated. Fire protection systems are also provided as discussed in Section 9.13.

- o Local Explosions and Missiles

All RSS equipment essential for reactor trip is redundant. Physical separation (distance or mechanical barriers) and electrical isolation exists between redundant components. This physical separation of redundant components minimized the possibility of a local explosion or missile damaging more than one redundant component. The remaining redundant components are still capable of performing the required protective functions.

- o Earthquakes

All RSS equipment, including sensors, actuators, signal conditioning equipment, wiring, scram breakers and structures (e.g., cabinets) housing such equipment, is classed as Seismic Category I. As such, all RSS equipment is designed to remain functional under OBE and SSE conditions. The characteristics of the OBE and SSE used for the evaluation of the RSS are found in Section 3.7.

### 7.2.2 Analysis

The Reactor Shutdown System meets the safety related channel performance and reliability requirements of the NRC General Design Criteria, IEEE Standard 279-1971, applicable NRC Regulatory Guides and other appropriate criteria and standards.

The RSS Logic is designed to conform to the IEEE Standards listed in Table 7.2-4.

#### General Functional Requirement

The Plant Protection System is designed to automatically initiate appropriate protective action to prevent unacceptable plant or component damage or the release or spread of radioactive materials.

## Single Failure

No single failure within the Plant Protection System nor removal from service of any component or channel will prevent protective action when required.

57| Two independent, diverse reactor shutdown systems are provided, either of which is capable of terminating all excursions without allowing plant parameters to exceed specified limits. Each system uses three redundant instrument channels and logic trains. The Primary RSS is configured  
57| using local coincidence logic while the Secondary RSS uses general coincidence logic. To provide further assurance against potential degradation of protection due to credible single events, functional and/or equipment diversity are included in the hardware design.

## Bypasses

Bypasses for normal operation require manual instating. Bypasses will be automatically removed whenever the subsystem is needed to provide protection. The equipment used to provide this action is part of the PPS. Administrative procedures are used to assure correct use of bypasses for infrequent operations such as two loop operation. If the protective action of some part of the system has been bypassed or deliberately rendered inoperative, this fact will be continuously indicated in the control room.

## Multiple Setpoints

Where it is necessary to change to a more restrictive setpoint to provide adequate protection for a particular normal mode of operation or set of operating conditions, the PPS design will provide automatic means of assuring that the more restrictive setpoint is used. Administrative procedures assure proper setpoints for infrequent operations.

For CRBRP, power operation on two-loops will be an infrequent occurrence, and will only be initiated from a shutdown condition. While the reactor is shutdown, the PPS equipment will be aligned for two-loop operation which will include set down of the appropriate trip points. Sufficient trip point set down is being designed into the PPS equipment to adequately cover the possible range (conceptually from 2% to 100%) of trip point adjustment required. In addition, administrative procedures (specifically the pre-critical checkoff) will be invoked during startup to ensure that the proper PPS trip points have been set.

The analysis of plant performance during two-loop operation has not been completed to date. Therefore, the exact trip point settings for two-loop operation cannot be specified at this time. However, the range of trip point settings indicated above is adequate to ensure that trip points appropriate for the anticipated lowest two-loop operating power can be achieved.

In summary, the design of the PPS equipment trip point adjustments and other features for two-loop operation coupled with the anticipated two-loop operating power level and administrative procedures assure full compliance with Branch Technical Position EICSB 12 and satisfy Section 4.15 of IEEE std 279-1971.

## Access

Administrative control of access to all setpoint adjustments, module calibration adjustments, test points and the means for establishing a bypass permissive condition is provided by locking cabinets and other access design features of the control room and the equipment racks.

## Information Read-Out

Indicators and alarms are provided as an operating aid and to keep the plant operator informed of the status of the RSS. Except for the IHX primary outlet temperature analog indicators which are part of the accident monitoring system, all indicators and alarms are not safety-related. The following items are located on the Main Control Panel for operator information.

## Analog Indication

- A. Secondary Wide Range Log MSV Power Level
- B. Secondary Wide Range Linear Power Level
- C. Primary Power Range Power Level
- D. Reactor Vessel Level
- E. HTS Pump Speeds
- F. HTS Loop Flows
- G. Reactor Inlet Pressure
- H. IHX Primary Outlet Temperature
- I. Evaporator Outlet Temperature
- J. Steam Flows
- K. Feedwater Flows
- L. Steam Drum Level

## Indicating Lights

- A. Instrument Channel Bypass Permissive Status
- B. Instrument Channel Bypass Status
- C. Logic Train Trip/Reset Status
- D. HTS Loop Trip/Reset Status
- E. HTS Loop Test Status

## Annunciators

- A. Instrument Channel Trip/Reset information is provided for each function listed in Table 7.2-1
- B. Logic Train Power Supply Failure
- C. Two Loop Bypasses Instated

Most information is also available to the operator via the Plant Data Handling and Display System.

## Annunciator for PPS Alarm Trips

A visual and audible indication of all alarm conditions within the PPS will be provided in the control room. These alarm conditions include any tripped PPS comparators in the Primary RSS, Secondary RRS, Containment Isolation System and Shutdown Heat Removal System. The Plant Data Handling and Display system

alerts the operator to significant deviations between redundant RSS analog instrumentation used to monitor a reactor or plant parameter for the RSS.

#### Control and Protection System Interaction

The Plant Protection System and the Plant Control System have been designed to assure stable reactor plant operation and to protect the reactor plant in the event of worst case postulated Plant Control System failures. The Plant Protection System is designed to protect the plant regardless of control system action or lack of action. Isolation devices will be used between protection and control functions. Where this is done, all equipment common to both the protection and control function is classified as part of the Plant Protection System. Equipment sharing between protection and control is minimized. Where practical, separate equipment (sensors, signal conditioning, cabling penetrations, raceways, cabinets, monitoring etc.) is provided. The sharing of components does not lead to a situation where a single event both initiates an incident through Plant Control System malfunction and prevents the appropriate Plant Protection System.

#### Periodic Testing

The Plant Protection System is designed to permit periodic testing of its functioning including actuation devices during reactor operation. In the Primary RSS, a single instrument channel is tested by inserting a test signal at the sensor transmitter and verifying it at the comparator output. A logic train is tested by inserting a very short test signal in 2 comparator inputs and verifying that the voltage on the scram breaker trip coils decrease. Because of the time response of the undervoltage relay coils of the scram breakers and very short duration of the test signal, the reactor does not trip. In the Secondary RSS, an instrument

channel can be tested from sensor to scram actuator by inserting a single test signal because of the general coincidence configuration of the 3 redundant channels. The primary and secondary rod actuators cannot be tested during reactor operation since dropping a single control rod will initiate a reactor scram. Scram actuators and control rod drop will be tested and maintained when the plant is shutdown (See Section 7.1-2). Whenever the ability of a protective channel to respond to an accident signal is bypassed such as for testing or maintenance, the channel being tested is placed in the tripped state and its tripped condition is automatically indicated in the control room.

#### Failure Modes and Effects Analysis

A Failure Modes and Effects Analysis (FMEA) has been conducted to identify, analyze and document the possible failure modes within the Reactor Shutdown System and the effects of such failures on system performance (see Appendix C, Supplement 1). Components of the RSS analyzed are:

- Reactor Vessel Sodium Level Input
- PPS Sodium Flow Input
- Pump Electric Power Sensor
- Compensated Ion Chamber Nuclear Input
- Fission Chamber Nuclear Input
- Primary Loop Inlet Plenum Pressure Input
- Sodium Pump Speed (Primary and Intermediate)
- Steam Mass Flow Rate Input
- Feedwater Mass Flow Rate Input
- Steam Drum Level Input
- Primary Comparator
- Secondary Comparator
- Primary Logic Train
- Secondary Logic Train
- Primary Computational Unit
- Secondary Computational Unit

Table 7.2-2 (Continued)

<u>Fault Events</u>	<u>Primary Shutdown System</u>	<u>Secondary Shutdown System</u>
Failure of Steam Dump System	Steam-Feedwater Flow Mismatch	Steam Drum Level
Sodium Water Reaction in Steam Generator	Steam-Feedwater Flow Mismatch	Sodium-Water Reaction

III. Extremely Unlikely

A. Reactivity Disturbances

Positive Ramps \$2.0/sec

Startup	Flux-Delayed Flux	Startup Nuclear
5-40% Power	Flux-Delayed Flux or Flux- Pressure	Modified Nuclear Rate or Flux-Total Flow
40-100% Power	Flux- Pressure	Flux-Total Flow
Full Power	High Flux	Flux-Total Flow

- (1) The maximum anticipated reactivity fault results from a single failure of the control system with a maximum insertion rate of approximately 4.1 cents per second.
- (2) The maximum unlikely reactivity faults result from multiple control system failures leading to withdrawal of six rods at normal speed or one rod at the maximum mechanical speed.
- (3) The PPS is required to terminate the results of these extremely unlikely events within the umbrella transient specified as emergency for the design of the major components.

7.2-22

Amend. 62  
Nov. 1981

TABLE 7.2-3

## ESSENTIAL PERFORMANCE REQUIREMENTS FOR RSS INSTRUMENTATION CHANNELS\*

<u>Plant Parameter</u>	<u>Accuracy (% of span)</u>	<u>Response Time (msec)</u>
Neutron Flux		
Primary	±1.0	<10
Secondary	±1.0	<10
Reactor Inlet Plenum Pressure	±2.0	<150
Sodium HTS Pump Speeds	±2.0	<20
Sodium HTS Flow	±5.0	<500
Reactor Vessel Sodium Level	±5.0	<500
Undervoltage Relay	±1.0	<230
Steam Flow	±2.0	<500
Feedwater Flow	±2.5	<500
Evaporator Outlet Sodium Temperature	±2.0	<5000
Steam Drum Level	±1.0	<1000
IHX Primary Outlet Temperature	±2.0	<5000
Underfrequency Relay	±2.0	<200

\* Note that these accuracy and response times relate to the performance of the instrumentation channels from the sensors up to the signal conditioning output.

In addition, as noted in Section 7.2.1.2.3, the reactor shutdown system logic, actuators and rod unlatch features require a further response time delay of 200 msec.



TABLE 7.2-4

LIST OF IEEE STANDARDS APPLICABLE TO  
THE REACTOR SHUTDOWN SYSTEM LOGIC (1)

IEEE 279-1971	IEEE Standard: Criteria for Protection Systems for Nuclear Power Generating Stations
IEEE 308-1974	Criteria for Class 1E Power Systems for Nuclear Power Generating Stations
IEEE 317-1976	Electric Penetration Assemblies in Containment Structures for Nuclear Power Generating Stations
IEEE 323-1974	IEEE Trial-Use Standard: General Guide for Qualifying Class 1E Electric Equipment for Nuclear Power Generating Stations
IEEE 323-A-1975	Supplement to the Foreward of IEEE 323-1974
IEEE 336-1971	IEEE Standard: Installation, Inspection and Testing Requirements for Instrumentation and Electric Equipment During Construction of Nuclear Power Generating Stations
IEEE 338-1977	IEEE Trial Use Criteria for the Periodic Testing of Nuclear Power Generating Station Protection Systems
IEEE-344-1975	IEEE Standard 344-1975, IEEE Recommended Practices for Seismic Qualification of Class 1 Equipment for Nuclear Power Generating Stations
IEEE 352-1975	IEEE Guide for General Principles for Reliability Analysis of Nuclear Power Generating Station Protection Systems
IEEE 379-1972	IEEE Trial-Use Guide for the Application of the Single Failure Criterion to Nuclear Power Generating Station Protection Systems
IEEE 384-1974	IEEE Trial Use Standard Criteria for Separation of Class 1E Equipment and Circuits
IEEE 494-1974	IEEE Standard Method for Identification of Documents Related to Class 1E Equipment and Systems for Nuclear Power Generating Station

(1) IEEE Standards applicable to the instrumentation and monitoring systems are listed in Section 7.5.

### Head Access Area Radiation

The Head Access Area Radiation Subsystem initiates closure of the containment isolation valves in the event of large radiation releases in the head access area. Three radiation sensors are located in the head access area to provide early initiation and closure of the isolation valves to assure that releases from design basis events do not exceed the guideline values of 10CFR100.

#### 7.3.1.2.2 Essential Performance Requirements

To implement the required isolation function within the specified limits, the CIS must meet the functional requirements specified below:

The closure time requirement for the inlet and exhaust isolation valves is 4 seconds with a three second or less detection time in the heating and ventilating system. A 10 second transport time from sensing point to the valve exists (see Section 15.1.1). The 3 seconds includes sensor time response, comparator and logic time delays.

The CIS is designed to meet these requirements for the environmental conditions described in Section 7.2.1.

#### 7.3.2 Analysis

The design of the CIS provides the necessary design features to meet the functional and performance requirements as described below. The CIS logic is designed to conform to the IEEE Standards listed in Table 7.3-2.

##### 7.3.2.1 Functional Performance

The analyses in Sections 15.5 and 15.6 shows the results of the postulated fault conditions. These analyses assumed a closed containment where the events occurred with the containment hatch closed. For the limiting event, primary drain tank fire during maintenance, scoping analyses have been performed to determine the required closure time of the containment isolation valves. For the primary drain tank fire, closure within 20 minutes is adequate. Further, analyses to determine the required closure time under postulated accident conditions have been performed and are discussed in Section 15.1.1. These analyses are used to determine the available design margin. The results of this assumed condition do not exceed the guideline values of 10CFR100 if the main exhaust and inlet valves are closed within 4 seconds assuming the normal air transport time from the detector to the valve is 10 seconds or more, a 14,000 Cfm normal ventilation rate.

Since the automatic Containment Isolation System is designed to isolate within the above time response requirements, all of the design basis conditions are terminated within the necessary limits for the present design concept.

##### 7.3.2.2 Design Features

The CIS instrumentation, controls and actuators are designed to meet the requirements of IEEE-279-1971. The analyses of compliance with these are summarized below.

### Single Failure

No single failure within the CIS nor removal from service of any component or channel will prevent protective action when required. There are three independent instrument channels for each necessary measurement, two independent 2/3 logics, and two independent actuators provided (as shown in Figure 7.3-1).

### Bypasses

No bypasses are provided.

### Multiple Setpoints

Multiple setpoints are not required.

### Completion of Protective Action

The automatic CIS is designed so that, once initiated, protective action at the system level must go to completion. Return to normal operation requires manual reset of the CIS breakers by the operator.

### Manual Initiation

The CIS includes means for manual initiation of containment isolation at the system level. No single failure will prevent manual initiation of the containment isolation action.

### Control and Protection Interaction

There are no shared components between the control system and the CIS.

The provisions for access, information read-out, annunciation of trips, and periodic testing are as specified for the Reactor Shutdown System in Section 7.2.2.

### Physical Separation

The following criteria assure physical separation for the CIS.

There will be at least one containment penetration for each of the three Primary PPS instrument channel conduits and each of the three Secondary PPS instrument channel conduits which exit containment. All requirements for separation of PPS wiring through conduits will also apply to separation of PPS wiring through containment penetrations.

TABLE 7.3-1

## CONTAINMENT ISOLATION SYSTEM DESIGN BASIS

<u>Event</u>	<u>Applicable Federal Regulation</u>	<u>Limit</u>
<u>Anticipated Fault</u>	10CFR20 § 105	<2 millirem in any one hour
No examples of anticipated faults which lead to release of activity have been identified.		<100 millirem in any one week
<u>Unlikely Fault</u>	10CFR20 § 403b	<5 rem in any two hours
No examples are presently identified for the automatic containment isolation system design basis.		
<u>Extremely Unlikely Faults &amp; Design Margin*</u>	10CFR100	<25 rem in any two hours
Examples include major sodium fires		<300 rem iodine doses in the thyroid in any two hours
		<75 rem to the lung
		<150 rem to the bone

\*The design basis for the CIS includes limiting the results of postulated accidents within the guideline values of 10CFR100. See Section 15.1.1.

TABLE 7.3-2

LIST OF IEEE STANDARDS APPLICABLE TO  
THE CONTAINMENT ISOLATION SYSTEM LOGIC

IEEE 279-1971	IEEE Standard: Criteria for Protection Systems for Nuclear Power Generating Stations
IEEE 308-1974	Criteria for Class 1E Power Systems for Nuclear Power Generating Stations
IEEE 317-1976	Electric Penetration Assemblies in Containment Structures for Nuclear Power Generating Stations
IEEE 323-1974	IEEE Trial-Use Standard: General Guide for Qualifying Class 1E Electric Equipment for Nuclear Power Generating Stations
IEEE 323-A-1975	Supplement to the Foreward of IEEE 323-1974
IEEE 336-1971	IEEE Standard: Installation, Inspection and Testing Requirements for Instrumentation and Electric Equipment During Construction of Nuclear Power Generating Stations
IEEE 338-1977	IEEE Trial Use Criteria for the Periodic Testing of Nuclear Power Generating Station Protection Systems
IEEE 344-1975	IEEE Standard 344-1975, IEEE Recommended Practices for Seismic Qualification of Class 1 Equipment for Nuclear Power Generating Stations
IEEE 352-1975	IEEE Guide for General Principles for Reliability Analysis of Nuclear Power Generating Station Protection Systems
IEEE 379-1972	IEEE Trial-Use Guide for the Application of the Single Failure Criterion to Nuclear Power Generating Station Protection Systems
IEEE 384-1974	IEEE Trial Use Standard Criteria for Separation of Class 1E Equipment and Circuits
IEEE 494-1974	IEEE Standard Method for Identification of Documents Related to Class 1E Equipment and Systems for Nuclear Power Generating Station

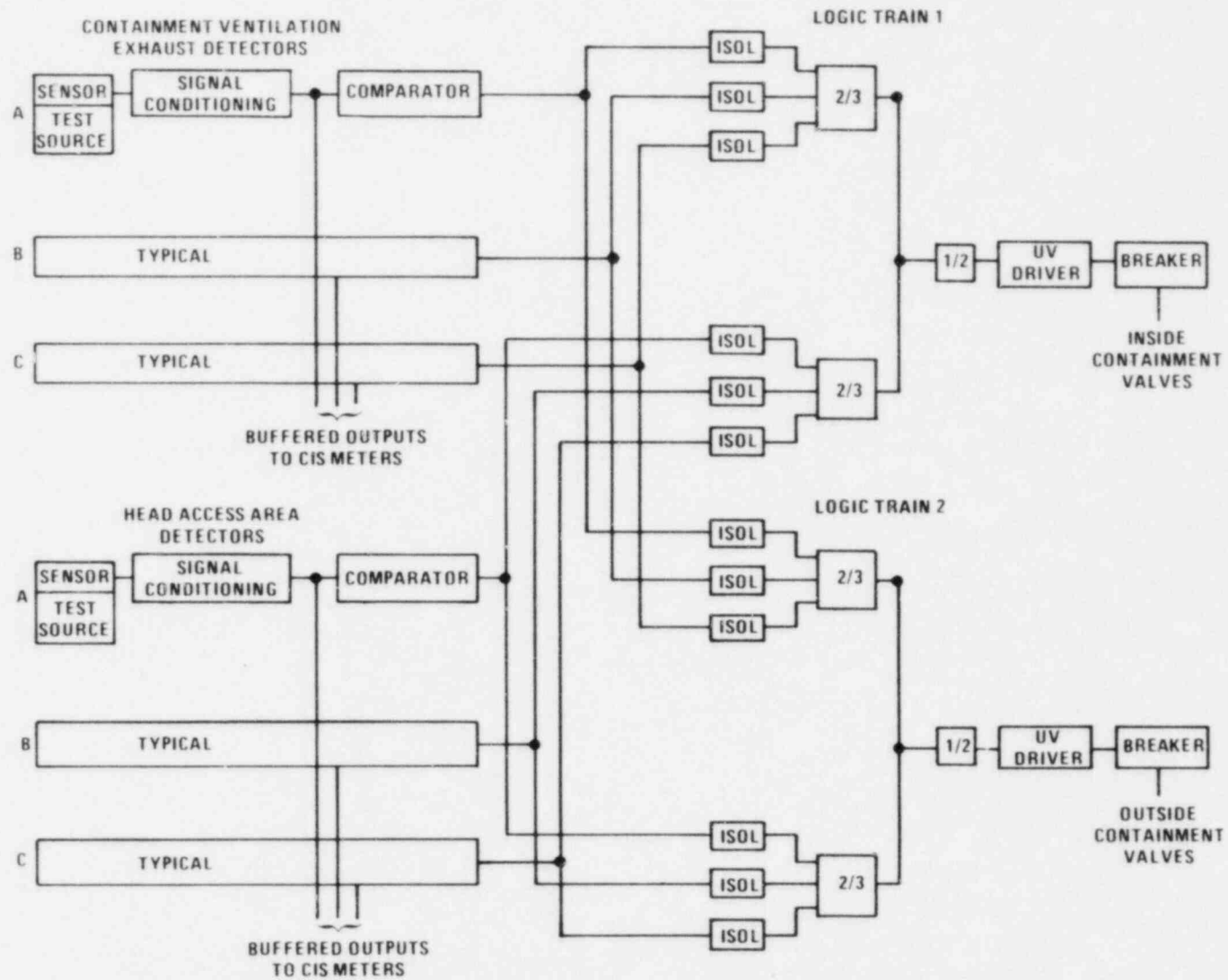


Figure 7.3-1. Containment Isolation System Block Diagram

## 7.4 INSTRUMENTATION AND CONTROL SYSTEMS REQUIRED FOR SAFE SHUTDOWN

The Instrumentation and Control Systems necessary for safe shutdown are those associated with monitoring of core criticality, decay heat removal (SGAHRs portion), outlet steam isolation, and control room habitability.

Monitoring of core criticality is effected by the Flux Monitoring System (Section 7.5.1). The control room habitability is covered in Chapter 6. Thus, this section treats the control and instrumentation needs for decay heat removal by the Steam Generator Auxiliary Heat Removal System (SGAHRs) and outlet steam isolation by the Outlet Steam Isolation System (OSIS); control and instrumentation for Direct Heat Removal Service (DHRS) is discussed in Section 7.6.

### 7.4.1 Steam Generator Auxiliary Heat Removal Instrumentation and Control System

#### 7.4.1.1 Design Description

##### 7.4.1.1.1 Function

The SGAHRs (fluid system and mechanical components as described in Section 5.6.1, and electrical components as described below) provides the heat removal path and heat sink for the nuclear steam supply system following upset, emergency, or faulted events which render the normal heat sink unavailable.

The SGAHRs Instrumentation and Control System in conjunction with the PPS detects the need for, initiates, and controls the alternate heat removal path when the normal heat sink is unavailable. The SGAHRs nominal control setpoints shown in Table 7.4-2 are discussed in the following subsections.

The SGAHRs Instrumentation and Control System is designed to the IEEE Standards listed in Table 7.4-3.

##### 7.4.1.1.2 Equipment Design

The mechanical system for which the SGAHRs I&C is provided is briefly described below.

When actuated, the SGAHRs draws water from a Protected Water Storage Tank and pumps it to each steam drum. Two supply lines are provided for each steam drum. One line is supplied by two half-sized, motor-driven feedwater pumps while the other is supplied by a full-sized, turbine-driven pump. Each supply line provides a flow control valve and an isolation valve at the inlet to each steam drum. The isolation valves are provided to isolate the auxiliary feedwater system from the steam generator system during power operation and to provide leak isolation during SGAHRs operation.

In addition, a Protected Air Cooled Condenser (PACC) supplied with each steam drum is placed into operation. This system rejects heat to the atmosphere via convection. Saturated steam is supplied to the condenser from the steam drum

and saturated water is returned. This steam and water loop is driven by natural circulation. Each PACC unit consists of two tube bundles, two sets of louvers and two fans. Regulation of heat rejection is accomplished by controlling the air flow across the condensing tubes through adjustment of inlet louver and fan blade pitch positions. The air side flow is driven by either forced or natural convection.

The arrangement of SGAHRS equipment is shown in Figure 5.1-5 (SGAHRS P&ID). Instrumentation and controls are provided for the components described below:

- o Auxiliary Feedwater Pump Control - Upon receipt of the SGAHRS initiation signal, (see Section 7.4.1.1.3), the two motor driven pumps are started, resulting in both pumps coming on line and operating at constant speed. In addition, the isolation valves in the steam supply lines from the steam drums to the turbine driven pump are opened. At the turbine inlet a pressure regulating valve reduces the steam supply pressure to the 1000 psig required by the turbine drive. The turbine drive mechanism is equipped with a governor to provide speed regulation. Each auxiliary feedwater pump can also be actuated manually at the operator's discretion.

Each pump control includes a "Normal Long Term Cooldown (LTC)" mode selector. In "normal" mode, the pumps start on SGAHRS initiation. In the "LTC" mode, the operator may shutdown any or all AFW pumps provided the steam drum water level is above the trip point setting. When in the "LTC" mode, the pumps come on line automatically when the steam drum water level drops to a low level trip point.

- o Auxiliary Feedwater Flow Control - The Auxiliary Feedwater Isolation Valves are opened upon receipt of the SGAHRS initiation signal. During SGAHRS operation, these valves close automatically upon indication of a sodium/water reaction, a high steam drum level, a steam drum pressure less than 200 psig, or AFW flow greater than 150% of full flow for 5 sec. This automatic closure occurs only in the affected loop. If the valves are closed by a high drum level signal they will reopen automatically when the drum level falls to the low drum level trip point. The flow to the steam drum is controlled with a control valve that is positioned by a single controller. Manual control of the Auxiliary Feedwater Flow Control valves is provided at the main control panel and at the local SGAHRS panel.



#### 7.4.1.1.9 Operator Information

Indicators and alarms are provided to keep the plant operator informed of the status of the SGAHRS. The following items are located on the Main Control Panel for operator information.

##### Analog Indication

- o Protected Water Storage Tank Level
- o Protected Water Storage Tank Temperature
- o Auxiliary Feedwater Flow (each loop)
- o Auxiliary Feedwater Pump Discharge Pressure
- o Drive Turbine Steam Inlet Pressure
- o Drive Turbine Speed
- o PACC Outlet Air Temperature
- o PACC Outlet Water Flow and Temperature
- o PACC Inlet Louver Position
- o PACC Fan Blade Pitch Position
- o Steam Drum Pressure and Water Level

##### Indicating Lights

- o PACC Outlet Louver Position
- o Position of all Isolation and Control Valves
- o Operating Status of all Motors
- o SGAHRS Initiation Logic Reset

##### Annunciators

- o Low Protected Water Storage Tank Level
- o Low Low Protected Water Storage Tank Level
- o High PWST Temperature
- o Simultaneous Opening or Closure of the AFW Pump Inlet Valve and the AFW Pump Alternate Inlet Valve
- o Flow Limiting of AFW
- o High AFW Supply Temperature
- o High/Low Drive Turbine Speed
- o High Drive Turbine Steam Inlet Pressure
- o Drive Turbine Group Alarm (Bearing and Lube Oil System)
- o AFW Pump Group Alarm (Bearing Temperature and Seal Cavity Pressure)
- o High Motor Bearing Temperatures
- o Transfer Switches on Local
- o SGAHRS Initiation Logic Trip
- o Na Aerosol Concentration High
- o Na Aerosol Control Bypassed
- o PACC Startup on Reactor Trip "on Test"
- o PACC Start-up Delay

Additional indicators and alarms are provided at the local instrumentation and control panels. Most information is also available to the operator via the Plant Data Handling and Display System (PDH&DS).

#### 7.4.1.1.10 Instrumentation

##### Protected Water Storage Tank (PWST) Level

The PWST level is measured to monitor the water inventory available to be supplied to the steam drums in the event of loss of normal feedwater or the normal heat sink. The level is redundantly measured by two differential pressure sensors mounted across tap lines near the top and bottom of the tank. A PWST level measurement signal is provided to the Plant Control System (PCS), PDH&DS, Plant Annunciator System (PAS) and to a PAM recorder.

##### PWST Temperature

The PWST water temperature is measured to monitor the capacity of the water inventory to provide an efficient heat sink. The temperature is measured by a single chromel-alumel thermocouple. The temperature signal from the transmitter is provided to the PCS, PDH&DS and PAS.

##### Auxiliary Feedwater (AFW) Flow

The AFW flow is monitored to provide input to (a) restrict maximum flow through each control valve to less than  $105 \pm 5\%$  rated AFW flow, and, (b) initiate automatic closure of AFW isolation valves in loops with AFW flow greater than  $150\%$  for 5 seconds. The flow in each of the AFW lines is redundantly measured by two differential pressure sensors across one venturi. This provides capacity for four flow measurements per loop. A flow measurement signal is provided to the PCS, PDH&DS, PAS and to a PAM recorder.

##### AFW Pump Discharge Pressure

The pressure of the water in the discharge line of the AFW pump is measured to provide the control of the valve in the recirculation line for AFW pump reduced flow operation. One pressure transmitter monitors the line pressure on the discharge side of each AFW pump. The pressure measurements are provided to the PCS and PDH&DS.

##### Drive Turbine Steam Inlet Pressure

The AFW Drive Turbine steam inlet pressure is measured to provide a control signal to modulate the pressure control valve. A single pressure transmitter is located between the turbine inlet and the control valve. The signal is provided to the PCS, PDH&DS and PAS.

##### Drive Turbine Speed

The AFW Drive Turbine speed is measured to provide a signal to the turbine speed governor and for initiating an overspeed trip. A single magnetic pickup provides signals to the PCS, PDH&DS and PAS.

### Protected Air Cooled Condensor (PACC)

- o PACC Outlet Water Flow - sensed by one differential pressure sensor per loop across a venturi. Signals are provided to the PCS and the PDH&DS.
- o PACC Outlet Water Temperature - sensed by one chromel-alumel thermocouple per loop. Signals are provided to the PCS and the PDH&DS.
- o PACC Outlet Air Temperature - sensed by three chromel-alumel thermocouples per loop. Signals are provided to the PCS from only the "A" outlet.
- o PACC Inlet Louver Position - sensed by two louver position sensors per loop. Signals are provided to the PCS and the PDH&DS.
- o PACC Outlet Louver Position - sensed by two switches per louver. Signals are provided to the PCS and the PDH&DS.
- o PACC Fan Blade Pitch Position - sensed by one pitch position sensor per fan (i.e. - two per loop). Signals are provided to the PCS and the PDH&DS.

### Isolation and Control Valve Positions

The position of each valve is sensed by two limit switches; one indicates the valve is open, one indicates the valve is closed. The "Open/Closed" position signal is provided to the PCS and the PDH&DS. The monitored valves are:

- PWST Fill Valve
- Alternate AFW Supply Valve
- AFW Pump Inlet Valve
- AFW Pump Alternate Inlet Valve
- AFW Pump Recirculation Valve
- AFW Control Valve
- AFW Isolation Valve
- AFW Pump Test Loop Isolation Valve
- Drive Turbine Steam Supply Isolation Valve
- Drive Turbine Pressure Control Valve
- Superheater Vent Control Valve
- Steam Drum Vent Control Valve
- Turbine Drive Governor Valve
- PACC Noncondensable Vent Valve

#### 7.4.1.2 Design Analysis

To provide a high degree of assurance that the SGAHRS will operate when necessary, and in time to provide adequate decay heat removal, the power for the system is taken from energy sources of high reliability which are readily available. As a safety related system, the instrumentation and controls critical to SGAHRS operation are subject to the safety criteria identified in Section 7.1.2.

Redundant monitoring and control equipment will be provided to ensure that a single failure will not impair the capability of the SGAHRS Instrumentation and Control System to perform its intended safety function. The system will be designed for fail safe operation and control equipment where practical and will, in the event of a failure, assume a failed position consistent with its intended safety function.

Because there are three redundant decay heat removal loops, the instrumentation and controls associated with each individual loop (e.g., auxiliary feedwater flow and air cooled condenser control systems) do not independently meet single failure criteria. However, when taken collectively as a system, they provide the single failure capability required.

#### 7.4.2 Outlet Steam Isolation Instrumentation and Control System

##### 7.4.2.1 Design Description

###### 7.4.2.1.1 Function

The Outlet Steam Isolation Subsystem (OSIS) provides isolation of steam system pipe breaks. Steam system isolation is a necessary function for safe shutdown in those pipe break conditions affecting the three steam supply systems and is provided if needed on a per loop basis. By definition, this zone of protection will include the high pressure steam supply system downstream from the individual loop check valves.

The OSIS Controls are designed to the IEEE Standards listed in Table 7.4-3.

#### 7.4.2.1.2 Equipment Design

A high steam flow-to-feedwater flow ratio is indicative of a main steam supply leak down stream from the flow meter or insufficient feedwater flow. The superheater steam outlet valves and superheater bypass valves shall be closed with the appropriate signal supplied by the heat transport instrumentation system (Section 7.5). This action will assure the isolation of any steam system leak common to all three loops and also provide protection against a major steam condenser leak during a steam bypass heat removal operation.

#### 7.4.2.1.3 Initiating Circuits

The OSIS is initiated by the SGAHRS initiation signal coincident with either a low superheater steam pressure signal or a high feedwater header pressure signal. The SGAHRS initiation signal is described in 7.4.1.1.3. This initiation signal closes the superheater outlet isolation valves in all 3 loops when a high steam-to-feedwater flow ratio or a low steam drum level occurs in any loop. In each Steam Generator System loop, the three trip signals for high steam-to-feedwater flow ratio and the low steam drum level are input to a two of three logic network. If two of three trip signals occur in any of the 3 loops, the OSIS is initiated, and all 3 loops are isolated from the main superheated steam system by closure of the superheater outlet isolation valves and superheater bypass valves.

#### 7.4.2.1.4 Bypasses and Interlocks

Control interlocks and operator overrides associated with the operation of the superheater outlet isolation valves have not been completely defined.

Bypass of OSIS may be required to allow use of the main steam bypass and condenser for reactor heat removal. In case the OSIS is initiated by a leak in the feedwater supply system, the operator may decide to override the closure of certain superheater outlet isolation valves.

#### 7.4.2.1.5 Redundancy and Diversity

Redundancy is provided within the initiating circuits of OSIS. The primary trip function takes place when a high steam-to-feedwater flow ratio is sensed by two of three redundant subsystems on any one SGS loop. The low steam drum level sensed by two of three

redundant channels in any one loop provides a backup trip function. Additional redundancy is provided by three independent SGS steam supply loops serving one common turbine header. Any major break in the high pressure steam system external from the individual loop check valves will be sensed as a steam feedwater flow ratio trip signal in all three loops.

#### 7.4.2.1.6 Actuated Device

The superheater outlet isolation and superheater bypass valves utilize a high reliability electro-hydraulic actuator. These valves are designed to fail closed upon loss of electrical supply to the control solenoid.

#### 7.4.2.1.7 Separation

The OSIS Instrumentation and Control System, as part of the Decay Heat Removal System is designed to maintain required isolation and separation between redundant channels (see Section 7.1.2).

#### 7.4.2.1.8 Operator Information

Indication of the superheater outlet isolation valve position is supplied to the control room. Indicator lamps are used for open-close position indication to the plant operator.

#### 7.4.2.2 Design Analysis

To provide a high degree of assurance that the OSIS will operate when necessary, and in time to provide adequate isolation, the power for the system is taken from energy sources of high reliability which are readily available. As a safety related system, the instrumentation and controls critical to OSIS operation are subject to the safety criteria identified in Section 7.1.2.

Redundant monitoring and control equipment will be provided to ensure that a single failure will not impair the capability of the OSIS Instrumentation and Control System to perform its intended safety function. The system will be designed for fail safe operation and control equipment, where practical, will assure a failed position consistent with its intended safety function.

#### 7.4.3 Pony Motors and Controls

There are six pony motors, one in each primary and intermediate heat transport loop to provide sodium flow for decay heat removal. These motors through the use of a gear box are capable of providing five to ten percent sodium flow in five discrete steps by gear changes. Section 5.6 describes the interaction of the primary and intermediate heat transport loops with the SGAHRS to provide decay heat removal.

#### 7.4.3.1 Design Description

The pony motors are 75 horsepower, 480 VAC, 3 phase, 60 Hz, totally enclosed fan cooled Class 1E motors. These motors are mounted on top of the sodium pump vertical drive motor. They are 1800 rpm motors which deliver power to the sodium pump via a reducing gear, an overrunning clutch, and the vertical motor shaft.

The overrunning clutch allows the pony motor to run continuously during all modes of plant operation and automatically drives the pump when the vertical motor speed decreases below the output speed of the reducing gear. Thus, after a reactor trip and pump (vertical drive motor) trip sodium flow does not decrease below pony motor flow.

During normal operation at pony motor speeds the external oil cooling system is in operation. However, the vertical drive motor bearings are designed to start and operate continuously at pony motor speed without the external oil cooling system or high pressure lift pump.

The pony motor is controlled using both Non-class 1E and Class 1E circuit. The Non-class 1E circuit is isolated from the Class 1E circuit and is overridden by the Class 1E circuit.

Normal pony motor start is through a Non-1E permissive sequence circuit which first starts the vertical drive motor external circuit which first starts the vertical drive motor external lubricating oil cooling system and high pressure lube oil pump. When the oil system achieves flow and pressure the pony motor starts. Once started the Class 1E circuit takes over and the loss of the external lubricating oil system will not result in a pony motor trip. This method of starting is not classified as safety-related and is used for starting the pony motor during reactor shutdown periods after maintenance which requires the pony motor to be off.

The Class 1E controls start the pony motors without the use of the external lubricating oil cooling system or high pressure lube oil pump. This function is carried out by a start-stop switch on the main control panel in the control room. Once started by either the Class 1E or Non-class 1E control the pony motor will automatically restart following the loss of off-site power on the Class 1E diesels.

#### 7.4.3.2 Initiating Circuits

The pony motor runs continuously during all modes of plant operations except during reactor shutdown for maintenance. During maintenance only one loop is permitted to be out of service. Therefore, there is no need for automatic or manual initiation circuits. However, the Class 1E start-stop switch is located on the main control panel.

#### 7.4.3.3 Bypasses and Interlocks

There are no bypasses in the Class 1E control circuit.

The only condition which results in an interlock/automatic pony motor trip is a sodium-to-water leak in the steam generator modules. This results in an automatic trip of the affected intermediate heat transport loop pony motor only. The sodium-to-water leak trip is described in 7.5.6.

#### 7.4.3.4 Analysis

The pony motor and the Class 1E control circuit is designed to the IEEE Standards listed in Table 7.4-3 and is qualified in accordance with Section 1.6 Reference 9.

#### | 7.4.4 Remote Shutdown System

##### | 7.4.4.1 Design Description

###### | 7.4.4.1.1 Function

The Remote Shutdown System provides the means by which (1) safe shutdown conditions of the reactor plant can be established and maintained from locations outside of the Control Room in the event that the Control Room must be vacated; (2) hot shutdown conditions can be achieved and maintained; and, (3) if desired, the plant can be cooled to and maintained at the refueling temperature.

###### | 7.4.4.1.2 Design Basis

The Remote Shutdown system is designed to use equipment located outside of the Control Room to place the reactor and plant into a safe shutdown condition under the following conditions:

- (a) The evacuation of the Control Room is not coincident with any other abnormal plant condition with the one exception that loss of offsite power may occur.
- (b) No severe natural phenomena such as earthquake, tornadoes, hurricanes, floods, tsunami and seiches (from 10CFR50, Appendix A, Criterion 2) occur coincidentally with the excavation of the Control Room.
- (c) The plant remains in an orderly shutdown status from the initiation of the evacuation of the Control Room to the time that command of the shutdown is re-established outside of the Control Room.
- (d) The remote shutdown operations will be commanded from one location and will use plant systems operated in their local mode to effect the shutdown and decay heat removal.
- (e) Plant instrumentation and control systems required for remote shutdown operations will have transfer switches located at the local panels to permit the plant operating personnel to select to operate from the local panels while isolating the remote controls or, conversely, to operate from the control room while isolating the local controls. The transfer of control of a plant system from the remote to the local mode is annunciated in the control room.
- (f) Communications between the Remote Shutdown Monitoring Panel (RSMP), the command location for remote shutdown operations, and the SGAHRS panels and other local panels during remote shutdown operations will be by the Maintenance Communication Jacking (MCJ) system utilizing a sound-powered telephone.



#### 7.4.4.1.3 Remote Shutdown Operations

The RSMP will be located in Cell 271 of the 836'-0" level of the SGB. The RSMP will have indications (see Section 7.4.4.1.4) from which an operator can assess the progress of the shutdown, and it will be the location from which that operator will command the operation of the plant systems being operated in their local mode to effect shutdown.

The Division 1, 11 and 111 SGAHRS (Section 7.4.1) local panels will be located in Cells 272A, B and C respectively, in close proximity to the RSMP, on the 836'-0" level of the SGB-1B. The SGAHRS, operated in its local mode, will be used to control the removal of heat from the reactor plant to achieve and stabilize the plant at the desired plant temperature (hot shutdown or refueling temperature). The local SGAHRS panels will have all of the controls and indications necessary to completely control the system. All signals from the Control Room to the SGAHRS panels are buffered to prevent faults occurring in the Control Room from propagating back to the SGAHRS panels. All SGAHRS component controls can be transferred to local at the local SGAHRS panels. Placing the transfer switches in "local" overrides all control functions in the Control Room.

The Division 1, 11 and 111 OSIS local panels are located in SGB Cells 272A, B and C with the SGAHRS panels, and will be operated in the local mode when required to control heat removal from the plant in conjunction with the operation of SGAHRS. Isolation of OSIS panel controls from the Control Room is incorporated in the design. Steam drum drain and superheater outlet isolation valve controls can be transferred to local at the local OSIS panels.

Whenever any SGAHRS component control transfer switch is placed in the "local" position an alarm is initiated in the Control Room to alert the Control Room operator. The same statement is true for the steam drum drain controls and superheat outlet isolation valve controls on the OSIS panels.

If offsite power is lost coincident with having to achieve a safe shutdown condition in the reactor plant from outside of the Control Room, the diesel generators will start and function in accordance with the design provided by the Building Electrical Power System. Any operator actions required in conjunction with operating and loading the diesel generators will be done in the local operating mode at the DG local panels.

In the event that the Control Room must be vacated, reactor scram and SGAHRS operation will be initiated manually. The operating personnel will move to the 836'-0" level of the SGB where the SGAHRS in the local mode will effect heat removal and stabilization of the plant temperatures. Operation of the SGAHRS in the local mode will effect heat removal and stabilization of the plant temperatures. The plant shutdown will be directed by the operator at the RSMP who will also assign operating personnel not continuously occupied in operating SGAHRS to oversee or operate other systems as required.

Movement of personnel within the plant and access to building cells and local panels will be controlled by the facilities and procedures of the Industrial Security System.

#### 7.4.4.1.4 Equipment Design

The RSMP is the only piece of equipment provided by the Remote Shutdown System. It will be a vertical sided, non-Class 1E cabinet assembly containing meters and a phone jack panel. The meters will receive buffered signals from the initiating systems and, thus, do not require transfer switches to isolate them from the Control Room. The phone jack panel will permit the operator at the RSMP to communicate with the five NSSS or Nuclear Island buildings by means of any of the three MCJ circuits provided in each of the buildings. In addition, communications among the buildings can be established through the phone jack panel on the RSMP.

The indications provided on the RSMP are as follows:

- o For each primary heat transport system loop,
  - 1 - Pump outlet sodium temperature indicator (3 total)
  - 1 - Reactor inlet sodium temperature indication (3 total)
  - 1 - Sodium pump shaft speed indication (3 total)
- o For each intermediate heat transport system loop,
  - 1 - IHX outlet sodium temperature indication (3 total)
  - 1 - IHX inlet sodium temperature indication (3 total)
  - 1 - Sodium pump shaft speed indication (3 total)
- o For each superheated steam loop,
  - 1 - Temperature indication (3 total)
  - 1 - Steam flow indication (3 total)
- o One reactor vessel sodium level meter (long probe)
- o For each Diesel Generator (3 total)
  - 1 - Wattmeter
  - 1 - Frequency meter
  - 1 - Varmeter
  - 1 - Voltmeter with phase selector switch
  - 1 - Ammeter with phase selector switch

In addition to the foregoing indications, other indications used during remote shutdown operations that are not on the RSMP will be available as follows:

- o SGAHRs

Controls and indicators used for the operation of each SGAHRs division are located on the three separate SGAHRs panels in cells 272A, B, and C. Each SGAHRs division is separate and redundant from the other divisions. See the response to Question CS421.04 for additional information about SGAHRs division assignments.

The following controls, indicators and alarms are on each SGAHRS panel.\*

### Controllers

Auxiliary Feedwater Flow  
AFW Steam Turbine Steam Inlet Pressure  
PACC Inlet Louver Position  
PACC Fan Blade Position  
Steam Drum Level  
Steam Drum Vent  
Superheater Vent

### Analog Indicators

Protected Water Storage Tank Level  
Protected Water Storage Tank Temperature  
Auxiliary Feedwater Flow  
Auxiliary Feedwater Pump Discharge Pressure  
Steam Driven Turbine Steam Inlet Pressure  
Steam Driven Turbine Speed  
PACC Outlet Air Temperature  
PACC Outlet Water Flow and Temperature  
PACC Inlet Louver Position  
PACC Fan Blade Pitch Position  
Steam Drum Pressure and Water Level

### Annunciators

Protected Water Storage Tank Level  
PWST Temperature  
AFW Supply Temperature  
Steam Driven Turbine Speed  
Driven Turbine Steam Inlet Pressure  
Steam Driven Turbine Bearing and Lube Oil Temperature  
High Motor Bearing Temperatures  
SGAHRS Initiation

- o Diesel speed and fuel oil indications will be available at the diesel generator local control panels in the Diesel Generator Building Cells 511 and 512.

\*Each indicator, alarm and controller is repeated on each of the SGAHRS panels except for those associated with the AFW pumps. Panels A and B have the controls, alarms and indicators for motor driven AFW pumps A and B; Panel B has those associated with the steam driven AFW pump.

#### 7.4.4.2 Design Analysis

The Remote Shutdown System provides the RSMP from which an operator can assess the progress of the plant shutdown and command the local operation of the plant systems (primarily SGAHRS) to effect the shutdown. It should be noted that the PACC subsystem of SGAHRS is automatically initiated by all reactor trips, and it remains in operation for the duration of the plant shutdown or as long as the reactor generates significant decay heat.

The Remote Shutdown System imposes no special requirements on the plant systems, but takes advantage of the following system design features:

- o The ability to operate in both local and remote modes with isolation from and annunciation in the Control Room when operating in the local mode.
- o The redundancy diversity, separation, isolation and reliability of the safety grade systems.
- o The design and location of safety grade systems equipment that minimize the probability and effect of fires and explosions on the ability of the systems to perform their safety function.
- o The redundant safety grade SGAHRS provides the capability to achieve and maintain hot shutdown and, if desired, to cool the plant to and maintain the plant at refueling conditions.
- o When transferring SGAHRS to the local mode, the operator manually starts SGAHRS. Once started, SGAHRS automatically controls those parameters used to remove decay heat.

The RSMP is a non-Class 1E Seismic Class III assembly and therefore, is not subject to the separation requirements of IEEE 384-1974, or to the seismic qualification requirements of IEEE 344-1974, or to any of the other IEEE Standards listed in Table 7.1-3.

TABLE 7.4-2  
NOMINAL SET POINTS (Cont'd)

NOTES:

1. The capability for the operator to assume manual control of the indicated functions from either the control room or the local panel is provided.
2. Valves will reopen should steam drum level fall to the low level trip (-8 in. from normal water level). Valves in the motor-driven AFW pump loops close at +8 in. from normal water level while the valves in the turbine-driven AFW pump loops close at +12 in. from normal water level.
3. In the long term cooldown mode, the second motor driven pump automatically restarts after a 1-minute delay if steam drum level remains at -7 in. or lower.
4. Steam drum pressure must be above 1000 psig to initiate turbine operation.
5. PACC vent control valves are controlled by the temperature differential between the noncondensable gas collection pipe and the steam saturation temperature measured in the PACC outlet header.
6. Normal steam drum water level is 1 inch above drum centerline.

TABLE 7.4-3

LIST OF IEEE STANDARDS APPLICABLE TO  
SGAHS AND OSIS INSTRUMENTATION AND CONTROL SYSTEMS

IEEE-279-1971	IEEE Standard: Criteria for Protection Systems for Nuclear Power Generating Stations
IEEE-308-1974	Criteria for Class 1E Power Systems for Nuclear Power Generating Stations
IEEE-323-1974	IEEE Trial-Use Standard: General Guide for Qualifying Class 1E Electric Equipment for Nuclear Power Generating Stations
IEEE-323-A-1975	Supplement to the Foreword of IEEE 323-1974
IEEE-336-1971	IEEE Standard: Installation, Inspection, and Testing Requirements for Instrumentation and Electric Equipment During Construction of Nuclear Power Generating Stations
IEEE-338-1977	Criteria for the Periodic Testing of Nuclear Power Generating Station Protection Systems
IEEE-344-1975	IEEE Standard 344-1975, IEEE Recommended Practices for Seismic Qualification of Class 1 Equipment for Nuclear Power Generating Stations
IEEE-352-1975	General Principles for Reliability Analysis of Nuclear Power Generating Station Protection Systems
IEEE-379-1972	IEEE Trial-Use Guide for the Application of the Single-Failure Criterion to Nuclear Power Generating Station Protection Systems
IEEE-382-1980	IEEE Standard for Qualification of Safety-Related Valve Actuators
IEEE-384-1974	IEEE Trial Use Standard Criteria for Separation of Class 1E Equipment and Circuits
IEEE-494-1974	IEEE Standard Method for Identification of Documents Related to Class 1E Equipment and Systems for Nuclear Power Generating Station

provide the required time response. The thermowell is also swaged at the tip. The thermocouples are spring loaded against the bottom of the well. Although failures of the wells are not expected, as confirmed by tests and analysis, the head of the thermowell, including the cable penetration, is sealed to provide a secondary boundary for the sodium. Tests have shown that this system will provide a time response less than 5 seconds. Flexible mica, polyimide and fiberglass insulated thermocouple extension wires in conduit are used to bring the signals out of the Heat Transport System Cell. The signals are then routed to the containment mezzanine into reference junctions and signal conditioning equipment. The conditioned signals are transmitted to the control room for the Reactor Shutdown System logic. The Reactor Shutdown System provides buffered signals to the PCS and PDH & DS.

#### Primary and Intermediate Hot and Cold Leg Temperature

The primary and intermediate hot and cold leg temperatures are measured to determine and record operating conditions and to calorimetrically calibrate the permanent magnet flowmeters. The measurement is made by two duplex element resistance temperature detectors (RTDs) per loop, installed in thermowells. Although failures of the wells are not expected, as confirmed by tests and analysis, the head of the thermowell, including the cable penetration, is sealed to provide a secondary boundary for the sodium. The signals from the RTDs are routed to signal conditioning equipment which converts the resistance variation to a standard signal level for transmission to the PDH & DS.

#### Primary and Intermediate Pump Discharge Pressure

The primary and intermediate pump discharge pressure measurements monitor pump performance. In addition the primary pump outlet in conjunction with the intermediate IHX outlet pressure provide the primary loop/intermediate loop differential pressure. The measurements are made by pressure elements installed in the elevated section of the drain line from the discharge piping of the sodium pump. NaK filled capillaries from the pressure elements are connected to pressure transducers which develop electrical signals proportional to the pressure. These pressure transducers provide a secondary boundary if the bellows in the pressure elements should fail. The conditioned signal is supplied to the PDH & DS. Since this pressure element is located in an inerted cell and replacement would require entry into the cell and draining of the loop, two pressure elements per loop are provided.

#### Intermediate IHX Outlet Pressure

The intermediate IHX outlet pressure measurement is used to monitor the loop and IHX operational performance history. The measurements are made by pressure elements installed in the intermediate loop piping between the IHX and the superheater. NaK filled capillaries from the pressure elements are connected to pressure transducers which develop electrical signals proportional to the pressure. The pressure transducers provide a secondary boundary if the bellows in the pressure elements should fail. The conditioned signal is supplied to the PDH and DS.

### IHX Differential Pressure

The primary sodium pump discharge pressure and the IHX Intermediate Loop outlet pressure detectors are used to provide a differential measurement of the IHX Primary/Intermediate pressure difference, which is maintained above 10 psi during normal operating conditions. The differential pressure measurement is alarmed if the intermediate loop pressure drops to 10 psi above the primary loop pressure to alert the operator for corrective action to assure intermediate to primary differential pressure is maintained above the minimum required.

### Intermediate Pump Inlet Pressure

The intermediate pump inlet pressure measurements provide a signal to monitor pump performance. Used with the pump outlet pressure, the differential pressure across the pump is obtained. In the primary loop, the reactor pressure is used for this surveillance. The measurements are made by pressure elements installed on the piping between the evaporators and the pump inlet. NaK filled capillaries from the pressure elements are connected to pressure transducers which develop electrical signals proportional to the pressure. The pressure transducers provide a secondary boundary if the bellows in the pressure elements should fail. The conditioned signal is supplied to the PDH & DS.

### Intermediate Expansion Tank Level

Two separate level measurement channels are provided; both channels are used for indication in the control room and DH & DS and for alarm. Alarm channels provide a broad range measurement that covers possible high and low levels during plant operation as well as the IHTS fill level. The PDH & DS uses measurements for intermediate loop sodium inventory (see also Section 7.5.5). The level probes are designed to be replaceable.

### Evaporator Sodium Outlet Temperature

Three thermocouple (as described above in the paragraph on IHX outlet temperature) channels are provided to measure the sodium temperature at the outlet of the evaporators in each loop. The thermocouples are placed just after the pipes from each evaporator join to form two single lines. These three signals are conditioned separately and provided to the Reactor Shutdown System logic. The Reactor Shutdown System in turn provides buffered signals to the PDH & DS.

#### 7.5.2.1.2 Sodium Pumps

##### Sodium Level

Sodium level is measured in each pump tank. The signal provides indication and alarm. The alarm is used to notify the operator of abnormal operation and allow initiation of action to prevent pump damage. The signal is also provided to the PDH & DS where it can be used in calculation of sodium inventory.



### Pony Motor

The pony motors are Class 1E motors and are supplied power from the Class 1E 480 VAC busses.

Non-class 1E signals are provided to the main control room to indicate the pony motors are running. These signals are pony motor speed indicators which are located in the main control panel and pony motor current which is available through the PDH & DS. Also start and stop lights are on the main control room panel which are from the pony motor starters.

During pony motor operation indication is available on the main control room panel from sodium flow.

### 7.5.2.1.3 Steam Generator

#### Sodium Flow

Venturi flowmeters are provided, one loop only, to accurately measure the sodium flow rate through each of the superheater outlet ports. The accurate flow data is used for determination of the performance characteristics typical of the superheaters and evaporators.

#### Sodium Temperature

The evaporator and superheater outlet temperature is monitored, on all three loops, by Resistance Temperature Detectors (RTD). The superheater inlet is monitored, on one loop only, also by an RTD for purposes of steam generator performance evaluation. These temperature sensors provide signals for the PDH & DS. The evaporator bulk outlet temperature is measured with three thermocouples and are part of the Reactor Shutdown System.

#### Sodium Pressure

For the purpose of steam generator performance evaluation, pressure is measured, in one loop only, at the superheater inlet, superheater outlet (both legs) and evaporator outlet. The type of pressure sensor used is the same as the one for Intermediate pump inlet pressure. These pressure measurements provide pressure signals to the PDH & DS.

#### Steam and Water Flow

- o Feedwater Mass Flow - sensed by three differential pressure elements across one venturi in the inlet line to each steam drum.

59|

- The temperature corrected feedwater flow signals are supplied to the Reactor Shutdown System logic. The Reactor Shutdown System provides buffered signals to PCS and PDH & DS.

59|29|

- Steam Mass Flow - sensed by three differential pressure elements across one venturi in the outlet of each superheater. The temperature and pressure corrected mass signals are supplied to the Reactor Shutdown System logic. The Reactor Shutdown System provides buffered signals to PCS and PDH & DS.

59|

- Steam Drum Blowdown Flow - sensed by flow orifice (differential pressure) in the blowdown line for each steam drum. The signal is provided to the PDH & DS.

- Evaporator Inlet Flow - sensed by a differential pressure element across a venturi in the inlet line to one of the evaporators in one loop only. This is to aid in the performance evaluation of a typical evaporator module.

#### Steam and Water Temperature

59|

- Feedwater Temperature - sensed by three resistance temperature detectors in the steam drum inlet line. The signal provides temperature compensation for the feedwater flow signal. Buffered signals are supplied to the PDH & DS.

59|

- Recirculating Water Temperature - sensed by a thermocouple detector in the recirculation pump discharge header. The signal is provided to the PDH & DS.

59|

- Saturated Steam Temperature - sensed by a thermocouple detector in the outlet header from the steam drum. The signal is provided to the PDH & DS.

59|

- Superheat Steam Temperature - sensed by three resistance temperature detectors in the superheater outlet line. The signal provides temperature compensation for the steam flow. Buffered signals are supplied for PCS and PDH & DS.

59|

- Evaporator and Superheater Inlet and Outlet Temperature - sensed by RTDs located at the inlet and outlet nozzles for one evaporator and superheater in one loop only. Used for performance evaluation for a typical generator module.
- Steam Drum Blowdown Temperature - sensed by a thermocouple located on the blowdown line. The signal provides temperature compensation for the steam drum blowdown flow and is also supplied to the PDH & DS.

#### 7.5.5.1.1 Design Bases and Design Criteria For the Liquid Metal-To-Gas Leak Detection System

The design bases of the Liquid Metal-to-Gas Leak Detection System arises from the need to protect plant equipment, considerations of maintenance and plant availability, and the corrosion effects of sodium compounds on stainless steels at high temperatures.

Considering the significance of corrosion with respect to piping integrity, it is appropriate that the design criteria assure that the Liquid Metal-to-Gas Leak Detection System provide reliable detection for the Primary and Intermediate Heat Transport In-Containment Systems in a small fraction of the nominal time to penetrate the pipe by local corrosion. The effects of corrosion on the CRBRP PHTS piping have been thoroughly assessed in WARD-D-185 "Integrity of the Primary and Intermediate Heat Transport System Piping In-Containment," Reference 1.6 of the PSAR. In summary, leaks of 100 gm/hr may cause local corrosion in 3600 hrs and general corrosion in 18,000 hours at temperatures near 1000°F. At temperatures less than 700°F, the corrosion rate becomes extremely slow. The Leak Detection System will detect leaks of 100 gm/hr in pipes and components operating at temperatures greater than 700°F in less than 250 hrs.

Design Criteria have been established to guarantee reliable plant operation with pipe temperatures greater than 700°F. These include:

1. The PHTS and in-containment IHTS shall be monitored for leaks by diverse methods each capable of providing the required time response.
2. Capability shall be provided to procure a filter sample for laboratory analysis to provide a highly reliable confirmation method. Filter samples should be analyzed a minimum of once every 1000 hrs.
3. The Liquid Metal-to-Gas Leak Detection System must operate after an operating basis earthquake (OBE).
4. The leak detection system shall be equipped with provisions to readily permit testing for operability and calibration during plant operation.
5. A reliable self-monitoring provision shall be provided to detect component failure.

6. Upon loss of ability to fulfill the specified time response, the plant will be placed in a hot shutdown condition.
7. The system shall be qualified to operate in its environment.

Additional Design Criteria of the Liquid Metal-To-Gas Leak Detection System required to protect plant and capital investment, limit maintenance and protect plant availability are outlined below:

1. The Liquid Metal-To-Gas Leak Detection System shall detect and locate liquid metal-to-gas leaks throughout the plant between the temperatures of 375 to 1000<sup>o</sup>F as required to fulfill continuous monitoring requirements of Appendix G, "CRBRP Plan For Inservice and Preservice Inspections."
2. The Leak Detection System shall be able to identify the general location of the leak.

This system is not needed for initiation of plant shutdown, for removal of decay heat or for reduction of off-site radiation exposure to acceptable levels; therefore, it is classified as a non-safety system. The safety related instrumentation provided to accommodate liquid metal leaks is described in Section 7.5.3.1.1. The passive engineered safety features provided to mitigate the effects of liquid metal leaks are described in Section 3.8.

The electrical sensing types of detectors (cables and contact) respond with an alarm when liquid metal causes an electrical short between the electrode and its protective sheath. The Sodium Ionization Detectors (SIDs) provide an alarm when the aerosol concentration reaches a level of about  $10^{-11}$  gm/cc. The PFADs, which are integrating devices, respond with an alarm when the differential pressure across a filter has increased by 2 inches of water. The time for this response is related to aerosol concentration as shown on Figure 7.5-7. For example, at  $1 \times 10^{-11}$  gm/cc, the time response is approximately 250 hours. Both SIDs and PFADs have filters which are chemically examined for sodium on a monthly basis so that leaks which result in aerosol concentrations lower than  $1 \times 10^{-11}$  gm/cc will also be detected. A leak resulting in a concentration of approximately  $2 \times 10^{-13}$  gm/cc is detectable by chemical examination of the filter pads. The sodium aerosol concentration resulting from a 100-gm/h leak in inerted CRBRP cells ranging in volume from 15,000 to 115,000 ft<sup>3</sup> is shown on Figure 7.5-8. In the operating temperature range of 700-1000°F, the leak detection criteria are easily met with either SIDs or PFADs. In addition, during reactor operation, the radiation particulate monitoring system will detect leaks resulting in aerosol concentration of approximately  $10^{-15}$  gm/cc in those cells containing primary sodium.

The aerosol detectors are connected to the PDH&DS so that the rate at which the signal is changing can be checked after a leak alarm is obtained. A rapid increase in PFAD differential pressure (less than 1 hour from normal reading to alarm) accompanied by leak alarms from other detectors in the same area would indicate a large leak (greater than 1 gpm). Conversely, a leak signal that took 10 to 100 hours or more to reach the alarm level would indicate a small (100-1000 gm/h) leak. The SIDs are calibrated so that aerosol concentration can be related to the signal level. Instruments are set to alarm at specific aerosol concentrations. The liquid metal-to-gas leak detection system is designed to function after an OBE. The radiation particulate monitoring system is designed to function after an SSE. All leak detection equipment will be tested periodically to demonstrate operability.

The increase in cell atmosphere temperature and pressure in the event leaks larger than 20 kg/min as detected by temperature and pressure sensors can provide an additional source of leak detection.

The ability to detect small leaks (100 gm/hr) by several methods in hours plus the ability to detect large leaks (>kg/min) in minutes will provide a highly reliable leak detection system that provides the operator information to enable shutdown to repair defects without extensive time for cleanup operations.

After a sodium or NaK leak has occurred, the Liquid Metal-to-Gas Leak Detection System equipment impacted by the leak will be either replaced or cleaned (pneumatic system rinsed with alcohol) to remove sodium leak residue products. The system will then be acceptance tested and calibrated in accordance with the preoperational test specification criteria utilized prior to initial plant startup.

Table 7.5-3 gives the primary and back-up methods of leak detection for the principal sodium systems and components in the plant. The methods shown in the table are related to the three sizes of leaks defined in Section 7.5.5.1.2. The principal methods of leak detection are described below.

#### Aerosol Monitoring

Aerosol monitoring will be performed by measuring the pressure drop across a membrane filter with a constant flow of gas sampled from the annular space between major piping and its insulation, from the space within guard vessels, and from cells containing liquid metal systems. Another cell aerosol monitoring method uses a sodium ionization detector. Liquid Metal aerosols or vapor are ionized by a hot filament and the ion current is measured. Increases in the ion current indicate a leak.

Based upon the experimental results, these methods provide for detection of leaks of 100 gm/hr and less, with a response time depending on temperature and the volume being monitored.

The major function of this instrumentation will be to provide indication of the presence of small leaks which do not present a significant contamination hazard, but which might result in undesirable long-term corrosion.

#### Contact Detectors (Spark-Plug)

Contact detectors consist of a stainless-steel-sheathed, mineral oxide-insulated, two-wire probe with the sensing end open and the wire ends exposed. Contact detectors are installed, for example, on bellows sealed valves with the sensing end between the bellows and the mechanical backup seal. A leak is detected by the reduction in circuit electrical resistance caused by sodium contacting the wire ends.

#### Cable Detectors

Cable detectors consist of stainless-steel-sheathed, mineral-oxide-insulated, cable with holes penetrating the sheath to permit leaked liquid metal to come in contact with the conductors. Cable detectors will be placed, for example, in the bottom of guard vessels and below large tanks.

#### Other Detection Methods

Pressure and temperature measurements available in the inerted cells (Section 9.5.1.5) will provide immediate indication of the presence of large leaks over the 20 kg/min size. In the case of systems containing radioactive sodium, the detection of airborne radioactivity arising from Na-24 or Na-22 in the aerosols will be performed by particulate radiation monitoring equipment (Section 11.4.2) which provides a sensitive detection method for aerosol concentrations as low as  $10^{-15}$  gm/cc.

Chemical analysis provides positive detection capability for aerosol concentrations of approximately  $10^{-13}$  gm/cc, depending on the leak integration period.

#### 7.5.5.1.1.1 Design Description

##### General

Detection equipment is provided to monitor the primary and intermediate sodium coolant boundaries to identify comparatively small leaks when they occur.

The leak detection methods selected for the following installations are:

1. Particulate monitors (radiation detectors), Sodium Ionization Detectors (aerosol detectors), and chemical analysis for atmosphere monitoring in selected cells.
2. Plugging filter aerosol detectors (PFADs) for Main Heat Transfer System piping and guard vessels, major components, and for inerted cell atmosphere monitoring.
3. Contact detectors in the space between the bellows and the stem packing of the bellows sealed sodium valves.
4. Cable detectors in guard vessels and under major liquid metal components.

Of the types of leak detection devices that comprise the Leak Detection System, only sodium aerosol leak detection devices show a difference in their response when operated in an air atmosphere as opposed to an inert atmosphere. The time for a detector to respond to a leak in air is generally shorter than in an inert atmosphere. The electrical sensing types such as cable and contact detectors show no difference in response due to operating atmospheres. However, the potential for higher moisture content in air can result in greater inhibition to sodium flow when the leak is very small.

Considerations which materially affect detection times include: sodium leak rate, sodium temperature, and cell size. Test data (See Reference 5) confirm that sodium leaks of 100 gm per hour in an air or inert atmosphere can be detected by aerosol detection over the operating temperature ranges, within the detection time periods identified in Figure 5.1.1 of WARD-D-0185, "Integrity of Primary and Intermediate Heat Transport System Piping in Containment", (Reference 2, PSAR Section 1.6). Larger leaks (on the order of kg/min) will be readily detected by two or more systems in minutes.

#### Other Backup Detection Method

Liquid Sodium Level Sensors in the reactor, the EVST, the IHTS expansion tank, and sodium storage tanks will provide indications of large leaks. Smoke detectors (Fire Protection System) will detect combustion products originating from sodium leaks in air (See Section 9.13.2).



### Indication in Control Room

An audible group alarm is sounded in the control room upon indication of a leak or certain failures of contact, cable, or aerosol channels. The channel number producing the alarm and the location of the region covered by this channel are displayed on an annunciator on a local panel. This information will identify the leak as occurring in a specific major component or series of pipe sections, or specific bellow-sealed valve, or the cell containing the leaking system. The leak detection system uses the Plant Data Handling System for channel failure monitoring, data and trend logging; the sampling time interval will nominally be approximately 30 seconds.

No automatic isolation functions or reactor scram are initiated by the Liquid Metal-To-Gas Leak Detection System. Isolation or shutdown of a system showing a leak will be performed manually, following verification of the leak and review of the operating conditions.

#### 7.5.5.1.2 Design Analysis

The Liquid Metal-to-Gas Leak Detection System will meet the appropriate requirements of CRBR Design Criterion 30, "Inspection and Surveillance of Reactor Coolant Boundary and Criterion 33, "Inspection and Surveillance of Reactor Coolant Boundary. Criterion 30 requires that means be provided for detecting and identifying the location of the source of reactor coolant leakage from the reactor coolant boundary to the extent necessary to assure that timely discovery and correction of leaks which could lead to accidents whose consequences could exceed the limits prescribed for protection of the health and safety of the public. Criterion 33 requires that means be provided for detecting intermediate coolant leakage from the intermediate coolant boundary. In order to demonstrate how the intent of the criteria will be satisfied, the instrumentation requirements met by this system for three different ranges of leaks are discussed. These ranges have been selected to analyze situations which cover the complete range of leak detection instruments. Section 15.6 discusses the consequences of leaks for the health and safety of the public.

### Large Leaks

This category covers failures up to those resulting in a leak of 30 gpm or 100 kg/min. A significant physical characteristic of leaks of this size is that they would result in pressure and temperature changes in the primary cells if the leak occurs in PHTS pipe sections. This feature sets the lower boundary of the leak at about 20 kg/min; this being an estimate of the amount of sodium which would result in measurable changes in cell pressure and temperature. If the leak occurs in a guard vessel, continuity detectors will provide detection

of these large leaks. Leaks of this magnitude would be detected in five minutes or less for the primary and intermediate heat transport system. The operator would then be able to initiate and complete plant shutdown within ten minutes after the start of the leak.

The pressure and temperature measurements available in the inerted cells will, in conjunction with the aerosol detectors, continuity detectors and radiation monitors, provide the response required for proper operator action in case of leaks of this magnitude.

#### Intermediate Leaks

Intermediate leaks were defined as those leaks which would not result in significant changes in cell pressures and temperatures but where the extent of the resulting contamination and plant maintenance makes plant shutdown desirable. The range of leak rates covered extends from the lower limit of the large leaks previously considered down to a leak of 100 gm/hr. The detection times for the wide range of leaks in this group would vary from a few minutes to several hours depending on the rate of leakage. Based upon experimental results, it is concluded that several systems would detect a leak of this magnitude in several hours at least and possibly in minutes.

Instrumentation capable of detecting leaks of this magnitude include radiation monitors, continuity detectors, and the different types of aerosol detectors.

#### Small Leaks

Small leaks at or below 100 gm/hr were defined as those events resulting in releases of sodium which do not pose a contamination or maintenance problem but might result in undesirable long-term corrosion (see Section 5.3.3). The methods for detecting leaks of this range are aerosol detectors and radiation monitors in the case of the primary system.

In the course of test programs, aerosol concentrations produced by leaks of down to 5 gm/hr were found to be within the detection capability of both a Sodium Ionization Detector and a Plugging Filter Aerosol Detector in test chambers. The test results show that leaks of this size can be detected in the range of one hour to 24 hours by annuli monitors depending upon the sodium temperature and gas environment. It is deduced from the test results that very small leak (<1 gm/hr) will be detected by annuli monitors in several days.

Tests during 1975 and 1976 showed that under environmental conditions typical of LMFBR operation, small leaks from typical piping configurations can be detected by both Sodium Ionization and Plugging Filter Aerosol Detectors. Continuity (cable or contact) detectors did not reliably detect small pipe leaks under these conditions. Testing in 1978 verified the performance of aerosol detectors using prototypic CRBRP cell atmosphere recirculation as well as pipe/insulation design.

It is deduced from the test results that the sodium vapor/aerosol systems will, in conjunction with existing radiation monitoring technology, provide adequate indication of the smallest sizes of leaks of interest.

#### Sodium Leaks into an Air Atmosphere

Test results indicate that the methods applicable to sodium leaks in inerted cells will also operate when applied in an air atmosphere. The additional use of smoke detectors and the accessibility of piping located in an air atmosphere to visual inspection assist in the selection of an effective sodium-to-air leak detection system.

#### 7.5.5.2 Intermediate to Primary Heat Transport System Leak Detection

##### 7.5.5.2.1 Design Description

The IHTS pressure is maintained at least 10 psi higher than the Primary Heat Transport System at the IHX to prevent radioactive primary sodium from entering the IHTS in the event of a tube leak. Maintaining a positive pressure differential across the IHX is a limiting condition for operation of the plant (Chapter 16 - Technical Specifications). This provides assurance that a zero or negative differential will not exist during any extended interval. A loss of this pressure or a reversal of it is not expected to occur except during accident conditions. Such an occurrence would necessitate an orderly plant shutdown to correct the problem. Since a reverse differential cannot occur for a significant interval, the potential leakage of primary sodium into the intermediate system, through an IHX tube leak, is small.

Leakage of primary sodium into the IHTS, should it occur, will be detected by radiation monitors provided on the IHTS piping within the SGB. The radiation monitor system will provide an indication of the radiation level and will provide alarms for conditions of excessive radiation indicative of ingress of primary sodium. Since the only activity expected in the IHTS is a low level of tritium, the radiation monitors will be very sensitive to the presence of significant amounts of radioactive primary sodium in the intermediate system. For accidents which involve a loss of IHTS boundary integrity the radiological effects have been evaluated. The results of these evaluations are presented in Sections 15.3.2.3, 15.3.3.3 and 16.6.1.5.

Maintaining a positive pressure differential across the IHX assures that the leakage across the IHX tube barrier will result in an inflow of sodium into the primary system causing a loss of sodium inventory in the IHTS. The sodium inventory in the IHTS is monitored by tracking the sodium levels and correcting for loop temperature effects. Alarms are provided in the control room to alert the operator upon detection of a large loss of IHTS sodium inventory.

#### 7.5.5.2.2 Design Analysis

Intermediate to Primary Heat Transport System leak detection is provided to comply with CRBRP General Design Criterion 36 "Inspection and Surveillance of Intermediate Coolant Boundary". In order to demonstrate now the intent of this criterion will be satisfied, an analysis of the minimum detectable leaks in the IHX is provided below.

The minimum detectable level change of sodium in the IHTS pump and expansion tank is approximately 3 inches which corresponds to about 150 gallons. In the event of a full-circumferential break of an IHX tube, the leak rate of intermediate sodium to the primary side of the IHX would be approximately 150 gpm. At this leak rate, the detection time would be about one minute assuming steady state temperature conditions.

Based upon a 3-inch level change, leakage of as low as 6.25 gph would fall within the detection threshold. Over long time periods, the sensitivity of the detection system will be reduced by an insignificant amount due to other potential leakages from the system. If leakage occurs due to piping or component leaks, the external leak detection system will detect the leakage. A second potential source is leakage through the four sets of dump valves which has a maximum expected rate of one to two gallons per day. Since this leakage rate is essentially two orders of magnitude smaller than the leakage threshold, it will not have a consequential effect on the detection sensitivity.

#### 7.5.5.3 Steam Generator Leak Detection System

A Steam Generator Leak Detection System is provided to detect small (as low as  $10^{-5}$  lb/sec) water-to-sodium and steam-to-sodium leaks in the steam generator modules, to identify the module in which the leak has occurred, and to alert the control room operator enabling him to take manual corrective action to prevent the leak rate from increasing. Leak detection instrumentation is provided for:

1. Sodium exiting from the superheater and the evaporators.
2. Sodium filled vent lines from the evaporator vents and the superheater vent.

features, or their power sources, concurrent with the failures that are a condition of, or a result of a specific accident, will prevent the operator from being presented the required information.

- o The Principal Instruments from sensor to indicator, and the Redundant Backup instruments from sensor through the indication device will be qualified in accordance with PSAR Section 1.6 Reference 13, "Requirements for Environmental Qualification of Class 1E Equipment." They are qualified to provide the information needed by the operator to assess plant and environs conditions during and following design basis events.
- o Instrumentation will continue to read within the required accuracy following, but not necessarily during, a Safe Shutdown Earthquake (SSE).
- o The Principal Instrument (from sensor to indicator) and Redundant Backup Instrument (from sensor through the isolation devices) will be energized from Class 1E power and be supplied with battery backing where momentary interruption of the indication is not tolerable.

#### | 7.5.11.2.2 Category 2

- o Each Category 2 Instrument signal, will be, as a minimum, processed for display on demand.
- o The Category 2 instrument indicators will be located to effectively support normal and emergency plant operations.
- o The Category 2 instruments from sensor to indicator will as a minimum be qualified in accordance with Reference 13, PSAR Section 1.6, "Requirements for Environmental Qualification of Class 1E Equipment" except for seismic. They will be qualified to provide the information needed by the operator to assess plant and environs conditions during and following design basis events.
- o The instrumentation will be energized from a highly reliable power source (not necessarily a Class 1E power supply). Where interruption of the power supply is acceptable station AC power may be used. Where momentary interruption is not tolerable, the non-1E UPS is used.

#### 7.5.11.2.3 Category 3

- o Each Category 3 Instrument signal, will be, as a minimum, processed for display on demand.
- o The location of the Category 3 Instrument Indication will be chosen to support normal and off-normal operations.
- o The Category 3 Instrumentation will be a high quality commercial grade.

#### 7.5.11.2.4 General Requirements to Category 1, 2, and 3

- o Servicing, testing, and calibration programs will be specified to maintain the capability of the monitoring instrumentation. For those instruments where the required interval between testing shall be less than the normal time interval between generating station shutdowns, a capability for testing during power operation shall be provided.
- o Whenever means for removing channels from service are included in the plant design, the plant design will facilitate administrative control of the access to such removal means.
- o The plant design will facilitate administrative control of the access to all setpoint adjustments, module calibration adjustments, and test points.
- o The monitoring instrumentation design will minimize the development of conditions that would cause meters, annunciators, recorders, alarms, etc., to give anomalous indications potentially confusing to the operator.
- o The instrumentation will be designed to facilitate the recognition, location, replacement, repair, or adjustment of malfunctioning components or modules.
- o To the extent practicable, monitoring instrumentation inputs will be from sensors that directly measure the desired variables. An indirect measurement will be made only when it can be shown by analysis to provide unambiguous information.

References to Section 7.5

1. Ford, J. A., "A Recent Evaluation of Foreign and Domestic Wastage Data from Sodium Water Reaction Investigation", APDA CTS-73-05, January, 1973.
2. Morejon, J. A., "Sodium-to-Gas Leak Detection Mockup Tests", N707-TR-520-004, September 17, 1975. (Atomics International)
3. Greene, D. A., J. A. Gudahl and J. C. Hunsicker, "Experimental Investigation of Steam Generator Materials by Sodium-Water Reactions, Volume 1, GEAP-14094, January 1976.
4. Gudahl, J. A. and P. M. Magee, "Microleak Wastage Test Results", GEFR-00352, March 1978.
5. Matlin, E., Witherspoon, J. E., Johnson, J. L., "Liquid Metal-to-Gas Leak Detection Instruments".

Figure 7.5-7 Liquid Metal/Gas Leak Detection System  
Response Time Vs. Sodium Aerosol Concentration (inerted Cells)

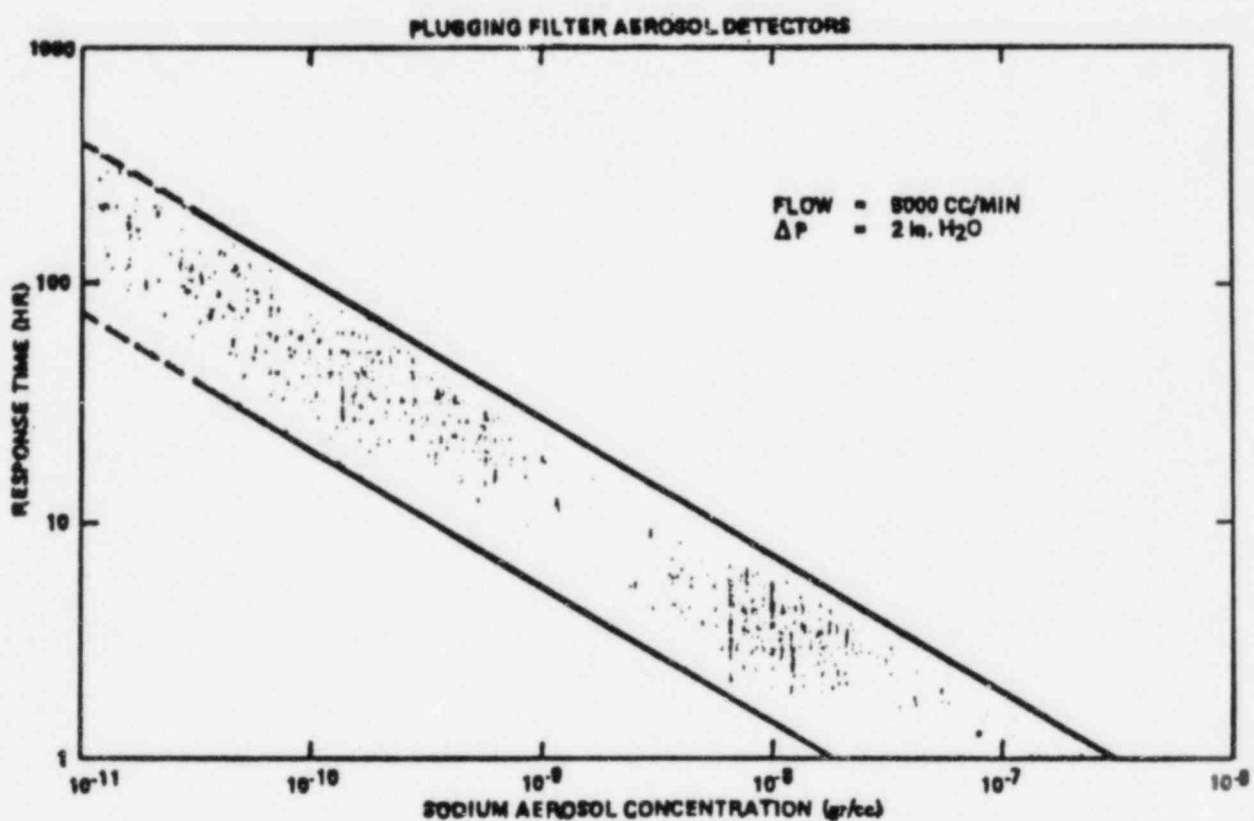
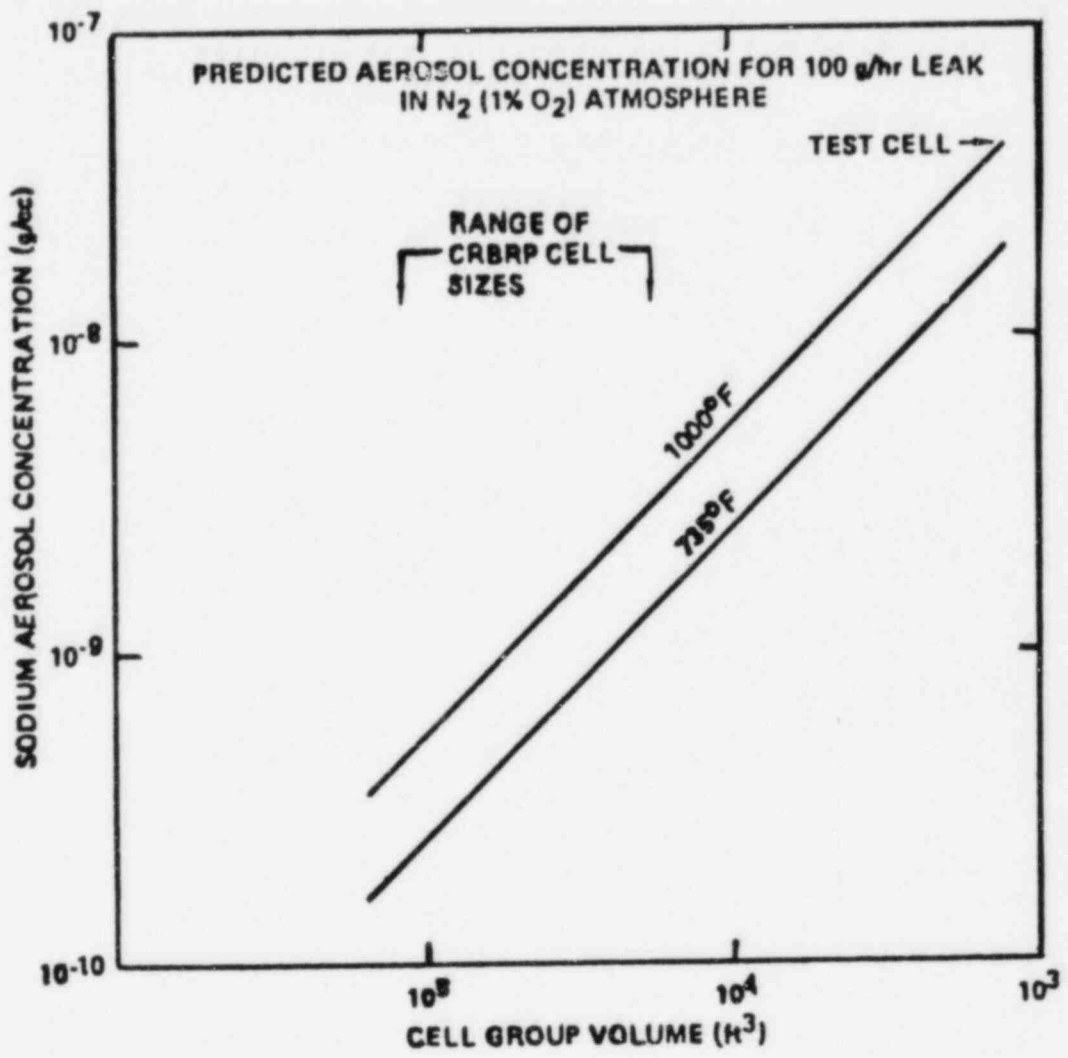




Figure 7.5-8 Liquid Metal/Gas Leak Detection System  
 Predicted Aerosol Concentration for 100 g/HR  
 Leak In N<sub>2</sub>(1% O<sub>2</sub>) Atmosphere



## 7.6 OTHER INSTRUMENTATION AND CONTROL SYSTEMS REQUIRED FOR SAFETY

The additional instrumentation and control systems required for safety which have not been discussed earlier in Chapter 7 are identified as the Emergency Plant Service Water, Emergency Chilled Water, Recirculating Gas Cooling, Heating, Ventilating, Air Conditioning, Instrumentation and Control Systems, and the Direct Heat Removal Service Instrumentation and Control. The Radiation Monitoring System also contains safety related components which are discussed in Chapter 11. The Emergency Plant Service Water, Emergency Chilled Water, Recirculating Gas Cooling, Heating Ventilating, Air Conditioning Systems, Fuel Handling, and DHRIS Instrumentation and Control are discussed in this Section. Review of the functional control diagrams will require reference to the symbols, notes and abbreviations as shown in Table 7.6-1.

### 7.6.1 Emergency Plant Service Water and Emergency Chilled Water Instrumentation and Control System

#### 7.6.1.1. Emergency Plant Service Water System (EPSW)

The EPSW System consists of two redundant divisions which supply cooling water to the diesel generators, the Emergency Chilled Water System and seismically qualified Non-Sodium Fire Protection System.

The Instrumentation and Control System is provided for automatic control of the Emergency Plant Service Water System, to monitor and indicate system process parameters during normal and off-normal conditions, and to provide signal inputs to Plant Data Handling and Display System.

Functional Control Diagrams for Emergency Plant Service Water System are identified in Figures 7.6-1, 7.6-2, 7.6-3 and 7.6-4.

#### 7.6.1.2 Design Criteria

Design criteria that are applicable to Emergency Plant Service Water Instrumentation and Control System are as follows:

- A. EPSW System is provided with Class 1E power supply, and is backed up by Diesel Generators to provide power during off-normal conditions.
- B. No single failure of an instrument, interconnecting cable or panel will prevent a key process variable from being controlled or monitored in both redundant divisions.
- C. Physical and electrical separation of redundant portions of Emergency Plant Service Water is provided.
- D. System level manual initiation capabilities are provided in both divisions to perform all the actions performed by automatic initiation.
- E. Instrumentation used in the control of Emergency Plant Service water will function during and after an SSE.

- F. Instrumentation used in the control of Emergency Plant Service Water will function during normal environmental conditions and during environmental conditions created by any design basis accident.
- G. Capabilities for periodic testing and calibration of all instruments are provided.
- H. Capabilities are provided for remote shutdown, should the control room become uninhabitable.
- I. Capabilities are provided to monitor the inoperable status of components in accordance with Reg. Guide 1.47.
- J. Capabilities are provided to monitor the process variables to assess plant and environs conditions during and following an accident.

#### 7.6.1.3 Design

Instrumentation and controls are provided for the following equipment in the EPSW System: EPSW Pumps; EPSW Makeup Water Pumps; Emergency Cooling Tower Fans and Temperature Control Valves. For a complete description of the EPSW System refer to Chapter 9.9.2.

##### 7.6.1.3.1 Control System

- A. Remote, auto and manual controls are provided in Control Room for EPSW Pumps, EPSW Makeup Water Pumps; Emergency Cooling Tower Fans.
- B. Local, auto and manual controls are provided in Local Panels for EPSW Pumps; EPSW Makeup Water Pumps; Emergency Cooling Tower Fans; and Temperature Control Valves.
- C. EPSW will start automatically under the following conditions:
  - i) On an Emergency Chilled Water System start demand;
  - ii) 20 seconds after the Diesel Generator Load Sequencer is actuated;
  - iii) when the system level manual control is initiated from Control Room.

##### 7.6.1.3.2 Monitoring Instrumentation

The following process variables are monitored through indication and alarms:

- A. EPSW Pump Discharge Temperature
- B. EPSW Pump Discharge Pressure
- C. EPSW Pump Pit Level
- D. EPSW Makeup Pump Flow

- E. Operating Basin Overflow
- F. EPSW Makeup Pump Discharge Pressure
- G. Emergency Cooling Tower Basin Level
- H. EPSW Flow to Emergency Chillers
- I. EPSW Temperature at the Discharge of Emergency Chillers
- J. EPSW Flow from Diesel Generators Heat Exchangers
- K. EPSW Temperature at the Discharge of Diesel Generators Heat Exchangers
- L. Diff. Pressure Across Emergency Chillers
- M. Transfer of Controlling Capabilities from Control Room to Local Panels
- N. Pump and Fan Status

Process variables identified above with 'A' and 'H' are designated as accident monitoring variables to assess plant and environs conditions during and following an accident. Refer to Section 7.5.11 of PSAR for detailed requirements on Accident Monitoring.

#### 7.6.1.3.3 Inputs to PDH&DS

The following process variables are provided as Inputs to Plant Data Handling & Display System (Non-Safety System):

- A. EPSW Discharge Temperature
- B. Emergency Cooling Tower Basin Level
- C. EPSW Temperature at the Discharge of Emergency Chiller
- D. EPSW Temperature at the Discharge of Diesel Generator Heat Exchanger
- E. EPSW Flow to Emergency Chiller

Inoperable status of EPSW Pumps; Makeup Pumps; and Cooling Tower Fans is also monitored through Inoperable Status Monitoring System.

#### 7.6.1.1.3.4 Design Analysis

EPSW System is designed to operate automatically. The system is operated only during emergency conditions. EPSW System components are cascaded to operate in sequence. Starting of EPSW Pumps will operate EPSW Makeup Pumps and Cooling Tower Fans. System will not operate when the EPSW Pump pit level is low or when electrical fault exists.

The design of the EPSW System is in conformance with the following IEEE standards listed in Table 7.6-2.

## 7.6.2 Emergency Chilled Water (ECW) System

The ECW System consists of two redundant divisions which supply chilled water. Controls are provided for the following equipment in the ECW System: Emergency Chillers, Circulating Pumps, Expansion Tank Valve, Normal-to-Emergency Isolation Valves, Temperature Control Valves, and "Recirculating Gas Cooling System Heat Exchanger and Secondary Coolant Heat Exchanger" Leak Isolation Valves. Detailed description of these controls is given in the following paragraphs. For a complete description of the ECW System, refer to Chapter 9.7.2.

The ECW System cannot operate without support from the Plant Electrical Power System and the Emergency Plant Service Water (EPSW) System. The ECW System power supply is Class 1E and requires a diesel generator back-up. A detailed description of the diesel generators and the Plant Electrical Power System is given in Chapter 8. The EPSW System supplies service water to the ECW Chiller. A detailed description of the EPSW System is given in Chapter 9.9.2.

Functional Control Diagrams for Emergency Chilled Water System are identified in Figures 7.6-5, 7.6-6, 7.6-7, 7.6-8, 7.6-9 and 7.6-10.

### 7.6.2.1 Design Criteria

Design criteria that are applicable to Emergency Chilled Water Instrumentation and Control System are as follows:

- A. ECW System is provided with Class 1E power supply, and is backed up by diesel generators to provide power during off-normal conditions.
- B. No single failure of an instrument, interconnecting cable or panel will prevent a key process variable from being controlled or monitored in both redundant divisions.
- C. Physical and electrical separation of redundant portions of Emergency Chilled Water is provided.
- D. System level manual initiation capabilities are provided in both divisions to perform all the actions performed by automatic initiation.
- E. Instrumentation used in the control of Emergency Chilled Water will function during and after an SSE.
- F. Instrumentation used in the control of Emergency Chilled Water will function during normal environmental conditions and during environmental conditions created by any design basis accident.
- G. Capabilities for periodic testing and calibration of all instruments are provided.
- H. Capabilities are provided for remote shutdown, should the control room become uninhabitable.

#### 7.6.2.2.3 Inputs to PDH&DS

The following process variables are provided as Inputs to Plant Data Handling & Display System (Non-Safety System):

- A. ECW Temperature at the Inlet of Emergency Chiller
- B. ECW Temperature at the Discharge of Emergency Chiller
- C. ECW Flow from Emergency Chiller
- D. ECW Chiller Trip Status
- E. ECW Containment Isolation Valves Status
- F. Secondary Coolant Expansion Tank DT-J Leakage

#### 7.6.2.2.4 Design Analysis

ECW System is designed to operate automatically. The system is operated only during emergency condition. ECW System components are cascaded to operate in sequence. Low flow of NCW to ECW loop signal will align ECW isolation valves and operate ECW Pumps, Emergency Plant Service Water Loops, and ECW Chillers. System will not operate when the EPSW flow through chiller is not established or when electrical fault exists.

The design of the ECW System is in conformance with the IEEE Standards listed in Table 7.6-2.

3. Unit cooler or HVAC unit supply air temperature high or air temperature entering cooling coil low.
  4. Smoke, ammonia, chlorine, fluorine or radiation present in Control Room main or remote air intake.
  5. Control switch in the local mode (Control Room only alarm only).
- C. Typically, process variables are provided as inputs to the Plant Data Handling & Display System as follows:
1. Control Room and computer room humidity.
  2. Containment differential pressure.
  3. Annulus differential pressure.
  4. RSB confinement differential pressure (four different cells).
  5. Control Room differential pressure.
  6. Air temperature entering and leaving each filter unit.
  7. Air temperature entering and leaving each HVAC unit.
  8. Cell temperature of each area being serviced by a unit cooler or HVAC unit.
  9. Inoperable or bypass status of components.
- D. The following process variables are classified as Accident Monitoring variables and are used to assess plant and environs conditions during and following an accident:
1. Annulus to atmosphere differential pressure.
  2. RSB confinement to atmosphere differential pressure.
  3. HVAC units discharge air temperature.
  4. Filter units adsorbent filter leaving air temperature.
  5. HVAC and filter units air flow low.
  6. Damper and valve position indication.
  7. Fan operation status indication.

#### 7.6.4.3 Design Analysis

The HVAC Instrumentation and Control System is designed to perform the functions described in Section 7.6.4 while meeting the criteria listed in Section 7.6.4.1. All HVAC I&C circuits shall meet the requirements of Section 7.1 with the exception of alarm circuits and inputs to the PDH&DS which are

Non-Class 1E circuits. The design of the HVAC Instrumentation and Control system is in conformance with the IEEE Standards and listed in Table 7.6-2.

Refer to PSAR Section 7.1.2 for conformance to applicable IEEE Standards.

### 7.6.5 Steam Generator Building (SGB) Flooding Protection Subsystem

#### 7.6.5.1 Design Basis

The SGB Flooding Protection Subsystem is provided to prevent flooding of SGAHRS equipment resulting from postulated SGS water/steam line ruptures, thereby assuring the availability of SGAHRS for reactor decay heat removal following water/steam line rupture events.

The SGB Flooding Protection Subsystem is designed to the IEEE Standards listed in Table 7.6-3.

#### 7.6.5.2 Design Requirements

The SGB Flooding Protection Subsystem is designed to perform the following functions:

- a) Detect the presence of large steam/water piping ruptures (see Section 15.3.3.1) by temperature and moisture sensors in each cell.
- b) Detect water level flooding conditions in each cell by water level sensing elements.
- c) Provide the signals to initiate the alarms and activate the equipment which provides the SGB flooding protection.

#### 7.6.5.3 Design Description

##### 7.6.5.3.1 Instrumentation

Instrumentation provided for this subsystem consists of Class 1E temperature, and moisture transducers. In addition, non-Class 1E level transducers are provided. The transducers and associated control logic are located in the SGB cells containing main feedwater or recirculation piping. Three independent moisture and temperature measurements in each cell are utilized for identifying a major water/steam line rupture. Water level measurements in each cell confirm a flooding condition and are annunciated in the main control room.

##### 7.6.5.3.2 Controls

Each heat removal loop isolates the main feedwater supply upon detection of a major pipe rupture. The start-up and main feedwater control valves close upon activation by a two-out-of-three logic using measurements of moisture and temperature in each cell. The main feedwater isolation valve is independently closed upon activation by a two-out-of-three logic using the same three moisture and temperature measurements from each cell. Separation and isolation is maintained between the control valve and isolation valve activation logic.



Small water/steam leaks are identified in each SGB cell by measuring water level. Manual corrective control of flooding is initiated by the operator upon annunciation in the main control room.

Inoperable status of subsystem fans (MA, MB, EA, EB) and Isolation valves (two per subsystem) is also monitored through Inoperable Status Monitoring System.

#### 7.6.6.2.4 Design Analysis

Refer to PSAR Section 7.1.2 for conformance to applicable IEEE Standards. RGC system is designed to operate automatically. The system and its safety-related subsystems are operated during normal as well as emergency conditions. The RGC system components are cascaded to operate in sequence. Starting a fan will open associated supply and return gas isolation valves. A subsystem will not operate when high water vapor or cooler high water level or electrical fault exists.

As discussed in Section 9.16 each subsystem of RGCs supplies cooling to redundant components, so no additional redundancy is provided in its components and instrumentation.

The systems are designed for fail safe operation and control equipment will assume a failed position consistent with its intended safety function.







The coolant supply to safety-related subsystems MA, MB, EA, EB is provided by Emergency Chilled Water System. The fan motors for these subsystems are provided with AC power from Class 1E power sources to continue operating during loss of offsite power, except for the booster fan of the subsystem EB which is not required to operate during loss of power condition. Subsystems MA and EA and the EM pumps cooled by these two subsystems are served by Class 1E power supply Division 1. Also, subsystems MA and EA are served by Emergency Chilled Water Loop "A". Subsystems MB and EB are served by Emergency Chilled Water Loop "B", and Class 1E power supply Division 2. The EM pumps cooled by subsystems MB and EB are also connected to Class 1E power supply Division 2. Automatic isolation valves are designed as fail open valves so as to be in their safety position upon loss of power.

Fan and Isolation Valve control switches are located in the local panels as well as in the back panels for subsystems MA, MB, EA and EB, except for booster fan. Thus, in case of control room evacuation the fans and valves can be controlled from outside the control rooms, using local panels.

The design of the Recirculating Gas System is in conformance with the IEEE Standards listed in Table 7.6-2.

TABLE 7.6-1

SYMBOLS

	ALARM
	INOPERABLE STATUS MONITORING
	RED IND LITE
	GREEN IND LITE
	WHITE IND LITE
	COMPUTER INPUT

NOTES:

- 1) Control switches are spring return to auto from start with a maintained stop unless otherwise stated.

ABBREVIATIONS

SSPLS	- Solid State Programmable Logic System
CR	- Control room (remote)
L	- Local (not control room)
T.D.	- Time delay
N.C.	- Normally closed
F.C.	- Fail closed
S.O.V.	- Solenoid operated valve
A.O.V.	- Air operated valve
MOD	- Motor operated damper
ZS	- Position switch
CIS	- Containment isolation signal
PPS	- Plant Protection System
E/H	- Electro-hydraulic

TABLE 7.6-1 (Continued)

TE	- Temp element
TT	- Temp transmitter
TIC	- Temp Ind controller
OAI	- Outside air intake
TMD	- Temp modulated damper
RA	- Return air
PDI	- Pressure differential indicator
PDC	- Pressure differential controller
PMD	- Pressure modulated damper
PDISH	- Pressure differential indicating switch high
FR	- Flow recorder
FIC	- Flow Indicating controller
FSL	- Flow switch low
FT	- Flow transmitter
FMD	- Flow modulated damper
FE	- Flow element
M	- Moisture
PB	- Pushbutton
MUX	- Multiplexing
AHU	- Air handling unit

TABLE 7.6-2

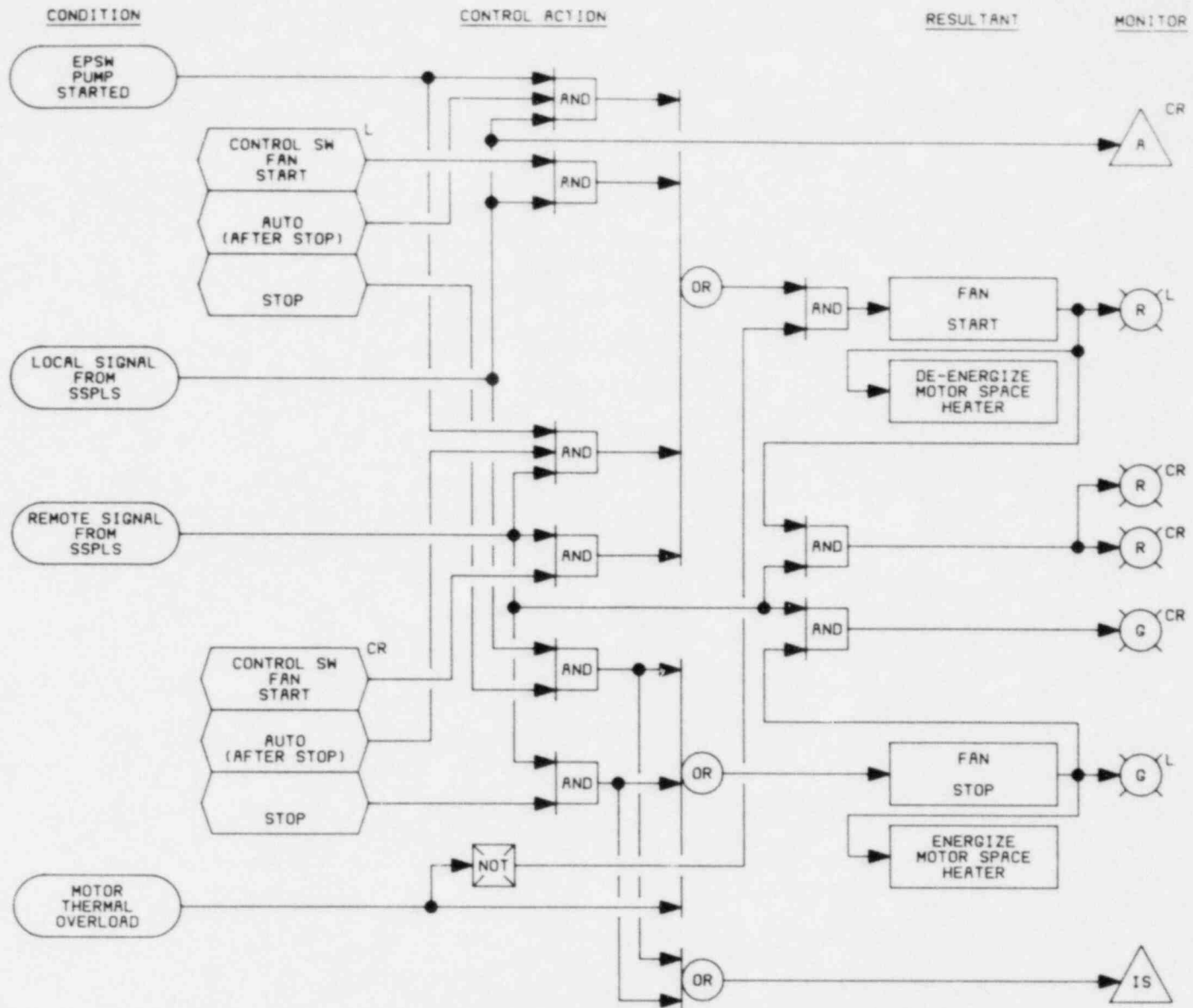
LIST OF IEEE STANDARDS APPLICABLE TO EMERGENCY  
PLANT SERVICE WATER, EMERGENCY CHILLED WATER, HVAC,  
AND RECIRCULATING GAS INSTRUMENTATION AND CONTROL SYSTEM

- a) IEEE Standard 279-1971  
IEEE Standard: Criteria for Protection Systems for Nuclear Power  
Generating Stations
- b) IEEE Standard 308-1974  
Criteria for Class 1E Power Systems for Nuclear Power Generating Stations
- c) IEEE Standard 323-1974  
Qualifying Class 1E Electrical Equipment for Nuclear Power Generating  
Stations
- d) IEEE Standard 338-1977  
Criteria for Periodic Testing of Nuclear Power Generating Station Safety  
Systems
- e) IEEE Standard 379-1972  
IEEE Trial-Use Guide for the Applicability of the Single-Failure Criterion  
to Nuclear Power Generating Station Protection Systems
- f) IEEE Standard 383-1974  
Standard for Type Test of Class 1E Electric Cables, Field Splices and  
Connections for Nuclear Power Generating Stations
- g) IEEE Standard 384-1974  
IEEE Trial-Use Standard Criteria for Separation of Class 1E Equipment and  
Circuits.

TABLE 7.6-3

LIST OF IEEE STANDARDS APPLICABLE TO  
SGB FLOODING PROTECTION SUBSYSTEM

IEEE-279-1971	IEEE Standard: Criteria for Protection Systems for Nuclear Power Generating Stations
IEEE-323-1974	IEEE Trial-Use Standard: General Guide for Qualifying Class 1E Electric Equipment for Nuclear Power Generating Stations
IEEE-323-A-1975	Supplement to the Foreword of IEEE-323-1974
IEEE-336-1971	IEEE Standard: Installation, Inspection, and Testing Requirements for Instrumentation and Electric Equipment During Construction of Nuclear Power Generating Stations
IEEE-338-1971	IEEE Trial-Use Criteria for the Periodic Testing of Nuclear Power Generating Station Protection Systems
IEEE-344-1975	IEEE Standard 344-1975, IEEE Recommended Practices for Seismic Qualification of Class 1 Equipment for Nuclear Power Generating Stations
IEEE-352-1972	IEEE Trial-Use Guide: General Principles for Reliability Analysis of Nuclear Power Generating Station Protection Systems
IEEE-379-1972	IEEE Trial-Use Guide for the Application of the Single-Failure Criterion to Nuclear Power Generating Station Protection Systems
IEEE-384-1974	IEEE Trial-Use Standard Criteria for Separation of Class 1E Equipment and Circuits
IEEE-494-1974	IEEE Standard Method for Identification of Documents Related to Class 1E Equipment and Systems for Nuclear Power Generating Station



7.6-19

Amend. 71  
Sept. 1982

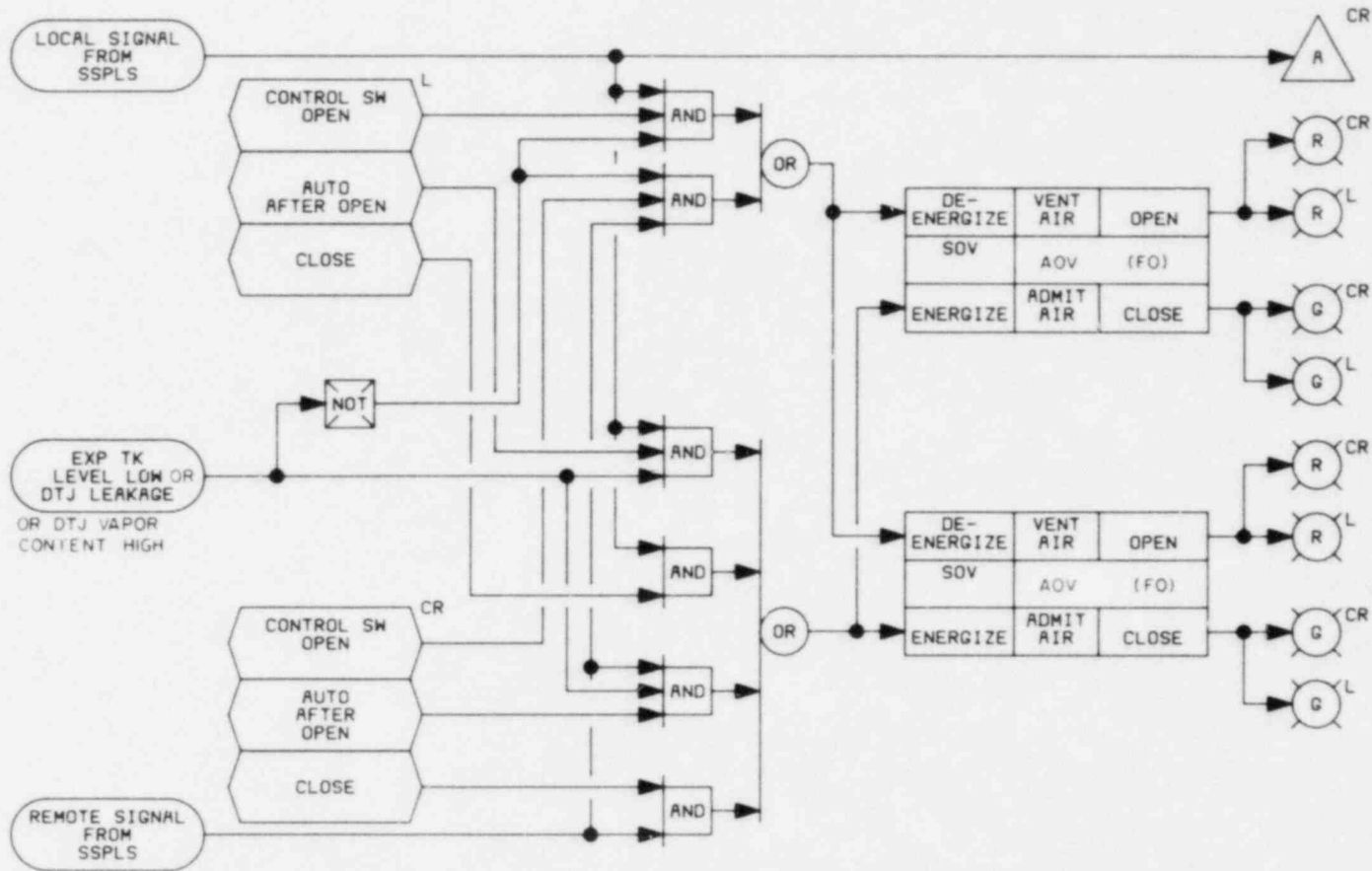
FIGURE 7.6-1  
EMERGENCY COOLING TOWER FAN

CONDITION

CONTROL ACTION

RESULTANT

MONITOR

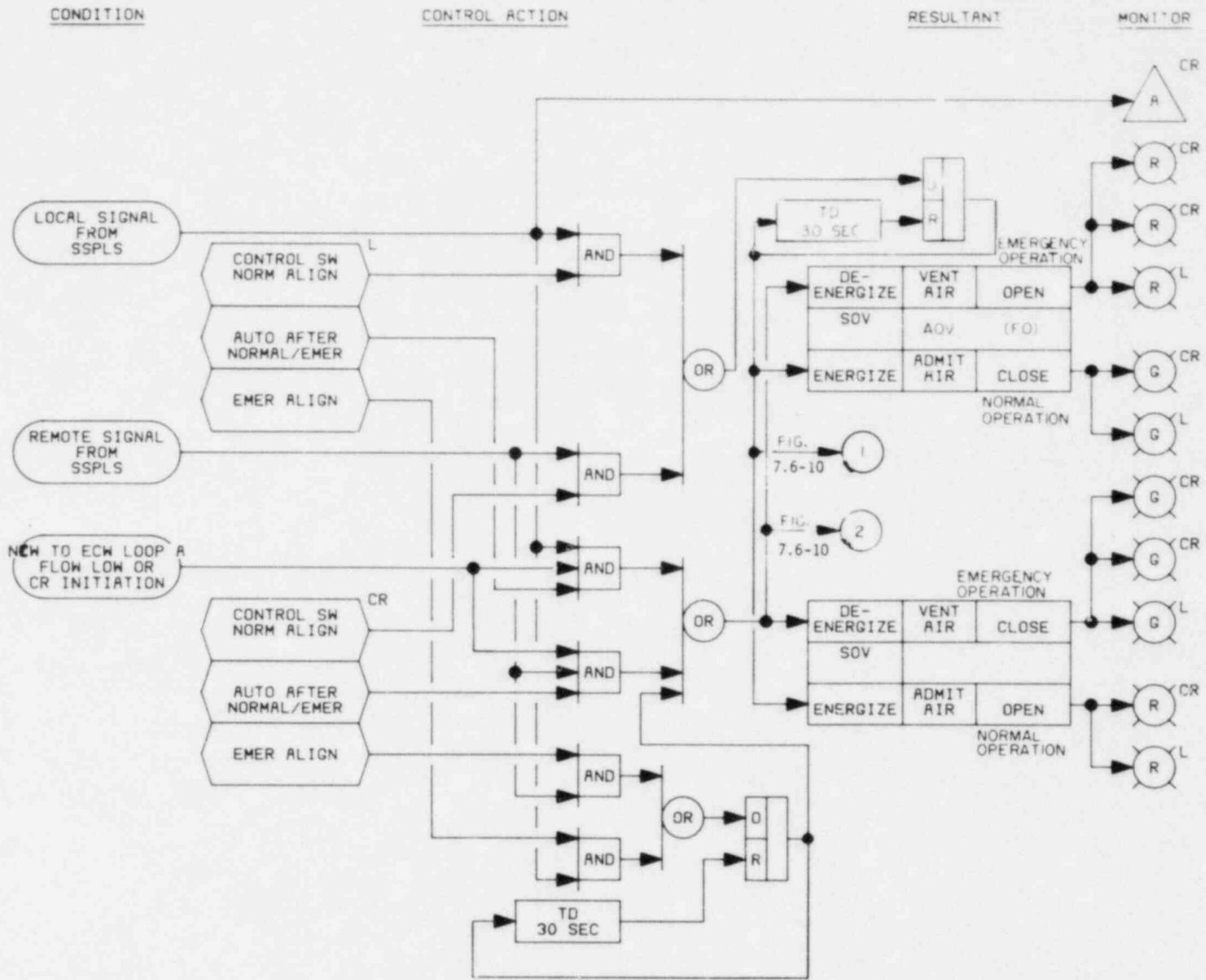


7.6-26

Amend. 71  
Sept. 1982

FIGURE 7.6-8  
EMERGENCY CHILLED WATER ISOLATION VALVES  
TO SECONDARY COOLANT LOOP



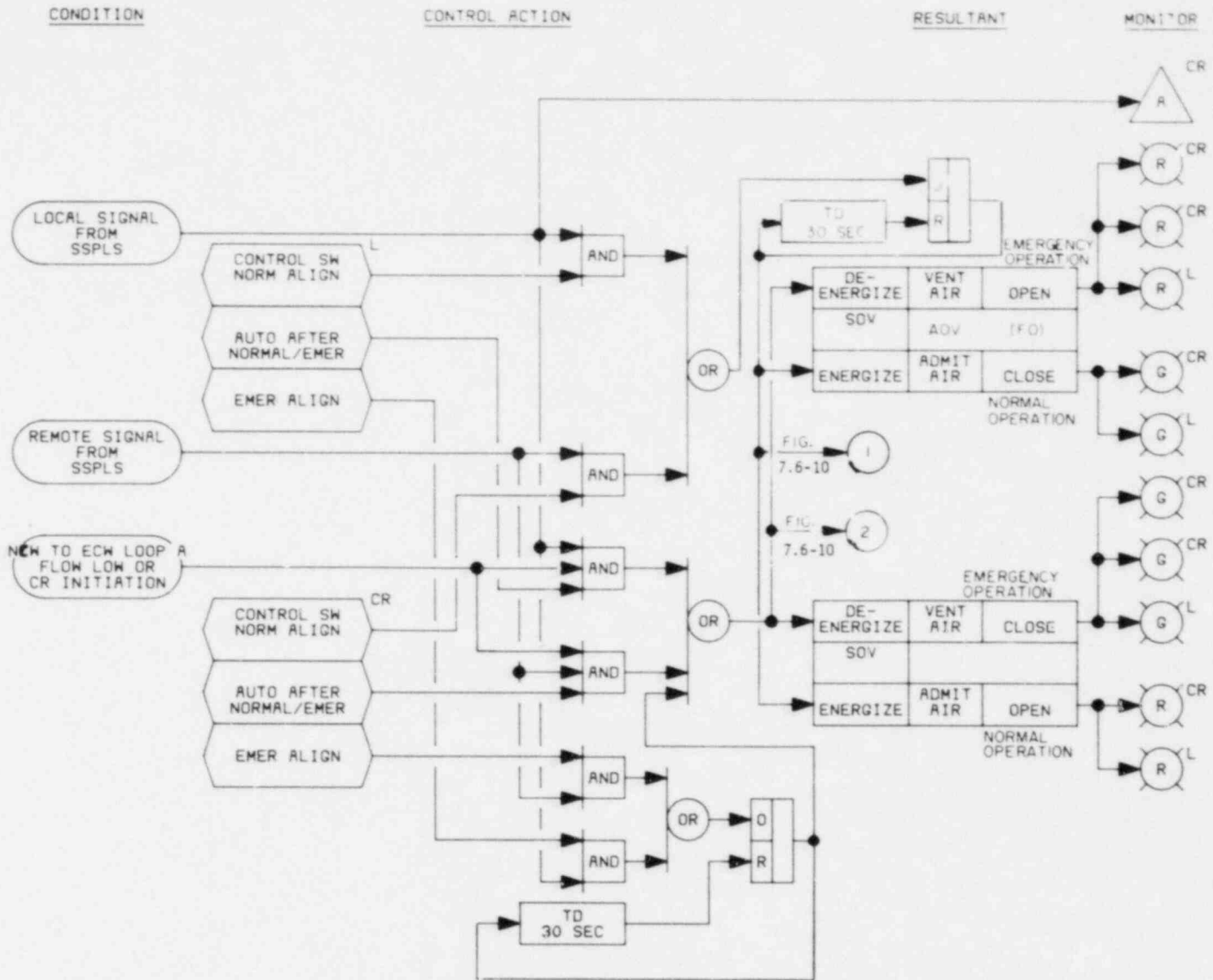


7.6-27

Amend. 72  
Oct. 1982

FIGURE 7.6-9  
 EMERGENCY CHILLED WATER SYSTEM **NEW** TO  
 ECW ISOLATION VALVES





7.6-27

Amend. 72  
Oct. 1982

FIGURE 7.6-9  
EMERGENCY CHILLED WATER SYSTEM NCV TO  
ECW ISOLATION VALVES

- o Steam Flow - Steam flow is sensed at a flow element in the outlet line from the superheater by a differential pressure transmitter. The differential pressure signal is compensated for temperature and pressure variations and linearized to provide a mass flow signal.
- o Feedwater Flow - Feedwater flow is sensed at a flow element in the inlet line to the steam drum by a differential pressure transmitter. The differential pressure signal is corrected for temperature variations and linearized to provide a mass flow signal.

#### 7.7.1.5.2 Main Feedwater Isolation

Isolation of the main feedwater supply is provided to mitigate the consequence of the loss of feedwater to a steam drum, a steam line break, or to prevent superheater flooding.

Isolation of the feedwater supply to the affected loop in the event of a steam generator system feedwater leak will ensure integrity of the feedwater supply to the two unaffected loops and mitigates the consequence of flooding damage to other equipment. This protection is provided by automatic closure of the steam drum isolation valve and both feedwater control valves upon sensing a low steam drum pressure (500 psig) signal and automatic closure of both feedwater control valves and feedwater valve isolation upon sensing a steam generator building flooding (temperature and humidity) signal.

In the event of a steam line break, steam drum dryout may occur and would result in damage to the steam generator loop upon re-introduction of feedwater. Protection against the re-introduction of feedwater is provided by the closure of the feedwater isolation, the steam drum isolation, and control valves on low steam drum pressure (500 psig) signal.

In the event of a failure in the drum water level control components, an overflowing condition might result in flooding of the steam drum and superheater. Protection against this is provided by three redundant water level sensors and by trip functions which close the feedwater valves at two steam drum levels. The first trip level, 8 inches above normal water level, closes the feedwater steam drum isolation valve, and the feedwater control valves. The second trip level, 12 inches above normal water level, closes the feedwater isolation valve.

Protection against flooding of the superheater during steam generator auxiliary heat removal is discussed in Section 5.6.1.

#### 7.7.1.5.3 Operational Considerations

##### Normal Operations

The steam drum level controller utilized for feedwater control valve operation is located in the control room back panels. The operator control station for the controller is located on the main control panel in the control room.

- o Control Building Fire Detection
- o Emergency Diesel Generators
- o Switchyard and Station Electrical Distribution
- o Direct Heat Removal Service

The layout of Section A of the main control panel is designed to minimize the time required for the operator to evaluate the system performance under accident conditions. Deviations from predetermined conditions are alarmed and/or indicated so that corrective action may be taken by the operator.

The control room also includes control and instrumentation equipment that is used infrequently or for which controlled access is desirable. Included in this control room back panel area are power distribution, chilled water, containment instrumentation, recirculating gas, heat transport, steam generator, heating ventilation and air conditioning, annunciator electronics, turbine, balance of plant, plant control, plant data handling and display system multiplexers, flux monitoring, radiation monitoring, reactor shutdown and containment isolation panels.

#### 7.9.2.4 Main Control Board Design

The Main Control Panel is an open U-shaped, stand up vertical panel as shown in Figures 7.9-1 (plan view) and 7.9-2 (side view). There are 3 significant features of the control board mechanical design: seismic capability; separation of redundant safety related equipment and wiring; and modular construction of switch, indicator and control equipment.

Since the Main Control Panel includes safety related equipment, the sections including this equipment are designed to Seismic Category I and qualified in accordance with IEEE Std. 323 and IEEE Std. 344. Structures, wiring, wireways, and connectors are designed and installed to ensure that safety related equipment on the control panel remains operational during and after the SSE. The Main Control Panel is constructed of heavy gauge steel within appropriate supports to provide the requisite stiffness.

Within the boundaries of the Main Control Panel Sections, modules are arranged according to control functions. Fire retardant wire is used. Modular train wiring is formed into wire bundles and carried to metal wire ways (gutters). Gutters are run into metal vertical wireways (risers). The risers are the interface between external wire trays feeding the panel and Main Control Panel wiring. Risers are arranged to maintain the separated routing of the external wire trays. (See Figures 7.9-3 and 7.9-4).

Mutually redundant safety train wiring is routed so as to maintain separation in accordance with the criteria of IEEE Std. 384. A minimum of six inches air separation is maintained between wires associated with different trains. Where such air separation is not available, mechanical barriers are provided in lieu of air space.

The Main Control Panel protection system circuits are designed and selected to ensure that system performance requirements are met and channel integrity and independence are maintained as required by IEEE Std. 279. Power division separation and isolation are maintained in accordance with the requirements of IEEE Std. 308.

### 7.9.3 Local Control Stations

Local control panels are provided for systems and components which do not require full time operator attendance and are not used on a continuous basis. In these cases, however, appropriate alarms are activated in the Control Room to alert the operator of an equipment malfunction or approach to an off-normal condition.

### 7.9.4 Communications

Communications are provided between the Control Room and all operating or manned areas of the plant. In addition to public address and interplant communications and the private automatic exchange (used for in-plant and external communications) a sound powered maintenance communication jacking system is provided. Redundant and separate methods of communication between the control room and other TVA generating plants is also provided.

### 7.9.5 Design Evaluation

Following the Three Mile Island accident, a large task force was formed for the purpose of performing a thorough review of the CRBRP Control Room design. This overall review was divided into three parts; a planning phase, a review phase, and assessment and implementation phase. Following the task force effort, NUREG-0700 was issued. NUREG-0700 is similar in intent to the CRBRP Control Room design evaluation.

#### 7.9.5.1 Planning Phase

In the planning phase the objectives and scope of the task force were identified, and criteria were established for personnel selection. A charter was developed which contained the scope and objectives, and personnel selection was accomplished.

The task force charter required a review of the Control Room design and the operating procedure outlines to ensure that the systems designs, the integration of the systems, and the man-machine interfaces properly supported safe operations of the plant during both normal and abnormal conditions. A task analysis was established for observing the operator conducting various duties. Specific items included in the review are:

1. Overall Control Room and individual panel designs and features, and their interface with the operator.
2. System and overall plant operating procedure outlines.
3. Administrative approaches for plant operations.
4. Recommendations from other Key System Review Task Forces.\*
5. Recommendations made by NRC and other parties as a result of the Three Mile Island occurrence.
6. Computer utilization by the operators.
7. Operator training requirements.
8. Remote shutdown capabilities and safety system status indication in the Control Room.

Criteria were established for personnel selection of those to participate on the task force. Nuclear experience was considered necessary in the areas of design, analysis, operations, testing, maintenance, and training. Personnel whose background included sodium plants and light water plants were selected. Licensed and qualified operators were considered mandatory. Personnel with human factors education and experience both inside and outside the nuclear industry were included.

Human factors considerations were emphasized in the planning phase. Previous Control Room design efforts had attempted to optimize the man-machine interface. However, a major objective of the Control Room Task Force was to re-evaluate this interface. Prior to the evaluation effort a seminar was held, under the direction of three leading human factors personnel, to teach the Task Force disciplined methods for considering human factors. Based on this training and further assistance from human engineers, check lists were prepared to evaluate the man-machine interface.

\*See Reference 7.9-1

#### 7.9.5.2 Review Phase

In the review phase extensive analysis of plant events were conducted. Functional analyses were made of the operator in his response to automatic equipment actions, manual actions which had to be performed in the Control Room, and manual actions required by operators external to the Control Room. More than 200 walk-throughs of plant events were conducted.

The Control Room design and operating instructions were thoroughly reviewed in four areas:

1. Proper identification of systems to be operated from the Main Control Room.
2. Proper staffing of the Control Room.
3. Proper overall layout of the Control Room to enhance the man-machine interfaces and support the integrated operation of plant's systems.
4. Proper layout and design of individual Control Room panels, instruments, indicators, and controls to enhance the man-machine interface and support the integrated operations of the plant's systems.

A full scale mockup of the Control Room was used. The events chosen to be evaluated were carefully selected so they would umbrella all of the operations that are either expected to occur or might be postulated to occur over the life of CRBRP. The off-normal events include plant responses to single and multiple failures.

The methodology of performing this review consisted of using three groups of people; simulators, operators, and evaluators.

The Simulators analyzed the events which were to be evaluated prior to the walk-throughs and then, during the walk-through evaluations, simulated the control panel indicators. Some of these events had previously been analyzed via computer while other events required additional computer runs to enable mocking up the panel as it would appear to the operator. The control panels were mocked up by the Simulators to represent the changing plant conditions and the information flow into the Control Room during the event. This made the walk-through as realistic as possible.

The Operators played the part of the Control Room operators and carried out the steps of the procedure being evaluated. They touched each switch they were required to operate, and observed each indicator which was part of the particular event.

The Evaluators included a Human Factors Engineer and a Systems Engineer. Their function was to fill out the Operating Sequence Diagram and the evaluation sheets for each procedure and event reviewed.



As problems or concerns were encountered, recommendations were made. These were, in some cases, of a broad nature and reflected the need for reconsideration of decisions made in the four most important evaluation areas described above. Other problems and concerns related to specific details of the Control Room design or the procedure outlines.

#### 7.9.5.3 Assessment and Implementation Phase

The evaluation and implementation of the recommendations started with a check of the consistency of all of the recommendations by the task force. Small models of the overall Control Room and Main Control Panel were made assuming all recommendations were incorporated into the design. The recommendations were modified based on the small model to provide a coordinated and consistent set of final recommendations. Senior Project Management reviewed the final set of recommendations and issued them to the Project line organization for assessment and implementation. The cognizant design engineers have two choices. They can either accept the recommendation if it is valid, and include it into the plant design via normal procedures, or reject the recommendation and provide adequate justification if the recommendation is invalid. Each assessment is reviewed and approved by senior project management.

#### 7.9.5.4 Conclusions

The Control Room Task Force Design Review is documented in further detail in Reference 7.9-1. In September 1981, NUREG-0700 entitled "Guidelines for Control Room Design Review" was issued. A comparison between these two documents leads to the conclusion that although NUREG-0700 was issued after the Control Room Task Force Review, the intent of the NRC in promulgating NUREG-0700 is similar to the Project's intent in performing the Control Room Task Force Review, and the intent of NUREG-0700 is believed met by CRBRP.

Reference:

1. Summary Report on the Conduct of the Clinch River Breeder Reactor Plant (CRBRP) Key System Reviews, February 1982.

20 | 11 in. diameter opening. The increased thickness of the EVTM floor valve in radial and axial direction provide the additional shielding required for the much higher radiation source which passes through an EVTM floor valve (spent fuel assembly) compared to an AHM floor valve (IVTM port plug).

44 | The stepped upper and lower steel plates of the floor valves, concentric to the valve port, (see Figure 9.1-18) prevent diffusion and radiation streaming through the minimal mating surface gaps. These design features limit the transient dose rate at the surface to less than 200 mrem/hr during transfer of radioactive components, and 5 mrem/hr when closed over the reactor ports.

20 | The floor valve is sealed to the fuel transfer port adaptor by double seals, and bolted to the adaptor flange. The movable circular disk which closes off the port opening in the valves is also sealed by double seals.

#### 9.1.4.6.3 Safety Evaluation

44 | 49 | The radial shielding limits the dose rate on the floor valve surface to less than the criteria in Sections 12.1.1 and 12.1.2 during transfer of the highest powered spent fuel assembly (for the EVTM floor valve). The floor valve is considered a piece of equipment whose main function is to permit transfer of radioactive components, both fueled and non-fueled, between a machine and a facility. The radiation source is transient and short term (less than 1 min per transfer) in nature. Hence, it results in a low integrated dose.

44 | Another function of the floor valves is to provide axial shielding to replace that normally provided by the port plugs. The axial shielding limits the dose rate to personnel to 5 mrem/hr when placed over a reactor port and to 0.2 mrem/hr when placed over EVST or FHC ports. Personnel cannot receive a direct axial dose because of the large diameter of the floor valve. In addition, the valve is covered by a mating machine much of the time. In all cases, sufficient axial and radial shielding for the EVTM and AHM floor valves is provided to limit the integrated dose to less than 125 mrem/quarter, and dose rates to the zone criteria of section 12.1.

59 | The floor valve has adequate seals to prevent excessive radioactive release to the RCB and RSB operating floors. Accidental cover gas release through inadvertent opening of a floor valve in the absence of a mating fuel handling machine (EVTM, AHM) on top of the floor valve is prevented by interlocks. One interlock prevents energizing the valve operating motor unless a mating machine is on top of the floor valve. (Electrical power to the floor valve motor is supplied by connection to the mating machine.) Other interlocks prevent (1) depressurizing the buffer gas zone, and (2) raising the closure valve extender, unless both the closure valve and the floor valve are in their closed positions.

As discussed in Section 15.5.2.4, an unlikely accident releasing radioactive cover gas from the reactor leads to a site boundary dose well below the guideline value of 10CFR20.

#### 9.1.4.7 Safety Aspects of the Reactor Fuel Transfer Port Adaptor and Fuel Transport Port Cooling Inserts

The reactor fuel transfer port adaptor (see Figure 9.1-19) is positioned on top of the reactor fuel transfer port and extends from the reactor head to the bottom of the floor valve which is located at the elevation of the RO3 operating floor. It serves as an extension of the reactor cover gas containment and provides shielding when irradiated core assemblies are removed from the reactor. The adaptor also guides cooling air from an air blower to a cooling insert inside and below the adaptor.

The function of the cooling inserts, located around the EVST and FHC fuel transfer ports as well as the reactor port (see Figure 9.1-19), is to remove decay heat should an irradiated core assembly in a sodium-filled CCP become immobilized in a fuel transfer port during transfer between the reactor vessel, EVST or FHC and the EVTM.

##### 9.1.4.7.1 Design Basis

The design bases for shielding and radioactive release of the fuel transfer port adaptor are the same as for the EVTM (see 9.1.4.3.1). The reactor, EVST, and FHC fuel transfer port cooling inserts have the capacity to remove decay heat from 20 KW irradiated core assemblies in sodium-filled CCPs to prevent exceeding the 1500<sup>o</sup>F spent fuel cladding temperature limit specified for unlikely or extremely unlikely events (Table 9.1-2).

##### 9.1.4.7.2 Design Description

The reactor fuel transfer port adaptor extends from the upper surface of the fuel transfer port in the reactor head to the operating floor, see Figure 9.1-19. The upper surface of the reactor fuel transfer port adaptor consists of a flange which is bolted to the floor valve and provides the sealing surface for the double seals on the lower surface of the floor valve. Shielding is provided by a thick, annular lead cylinder surrounding the adaptor cover gas containment tube over its entire length to limit the dose rate at the shield surface to less than the limits given in Sections 12.1.1 and 12.1.2. The lower part of the adaptor is bolted to the reactor head during refueling only.

The reactor fuel transfer port cooling insert extends from the top flange of the adaptor to the fuel transfer port nozzle. The cooling insert uses a cold wall cooling concept, similar to the EVTM. The CCP containing a spent fuel assembly is cooled by thermal radiation and conduction across the argon gas gap to the cold wall which forms the confinement barrier for the reactor cover gas. Ambient air is blown down the outside annulus of the cooling insert, and discharges into the reactor head access area. Air flow from the blower is adequate to limit the cladding temperature of a 20 KW fuel assembly to less than 1500<sup>o</sup>F.

#### 9.6.5.4 Testing and Inspection Requirements

All components are tested and inspected as separate components and as integrated systems. Velometer readings are taken to ensure that all systems are balanced to deliver and exhaust the required air quantities. All water coils are hydraulically tested for leakage prior to being placed in service. Capacity and performance of the fans are tested according to the Air Moving and Conditioning Association requirements prior to operation of the plant.

#### 9.6.6 Steam Generator Building HVAC System

##### 9.6.6.1 Design Basis

##### 9.6.6.1.1 Steam Generator and Auxiliary Bay HVAC System

The Steam Generator and Auxiliary Bay HVAC System is a safety-related system designed to provide filtered and conditioned air to the Steam Generator Loop Cells, the Auxiliary Bay Cells and the Intermediate Bay IHTS Cells to permit continuous routine personnel access during normal operation and to ensure operability of the equipment under all conditions. The HVAC System serving these areas is designed to:

- a) Maintain 100°F max. within all areas during normal operation.
- b) Maintain 120°F max. within all areas under single failure of an HVAC System component.
- c) Maintain 120°F max. within all areas under loss of cooling from the Normal Chilled Water System.
- d) Maintain the ventilation rate within all areas under all operating conditions.
- e) Comply with the single failure criterion of Regulatory Guide 1.53.
- f) Operate from the Class IE AC power supply during loss of off-site power.
- g) Maintain 120°F max. within the Auxiliary Feedwater Pump Cells during off-normal conditions.
- h) Provide ducted cool air directly to the lube oil cooling panels.
- i) Provide exhaust ductwork for the Intermediate Sodium Pump Drive to exhaust hot discharge air directly outside to atmosphere.
- j) Provide ducted exhaust from the Intermediate Sodium Cold Trap.
- k) Provide design features to mitigate the consequences of a sodium fire.

##### 9.6.6.1.2 Steam Generator Building Intermediate Bay HVAC Systems

The Steam Generator Building Intermediate Bay HVAC Systems are safety-related systems designed to provide filtered and conditioned air throughout the

Intermediate Bay (except IHTS cells) to permit continuous routine personnel access and to ensure operability of the equipment during normal operation. The HVAC System serving these areas is designed to:

- a) Maintain 95°F max. within all areas during normal operation.
- b) Maintain 120°F max. within all areas under single failure of an HVAC system component.

The Air Handling Unit with its two (2) 100% capacity redundant supply fans are located in Steam Generator Loop 1 Cell on a platform at E1. 852'-6". Identical arrangement of Air Handling Units and their supply fans exist in Loops 2 and 3 respectively. Each Air Handling Unit is connected to an independent missile protected air intake structure located on the north side of the SGB-IB roof by ductwork with redundant fire dampers. Each air handling unit consists of a mixing plenum with an outside and return air intake damper, pre and after filter, cooling coil and access sections. Downstream of the cooling coil section, a sufficiently long end access section is provided for the connection of the 100% supply fans. The length of the end access section is selected to permit equalization of the air flow through the cooling coils required by the off-center location of the fans. The length of the other access sections is determined by the maintenance requirements of the individual components. The fan sections are connected to the end access section and are followed by manual dampers (normally locked open), flexible connections, fans, flexible connections and automatic isolation dampers. The "Y" duct section connects with the supply ductwork which serves the respective cell. In cells 244, 245, and 246, a branch duct is connected to the sodium pump drive lube oil cooling panels from the main supply duct. The air is then relieved to the cell.

Two (2) Unit Heaters are located in each SG Loop Cell at E1. 816'-0". One Unit Heater is located in each Steam Drum Cell at E1. 846'-0".

The return air is transferred from cell to cell to one of two (2) 100% redundant exhaust fans, located in each of the three (3) SGB Loop Cells at E1. 851'-6" and 861'-0". The discharge side of each fan is connected to a flexible connection and followed by ductwork and an automatic isolation damper. The damper section is connected to the discharge ductwork which either returns the air to the cell for recirculation in the system or exhausts it to atmosphere through a missile protected exhaust structure. The exhaust ductwork is provided with redundant fire dampers to create a controlled vent path. The exhaust stack is provided with redundant motorized dampers to allow closure after initial venting. A tritium sampler, monitors the air discharge for release of tritium.

Exhaust from the two (2) cold traps located in each Steam Generator Cell at E1. 806'-0" connects to the Steam Generator Cell exhaust ductwork.

The IHTS pump motor draws the air required for cooling from the cell. Exhaust ducts are provided with redundant fire dampers and are connected to the air discharge flanges of the IHTS pump motor and discharge the hot air to the atmosphere through the steam vent structure.

The Steam Generator Building Aerosol Release Mitigation System, an engineered safety feature whose operation is described in Section 6.2.7, is located in each SGB loop. The ESF consists of redundant safety-related closure dampers, relief vent dampers, and aerosol detectors. The closure dampers are fire dampers preceding each loop's air handling unit, following each loop's IHTS pump motor and exhaust fans, and clutch-type motorized exhaust dampers. Controlled release of aerosols from the SGB is accomplished by closure of the fire dampers and the controlled venting of the aerosols through the vent stack until terminated by the clutch-type motorized exhaust dampers. Additionally, the HVAC systems of the remaining Nuclear Island Buildings will be isolated

from the outside atmosphere by either closing dampers or shutting off supply and exhaust fans. These actions are initiated by redundant sets of safety-related aerosol smoke detectors in the SGB. The relief vent dampers are also fire actuated dampers. The P&ID for SGB Loop 1, 2 and 3 is Figure 9.6-12, 9.6-13, and 9.6-14, respectively.

Two (2) Unit Coolers provide conditioned air for the electric driven Auxiliary Feedwater Pump cells (one cooler for each cell).

The supply air is distributed to the cells by an independent ductwork system to satisfy the cooling requirements.

The unit cooler filters maintain the cleanliness of the air supply (for initial start-up only). The cooling coils provided in the unit coolers, along with their instrumentation and controls, maintain the Indoor Design Conditions.



The Unit Coolers are located in the Auxiliary Feedwater Pump Cells 204A and B at El. 733'-0". The unit coolers consist of disposable filters, cooling coils and a V-belt driven centrifugal fan. The fan discharge is connected to an independent ductwork that serves the SGAHRS water storage tank at El. 746'-0", Auxiliary Feed Pump Cells 204A and B and Cell 204 at El. 733'-0". The return air to the unit coolers is not ducted.

An outside air duct connected to a missile protected outside air intake located at SGB auxiliary bay wall at El. 880'-0" with a supply fan provides the necessary ventilation for the auxiliary feedwater pump (electric driven) cells. An electric duct heater is installed in the outside air duct downstream of the supply fan to preheat the outside air during winter operation. An outside air filter is installed in the outside air duct to maintain the cleanliness of the outside air supply.

Two (2) 100% capacity unit coolers provide conditioned air to the Turbine Driven Auxiliary Feedwater Pump cell. The supply air is distributed to the cell by an independent ductwork system to satisfy the cooling requirements. The unit cooler filters maintain the cleanliness of the supply air (for initial start-up only). The cooling coils provided in the unit coolers along with their instrumentation and controls, maintain the supply air temperature to satisfy the Indoor Design Conditions.

The 100% unit coolers are located on a platform at El. 746'-0" in Cells 202 and 202B. One of the unit coolers is enclosed with a 3 hour fire rated wall. Each unit cooler consists of a disposable filter, cooling coil, and a V-belt driven centrifugal fan. Each unit cooler discharges air to the cell independently. Return air to the unit cooler is not ducted.

An outside air duct connected to a missile protected outside air intake located at the SGB auxiliary bay west wall at El. 880'-0" with a supply fan provides the necessary ventilation for the auxiliary feedwater pump (turbine driven) cells. An electric duct heater is installed in the outside air duct downstream of the supply fan to preheat the outside air during winter operation. An outside air filter is installed in the outside air duct to maintain the cleanliness of the outside air supply.

## 2. Intermediate Bay (SGB-IB) System

One of the two recirculating type Air Handling Units with two (2) 100% capacity supply fans provides conditioned supply air to the SGB-IB areas above El. 836'-0" and the normal chiller rooms. The supply air is distributed by supply ductwork to the various areas to satisfy the Ventilation Requirements. The Air Handling Unit

All Normal Chilled Water piping and piping components located outside of the RCB are built to the requirements of ANSI B31.1, "Power Piping", whereas heat exchangers and pressure vessels outside the RCB are built to the requirements of ASME Boiler and Pressure Vessel Code, Section VIII.

The Normal Chilled Water System is terminated by two sets of ASME, Section III, Class 3 isolation valves, where cross-connections are made to the Emergency Chilled Water System. Upon loss of Normal Chilled Water Supply to the Emergency Chilled Water System headers, the isolation valves are closed automatically, and the Emergency Chilled Water System starts. Where the Normal Chilled Water System penetrates the RCB, one remote manually actuated ASME Section III, Class 2 isolation valve is provided on each line. The piping on the RCB side of this valve up to the next manual isolation valve is ASME Section III, Class 2.

The components served by the Normal Chilled Water System are listed in Table 9.7-1. The major system component design data are listed in Table 9.7-2.

#### 9.7.1.3 Safety Evaluation

One 20 percent capacity standby chiller unit is provided to ensure continuous cooling capability in case of a malfunction of a chiller unit. One 20 percent capacity standby chilled water circulation pump is also provided for the same purpose. The diversity of the cooling loads provides additional refrigeration margin for the system.

In addition to these considerations, Section 9.7.3 lists system design features intended to prevent water/sodium interactions. Pipe break analysis for this moderate energy fluid system will be provided in the FSAR.

#### 9.7.1.4 Tests and Inspections

The system is tested and inspected as separate components at the manufacturer's facilities and as an integrated system prior to plant operation. All water flow rates are balanced and set to the design flow conditions. Periodic inspection of the equipment is scheduled to ensure the proper operation of the system.

All chilled water lines penetrating the containment shall be provided with vents and drains to permit drainage. Normal chilled water supply and return headers immediately upstream and downstream of the containment isolation valves shall be drainable.

Vents and drains will be opened to permit drainage and to permit transmission of containment test pressure to the closed isolation valves.

### 9.7.1.5 Instrumentation Application

Chilled water system control panels are located in the area of the water chillers. These panels include control switches, monitors, and system alarms. Local alarms are provided for the following conditions:

- a. Expansion tank high water level
- b. Expansion tank low water level
- c. Leak detection and isolation (described in Section 9.7.3)
- d. High chilled water discharge temperature
- e. Water chiller trip alarm (includes following chiller malfunctions):
  1. low chilled water temperature
  2. high condensing pressure
  3. low refrigerant temperature or pressure
  4. low chilled water flow
  5. low condenser water flow
  6. low oil pressure
  7. high shaft vibration
  8. high bearing temperature
  9. high motor temperature

59 | 15 A common system annunciator for "a" through "e" above is provided in the control room to indicate trouble in the Normal Chilled Water System. In addition, an annunciator alarm is provided for condition "e" in the control room, with first out indication locally for conditions "e.1" through "e.9" above. 44

### 9.7.2 Emergency Chilled Water System

#### 9.7.2.1 Design Basis

59 | The function of the Emergency Chilled Water System is to provide chilled water for systems listed in Table 9.7-3. The Emergency Chilled Water System has a chilled water operating temperature of less than 60°F and an operating pressure of less than 150 psig. The system is designed to meet the following design criteria: 44

If during normal operation normal chilled water supply is interrupted, flow switches in the emergency chilled water supply header will close the ASME III Class 3 isolation valves between the two systems and automatically start the Emergency Plant Service Water System and then the Emergency Chilled Water System.

In addition to these considerations, Section 9.7.3 lists system design features which are provided to prevent a water/sodium reaction. Pipe break analysis for this moderate energy fluid system will be provided in the FSAR.

#### 9.7.2.4 Tests and Inspections

After testing each individual component of the system, the entire system is tested prior to plant operation. Instruments and controls are provided for periodically testing the performance of the system during normal plant operation or scheduled shutdown. All water flow rates are balanced and set to the design flow conditions. Periodic inspections of equipment are scheduled to ensure the proper operation of the system. In-service inspections will be conducted according to ASME XI, as described in Section 9.7.2.1.g.

All chilled water lines penetrating containment shall be provided with vents and drains to permit drainage. Emergency chilled water supply and return lines immediately upstream and downstream of the containment isolation valves shall be drainable. Vents and drains will be opened to permit drainage and to permit communication of containment test pressure to the closed isolation valves.

#### 9.7.2.5 Instrumentation Application

Chilled water system control panels are located in the area of the water chillers. The panels include the control switches, monitors, and system alarms. Local alarms are provided for the following conditions:

- a. High chilled water temperature
- b. Low chilled water flow
- c. Normal chilled to emergency chilled changeover valve malfunction
- d. Expansion tank high water level
- e. Expansion tank low water level
- f. Leak detection and isolation (described in Section 9.7.3)
- g. Water chiller trip alarm (includes following chiller malfunctions):

1. low chilled water temperature
2. high condensing pressure
3. low refrigerant temperature or pressure
4. low chilled water flow
5. low condenser water flow
6. low oil pressure
7. high shaft vibration
8. high bearing temperature
9. high motor temperature

59 | Individual annunciator alarms are provided for conditions "a" through "c" above in the control room main control board and locally for both loops A and B. A common system annunciator alarm for conditions "d" through "g" is provided on the control room main control board and locally for both loops A and B. In addition, an individual annunciator alarm is provided for condition "g" on back panel with first out indication locally for conditions "g.1" through "g.9" listed above. 44

Amend. 59  
Dec. 1980

TABLE 11.2-5

## EQUIPMENT DESCRIPTION OF LIQUID RADWASTE SYSTEM

Equipment Description	Capacity (gal)	Number of Components	Throughput Rate (gpm)	Quality Class (RG 1-26)*	Seismic Category (RG 1-29)*	Codes	Material	Design Temperature °F	Design Pressure
Piping and Valves	-	-	1-125	D	III	ANS B31.1	SS	200	150 PSI
IALL/LALL Filters	-	2/2	125/50	D	III	ASME VIII	SS	200	150 PSI
IALL Collection Tank	24700	2	-	D	III	API 650	SS	200	Atmos.
LALL Collection Tank	2400	2	-	D	III	API 650	SS	200	Atmos.
Evaporator Prefilters	-	4	10	D	III	ASME VIII	SS	200	150 PSI
Evaporators	-	2	10	D	III	ASME VIII	SS	200	150 PSI
Distillate Demineralizer	-	4	10	D	III	ASME VIII	SS	200	150 PSI
Resin Traps	-	4	10	D	III	ASME VIII	SS	200	150 PSI
IALL Distillate Storage Tank	24700	2	-	D	III	API 650	SS	200	Atmos.
LALL Monitoring Tank	2400	2	-	D	III	API 650	SS	200	Atmos.
Pumps	-	-	1-125	D	III	Manufacturers Std.	SS	200	Atmos.
Caustic Neutralizing/Storage Tank	2500	1	-	D	III	API 650	SS	200	Atmos.
Caustic Feed Tank, Antifoam Tank, Resin Feed Tank	150								
Acid Feed Tank	700	1	-	D	III	API 650	HNA	200	Atmos.

\* RG - Regulatory Guide

11.2-20

Amend. 72  
Oct. 1982

TABLE 11.2-5A

INDOOR RADIOACTIVE WASTE TANKS - PROVISIONS TO  
PREVENT AND CONTROL OVERFLOW CONDITIONS

Tanks	Provisions
<p>1. <u>Intermediate Activity Level Liquid (IALL) Collection Tank A &amp; B</u></p>	<p>(a) Liquid Level Indicator in Radwaste Control Room.</p> <p>(b) High and Low Liquid Level Annunciator Alarms in Radwaste Control Room.</p> <p>(c) IALL Collection Tanks sized so that the two of them can hold the entire system inventory overflow for both tanks is connected to the radwaste sump.</p> <p>(d) Cell walls are capable of containing any leakage. The contained liquid is returned to the radwaste sump via floor drains.</p> <p>(e) A common Main Control Room alarm from the Radwaste Control Room to annunciate abnormal system conditions in the Radwaste Area.</p>
<p>2. <u>Low Activity Level Liquid (LALL) Collection Tank A &amp; B</u></p>	<p>(a) Liquid Level Indicator in Radwaste Control Room.</p> <p>(b) High and Low Liquid Level Annunciator/ Alarms in Radwaste Control Room.</p> <p>(c) Overflow for both tanks is connected to the radwaste sump.</p> <p>(d) Floor drains are provided to collect and return any leakage to the radwaste sump.</p>

## 11.4 PROCESS AND EFFLUENT RADIOLOGICAL MONITORING SYSTEM

### 11.4.1 Design Objectives

Process radiation monitors are provided to allow the evaluation of plant equipment performance and to measure, indicate and record the radioactive concentration in plant process and effluent streams during normal operation and anticipated operational occurrences. The monitors are provided in accordance with CRBRP (Section 3.1) Design Criterion 56.

Radiation monitoring of process systems provides early warning of equipment malfunctions, indicative of potential radiological hazards, and prevents release of activity to the environment in excess of 10CFR 20 limits. Each monitor will be equipped with a loss-of-signal instrument failure alarm and a high level alarm, (a high-high level alarm is also provided when required). These alarms alert operating personnel to channel malfunction and excessive radioactivity. Corrective action will then be manually or automatically performed.

Monitoring of liquid and gaseous effluents under normal operating conditions will be in accordance with NRC Regulatory Guide 1.21 and any activity released will be within limits established in 10CFR20.

The number, sensitivities, ranges, and locations of the radiation detectors will be determined by requirements of the specific monitored process during normal and postulated abnormal (accident) conditions. All monitors will be designed so that saturation of detectors during a severe accident condition will not cause erroneously low readings. Monitoring during severe post accident conditions will be accomplished by the high-range gamma area monitors discussed in Section 12.1.4, in conjunction with the sampling lines described in Section 11.4.2.2.1.

Radioactivity in the low level waste releases will be integrated and recorded. Control signals will be provided by the radiation monitor(s) to terminate liquid or gaseous effluent if an out-of-limit signal is recorded. The monitoring and control exerted by the process radiation monitoring equipment and the operator during any release will also be verified by periodic manual sampling and laboratory analysis in accordance with Technical Specifications. For tritiated process liquids, tritium surveillance will be by sampling and lab analysis.

All detectors will be shielded against ambient background radiation levels so that required activity measurements can be maintained. Monitors associated with accident conditions are also discussed in 3.A.3.1. Area monitors and airborne radioactivity monitors are discussed in 12.1.4 and 12.2.4, respectively. The radiological effluent sampling program is discussed in Section 11.4.3 and meets the reporting requirements of Regulatory Guide 1.21.



## 11.4.2 Continuous Monitoring/Sampling

### 11.4.2.1 General Description

The descriptive tabulation of the various continuous monitors/samplers for process and effluent radioactivity monitoring, which includes those gas and liquid monitoring devices in or associated with liquid or gas process streams considered in this discussion, is found in Table 11.4-1. The basis for selecting the locations as well as the control functions associated with the monitor, are described below.

Each continuous monitor will be equipped with power supplies, micro-processor and accessories, indication and local alarm indicator lights. Each monitor will transmit radioactivity level and alarm status information for display and logging by Radiation Monitoring equipment located in the Control Room with redundant display and logging equipment located in the Health Physics Area of the Plant Service Building. The alarms are provided to indicate instrument malfunctions or a radioactivity level in excess of the monitor's alarm setpoint. Each continuous monitor has a local indicator at the detector location to facilitate the testing and/or calibration of the equipment.

The lowest scale division of each continuous monitor's range is the maximum detector sensitivity deemed appropriate for the intended service. The range of the monitor will be a minimum of five decades above the maximum sensitivity level; and will allow for a minimum of one decade span above the monitor high-high setpoint (when high-high setpoints are employed). The effluent alarm setpoint corresponds to the alarm annunciation level dictated by the CRBRP Technical Specifications (Chapter 16.) For each monitor, a sample chamber and/or detector is selected and will be installed in such a way as to minimize sampling losses and electromagnetic and background interferences. The output of all effluent monitors will be continuously sampled and recorded by the CRBRP Plant Data Handling and Display System. The Reactor Containment Isolation Monitors (PPS), Control Room Air Intake monitors and other safety-related monitors will be powered by Class IE, redundant 120 VAC power.

### 11.4.2.2 Gaseous System Description

#### 11.4.2.2.1 Post-Accident Containment Atmosphere Monitors

The capability to monitor the containment atmosphere radioactivity level following containment isolation during an accident condition shall be provided. Three pair of penetrations, located 120° apart around the containment structure will allow air samples to be taken by mobile or portable monitors and sampling equipment. The penetrations design and locations will consider the following criteria:

1. The penetration opening on the inside of containment will be positioned to obtain a representative sample.
2. The penetration opening on the outside of containment will be positioned in an accessible area to enable connection of the monitoring and/or sampling equipment.

3. Each penetration will have two isolation valves; a remote manual controlled valve inside containment and a manual, locked valve outside containment with a blind flange.
4. The penetration design will comply with CRBRP Design Criteria Numbers 45 and 47 (Section 3.1)

Each pair of penetrations can be connected to a mobile monitor which will be utilized for continuous monitoring of the containment atmosphere. The sample is withdrawn from containment, passes through the monitor for radiation detection and returned to containment. Grab samples will also be obtained for further laboratory analysis.

#### 11.4.2.2.2 Reactor Containment Isolation Monitors

The radiation level in the head access area will be monitored by three detectors for direct gamma activity. The output of these detectors is routed to the plant protection system to initiate closure of containment isolation valves if a preset limit is reached by two out of three of the detectors.

In addition, the radiation level in containment exhaust, upstream of the isolation valves will be isokinetically monitored for gaseous activity by three gas monitors. Their output will also be provided to the PPS for initiation of containment isolation when a preset radiation level is reached by two of the three detectors.

The monitoring system will be designed to comply with IEEE 279-1971. The overall containment isolation system design and protection logic is discussed in Section 7.3. Figure 12.2-1 shows a typical block diagram of these channels and Figure 7.3-1 shows the trip logic configuration.

#### 11.4.2.2.3 Building Ventilation Exhaust Monitors

The number and location of building exhaust plenums from which potentially radioactive plant gaseous release may emanate are: One located in the Intermediate Bay (SGB-IB), nine located near the top of the RCB dome, two located in the Reactor Service Building (RSB), one located in the Radwaste Area (Bay), one located in the Plant Service Building (PSB), fourteen in the Turbine Generator Building (TGB), and three located in the Steam Generator Building (SGB). Continuous monitoring will be performed at those exhausts which could conceivably undergo a significant increase in detectable levels in radioactivity. The remaining exhausts will be sampled periodically.

The exhaust plenum located in the IB receives ventilation exhaust air from the Intermediate Bay area. A continuous air monitor (CAM) will be provided to detect particulate, radioiodine and gaseous activity in the effluent stream. The air sample will be obtained isokinetically from the exhaust, on a continuous basis. The operation of the three-channel CAM unit is described in Section 12.2.4.2.1.

The exhaust plenum located on the Radwaste Building receives ventilation exhaust air from the radwaste area. A Continuous Air Monitor (CAM) will be provided to detect particulate, iodine and gaseous activity in the effluent stream. The air sample will be obtained isokinetically from the exhaust, on a continuous basis. The operation of the three channel CAM unit is described in Section 12.2.4.2.1.

The two RSB exhausts will be continuously monitored for radioactivity releases. The first exhaust plenum located on the RSB roof which receives ventilation exhaust from the RCB will be continuously monitored for particulates, radio gases, and radioiodine activity in the effluent stream. The second exhaust plenum located on the RSB which receives ventilation exhaust from the RSB via the RSB clean-up filtration units will also be continuously monitored for particulate, gaseous and radioiodine activity.

The exhaust plenum located near the top of the RCB dome, which receives exhaust from the Containment Clean-up and Annulus Pressure Maintenance and Filtration System will be continuously monitored for particulate, radioiodine, radiogases, and plutonium activity in the effluent stream.

The 8 exhausts located at the top of the RCB dome for the Annulus Cooling Air become potential radioactivity release points only in the event of very low probability accidents beyond the design basis (e.g., Thermal Margin Beyond the Design Base). On line monitoring for particulates, radioiodines and radiogases have been provided for these exhausts in the event of such an accident.

TGB areas will be periodically grab sampled and samples will be analyzed for tritium activity.

The exhaust in the PSB receives ventilation from the combined laboratory. Samples will be collected isokinetically by a particulate (and iodine, if required) filter and analyzed for isotopic content in the Counting Room.

Certain effluent radiation monitors are identified as Accident Monitoring Instrumentation in Table 11.4-1. As such, these monitors will meet the requirements of Section 7.5.11 of the PSAR.

The reporting of effluent radioactivity released from the CRBRP will be consistent with the guidelines established in Regulatory Guide 1.21. This reporting will be based upon the results of Counting Room analysis of effluent samples obtained at each location listed above.

#### 11.4.2.2.4 Condenser Vacuum Pump Exhaust, Deaerator Continuous Vents and Turbine Steam Packing Exhauster Tritium Samplers

A gas sample will be continuously withdrawn from each one of the condenser vacuum pump air, deaerator exhaust, and turbine steam packing exhauster air into tritium samplers comprised of silica gel dessicant column to enable determination of tritium activity to indicate unacceptable tritium diffusion in the steam generators. The sample will be analyzed using liquid scintillation techniques in the counting room.

#### 11.4.2.2.5 Control Room Inlet Air Monitors

The main and remote Control Room air intakes will each be continuously monitored by two redundant monitors. These three channel (particulate/radioiodine/radlogas) CAMs will detect radioactivity in the air intakes and will determine which intake should be used during the Control Room Isolation condition. Details concerning the sequence of operation during Control Room Isolation are given in Section 9.6.1.3.4.13. A fifth three channel CAM will be installed downstream of the parallel HVAC make-up air filters to monitor the performance of the HEPA filter trains. A detailed description of the operation of each of these CAM units is given in Section 12.2.4.2.1.

#### 11.4.2.2.6 Inerted Cell Atmosphere Monitors

The capability for monitoring the atmosphere of each individual inerted cell for high radioactivity will be accomplished by three methods. One method is the sequential sampling of groups of cells with on-line gas monitors as described in 3.A.1.4.2. Each monitor shall have a trip signal determined by the process system to initiate activation of cell purging equipment. In addition, mobile particulate, iodine and gas monitors are provided to sample any individual inerted cells atmosphere, as described in 12.2.4.

Finally to provide a sensitive method of sodium leak detection, particulate monitors are provided for continuous monitoring of inerted cells within the RCB containing components contacting radioactive sodium. These monitors will alarm for activated sodium present in the cells atmosphere. The individual inerted cells that are continuously monitored for sodium leak detection are listed in Table 3.A.1-3.

#### 11.4.2.2.7 RAPS and CAPS Monitoring

Gas monitors will be provided for the Radioactive Argon Processing System (RAPS) and Cell Atmosphere Processing System (CAPS). A monitor will be located at the CAPS inlet for controlling the rate of radioactivity input. Monitors will also be located at the output of these systems to ascertain that the radionuclide activity of the processed gas is within limits for reuse in RAPS or within 10 CFR 50, App. I and ALARA limits for those gases exhausted to the H&V system by CAPS.

#### 11.4.2.2.8 Safety-Related Monitors

Certain monitors which provide control signals to safety related process systems or are used to monitor safety related systems are classified as safety related monitors. These monitors will be supplied with Class 1E power from redundant vital AC buses and will meet the requirements described in Section 7.1. Safety related monitors are identified in Table 11.4-1.

These monitors will each have a dedicated Display and Control Unit (DCU) in the Control Room. The DCU will also meet the requirements described in Section 7.1 and will be supplied with Class 1E power. The DCU's will be located in the back panel area of the Control Room adjacent to the Radiation Monitor Console (computer).

### 11.4.2.3 Liquid Systems Description

#### 11.4.2.3.1 Radwaste Disposal System Liquid Effluent Monitor

Effluents from the Liquid Radwaste Disposal System are discharged into the cooling tower blowdown. A liquid radioactivity detector will continuously monitor, record, and control the activity released to the cooling tower blowdown stream. The blowdown flow rate available for liquid waste dilution and compliance with 10CFR20 will be considered in establishing a high radiation set-point for this monitor. A high radiation signal will automatically close the isolation valve in the discharge line and alarm in the control room.

Frequent composite samples of the blowdown downstream of the radioactive liquid input will be taken for radionuclide determination including tritium.

#### 11.4.2.4 Maintenance and Calibration

54 | On completion of the monitoring system installation, each process  
6 | monitor will be checked for proper operation and calibrated against a radiation check source(s) traceable back to the National Bureau of Standards or from an equally acceptable source. This initial calibration, and subsequent calibration at six month intervals will verify the electronic operation of both local and Control Room indications and also all annunciation points (loss-of-signal), loss-of-sample flow, high radiation, etc. In addition, each monitor is supplied with a built-in check source to provide rapid functional tests at periodic intervals.

### 11.4.3 Sampling

This section provides information on the CRBRP process and effluent sampling program. Process sampling provides the means for determining and monitoring various plant systems containing radioactive and potentially radioactive fluids. Effluent sampling provides the means for the reporting of radioactive releases to the environment. The effluent sampling will meet the reporting requirements of Regulatory Guide 1.21 and will provide data necessary for the semiannual report required by 10CFR50.

Amend. 54  
May 1980

#### 11.4.3.1 Process Sampling

Periodic sampling is conducted to alert the operator of any abnormal condition that may be developing. Both local and remote liquid samples are taken. Gaseous samples are taken directly at the sample station adjacent to the gas analyzer. The locations for gaseous sample instrumentation are given in Section 11.3.3.3. Operating procedures and performance tests of gaseous samples are discussed in Section 11.3.4. Sampling of primary sodium, secondary sodium, ex-vessel sodium and cover gas is discussed in detail in Section 9.8, entitled "Impurity Monitoring System". This section also discusses the location of samples, expected composition and concentration, sampling frequency and procedures.

The basis for selecting the locations for sample stations is to provide an indication of the effectiveness of key process operations. Analyses of these samples are related to the process sequence from which they were obtained to evaluate specific equipment performance.

Gaseous samples are monitored for gross activity and periodically analyzed for isotopic content. Tables 11.3-1 through 11.3-15 list inventories of the expected concentration and composition of the effluent gas samples.

Sections 11.4.3.1.1 through 11.4.3.1.5 describe in detail each of the liquid sampling points in the Radioactive Waste Systems. Sampling procedure, analytical procedure, and sensitivity for each sample point are the same and are discussed in detail in the following paragraphs.

**Sampling Procedure:** Samples are collected in a sampling station located on the operating floor of the radwaste building. Sample circulating lines run through this sampling station. The upstream side of the sample lines are connected to the discharge of the pumps serving the tanks. After passing through the sampling station, the circulating sample fluid is returned to the tank from which it was drawn.

**Analytical Procedure and Sensitivity:** The quantity of sample to be counted for gross beta-gamma is pipetted onto a planchet. The planchet is placed on a turntable and evaporated to dryness under an infrared bulb. The rotation insures a uniformly distributed dried sample for reproducible counting. The height of the infrared bulb is adjustable to obtain a moderate rate of evaporation. Counting is done by means of an internal proportional counter.

The isotopic analysis is performed by a completely automated Pulse Height Analysis System. A shielded Ge (Li) detector is used with a computer-based pulse height analysis system. The system satisfies the reporting requirements of Regulatory Guide 1.21.

Provisions will also be made for alpha and tritium assay.

#### 11.4.3.1.1 Intermediate Level Activity Liquid Waste Collection Tanks

These tanks receive decontamination waste from the Large Component Cleaning Cell. The analysis of this waste provides a check on the decontamination procedure.

The composition is expected to be sodium hydroxide solution, nitric acid solution and water rinses. After neutralization a solution of sodium sulfate or sodium nitrate results. Activity will be  $\sim 1$   $\mu\text{Ci/cc}$ .

The quantity to be measured is the gross  $\beta$ - $\gamma$  activity.

Additional rinses would be required if the activity of the component is higher than expected. Additional passes through the purification equipment would be required if the activity of the product from the evaporator is too high. Corrective action would be taken if the DF is lower than the expected value. The expected recirculation flow through the sample line is 10 gpm.

#### 11.4.3.1.2 Process Distillate Storage Tanks

These tanks receive the distillate from the Process Waste Evaporator. The sample provides the check on the DF of the evaporator and purity of the product to be recycled for plant uses or released to the environment after dilution with cooling tower blowdown. The composition is expected to be very dilute sodium sulfate or sodium nitrate with an activity  $\sim 10^{-6}$   $\mu\text{Ci/cc}$ .

The quantity to be measured is the gross  $\beta$ - $\gamma$  activity, if no excess inventory exists. If excess inventory exists and a portion of the content is to be released to the low activity liquid system, an isotopic analysis will be performed consistent with reporting requirements of Regulatory Guide 1.21. If the activity of the sample is unacceptably high, the contents of the tank are reprocessed through another evaporator-ion exchange cycle. Corrective measures would be taken if the DF is much lower than the expected value.

The expected recirculation flow through the sampling line is 10 gpm.

#### 11.4.3.1.3 Low Level Activity Liquid Waste Collection Tanks

These tanks receive laboratory drains, floor drains, lavatory drains, and shower drains from areas that may contain radioactivity. An activity check at these points determines the possibility of the need for further processing. It also permits a check on the DF of the purification equipment by comparing it with the activity of the purified waste.

These tanks receive waste from several sources, hence the composition is not well defined. The conductivity will be measured to determine impurity level. The expected activity is  $10^{-4}$   $\mu\text{Ci/cc}$ . The quantity to be measured is the gross  $\beta$ - $\gamma$  activity.

The sampling frequency will be in accordance with reporting requirements of Regulatory Guide 1.21.

Higher sample activity indicates abnormal operations elsewhere in the plant. Corrective measures at those locations would be taken. Also, higher activity indicates that a second pass through the equipment would be required.

The expected recirculation flow of the sampling line is 10 gpm.

#### 11.4.3.1.4 Low Level Activity Distillate Monitoring Tanks

Since these tanks are holding tanks for the purified product from the low level waste evaporator, pending release to the discharge canal, sample analysis is mandatory. The composition is expected to be equivalent to grade C water or comply with federal and state regulations and have an average activity of  $10^0 \mu\text{Ci/cc}$ .

A gross  $\beta$ - $\gamma$ - $\alpha$  count is made before releasing to the environment. Tritium content will also be sampled. An isotopic analysis is performed for record purposes as required by Regulatory Guide 1.21. Sampling frequency will be determined by reporting requirements of Regulatory Guide 1.21.

High sample activity indicates the need for reprocessing the batch. Corrective measures would be taken if DF is lower than the expected level. No particular process flow is associated with this sample point.

#### 11.4.3.1.5 Concentrated Waste Collection Tank

The material in this tank is intended to be solidified and shipped to the disposal site. To determine the type of packaging and degree of shielding required to meet the shipping regulation CFR Title 49, the analysis of sample is necessary. The composition is expected to be a solution of sodium sulfate or sodium nitrate and an activity of  $\sim 50 \mu\text{Ci/cc}$ . The quantity to be measured is the gross  $\beta$ - $\gamma$  activity.

The sampling frequency will be determined in the FSAR. No process flow is associated with this sampling procedure.

#### 11.4.3.2 Effluent Sampling

The radioactive effluents are continuously monitored or sampled as indicated in Section 11.4.2.2.3 by activity and by flow. The sampling system is designed to obtain a representative effluent sample to establish concentrations of radioactivity and to facilitate radioisotopic analysis to assure compliance with recognized codes and standards for radiation protection. The samples are taken before the effluent release to the environment. The gaseous effluents are discussed in detail in Section 11.3 and liquid effluents are discussed in Section 11.2.



The Cooling Tower blowdown, wastes and drains and other normally non-radioactive liquid effluent streams will be sampled for suspended/dissolved activity including tritium. The problem associated with continuous monitoring of low level  $\beta$  activity in tritium is recognized and therefore, periodic batch samples from each liquid effluent stream will be taken and analyzed in the laboratory.

Building Storm drains and Plant Service Building liquid effluents are normally non-radioactive and will not be monitored, but will be periodically sampled for radioisotopic analysis as necessary.

To satisfy Regulatory Guide 1.21 requirements for gamma spectroscopy and sensitivity, a high resolution automated radioisotopic analysis system will be provided at the plant site to facilitate precise identification and analysis of complex radionuclide concentrations.

#### 11.4.4 Reporting

An automated Report Processor will be provided which will generate the Effluent Radioactivity Release Reports in accordance with Appendix B of NRC Regulatory Guide 1.21. This computer based processor will be interfaced with the Radiation Monitoring System Controllers and the CRBRP Environmental Computer. The Report Processor will also accept manual entry of analyses performed by the Health Physicist.

TABLE 11.4-1 PROCESS & EFFLUENT MONITORING AND SAMPLING

Description	Bldg.	Elev.	Sample or Cont.	Range (uCi/cc) UOS	Expected Concent.	Quant. Meas.	Remarks
Reactor Containment Isolation Monitors (PPS):							
-Containment Ventilation (3) Exhaust (Gaseous) CAM	RCB	842	Continuous	$10^{-7}$ - $10^{-2}$ Cs <sup>137</sup>	See Section 11.3.2.6	Gross Concent.	Safety-related Class 1E PPS Related
-Head Access Area (3) Direct Gamma	RCB	802	Continuous	$10^{-1}$ - $10^{-4}$ mR/hr		Direct Gamma	See Section 7.3.1.2
Radwaste Monitor:							
-LALL Evaporator, Heating Element; Heating Water Out (Liquid)	RWA	775	Continuous	$4 \times 10^{-7}$ - $4 \times 10^{-2}$ Cs <sup>137</sup>		Gross Concent.	
-LALL Evaporator, Heating Element; Heating Water Out (Liquid)	RWA	775	Continuous	$4 \times 10^{-7}$ - $4 \times 10^{-2}$ Cs <sup>137</sup>		Gross Concent.	
-LALL Evaporator, Distill. Cooler; Cooling Water Out (Liquid)	RWA	775	Continuous	$4 \times 10^{-7}$ - $4 \times 10^{-2}$ Cs <sup>137</sup>		Gross Concent.	
-LALL Evaporator, Distill. Cooler; Cooling Water Out (Liquid)	RWA	775	Continuous	$4 \times 10^{-7}$ - $4 \times 10^{-2}$ Cs <sup>137</sup>		Gross Concent.	
-LALL Effluent	RWA	795	Continuous	$4 \times 10^{-7}$ - $4 \times 10^{-2}$ Cs <sup>137</sup>		Gross Concent.	
RAPS & CAPS Process Monitors:							
-Gas Entering RAPS Cold Box (Gaseous)	RCB	733	Continuous	$2.7$ - $2.7 \times 10^5$ Kr <sup>85</sup>		Gross Concent.	
-Coolant Leaving RAPS Cold Box (Gaseous) (2)	RSB	779	Continuous	$2.7 \times 10^{-6}$ - $2.7 \times 10^{-1}$ Kr <sup>85</sup>		Gross Concent.	In-Line Monitoring
-Gas Leaving RAPS Cold Box (Gaseous)	RCB	733	Continuous	$2.7 \times 10^{-3}$ - $2.7 \times 10^{+2}$ Kr <sup>85</sup>		Gross Concent.	
-Gas Leaving CAPS Surge Vessel (Gaseous Iodine)	RSB	779	Continuous	$2.7 \times 10^{-4}$ - $2.7 \times 10^{+1}$ Kr <sup>85</sup> $10^{-5}$ - $10^0$ I <sup>131</sup>		Gross Concent.	
-CAPS Header Serving RCB Cells (Gaseous)	RCB		Continuous	$2.7 \times 10^{-6}$ - $2.7 \times 10^{-1}$ Kr <sup>85</sup>		Gross Concent.	

11.4-10

Amend. 72  
Oct. 1982

TABLE 11.4-1 PROCESS &amp; EFFLUENT MONITORING AND SAMPLING

Description	Bldg.	Elev.	Sample or Cont.	Range ( $\mu\text{Ci/cc}$ ) UOS	Expected Concent.	Quant. Meas.	Remarks
-Gas From Nitrogen Cell Atmosphere Sampling Unit (Gaseous)	RSB	755	Continuous	$2.7 \times 10^{-6}$ - $2.7 \times 10^{-1}$	Kr <sup>85</sup>	Gross Concent.	
-Gas From Nitrogen Cell Atmosphere Sampling Unit (Gaseous)	RCB	752	Continuous	$2.7 \times 10^{-6}$ - $2.7 \times 10^{-1}$	Kr <sup>85</sup>	Gross Concent.	
CAPS Process Gas Effluent to HVAC (Gaseous) (2) (Iodine)	RSB	779	Continuous	$2.7 \times 10^{-5}$ - $2.7 \times 10^0$ $10^{-10}$ - $10^{-5}$	Kr <sup>85</sup> I <sup>131</sup>	Gross Concent.	
Effluent Gas From (2) Inerted Cells to HVAC (Gaseous)	RSB	800	Continuous	$2.7 \times 10^{-6}$ - $2.7 \times 10^{-1}$	Kr <sup>85</sup>	Gross Concent.	
HVAC Duct Monitoring (CAM of RAPS/CAPS Cells:							
-RAPS Cold Box & Valve Gallery Cells (Gaseous)	RCB	733	Continuous	$2.7 \times 10^{-6}$ - $2.7 \times 10^{-1}$	Kr <sup>85</sup>	Gross Concent.	In-Line Monitoring & Cell Isolation
-RAPS Noble Gas Storage Vessel Cell (Gaseous)	RCB	733	Continuous	$2.7 \times 10^{-6}$ - $2.7 \times 10^{-1}$	Kr <sup>85</sup>	Gross Concent.	In-Line Monitoring & Cell Isolation
-RAPS Compressor and Aftercooler Cells (2) (Gaseous)	RCB	733	Continuous	$2.7 \times 10^{-6}$ - $2.7 \times 10^{-1}$	Kr <sup>85</sup>	Gross Concent.	In-Line Monitoring & Cell Isolation
-RAPS Vessels (Gaseous)	RCB	733	Continuous	$2.7 \times 10^{-6}$ - $2.7 \times 10^{-1}$	Kr <sup>85</sup>	Gross Concent.	In-Line Monitoring & Cell Isolation
-RAPS/CAPS Pipeway (Gaseous)	RCB	780	Continuous	$2.7 \times 10^{-6}$ - $2.7 \times 10^{-1}$	Kr <sup>85</sup>	Gross Concent.	In-Line Monitoring & Cell Isolation
-CAPS Cold Box Cell (Gaseous)	RSB	792	Continuous	$2.7 \times 10^{-6}$ - $2.7 \times 10^{-1}$	Kr <sup>85</sup>	Gross Concent.	In-Line Monitoring & Cell Isolation
-CAPS Vessel Cells & Gallery (Gaseous)	RSB	755	Continuous	$2.7 \times 10^{-6}$ - $2.7 \times 10^{-1}$	Kr <sup>85</sup>	Gross Concent.	In-Line Monitoring & Cell Isolation

11.4-11

Amend. 72  
Oct. 1982

TABLE 11.4-1 PROCESS & EFFLUENT MONITORING AND SAMPLING

Description	Bldg.	Elev.	Sample or Cont.	Range (uCi/cc) UOS	Expected Concent.	Quant. Meas.	Remarks
-CAPS Compressor & (2) After Cooler Cells (Gaseous)			Continuous	$2.7 \times 10^{-6}$ - $27 \times 10^{-1}$ Kr <sup>85</sup>		Gross Concent.	In-Line Monitoring & Cell Isolation
-RAD Water Holding Vessel & Pump Cell (Gaseous)			Continuous	$2.7 \times 10^{-6}$ - $27 \times 10^{-1}$ Kr <sup>85</sup>		Gross Concent.	In-Line Monitoring & Cell Isolation
-Access Areas (4) (Gaseous)			Continuous	$2.7 \times 10^{-6}$ - $27 \times 10^{-1}$ Kr <sup>85</sup>		Gross Concent.	In-Line Monitoring & Cell Isolation
-Cover Gas Monitoring Cells (Gaseous)			Continuous	$2.7 \times 10^{-6}$ - $27 \times 10^{-1}$ Kr <sup>85</sup>		Gross Concent.	In-Line Monitoring & Cell Isolation
-Pipe Chase & Vapor Trap Cell (Gaseous)	RSB	772	Continuous	$2.7 \times 10^{-6}$ - $27 \times 10^{-1}$ Kr <sup>85</sup>		Gross Concent.	In-Line Monitoring & Cell Isolation
-HVAC Common Header For Various Cells (Gaseous)	RCB	766	Continuous	$2.7 \times 10^{-6}$ - $27 \times 10^{-1}$ Kr <sup>85</sup>		Gross Concent.	In-Line Monitoring & Cell Isolation
Main HVAC Duct From All RAPS/CAPS Cells (Gaseous) CAM (Iodine)	RSB	779	Continuous	$2.7 \times 10^{-6}$ - $2.7 \times 10^{-1}$ Kr <sup>85</sup> $10^{-10}$ - $10^{-5}$ I <sup>131</sup>		Gross Concent.	
Sodium Leak Detection For Following Reclrc. Gas Cooling Subsystems: (All Particulate)							
Reactor Cavity	RCB	733	Continuous	$2.94 \times 10^{-13}$ - $2.94 \times 10^{-5}$ Na <sup>24</sup>		Gross Concent.	Alarm Only
PHTS Loop 1	RCB	766	Continuous	$2.94 \times 10^{-13}$ - $2.94 \times 10^{-5}$ Na <sup>24</sup>		Gross Concent.	Alarm Only
PHTS Loop 2	RCB	766	Continuous	$2.94 \times 10^{-13}$ - $2.94 \times 10^{-5}$ Na <sup>24</sup>		Gross Concent.	Alarm Only
PHTS Loop 3	RCB	766	Continuous	$2.94 \times 10^{-13}$ - $2.94 \times 10^{-5}$ Na <sup>24</sup>		Gross Concent.	Alarm Only
Na Makeup Pump & Vessels	RCB	752	Continuous	$2.94 \times 10^{-13}$ - $2.94 \times 10^{-5}$ Na <sup>24</sup>		Gross Concent.	Alarm Only
Na Makeup Pump & Pipeway	RCB	752	Continuous	$2.94 \times 10^{-13}$ - $2.94 \times 10^{-5}$ Na <sup>24</sup>		Gross Concent.	Alarm Only

11.4-12

Amend. 72  
Oct. 1982

TABLE 11.4-1 PROCESS & EFFLUENT MONITORING AND SAMPLING

Description	Bldg.	Elev.	Sample or Cont.	Range (uCi/cc) UOS	Expected Concent.	Quant. Meas.	Remarks
Cold Trap, Nak Cells	RCB	794	Continuous	$2.94 \times 10^{-13}$ - $2.94 \times 10^{-5}$	Na <sup>24</sup>	Gross Concent.	Alarm Only
Control Room Main (2) Air Intake (Gaseous) CAM (Iodine) (Particulate)	CB	863	Continuous	$3 \times 10^{-7}$ - $3 \times 10^{-2}$ Kr <sup>85</sup> $4 \times 10^{-12}$ - $4 \times 10^{-7}$ I <sup>131</sup> $2 \times 10^{-10}$ - $2 \times 10^{-5}$ Cs <sup>137</sup>	See Section 12.2	Gross Concent.	Initiate C/R Isolation, see Sec. 7.6.4.5.6 Safety-Related (1E)
Control Room Remote (2) Air Intake (Gaseous) CAM (Iodine) (Particulate)	SGB	851	Continuous	$3 \times 10^{-7}$ - $3 \times 10^{-2}$ Kr <sup>85</sup> $4 \times 10^{-12}$ - $4 \times 10^{-7}$ I <sup>131</sup> $2 \times 10^{-10}$ - $2 \times 10^{-5}$ Cs <sup>137</sup>	See Section 12.2	Gross Concent.	Initiate C/R Isolation, see Sec. 7.6.4.5.7 Safety-Related (1E)
Control Room Common Duck Downstream of Filter Units (Gaseous) CAM (Iodine) (Particulate)	CB	847	Continuous	$3 \times 10^{-7}$ - $3 \times 10^{-2}$ Kr <sup>85</sup> $4 \times 10^{-12}$ - $4 \times 10^{-7}$ I <sup>131</sup> $5 \times 10^{-10}$ - $5 \times 10^{-5}$ Cs <sup>137</sup>	See Section 12.2	Gross Concent.	Monitor Only
IHTS Loop 1 (Direct Gamma)	SGB	765	Continuous	$10^{-2}$ - $10^3$ mR/hr		Gross Activity	
IHTS Loop 2 (Direct Gamma)	SGB	765	Continuous	$10^{-2}$ - $10^3$ mR/hr		Gross Activity	
IHTS Loop 3 (Direct Gamma)	SGB	765	Continuous	$10^{-2}$ - $10^3$ mR/hr		Gross Activity	
Large Component Cleaning Cell (LCCC)	RCB	756	Continuous	$10^{-1}$ - $10^4$ mR/hr		Gross Activity	
LCCC Cooling Water (Liquid)	RCB	733	Continuous	$4 \times 10^{-7}$ - $4 \times 10^{-2}$ Cs <sup>137</sup>		Gross Concent.	
LCCC Process Gas Effluent (Gaseous)	RCB		Continuous	$10^{-6}$ - $10^{-1}$ Kr <sup>85</sup>		Gross Concent.	
Fuel Handling Cell (FHC) Argon Gas (Gaseous) (Iodine) (Particulate)	RSB	779	Continuous	$10^{-6}$ - $10^{-1}$ Kr <sup>85</sup> $10^{-10}$ - $10^{-5}$ I <sup>131</sup> $10^{-10}$ - $10^{-5}$ Cs <sup>137</sup>		Gross Concent.	
EVST Argon Cover Gas (Gaseous)	RSB	842	Continuous	$10^0$ - $10^4$ Kr <sup>85</sup>		Gross Concent.	

11.4-13

Amend. 72  
Oct. 1992

TABLE 11.4-1 PROCESS & EFFLUENT MONITORING AND SAMPLING

Description	Bldg.	Elev.	Sample or Cont.	Range ( $\mu\text{Ci/cc}$ ) UOS	Expected Concent.	Quant. Meas.	Remarks
FHC Utility Monitor (Direct Gamma)	RSB	779	Continuous	$10^{-1}$ - $10^7$ mR/hr		Gross Activity	
Radwaste Building Exhaust (Gaseous) CAM (Iodine) (Particulate)	RWB	867	Continuous	$3 \times 10^{-7}$ - $10^3$ Kr <sup>85</sup> $10^{-10}$ - $10^2$ I <sup>131</sup> $10^{-10}$ - $10^2$ Cs <sup>137</sup>		Gross Concent.	Initiate Filtering of Effluent from RWB
RSB Operating Floor (2) HVAC Exhaust (Gaseous) CAM (Iodine) (Particulate)	RSB	816	Continuous	$3 \times 10^{-7}$ - $3 \times 10^{-2}$ Kr <sup>85</sup> $4 \times 10^{-12}$ - $4 \times 10^{-7}$ I <sup>131</sup> $10^{-6}$ - $10^{-1}$ Cs <sup>137</sup>		Gross concent.	Initiate RSB Confinement see Section 7.6.4.3.3 (4) Safety related (1E)
Fuel Handling Cell (2) HVAC Exhaust (Gaseous) (Iodine) (Particulate)	RSB	779	Continuous	$3 \times 10^{-7}$ - $3 \times 10^{-2}$ Kr <sup>85</sup> $4 \times 10^{-12}$ - $4 \times 10^{-7}$ I <sup>131</sup> $10^{-6}$ - $10^{-1}$ Cs <sup>137</sup>		Gross Concent.	- same -
Annulus Filter (2) Discharge (Gaseous) (Iodine) (Particulate)	RSB	840 851	Continuous	$4.4 \times 10^{-6}$ - $4 \times 10^{-1}$ Kr <sup>85</sup> $1.1 \times 10^{-7}$ - $1.1 \times 10^{-2}$ I <sup>131</sup> $1.2 \times 10^{-10}$ - $1.2 \times 10^{-5}$ Cs <sup>137</sup>		Gross Concent.	Select Filter train Section 7.6.4.2.2 (1) Safety Related (1E)
Annulus Filter Inlet/(2) Annulus Cooling Exhaust CAM (Gaseous) (Iodine) (Particular)	RSB	840 861	Continuous	$3 \times 10^{-7}$ - $1 \times 10^4$ Kr <sup>85</sup> $1 \times 10^{-10}$ - $1 \times 10^2$ I <sup>131</sup> $1 \times 10^{-6}$ - $1 \times 10^2$ Cs <sup>137</sup>		Gross Concent.	1) Start Filter see 7.6.4.2.2 (6) 2) Monitor Exhaust see 11.4.2.2.3 (Accident (Monitor)
RSB Clean Up Filter Discharge (Gaseous) (Iodine) (Particulate)	RSB	816 794	Continuous	$3 \times 10^{-7}$ - $3 \times 10^{-2}$ Kr <sup>85</sup> $1 \times 10^{-10}$ - $1 \times 10^{-5}$ I <sup>131</sup> $1 \times 10^{-6}$ - $1 \times 10^{-1}$ Cs <sup>137</sup>		Gross Concent.	Select Filter Train See Section 7.6.4.3.3(1) Safety Related (1E)
Radwaste Ventilation Exhaust Effluent (Gaseous) (Iodine) (Particulate)	RSB	867	Continuous	$1 \times 10^{-6}$ - $1 \times 10^3$ Kr <sup>85</sup> $1 \times 10^{-10}$ - $1 \times 10^2$ I <sup>131</sup> $1 \times 10^{-10}$ - $1 \times 10^2$ Cs <sup>137</sup>	See Section 11.3.6	Gross Concent.	Effluent, Accident Monitor

11.4-14

Amend. 72  
Oct. 1982

TABLE 11.4-1 PROCESS &amp; EFFLUENT MONITORING AND SAMPLING

Description	Bldg.	Elev.	Sample or Cont.	Range ( $\mu\text{Ci/cc}$ ) UOS	Expected Concent.	Quant. Meas.	Remarks
RCB Ventilation Exhaust Effluent (Gaseous) (Iodine) (Particulate)	RSB	861	Continuous	$1 \times 10^{-6}$ - $1 \times 10^{-1}$ Kr <sup>85</sup> $1 \times 10^{-10}$ - $1 \times 10^{-5}$ I <sup>131</sup> $1 \times 10^{-10}$ - $1 \times 10^{-5}$ Cs <sup>137</sup>	See Section 11.3.2.6	Gross Concent.	
RCB Annulus/TMBDB (2) Effluent (Gaseous) (Iodine) (Particulate) (Plutonium/Alpha)	RSB	840 861	Continuous	$1 \times 10^{-6}$ - $1 \times 10^{-5}$ Kr <sup>85</sup> $1 \times 10^{-10}$ - $1 \times 10^{-2}$ I <sup>131</sup> $1 \times 10^{-10}$ - $1 \times 10^{-2}$ Cs <sup>137</sup> $1 \times 10^{-12}$ - $1 \times 10^{-7}$ Pu <sup>239</sup>			Accident Monitor Safety Related (1E)
RSB Exhaust Effluent (Gaseous) (Iodine) (Particulate)	RSB	816	Continuous	$1 \times 10^{-6}$ - $1 \times 10^{-1}$ Kr <sup>85</sup> $1 \times 10^{-10}$ - $1 \times 10^{-2}$ I <sup>131</sup> $1 \times 10^{-10}$ - $1 \times 10^{-2}$ Cs <sup>137</sup>			Accident Monitoring
SGB-IB Exhaust Effluent (Gaseous) (Iodine) (Particulate)	SGB	836	Continuous	$1 \times 10^{-6}$ - $1 \times 10^{-3}$ Kr <sup>85</sup> $1 \times 10^{-10}$ - $1 \times 10^{-2}$ I <sup>131</sup> $1 \times 10^{-10}$ - $1 \times 10^{-2}$ Cs <sup>137</sup>	See Section 11.3.2.6		Accident Monitoring
Hot Laboratory, Counting Room, and Decontamination Area Ventilation Exhaust Particulate Sampler	PSB		Sample**			Gross Concent.	
Plant Discharge Canal Liquid Sampler	YARD	-	Sample***		See Section 11.2.5	Concent.	

\*\* Particulate collection on filter, analysis by proportional counters and spectroscopy system.  
 \*\*\* Liquid Samples collected in container. Analysis by proportional and liquid scintillation counters and spectroscopy system.

11.4-15

Amend. 72  
Oct. 1982

### LALL Distillate Demineralizers

The Activity Inventory of the LALL demineralizers is provided in Table 12.1-39a. This inventory is assumed to contain the activity inventory of the LALL Collection Tank (Table 12.1-35). This is based on accumulation in the demineralizers of the activity in one 2400 gal. batch of filtered LALL process fluid (assuming the evaporator are bypasses).

### IALL and LALL Resin Traps

The purpose of the resin traps downstream of the distillate demineralizers is to catch resins which may be contaminated which have broken away from the demineralizer beds. The source term for each resin trap is assumed to contain 6% of the activity inventory of the demineralizers (Tables 12.1-39 and 12.1-39A). This reflects the activity that would be present in the resin traps, should a rupture of the demineralizer resin retention devices occur. The activity inventory of the IALL resin trap is provided in Table 12.1-40, and the inventory of the LALL resin trap is provided in Table 12.1-40A.

### Concentrated Waste Tank

The Concentrated Waste Tank in the SRWS receives the concentrated radioactive wastes from the IALL and LALL evaporators. The activity inventory is given in Table 12.1-43.

### Decanting Tank

The Decanting Tank collects the powdered resin waste from the spent IALL and LALL Distillate Demineralizer resins. The activity inventory for the Decanting Tank is based on isotope inventory of the spent Distillate Demineralizer resins in Table 12.1-39 and 12.1-39A. The activity inventory is given in Table 12.1-44.

### Decantate Filters

The Decantate Filters remove undissolved solids from the liquid decanted off the Decanting Tank. These filters are assumed to contain 1% of the activity of the Decanting Tank. The activity inventory is given in Table 12.1-45.

### Solid Radwaste Drums

Concentrated liquid radwaste and spent resins will be drummed, solidified and stored in the SRS in the Radwaste Building. Up to 136 drums per year containing concentrated liquid waste will be stored in the high activity drum storage vault. Each drum will contain 30 gallons of concentrate from the Concentrated Waste Tank. The activity inventory per drum is shown in Table 12.1-46. Up to 17 drums per year containing spent demineralizer resins will be stored. Each drum will contain 17 gallons of spent resins and from the Decanting Tank. The activity inventory per drum is shown in Table 12.1-47.



#### 12.1.4 Area Radiation Monitoring

##### 12.1.4.1 Design Criteria

Area monitors are provided in selected building locations to continuously detect, measure, and indicate the radiation level and to initiate alarms (audible and visual) for radiation levels above preset values. In high or varied noise level areas ( $\geq 95$ db) strobe lights are also provided in addition to the audible alarms. These monitors advise plant personnel of existing radiation levels during normal operation and warn them of potential radiation hazards that may cause higher exposure levels than expected.

The detector ranges of these monitors are chosen to provide continuous monitoring of gamma radiation levels ranging from one decade below to three decades above the design background level at each monitor location.

The basis for location of the various personnel protection monitors shall consider the following factors:

1. The anticipated radiation level under operation, shutdown maintenance, and abnormal conditions.
2. The frequency and duration of occupancy, and the flow of traffic under normal and accident conditions.
3. The proximity of high radiation sources.
4. The consequence of an undetected increase in radiation level.

In addition to the personnel protection monitoring utilized during normal plant conditions, accident area monitoring will also be provided. Area monitoring for range  $10^{-1}$  to  $10^4$  R/hr will be provided in the following areas:

1. Inside buildings or areas which are in direct contact with primary containment where penetrations and hatches are located.
2. Inside buildings or areas where access is required to service equipment important to safety and the threat of radiation contamination exists.

Three high-range monitors of range 1 to  $10^7$  R/hr will be provided to monitor the levels of gamma radiation in the Containment Area. The detectors for these monitors will be located approximately  $120^\circ$  apart around the Containment vessel periphery in the Annulus space so as to allow a measurement of gamma activity being radiated from containment. The location of these monitors is in the more benign environment of the Annulus rather than in containment to avoid the severe temperature transient and direct sodium aerosol which may occur during and following an accident. These monitors are safety-related and each is supplied with a separate division of Class 1E power.

The Accident Monitors as identified in Table 12.3-5, will meet the requirements of Section 7.5.11 of the PSAR

The locations of the area monitors provided for the CRERP are shown on Figs. 12.1-1 to 12.1-19d and are listed in Table 12.3-5.

#### 12.1.4.2 Monitoring System Description

Each area monitoring channel consists of a gamma detector, microprocessor and accessories, local indicators, alarms, and Control Room indication. The gamma detector energy dependence will be flat within  $\pm 20\%$  for incident radiation above 100 KeV. Local monitor display includes loss-of-signal, high and high-high radiation indicator lights, high and high-high radiation audible alarms and mR/hr rate meter. Also, an essential feature of each monitoring channel will be its ability to avoid "foldover" following saturation in high radiation fields.

The detector signal is also displayed on redundant Radiation Monitoring System CRTs located in the Control Room and Health Physics Area of the Plant Service Building via their respective Central Processing Units and Mini-Computers(System Controllers). The indicating analog meter in each local monitor indicates exposure levels on a suitable multi-decade logarithmic scale. The alarm signals are also permanently recorded by the redundant Radiation Monitoring System Line-Printers located in the Control Room and Health Physics Area.

Group annunciation is also provided on the Main Control Board.

Each area monitor will contain a built-in solenoid actuated shielded check source which can be actuated from the remote process station in the vicinity. All monitor components will be modular, commercially available units designed for rapid replacement upon failure. Electronic components will be exclusively solid-state, as available; and power will be supplied from the Instrument AC (120V, 60Hz) busses for the non-safety monitors. Area monitors performing containment isolation functions (PPS) will be supplied with Class 1E power from redundant vital AC busses.

The high radiation alarms of all area monitors are transmitted from the local monitors to the Remote Data Acquisition Terminal units in the vicinity. The Plant Data Handling and Display system will display and log all high alarms.

Figure 12.1-21 shows a functional block diagram of an area radiation monitor. Locations, design dose rates and ranges of sensitivities of the monitors are provided in Table 12.3-5.

#### 12.1.4.3 Maintenance and Calibration

On completion of the monitoring system installation, each area monitor will be checked for proper operation and calibrated against a radiation checksource traceable to the National Bureau of Standards or from an equally acceptable source. The initial calibration and subsequent calibrations at six month intervals will utilize a minimum of two source strengths to verify the linearity of detector output. In addition, each monitor is supplied with a built-in check source to provide a rapid functional test at periodic intervals.

#### 12.1.5 Estimates of Exposure

##### Peak External Dose Rates and Annual Doses at Unrestricted Locations

The peak dose rates and annual doses at the site boundary and control room due to direct plant radiation are low and considered small relative to the natural background radiation. These doses have been estimated and are shown in Table 12.1-49, Parts I, II, and III.

TABLE 12.1-1  
PLANT RADIATION ZONE CLASSIFICATION

Zone	Area Type	Access	Design Dose Rate (mrem/hr)	Zone Dose Rate Specification (mrem/hr)	Type of Control
-	Unrestricted Area	Continuous	-	**	Uncontrolled
I	Restricted Area	Continuous Routinely Occupied	0.2	≤0.2	Administrative Control
II	Restricted Area	Continuous, Not Routinely Occupied	2.0	>0.2 to <5	Administrative Control
III	Radiation Area	Periodic Limited Access for Routine Tasks	10***	>5 to ≤100	Administrative Control
IV	High Radiation Area	Unoccupied* Limited Access for Non-routine or infrequent Tasks	100	>100 to <5000	Special Work Permits, Locked Doors, Signs, Temporary Barricades, Health Physics Surveillance
V	Extremely High Radiation Area	Unoccupied*	Unlimited	>5000	Positive exclusion, Locked Doors, Special Work Permits, Continuous Health Physics Monitoring

\* 10CFR20 criteria.

\*\* Approaching background radiation.

\*\*\* 25 mrem/hr within HAA

12.1-28

Amend. 72  
Oct. 1982

TABLE 12.1-2

## SHIELD PARAMETERS FOR THE HEAD ACCESS AREA

<u>Radiation Zone</u>	<u>Predominant Sources of Radiation</u>	<u>Specific Design Considerations Applying to Sources</u>	<u>Type of Shielding Required</u>	<u>Nominal Thickness of Shield</u>
III	Na <sup>24</sup> gammas from primary Inlet and outlet coolant piping	Major Source Geometries: (a) 36" Pipe (b) 24" Pipe	Concrete Walls Along Periphery of HAA, Above Support Ledge	5'
III	Na <sup>24</sup> gammas from In-vessel sodium pool and primary sodium coolant piping. In-vessel neutron leakage through sodium pool; ex-vessel neutron leakage	(a) In-Vessel Sodium Pool (b) 36" Pipe (c) 24" Pipe (d) Reactor Cavity (e) cover Gas Pool	Concrete Support Ledge; Carbon Steel Reactor Vessel Support Structure	6' (serpentine concrete) 9" (steel)
III	Same as Above	Same as Above	Steel/Inconel Reactor Vessel Closure Head Assembly	53"
III	Ex-Vessel Neutron Leakage	Major Source Geometries; Reactor Cavity	B <sub>4</sub> C Annular Neutron Shield Ring	14"
III	Radioactive cover gas gamma sources; Gamma streaming (Na <sup>24</sup> ); Neutron streaming	Major Source Geometries; (a) Annular Gaps (b) In-vessel sodium Pool (c) Cover Gas Volume Above Sodium Pool (d) Reactor Cavity	Penetration Shields CRDM's (15) EVTM - Nozzle port IVTM - Nozzle port Others: UIS Jacks (4) Liquid Level Ports (4) Risers (3)	Local Shadow Shields (steel) as required

12.1-29

TABLE 12.1-47

SOLID RADIOACTIVE WASTE RADWASTE DRUM  
(SPENT RESINS) RADIOISOTOPE INVENTORY

ISOTOPE	INVENTORY (CURIES)	ISOTOPE	INVENTORY (CURIES)
Cr-51	4.2(-2)	Ce-141	3.02(-1)
Mn-54	3.02(-1)	Ce-143	1.35(-1)
Fe-59	2.06(-3)	Pr-143	1.35(-1)
Co-58	2.8(-1)	Ce-144	2.15(-1)
Co-60	9.0(-2)	Pr-144	2.15(-1)
Sr-89	4.62(-1)	Nd-147	6.51(-2)
Sr-90	3.39(-1)	Pm-147	1.22(-1)
Y-90	3.39(-1)	Pm-149	3.6(-3)
Y-91	1.34(-1)	Eu-155	1.58(-2)
Zr-95	2.54(-1)	Eu-156	6.0(-3)
Nb-95	2.54(-1)	Ta-182	1.33(-2)
Mo-99	2.82(-2)	Pu-238	2.8(-3)
Ru-103	3.36(-1)	Pu-239	7.04(-4)
Ru-106	2.72(-1)	Pu-240	9.39(-4)
Rh-106	2.72(-1)	Pu-241	8.28(-2)
Ag-111	8.8(-3)	Pu-242	1.76(-6)
Te-127	9.25(-1)	Np-238	5.87(-8)
Te-127m	9.25(-1)	Np-239	4.09(-4)
Te-129m	2.79(0)	Am-241	7.54(-4)
Te-129	2.79(0)	Am-242m	2.93(-5)
Te-132	1.98(0)	Am-242	1.35(-10)
I-131	1.3(-3)	Am-243	1.17(-5)
I-132	1.99(0)	Cm-242	1.43(-4)
Cs-134	2.6(-3)	Cm-243	5.86(-6)
Cs-136	2.5(-3)	Cm-244	1.64(-4)
Cs-137	1.88(-2)		
Ba-140	1.83(-1)		
La-140	1.83(-1)		

TOTAL 16.52

| TABLE 12.1-48 HAS BEEN INTENTIONALLY DELETED





### GENERAL NOTES

1. THE FIRST RADIATION ZONE DESIGNATION REFERS TO THE RADIATION LEVEL IN A CELL WHILE OPERATING. THE SECOND DESIGNATION DURING CELL SHUTDOWN. THE SHUTDOWN CONDITION REQUIRES THAT THE PIPE AND/OR EQUIPMENT IN A CELL BE DRAINED, PLUGGED OR VOIDED OF RADIOACTIVE SOURCES AS NECESSARY. RADIATION SOURCES INTERNAL AND EXTERNAL TO A CELL ARE CONSIDERED.

### 2. PLANT RADIATION ZONE CLASSIFICATION

ZONE CLASS	DESIGN DOSE RATE RANGE (MR/HR)	ZONE DESCRIPTION	DESIGN OCCUPANCY CRITERIA
I	≤ 0.2	RESTRICTED AREA ROUTINELY OCCUPIED	24/7
II	> 0.2 TO ≤ 5	RESTRICTED AREA NOT ROUTINELY OCCUPIED	100FR20
III	> 5 TO ≤ 100	RADIATION AREA LIMITED ACCESS FOR ROUTINE TASKS	100FR20
IV	> 100 TO ≤ 5000	HIGH RADIATION AREA ACCESS TO PERFORM SPECIFIC NON-ROUTINE TASKS	100FR20
V	> 5000	INACCESSIBLE	100FR20

3. THESE RADIATION ZONE DIAGRAMS ARE TO BE USED ONLY FOR RADIATION ZONE INFORMATION.

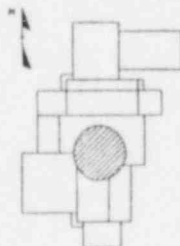
-777 FILTER

P/G/I Mobile Monitor

Alpha Mobile Monitor

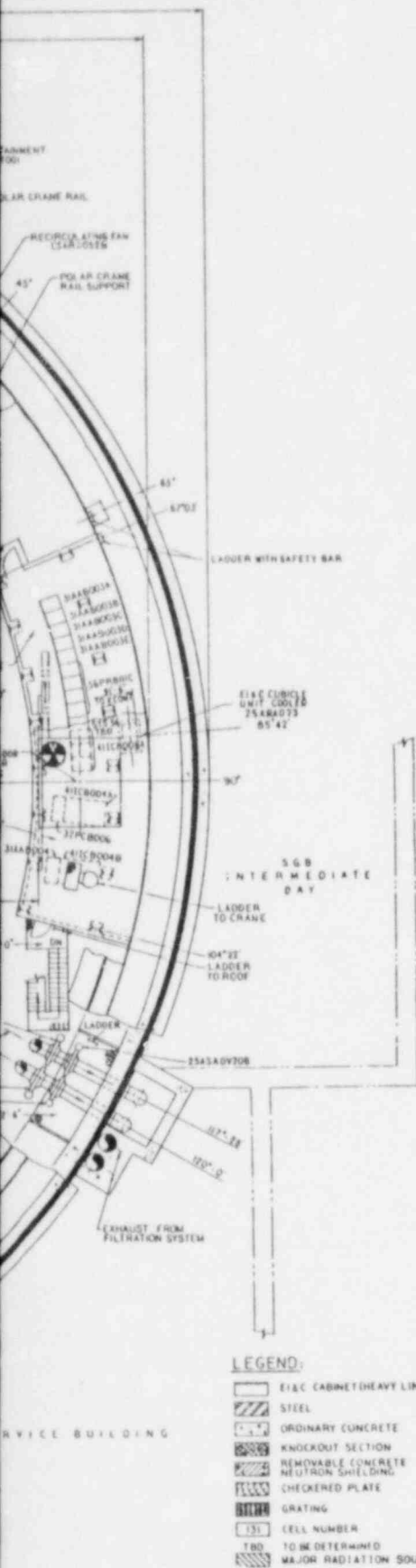
### REFERENCE DRAWINGS

- NH7400 - DESIGN RADIATION DOSE RATES RCB PLAN ABOVE EL 816'-0"
- NH7401 - DESIGN RADIATION DOSE RATES RCB PLAN ABOVE EL 794'-0"
- NH7402 - DESIGN RADIATION DOSE RATES RCB PLAN ABOVE EL 780'-0"
- NH7403 - DESIGN RADIATION DOSE RATES RCB PLAN ABOVE EL 768'-0"
- NH7404 - DESIGN RADIATION DOSE RATES RCB PLAN ABOVE EL 752'-0"
- NH7405 - DESIGN RADIATION DOSE RATES RCB PLAN ABOVE EL 733'-0"



KEY PLAN

Figure 12.1-1 Plant Radiation Protection

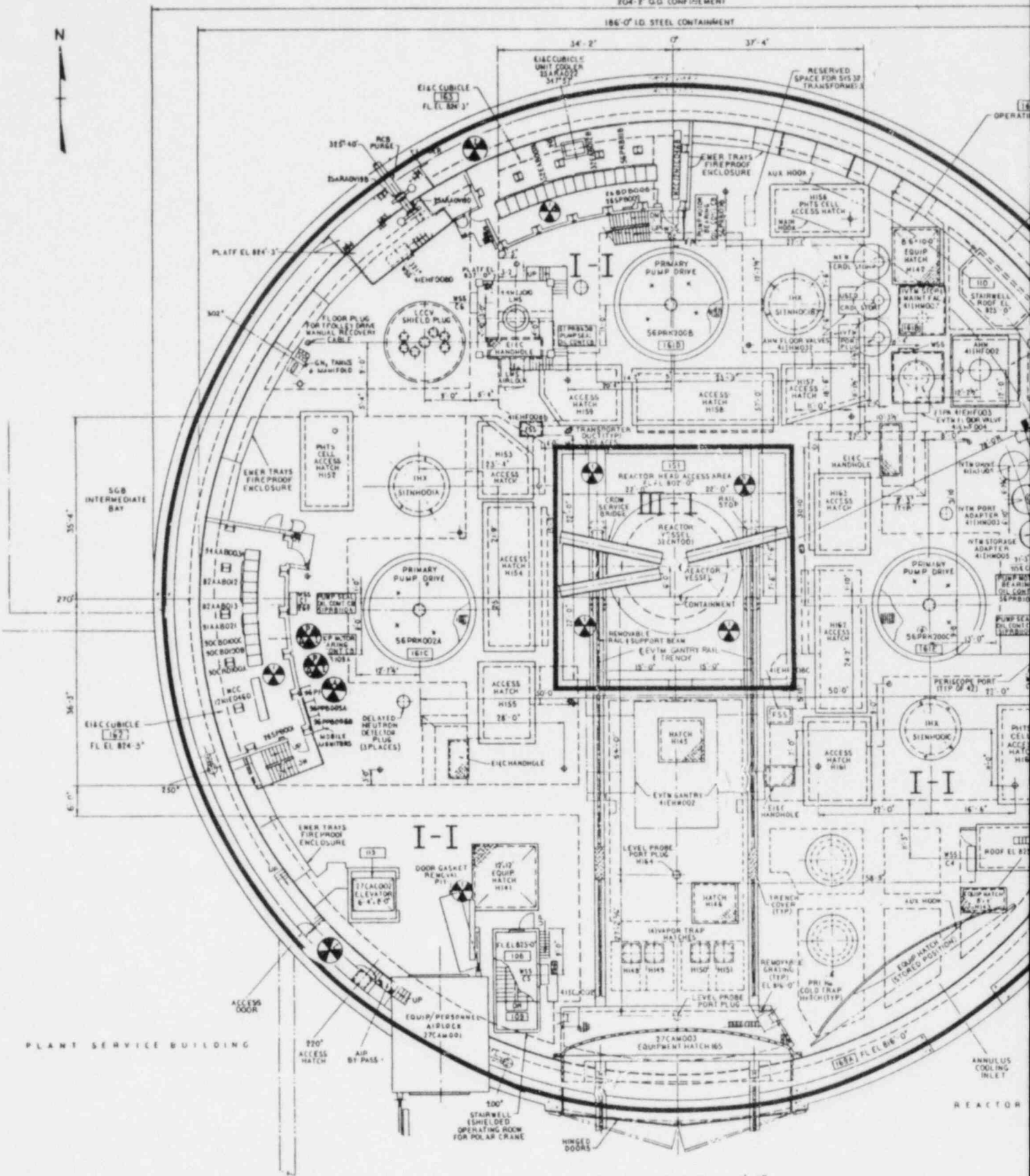


### LEGEND:

- E1&C CABINET (HEAVY LINE FRONT)
- STEEL
- ORDINARY CONCRETE
- KNOCKOUT SECTION
- REMOVABLE CONCRETE NEUTRON SHIELDING
- CHECKERED PLATE
- GRATING
- CELL NUMBER
- TO BE DETERMINED
- MAJOR RADIATION SOURCES

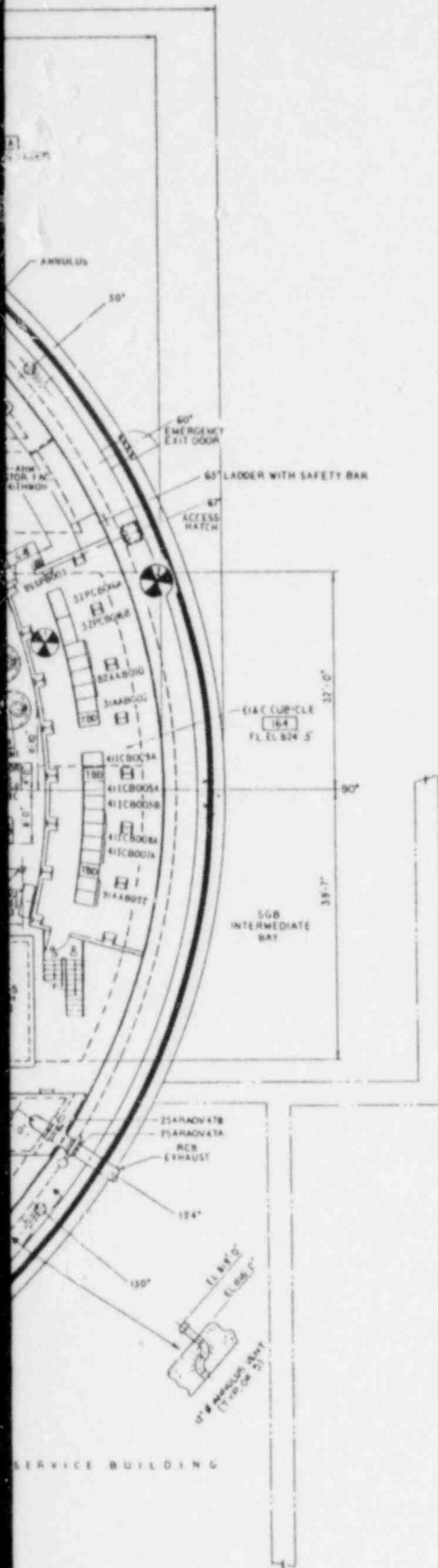
204'-1" O.D. CONFINEMENT

186'-0" I.D. STEEL CONTAINMENT

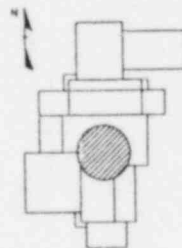
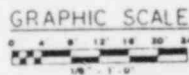


PLANT SERVICE BUILDING

PLAN ABOVE EL 816'-0"



REFERENCE DRAWINGS  
SEE DRAWING NH7399



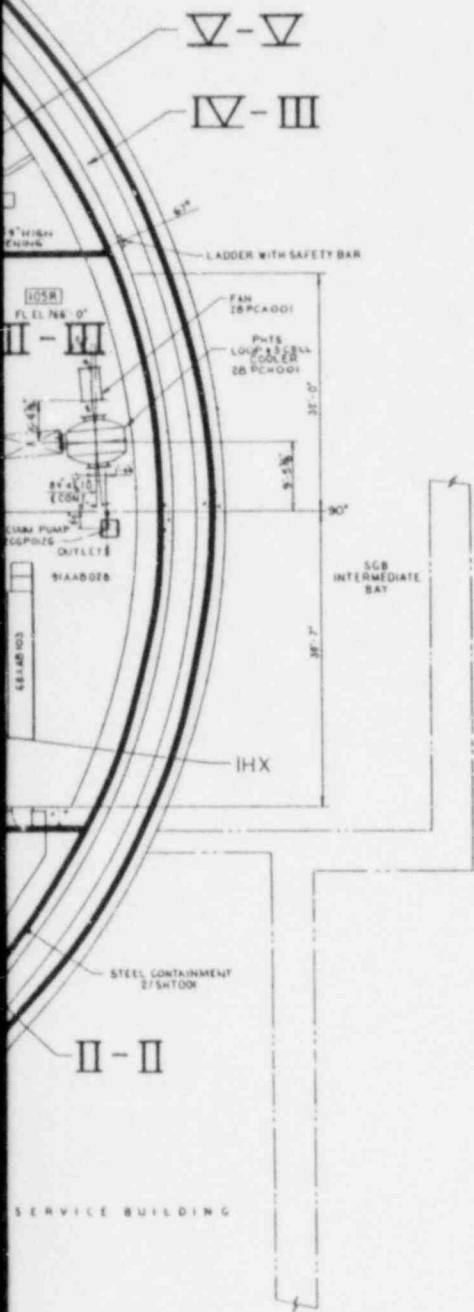
KEY PLAN

Figure 12.1-2 Plant Radiation Protection

12.1-82

Amend. 72  
Oct. 1982





REFERENCE DRAWINGS  
SEE DRAWING NH7350

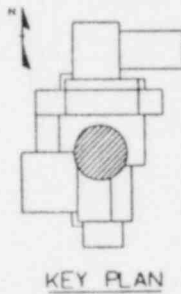
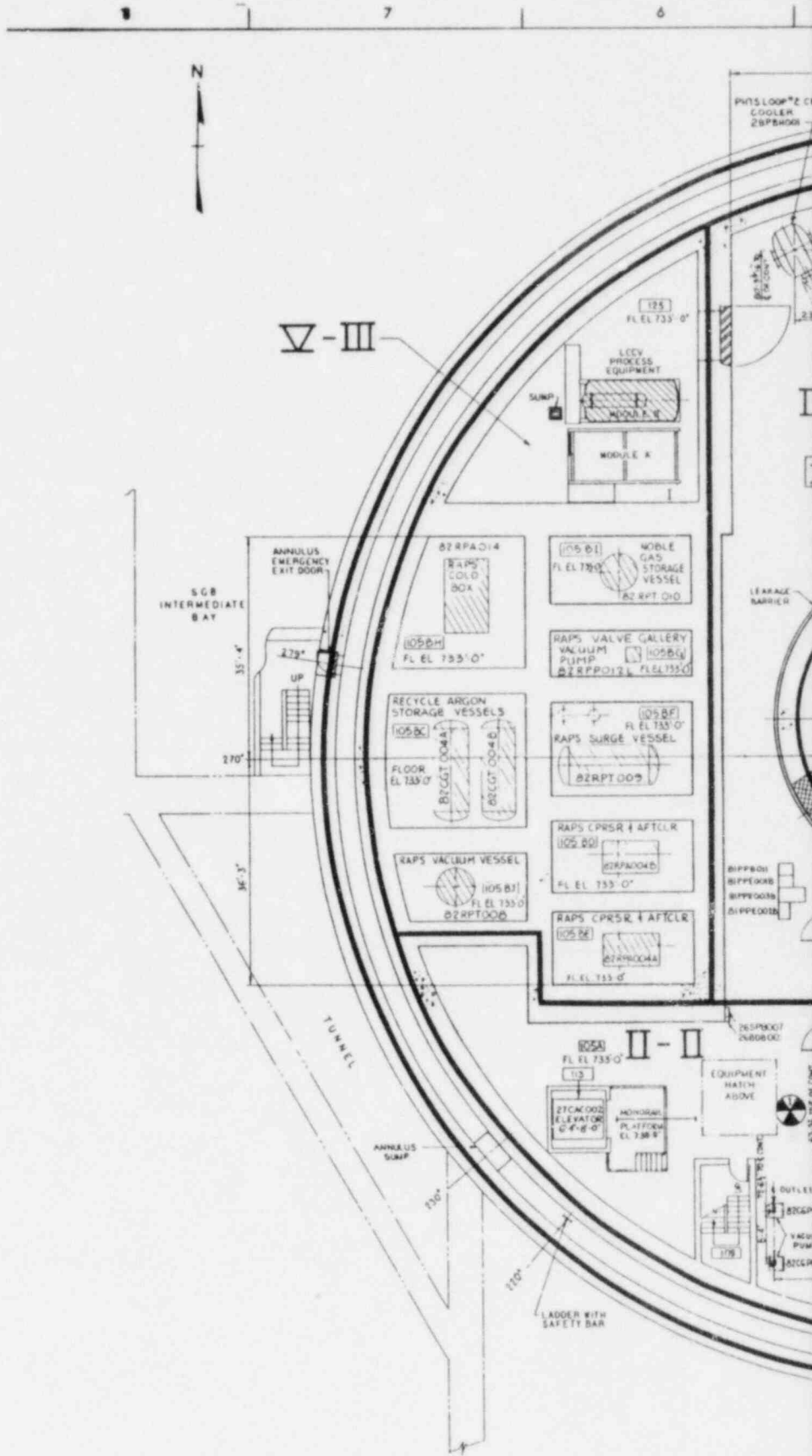


Figure 12.1-5 Plant Radiation Protection

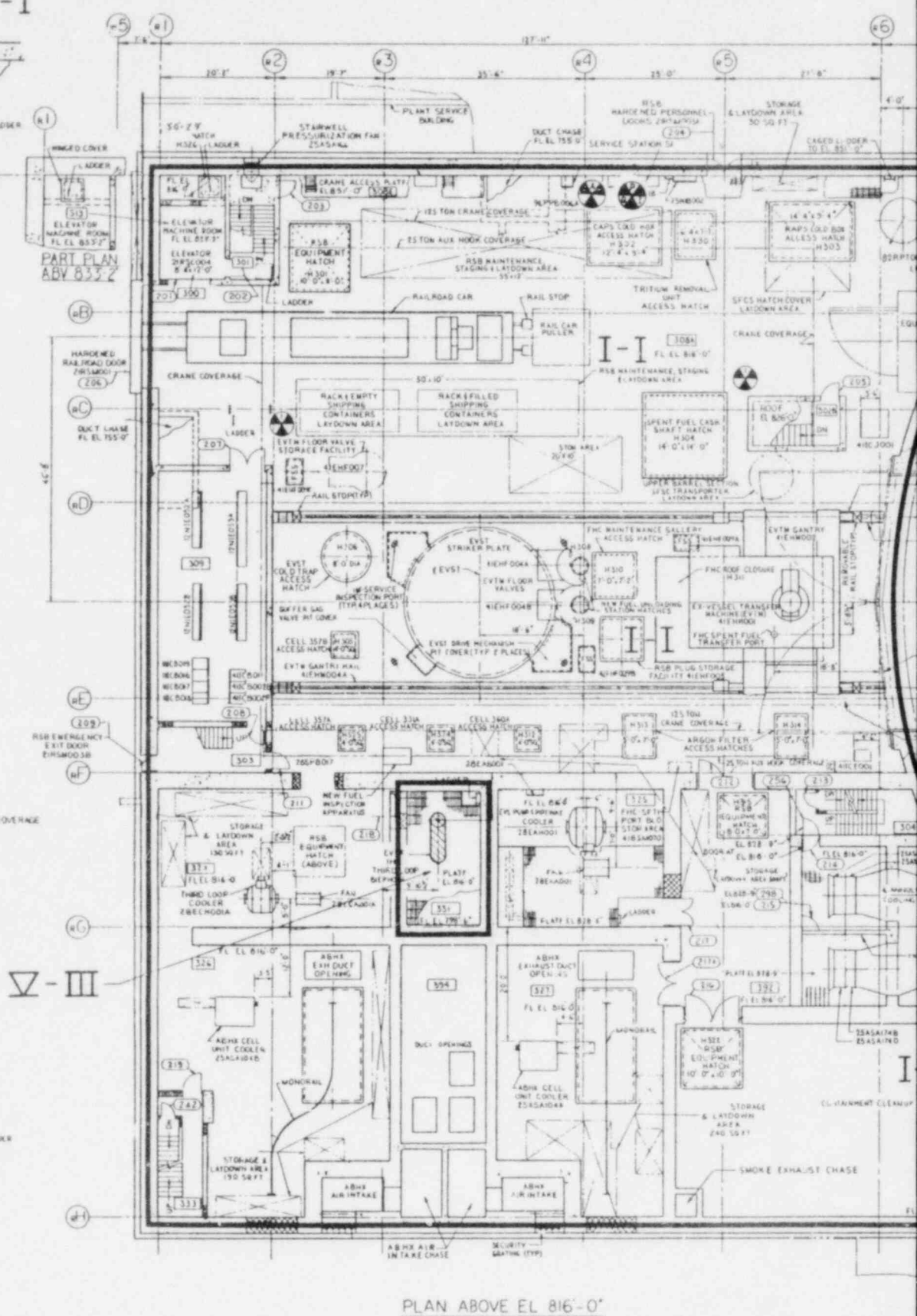
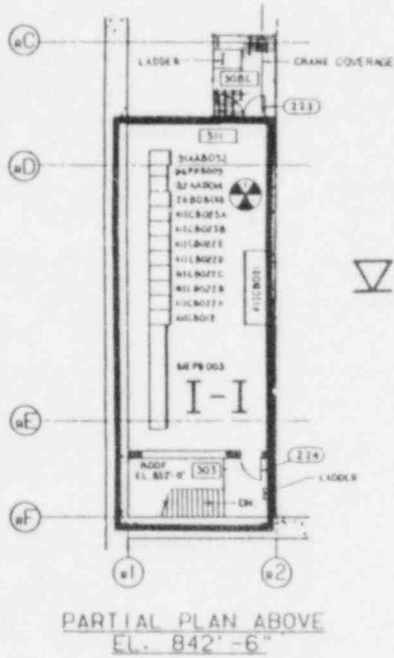
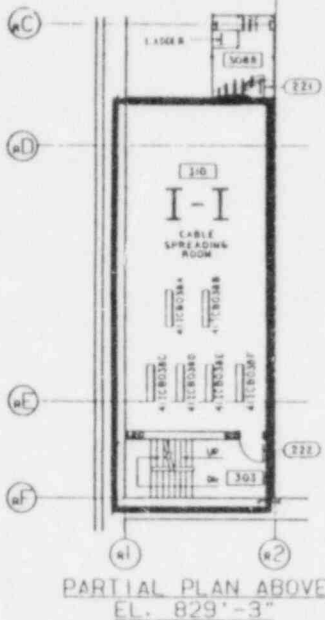
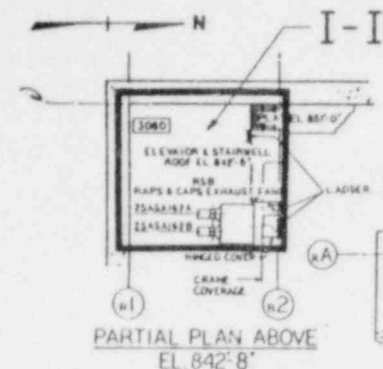
12.1-85

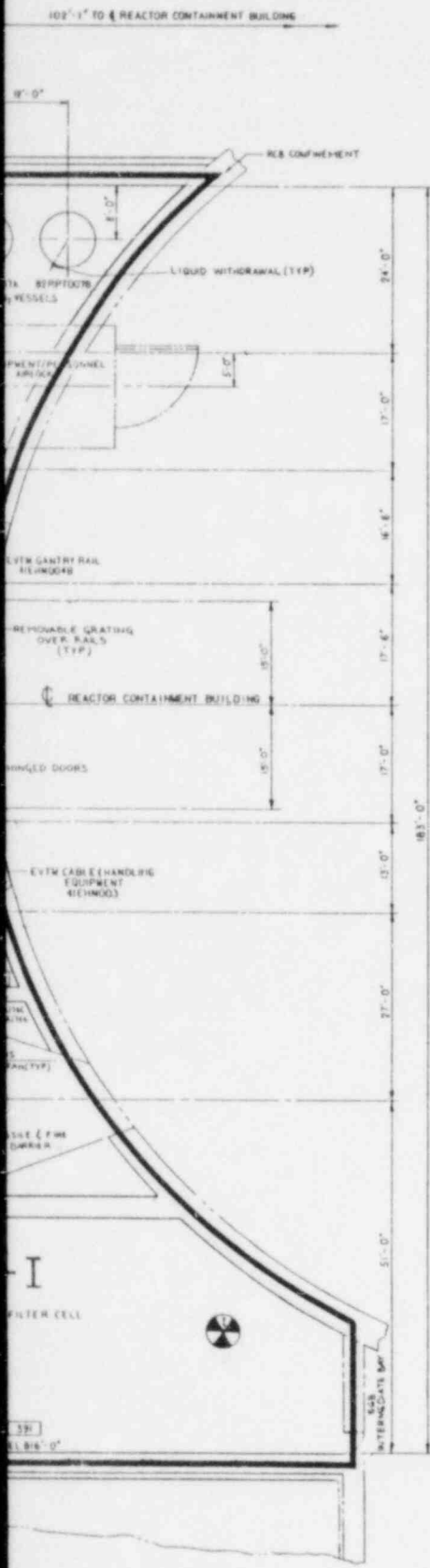
Amend. 72  
Oct. 1982



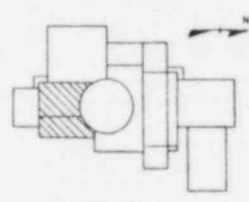








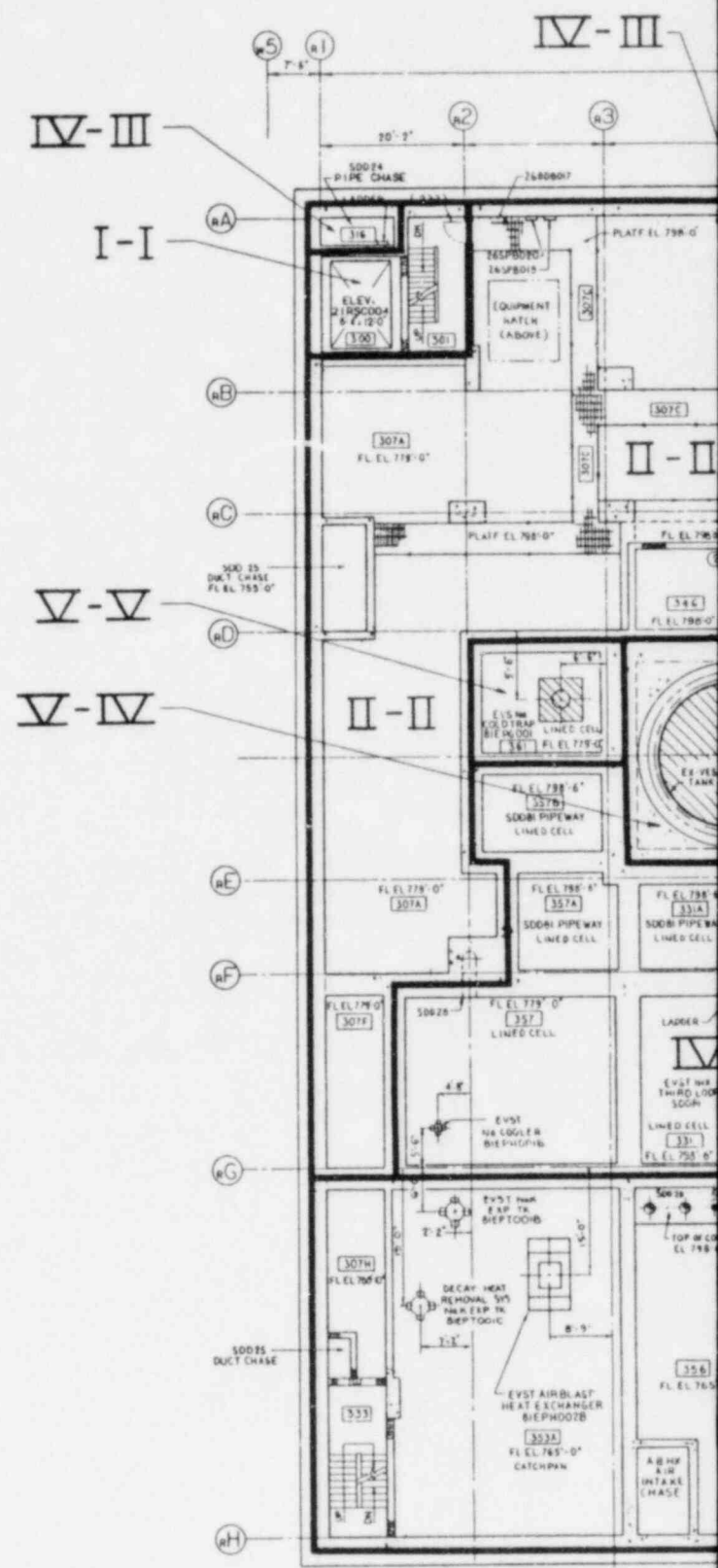
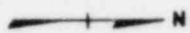
REFERENCE DRAWINGS  
SEE DRAWING NN7459

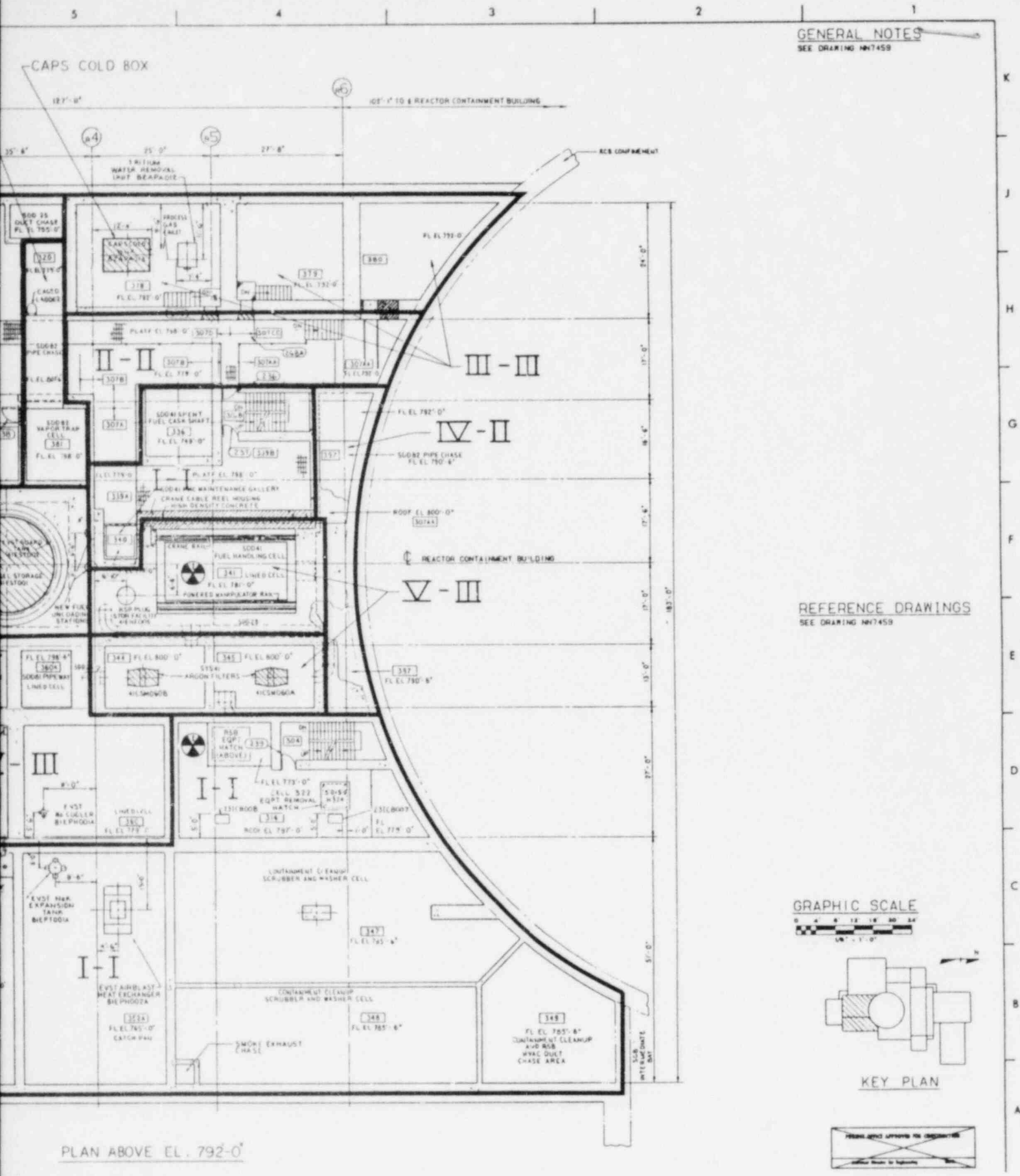


KEY PLAN

Figure 12.1-9 Plant Radiation Protection

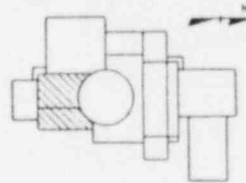
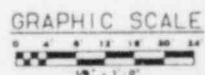
12.1-89 Amend. 72  
Oct. 1982





GENERAL NOTES  
SEE DRAWING NH7459

REFERENCE DRAWINGS  
SEE DRAWING NH7459

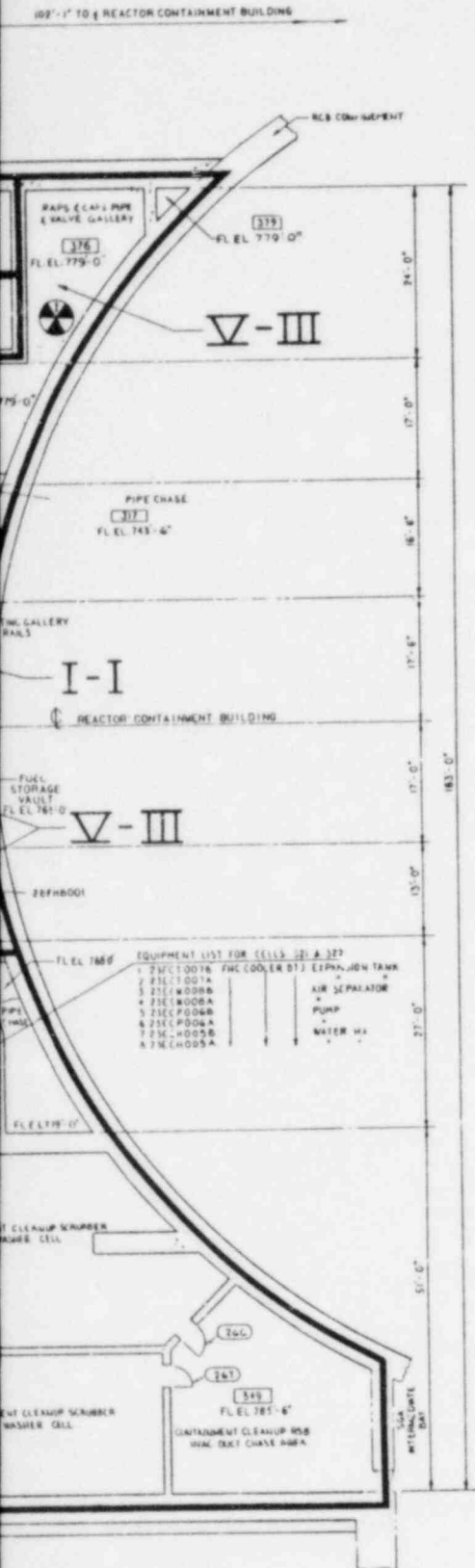


KEY PLAN

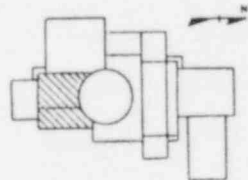
PLAN ABOVE EL. 792'-0"

Figure 12.1-10 Plant Radiation Protection





REFERENCE DRAWINGS  
SEE DRAWING NW458



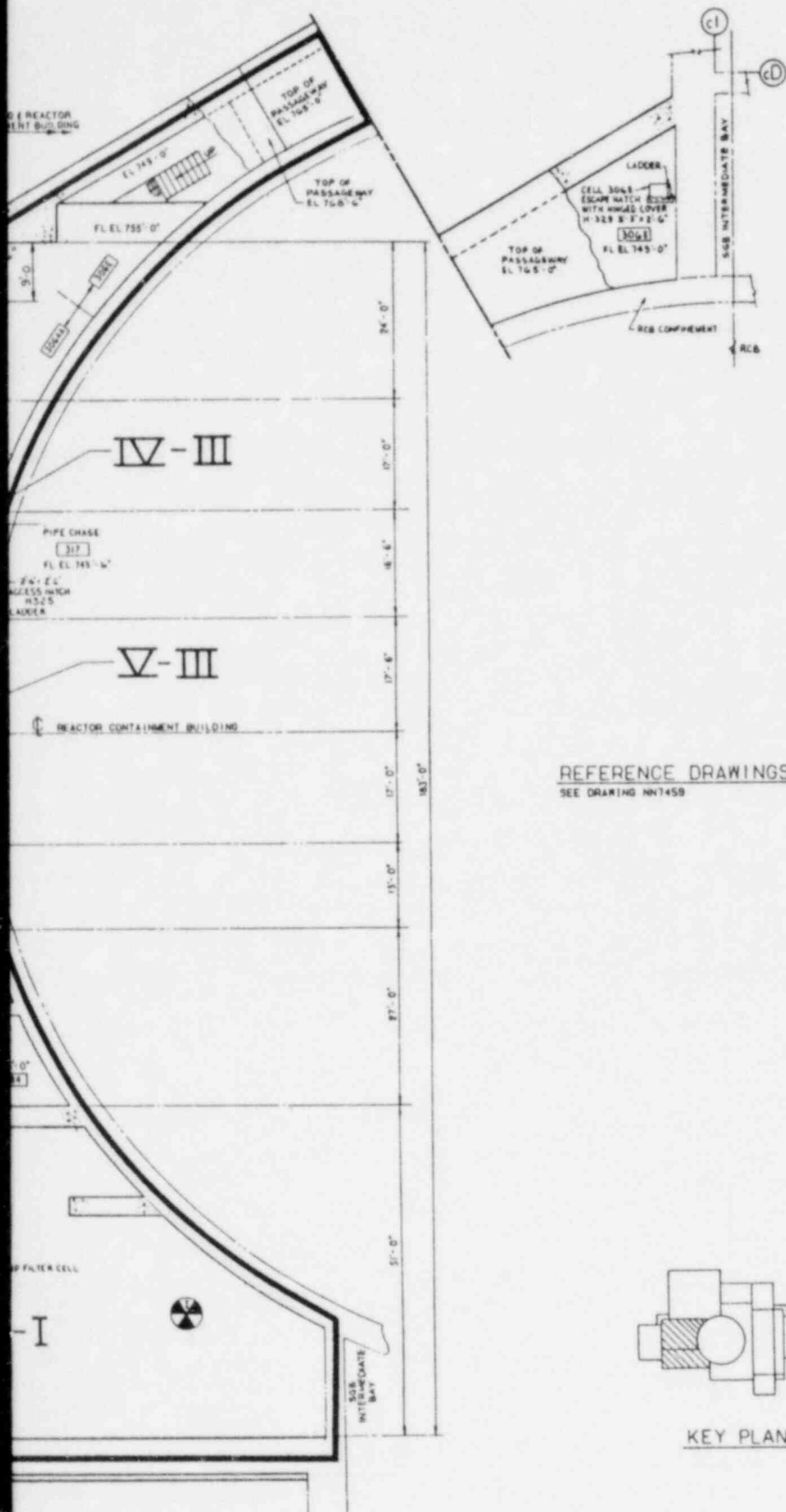
KEY PLAN

Figure 12.1-11 Plant Radiation Protection

12.1-91

Amend. 72  
Oct. 1982





REFERENCE DRAWINGS  
SEE DRAWING NN745B

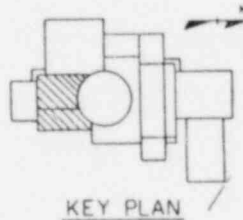


Figure 12.1-12 Plant Radiation Protection

12.1-92 Amend. 72  
Oct. 1982





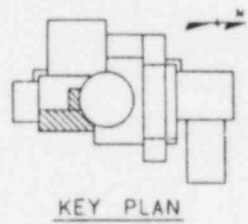
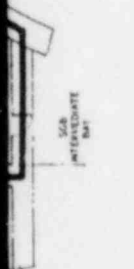
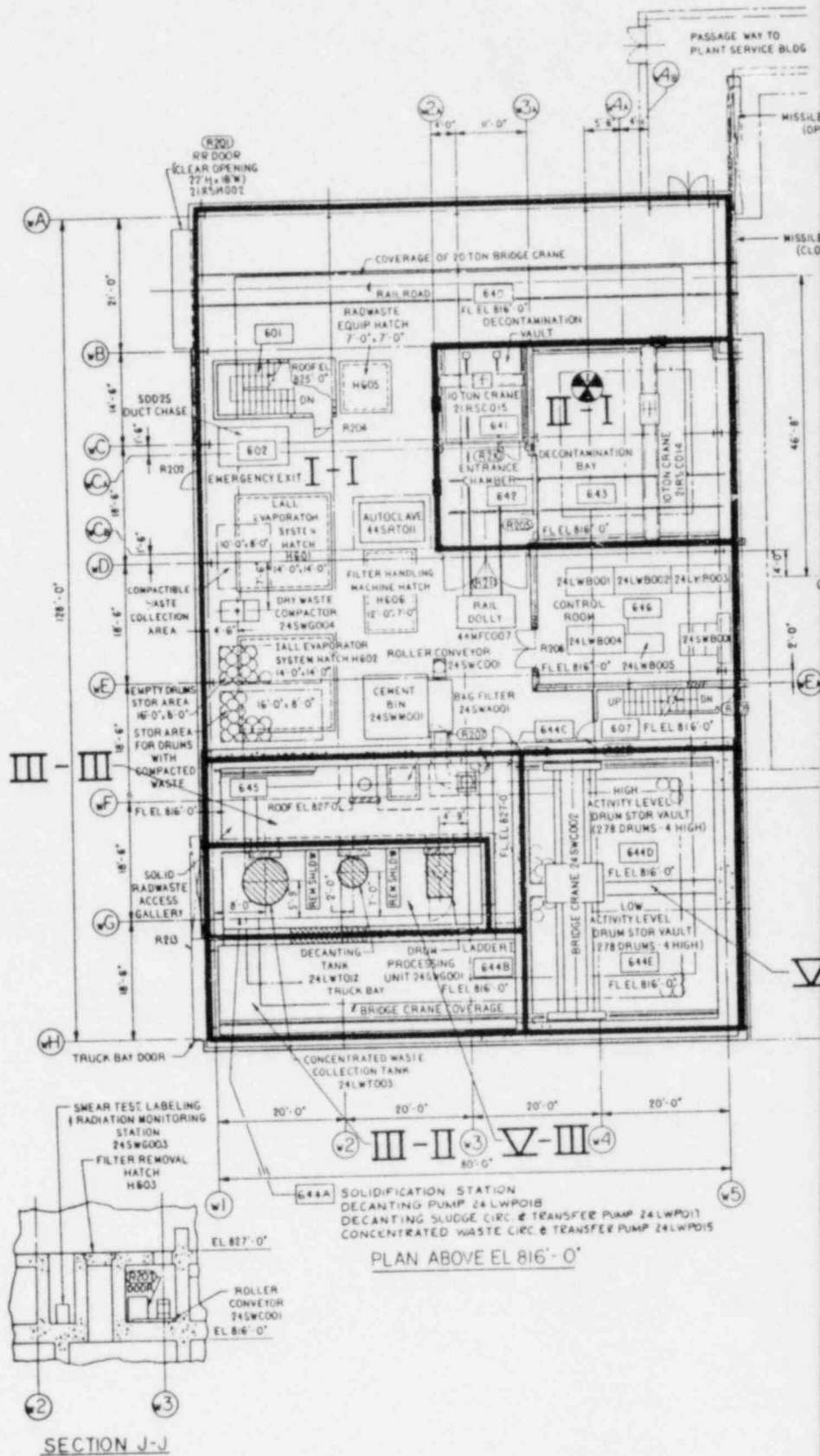


Figure 12.1-13 Plant Radiation Protection

12.1-93      Amend. 72  
Oct. 1982



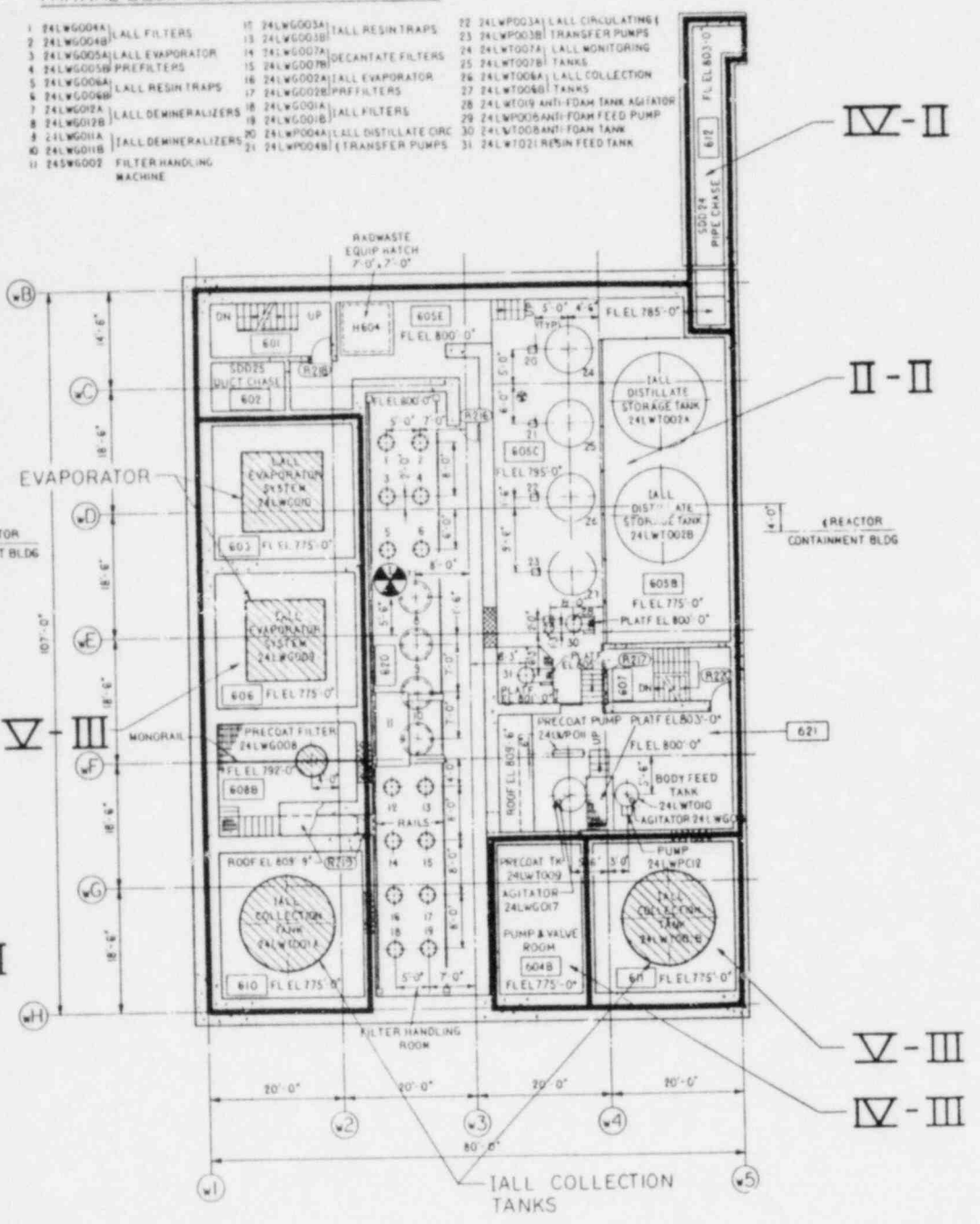




PARTIAL EQUIPMENT LIST - PLAN ABOVE EL 795'-0"

1 24LW0004A	LALL FILTERS	15 24LW0003A	LALL RESIN TRAPS	22 24LW0003A	LALL CIRCULATING
2 24LW0004B	LALL FILTERS	16 24LW0003B	LALL RESIN TRAPS	23 24LW0003B	TRANSFER PUMPS
3 24LW0005A	LALL EVAPORATOR	17 24LW0007A	DECANTATE FILTERS	24 24LW0007A	LALL MONITORING
4 24LW0005B	PREFILTERS	18 24LW0007B	DECANTATE FILTERS	25 24LW0007B	TANKS
5 24LW0006A	LALL RESIN TRAPS	19 24LW0002A	LALL EVAPORATOR	26 24LW0006A	LALL COLLECTION
6 24LW0006B	LALL RESIN TRAPS	20 24LW0002B	PREFILTERS	27 24LW0006B	TANKS
7 24LW0002A	LALL DEMINERALIZERS	21 24LW0001A	LALL FILTERS	28 24LW0009	ANTI-FOAM TANK AGITATOR
8 24LW0002B	LALL DEMINERALIZERS	22 24LW0001B	LALL FILTERS	29 24LW0008A	ANTI-FOAM FEED PUMP
9 24LW0001A	LALL DEMINERALIZERS	23 24LW0004A	LALL DISTILLATE CIRC	30 24LW0008A	ANTI-FOAM TANK
10 24LW0001B	LALL DEMINERALIZERS	24 24LW0004B	LALL DISTILLATE CIRC	31 24LW0021	RESIN FEED TANK
11 24LW0002	FILTER HANDLING MACHINE				

DOOR (H)  
DOOR (E)



REFERENCE DRAWINGS  
SEE DRAWING HW1470

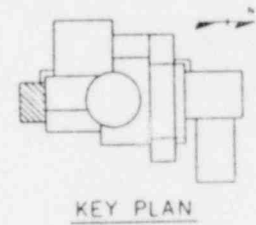
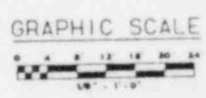
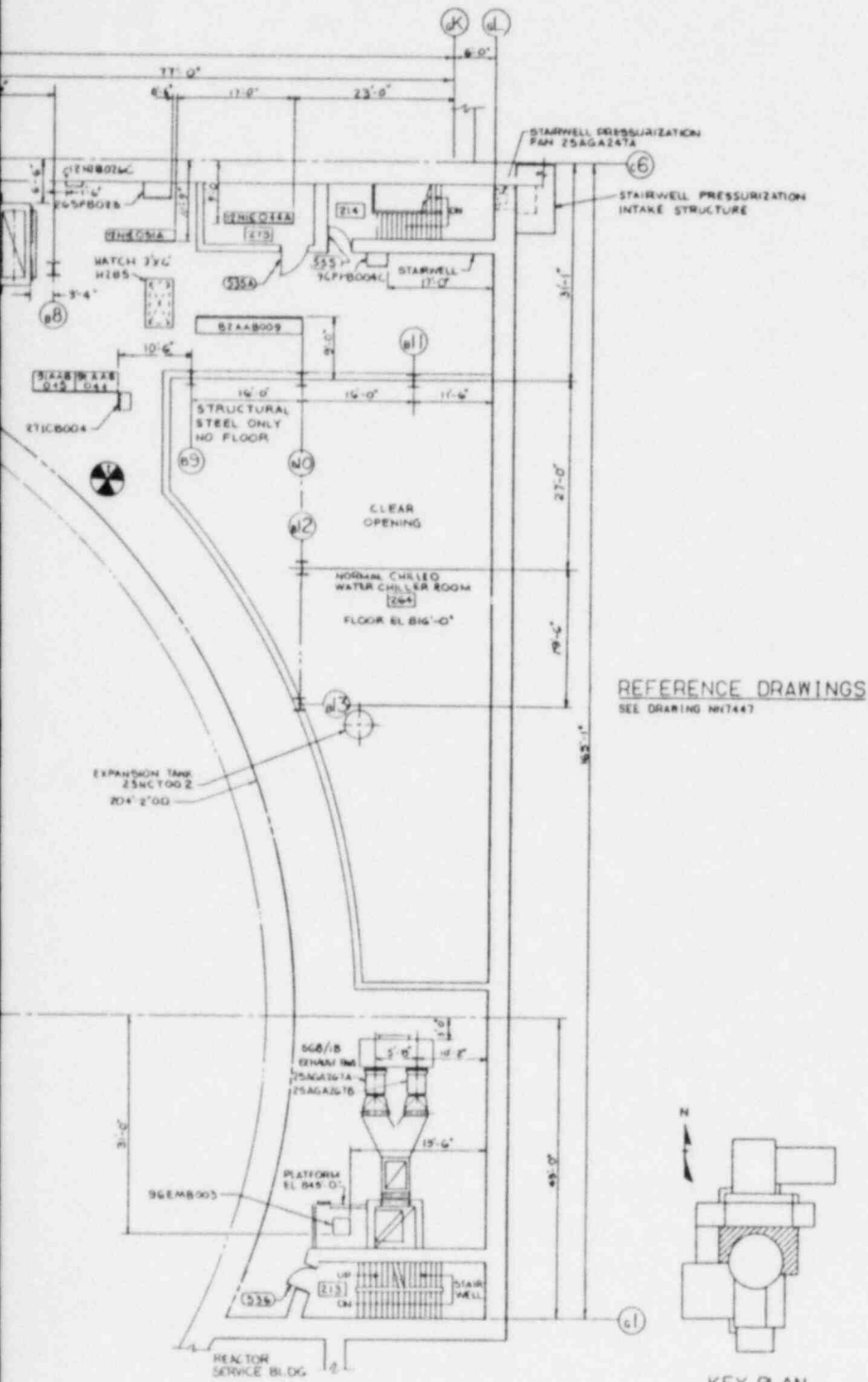


Figure 12.1-16 Plant Radiation Protection





REFERENCE DRAWINGS  
SEE DRAWING M7447

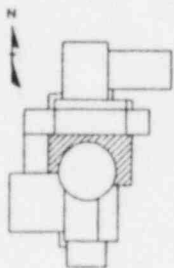


Figure 12.1-19 Plant Radiation Protection

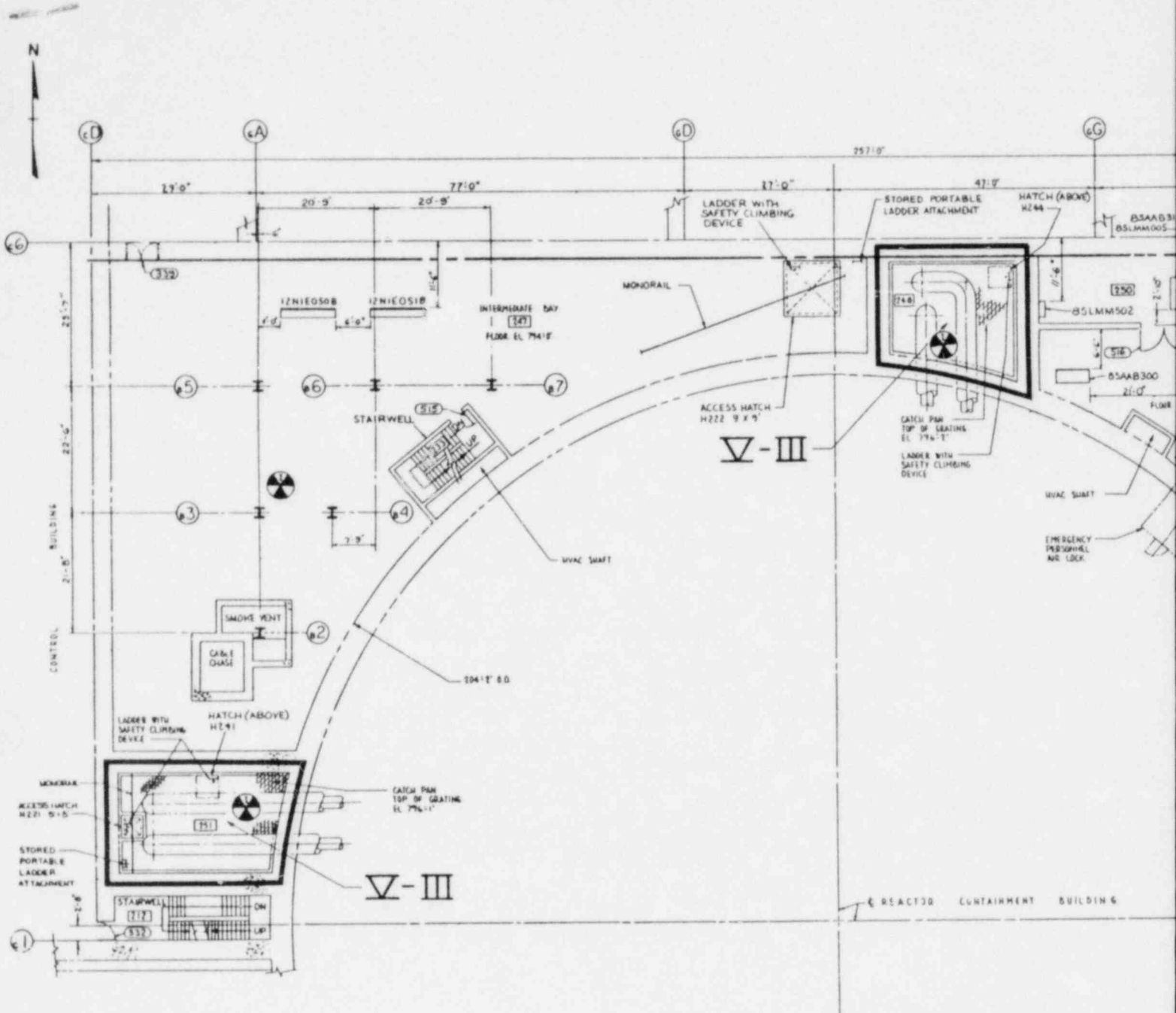
12.1-99

Amend. 72  
Oct. 1982









PLAN ABOVE EL 794'-0"

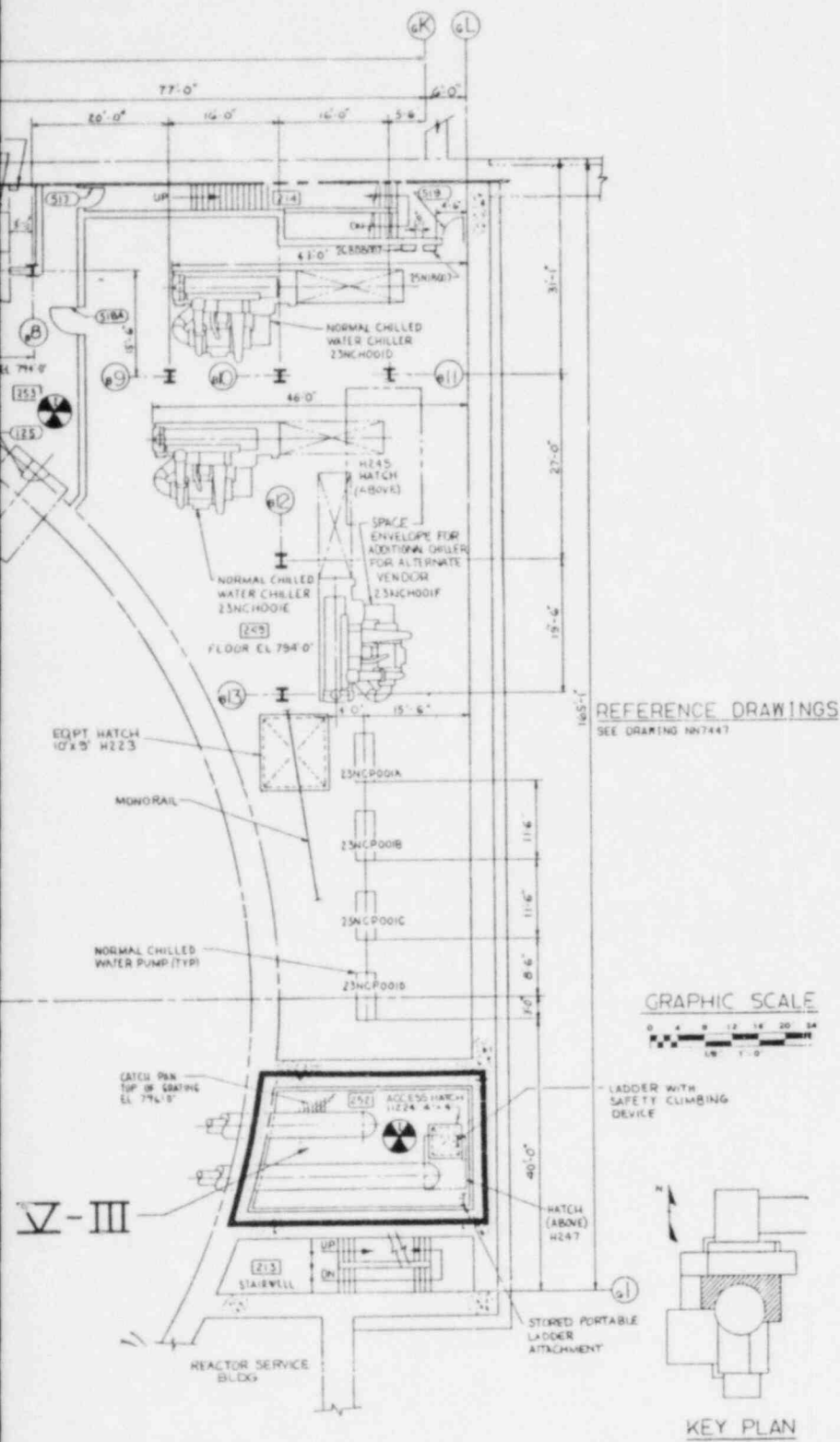


Figure 12.1-19b Plant Radiation Protection

12.1-99b Amend. 72  
Oct. 1982

12.1-101

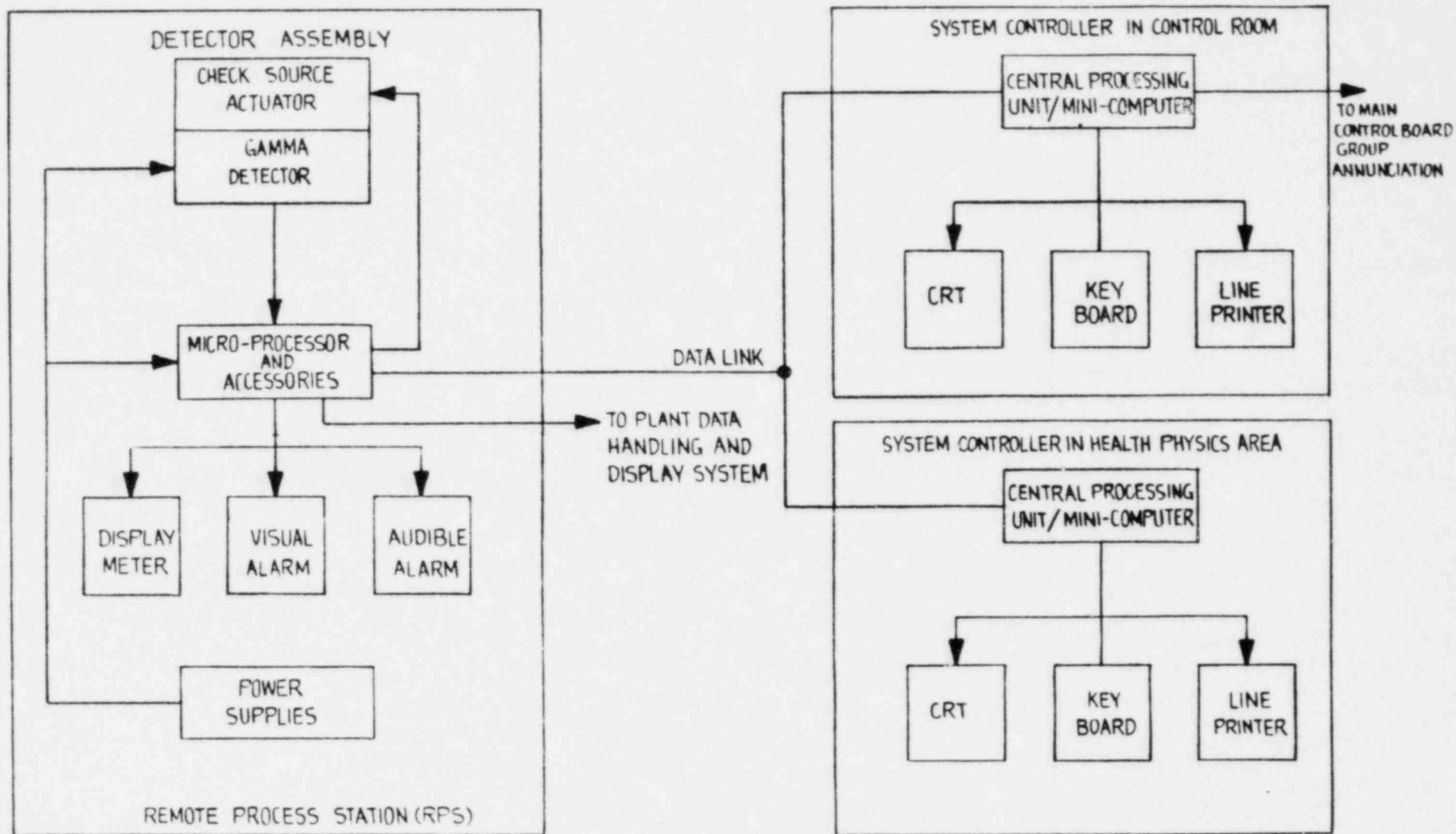


FIGURE 12-1-21 FUNCTIONAL BLOCK DIAGRAM OF AN AREA RADIATION MONITOR

18 |

Sections 9.6.1 through 9.6.5 describe the ventilation systems for each building and the main control room. The conceptual design for the RCB provides 14,000 cfm of outside air. This is adequate to meet the design objectives for radiation protection. The conceptual design flow rate to each of the IHTS piping cells is 1000 cfm, which is sufficient to meet the design objective for radiation protection and to satisfy personnel access requirements. Other plant areas will be designed in accordance with conventional heating and ventilation requirements. Analysis of design requirements for other areas involving potential radioactive release will be undertaken and results incorporated, as necessary, in the heating and ventilation requirements for these areas.

12.2.3 Source Terms

The sources of radioactivity originate from the reactor cover gas leakage and H<sup>3</sup> diffusion. The estimated radioactive leakages rates into normally accessible cells are presented in Table 12.2-1. The basis of the table is provided in Section 11.3.

12.2.4 Airborne Radioactivity Monitoring

12.2.4.1 Design Criteria

49 |

Fixed and mobile continuous air monitors (CAM) will be employed in conjunction with portable air sampling equipment to satisfy the requirements of CRBRP General Design Criteria 17 and 56 and the relevant sections of 10CFR20; and to verify that radioactive atmospheric contamination within the CRBRP remains normally "as low as reasonably achievable".

49 |

The above radioactivity monitoring which is provided for the CRBRP reflects a design philosophy which identifies the following levels of radiation protection (exclusive of the portable personnel monitoring provisions described in Section 12.3).

18 |

1. Continuous monitoring (fixed) performed on the ventilation which serves the Reactor Containment Building (RCB) and Reactor Service Building (RSB) operating areas. Continuous monitoring is also performed to verify Control Room habitability.
2. Continuous monitoring (mobile) is performed in frequently occupied Nuclear Island operating areas adjacent to potential radioactivity sources. Frequently occupied areas include radiation zone I and II (Figures 12.1-1 through 12.1-19) cells which house numerous process system control panels.

49 |

1

3. Low-volume (integrating) air sampling is performed in infrequently occupied operating areas within the Nuclear Island. Infrequently occupied areas include radiation zone II and III cells where routine tasks are performed on a limited access basis.
4. High-volume grab sampling is performed (with accompanying Counting Room analysis) prior to personnel entry into Zone IV radiation zones; and whenever a gross determination of short-lived airborne radioactivity in lower radiation zoned areas is desired.

Fixed CAM's are provided as effluent and process monitors (described in Section 11.4) at locations which could conceivably be subject to increases in radioactivity levels during various plant evolutions. The process monitors are used to monitor the ventilation exhaust from a particular cell or group of cells. Upon detection of radioactivity above desired levels the radiation monitor will produce an alarm at the process system local panel (in addition to the Control Room) and some monitors will initiate a signal to automatically isolate the affected area. The effluent monitors perform surveillance functions and provide (in the Control Room) indication of an abnormal occurrence warranting investigation by Health Physics personnel. Since the effluent monitors don't perform initiation of isolation the ranges have been selected to provide monitoring during normal and accident conditions. These monitors are included in Table 11.4-1. Fixed CAMs, except those downstream of HEPA filters will withdraw the samples isokinetically in accordance with ANSI N13.1. In addition, the monitors will be located as close as practical to the sample point, and sample line bends are minimized to avoid plate out.

Fixed CAM's are also provided to ensure adequate protection against contamination of the Control Room atmosphere due to airborne radioactivity following an accident condition. This monitoring arrangement is described in Section 11.4. Fixed radiogas monitors (PPS) are also used to initiate Reactor Containment Isolation as discussed in Section 7.3.1.

Mobile CAM's will be provided in select locations throughout the CRBRP to perform the following functions:

1. Continuously monitor the atmosphere at any specific location where maintenance is performed.
2. Continuously monitor the atmosphere at any specific location where a process system failure is suspected of causing airborne radioactivity leakage.
3. Continuously monitor individual inerted cell purging activities as required by the Heating, Ventilating and Air Conditioning System.
4. Continuously monitor the RCB atmosphere following containment isolation, after connection to the post-accident containment sampling penetrations discussed in Section 11.4.2.2.1.
5. Provide backup support to inoperative stationary airborne radioactive monitors.

The mobile CAM's will provide local audible and visual alarm indication of airborne radioactivity levels which exceed the monitor setpoint(s). Locations and design parameters of the various mobile airborne activity monitors are given in Table 12.2-3.

High and low volume portable air samplers will be employed to obtain representative samples of breathing air at infrequently occupied operating areas of the CRBRP. Samples obtained will be analyzed in the Counting Room for gross activity and radioisotopic identification, as required. The portable air samplers will be supplied as health physics equipment, and their frequency of use will be governed by the operational procedures of the CRBRP Health Physics Program.

#### 12.2.4.2 Monitoring System Description

##### 12.2.4.2.1 Continuous Air Monitors

Continuous air monitors (CAM) are used to provide detection of radiogas, particulate, radioiodine and alpha (Pu) activity as indicated in Table 12.2-3. A combination of single and multichannel instruments are used to perform the required monitoring functions. The following is a description of each type of monitor provided:

##### Gaseous Radioactivity Monitors

Each radiogas CAM continuously draws gas/air samples through a particulate filter into a shielded 4-Pi sample chamber where the gas is viewed by a beta detector, and then returns the gas/air back to the original source. A regulated vacuum pump is used to maintain desired flow rate through the monitor. Samples withdrawn from process or effluent flow will be obtained isokinetically from the source stream. Each monitor consists of a radiogas detector, vacuum pump, microprocessor and accessories, local indicator and alarms. The detector will have a minimum sensitivity of  $3 \times 10^{-7}$   $\mu\text{Ci/cc}$  for Kr-85, at the 95% confidence level. Each monitor cabinet will include local loss-of-signal, high and high-high radiation indicator lights, gas/air sample flowmeter and count-rate meter. Taps will be provided to allow samples to be withdrawn for analysis in the Counting Room. For stationary monitors, the detection signal is continuously provided for display on redundant Radiation Monitoring System CRTs located in the Control Room and the Health Physics Area of the Plant Service Building, via their respective Central Processing Units and Mini-Computers (System Controllers). All control signals from monitors which are transmitted to interfacing systems will originate from Process Stations which are part of the local monitor cabinet. The alarm signals are permanently recorded by the redundant Radiation Monitoring System Line Printers located in the Control Room and Health Physics Area.



### Iodine and Gaseous Radioactivity Monitors

Radiiodine and radiogas CAM's provide two distinct detection channels within a single monitor housing. A regulated vacuum pump continuously draws a gas/air sample at a measured flow rate into the monitor assembly.

The sampled gas/air flows through a fixed iodine filter, where a gamma detector observes radiiodine activity through a discriminator window. The minimum radiiodine sensitivity is  $10^{-10}$   $\mu\text{Ci/cc}$  for I-131 at the 95% confidence level.

From the iodine filter the air sample passes into a 4-Pi shielded chamber where a beta detector observes gaseous activity with a minimum sensitivity of  $10^{-6}$   $\mu\text{Ci/cc}$  for Kr-85 at the 95% confidence level. The gas/air sample is then exhausted to the original source.

Each monitor contains the detectors, vacuum pump, microprocessor and accessories, and indicators. Display provisions at each monitor cabinet include (common for each detection channel) loss-of-signal, high and high-high radiation indicator lights, and (separate for each detection channel) count-rate meters. A sample flow rate gauge is also provided.

The detection signal is continuously provided for display on redundant Radiation Monitoring system CRTs located in the Control Room and the Health Physics Area of the Plant Service Building, via their respective Central Processing Units and Mini-Computers (system Controllers). All Control signals from monitors which are transmitted to interfacing systems will originate from Remote Process Stations which are part of the local monitor cabinet. The alarm signals are permanently recorded by the redundant Radiation Monitoring System Line Printers located in the Control Room and Health Physics Area.

### Particulate, Iodine and Gaseous Radioactivity Monitors

Particulate, radiiodine and radiogas CAM's provide three distinct detection channels within a single monitor housing. A regulated vacuum pump continuously draws a gas/air sample at a measured flow rate into the monitor assembly. If process or effluent flow is being monitored, the sample is obtained isokinetically from the source stream. Particulates are collected on a filter paper having an efficiency of 99.0% for 0.3 microns particle sizes and viewed by a beta detector of minimum sensitivity of  $10^{-10}$   $\mu\text{Ci/cc}$  for Cs-137 at the 95% confidence level, during an integrating time determined by sample flow rate. From the particulate filter, the sampled gas/air flows through a fixed iodine filter, where a gamma detector observes radiiodine activity through a discriminator window. The minimum radiiodine sensitivity is  $4 \times 10^{-12}$   $\mu\text{Ci/cc}$  for I-131 at the 95% confidence level.

From the Iodine filter the air sample passes into a 4-Pi shielded chamber where a beta detector observes gaseous activity with a minimum sensitivity of  $3 \times 10^{-7}$   $\mu\text{Ci/cc}$  for Kr-85 at the 95% confidence level. The gas/air sample is then exhausted to the original source.

Each monitor contains the detectors, vacuum pump, microprocessor and accessories, and indicators. Display provisions at each monitor cabinet include (common for each detection channel) loss-of-signal, high and high-high radiation indicator lights, and (separate for each detection channel) count-rate indicators. Mobile monitors are provided with a multipoint strip-chart recorder and audible and visual alarms for high and high-high radiation conditions.

For stationary monitors, the detection signal is continuously provided for display on redundant Radiation Monitoring System CRTs located in the Control Room and the Health Physics Area of the Plant Service Building, via their respective Central Processing Units and Mini-Computers (System Controllers). All control signals from monitors which are transmitted to interfacing systems will originate from Remote Process Stations which are part of the local monitor cabinet. The indicating analog meter in the Remote Process Station will indicate counts per minute on a five decade logarithmic scale. The alarm signals are permanently recorded by the redundant Radiation Monitoring System Line Printers located in the Control Room and Health Physics Area.

#### Gaseous In-Line Monitors

Gaseous in-line monitors provided to monitor radioactivity in some process systems including HVAC. The Monitor consists of a shielded section of pipe which is mounted by end flanges in the process line. A penetration through the pipe wall allows a beta scintillation detector to be placed in the process system flow. The detector will have a minimum sensitivity of  $10^{-6}$   $\mu\text{Ci/cc}$  for Kr-85, at the 95% confidence level. Each monitor will have a local microprocessor with local indicator and alarms.

The detection signal is continuously provided for display on redundant Radiation Monitoring System CRTs located in the Control Room and the Health Physics Area of the Plant Service Building, via their respective Central Processing Units and Mini-Computers (System Controllers). All control signals from monitors which are transmitted to interfacing systems will originate from Remote Process Stations which are part of the local monitor cabinet. The alarm signals are permanently recorded by the redundant Radiation Monitoring System Line Printers located in the Control Room and Health Physics Area.

#### Alpha Radioactivity Monitors

Each alpha CAM (mobile units) provided will have the capability to differentiate plutonium alpha readings from the natural radon thoron alpha background through delayed detection techniques. Each alpha CAM continuously draws air samples into a shielded chamber where particulates greater than 0.3 microns are deposited on a filter with an efficiency of 99.0% and viewed by  $\alpha$  detector(s). A regulated vacuum pump will be used

to maintain desired flow rate through the monitor arrangement, and return the air sample back to the original source. Each monitor contains the alpha detector(s), vacuum pump, microprocessor and accessories and indicators. The detector(s) will have a minimum sensitivity of  $10^{-12}$   $\mu\text{Ci/cc}$  for Pu-239 at the 95% confidence level for a collection time of 8 hours. Display provisions at each monitor cabinet include loss-of-signal, loss-of-sample flow, high and high-high radiation indicator lights, sample flow-meter, count-rate meter, strip-chart recorder and audible alarms for high and high-high radiation conditions. These monitors shall have the capability to transmit data to the radiation monitoring consoles in the control room and health physics area when linked to the communication loop at the option of plant operators.

Figures 12.2-1 and 12.2-2 show typical block diagrams of the containment exhaust (PPS) and typical fixed (non-PPS) continuous air radiation monitoring channels. The PPS radiogas monitors used for Containment Isolation differ from the radiogas CAM described previously in the following manner:

1. Each Class 1E Monitor is individually wired to a dedicated Display and Control Unit (DCU) in the Control Room.
2. An analog output is provided by each monitor to the Plant Protection System (Containment Isolation System) Comparators, Logic and Safety Circuits.
3. The buffered output of each monitor is available for display on the Radiation Monitoring System CRTs and logging on Line Printers.

All CAM components will be modular, commercially available units designed for rapid replacement upon failure. Electric components will be exclusively solid-state, as available, and power will be supplied from the Instrument AC busses (120V, 60Hz), with the exception of Class 1E monitors. These latter CAM's will receive Class 1E power (120 Vac, 60Hz) from redundant vital instrument AC busses. Certain design parameters, as well as locations of the various airborne activity monitors are given in Table 12.2-3.

#### 12.2.4.2.2 Portable Air Samplers

Portable air samplers will be used to obtain representative samples of both long and short-lived airborne radioactive contaminants in operating areas of the plant. Their use and placement will be under the direction of the CRBRP site Health Physicist.

##### Low Volume Samplers

Each sampling station consists of a regulated air pump and filter arrangement to deposit particulates greater than 0.3 microns in size, and/or radiiodine, as required. The sample flow rate is set locally and recorded to enable an accurate determination of activity. The filters will be collected after a suitable integrating time interval, and brought to the Counting Room for analysis. The only local output from the sampler unit is the pump flow signal. The complete pump and filter(s) arrangement are standard, commercially available units designed for ease of maintenance and interchangeability of components.

### High Volume Samplers

High volume samplers will employ high speed air blowers to enable grab samples to be obtained in the 20-35 cfm range. Particulate and/or charcoal filters will be used for sample collection, and analysis in the Counting Room will be performed. This type of sampler will be used to determine the airborne radioactivity contribution due to shorter lived isotopes.

#### 12.2.4.3 Maintenance and Calibration

On completion of the monitoring system installation, each CAM will be checked for proper operation and calibrated against a radiation check source(s) traceable back to the National Bureau of Standards or from an equally acceptable source. This initial calibration, and subsequent calibration at six month intervals will verify the electronic operation of both local and Control Room ratemeters and also all annunciation points (loss-of-signal, high radiation, etc.) In addition, each monitor is supplied with a built-in check source to provide rapid functional tests at periodic intervals.

#### 12.2.5 Inhalation Doses

Inhalation doses to plant personnel will be limited and controlled consistent with 10CFR20 requirements via the heating and ventilation system design. Resulting doses will be kept as low as practicable during operation and maintenance and exposures will be compatible with existing regulations (10CFR20).

The expected annual inhalation doses to plant personnel in normally accessible cells can be determined from the leakage rates given in Table 12.2-1 and the design flow rates for ventilation air in the Heat Access Area and Intermediate Sodium Piping cells.

The concentration in these cells, for the expected leakage rates, is estimated by assuming that there is a uniform concentration in the cell atmosphere and the ventilation air stream. Thus, an equilibrium concentration will exist when the curie content discharged per day is equal to the leakage into the cell. The expected concentrations in the accessible cells are given in Table 12.2-4. The doses from the expected concentration can be estimated by assuming the ratio of the concentration to MPC occupational limits for each isotope present and multiplying this by 5 rem, the annual dose which would result from exposure to the MPC for 40 hours per week for 50 weeks of the year.

As shown in Table 12.2-4, the combined expected activity level for the isotopes present is about 0.01 MPC (occupational) in the Head Access Area. Thus, the corresponding annual dose would be about 5mrem/year.

The release to the Intermediate Sodium Piping cells is tritium and the resulting equilibrium concentration is 0.0008 MPC. The resulting expected yearly dose would be about 4mrem/year.

Both of the above annual dose estimates are conservative since each assumes occupancy in the cells by an individual of 40 hours per week for 50 weeks of the year. The expected occupancy is considerably less.

The control room will be designed to assure continued occupancy during postulated accident conditions. The expected radioactivity in the control room during normal plant operations is background level. Additional discussion is provided in Section 12.1.5.

TABLE 12.2-3  
LOCATION OF CONTINUOUS AIR MONITORS

LOCATION			TYPE OF MONITOR	MONITOR AREA DESCRIPTION	BASIS FOR LOCATION/FUNCTION	REMARKS
BLDG.	ELEV.	CELL NO.				
RCB	B16	161A	Particulate/Radio-Iodine/Gaseous	Operating Floor	Mobile monitor to provide monitoring of work areas within containment	See Figure 12.2-2, See Sections 12.2.4.1 & 12.2.4.2.1. This location is the normal storage position of the mobile monitor.
RCB	B16	161A	Particulate/Radio-Iodine/Gaseous	Operating Floor	Mobile monitor to provide monitoring of work areas and inerted cells in the containment	See Figure 12.1-2, See Sections 12.2.4.1 & 12.2.4.2.1. This location is the normal storage position of the mobile monitor.
RCB	B16	161A	Alpha	Operating Floor	Mobile monitor to provide monitoring of work areas within containment	See Figure 12.1-2, See Sections 12.2.4.1 & 12.2.4.2.1. This location is the normal storage position of the mobile monitor.
RCB	766	105M	Particulate/Radio-Iodine/Gaseous	Operating Floor	Mobile monitor to provide monitoring of work areas and inerted cells in the containment	See Figure 12.2-5, See Sections 12.2.4.1 & 12.2.4.2.1. This location is the normal storage position of the mobile monitoring.

12.2-9

Amend. 72  
Oct. 1982

TABLE 12.2-3 (Cont'd)

LOCATION			TYPE OF MONITOR	MONITOR AREA DESCRIPTION	BASIS FOR LOCATION/FUNCTION	REMARKS
BLDG.	ELEV.	CELL NO.				
RSB	779	307B	Particulate/Radioiodine/Gaseous	Operating Floor	Mobile monitor to provide monitoring of local work areas and post-accident monitoring of containment atmosphere	See Figure 13.1-11, See Sections 12.2.4.1, 12.2.4.2.1 & 11.4.2.2.1. This location is the normal storage position of the mobile monitor.
RSB	816	308A	Alpha	Operating Floor	Mobile monitor to provide monitoring of local work areas and post-accident monitoring of containment atmosphere	See Figure 12.1-9, See Sections 12.2.4.1, 12.2.4.2.1, & 11.4.2.2.1. This location is the normal storage position of the mobile monitor.
RSB	816	308B	Particulate/Radioiodine/Gaseous	Operating Floor	Mobile monitor to provide monitoring of local work areas	See Figure 12.1-9, See Sections 12.2.4.1 & 12.2.4.2.1. This location is the normal storage position of the mobile monitor.
SGB-IB	816	262	Particulate/Radioiodine/Gaseous	Operating Floor	Mobile monitor to provide monitoring of SGB-IB local work areas and post-	See Figure 12.1-19a, See accident monitoring of containment Sections 12.2.4.1, atmosphere 12.2.4.2.1 & 11.4.2.2.1. This location is the normal storage position of the mobile monitor.

12.2-10

Amend. 72  
Oct. 1982

TABLE 12.2-3 (Cont'd)

LOCATION			TYPE OF MONITOR	MONITOR AREA DESCRIPTION	BASIS FOR LOCATION/FUNCTION	REMARKS
BLDG.	ELEV.	CELL NO.				
CB	816	431	Particulate/Radio-iodine/Gaseous	Operating Floor	Mobile monitor to provide monitoring of control room and local work areas	See Section 12.2.4.1 & 12.2.4.2.1. This location is the normal storage position of the mobile monitor.

12.2-10a

Amend. 72  
Oct. 1982



TABLE 12.2-4

## EXPECTED\* ANNUAL EXPOSURE IN NORMALLY ACCESSIBLE CELLS

Head Access Area

Isotope	Expected Concentration ( $\mu\text{Ci/ml}$ )	MPC+ ( $\mu\text{Ci/ml}$ )	Expected Concentration : MPC
Xe 131m	9.7 E-13	2.0 E-05	4.8 E-8
133m	3.0 E-11	1.0 E-05	3.0 E-6
133	5.5 E-10	1.0 E-05	5.5 E-5
135m	9.4 E-12	1.0 E-06	9.4 E-6
135	1.3 E-9	4.0 E-06	4.5 E-4
138	1.6 E-11	1.0 E-06	1.6 E-5
Kr 83m	2.9 E-11	1.0 E-06	2.9 E-5
85m	1.1 E-14	6.0 E-06	1.9 E-5
85	1.7 E-14	1.0 E-05	1.7 E-9
87	6.0 E-11	1.0 E-06	6.0 E-5
88	1.7 E-10	1.0 E-06	1.7 E-4
Ar 39	3.5 E-9	5.0 E-06	7.0 E-4
49   41	6.4 E-11	2.0 E-06	3.2 E-5
H 3	9.2 E-15	5.0 E-06	1.8 E-9
49   TOTAL	5.84 E-9		0.0015

Intermediate Sodium Piping Cells

49   H3	4.0 E-09	5.0 E-06	7.9 E-04
---------	----------	----------	----------

+MPC = MPC for Restricted Areas

\*Failed Fuel Fraction = 0.1 percent at 1 year operation

Amend. 49  
April 1979

12.2-12

Amend. 72  
Oct. 1982

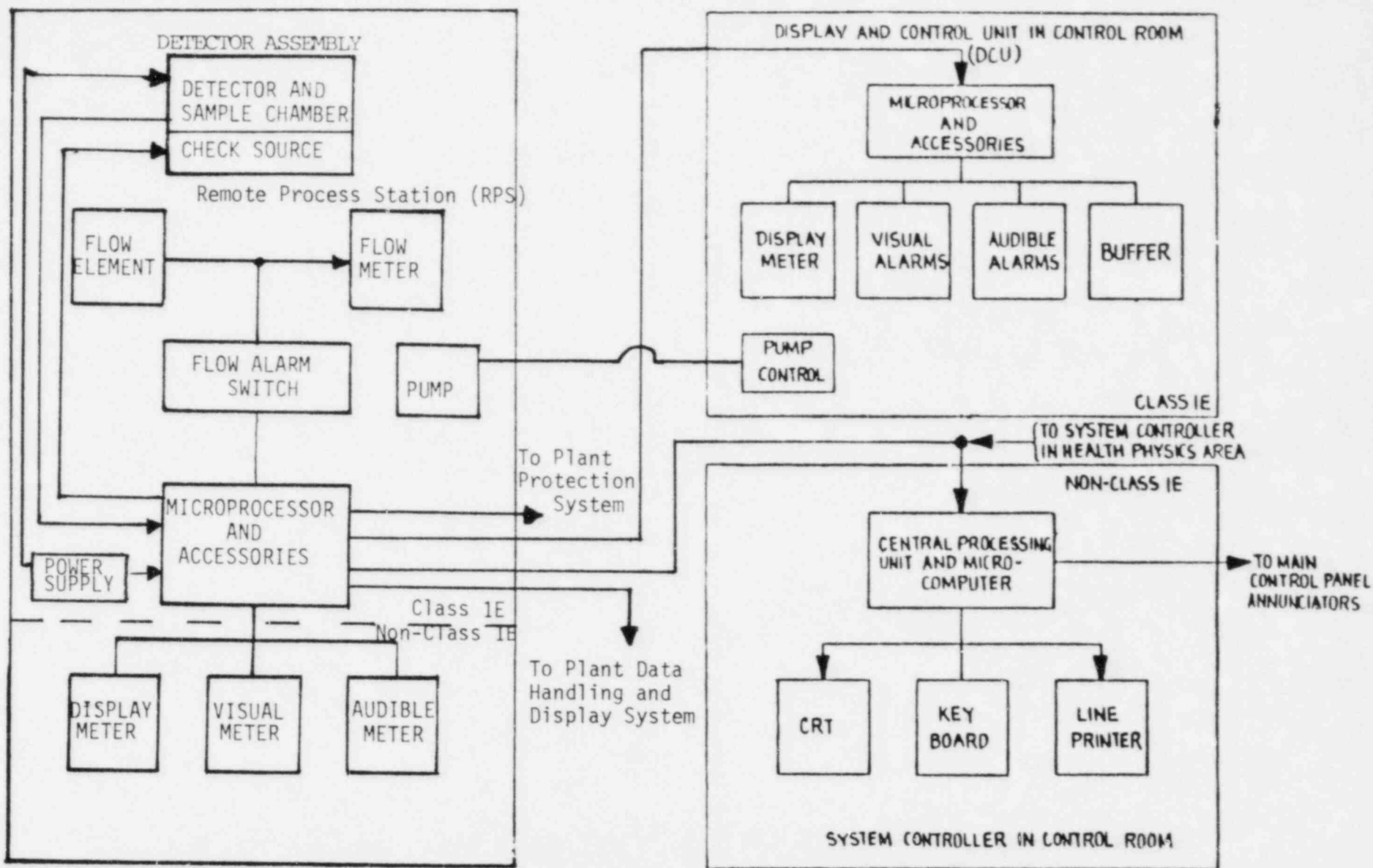


FIGURE 12-2-1 PPS CONTAINMENT EXHAUST RADIATION MONITORING CHANNEL (CLASS 1E)

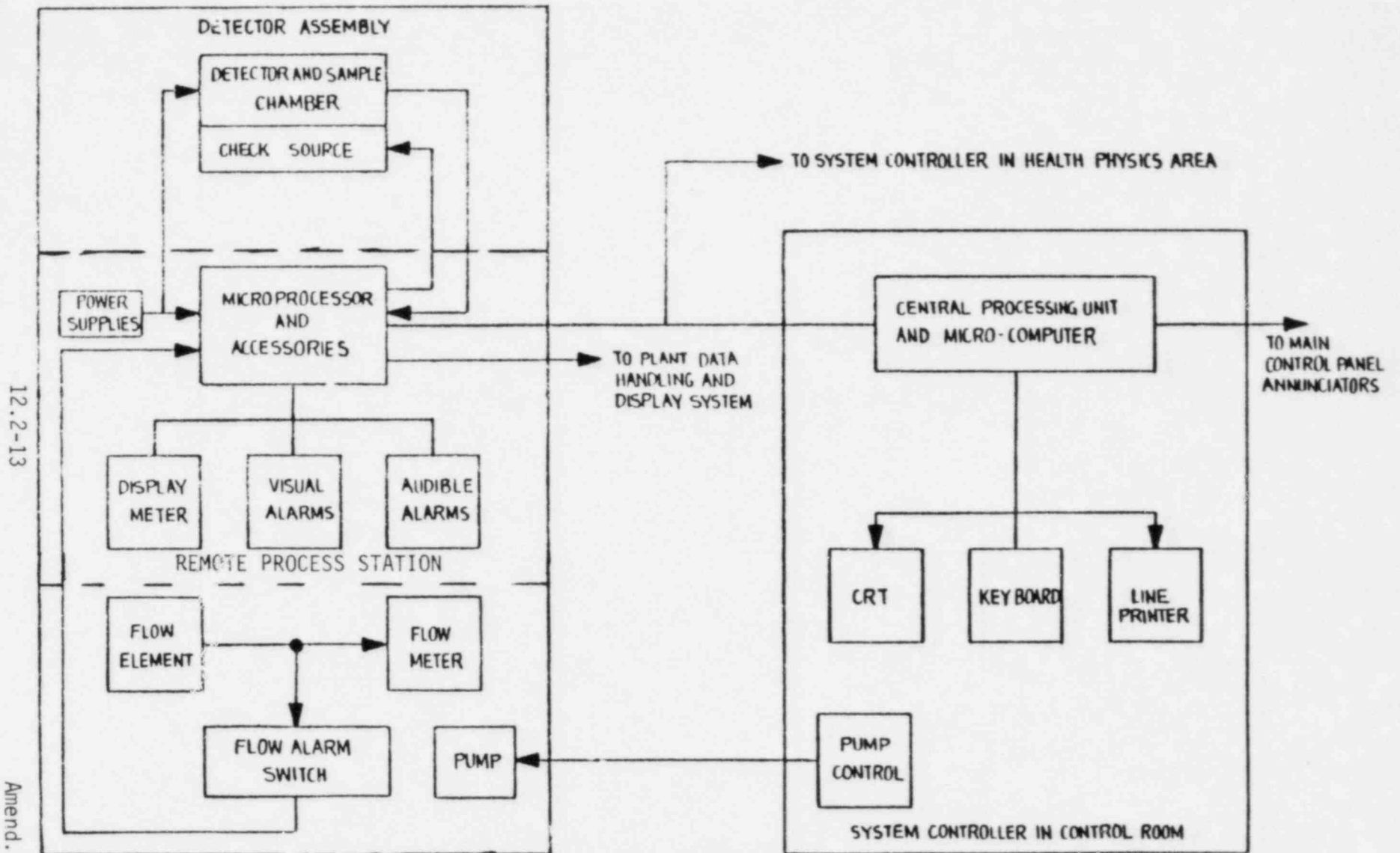


FIGURE 12-2-2 NON PPS AIR RADIATION MONITORING CHANNEL

TABLE 12.3-5

## PERSONNEL PROTECTION MONITOR - AREA MONITORS

BLDG.	LOCATION		AREA AND/OR PROCESS MONITORED	MONITOR TYPE	METER RANGE mR/hr	OPERATIONAL BACKGROUND (mR/hr)	MONITOR OUTPUT**	BASIS FOR LOCATION*
	ELEV.	CELL						
RCB	824'	162	I&C Cubicle	Direct Gamma	0.01-10 <sup>3</sup>	0.2	A	1.
RCB	824'	163	I&C Cubicle	Direct Gamma	0.01-10 <sup>7</sup>	0.2	A	1,5
RCB	824'	164	I&C Cubicle	Direct Gamma	0.01-10 <sup>7</sup>	0.2	A	1.,4,3
RCB	780'	105U	Primary PTI Operating Area	Direct Gamma	0.1-10 <sup>4</sup>	2.0	A	1.,2
RCB	766'	105S	Operating Floor	Direct Gamma	0.1-10 <sup>4</sup>	2.0	A	1.,2.,5
RCB	780'	161G	Operating Floor	Direct Gamma	0.1-10 <sup>4</sup>	2.0	A	1.,2.
RCB	794'	152	Operating Floor	Direct Gamma	0.1-10 <sup>4</sup>	2.0	A	1.,2.
RCB	752'	105H	Operating Floor	Direct Gamma	0.1-10 <sup>4</sup>	2.0	A	1.,2.
RCB	766'	105Q	Operating Floor	Direct Gamma	0.1-10 <sup>4</sup>	2.0	A	1.,2
RCB	733'	105A	Operating Floor	Direct Gamma	0.1-10 <sup>4</sup>	2.0	A	1.,2,5
RSB	842'6"	311	Refuel. Comm. Center	Direct Gamma	0.01-10 <sup>3</sup>	0.2	B	1.,3
RCB	802'	151	Head Access Area	Direct Gamma	0.1-10 <sup>7</sup>	25.0	A	1.,2.,4.
RSB	816'	308A	Operating Floor	Direct Gamma	0.01-10 <sup>3</sup>	0.2	B	1.,2.,3,6
RSB	816'	308A	Operating Floor	Direct Gamma	0.01-10 <sup>3</sup>	0.2	B	1.,3,6
RWB	816'	643	Decontamination Bay	Direct Gamma	0.1-10 <sup>4</sup>	2.0	B	1.,2
RCB	794'	105V	Operating Floor	Direct Gamma	0.1-10 <sup>4</sup>	2.0	A	1.,2,5
RSB	779'	307A	Ex-Vessel SSP Operating Area	Direct Gamma	0.1-10 <sup>4</sup>	2.0	A	1.
RCB	752'	105K	Operating Area	Direct Gamma	0.1-10 <sup>4</sup>	2.0	A	1.
RSB	755'	306A	Ex-Vessel PTI Operating Area	Direct Gamma	0.1-10 <sup>4</sup>	2.0	A	1.
SGB	836'	27'	SGB(IB) Remote Shutdown Panels Area	Direct Gamma	0.01-10 <sup>7</sup>	Unrestricted (See NOTE 2)	A	1.

12.3-13

Amend. 72  
Oct. 1982

TABLE 12.3-5 (Cont'd)

BLDG.	LOCATION		AREA AND/OR PROCESS MONITORED	MONITOR TYPE	METER RANGE mR/hr	OPERATIONAL BACKGROUND (mR/hr)	MONITOR OUTPUT**	BASIS FOR LOCATION*
	ELEV.	CELL						
RCB	733'	105F	Make-up Pump Valve Operating Gallery	Direct Gamma	0.1-10 <sup>4</sup>	2.0	A	1,5
RCB	733'	105D	Operating Area	Direct Gamma	0.1-10 <sup>4</sup>	2.0	A	1.
RCB	766'	105M	Primary SSP Operating Area	Direct Gamma	0.1-10 <sup>4</sup>	2.0	A	1.,2.
RWB	795'	605C	IALL Distillate Storage Tank Area	Direct Gamma	0.1-10 <sup>4</sup>	2.0	A	1
RWB	795'	620	Filter Handling Room	Direct Gamma	0.1-10 <sup>4</sup>	2.0	A	1
RSB	733'	305B	Operating Areas	Direct Gamma	0.1-10 <sup>4</sup>	2.0	A	1
RSB	779'	307A	Operating Floor	Direct Gamma	0.1-10 <sup>4</sup>	2.0	B	1.,2
RSB	781'	341	Fuel Handling Cell	Direct Gamma	0.01-10 <sup>8</sup>	2.0x10 <sup>8</sup>	B	3.
RSB	779'	339A	FHC Operating Gallery	Direct Gamma	0.01-10 <sup>3</sup>	0.2	B	1.,2.
RSB	749'	336	Spent Fuel Cask Corridor and Shaft	Direct Gamma	0.01-10 <sup>8</sup>	5.0x10 <sup>4</sup>	B	3.
RSB	755'	306AA	Operating Areas	Direct Gamma	0.1-10 <sup>4</sup>	2.0	A	1.,2.
RSB	733'	335	SFSC Service Station Equipment	Direct Gamma	0.1-10 <sup>4</sup>	10.0	B	1.,2.,3
SGB	816'	262	Operating Areas	Direct Gamma	0.1-10 <sup>7</sup>	Unrestricted (See NOTE 2)	A	1.,4
SGB	794'	253	Emerg. Airlock/Analysis Operating Area	Direct Gamma	0.1-10 <sup>4</sup>	Unrestricted (See NOTE 2)	A	1.,4,6
CB	816'	431	Control Room	Direct Gamma	0.1-10 <sup>7</sup>	Unrestricted (See NOTE 2)	A	1.
PSB	816'	146	Combined Lab	Direct Gamma	0.01-10 <sup>3</sup>	Unrestricted (See NOTE 2)	A	1.
RWB	775'	605A	IALL Distillate Storage Tank Area	Direct Gamma	0.01-10 <sup>7</sup>	2.0	A	1.

12.3-14

Amend. 72  
Oct. 1982

TABLE 12.3-5 (Cont'd)

BLDG.	LOCATION		AREA AND/OR PROCESS MONITORED	MONITOR TYPE	METER RANGE mR/hr	OPERATIONAL BACKGROUND (mR/hr)	MONITOR OUTPUT**	BASIS FOR LOCATION*
	ELEV.	CELL						
RCB	816'	161A	Equipment/Personnel Airlock Area	Direct Gamma	$0.01-10^3$	0.2	A	1.
RCB	816'	169A	RCB Annulus	Direct Gamma	$10^0-10^7$	0.2	A	4
RCB	816'	169A	RCB Annulus	Direct Gamma	$10^0-10^7$	0.2	A	4
RCB	816'	169A	RCB Annulus	Direct Gamma	$10^0-10^7$	0.2	A	4
RCB	794'	161E	Primary Pump Drive	Direct Gamma	$10^{-1}-10^4$	2.0	A	5
RCB	794'	161D	Primary Pump Drive	Direct Gamma	$10^{-1}-10^4$	2.0	A	5
RCB	794'	161C	Primary Pump Drive	Direct Gamma	$10^{-1}-10^4$	2.0	A	5
RCB	766'	105Y	Valve Operating Gallery	Direct Gamma	$10^{-1}-10^4$	2.0	A	5
RCB	733'	111	Stairwell	Direct Gamma	$10^{-1}-10^4$	2.0	A	5
RCB	733'	105E	Access Area	Direct Gamma	$10^{-1}-10^4$	10.0	A	5
RCB	825'	106	Polar Crane Operating	Direct Gamma	$10^{-1}-10^4$	0.2	A	5
RCB	842'	165	EI&C Cubicle	Direct Gamma	$10^{-1}-10^4$	0.2	A	5
RCB	842'	167	EI&C Cubicle	Direct Gamma	$10^{-1}-10^4$	0.2	A	5
SGB	794'	247	Power Distrib. Panel Area	Direct Gamma	$10^{-1}-10^4$	Unrestricted	A	5,6
SGB	794'	271	Operating Area	Direct Gamma	$10^{-1}-10^4$	Unrestricted	A	5,6
SGB	794'	271	Operating Area	Direct Gamma	$10^{-1}-10^4$	Unrestricted	A	5,6
SGB	794'	262	Operating Area	Direct Gamma	$10^{-1}-10^4$	Unrestricted	A	5,6
SGB	794'	262	Operating Area	Direct Gamma	$10^{-1}-10^4$	Unrestricted	A	5,6
SGB	794'	211A	Valve Gallery	Direct Gamma	$10^{-1}-10^4$	$5 \times 10^2$	A	6
SGB	794'	248	IHTS Pipe Chase	Direct Gamma	$10^{-1}-10^4$	$1 \times 10^4$	A	6
SGB	794'	251	IHTS Pipe Chase	Direct Gamma	$10^{-1}-10^4$	$1 \times 10^4$	A	6
SGB	794'	252	IHTS Pipe Chase	Direct Gamma	$10^{-1}-10^4$	$1 \times 10^4$	A	6

12.3-14a

Amend. 72  
Oct. 1982

TABLE 12.3-5 (Cont'd)

BLDG.	LOCATION		AREA AND/OR PROCESS MONITORED	MONITOR TYPE	METER RANGE mR/hr	OPERATIONAL BACKGROUND (mR/hr)	MONITOR OUTPUT**	BASIS FOR LOCATION*
	ELEV.	CELL						
RSB	785'	348	Cont. Cleanup Scrubber	Direct Gamma	$10^{-1}-10^4$	0.2	A	6
RSB	785'	349	Cont. Cleanup & HVAC Duct	Direct Gamma	$10^{-1}-10^4$	0.2	A	6
RSB	840'	332	NDHX 3rd Loop Cell	Direct Gamma	$10^{-1}-10^4$	0.2	A	5
RSB	864'	395A	Annulus Filter	Direct Gamma	$10^{-1}-10^4$	0.2	A	6
RSB	733'	350	NAP Storage Vessel Cell	Direct Gamma	$10^{-1}-10^4$	2.0	A	6
RSB	733'	305M	Access Area	Direct Gamma	$10^{-1}-10^4$	2.0	A	6
RSB	733'	305C	RSB/SGB Passageway	Direct Gamma	$10^{-1}-10^4$	2.0	A	6
RSB	743'	311	SDD 82, 85 & 94 Area	Direct Gamma	$10^{-1}-10^4$	$1 \times 10^2$	A	6
RSB	797'	314	SDD 23 Instru. Area	Direct Gamma	$10^{-1}-10^4$	0.2	A	5
RSB	755'	359	Cont. Cleanup Filter Cell	Direct Gamma	$10^{-1}-10^4$	0.2	A	6
RSB	779'	376	RAPS Pipe Gallery	Direct Gamma	$10^{-1}-10^4$	$5 \times 10^3$	A	6
RSB	775'	3511	EVS Cooling Pipeway	Direct Gamma	$10^{-1}-10^4$	$2 \times 10^3$	A	6

LEGEND

RCB - Reactor Containment Bldg.  
 RSB - Reactor Service Bldg.  
 SGB - Steam Generator Bldg.  
 CB - Control Bldg.  
 PSB - Plant Service Bldg.  
 RWB - Radwaste Area (Bay)

\*BASIS FOR LOCATION

1. Provide personnel protection in trafficked area.
2. Monitor adjacent high radio-activity area.
3. Monitor refueling operations.
4. High level reactor containment radiation monitor (Accident Monitor).
5. Monitor areas containing safety-related equipment (Accident Monitor).
6. Monitor areas with hatches or penetrations from containment (Accident Monitor).

\*\*MONITOR OUTPUT

- A. Local and Control Room: Loss of signal indicator light, high level radiation alarm, high-high level radiation alarm, exposure meter (mR/hr).
- B. Local, Control Room and Refueling Communication Center: (same as above).

NOTES:

Unrestricted: Defined by 10 CFR 20, Paragraph 20.105.

Background specified in table is maximum design background value during operation, based on Na-24 gamma field.

12.3-14b

Amend. 72  
 Oct. 1982

#### 15.1.4 Effect of Design Changes on Analyses of Accident Events

The design of the CRBRP has made significant progress since the consequences of design basis events reported in the remainder of this chapter were first analyzed. A review of approved design changes to determine which may affect the reported results and a qualitative evaluation of the effects of these changes has been made. A primary example is the change in core design from a homogeneous to a heterogeneous configuration. The results of this effort are discussed in the following sections.

##### 15.1.4.1 Reactivity Insertion Design Events

Section 15.2 covers the analyses of reactivity insertion design events. The format progresses from anticipated up through faulted design transients with each accident scenario providing:

- o identification of causes and accident description;
- o analysis of effects and consequences;
- o conclusions.

With regard to accident scenarios, there have been no changes to Section 15.2 since the original PSAR submittal. However, various pieces of design data have changed and have subsequently been incorporated into the appropriate design sections of the PSAR. Modifications to the nuclear and thermal-hydraulic information affect the maximum temperatures attained and the temperature/time traces shown. The purpose of this section is to indicate the effect of these various changes to the Section 15.2 results.

Reactivity insertion accidents typically result in overpower transients that are characterized by an increase in power such that a proportionately larger increase occurs in fuel temperature than in cladding temperature. This is opposed to undercooling design events which have a very small fuel temperature increase as compared to that of the cladding. Worst case overpower conditions commonly have a rapid increase in power which institutes scram of the Plant Protection System (PPS). For events having a rapid power burst, the period of the overpower conditions is typically less than one second (see Figure 15.2.3.3-3, for example). Although the shutdown occurs quickly, effects such as fuel melting and the potential for fuel/cladding interaction are of prime importance in the fuel pin performance evaluations.

To demonstrate temperatures that envelope overpower events with current data applied, a worst case event was reanalyzed and the results are herein described relative to the former values. This worst case selected previously was the Seismic Reactivity Insertion (SSE) (see Section 15.2.3.3.1) with primary control system shutdown (which is an extremely unlikely event).



As with the past analyses, the following conservative assumptions were made:

- 1) All full power cases are for the reactor operating at thermal hydraulic design conditions with a power generation of 975 MWt at three-loop operation. (Power uncertainties are discussed in Section 4.4.3.2.)
- 2) Since the smallest Doppler coefficient occurs at the beginning-of-equilibrium cycle, the transient reactor power calculation was made for this particular phase in core life. This results in the highest possible reactor power changes being calculated. For overpower transients, the smallest Doppler coefficient of all core cycles is used (see Section 4.3.2.3) and this value is reduced 30% to account for 3 $\sigma$  uncertainties.
- 3) The highest cladding and fuel temperature hot rod occurs at the beginning of the first cycle of operation (in F/A #52 and 101). The conservative reactor power calculation from Item 2 above was applied to this particular rod. With burnup, the power generation and steady-state temperatures decrease (flows are constant) in the hottest fuel assemblies, and consequently, the temperatures, due to the transients, would decrease after beginning of cycle.
- 4) As described in Chapter 7.0 and Section 4.2, the maximum allowable time delays for PPS logic and electrical/mechanical delays have been conservatively enveloped by using a 200 millisecond delay between the instrument channel output going beyond the trip level and the start of control rod insertion.\*
- 5) Three sigma (3 $\sigma$ ) hot channel factors were used for all the analyses and the cladding temperatures shown are the inner surface of the hot pin cladding at the highest temperature position, both axially and circumferentially on the fuel rods. (Position is under the wire wrap.)
- 6) The most rapid flow decay after de-energizing the primary pumps was used. (See Figure 5.3-22.)
- 7) Maximum decay heats were used for the hot rods considering 3 $\sigma$  uncertainties.

Results from FORE-2M analysis are given in Figures 15.1.4-1, 2 and 3 and Table 15.1.4-1 for a 60% step reactivity insertion occurring at the worst time during the SSE (see Section 15.2.3.3.1). Comparisons of the heterogeneous core results are made with data for a homogeneous core previously reported in this section. This previously reported data updated earlier data for the homogeneous core analyzed in Section 15.2.3.3. The figures show the

\*In this instance the sensor delay has been encompassed by the 200 msec PPS logic and control rod unlatch delay. This is justified by the small magnitude of the flux sensor delay which is estimated at less than 10 msec.

### 15.3.1 Anticipated Events

#### 15.3.1.1 Loss of Off-Site Electrical Power

##### 15.3.1.1.1 Identification of Causes and Accident Description

The off-site power supply to the 13.8 KV buses is available from the generating switchyards and the reserve switchyard both of which are powered by outside sources as described in Chapter 8.0. Hence, the postulated loss of power would result only from simultaneous, multiple failures.

The loss of all off-site power trips all primary and intermediate sodium pumps, commencing a flow coastdown. It also initiates starting of the emergency diesel generators. Action of the Plant Protection System (PPS) trips the control rods thus limiting core over temperatures from reduced flow. Either emergency diesel provides power to the primary and intermediate sodium pump pony motors and SGAHRS Auxiliary Feedwater Pumps for decay heat removal. Additionally, a third power supply (250 VDC Diverse Battery and Inverter) provides power to the third loop pony motors. To provide conservatism in the analysis, the most rapid core flow coastdown was assumed by using the minimum pump rotating kinetic energy and the maximum primary system flow resistance specified in the design.

The action of the Primary and Secondary Shutdown Systems (SDS) are as follows:

- a. Primary trip - Loss of electrical power trip occurring in 0.5 seconds. The 0.5 second delay includes measurement and trip function lags. These lags include bus voltage decay and instrument delay but not the RSS logic and control rod unlatching delays.
- b. Secondary trip - Flux-Total Flow trip occurring 2 seconds after loss of electrical pumping power. This lag includes time for the flow to coastdown as well as the measurement lags.

##### 15.3.1.1.2 Analysis of Effects and Consequences

The loss of off-site electrical power event was analyzed with the DEMO computer code. The overall results of the analysis are summarized in Figures 15.3.1.1-1 and 15.3.1.1-2. As shown, the Primary PPS loss of electrical power trip limits the maximum core hot spot temperature to 1410°F.

In the event the primary shutdown system does not operate, Figure 15.3.1.1-1 shows that the secondary shutdown system limits the worst case clad hot spot temperature to 1630°F. While the transient temperature exceeds the design basis emergency transient envelope temperature by 30°F, the time above the normal operating temperature is only 6 second as compared to 150 seconds for

the design basis transient (see Figure 15.3.1.1-3). Consequently, the cladding damage due to the transient is less than that due to the design basis transient for which, as shown in Section 4.2, cladding integrity limits are satisfied.

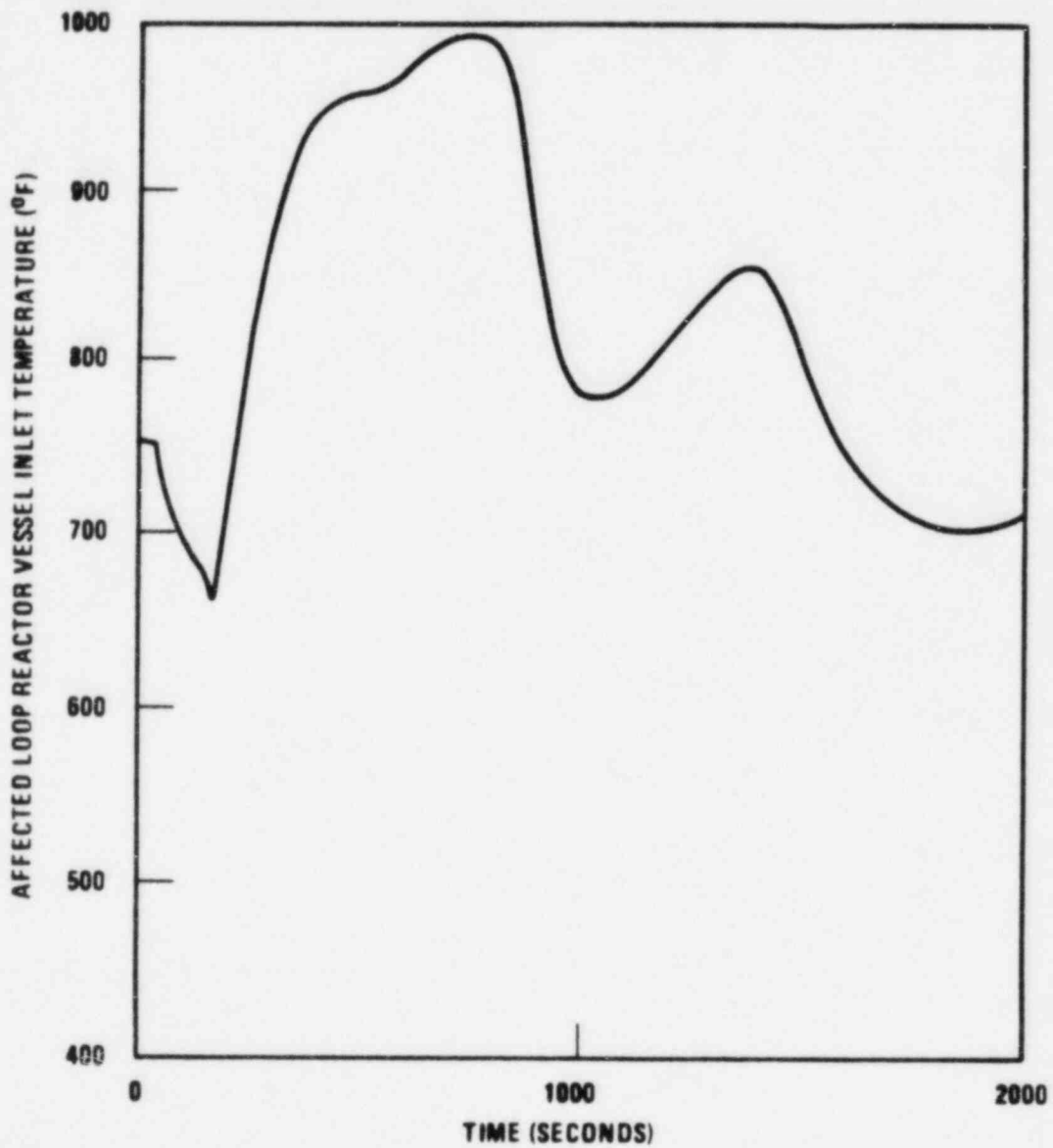
The capability of the CDF procedure to conservatively predict the results of Fuel Clad Transient Test (FCTT) is demonstrated below. The range of the FCTT temperatures and fluences considered exceeded the data base of the FURFAN CDF computer code. Despite this, the CDF analyses conservatively predicted the test results with peak cladding temperatures in excess of 1900°F, and cladding fluence exposures in excess of  $3 \times 10^{22}$  n/cm<sup>2</sup>.

The quantitative criteria in terms of Temperature versus Time for transient events which do not affect cladding integrity is shown in Figure 4.2-31. The shape of the emergency transient considered in this plot envelopes the loss of off-site electrical power with scram by the secondary PPS event. The minimum cladding lifetime is determined by the intersection of the peak transient cladding temperature versus time curve and the transient limit curve with maximum design temperatures and maximum uncertainty in properties. Note that the maximum peak cladding temperature occurs at beginning-of-life, and the cladding temperature increment due to the transient is assumed constant throughout life. Thus, for an emergency transient with a maximum peak cladding temperature of 1630°F, the peak clad temperature versus time curve would lie parallel to and 30°F above the peak clad temperature versus time curve shown in Figure 15.3.1.1-4. The intersection of this curve with the minimum transient limit curve gives a cladding lifetime of 450 days or 35 days less than the 1600°F peak cladding temperature transient. In all calculations involved in generating Figure 15.3.1.1-4, cumulative cladding damage is continuously accounted for in the cladding property considerations.

It should be noted that the anticipated time temperature curve for the loss of off-site electrical power is considerably less than the time envelope used to develop the transient limit curves. Therefore, the above loss of 35 days due to the additional 30°F is believed to be an overestimate of the transients actual effect. This notwithstanding, the design lifetime based on the above analysis for the loss of offsite power is still in excess of the 411 day goal lifetime.

As discussed earlier, the most realistically severe combination of possibilities allowed in the design specifications were selected to analyze this event. Figure 15.3.1.1-2 shows the effects of a possible longer flow coastdown, enhanced secondary control rod dynamics, and using "minimum required" instead of "expected" primary control rod shutdown rates. Lower possible core flow resistances and higher pump rotating kinetic energies, decrease the core hot spot temperature 10°F for a primary PPS trip and 15°F for the secondary shutdown system trip. Additionally, increasing the initial secondary control rod insertion rate to match the primary rates decreases the clad temperature 35°F for the secondary trip.

Figure 15.3.1.7-1.a Temperatures of Pertinent Parameters as a Function of Time After Inadvertent Actuation of the Water/Steam Side of the Sodium/Water Reaction Pressure Relief System.



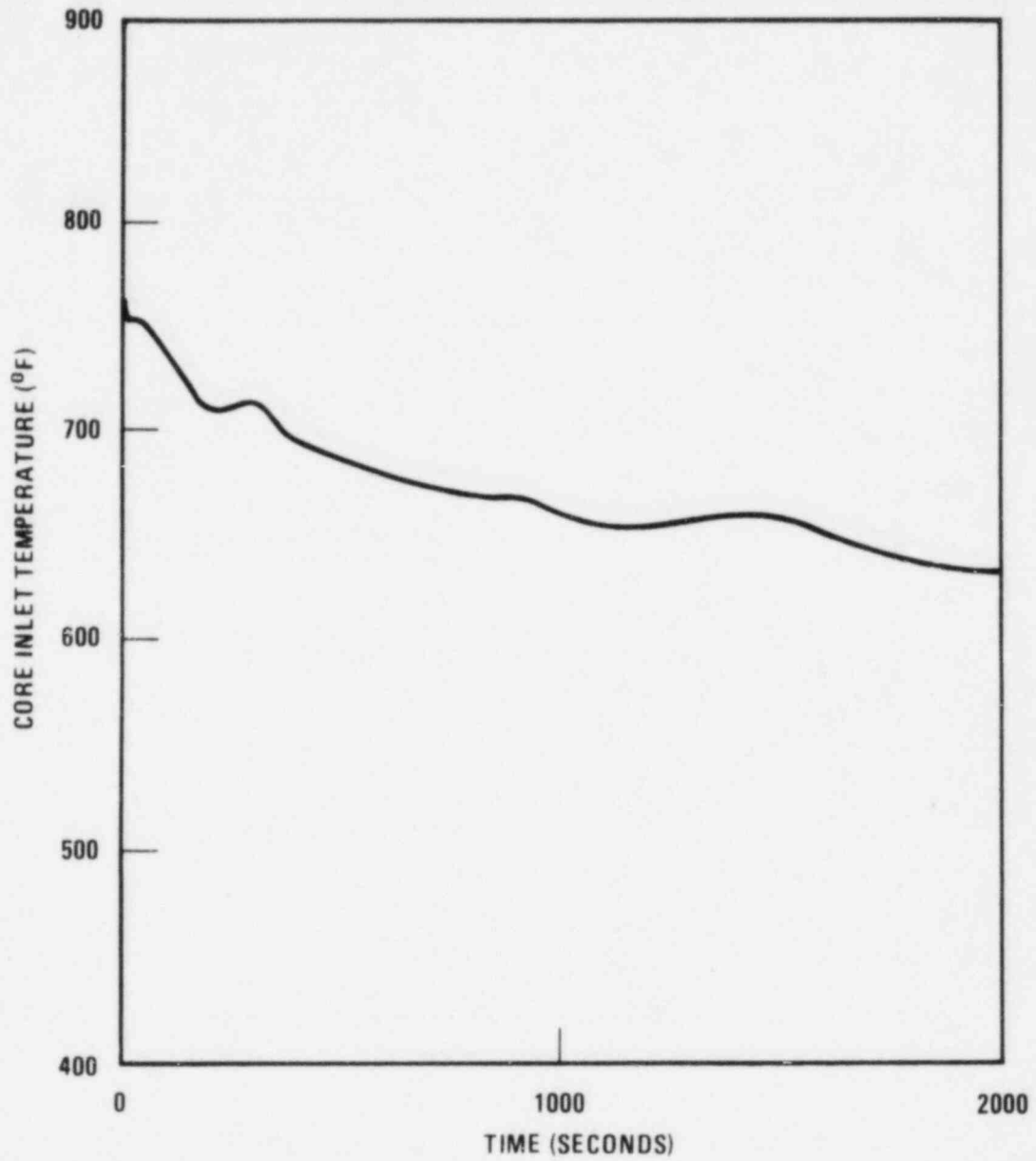


Figure 15.3.1.7-1B. Temperature of Core Inlet as a Function of Time After Inadvertant Actuation of the Water/Steam Side of the Sodium/Water Reactor Pressure Relief System

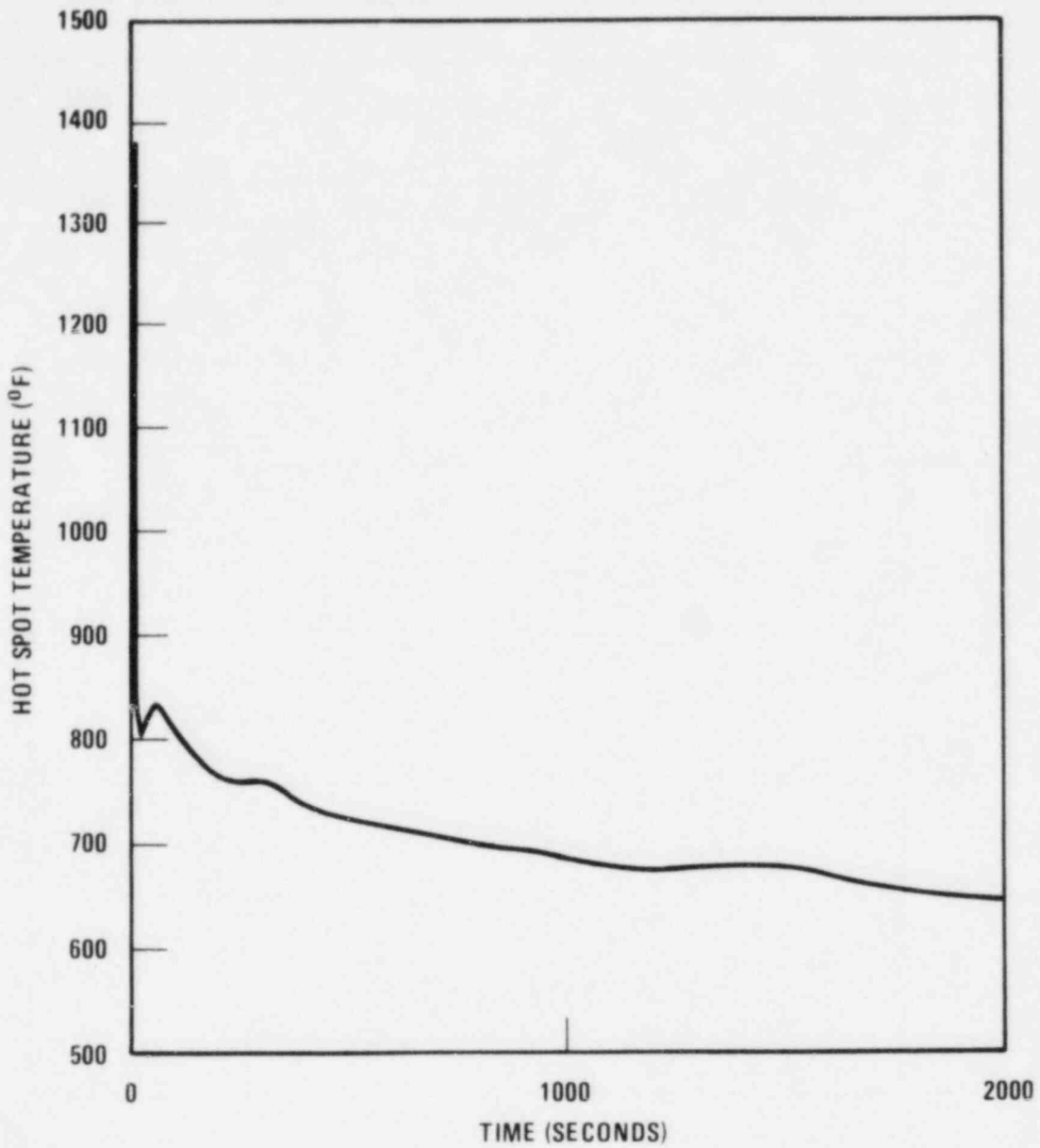


Figure 15.3.1.7-1C Temperature of Hot Spot as a Function of Time After Inadvertant Actuation of the Water/Steam Side of the Sodium/Water Reactor Pressure Relief System

### 15.3.2.3 Small Water-to-Sodium Leaks In Steam Generator Tubes

#### 15.3.2.3.1 Identification of Causes and Accident Description

The probability of a tube leak in the steam generators is expected to be quite small as a result of careful design supported by development and testing of the steam generators. However, the Steam Generator Leak Detection System, described in Section 7.5.5, has been provided to allow operator action to limit the consequences of a small leak in a steam generator tube.

The water-to-sodium leak detection system is designed to alert the operator to the existence of very small leaks, as small as approximately  $2 \times 10^{-5}$  lb. water/sec. For initial very small leaks which can be realistically expected (up to about  $5 \times 10^{-5}$  lb. water/sec.), the reactor will be shut down normally followed by a controlled cooldown and depressurization of the affected steam generator. The affected IHTS loop would then be drained to allow repair of the steam generator.

However, in the unlikely event of a small leak exceeding approximately  $5 \times 10^{-5}$  lb. water/sec, the operator may elect to scram the reactor and isolate and blowdown all three steam generator modules in the affected loop. The operator would also drain the affected IHTS loop, resulting in flow stoppage in that loop.

#### 15.3.2.3.2 Analysis of Effects and Consequences

It is assumed that the reactor is operating at rated conditions when a leak occurs in a steam generator of such a nature that the operator elects to manually shutdown the reactor, isolate and depressurize the water side of the affected loop, and drain the sodium side of that loop. Dynamic analyses have not been completed for this event; however, the primary system response can be conservatively bounded by assuming that all heat removal capability is instantaneously lost in the IHX of the affected loop at the time when intermediate flow stops. The IHX primary outlet temperature increases rapidly to the primary inlet temperature. Core flow rate and the resulting fuel cladding and core coolant exit temperatures are identical to those for normal scram until the hot sodium from the affected IHX reaches the core. This is calculated to occur about 60 seconds after reactor scram, assuming a normal flow coast down. The hot sodium from the affected loop mixes with the sodium from the other two loops in the reactor vessel inlet plenum. Assuming perfect mixing in the core inlet region, the core inlet temperature increases about  $90^{\circ}\text{F}$ . If this increase in core temperatures 60 seconds after scram is conservatively added to the hot-channel coolant exit temperature for the normal scram, the hot-channel clad temperature would increase from about

810°F to 900°F. This increase in temperature would be somewhat larger if incomplete mixing occurs in the reactor vessel inlet plenum. However, even for the extreme assumption of zero mixing, the hot-channel coolant temperature could increase a maximum of only 265°F to about 1125°F, still well below the normal steady-state operating value. The core exit temperatures would then decrease as the reactor was cooled by the operable loops.

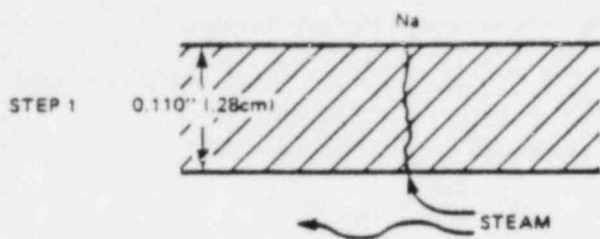
If it is assumed that this event occurs following operation with the maximum undetected intermediate-to-primary sodium leak rate there will be insignificant radiological release. Leakage of primary sodium into the IHTS is prevented by pressurizing the IHTS such that a pressure differential across the IHX (intermediate-to-primary) of at least 10 psi exists during plant operation. This pressure differential could be lost during the sodium dumping process and it is possible that primary sodium could enter the IHTS. Leak rates of approximately 6 gph will be detected during normal operation (Section 7.5.5) and therefore only small amount of primary sodium could be introduced into the IHTS during the pump coast down. This small amount of primary sodium would mix with the intermediate sodium and either remain in the non drainable sections of the IHTS, steam generators, and IHX, or be drained to the sodium dump tank. Over pressurization of this tank is prevented by either the equalization line or the pressure relief valve, the gases vented through this system will be the inert gas displaced by the sodium entering the dump tank. No sodium will be released in this process and the radiological consequences of this event are insignificant.

22

#### 15.3.2.3.3 Conclusion

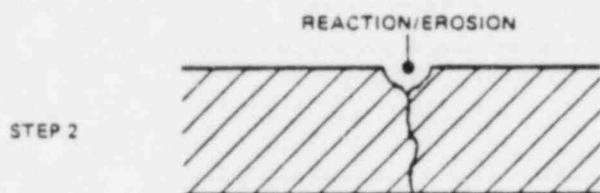
Core temperatures following a steam generator tube leak are well within the normal operating temperature range for the fuel and core. Residual heat removal is provided by the operable loops. This event is included in the overall plant duty cycle list that provides the basis for the thermal transient design conditions for the reactor and the main heat transport system.





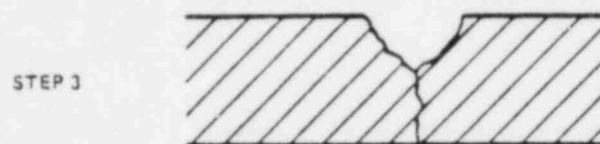
VERY SMALL INITIAL H<sub>2</sub>O LEAK FLOW

$1 \cdot 10^{-2}$  g/s ( $1.2 \cdot 10^{-5}$  lbs/sec)  
Leakage probably plugs, or is no higher prior to step 5 below.



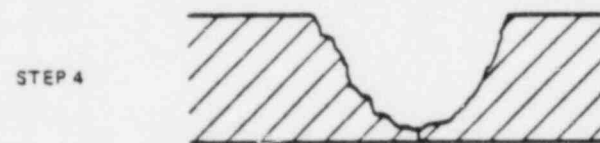
EROSION BEGINS, BRIEF INTERMITTENT LEAKS

Probably plugged for long periods



DEVELOPMENT OF LARGE CRATER

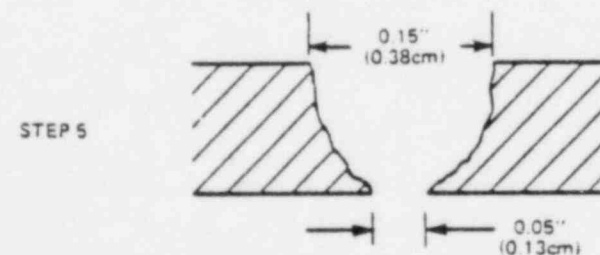
Leakage path may open for longer periods



CRATER NEARS STEAM SIDE

Leakage continuous but variable, still no higher than step 1.

ELAPSED TIME FROM STEP 1: HOURS, DAYS TO MONTHS



RAPID EROSION AT INNER WALL

Rapid increase in leakage to 15 g/s ( $3 \cdot 10^{-2}$  lbs/sec)

ELAPSED TIME FROM STEP 4: ONE MINUTE OR LESS (SUPERHEATER CONDITIONS)

Figure 15.3.3.3-1. Development of a Large Leak From a Small Steam Leak in 2 1/4Cr-1Mo Tubing Exposed to Sodium

AMENDMENT 72

List of Responses to NRC Questions  
Received Since the Fall of 1981 and  
Located Chronologically in PSAR Volumes 25 and 26

QCS220.25	QCS760.13
QCS421.9	QCS760.28
QCS421.17	QCS760.30
QCS421.22	QCS760.36
QCS421.27	QCS760.105
QCS421.30	QCS760.110
QCS421.31	QCS760.116
QCS421.34	QCS760.131
QCS421.36	QCS760.166
QCS421.37	QCS760.172
QCS421.42	QCS760.175
QCS421.47	QCS760.176
QCS421.48	QCS760.177
QCS421.58	QCS760.178
QCS721.1	

Question 220.25 (3.8.2.2)

On page 3.8-1, it is stated that ASME Section III Division 1, 1974 Edition with Addenda through winter 1974 and ASME Section III Division 2, 1974 Edition will be used for the design of the steel containment and the steel-lined concrete containment foundation mat, respectively. Indicate what will be the effect on the design if the latest editions of the ASME Section III Divisions 1 and 2 including Code Case N-284 (1980) are used.

Response:

The PSAR design was performed to the requirements of the 1974 Code edition specified in the design specifications. The specific criteria related to buckling are described in the PSAR Appendix 3.8-A. The intent of these criteria is similar to the Code Case N-284 criteria, in that these address buckling modes based on classical analysis, provide capacity reduction factors, factors of safety, and interaction equations for buckling. A significant reanalysis would be required to demonstrate that the Containment Vessel meets the requirements of the new Code and Code Case N-284. However, the applicant has compared the PSAR to the ASME code and N-284. The significant differences have been evaluated and are provided as parts 6.0 and 7.0 of this response.

In addition the applicant has performed an analysis of the critical buckling region just above the operating floor using N-284 criteria and the appropriate loads. This analysis demonstrated that the design margin exceeds the requirements of Code Case N-284. See part 7.0.

INDEX

CRBRP CONTAINMENT VESSEL

COMPARISON AND EVALUATION OF PSAR AND 1980 EDITIONS OF

ASME B&PV CODE/CODE CASE N-284

	<u>Page No.</u>
1.0 SUMMARY .....	3
2.0 COMPARISON OF SECTION III, SUBSECTION NCA .....	4
.1 NCA-3000 Responsibilities and Duties .....	5
3.0 COMPARISON OF SECTION III, DIVISION 1 SUBSECTION NE, CLASS MC COMPONENTS .....	9
.1 NE-1000 General Requirements .....	10
.2 NE-2000 Materials .....	11
.3 NE-3000 Design .....	16
.4 NE-3000 List of NE-3000 Subarticles Not Evaluated .....	37
.5 NE-4000 Fabrication & Installation.....	38
.6 NE-5000 Examination .....	45
.7 NE-6000 Testing .....	47
.8 NE-7000 Protection Against Overpressure .	52
.9 NE-8000 Nameplates, Stamping, & Reports .	53
4.0 COMPARISON OF SECTION III, DIVISION 2 FOUNDATION MAT AND BOTTOM LINER .....	54
.1 CC-2000 Material .....	55
.2 CC-3000 Design .....	57
.3 CC-4000 Fabrication and Construction ....	59
.5 CC-5000 Construction Testing and Examination .....	60
5.0 COMPARISON OF CODE CASE N-284, BUCKLING CRITERIA	61
6.0 EVALUATION OF KEY DIFFERENCES 1980 ASME CODE ..	71
7.0 EVALUATION OF KEY DIFFERENCES CODE CASE N-284 .....	79

## 1.0 SUMMARY

This section summarizes the differences in the containment design requirements between the PSAR and the 1980 Edition (Including Winter 1981 Addenda) of the ASME B&PV Code Section III, Division 1 and the 1975 Edition of the ASME B&PV Code Section III, Division 2 and the 1980 Edition (Including Winter 1981 Addenda) of the ASME B&PV Code Section III, Division 2. Specific differences, both design and documentation, are noted in subsequent sections of this attachment. Key differences in the containment design requirements are identified below:

### 1.1 ASME B&PV Code Section III, Subsection NCA

1. No Impact on the design of the containment. Specific documentation changes are identified in Section 2.0 of Attachment II.

### 1.2 ASME B&PV Code Section III, Division 1

1. Buckling criteria are added to the design by analysis criteria giving general rules for buckling conditions not covered by the design by formula criteria.
2. Service Level Limits are introduced. By including accident conditions under Levels A and B, the Code now requires the evaluation of primary plus secondary stress intensity range for accident conditions and provides an allowable stress limit. Since this requirement was not in the 1974 Code, calculations of secondary stresses in different areas would now be needed.
3. Additional requirements are imposed on nozzles, by changing the classification of stresses at the nozzle piping transition and also rules governing opening and reinforcement.
4. Additional requirements are imposed on the spacing of areas of primary local membrane stress intensity at brackets.

### 1.3 ASME B&PV Code Section III, Division 2 (Affecting the Foundation Mat)

1. The concrete strain corresponding to the maximum allowable primary plus secondary membrane and bending compressive stress of  $0.85 f'_c$  has been reduced.

### 1.4 CONCLUSION

These differences have been reviewed by the applicant and compared to the criteria in the PSAR. None of these differences require a change in the present design in the opinion of the applicant. The detailed logic for this conclusion is provided in Section 6.0 of the document.

2.0 COMPARISON OF SECTION III, SUBSECTION NCA

.1 NCA-3000 Responsibilities and Duties

2.1 SUMMARY

Changes in this section have no impact on the design.

CONTAINMENT VESSEL - ASME B&PV CODE COMPARISON

SECTION III - ARTICLE NCA-3000 RESPONSIBILITIES AND DUTIES

<u>PARAGRAPH/TITLE</u>	<u>74 EDITION - W74 ADDENDA</u>	<u>80 EDITION - W81 ADDENDA</u>	<u>IMPACT ON DESIGN</u>
1. NCA-3125 Subcontracted Services	No provisions for subcontracted services.	Services covered by Section III may only be subcontracted to appropriate certificate holders. An N Type Certificate Holder may subcontract to another organization the Surveying and auditing functions, but must retain the responsibilities for these activities and qualifications	None.
2. NCA-3130 Welding and Subcontract- ing during Construction	Provides that construction includes materials, design, fabrication, examination, testing, inspection and certification	The term "construction" is no longer defined.	None.
3. NCA-3131 Welding during Con- struction	Provides conditions that must be met for the performance of welding for shop or field work during Code construction.	Adds the exception for furnace brazing operations as specified in NCA-3561 (c), NCA-3661 (b), and NCA-3761 (b)	None.
4. NCA-3220 Categories of the Owners Responsibili- ties	Owners responsibilities included eight (8) specific items.	Owners responsibilities for Division 1 increased to 19 specific items of which 10 are new responsibilities. All but 4 can be assigned to the Owner Designee	None.
5. Deleted			

QCS220.25-5

Amend. 72  
Oct. 1982

CONTAINMENT VESSEL - ASME B&PV CODE COMPARISON

SECTION III - ARTICLE NCA-3000 RESPONSIBILITIES AND DUTIES

<u>PARAGRAPH/TITLE</u>	<u>74 EDITION - W74 ADDENDA</u>	<u>80 EDITION - W81 ADDENDA</u>	<u>IMPACT ON DESIGN</u>
6. NCA-3240 Provision of Adequate Supporting Structure	Provides that the Owner shall be responsible for adequate structural support and definition of boundary interfaces	The Owner has the additional requirement to determine allowable bearing pressure or load per caisson or pile and furnish same to designer.	None.
7. NCA-3252 Contents of Design Specification	Provides 8 items to be included in Design Specification.	Adds 2 additional items which include: 1-specifying operating requirements of a component 2-specifying effective Code Edition & Addenda & Code Case	None.
8. NCA-3256 (a) Filing of Design Specification	Design Specifications shall be made available to the Inspector at the construction site for all but parts and piping assemblies	Provides that in addition, the applicable data for parts, piping assemblies and appurtenances shall be made available to the Inspector at the fabrication site.	None.
9. NCA-3270 Owners Data Report and Filing	1-Owner or designee shall prepare Form N-3 2-Owner shall certify, by signing the form that each organization was a Holder of Certificate of Authorization 3-Form N-3 shall be filed in accordance with NA-8430	Owner or designee shall prepare Form N-3. The other requirements have been deleted	None.
10. NCA-3280 Owner's Responsibility for Records	No Requirement	Owner shall be responsible for designating and maintaining records.	None.

QCS220.25-6

Amend. 72  
Oct. 1982



CONTAINMENT VESSEL - ASME B&PV CODE COMPARISON

SECTION III - ARTICLE NCA-3000 RESPONSIBILITIES AND DUTIES

<u>PARAGRAPH/TITLE</u>	<u>74 EDITION - W74 ADDENDA</u>	<u>80 EDITION - W81 ADDENDA</u>	<u>IMPACT ON DESIGN</u>
11. NCA-3500 Responsibility of an N Certificate Holder - Division 1	Manufacturer's Responsibilities	Manufacturer has been changed to read N Certificate Holder. Some changes in the definition wording have been made.	None.
12. NCA-3520 Categories of the N Certificate Holders Responsibilities	Manufacturer is charged with nine (9) specific responsibilities	Certificate holder charged with 15 times of responsibilities that includes 6 additional.	None.
13. NCA-3551 Design Documents		This paragraph has been rewritten in its entirety without significant alteration of its content	None.
14. NCA-3561 (c) Scope of Responsibility	No provision for brazing operations performed by organizations not holding certificate of authorization.	Permits the N Certificate holder to subcontract furnace brazing to non-Certificate Holders.	None.
15. NCA-3620 Categories of the NPT Certificate Holders Responsibilities		NPT Certificate Holders responsibilities have been added (16 items) and includes scope of the NPT Certificate Holders Responsibility for Quality Assurance.	None.

QCS220.25-7

Amend. 72  
Oct. 1982

CONTAINMENT VESSEL - ASME B&PV CODE COMPARISON

SECTION III - ARTICLE NCA-3000 RESPONSIBILITIES AND DUTIES

PARAGRAPH/TITLE	74 EDITION - W74 ADDENDA	80 EDITION - W81 ADDENDA	IMPACT ON DESIGN
16. NCA-3700 Responsibilities of an NA Certificate Holder	Installers responsibilities Includes six (6) specific Items	NA Certificate Holders responsibilities Includes 12 specific Items, six (6) of which are additional	None.
17. NA-3500 Responsibilities of Inspection Agencies, Inspection Specialists and Inspectors	These two Subarticles have been deleted from the later code Editions		None.
18. NA-3600 Engineering Organization's Responsibilities	" " " " " " " " " "		
19. NCA-3800 Metallic Material Manufacturer's and Material Supplier's Quality System Program	NA-3700 contains provisions for a similar Quality Systems program	NCA-3800 is similar to NA-3700	None.
20. NCA-3900 Nonmetallic Material Manufacturer's and Constituent Suppliers Quality System Program	Not included in the earlier Code Editions	New Quality Assurance Provision for non-metallic materials which is similar to NCA-3800 but not as comprehensive	None.

QCS220.25-8

Amend. 72  
Oct. 1982

3.0 COMPARISON OF SECTION III, DIVISION 1 SUBSECTION NE, CLASS MC COMPONENTS

- .1 NE-1000 General Requirements
- .2 NE-2000 Materials
- .3 NE-3000 Design
- .4 NE-3000 List of NE-3000 Subarticles Not Evaluated
- .5 NE-5000 Examination
- .6 NE-6000 Testing
- .7 NE-7000 Protection Against Overpressure

CONTAINMENT VESSEL - ASME B&PV CODE COMPARISON

SECTION III - ARTICLE NE-1000 GENERAL REQUIREMENTS

<u>PARAGRAPH/TITLE</u>	<u>74 EDITION - W74 ADDENDA</u>	<u>80 EDITION - W81 ADDENDA</u>	<u>IMPACT ON DESIGN</u>
1. NE-1132 Boundaries of the Contain- ment System	<p>Jurisdiction of Subsection NE shall conform as follows:</p> <p>It is intended that the jurisdiction of this Subsection for the containment vessel shall conform to the provisions of (a) and (b) below.</p> <p>(a) Connections for the attachments by welding of piping or of penetration assemblies (NA-1262) shall terminate at a circumferential joint exclusive of the connecting weld located at least the greater of the distances normal to the surface of the vessel (Fig. NE-1132-1) as given in (1) and (2) below:</p> <p>(1) the limits of reinforcement given in NE-3334; or</p> <p>(2) the boundary of the connection as given in the Design Specification (NA-3251) and included in the Manufacturer's test (NE-6000) and certification (NE-8000).</p> <p>(b) Connections for the attachment of locks or hatches shall include all required doors, covers, or other attachments required for the containment function. Piping, pumps, or valves attached to the locks or hatches shall be classified in the Design Specification (NE-1131).</p>	<p>The Design Specification shall define the boundary of a containment vessel to which piping or another component is attached. The boundary shall not be closer to the containment vessel than:</p> <p>(a) the first circumferential joint in welded connections (the connecting weld shall be considered part of the piping);</p> <p>(b) The face of the first flange in bolted connections (the bolts shall be considered part of the piping);</p> <p>(c) the first threaded joint in screwed connections.</p>	None.

QCS220.25-10

Amend. 72  
Oct. 1982

CONTAINMENT VESSEL - ASME B&PV CODE COMPARISON

SECTION III - ARTICLE NE-2000 MATERIALS

<u>PARAGRAPH/TITLE</u>	<u>74 EDITION - W74 ADDENDA</u>	<u>80 EDITION - W81 ADDENDA</u>	<u>IMPACT ON DESIGN</u>
1. NE-2110 Scope of Principle Terms Employed		Thickness definitions added	None.
2. NE-2121 (B) & (C) Permitted Material Specification	Material which need not be tested per NE-2320	1. List of items not covered by this article expanded. 2. Permits pressure-retaining material of ferritic steel to be quenched and tempered. 3. Corrects reference of material which need not be tested to NE-2311.	None.
3. NE-2180 Procedures for Heat Treating of Materials	None	Requires temperature surveyed and calibrated furnaces.	None.
4. NE-2190 (b) Nonpressure-Retaining Material	None	Provides for the repair welding of structural steel rolled shapes.	None.
5. NE-2223.1 Location of Coupons	Provides test specimen orientation for forgings of 2" maximum thickness and forgings greater than 2" maximum thickness.	Combines into one paragraph requirements for test specimen orientation for forging under 2" and forgings over 2".	None.
6. NE-2224 Location of Coupons	Provides Test specimen orientation for bars of 2" maximum thickness and bars greater than 2" maximum thickness.	Combines into one paragraph requirements for test specimen orientation for bars of all thicknesses.	None.
7. NE-2225 Tubular Products and Fittings	Same as above	Same as above	None.

QCS220.25-11

Amend. 72  
Oct. 1982

CONTAINMENT VESSEL - ASME B&PV CODE COMPARISON

SECTION III - ARTICLE NE-2000 MATERIALS

PARAGRAPH/TITLE	74 EDITION - W74 ADDENDA	80 EDITION - W81 ADDENDA	IMPACT ON DESIGN
8. NE-2311 Material for which Impact Testing is Required	Provides a listing of materials not required to be impact tested	<ol style="list-style-type: none"> <li>1. Provides definitions of thicknesses for materials not required to be impact tested.</li> <li>2. Provides Table NE-2311(a)-1 which list material exempt from impact testing based on TNDT and lowest service temperature and where LST exceeds 150°F.</li> <li>3. Requires design specification to state LST.</li> <li>4. Provides exemptions for drop weight test.</li> </ol>	None.
9. NE-2321.1 Drop Weight Tests	Restricts drop weight tests to 5/8" thick and greater and where Charpy V notch testing is not successful, drop weight testing may not be used as an alternate to the Charpy V - notch test where the heat-affected zone of the crack starter weld is tougher than the base metal	No restrictions identified	None.
10. NE-2322.1 Location of Test Specimens	Location of test specimens shall be as specified in NE-2220 or material specification. The number of test specimens shall be per NE-2340.	Impact specimens shall be as far from the material surface as is specified for tensile specimens in the material specifications. For bolting, the impact specimen shall be located at 1/2 radius or 1" below surface. Fracture plane shall be one diameter from the heat treated end.	None.
11. NE-2322.2 Orientation of Test Specimen		Added requirement that drop weight specimens may be oriented in any direction.	None.
12. NE-2322.3 & NE-2322.4	Preparation of test specimens and impact test temperature.	Not specified in this section	None.

QCS220.25-12

Amend. 72  
Oct. 1982

CONTAINMENT VESSEL - ASME B&PV CODE COMPARISON

SECTION III - ARTICLE NE-2000 MATERIALS

PARAGRAPH/TITLE	74 EDITION - W74 ADDENDA	80 EDITION - W81 ADDENDA	IMPACT ON DESIGN
13. NE-2330 Test Requirements and Acceptance Standards		<p>Requirements expanded considerably to include (a) Charpy V-notch testing at or below the Lowest Service Metal temperature. (b) Drop weight testing at (LST-TNDT) (c) Charpy V-notch testing at or below lowest specified vessel test temperature when hydrostatic or pneumatic test temperature is lower than LST. (d) Charpy V-notch testing for MILs Lateral Expansion Values (e) Charpy V-notch testing for absorbed energy values (f) Drop weight testing for two no-break specimens.</p> <p>Tests are specified according to material thickness and other criteria.</p>	
14. NE-2351 Retests for Material other than bolting	Retest for Charpy V-notch test require that the results meet minimum requirements. Where a test result is below, it shall not be lower than 10'-lbs. below.	Minimum requirements is changed to average three of table NE-2332.1, NE-2332.1-2 or NE-2333.1-1 as applicable. Also the test result below the average may not be lower than 5'-lbs below.	None.
15. NE-2552 Retests for Bolting Material	Not specified	Requirements for retest have been added	None.
16. NE-2420(d) & (f) Required Tests		Definitions of lots of covered, flux cored, or fabricated electrode and carbon or low alloy steel barred electrodes have been expanded considerable	None.
17. NE-2431.(b) & (c) General Test Requirements		<ol style="list-style-type: none"> <li>Provides for deposition of weld metal by the electroslag process and</li> <li>Post weld heat treat of the electroslag process weld deposits</li> </ol>	None.

NCS220.25-13

Amend. 72  
Oct. 1982

## CONTAINMENT VESSEL - ASME B&amp;PV CODE COMPARISON

## SECTION III - ARTICLE NE-2000 MATERIALS

PARAGRAPH/TITLE	74 EDITION - W74 ADDENDA	80 EDITION - W81 ADDENDA	IMPACT ON DESIGN
18. NE-2432.1(a) &(c) Test Methods	Requires chemical analysis for A-No. 8 welding material used with GTAW and PAW processes and any other welding material used with any GMAW process	Requires in addition chemical analysis for any other welding material used with any GTAW and PAW processes.	None.
19. NE-2433 Delta Ferrite Determination	Delta ferrite determination shall be performed by comparison of chemical analysis to Schaeffer diagram.	1. Delta ferrite determination shall be performed by comparison of chemical analysis to Schaeffler diagram or 2. By magnetic determination by instrument calibrated to AWS-A4.2-74	None.
20. NE-2550 Examination of Wrought Seamless and welded (without Filler Metal) Tubular Products and Fittings	Seamless and welded (without filler metal) tubular products and fittings shall meet requirements of SA-249, SA-312, SA-333, and SA-334 plus one of the following weld inspections (a) Ultrasonic, (b) eddy current (c) radiographs or (d) magnetic particle or liquid penetrant.	1. Wrought seamless and welded (without filler metal) pipe and tubing shall comply with requirements of Class 2 components and SA-655 2. Similar fittings shall comply with requirements of Class 2 components and SA-652	None.
21. NE-2560 Examination and Repair of Tubular Products and Fittings Welded with Filler Metals	All welds shall be examined radiographically in addition to material requirements in accordance with NE-5110	In addition to material requirements, pipe shall meet SA-655 and fittings shall meet SA-652	None.
22. NE-2570 Examination and Repair of Static-ly and Centrifugally cast products	Cast material shall be examined by either radiographic or ultrasonic methods to the acceptance standards of SA-609	Cast products shall meet all the requirements of SA-613	None.

QCS220.25-14

Amend. 72  
Oct. 1982



CONTAINMENT VESSEL - ASME B&PV CODE COMPARISON

SECTION III - ARTICLE NE-2000 MATERIALS

<u>PARAGRAPH/TITLE</u>	<u>74 EDITION - W74 ADDENDA</u>	<u>80 EDITION - W81 ADDENDA</u>	<u>IMPACT ON DESIGN</u>
23. NE-2580 Examination of Bolts, Studs and Nuts	Bolts, studs and nuts shall be examined in accordance with requirements of material specification	Bolts, studs and nuts shall meet the requirements of SA-614	None.

QCS220.25-15

Amend. 72  
Oct. 1982

CONTAINMENT VESSEL - COMPARISON OF 1974 EDITION AND 1980 EDITION OF ASME B&PV CODE

SECTION III - DIVISION 1 ARTICLE NE-3000 DESIGN

PARAGRAPH/TITLE	74 EDITION - W74 ADDENDA	80 EDITION - W81 ADDENDA	IMPACT ON DESIGN
1. NE-3111 Loading Conditions		Changes some load definitions editorially and adds a few typical loadings to be considered in a vessel design.	None.
2. NE-3112	Design Conditions	New Title: "Design Loadings"  Design loads redefined	None.
3. NE-3112.1 Design Pressure	i)  ii) "Stability of the vessel shell may be provided by <u>internal concrete</u> structures bearing directly against the shell."  iii) Requirements related to design pressure are: "The design pressure shall be used in the design formulas of NE-3300 for thickness of components when pressure is the only substantial load and also in the computations made to show compliance with the stress-intensity limits of NE-3221, NE-3227.1, NE-3227.2, NE-3227.4, NE-3228 and NE-3231."	Deletes the following note: "Maximum containment internal pressure is intended to include a margin above the maximum calculated peak internal pressure under which conditions the containment function is required..."  Deletes the words " <u>internal concrete</u> ". Hence, shell stability can be provided by internal or external structures.  Deletes the requirements in NE-3112.1. Similar requirements are given in NE-3131.	None.  None.  None.

QCS220.25-16

Amend. 72  
Oct. 1982

CONTAINMENT VESSEL - COMPARISON OF 1974 EDITION AND 1980 EDITION OF ASME B&PV CODE

SECTION III - DIVISION 1 ARTICLE NE-3000 DESIGN

<u>PARAGRAPH/TITLE</u>	<u>74 EDITION - W74 ADDENDA</u>	<u>80 EDITION - W81 ADDENDA</u>	<u>IMPACT ON DESIGN</u>
4. NE-3112.2 Design Mechanical Loads		Hydrostatic loads coincident with Design Pressure are designated as Design Mechanical Loads	None.
5a. NE-3112.4 Design Allowable Stress Values	Main provisions are: a) Use allowable stress-Intensity for design from Table I-10.0, b) Criteria on the maximum allowable compressive stresses, c) Stress in the wall of a vessel should be less than the maximum allowable stress value at the temperature	Revised provisions are stated in a more comprehensive way, as below:  "The rules for allowable stresses are given in NE-3200 for vessels designed by analysis where the allowable stress-Intensity $S_{mc}$ is the $S_m$ value given in Table I-10.0 of Appendix I. The allowable stress $S$ to be used in the equations of NE-3300 shall be those listed in Table I-10.0 of Appendix I."	See Items 9 through 27.
5b. NE-3112.4 NE-3134.6 (New Code)	$S_m$ is Design Stress Intensity	Codes use $S_{mc}$ or $S_{mI}$ instead of $S_m$ .  $S_{mc}$ from Table I-10.0. Used for primary stresses.  $S_{mI}$ from Table I-10.0. Used for primary plus secondary stresses.	None.

QCS220.25-17

Amend. 72  
Oct. 1982

CONTAINMENT VESSEL - COMPARISON OF 1974 EDITION AND 1980 EDITION OF ASME B&PV CODE

SECTION III - DIVISION 1 ARTICLE NE-3000 DESIGN

<u>PARAGRAPH/TITLE</u>	<u>74 EDITION - W74 ADDENDA</u>	<u>80 EDITION - W81 ADDENDA</u>	<u>IMPACT ON DESIGN</u>
6. NE-3113 Normal Operating Conditions for Nozzles (1974) Service Limits (1980)	<p>Requirements are specified for nozzles attached to Class 1 piping during Normal Operating Conditions.</p> <p>The Code considered only Operating and Design Conditions.</p> <p>OBE was within Design or Operating Conditions.</p> <p>SSE was within Design Conditions with higher allowable stress intensity.</p> <p>DBA was within Design Conditions.</p>	<p>The requirements for nozzles are deleted from this section. The subsection has a new subject "Service Limits". It specifies four different Service Limits.</p> <p>See Table 1 for comparison of requirements.</p>	See evaluation in 6.0 for Item 14
7. NE-3131 General Requirements	<p>General requirements includes design by analysis and by formula and deals with load classification and stress intensity limits. Includes requirements for configuration having compressive stresses (NE-3133), jet impingement effects, other pressure loads.</p>	<p>More emphasis on NE-3200 (Design by Analysis) than on NE-3300 (Design by Formula). For vessels subjected to compressive stresses or external loads, code places emphasis on the new rules NE-3222 (Buckling Stress Values). When applicable, NE-3133 may be used.</p>	See evaluation in 6.0 for Item 21

QCS220.25-18

Amend. 72  
Oct. 1982

CONTAINMENT VESSEL - COMPARISON OF 1974 EDITION AND 1980 EDITION OF ASME B&PV CODE

SECTION III - DIVISION 1 ARTICLE NE-3000 DESIGN

<u>PARAGRAPH/TITLE</u>	<u>74 EDITION - W74 ADDENDA</u>	<u>80 EDITION - W81 ADDENDA</u>	<u>IMPACT ON DESIGN</u>
8. NE-3133 Components Under External Loading		The rules have been revised. They are more extensive. More specific rules are provided for the ellipsoidal and the torispherical heads. Rules are also provided for the cylinders with the diameter to the thickness ratio less than 10.	See evaluation in 6.0
9. NE-3200 Design by Analysis			
Revised Terms	Operation  Operational Cycle  Operating Conditions	Service  Service Cycle  Service Loadings	None.
10. NE-3211 General Requirements for Accept- ability	i)          ii) Requires that the critical buckling stress shall be taken into account for the configurations where compressive stresses occur.  Does not given specific safety factors.	Following requirements are deleted from NE-3211:  "The design details shall conform to the rules given in NE-3100 (General Design)."  "In case of conflict between NE-3200 and NE-3300, the requirements of NE-3300 shall govern when considering pressure alone."  Following requirement is added in NE-3211:  "The buckling stress shall be considered in accordance with NE-3222."  Specifies new rules for the buckling consideration of vessel.	None.  None.  See evaluation in 6.0 for item 21.

QCS220.25-19

Amend. 72  
Oct. 1982

CONTAINMENT VESSEL - COMPARISON OF 1974 EDITION AND 1980 EDITION OF ASME B&PV CODE

SECTION III - DIVISION 1 ARTICLE NE-3000 DESIGN

PARAGRAPH/TITLE	74 EDITION - W74 ADDENDA	80 EDITION - W81 ADDENDA	IMPACT ON DESIGN
11. NE-3213.10 Local Primary - Membrane Stress	<p>i) Rule for Local Primary Membrane Stress is as below:</p> <p>"A stressed region may be considered local if the distance over which the stress intensity exceed 1.1 Sm does not extend in the meridional direction more than <math>0.5 R_t</math> and if it is <u>not closer in the meridional direction than <math>2.5 R_t</math> to another region</u> where the limits of general primary membrane stress are exceeded, where R is the mean radius of the vessel and t is the wall thickness."</p>	<p>Rule is modified and is stated below:</p> <p>"A stressed region may be considered local if the distance over which the membrane stress intensity exceeds 1.1 Smc does not extend in the meridional direction more than <math>1.0 R_t</math>, where R is the minimum midsurface radius of curvature and t is the minimum thickness in the region considered. Regions of local primary stress intensity <u>involving axisymmetric membrane stress distributions which exceed 1.1 Smc shall not be closer in the meridional direction than <math>2.5 R_t</math></u>, where R is defined as <math>(R_1 + R_2)/2</math> and t is defined as <math>(t_1 + t_2)/2</math>, where <math>t_1</math> and <math>t_2</math> are the minimum thicknesses at each of the 2 regions considered, and <math>R_1</math> and <math>R_2</math> are the minimum midsurface radii of curvature at these regions where the membrane stress intensity exceeds 1.1 Smc."</p>	None.
	<p>ii)</p>	<p>The following new requirement is added:</p> <p>"Discrete regions of local primary membrane stress intensity, such as those resulting from concentrated loads acting on brackets, where the membrane stress intensity exceeds 1.1 Smc shall be spaced so that there is no overlapping of the areas in which the membrane stress intensity exceeds 1.1 Smc."</p>	See evaluation in 6.0

QCS220.25-20

Amend. 72  
Oct. 1982



CONTAINMENT VESSEL - COMPARISON OF 1974 EDITION AND 1980 EDITION OF ASME B&PV CODE

SECTION III - DIVISION 1 ARTICLE NE-3000 DESIGN

PARAGRAPH/TITLE	74 EDITION - W74 ADDENDA	80 EDITION - W81 ADDENDA	IMPACT ON DESIGN
13. NE-3220 Title Changed	"Stress Limits for Other Than Bolts"	"Stress Intensity and Buckling Stress Values for Other Than Bolts"	None.
14. Revised Title for Figure NE-3222-1 (Old Code), Figure NE-3221-2 (New Code)	Stress Categories and Limits of Stress Intensity for <u>Operating Conditions</u>	" <u>Operating Conditions</u> " changed to "Levels A and B Service Limits"; and for Level C Service Limits where the structure is not integral and continuous."  Accidental pressure and temperatures are within Level A. Primary plus secondary stresses intensity range must be evaluated, while before only primary stresses were considered.	See evaluation in 6.0

QCS220.25-22

Amend. 72  
Oct. 1982



CONTAINMENT VESSEL - COMPARISON OF 1974 EDITION AND 1980 EDITION OF ASME B&PV CODE

SECTION III - DIVISION I ARTICLE NE-3000 DESIGN

<u>PARAGRAPH/TITLE</u>	<u>74 EDITION - W74 ADDENDA</u>	<u>80 EDITION - W81 ADDENDA</u>	<u>IMPACT ON DESIGN</u>
15a. Added New Figures		<p>Figures NE-3221-3 and 3221-4 added as described below:</p> <p>Figure NE-3221-3 "Stress Categories and Limits of Stress Intensity for Level C Service Limits where the structure is integral and Continuous, and for Level D Service Limits where the structure is not Integral and continuous and at Partial Penetration Welds."</p> <p>Figure NE-3221-4 "Stress Categories and Limits of Stress Intensity for Level D Service Limits where the structure is Integral and Continuous."</p>	<p>None.</p> <p>None.</p>
15b. Added New Table		Table NE-3221-1 presents summary of Stress Intensity Limits on Design Limits and Levels A, B, C and D and Service Limits	See evaluation in 6.0 for Item 14
16. NE-3221	Gives allowable stress intensities for "Design Conditions."	<p>Gives stress intensity values for "Design Conditions" and Service Limits A through D. Table NE-3221-1 provides summary of stress Intensity Limits. See New Figures NE-3221-1 to NE-3221-4, to cover all conditions.</p> <p>imposes limits on primary membrane plus primary bending stress Intensity when the local primary membrane stress Intensity exceed 0.67 of yield</p>	<p>See evaluation in 6.0 for Item 14</p> <p>See evaluation in 6.0</p>

QCS220.25-23

Amend. 72  
Oct. 1982

CONTAINMENT VESSEL - COMPARISON OF 1974 EDITION AND 1980 EDITION OF ASME B&PV CODE

SECTION III - DIVISION I ARTICLE NE-3000 DESIGN

PARAGRAPH/TITLE	74 EDITION - W74 ADDENDA	80 EDITION - W81 ADDENDA	IMPACT ON DESIGN
17. NE-3222	Gives limits for Operating Conditions	Gives buckling requirement. Does not recognize Operating Conditions. Instead it provides Service Limits.	See evaluation in 6.0, Item 14
18. NE-3221 and NE-3222 (Old Code) NE-3221 (New Code)	i) Primary stresses produced only by mechanical loads (Figure NE-3221-1)	Deletes the restriction	None.
	ii) Refer to Figure NE-3221-1. Expansion Stresses treated as secondary	Definition of expansion stresses as secondary has been removed. Considered now as primary (see also NE-3227.5).	See evaluation in 6.0 for NE-3227.5 (Item 24)
	iii) Primary stresses are produced by pressure and mechanical loads for general membrane and by pressure, mechanical loads and inertia effects for local membrane and primary bending (Figure NE-3222-1)	The restriction deleted.	None.
19. NE-3222.2 (1974 Code) NE-3221.4 (1980 Code)		The following note is added to the subsection: "The concept of stress differences discussed in NE-3216 is essential to determination of the maximum range, since algebraic signs must be retained in the computation. Note that this limitation on range is applicable to the entire history of service conditions, not just to the stresses resulting from each individual service condition."	None.

QCS220.25-24

Amend. 72  
Oct. 1982

CONTAINMENT VESSEL - COMPARISON OF 1974 EDITION AND 1980 EDITION OF ASME B&PV CODE

SECTION III - DIVISION 1 ARTICLE NE-3000 DESIGN

PARAGRAPH/TITLE	74 EDITION - W74 ADDENDA	80 EDITION - W81 ADDENDA	IMPACT ON DESIGN
20. NE-3222-4(d) 1974 Code NE-3221.5(d) 1980 Code Analysis for Cyclic Operation Temperature Difference	<p>i) Paragraph 2:  By Note, adjacent points are defined as follows: "Adjacent points are defined as points which are spaced less than the distance <math>2 Rt</math> from each other, where <math>R</math> and <math>t</math> are the mean radius and thickness, respectively, of the vessel, nozzle, flange or other component in which the points are located."</p>	<p>Paragraph 2:  By Note, adjacent points are defined as follows: "a) For surface temperature differences:  1) On surfaces of revolution in the meridional direction, adjacent points are defined as points which are less than the distance <math>2 Rt</math>, where <math>R</math> is the radius measured normal to the surface from the axis of rotation of the midwall and <math>t</math> is the thickness of the part at the point under consideration. If the product of <math>Rt</math> varies, the average value of the points shall be used.  2) On surfaces of revolution in the circumferential direction, and on flat parts as flanges and flat heads, adjacent points are defined as any two points on the same surface.  b) For through-thickness temperature differences, adjacent points are defined as any two points on a line normal to any surface."</p>	None.
	<p>ii) Paragraph (d)-2 provides requirements for Normal Operation Pressure Fluctuation.</p>	<p>The stress intensity "<math>S_m</math>" is changed to "<math>S_n</math>". Also, "Normal Operation Pressure" is now called "Normal Service Pressure."</p>	None.

QCS220.25-25

Amend. 72  
Oct. 1982

CONTAINMENT VESSEL - COMPARISON OF 1974 EDITION AND 1980 EDITION OF ASME B&PV CODE

SECTION III - DIVISION 1 ARTICLE NE-3000 DESIGN

<u>PARAGRAPH/TITLE</u>	<u>74 EDITION - W74 ADDENDA</u>	<u>80 EDITION - W81 ADDENDA</u>	<u>IMPACT ON DESIGN</u>
21. NE-3222 Operating Conditions (1974 Code) Buckling Stress Values (1980 Code)		<p>Operating Conditions were deleted and replaced by buckling requirements.</p> <p>For Level A and B; the maximum buckling stress value shall be either of the following:</p> <p>a) One third the value of critical buckling stress determined by one of the methods given below:</p> <p>1) rigorous analysis which considers the effects of gross and local buckling, geometric imperfections, nonlinearities, large deformations, and inertial forces (Dynamic loads only);</p> <p>2) classical (linear) analysis reduced by margins which reflect the difference between theoretical and actual load capacities (knockdown factors)</p> <p>3) tests of physical models under conditions of restraint and loading the same as those to which the configuration is expected to be subjected;</p> <p>b) the value determined by the applicable rules of NE-3133. (This covers only cylindrical shells under uniform axial compression and cylindrical and other shells under uniform external pressure).</p> <p>For Level C and D, Level A and B buckling allowables may be increased by 20% and 50%, respectively.</p>	See evaluation in 6.0

QCS220.25-26

Amend. 72  
Oct. 1982

CONTAINMENT VESSEL - COMPARISON OF 1974 EDITION AND 1980 EDITION OF ASME B&PV CODE

SECTION III - DIVISION 1 ARTICLE NE-3000 DESIGN

<u>PARAGRAPH/TITLE</u>	<u>74 EDITION - W74 ADDENDA</u>	<u>80 EDITION - W81 ADDENDA</u>	<u>IMPACT ON DESIGN</u>
22. NE-3226 Testing Limits (1980 Code)	Requirements given in NE-6222 and NE-6322. vessel.	Limits on maximum permissible test pressure are given based on stress limits for the	See evaluation in 6.0
23. NE-3227.1 Bearing Loads	i) The average bearing stress under the maximum load, experienced as a result of design conditions or of any of the operating or testing conditions other than faulted conditions is limited to Sy.	Eliminates the exception "other than faulted conditions" and uses "Service Loading" instead of "Operating Conditions".	None.

QCS220.25-27

Amend. 72  
Oct. 1982

CONTAINMENT VESSEL - COMPARISON OF 1974 EDITION AND 1980 EDITION OF ASME B&PV CODE

SECTION III - DIVISION 1 ARTICLE NE-3000 DESIGN

PARAGRAPH/TITLE	74 EDITION - W74 ADDENDA	80 EDITION - W81 ADDENDA	IMPACT ON DESIGN
24. NE-3227.5 Nozzle Piping Transition			
a) Within the Limits of Reinforcement	1) Primary membrane stress classification in nozzles applies to those resulting from pressure, external load and moment.	i) Additional requirements are added for primary membrane stress classifications.  Stresses attributed to restrained end displacement of attached piping should be added to stresses due to pressure, external loads and moments.  Also, states that primary membrane stresses do not include discontinuity stresses.	See evaluation in 6.0    None.
		ii) Expands classification of local primary membrane stress intensity due to discontinuity effects resulting from pressure, external loads and moments to include those attributable to restrained free end displacements of the attached pipe.	See evaluation in 6.0
		iii) Adds classification of primary local plus primary bending plus secondary stress intensities for those resulting from a combination of pressure, external load and moments, and temperatures and restrained free end displacements of attached pipe.	See evaluation in 6.0
b) Beyond the Limits of Reinforcement	$P_L + P_D + Q$ classification is applied to primary plus secondary stress intensities resulting from all <u>operating conditions</u> loads.	Instead of "Operating Conditions", code requires to consider all pressure, temperature external loads and moments. This would include accident conditions.	See evaluation in 6.0

QCS220.25-28

Amend. 72  
Oct. 1982

CONTAINMENT VESSEL - COMPARISON OF 1974 EDITION AND 1980 EDITION OF ASME B&PV CODE

SECTION III - DIVISION 1 ARTICLE NE-3000 DESIGN

PARAGRAPH/TITLE	74 EDITION - W74 ADDENDA	80 EDITION - W81 ADDENDA	IMPACT ON DESIGN
25. NE-3228.4 Impulsive Loads (1980 Code)	No provisions in the Code.	This is a new section. New provisions are added.	None.
26. NE-3229 Design Stress Values (1974 Code)		Deleted from the Code. However, parts are included in other subsections, NE-3112.4, Design; NE-3134, Material Properties.	None.
27. NE-3232	i) Title: Operating Conditions  ii) Stress limits for bolting material based on Table I-1.3.  iii) Fatigue analysis based on $S_m$	New Title: "Combined Loads".  Stress limits based on Table I-10.3  Stress limits based on $S_m$	None.  See evaluation in 6.0
28. NE-3311 Requirements for Acceptability (Subsection) of Design by Formula)	The requirements for acceptability of a vessel design are given under General Design Rules (NE-3130).	If the approach of "NE-3300 Design by Formula" is used, the rules are applicable to Level A and B Service Loadings which do not include substantial mechanical or thermal loads other than pressure. Substantial loads are mechanical or thermal loads with cumulative result on stresses that exceed 10% of the primary stresses induced by design pressure.	None.
29. NE-3324.3 Cylindrical Shell (Under Internal Pressure)	There are two equations to determine the minimum thickness (t) of the cylindrical shells subjected to internal pressure.	In addition to the previous two equations, additional equations to determine the minimum thickness are provided.	None.

QCS220.25-29

Amend. 72  
Oct. 1982

CONTAINMENT VESSEL - COMPARISON OF 1974 EDITION AND 1980 EDITION OF ASME B&PV CODE

SECTION III - DIVISION 1 ARTICLE NE-3000 DESIGN

<u>PARAGRAPH/TITLE</u>	<u>74 EDITION - W74 ADDENDA</u>	<u>80 EDITION - W81 ADDENDA</u>	<u>IMPACT ON DESIGN</u>
30. NE-3324.4 Spherical Shells (Under Internal Pressure)	There is only one equation to determine the minimum thickness "t". The restriction imposed on the equation is that $t < 0.356R$ and $P < 0.665S$ .	Several additional equations are provided to determine the minimum "t". The main difference is that the code now provides a set of equations for the conditions when $t > 0.356R$ or $P > 0.665S$ .	None.
31. NE-3324.5 Formed Heads, General Require- ments	There are three requirements.	There are six requirements. The following are the additional three:  i) The inside crown radius $t_c$ which a head is dished shall be not greater than the outside diameter of the skirt of the head. The inside knuckle radius of a torispherical head shall be not less than 6% of the outside diameter of the skirt of the head but in no case less than three times the head thickness.  ii) If a torispherical, ellipsoidal, or hemispherical head is formed with a flattened spot or surface, the diameter of the flat spot shall not exceed that permitted for flatheads as given by Eq. (1) or (2) of NE-3225.2 using $C = 0.25$ .  iii) Openings in formed heads under internal pressure shall comply with the requirements of NE-3330.	None.

QCS220.25-30

Amend. 72  
Oct. 1982



CONTAINMENT VESSEL - COMPARISON OF 1974 EDITION AND 1980 EDITION OF ASME B&PV CODE

SECTION III - DIVISION 1 ARTICLE NE-3000 DESIGN

PARAGRAPH/TITLE	74 EDITION - W74 ADDENDA	80 EDITION - W81 ADDENDA	IMPACT ON DESIGN
32. NE-3324.6 Ellipsoidal Heads		An additional equation is provided to determine "t" for ellipsoidal shells of other than a 2:1 ratio.	None.
33. NE-3324.8 (1980 Code) Torispheri- Heads	No provisions in the code.	A new subsection NE-3324.8 is added which provides new rules for Torispherical Heads.	None.
34. NE-3324.11 (1974 Code) NE3324.12 (1980 Code) Nozzles		The Code sets an additional requirement on shear as stated below:  "The allowable stress value for shear in a nozzle neck shall be 70% of the allowable tensile stress for the vessel material".	See evaluation in 6.0
NE-3326.2	i) Title: " <del>Circular</del> Spherically Dished Heads with Bolting Flanges, <del>Concave</del> to Pressure".  ii) Rules of this section are applicable to the spherically dished heads which are concave to pressure.	New Title: "Spherically Dished Heads with Bolting Flanges"  Rules are now applicable to spherically dished heads either concave or convex to pressure. Some revisions were made, but are not applicable to CRBRP.	None.  None.
36. NE-3326.3	"Circular Spherically Dished Covers with Bolting Flanges, Convex to Pressure".	Deleted.	None.

QCS220.25-31

Amend. 72  
Oct. 1982

CONTAINMENT VESSEL - COMPARISON OF 1974 EDITION AND 1980 EDITION OF ASME B&PV CODE

SECTION III - DIVISION 1 ARTICLE NE-3000 DESIGN

<u>PARAGRAPH/TITLE</u>	<u>74 EDITION - W74 ADDENDA</u>	<u>80 EDITION - W81 ADDENDA</u>	<u>IMPACT ON DESIGN</u>
37. NE-3331 General Require- ments for Openings	<p>Requirement (b) of NE3331 states as follows:</p> <p>"For vessels or parts thereof which are in cyclic service and do not meet the requirements of NE-3222.4(d) for operating loads so that a fatigue analysis is required, the rules contained in NE-3330 assure satisfaction of the requirements of NE-3221 in the vicinity of openings, and no specific analysis showing satisfaction of those stress limits is required."</p>	<p>Requirement (b) is modified and is more restricted.</p> <ul style="list-style-type: none"> <li>o Rules contained in NE-3330 assure satisfaction for pressure load only.</li> <li>o An additional following requirement is imposed:                             <p>"The requirements of NE-3221.4 may also be considered to be satisfied if, in the vicinity of the nozzle, the stress intensity resulting from external nozzle loads and thermal effects, including gross but not local structural discontinuities, is shown by analysis to be less than <math>1.5 S_m</math>. In this case, when evaluating the requirements of NE-3221.5 (e), the peak stress intensities resulting from pressure loadings may be obtained by application of the stress Index method of NE-3338."</p> </li> </ul>	See evaluation in 6.0
37a. NE-3335.1 (1974 Code) Pad-Type Reinforcement		Change to NE-3335(e) in the 1980 Code replaces the requirements of NE-3335.1 in the 1974 Code.	None

QC5220.25-32

Amend. 72  
Oct. 1982

CONTAINMENT VESSEL - COMPARISON OF 1974 EDITION AND 1980 EDITION OF ASME B&PV CODE

SECTION III - DIVISION 1 ARTICLE NE-3000 DESIGN

PARAGRAPH/TITLE	74 EDITION - W74 ADDENDA	80 EDITION - W81 ADDENDA	IMPACT ON DESIGN
38. NE3332.2 Required Area of Reinforcement		The following requirement is added:  "At least one-half of the required reinforcing shall be on each side of the centerline of the opening".	None.
39. NE-3334.1 Limit of Reinforcement Along the Vessel Wall	Two requirements on the limit of reinforcement. In addition to that, requirements are provided in NE-3332.3 "Compact Reinforcing in Vessel Wall".	NE-3332.3 is deleted, however, its intention is carried to NE-3334.1. There is an additional requirement set as described below:  "Two-thirds of the required reinforcement shall be within a distance on each side of the axis of the opening equal to the greater of the following:  1) $r + 0.5 / Rt$ , where R is the mean radius of shell or head, t is the nominal vessel wall thickness, and r is the radius of the finished opening in the corroded condition;  2) the radius of the finished opening in the corroded condition plus two-thirds the sum of the thickness of the vessel wall and the nozzle wall (new equipment)".	See evaluation in 6.0

QCS220.25-33

Amend. 72  
Oct. 1982

CONTAINMENT VESSEL - COMPARISON OF 1974 EDITION AND 1980 EDITION OF ASME B&PV CODE

SECTION III - DIVISION 1 ARTICLE NE-3000 DESIGN

<u>PARAGRAPH/TITLE</u>	<u>74 EDITION - W74 ADDENDA</u>	<u>80 EDITION - W81 ADDENDA</u>	<u>IMPACT ON DESIGN</u>
40. NE-3336 Strength of Rein- forcing Material	"Material in the nozzle wall used for reinforcement shall preferably be the same as that of the vessel wall. If material with a lower design stress value, $S$ , is used, the area provided by such material shall be increased in proportion to the inverse ratio of the stress values of the nozzle and the vessel wall material."	Revised provision:  "Material used for reinforcement shall preferably be the same as that of the vessel wall. If the material of the nozzle wall or reinforcement has a lower design stress value $S$ than the vessel material, the amount of area provided by the nozzle wall or reinforcement in satisfying the requirements of NE-3332 shall be taken as the actual area provided multiplied by the ratio of the nozzle or reinforcement design stress value to the vessel material design stress value."	See evaluation In 6.0
41. NE-3367 Closures On Small Pene- trations		Dimensional standards are updated to the latest applicable standards.	See evaluation In 6.0

QCS220.25-34

Amend. 72  
Oct. 1982

CONTAINMENT VESSEL - COMPARISON OF 1974 EDITION AND 1980 EDITION OF ASME B&PV CODE

SECTION III - DIVISION 1 ARTICLE NE-3000 DESIGN

<u>PARAGRAPH/TITLE</u>	<u>74 EDITION - W74 ADDENDA</u>	<u>80 EDITION - W81 ADDENDA</u>	<u>IMPACT ON DESIGN</u>
42. NE-3720 Design Rules for Electrical and Mechanical Pene- tration Assemblies		<p>The following is an additional requirement imposed:</p> <p>"For closing seams in electrical and mechanical penetrations meeting the requirements of NE-4730(c), the closure head shall meet the requirements of NE-3325 using a factor <math>C = 0.30</math>. The fillet weld shall be designed using an allowable stress of <math>0.55S_m</math>."</p> <p>Design of the pressure retaining portion of the electrical and mechanical penetration assemblies shall be the same as for vessels. There is no exemption to this rule.</p>	See evaluation in 6.0

QCS220.25-35

Amend. 72  
Oct. 1982

TABLE I  
STRESS INTENSITY LIMITS FOR STEEL CONTAINMENTS

LOAD COMBINATIONS	PRIMARY STRESS INTENSITIES										
			GENERAL MEMBRANE $P_m$		LOCAL MEMBRANE $P_L$		BENDING PLUS LOCAL MEMBRANE $P_b + P_L$		PRIMARY PLUS SECONDARY STRESS INTENSITY RANGE $P_L + P_b + Q$		
	1974 Code	1980 Code	1974 Code	1980 Code	1974 Code	1980 Code	1974 Code	1980 Code	1974 Code	1980 Code	
D+L+T+PI/Po/R	Design	Design	Sm	Sec	1.5Sm	1.5Sec	1.5Sm	1.5Sec	N/A	N/A	
**D+L+T+PI/Po/R	Design	Level A	Sm	Sec	1.5Sm	1.5Sec	1.5Sm	1.5Sec	N/A	3.0 Sm	
**D+L+T <sub>o</sub>	Operating	Level A	N/A	Sec	N/A	1.5Sec	N/A	1.5Sm	3.0Sm	3.0 Sm	
**D+L+T+PI/Po/R+OBE	Design	Level B	Sm	Sec	1.5Sm	1.5Sec	1.5Sm	1.5Sec	N/A	3.0 Sm	
**D+L+T <sub>o</sub> +OBE	Operating	Level B	N/A	Sec	N/A	1.5Sec	N/A	1.5Sm	3.0Sm	3.0 Sm	
D+L+T+PI/Po/R+SSE and D+L+T <sub>o</sub> +SSE	Design	Level C	When not integral and Continuous	Sm	Sec	1.5Sm	1.5Sec	1.5Sm	1.5Sec	N/A	N/A
			When integral and Continuous	1.2Sm or Sy*	1.2Sec or Sy*	1.8Sm or 1.5Sy*	1.8Sec or 1.5Sy*	1.8Sm or 1.5Sy*	1.8Sec or 1.5Sy*	N/A	N/A

\* Larger of 2 values.

\*\* See evaluations in 6.0, Item 14 under NE-3000

- NOTES: (1) PI/Po/R represents consideration of PI, Po or R in the load combination at a time. However, all three situations need to be evaluated.  
(2) Notations are as per PSAR 3.8.  
(3) Level D service limit not evaluated as such loads are not specified for the vessel design.

QCS220.25-36

Amend. 72  
Oct. 1982

## LIST OF ITEMS NOT EVALUATED

The following is a list of sections from the 1974 Code which have not been evaluated against the 1980 Code because either the items are not applicable to ORERP Containment or the containment vessel design does not adopt the techniques or the concepts described by the Code Sections. Further in the evaluation, consideration was given to only those loading conditions which are specified for the design of the vessel.

- 1) NE-3122 Cladding
- 2) NE-3131.2 Jet Impingement Effects
- 3) NE-3133.7 Conical Heads
- 4) NE-3213.21 Limit Analysis - Collapse Load
- 5) NE-3213.22 Collapse Load - Lower Bound
- 6) NE-3216.2 Varying Principal Stress Direction
- 7) NE-3222.5 Thermal Stress Ratchet
- 8) NE-3228 Applications of Plastic Analysis
- 9) NE-3324.7 Hemispherical Heads
- 10) NE-3324.8 Conical Heads
- 11) NE-3324.9 Reducer Sections
- 12) NE-3325 Flat Heads and Covers
- 13) NE-3333 Reinforcement Required for Openings in Flat Heads
- 14) NE-3338.2 Stress Index Methods
- 15) NE-3352.4, Para. 3(d), 3(e), 3(f). 3(d) is on Attachment of Nozzles Using Partial Penetration Welds; 3(e) describes Attachment of Fittings with Internal Threads; 3(f) is on Attachment of Tube Connections
- 16) NE-3358.3 Head Attachments Using Corner Joints
- 17) NE-3358.4 Flat Heads with Hubs

CONTAINMENT VESSEL - ASME B&PV CODE COMPARISON

SECTION III - ARTICLE NE-4000 FABRICATION AND INSTALLATION

PARAGRAPH/TITLE	74 EDITION - W74 ADDENDA	80 EDITION - W81 ADDENDA	IMPACT ON DESIGN
1. NE-4131 Elimination and Repair of Defects	No requirement for the time of examination of weld repair to weld edge preparation	Requires that examination of weld repair to weld edge preparation be in accordance with NE-5130.	None.
2. NE-4213.2(c) Procedure Qualifica- tion Test (Impact Testing)	Percent strain for spherical or dished surfaces  % strain = 65†	Changed constant 65 to 75.  % strain = 75†	None.
3. NE-4213.2(e)	Does not cross-reference base material impact testing of NE-2300	Imposes base material impact test requirements of NE-2300.	None.
4. NE-4213.2(f)	Determine maximum loss of impact energy and maximum NDT temperature change	Determine maximum lateral expansion or maximum change in temperature, plus, maximum changes NDT temperature.	None.
5. NE-4221.2(a) Maximum Deviation from True Theoretical Form for External Pressure	(a) Maximum arc length need not be greater than 0.250 <sub>o</sub> for determining deviation from the true circle	(a) Maximum arc length need not be greater than 0.300 <sub>o</sub> .	None.
6. NE-4221.2-1 Curves for Maximum Permissible Deviation, from a true Circular Form	(b)	(b) Curves are shifted slightly from 1974 version.	None.
7. NE-4221.2-2 Curves for Maximum Arch Length for Determining Plus or Minus Deviation	(c)	(c) Curves are shifted significantly to right.	None.

QCS220.25-38

Amend. 72  
Oct. 1982



CONTAINMENT VESSEL - ASME B&PV CODE COMPARISON

SECTION III - ARTICLE NE-4000 FABRICATION AND INSTALLATION

<u>PARAGRAPH/TITLE</u>	<u>74 EDITION - W74 ADDENDA</u>	<u>80 EDITION - W81 ADDENDA</u>	<u>IMPACT ON DESIGN</u>
8. NE-4221.2(c) The Value of Cylinder Length (L)	(d) Provides definition of length without reference to NE-3133.2	(d) Clarifies definition of length to be consistent with NE-3133.2.	None.
9. NE-4222.1(a) Deviation for (from) Specified Shape		Provides tighter constraints on the deviation of the head from the nominal diameter of the vessel.	None.
10. NE-4222.1(b)	Provides for skirts of heads to be within 1% of nominal diameter	Provides that hemispherical heads and any spherical portion thereof shall meet NE-4221.2.	None.
11. NE-4222.1(c)		Provides that measurements shall be taken on base metal and not on welds.	None.
12. NE-4222.2 Tolerance on Forged Heads	Forged heads shall conform to drawing shape as is practicable	None.	None.
13. NE-4232-1 Fairing of Offsets	Provides for fairing of offsets over the width of the finished weld	1. Fairing of offset shall be at least a 3:1 taper over the width of the finished weld.  2. Offsets greater than those in Table NE-4232-1 are acceptable provided the requirements of NE-3200 are met.	None.
14. NE-4243 Category C Weld Joints		Category C welds include the exception that socket welded flanges are 2" nominal pipe size and less and slip-on flanges may be used.	None.
15. NE-4244(d) Category D Weld Joints		Partial Penetration welds for Attachment of Nozzles are also limited by additional requirements of NE-3359, which provides for sufficient weld strength and percent of allowable stress valves.	None.

QCS220.25-39

Amend. 72  
Oct. 1982

CONTAINMENT VESSEL - ASME B&PV CODE COMPARISON

SECTION III - ARTICLE NE-4000 FABRICATION AND INSTALLATION

PARAGRAPH/TITLE	74 EDITION - W74 ADDENDA	80 EDITION - W81 ADDENDA	IMPACT ON DESIGN
16. NE-4244(e) Attachment of Fittings With Internal Threads	(a) Internally threaded fitting and bolting pads not exceeding 2" pipe size may be attached to vessels	The 2" pipe size limitation has been corrected to read 3" pipe size.	None.
16a. NE-4244(g) (1974)		Nozzles with integral reinforcing have been deleted.	None.
17. Figure NE-4244(d)-1	Acceptable types of welded nozzles using partial penetration welds shows examples of reinforced weldments (e), (f) and (g)	The reinforced examples are no longer shown as acceptable types. New acceptable types are shown in (e) and (f).	None.
18. NE-4311.1 Stud Welding Restrictions	Stud cross-sectional area is limited to 1/2" maximum diameter for stud welding	The cross-sectional area is now limited to 1" for flat position and 3/4" diameter for all other positions.	None.
19. NE-4311.2 & NE-4311.3 Capacitor Discharge Welding		Capacitor Discharge Welding and Low Energy Discharge Welding provisions have been added.	
20. NE-4322.1 Identification of Joints by Welder or Welding Operator		Requires the marking be done with blunt Nose continuous or interrupted dot die stamp and provides relaxations where multiple welders are involved. Identification of tack welders not required. Deletes reference to NE-4122.1.	None.
21. NE-4332 Base Material to be Employed	Base material used for weld qualification shall be same as type and grade except that any P- Number 1 material in a Group qualifies for all P- Number 1 of the same grouping	Base material shall be in accordance with the applicable requirements of QW-403.4 and QW-403.5 of Section IX.	None.
22. NE-4334.1 Coupons Representing the Weld Deposits		Additional requirement that where the postweld heat treatment temperature exceeds the maximum temperature specified in NE-4620, and the test assembly is cooled at an accelerated rate, the longitudinal axis of the specimen shall be a minimum of t from the edge of the test assembly. Otherwise the axis of the specimen shall be not	None.

QCS220.25-40

Amend. 72  
Oct. 1982

CONTAINMENT VESSEL - ASME B&PV CODE COMPARISON

SECTION III - ARTICLE NE-4000 FABRICATION AND INSTALLATION

<u>PARAGRAPH/TITLE</u>	<u>74 EDITION - W74 ADDENDA</u>	<u>80 EDITION - W81 ADDENDA</u>	<u>IMPACT ON DESIGN</u>
22. (Cont'd)		less than 3/8" from the weld surface if possible, but not less than 1/4t.  For drop weight specimens, the tension surface shall be parallel to the surface of the test weld assembly.	
23. NE-4334.2 Coupons Representing the Heat Affected Zone		1. Additionally, defines axis of the weld relative to plate or forgings.  2. Provides for comparison of heat affect zone values with base material values.	None.
24. NE-4335 Impact Test Require- ments		Specifically overrules certain exemptions of impact testing permitted by NE-2311(a)(8).	None.
25. NE-4335.1 Impact Testing of Weld Metal	Requires impact testing for welding procedure qualification for classification A-Number 1 weld analysis or any other ferritic weld analysis	Requires: 1. Impact testing is required for weld metal for the welding procedure for any weld repair to base metal that requires impact testing.  2. Impact test requirements and acceptance standards for welding procedure qualification weld metal shall be the same as specified in NE-2330 for the base material to be welded or repaired. Dissimilar metals shall be impact tested according to requirements for either metal except where otherwise specified by NCA-1230 or other parts of Section III.  3. Impact tests not required for austenitic and nonferrous metal.  4. Welding procedure qualified to impact testing requirements of Subsection NB or NC may be accepted as an alternate.	None.

QCS220.25-41

Amend. 72  
Oct. 1982

CONTAINMENT VESSEL - ASME B&PV CODE COMPARISON

SECTION III - ARTICLE NE-4000 FABRICATION AND INSTALLATION

PARAGRAPH/TITLE	74 EDITION - W74 ADDENDA	80 EDITION - W81 ADDENDA	IMPACT ON DESIGN
26. NE-4335.2(a) Impact Tests of Heat Affected Zone	Requires impact testing for base metal weld heat-affect zone for materials of P-Number 1 classification	1. Provides exemptions from impact testing for (a) the qualification for welds in P-Number 1 material that is post weld heat treated and made by any process other than electroslag, electrogas, or thermit (b) the qualification of weld deposits on weld cladding on any base material.	None.
27. NE-4335.2(b) Impact Tests of Heat Affected Zone		Greatly expanded requirements for impact testing for special case procedure qualification test for heat affected zone.	None.
28. NE-4335.2(c)		Retest of failed impact test results shall be at higher temperature until requirements are met.	None.
29. NE-4335.2(d)		A welding procedure specification qualified to impact testing requirements of Subsection NB or NC may be accepted as an alternate.	None.
30. Figure NE-4427-1 Fillet and Socket Weld Details and Dimensions		Figure was redrawn. Back weld added to (C-1) slip-on flange. Removed 2" pipe size limitation.	None.
31. NE-4429 Welding of Clad Parts	Weld deposited cladding shall be examined by a liquid penetrant method in accordance with the requirements of Article 6 of Section V and the acceptance standards of NE-5350	No reference to inspection methods.	None.
32. NE-4431 Materials for Perma- nent Structural Attachment	Material shall meet requirements of NE-4620 and impact tested to Table I-10.0. Material exempt from impact or not post weld heat treated may not be welded closer than 4" or 16 times thickness from weld joint of permanent structural attachment	Materials shall meet requirements of NE-2190 and impact tested to NE-2300 if exempt from post weld heat treatment.	None.

QCS220.25-42

Amend. 72  
Oct. 1982

CONTAINMENT VESSEL - ASME B&PV CODE COMPARISON

SECTION III - ARTICLE NE-4000 FABRICATION AND INSTALLATION

<u>PARAGRAPH/TITLE</u>	<u>74 EDITION - W/4 ADDENDA</u>	<u>80 EDITION - WB1 ADDENDA</u>	<u>IMPACT ON DESIGN</u>
33. NE-4333 Types of Permanent Structural Attachment Welds		Provides for full penetration, fillet, or partial penetration continuous or intermittent welds for attachment of Permanent Structures.	None.
34. E-4435 Welding of Non-Structural and Temporary Attachments	when required by NE-4620.	Also provides that (a) the welding material is identified and compatible with the materials joined (b) The welds are post-weld heat treated	None.
35. NE-4453.1 Defect Removal		Welds examination where defect removal removes essentially the full thickness of the weld in partial penetration and fillet welds.	None.
36. NE-4453.4 Examination of Repair Welds	Repair cavities which do not exceed 3/8" or 10% of weld thickness need only magnetic particle or liquid penetrant method for reexamination	Repair cavities not exceeding 1/3t for t ≤ 1/2", 1/4t for 1/2" < 2-1/2", 1/8" or 10%t for t > 2-1/2" need only magnetic particle or liquid penetrant method for reexamination, where t = thickness.	None.
37. NE-4622.1(a) General Require- ments	No requirement to include PWHT time after completion of component into total time at temperature for test specimen	<ol style="list-style-type: none"> <li>1. PWHT shall be performed in temperature - surveyed and - calibrated furnaces or with thermocouples in contact with the material or attached to blocks in contact with the material.</li> <li>2. PWHT time after completion of part shall be added to total time at temperature for test specimen.</li> </ol>	None.
37a. NE-4622.4(c) Holding Times at Temperature	Provides three (3) alternatives for lowering heat treat temperatures	Two alternatives for lowering heat treat temperatures are deleted.	None.

QCS220.25-43

Amend. 72  
Oct. 1982

CONTAINMENT VESSEL - ASME B&PV CODE EVALUATION

SECTION III - ARTICLE NE-4000 FABRICATION AND INSTALLATION

PARAGRAPH/TITLE	74 EDITION - W74 ADDENDA	80 EDITION - W81 ADDENDA	IMPACT ON DESIGN
38. NE-4622.7(f) Exemptions to Mandatory Requirements		Deleted exemption for PWHT of Type 405 or Type 410 with carbon less than 0.08% and modified some exemption requirements.	None.
39. NE-4640 Heat Treatment After Repair by Welding		Delete Heat Treatment after repair and placed in Table NE-4622.7(b)-1.	None.
40. NE-4660 Heat Treatment of Electroslag Welds		Added requirement for heat treatment of electroslag weld.	None.
41. NE-4730 Electrical and Mechanical Penetration Assemblies		Optional method for closing seam for the penetration assembly depicted in added Figure NE-4730-1 and in accordance with listed requirements.	None.
42. NE-4714 Stud Threading	No requirement	Provisions for stud threading has been added.	None.
43. NE-4740 Special Qualifica- tion Require- ments for Electrical and Mechni- cal Penetra- tion Assemblies	No requirement	Qualification requirements added.	None.

QCS220.25-44

Amend. 72  
Oct. 1982

CONTAINMENT VESSEL - COMPARISON OF 1974 EDITION AND 1980 EDITION OF ASME B&PV CODE

SECTION III - DIVISION 1 ARTICLE NE-5000 EXAMINATION

PARAGRAPH/TITLE	74 EDITION - W74 ADDENDA	80 EDITION - W81 ADDENDA	IMPACT ON DESIGN
1. NE-5130 Examination of Weld Edge Pre- paration Surfaces	No requirement for examination of weld edge preparation surfaces	1. All full penetration weld edge preparation surfaces shall be examined by magnetic or liquid penetrant method to the acceptance standards defined in NE-5130.  2. Laminar indications exceeding 1" in length shall be examined ultrasonically to the acceptance standards defined in NE-5130.  3. Weld repairs made to weld edge preparation shall be magnetic particle and liquid penetrant examined.	None.  None.  None.
2. NE-5232 Non butt- weld joint	No requirements for corner joints	Corner joint welds where one plate is more than 1/2" thicker, the cut edges of the plate shall be examined before welding adjacent to the intended weld by magnetic particle or liquid penetrant methods. After welding all exposed edges adjacent to weld shall be reexamined.	None.
3. NE-5270 Special	Clad plate and applied corrosion layers be radiographed.	Weld metal cladding shall be examined by the liquid penetrant method.	None.
4. NE-5278 Electroslag Weld	No requirement	All complete penetration welds made by the electroslag process in ferritic materials shall be ultrasonically examined	None.
5. NE-5320 Radio- graphic Acceptance Standards	Provides for radiographic acceptance standards	Permits, in addition to radiographic acceptance standards, internal root weld conditions as acceptable when the density change as indicated in the radiograph is not abrupt.	None.

QCS220.25-45

Amend. 72  
Oct. 1982

CONTAINMENT VESSEL - ASME B&PV CODE COMPARISON

SECTION III - ARTICLE NE-5000 Examination

<u>PARAGRAPH/TITLE</u>	<u>74 EDITION - W74 ADDENDA</u>	<u>80 EDITION - W81 ADDENDA</u>	<u>IMPACT ON DESIGN</u>
6. NE-5342 Acceptance Standards & NE-5352 Acceptance Standards	Does not provide for a lower limit of relevant indication	Provides that only indications with major dimensions greater than 1/16" shall be considered relevant	None.
7. NE-5520 Personnel Qualifica- tion, Certification and Verification	Qualification and Certification of Personnel based upon SNT-TC-1A	Qualification and Certification of personnel description greatly expanded but still based upon SNT-TC-1A	None.
8. NE-5600 Examination of Material	Defines some limited material requirements	Deleted as being redundant to NE-2000 requirements. Moved the requirements for materials forming a corner joint to NE-5232	None.

QCS220.25-46

Amend. 72  
Oct. 1982



CONTAINMENT VESSEL - ASME B&PV CODE COMPARISON

SECTION III - ARTICLE NE-6000 Testing

PARAGRAPH/TITLE	74 EDITION - W74 ADDENDA	80 EDITION - W81 ADDENDA	IMPACT ON DESIGN
1. NE-6110 Testing of MC Components	Requires all vessels & appurtenances constructed or installed per Sub-section NE to be pressure tested	Now requires <u>all pressure</u> retaining vessels etc. to be tested. Also washers have been <u>added</u> to list of items exempted from testing.	None.
2. NE-6111 Pneumatic or hydro- static Testing		Rearranged editorially	None.
3. NE-6112 Conditions for Pneumatic Testing		Rearranged editorially	None.
4. NE-6112.1 Precautions for Pneuma- tic Testing	Refers to "compressed gas" and states that precautions shall be taken	NE-6112.2 refers to "compressed gaseous fluid" and recommends that precautions be taken	None.
5. NE-6115 Time of Test	Required test to be done prior to stamping & provided instructions to Inspector for signing Data Report	Paragraph has been deleted from latest revision, however, new paragraph NE-6113 requires all testing done under this Article to be in the presence of the Inspector	None.
6. NE-6121 Exposure of Joints	Discusses leaving all mechanical and welded joints accessible for examination except as provided in NE-5211	Has expanded these requirements to <u>all</u> joints and left <u>uninsulated</u> and <u>exposed</u> for examination	None.
7. NE-6122 Temporary Supports	Allows use of temporary supports or stiffening to support weight of test liquid during test	Considers stiffening same as support	None.

QCS220.25-47

Amend. 72  
Oct. 1982

CONTAINMENT VESSEL - ASME R&PV CODE COMPARISON

SECTION III - ARTICLE NE-6000 TESTING

PARAGRAPH/TITLE	74 EDITION - W74 ADDENDA	80 EDITION - W81 ADDENDA	IMPACT ON DESIGN
8. NE-6123 Restraint or Isolation of Expansion Joints		Deletes option of Isolating expansion joint during the test. (Note: the title is not changed)	None.
9. NE-6125 Flanged Joints containing Blinds	Discusses not testing Flanged joints with Blanks installed until <u>after</u> the Blanks are removed	Allows these same Flanged joints to <u>not</u> be retested after removal of blanks	None.
10. NE-6211 Venting before Hydrostatic Testing	Requires vent at all high points to vent air pockets while filling	Reduces discussion to indicate venting shall be done to minimize air pockets	None.
11. NE-6212 Test Medium & Temp- erature	Limits hydro media to water & requires testing be done at temperatures above brittle fracture point	Expands requirements to allow use of "alternative liquid" as permitted by Design Specification	None.
12. NE-6123 & NE-6313 Check of Test Equip. (1974 Code)		NE-6127 - now contains these relocated requirements	None.
13. NE-6215 Examination for leakage (1974 Code)		Requirements are now given in NE-6224	None.

QCS220.25-48

Amend. 72  
Oct. 1982

CONTAINMENT VESSEL - ASME B&PV CODE COMPARISON

SECTION III - ARTICLE NE-6000 TESTING

PARAGRAPH/TITLE	74 EDITION - W74 ADDENDA	80 EDITION - W81 ADDENDA	IMPACT ON DESIGN
14. NE-6221 Min. Test Pressure	Required minimum of 1.35 Times Design Pressure multiplied by a factor dependent on stress for that particular material	Redefined min. pressure to be not less than 1.35 Times design pressure	None.
15. NE-6222 Max. Test Pressure	Provides lengthy discussion of considerations to determine max. pressure to be used	Requirements are now given by the stress limits of NE-3226 when determining max. pressure	See Evaluation in 6.0 for Item 22.
16. NE-6224 Holding Time (1974 Code)		Now numbered NE-6223	None.
17. NE-6224 Examination for leakage (1980 Code)	Requirements given in NE-6215	Now appears as NE-6224 and provides much more definitive guidance on pressures to be maintained during examination depending on what is being examined. It also provides for allowances of certain kinds of leakages during the test.	None.
18. NE-6510 Bellows Expansion Joints (1974 Code)		New Section NE-6320 is provided that now includes requirements for testing bellows. This change goes in hand with NE-6123 which no longer recognizes isolating expansion joints during hydro testing & is tied to changes made from old Section NE-6500	None.
19. NE-6311 General content of NE-6322		Only change is reference to NE-3226 for guidance on stress intensities in keeping with change in	See Evaluation in 6.0 for Item 22.
20. NE-6312 Test Temperature		Same comments as Test temperature portion of NE-6212 changes	

QCS220.25-49

Amend. 72  
Oct. 1982

CONTAINMENT VESSEL - ASME B&PV CODE COMPARISON

SECTION III - ARTICLE NE-6000 TESTING

PARAGRAPH/TITLE	74 EDITION - W74 ADDENDA	80 EDITION - W81 ADDENDA	IMPACT ON DESIGN
21. NE-6314 Procedure		NE-6313 now provides this guidance. It no longer contains the requirement to reduce pressure for the examination. This is now contained in NE-6324.	None.
22. NE-6315 Examination for leakage		Now appears as NE-6324. More allowance for reducing pressure during examination to the greater of Design Pressure or 3/4 Test Pressure vs. 4/5 Test Pressure	None.
23. NE-6321 Min. Test Pressure	Required minimum of 1.10 times design pressure multiplied by a factor dependent on stress for that particular material	Redefined min. pressure to be not less than 1.1 times design pressure	None.
24. NE-6322 Max. Test Pressure		Same comments as Max. Test Pressure of NE-6222 changes.	
25. NE-6324 Holding Time		Now numbered NE-6323	None.
26. NE-6411 Types & Location of Gages		Reduced <u>requirement</u> for using a recording gage to a <u>recommendation</u> to be used for vessels with large volumetric content	None.

QCS220.25-50

Amend. 72  
Oct. 1982

CONTAINMENT VESSEL - ASME B&PV CODE COMPARISON

SECTION III - ARTICLE NE-6000 TESTING

<u>PARAGRAPH/TITLE</u>	<u>74 EDITION - W74 ADDENDA</u>	<u>80 EDITION - W81 ADDENDA</u>	<u>IMPACT ON DESIGN</u>
27. NE-6500 Pressure Testing of Expan-	This Includes requirements that allow both hydrostatic or pneumatic testing of Expansion (Bellows Type) Joints.	This guidance is now relocated to Section NE-6320. New paragraph NE-6320 deletes direct reference to pneumatic testing of these joints.	None.

QCS220.25-51

Amend. 72  
Oct. 1982

CONTAINMENT VESSEL - ASME B&PV CODE COMPARISON

SECTION III - ARTICLE NE-7000 - PROTECTION AGAINST OVERPRESSURE

PARAGRAPH/TITLE	74 EDITION - W74 ADDENDA	80 EDITION - W81 ADDENDA	IMPACT ON DESIGN
1. NE 7000		<p>General Comment: Article NE-7000 has been completely rewritten. A subsection by subsection comparison is not possible in the strict sense. Section NE-7000 has been expanded from two pages to nine pages providing new guidance in the following areas.</p> <p>NE 7110 Scope                      NE 7111 General Definitions                      NE 7120 Integrated overpressure protection                      NE 7130 Provisions for check operation of pressure relief devices                      NE 7160 Unacceptable relief devices                      NE 7300 Relieving capacity requirements                      NE 7400 Set pressure of pressure relief devices                      NE 7500 Operating design requirements for pressure relief valves                      NE 7700 Certification requirements (specifically involve certifying capacity of relief devices)                      NE 7800 Marking, stamping and data reports                      NE 7141(b) - (d) New provisions for installation</p>	See evaluation in 6.0
2. NE 7113 Requirements when Pressure Relief Device are Permanently Installed		NE 7141(a) provides similar guidance only minor editorial change	None.
3. NE 7114 Requirements for Pressure Relief Devices	This allowed for <u>exceptions as indicated</u> in the article	NE 7151 now restricts all construction to Class 2 requirements	None.

QCS220.25-52

Amend. 72  
Oct. 1982

CONTAINMENT VESSEL - ASME B&PV CODE COMPARISON

SECTION III - ARTICLE NE-7000 - PROTECTION AGAINST OVERPRESSURE

<u>PARAGRAPH/TITLE</u>	<u>74 EDITION - W74 ADDENDA</u>	<u>80 EDITION - W81 ADDENDA</u>	<u>IMPACT ON DESIGN</u>
4. NE-7211 & NE-7212 Acceptable types of vacuum relief devices		These two sections are now addressed in NE-7152. NE-7152 contains only minor changes to regrouped content of previous paragraphs	None.
5. NE-7117 Intervening Step Valves	Discusses placement of step valves and interlocks and controls required if they are placed such that they might prohibit proper relief protection	NE-7142 - New requirement for means shall be provided such that the operation of controls and interlocks can be verified	None.

CONTAINMENT VESSEL - ASME B&PV CODE COMPARISON

SECTION III - ARTICLE NE-8000 - NAMEPLATES, STAMPING, & REPORTS

<u>PARAGRAPH/TITLE</u>	<u>74 EDITION - W74 ADDENDA</u>	<u>80 EDITION - W81 ADDENDA</u>	<u>IMPACT ON DESIGN</u>
1. NE-8100 Requirements		Provides similar guidance; only minor editorial changes	None.

QCS220.25-53

Amend. 72  
Oct. 1982

4.0 COMPARISON OF SECTION III, DIVISION 2 AFFECTING FOUNDATION MAT AND BOTTOM LINER

- .1 CC-2000 Materials
- .2 CC-3000 Design
- .3 CC-4000 Fabrication and Construction
- .4 CC-5000 Construction Testing and Examination



CC-2000 MATERIAL

LIST OF CHANGES

- CC-2122.3 Reports of tests, treatments, etc. to go to Authorized Inspector (AI). Provisions made for inspections by AI as required.
- CC-2131.4 Personnel Qualification. Laboratory personnel performing tests required by CC-2000 may be qualified using appropriate industry or laboratory standards. Appendix VII qualification not mandatory for laboratory tests for concrete constituents and concrete.
- CC-2160 Dimensional Standards. Dimensions of standard items for pipe, tube, fittings, etc. updated and enlarged in Table CC-2160-1.
- CC-2211 Consideration shall be given in the requirements of concrete to minimizing the heat of hydration in concrete, strength development with respect to form removal, and construction stresses. (Note these items are covered in Burns and Roe Specifications).
- CC-2221 Cement. Added ASTM C595, Type IP, (MS) or (MH) to other allowable types of cement. Enlarged on requirements for use of sulphate resistant cement.
- CC-2222.1(b) Coarse Aggregate. Added criteria and test for flat and elongated particles. Test is CRD-C 119, Method of Test for Flat and Elongated Particles in Coarse Aggregate.
- CC-2222.1(f) If tangential shear is to be carried by concrete, test aggregate loss of weight by ASTM C131, Resistance to Abrasion of Small Coarse Aggregate by Use of Los Angeles machine. Loss not to exceed 40%.
- CC-2224.1 Admixtures for Concrete. Each admixture shall not contribute more than 5 ppm, by weight, of chloride ions to the total concrete constituents.
- CC-2310(d) Only material listed in Table I-2.1 may be used for joining reinforcing bar to liner plate or structural steel shapes by welding.

- CC-2332 Bend tests revised by more explicit instructions. Pin diameter changed and listed.
- CC-2333 Chemical Analysis. Requirements for analysis revised and defined in more detail.
- CC-2535 Examination and requirements added for wrought seamless and welded tubular products and fittings.
- CC-2537 Examination and repair requirements added for statically and centrifugally case products.
- CC-2600 Welding Materials. Some changes in wording, format and tests.
- CC-2700 Material Manufacturer's Quality System Program. System program description and references have changed.

CONCLUSION. None of these changes impact the design.

FOR MAT FOUNDATION DESIGN

CC-3000 - DESIGN

CHANGES

IMPACT ON DESIGN

Effect of changes of ASME Section III, Division 2 from  
1975 Edition to 1980 Edition.

1. Load combination and load factors (P. 172 Table CC-3230-1)

See evaluation in 6.0

Construction Load Combination:

$$U = 1.0D + 1.0L + 1.0F + 1.0T_o + 1.0W$$

"1.0W" added in the load combination

2. Allowable Compression stresses for factored loads  
(Page 174, Table CC-3421-1)

- a. The maximum allowable primary-plus-secondary membrane and bending compressive stress of .85 f' corresponds to limiting strain of .002 in/in instead of .033 in/in in 1975 Edition
- b. The membrane portion of the calculated stress shall not exceed the allowable stress applicable when membrane stress act alone.
- c. The primary portion of the calculated stress shall not exceed the allowable stress applicable when primary stress acts alone.

See evaluation in 6.0

None.

None.

QCS220.25-57

Amend. 72  
Oct. 1982

FOR MAT FOUNDATION DESIGN

CC-3000 - DESIGN

CHANGES	REMARKS
3. CC-3121: "Liner behavior" changed to "Maximum strains"	No Impact.
4. CC-3136.3 thru 3136.5: Classification of primary and secondary stresses redefined. Notably the bending stress at a gross structural discontinuity due to external loads is reclassified from secondary to primary stress. (Note 3 of Table CC-3136.5-1)	No Impact.
5. CC-3222.3 and Table CC-3230-1: Defined the internal flooding load, $H_a$ , in the load combinations.	No Impact.
6. CC-3410: Add "primary" to factored loads to clarify general yield considerations.	No Impact.
7. CC-3422.1: Requirements for tension rebars have been expanded substantially.	No Impact.
8. Table CC-3431-1, subparagraph CC-3432.1 and 2: Changes may affect the added wind load "1.0W", secondary effects and test condition.	No Impact.
9. CC-3521.2.4 (deleted)	
10. CC-3531.1.2(e), (h) (3) & (h) (4): Changes in development length requirements.	No Impact.

QCS220.25-58

Amend. 72  
Oct. 1982

CC-4000 FABRICATION AND CONSTRUCTION

- CC-4240(a) Curing. Concrete shall be kept moist and protected through the minimum curing time specified in construction specifications. (Dropped "at least 7 days after placing"). Note: Burns and Roe specifications refer to ACI 301 and 308 which conforms to the above curing requirements.
- CC-4323.4 Fabrication of Reinforcing - Tolerances. Tolerances shown in Figures 4323-2 and 4323-3.
- CC-4330 Splicing of Reinforcing Bars. Added new types of mechanical splices and method of qualification of other systems by manufacturers.
- CC-4522.1 Liner Shell. Spacing of measurements for tolerance conformity increased from 10 feet to 12 feet.
- CONCLUSION. None of these changes impact the design.

CC-5000 CONSTRUCTION TESTING AND EXAMINATION

- CC-5221 Cement. Tests listed in Table 5220-1 enlarged, but are less than those given in Burns and Roe Specification 3066-10-4.
- CC-5222 Fly Ash. Tests listed in Table 5220-1 enlarged, but are less than those given in Specification 3066-10-5. Also, frequency is less in most cases (1000 tons instead of 200 tons).
- CC-5224 Aggregates. Frequency changed from time basis to volume basis. (once daily changed to each 2000 cubic yard concrete. Depending on production rate, may be increase or decrease in frequency.
- CC5225 Water. Soundness test dropped. Frequency decreased from monthly to every 6 months.
- CC-5232 Concrete, Slump. After initial testing, frequency of testing has been decreased from every 50 cubic yard to every 100 cubic yards.
- CC-5232 Air Content. After initial testing, frequency of testing has been decreased from every 50 cubic yards to every 100 cubic yards.
- Temperature: Ditto
- Weight/Yield. After initial testing, frequency has been decreased from every 100 cubic yards to every 200 cubic yards.
- Compressive Strength. Ditto
- CC-5500 Examination of Liners. More explicit instructions added for testing and examination of welds. Ultrasonic testing added as an allowable method of testing (added to radiographic, magnetic particle and liquid penetrant methods).

CONCLUSION. None of these changes impact the design.

## 5.0 COMPARISON OF CODE CASE N-284, BUCKLING CRITERIA

### i. Key items for Comparison

The comparison between the PSAR and the Code Case N-284 buckling criteria is based on a qualitative evaluation of both criteria. Only those items judged to be significant to the design considerations of the CRBRP containment vessel are included in the evaluation.

When one of the two criteria is identified as "more conservative" with respect to a particular item, the conservatism is meant to be relative to the other criteria for that particular item only. The evaluation is also based on loadings and geometries applicable to the CRBRP vessel design only.

Items for comparison are grouped in accordance with the following list:

- I. Classical buckling analysis for single stress component
  - A. Calculation by formulas
  - B. Analysis by shell of revolution computer programs
  - C. Analysis by three-dimensional finite-element or finite-difference computer programs
- II. Critical buckling stress for single stress component
  - A. Local buckling
    1. Unstiffened cylindrical shells and also cylinders between ring stiffeners
    2. Double curvature shells
    3. Thermal stress
    4. Membrane stress at structural discontinuity
    5. Curved panels between rings and stringers
  - B. Rings and stringers

QC5220.25-61

Amend. 72  
Oct. 1932

III. Interaction equations for local buckling

A. Cylindrical shells

1. Axial compression plus hoop compression
2. Axial or hoop compression plus shear
3. In combination with thermal

B. Double curvature shells

IV. Factors of safety

A. Stringer buckling and general instability

B. Local buckling

III. Description of Numerical Comparison

A brief description of the numerical comparison using BOSOR4 computer analyses is given in Section 7.0 following qualitative comparisons of the PSAR and N-284 criteria.

QCS220.25-62

Amend. 72  
Oct. 1982



CONTAINMENT VESSEL - BUCKLING CRITERIA COMPARISON

<u>ITEM</u>	<u>PSAR CRITERIA</u>	<u>CODE CASE N-284</u>	<u>COMMENTS</u>
i. Classical buckling analysis for single stress component			
IA. Calculation by formulas	Conservative	Methods of -1712 (Conservative)	Formulas for calculating classical buckling values under uniform loads are well established. Both criteria assume uniform distribution of the stress component in the circumferential and longitudinal (also meridional) directions. Generally the two criteria will yield similar values.  For a longitudinally varying stress component, a computer analysis for calculating the uniaxial classical buckling value is allowed in -1711.
iB. Analysis by shell of revolution computer programs	Not defined (Note: used BOSOR4 analyses as bases for thermal buckling criteria) Reference 1	Methods of -1720 (Conservative)	Paragraph -1720 permits use of shell of revolution computer analyses. Such analyses are capable of handling stress components which vary in the circumferential and/or longitudinal directions. This method provides relief from the conservatism inherent in the methods of -1712 wherein the peak value of the stress component is assumed to apply uniformly throughout the shell.

Reference 1: Response to NRC Question 220.43(a)

QCS220.25-63

Amend. /2  
Oct. 1982

CONTAINMENT VESSEL - BUCKLING CRITERIA COMPARISON

<u>ITEM</u>	<u>PSAR CRITERIA</u>	<u>CODE CASE N-284</u>	<u>COMMENTS</u>
IC. Analysis by three-dimensional finite-element or finite-difference computer programs	Not defined (Note: evaluation based on established engineering practices)	Methods of -1730 (Conservative)	Methods of -1730 permitted by N-284 are similar to methods of -1720 except the former methods allow modeling of material property variations in the circumferential direction (e.g. large penetration and reinforcements in a shell). The CRBRP containment vessel follows the ASME area replacement method for the penetration reinforcement design which assumes no reduction in buckling capacity for a properly reinforced opening based on established engineering practices.
II. Critical buckling stress for single stress component	Conservative	Conservative	The comparison between the PSAR and Code Case N-284 criteria is based on formulas given in both criteria which define the critical buckling stress for a stress component as the classical buckling value multiplied by the corresponding capacity reduction factor due to imperfection knock-down. These formulas given in both criteria are conservatively established from analyses and tests available in the literature.
IIA. Local buckling	Conservative	Conservative	N-284 defines local buckling as buckling of shell plate between stiffeners or boundaries. PSAR considers local buckling to be buckling associated with edge effects at a gross structural discontinuity.

QCS220.25-64

Amend. 72  
Oct. 1982

CONTAINMENT VESSEL - BUCKLING CRITERIA COMPARISON

<u>ITEM</u>	<u>PSAR CRITERIA</u>	<u>CODE CASE N-284</u>	<u>COMMENTS</u>
IIA1. Unstiffened cylindrical shells and also cylinders between ring stiffeners			
IIA1a. Axial compression	More conservative	Conservative	Both criteria use the same formula for calculating the classical buckling values. However, for cylinders between ring stiffeners typical of the CRBRP vessel construction, the capacity reduction factors used in the PSAR criteria are more conservative than those used in the N-284 criteria.
IIA1b. Bending	Conservative	Methods of -1720 & -1730 (Conservative)	The PSAR criterion uses higher critical buckling stresses due to bending for all longitudinal compressive stresses which can be represented by the first or higher Fourier harmonics and are not included in the axial compression. The methods of -1710 treat the peak stress as the uniform stress. However, for a cylinder between ring stiffeners typical of the CRBRP vessel construction, the critical buckling stress for bending in the PSAR criteria is comparable to the critical buckling stress for axial compression in the N-284 criteria because of the higher critical axial stress allowed in the N-284 criteria.
IIA1c. Radial pressure	Conservative	More conservative	Although formulas for circumferential compression due to radial pressure are permitted in the PSAR criteria, they are not used in the actual design. Instead, the formulas for hydrostatic pressure are used which are more conservative. For circumferential compression alone, the N-284 criteria are more conservative than the PSAR criteria.

QCS220.25-65

Amend. 72  
Oct. 1982

CONTAINMENT VESSEL - BUCKLING CRITERIA COMPARISON

<u>ITEM</u>	<u>PSAR CRITERIA</u>	<u>CODE CASE N-284</u>	<u>COMMENTS</u>
IIA1d. Hydrostatic pressure (external pressure with end pressure included)	More conservative	Conservative	For hydrostatic pressure alone, the N-284 criteria are less conservative than the PSAR criteria. The use of hydrostatic pressure case for radial pressure case in the PSAR criteria makes the PSAR criteria more conservative overall in dealing with the circumferential compression.
IIA1e. Shear/torsion	Conservative	More conservative	The increased critical buckling values for shear over torsion as permitted in the PSAR criteria are based on the recommendation of Reference 2. The critical shear stresses used in the N-284 criteria are mainly based on the torsional consideration, therefore, they are more conservative than the PSAR criteria.
IIA1f. Stiffening effect due to internal pressure	Not used	Not defined	Although the PSAR criteria include formulas to account for the stiffening effects due to internal pressurization, these formulas are not used because they could result in unconservative design. The N-284 criteria do not provide specific formula for these stiffening effects.
IIA2. Double curvature shells	Conservative	Conservative (For items defined)	PSAR criteria are based on criteria given in Welding Research Council (WRC) Bulletin No. 69. N-284 criteria do not provide sufficient guidelines to allow comparisons of all relevant items.

Reference 2: "Guide to Stability Design Criteria for Metal Structures", 3rd Edition, Structural Stability Research Council, Edited by B.G. Johnston.

QCS220.25-66

Amend. 72  
Oct. 1982

CONTAINMENT VESSEL - BUCKLING CRITERIA COMPARISON

<u>ITEM</u>	<u>PSAR CRITERIA</u>	<u>CODE CASE N-284</u>	<u>COMMENTS</u>
11A3. Thermal stress	Conservative	Conservative	Both criteria treat thermal stresses as primary buckling stresses which is conservative. The PSAR criteria use material yielding rather than imperfect shell capacity as critical buckling stress for thermal loading. This approach of using yield stress for thermal buckling is based on analyses by BOSOR4 and test data (see Reference 1 under Item 1B).
11A4. Membrane stress at structural discontinuity	Conservative	Conservative	Both criteria recognize the fact that the use of peak membrane stress at structural discontinuity as uniform buckling stress is overly conservative. Therefore, both criteria use the stress at $t/R$ (where $R$ = shell radius and $t$ = shell thickness) away from discontinuity as the basis for providing relief from the excessive conservatism.
11A5. Curved panels between rings & stringers			The following evaluations are based on a typical curved panel of the CFRP vessel which is located between the upper and lower crane girders and also between two gusset plates.
11A5a. Axial compression	Conservative	More conservative	N-284 criteria allow a lower critical buckling stress than the PSAR criteria.

QCS220.25-67

Amend. 72  
Oct. 1982

CONTAINMENT VESSEL - BUCKLING CRITERIA COMPARISON

<u>ITEM</u>	<u>PSAR CRITERIA</u>	<u>CODE CASE N-284</u>	<u>COMMENTS</u>
IIA5b. Circumferential compression due to hydrostatic pressure	More conservative	Conservative	N-284 criteria allow a higher critical buckling stress than the PSAR criteria.
IIA5c. Shear	Conservative	More conservative	N-284 criteria allow a lower critical buckling stress than the PSAR criteria.
IIB Rings & stringers	Conservative	Conservative	Both criteria use formulas which are sufficiently conservative to ensure that the shell plate or the shell-stringer combination will buckle before the shell-ring combination can buckle. In addition, N-284 criteria require 20% higher margin for the ring and/or stringer buckling than for the shell plate buckling between the stiffeners or supports.
III. Interaction equations for local buckling			
IIIA. Cylindrical shells			The following discussions on interaction equations for cylindrical shells are limited to elastic buckling only.
IIIA1. Axial compression plus hoop compression	More conservative	Conservative	The PSAR criteria use a linear relationship for the combination of axial compression (& also bending) & hoop compression. The N-284 criteria use a linear relationship between the pure hoop compression case and the hydrostatic pressure case and a square term for hoop compression for the rest of the axial and hoop combinations.

QCS220.25-68

Amend. 72  
Oct. 1982

CONTAINMENT VESSEL - BUCKLING CRITERIA COMPARISON

<u>ITEM</u>	<u>PSAR CRITERIA</u>	<u>CODE CASE N-284</u>	<u>COMMENTS</u>
IIIA2. Axial or hoop compression plus shear	Conservative	Conservative	Both criteria use a square term for the shear.
IIIA3. In combination with thermal	Conservative	Conservative	The PSAR criteria use a square term for the thermal while the N-284 criteria treat the thermal stress the same as pressure or mechanical load induced stresses. Since the predominant thermal effect is in hoop compression, the N-284 criteria basically follow the same relationship as the PSAR criteria for most cases.
IIIB. Double curvature shells	Conservative	Conservative	Both criteria use the approach of WRC 69 as the basis for defining interaction equations.
IV. Factors of safety			The factor of safety is defined as the ratio of the critical buckling stress over the allowable buckling stress.
IVA. Stringer buckling & general instability	Conservative	More conservative	The PSAR criteria consider the buckling of unstiffened or stringer stiffened shell away from the edge effects due to discontinuities (supports and ring stiffeners) as general buckling. The N-284 criteria classify the stringer and/or ring buckling as general buckling and require 20% higher margin than the safety factor for local buckling.

QC5220.25-69

Amend. 72  
Oct. 1982

CONTAINMENT VESSEL - BUCKLING CRITERIA COMPARISON

ITEM	PSAR CRITERIA	CODE CASE N-284	COMMENTS
IVB. Local buckling	Conservative	More conservative	The PSAR criteria consider any shell buckling within the edge effects due to discontinuities as local buckling while N-284 criteria consider the shell plate buckling between stringers and/or discontinuities as local buckling.

QCS220.25-70

Amend. 72  
Oct. 1982



6.0 EVALUATION OF KEY DIFFERENCES; PSAR TO 1980 ASME CODE

The following evaluation pertains to key items identified in Sections 2.0 through 5.0.  
(See table of content index)

As shown in this section, the 1980 Code criteria appear to be more conservative than the CRBRP criteria in some areas and less conservative in other areas. The intent of the 1980 Code has been implemented by the CRBRP criteria given in the PSAR. Evaluation of these differences reveals that the existing containment vessel design is adequate and provides a level of safety equivalent to that which would result from complete application of the 1980 Code and Code Case N-284.

QCS220.25-71

Amend. 72  
Oct. 1982

CONTAINMENT VESSEL - EVALUATION OF DIFFERENCES BETWEEN 1974 EDITION  
& 1980 EDITION OF ASME B&PV CODE

<u>ITEM NO. &amp; PARAGRAPH/TITLE</u>	<u>EVALUATION</u>
The following items pertain to NE-3000 as listed in 3.0.3:	
8. NE-3133 Component Under External Loading	External pressure can only occur for a short period of time late in an accident transient. Therefore, the loading combination given in the PSAR (Section 3.8) is overly conservative in that it specifies the combination of external pressure with an earthquake. The vessel as currently designed satisfies the design formulas for external pressure plus dead and live loads used in NE-3133 of the 1980 code for Level A Service Limits.
11. NE-3213.10 Local Primary Membrane Stress	The 1980 Code requires that discrete regions in the vicinity of brackets, in which the local primary membrane stresses exceed 1.1 S <sub>mc</sub> , shall not overlap. Although not required by the ASME Code, the CFRBP containment vendor has followed standard, conservative design practice which includes assuring that the local effects (e.g., primary membrane stresses greater than 1.1 S <sub>mc</sub> ) do not overlap. Therefore, the existing containment vessel design provides a level of safety equivalent to that which would result from complete application of the 1980 Code.
14. Figure NE-3222-1 (1974 Code), Figure NE-3221-2 (1980 Code)	The 1980 Code requires evaluation of secondary stresses for accidental pressure and temperature within Level A Service Limits and within Level B Service Limits when OBE is also combined. Secondary stresses occur at regions of discontinuity (including non-integral connections). Secondary stresses are small and even if not small, would not affect the overall safety margin for a single accident event with or without OBE effects.

QCS220.25-72

Amend. 72  
Oct. 1982

CONTAINMENT VESSEL - EVALUATION OF DIFFERENCES BETWEEN 1974 EDITION

& 1980 EDITION OF ASME B&PV CODE

<u>ITEM NO. &amp; PARAGRAPH/TITLE</u>	<u>EVALUATION</u>
14. (Cont'd)	The 1980 Code reclassified the operating conditions and required evaluation of primary membrane and bending stresses. Although the evaluation of this combination of stresses is not required in the 1974 Code, the normal practice of containment vendors including CB&I is to consider all of these stresses. Such consideration was made for the CRBRP vessel. Therefore, the current CRBRP containment vessel design provides a level of protection to public safety equivalent to that which would result from detail implementation of the 1980 Code.
16. NE-3221 Stress Intensity Values	The additional requirements of NE-3221.3(b)(1) and (c)(2) in the 1980 Code impose limits on the primary general or local membrane plus primary bending stress intensity when the primary general or local membrane stress exceeds 67% of the yield strength at temperature. For CRBRP, buckling considerations in general govern the design of the containment shell, and the primary general membrane stress does not exceed 67% of the yield strength at temperature. Therefore, the existing containment design provides a level of safety equivalent to that which would be expected to result from complete application of the 1980 Code.
21. NE-3222 Operating Conditions (1974 Code), Buckling Stress	In the 1974 Code, NE-3222 is used to specify requirements for operating conditions. In the 1980 Code, operating conditions have been deleted from NE-3222 and merged with accident conditions and put into service conditions. NE-3222 is now used exclusively for specifying buckling requirements for the design by analysis approach. See item 14 above for evaluation of operating conditions.

QCS220.25-73

Amend. 72  
Oct. 1982

CONTAINMENT VESSEL - EVALUATION OF DIFFERENCES BETWEEN 1974 EDITION  
& 1980 EDITION OF ASME B&PV CODE

<u>ITEM NO. &amp; PARAGRAPH/TITLE</u>	<u>EVALUATION</u>
21. (Cont'd)	Code Case N-284 is an expansion of the method of linear bifurcation analysis reduced by margins which reflect the difference between theoretical and actual load capacities (imperfection and plasticity reduction factors) as permitted by NE-3222.1(a)(2). By following the specific procedures and factors of safety given in the Code Case, a cylinder under external pressure load will result in similar allowables whether it is designed to the N-284 rules or the NE-3133 rules. For evaluation of differences between N-284 and the PSAR buckling criteria in addition to the NE-3133 rules, see Section 7.0.
22. NE-3226 Testing Limits (1980 Code)	Stress limits for testing conditions are modified somewhat in the 1980 Code. This Code requirement provides protection to the plant and on-site personnel during the containment test and assures that test performance will not effect the containment vessel design function. The CRBRP containment vessel design is controlled by considerations other than the internal pressure imposed during containment test. The stresses to which the containment is subjected during testing are well within the existing allowables. Therefore, current design of the containment vessel provides a level of protection to public safety equivalent to that which would result from detail implementation of the 1980 Code.

OCS220.25-74

Amend. 72  
Oct. 1982

CONTAINMENT VESSEL - EVALUATION OF DIFFERENCES BETWEEN 1974 EDITION  
& 1980 EDITION OF ASME B&PV CODE

<u>ITEM NO. &amp; PARAGRAPH/TITLE</u>	<u>EVALUATION</u>
24. NE-3227.5 Nozzle Piping Transition	In the 1980 Code, substantial changes are made to the stress classifications in the nozzle piping transition either within the limits of reinforcement or beyond the limits of reinforcements. Although a quantitative assessment of the effects of these changes would require additional detailed calculations, a qualitative assessment is provided as follows. Consistent with normal containment design practices, extremely conservative "enveloping" loads were specified for similar groups of penetrations. The vessel including the nozzle piping transitions were designed to accommodate these conservatively specified loads using simplified but conservative design approaches. This results in substantial design margin for a large fraction of the penetrations. For those penetrations in which design margin is not obvious, it is judged that the use of detailed analysis approaches would demonstrate that the current design has a capability that approaches, if not meets, the specified limits for the load combinations identified in the 1980 Code. Thus, the current design is judged to provide a level of safety equivalent to that which would result from full implementation of the 1980 Code.
27. NE-3232 Operating Conditions (1974 Code), Combined Loads (1980 Code)	In addition to requiring secondary stress evaluation for accident conditions, there are also changes to the stress limits for bolts in the 1980 Code. The only bolts covered by this provision of the 1980 Code would be the bolts that secure the refueling hatch cover in place on the containment shell. The only significant operating load is the deadload from the mass of the hatch cover itself. The only significant mechanical load is that resulting from an earthquake. The calculated stresses for the bolts under these conditions are well within the specified allowables (1974

QCS220.25-75

Amend. 72  
Oct. 1982

CONTAINMENT VESSEL - EVALUATION OF DIFFERENCES BETWEEN 1974 EDITION

& 1980 EDITION OF ASME B&PV CODE

<u>ITEM NO. &amp; PARAGRAPH/TITLE</u>	<u>EVALUATION</u>
27. (Cont'd)	Code version) for these loads and it is believed that the bolts would readily meet the requirements of the 1980 Code. Therefore, the current design provides the same level of safety as would result from implementation of the 1980 Code.
34. NE-3324.11 Nozzle Necks (1974 Code), NE-3324.12 Nozzles (1980 Code)	<p>The requirement of NE 3300 would not be mandatory for the CRBRP vessel. These requirements are applicable only when the internal pressure loading represents 90% or more of the total loading.</p> <p>The additional requirement in the 1980 Code, limiting the allowable shear stress to 70% of the allowable tensile stress in the nozzle neck, would require review of design calculations. Normal containment vendor practice limits shear stresses to less than 50 percent of the allowable tensile stress in the nozzle neck. Therefore, it is judged that the current design provides a level of protection to public health and safety equivalent to that which would result from implementation of the 1980 Code.</p>
37. NE-3331 General Requirements for Openings	<p>The requirement of NE 3300 would not be mandatory for the CRBRP vessel. These requirements are applicable only when the internal pressure loading represents 90% or more of the total loading.</p> <p>The changes in the 1980 Code regarding the opening and reinforcement would require review of design calculations. However, there are no areas for the CRBRP where the controlling load combinations include significant contribution from internal pressure. Therefore, this 1980 Code provision would not be applicable to CRBRP.</p>

QCS220.25-76

Amend. 72  
Oct. 1982

CONTAINMENT VESSEL - EVALUATION OF DIFFERENCES BETWEEN 1974 EDITION  
& 1980 EDITION OF ASME B&PV CODE

<u>ITEM NO. &amp; PARAGRAPH/TITLE</u>	<u>EVALUATION</u>
39. NE-3334.1 Limit of Reinforcement along the vessel wall	See evaluation of Item 37 above.
40. NE-3336 Strength of Reinforcing Material	See evaluation of Item 37 above.
41. NE-3367 Closures on small Penetrations	Dimensional standards are updated in the 1980 Code. This optional provision applies only to penetrations of 2" diameter or less. The smallest penetration in the CRBRP containment vessel is 4" in diameter. Therefore, this provision is not applicable to CRBRP.
42. NE-3720 Design Rules	The largest, and therefore the most critical, mechanical penetrations are designed for 30 psi. The electrical penetrations have been designed with even greater margin and are tested at 50 psi. Therefore, pressure capability is significantly greater than the 10 psi CRBRP design pressure and tens of times greater than the actual accident pressure of less than 2 psi. Therefore the existing design provides a level of safety equivalent to that which would result from complete application of the 1980 code.

QCS220.25-77

Amend. 72  
Oct. 1982

CONTAINMENT VESSEL - EVALUATING OF DIFFERENCES BETWEEN 1974 EDITION  
& 1980 EDITION OF ASME B&PV CODE

<u>ITEM NO. &amp; PARAGRAPH/TITLE</u>	<u>EVALUATION</u>
<p>The following item pertains to NE-7000 as listed in 3.0.7:</p> <ol style="list-style-type: none"><li>1. NE-7000 Protection against Over-Pressure (1974 Code), Overpressure Protection (1980 Code)</li></ol> <p>The following item pertains to CC-3000 as listed in 4.0.2:</p> <ol style="list-style-type: none"><li>1. CC-3000 Design</li></ol>	<p>Purchase of standard appurtenances only may be impacted. There is no effect on the containment vessel design.</p> <p>The changes in the 1980 Code impose modified requirements with respect to stress and strain in reinforced concrete design and also to rebar details. The modified requirements do not represent a significant departure from the design approach in the 1974 edition of the Code. Although the changes generally result in the 1980 Code being more conservative than the 1974 Code, the changes are relatively minor. It is believed that if there were areas of the existing CRBRP containment which have not already been demonstrated to accommodate specified loads within the revised criteria, the use of more refined analysis techniques would be expected to demonstrate that the existing design represents the capability which approaches that dictated by the 1980 Code. Therefore, it is judged that the current CRBRP design embodies a level of safety equivalent to that which would result from detailed implementation of the 1980 Code.</p>

QCS220.25-78

Amend. 72  
Oct. 1982



7.0 EVALUATION OF KEY DIFFERENCE; PSAR TO CODE CASE N-284

Code Case N-284 criteria appear to be more conservative than the PSAR criteria in some areas and less conservative in other areas. The Applicant has done an analysis of the critical region using N-284 criteria and appropriate loads. This analysis results in a design margin in excess of that required by N-284.

QCS220.25-79

Amend. 72  
Oct. 1982

CONTAINMENT VESSEL - EVALUATION  
OF DIFFERENCES BETWEEN PSAR  
& CODE CASE N-284

<u>ITEM</u>	<u>EVALUATION</u>
<p>The following item pertains to Code Case N-284</p> <p>As Listed in 5.0:</p> <ol style="list-style-type: none"><li>1. PSAR Buckling Criteria (Expanded from 1974 Code), Code Case N-284 (Published in 1980).</li></ol>	<p>Changing the buckling criteria from the PSAR criteria to the N-284 criteria would require reanalysis of the shell for buckling evaluation.</p> <p>The most critical region (just above the operating deck) has been analyzed using BOSOR4 computer program and selected critical loading combinations in order to verify the design adequacy of the CRBRP containment vessel against the N-284 buckling criteria. Since the BOSOR4 analyses do not include shear stresses, the effects of shear stresses are manually adjusted using the procedures of N-284 criteria. The results of these analyses show that the design margins of the vessel exceed the requirements of N-284.</p> <p>This analysis was performed using the PSAR load combinations for SSE and OBE, setting <math>P_e = 0</math> (External pressure is not postulated to exist during a seismic event, see Section 6, Item 8) and was evaluated against the ASME Level B and C service limits. The BOSOR4 model is as shown in Figure 7.0-1. In the analysis for each load combination, pre-buckling stresses are determined from actual hoop and axial stress distributions amplified by their corresponding imperfection knockdown factors. The results of this analysis yield an eigenvalue corresponding to the buckling of the critical region just above the operating deck.) The lowest buckling mode is shown in figure 7.0-2.</p>

(continued on next page)

QCS220.25-80

Amend. 72  
Oct. 1982

CONTAINMENT VESSEL - EVALUATION

OF DIFFERENCES BETWEEN PSAR

& CODE CASE N-284

ITEM

The following item pertains to Code Case N-284

EVALUATION

As Listed In 5.0:

1. PSAR Buckling Criteria (Expanded from 1974 Code), Code Case N-284 (Published In 1980). (Continued)

Since BOSOR4 analysis does not include shear, the results are adjusted to determine factors of safety including shear stresses. The adjustment is performed in accordance with the following formula:

$$\frac{FS}{\lambda} + \left( \frac{FS \cdot \sigma_{\phi\theta}}{\alpha_{\phi\theta} \cdot \sigma_{\phi\theta eL}} \right)^2 \leq 1$$

WHERE  $\lambda$  = EIGEN VALUE FROM BOSOR4 ANALYSIS

- $\sigma_{\phi\theta}$  = SHEAR STRESS
- $\alpha_{\phi\theta}$  = KNOCKDOWN FACTOR FOR SHEAR (=0.712, EL. 816' TO EL. 839')
- $\sigma_{\phi\theta eL}$  = CLASSICAL BUCKLING VALUE UNDER SHEAR LOAD BASED ON N-284 FORMULA
- FS = FACTOR OF SAFETY

RESULTING FACTOR OF SAFETY

LOAD COMBINATION	PSAR	N-284
D + L + T <sup>1</sup> + P <sub>e</sub> + SSE	1.9	1.67
D + L + T <sup>1</sup> + P <sub>e</sub> + OBE	2.5	2.0

QC5220.25-81

Amend. 72  
Oct. 1982

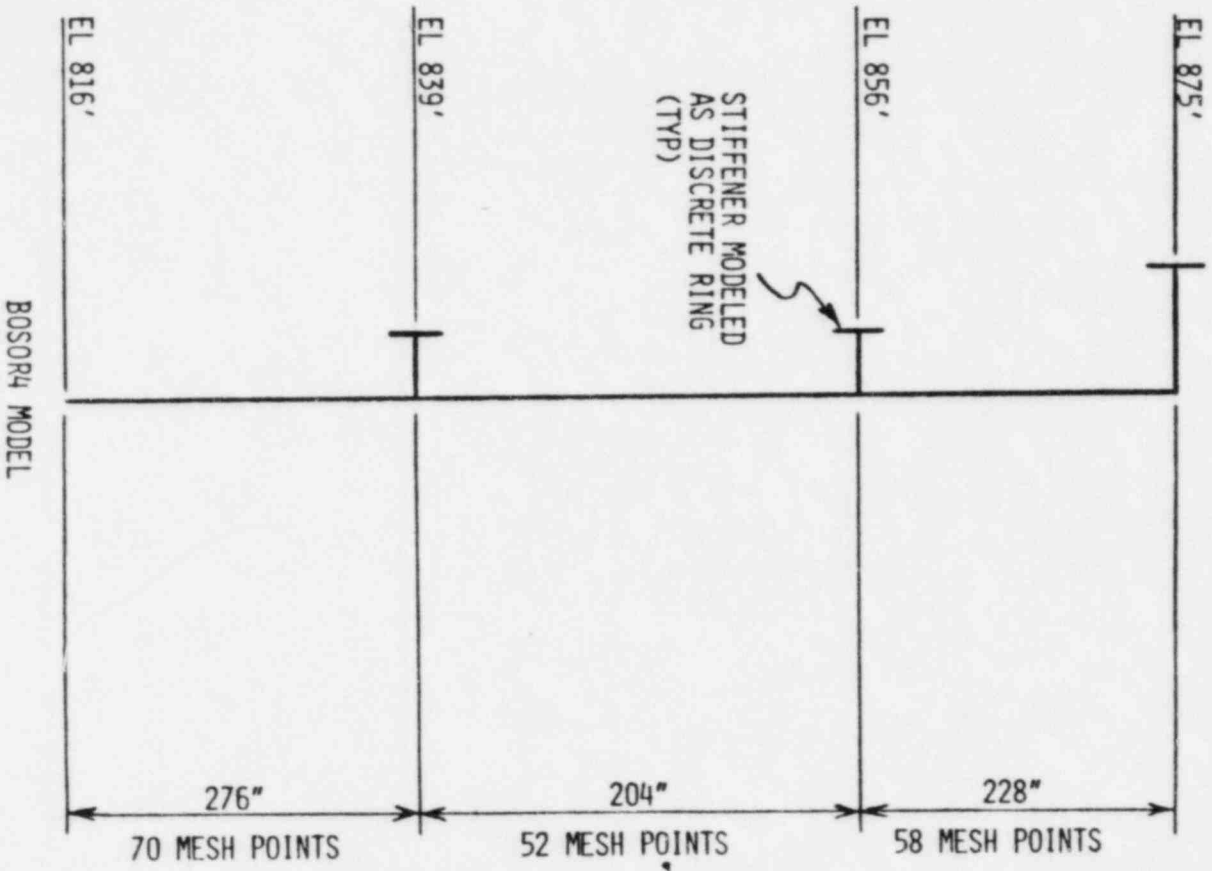
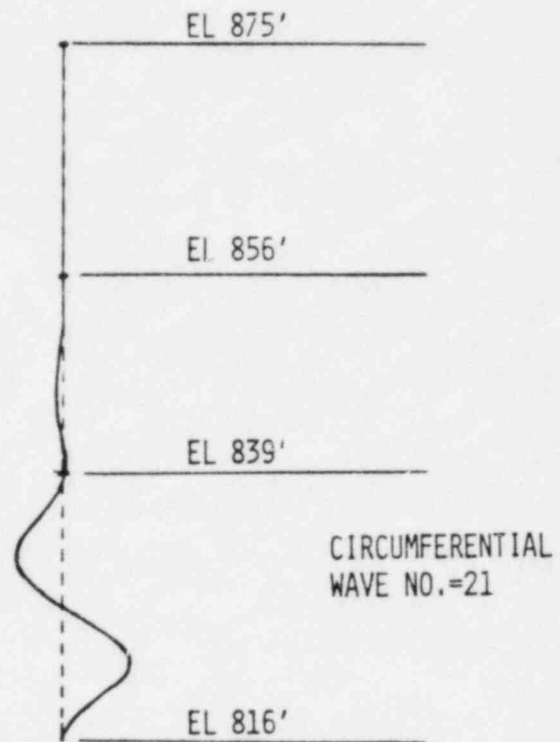


FIGURE 7.0-1

QCS220.25-82

Amend. 72  
Oct. 1982



BOSOR4 BUCKLE MODE  
 RADIAL DISPLACEMENT FOR  
 DL + LL + SSE + THERMAL +  $P_E$

FIGURE 7.0-2

Question CS421.9

Identify where instrument sensors or transmitters supplying information to more than one protection channel, to both a protection channel and control channel, or to more than one control channel, are located in a common instrument line or connected to a common instrument tap. The intent of this item is to verify that a single failure in a common instrument line or tap (such as break or blockage) cannot defeat required protection system redundancy.

Response:

Redundant protection channels, protection channels and control channels, or more than one control channel instrumentation sensors or transmitters are not located in common instrument lines or taps. Therefore, the required protection system redundancy will not be defeated by a blockage or breakage of an instrument line or tap.

Question CS421.17

The information supplied for remote shutdown (PSAR Section 7.4.3) from outside the control room is insufficient. Therefore, provide further discussion to describe the capability of achieving hot or cold shutdown from outside the control room. As a minimum, provide the following information:

- a) A table listing the controls and display instrumentation required for hot and cold shutdown from outside the control room. Identify the train assignments for the safety-related equipment.
- b) Design basis for selection of instrumentation and control equipment on the hot shutdown panel.
- c) Location of transfer switches and the remote control station.
- d) Description of transfer switches and the remote control station.
- e) Description of isolation, separation and transfer/override provisions. This should include the design basis for preventing electrical interaction between the control room and remote shutdown equipment.
- f) Description of control room annunciation of remote control or overridden status of devices under local control.
- g) Description of compliance with the staff's Remote Shutdown Panel position.

Response:

The response to this question is provided in the amended text for Section 7.4.4.

Question CS421.22

The information supplied in PSAR Section 7.5 concentrates on the information and monitoring systems but does not provide sufficient information to describe safety-related display instrumentation needed for all operating conditions. Therefore, please expand the PSAR to provide as a minimum additional information on the following:

1. ESF Systems Monitoring
2. ESF Support System Monitoring
3. Reactor Protective System Monitoring
4. Rod Position Indication System
5. Plant Process Display Instrumentation
6. Control Boards and Annunciators
7. Bypass and Inoperable Status Indication
8. Control Room Habitability Instrumentation
9. Residual Heat Removal Instrumentation

Response:

This response describes safety-related display information available to the operator in the control room.

Display instrumentation provided for ESFs is described below. Section 7.3 will be revised to include this information. The instrumentation for monitoring ESF support systems are described in the indicated sections of the PSAR: HVAC-7.6.4; Plant Service and Chilled Water Systems-7.6.1; Diesel Generator-8.3.3; Electric Power Systems-8.3.1.1.2, 8.3.1.1.5 and 8.3.2.1.1. The Reactor Protective Monitoring System is described in Section 7.2. Additional information about the display instrumentation has been inserted into Section 7.2 with this response. A description of the display instrumentation provided in the control room for operators for Rod Position Indication is provided in PSAR Section 7.7.1.3.2. Control Boards and Annunciators are detailed in Section 7.9. The Inoperable Status Monitoring System (including bypass monitoring) is discussed in PSAR Section 7.5.12. Section 7.4.1 discusses instrumentation and controls for the SGAHRS which is a part of the overall Shutdown Heat Removal system.

Safety-Related Display Information for ESF Systems

Reactor Containment Building Annulus Filtration System

Monitoring, including indications and alarms, is provided in the control room for the following parameters for each of the redundant trains:

- a. Annulus filter fan discharge flow;
- b. Annulus pressure maintenance fan discharge radiation;
- c. Annulus filter unit inlet radiation;
- d. Annulus filter unit relative humidity;
- e. Annulus differential pressure (3 monitors for each train);  
(alarm only);
- f. Annulus discharge to atmosphere, radiation (2 monitors for each train);
- g. Fan vibration (alarm only);
- h. Filter unit leaving air temperature (alarm only);



- i. Individual component differential pressure (alarm only);
- j. Filter unit differential pressure (alarm only).

Status of the following equipment is provided in the control room for each of the redundant trains:

- Annulus Filter Fan
- Annulus Pressure Maintenance Fan
- Annulus Filter Fan Discharge Damper
- Annulus Pressure Maintenance Fan Discharge Damper
- Annulus Filter Unit Recirc. Air Damper

#### RSB Filtration System

Monitoring including indications and alarms is provided in the control room for the following parameters for each of the redundant trains:

- a. RSB cleanup filter fan discharge flow and radiation;
- b. RSB cleanup filter train leaving air temperature (2 monitors in each train);
- c. RSB cleanup filter unit inlet flow;
- d. Fan vibration (alarm only);
- e. Individual component differential pressure (alarm only);
- f. Filter unit differential pressure (alarm only).

Also non-safety-related indications and alarms are provided in the control room for radiation detection in the roof air exhaust discharge.

Status of the following equipment is provided in the control room for each of the redundant trains:

- RSB Cleanup Filter Fan
- RSB Cleanup Filter Fan Discharge Damper
- RSB Cleanup Filter Recirc. Air Supply Damper
- RSB Cleanup Filter Recirc. Discharge Damper
- RSB Cleanup Filter Normal Exhaust Damper

#### Control Room Habitability System

Monitoring including indications and alarms is provided in the control room for the following parameters for each of the redundant trains:

- a. Main air intake radiation (control room outside air);
- b. Remote air intake radiation (control room outside air);
- c. Mixed air temperature (2 monitors in each train);
- d. Control room A/C unit supply air flow;
- e. Control room A/C unit discharge air temperature (2 monitors in each train);
- f. Toxic gas in main air intake (alarm only);
- g. Toxic gas in remote air intake (alarm only);
- h. Smoke in main air intake (alarm only);
- i. Smoke in remote air intake (alarm only);
- j. Filter unit air flow;
- k. Fan vibration (alarm only);

- l. Filter unit leaving air temperature (alarm only);
- m. Individual filter unit components differential pressure (alarm only);
- n. Filter unit differential pressure (alarm only).

Status of the following equipment is provided in the control room for each of the redundant trains:

- a. Control Room A/C Unit
- b. Control Room A/C Unit Discharge Damper
- c. Control Room A/C Unit Inlet Damper
- d. Control Room A/C Unit Supply Air Damper (two for each train)
- e. Control Room Filter Unit Supply Fan
- f. Control Room Filter Unit
- g. Control Room Filter Inlet Damper
- h. Control Room Filter Unit Supply Fan Discharge Damper

#### Guard Vessels, Cell Liners and Catch Pans

No instrumentation is required as none is provided for ESF guard vessels (for the reactor and the primary heat transport system), cell liners and catch pans.

#### Steam Generator Building Aerosol Release Mitigation System Instrumentation and Controls

The Steam Generator Building (SGB) Aerosol Release Mitigation System is designed to control the release of sodium aerosols from the Steam Generator Building in the event of a design basis leak in one of the three IHTS loops. The functional design of this system is discussed in Section 6.2.7. The following instrumentation is provided in the main control room for the SGB Aerosol Release Mitigation System.

#### Main Control Room Instrumentation for the Steam Generator Building Aerosol Release Mitigation System

- a. Aerosol Detector Alarm Indication
- b. SGB Loop #1, #2 and #3 Dampers Position Status Indication
- c. RCB Supply And Exhaust Fans Common Alarm
- d. RSB Dampers and CB Isolation Valves Position Status Indication
- e. CB Dampers and CB Isolation Valves Position Status Indication
- f. SGB-IB Damper Position Status Indication
- g. RSB-RWA Supply and Exhaust Fans and the Exhaust Filter Fan Common Alarm
- h. ABHX Intake and Exhaust Dampers Position Status Indication
- i. SGB-MB Outside Air Damper Common Alarm
- j. DGB Intake Tornado Damper and Outside Air Damper Position Status Indication

Question CS421.27

In the PSAR Section 7.3, the statement is made that the initiation of containment isolation is the only Engineered Safety Feature (ESF) identified which requires a description in this Section. Chapter 6 of the PSAR denotes several systems (Annulus Filtration System, Reactor Service Building Filtration System, and the Residual Heat Removal System including SGAHRS and OHRS) in addition to the Containment Isolation System as being part of the ESF System. Justify why these systems aren't included in Section 7.3 of the PSAR. Also, the staff believes that the Sodium-Water Reactor Pressure Relief System (SWRPS) should be classified as part of the ESF System. Describe the actions to be automatically initiated or to be initiated by operators to mitigate sodium-water reactions. The discussions should include actions necessary to protect public safety or avoid an unanalyzed plant upset.

Response:

Section 7.3 as modified by Amendment 71 provides a cross-reference to PSAR Section 6.1 which identifies Engineered Safety Features (ESFs) and the sections of the PSAR where they are discussed. Additional information is provided in the response to NRC Question CS421.22.

The Sodium/Water Reactor Pressure Relief System's (SWRPRS) safety function is accomplished by the mechanical actuation of the rupture discs by pressure generated from a sodium/water reaction occurring in a steam generator module (ref. PSAR Sections 5.5.2.4 and 5.5.2.6).

Subsequently, the SWRPRS instrumentation and control has two functions. These two electrical functions have different safety consequences, and therefore, one is classified as safety-related, and the other as non-safety-related.

- 1) Safety-related instrument and control function: Actuation of the SWRPRS is detected immediately downstream of the rupture discs (ref. PSAR Section 5.5.2.4). A safety-related (Class 1E) signal resulting from the sensors, is transmitted to the PPS (ref. PSAR Section 7.2.1.2.2). This initiates a reactor trip and is part of the Plant Protection System. As stated in Section 7.5.6.2 this complies with requirements stated in Section 7.1.2 and 7.2.2.
- 2) Non-safety-related instrument and control functions: A buffered signal initiates actions as described in Section 7.5.6.1.2. Since these actions only isolate the loop affected, the ability of any other loop to remove decay heat from the reactor is not compromised. Therefore, these functions are not considered safety-related.

For automatic and operator actions in case of sodium/water reactions, see Sections 5.5.2.8, 7.5.5.3, and 7.5.6.

Question CS421.30

To extend our review, the staff (ICSB & EC&G) each require a set of one line I&C Drawings for the safety related CRBR systems. Drawings should also be provided that indicate the separation used in the CRBR design.

Response:

The NRC Staff in a telecon with the Project on 9/13/82, confirmed that the requested information is currently in their possession.

Question 421.31

Address the adequacy of the Reactor Vessel Level gauges with emphasis on the lack of diversity, the level range chosen, the method selected, and the effects of temperature on the level accuracy. Provide this same discussion for the level probes in the sodium expansion tank, the sodium dump tank, and the sodium pump tank. Also, discuss provisions made for sodium level measurements in the intermediate system.

Response:

Mutual inductance type sodium level probes are used for all continuous sodium level measurements in the reactor vessel, sodium expansion tank, sodium dump tank and the sodium pump tank. This type of level probe has been shown to be superior to other types of level probes during sodium testing of various types of level probes. Other types of level probes which were evaluated in this test program include balanced bridge type inductive level probes, displacer-float type level transducers, delta P type level transducers and time domain reflectometry transducers. The advantage of using highly reliable mutual inductance type probes outweighs any advantage that could be obtained from type diversity.

The mutual inductance level probe has a primary and secondary inductance coil. Excitation is applied to the primary coil which develops a signal in the secondary coil. The signal magnitude in the secondary coil is dependent upon the height of the sodium.

To compensate for sodium temperature changes a temperature compensation circuit is integral with the signal condition equipment and works on the concept of resistance changing with temperature. The compensation circuit measures the voltage and current in the primary coil and evaluates changes to determine the resistance change and automatically adjusts the output of the signal conditioner based on the resistance change.

The reactor vessel contains four narrow range probes, three of which are used by the Primary Reactor Shutdown System, and two wide range probes which are designated to the part of the Accident Monitoring (AM) System. The measurement range chosen for the narrow range probes (30 inches) is based on a range which is wide enough to cover the normal operating ranges of the sodium level in the reactor vessel but is narrow enough that the uncertainty associated with the measurement is minimized.

The measurement range chosen for the wide range probes (189 inches) is based on the ability to monitor the sodium level down to the level of the reactor vessel outlet nozzles.

Each Primary pump contains two redundant wide range probes (80.5 inches) to monitor sodium level over the full elevation of the pump tank.

Sodium level measurement is accomplished in the intermediate system via the sodium pump and expansion tank, the intermediate sodium pumps have a single wide range probe (86.9 inches) installed in the pump tank which monitors the full range of the sodium level in the pump tank. Two level probes are installed in the sodium expansion tank, a wide range probe to measure the full range of anticipated steady state and transient sodium levels in the tank and a narrow range probe for accuracy during fill of the system. The wide range level probe in the expansion tank also provides a signal for a high and low level alarm. The pump tank level probe provides a signal for a high and low level alarm, and isolation of IHTS argon cover gas system.

Two wide range level probes are installed in each sodium dump tank. These probes are arranged with overlap to provide for monitoring sodium levels during sodium fill and drain operations of the Intermediate Heat Transport System.

Question CS421.34

PSAR Section 7.5.2.1.2 states in part that a signal is provided to the control room indicating that the pony motor is running. The staff requires more information with regard to the CRBR pony motor instrumentation and control system. In particular, the initiation signals for the pony motors, manual initiation capability, qualifications for the system, and the design criteria for the system should be discussed. PSAR Section 7.5.6.1.1 states in part that the sodium pony motor is tripped upon a large leak detection. Discuss the safety aspects of this trip and provide the staff information on other signals that will trip the pony motors.

Response:

The pony motor runs continuously during all modes of plant operation except during sodium pump or drive system maintenance. Therefore, there is no need for automatic or manual initiation signals except for the start-stop switch.

Normal pony motor start is through a permissive sequence circuit which starts the external lubricating oil cooling system and high pressure lube oil pump, and when the oil system achieved flow and pressure the pony motor starts. Once started the loss of flow or pressure will not result in a pony motor trip. This method of starting is not classified as safety-related.

In the safety-related mode, pony motor operation does not require the use of the external lubricating oil cooling system or high pressure lube oil pump. This function is carried out by a start-stop switch on the main control panel in the control room.

The non-safety permissive sequence starting circuit is isolated from the safety circuit and will not prevent the operation of the safety function. The safety circuit will be qualified per WARD-D-0165 (Ref. 13 of PSAR Section 1.6).

There is available in the control room, pony motor speed and current indications. Pony motor current indication is provided via the PDH&DS. These circuits are non-safety related.

The only condition which results in an automatic IHTS pony motor trip (the PHTS pony motor is not tripped) is a large sodium/water reaction which results in a rupture disc rupturing. The safety aspects of this trip are specifically addressed in the response to Question CS421.27.

Question CS421.36

Provide a more detailed discussion of the CRBR Leak Detection system and how it meets the provisions contained in the Light Water Reactor Regulatory Guide 1.45. The discussion should include detection methods, detector sensitivity, detector response time, signal correlations and calibration, seismic qualification, testability, and the provisions for technical specifications.

Response:

PSAR Section 7.5.5.1.1 has been revised to provide a more detailed discussion of the CRBRP Leak Detection Instrumentation System. A comparison to the provisions of Regulatory Guide 1.45 is contained in Section 5.3 of WARD-D-185, "Integrity of the Primary and Intermediate Heat Transport System Piping In Containment", (Reference 2 of PSAR, Section 1.6).

Technical Specifications will be developed at the FSAR stage. The Technical Specification will require that the plant will be placed in either the hot shutdown or refueling condition if there is a confirmed leak in either the primary or intermediate heat transport system.



Question CS421.37

Discuss the provisions made for alarming a zero or negative differential pressure (PSAR Section 7.5.5.2.1) as to sensor type, location, setpoints, testability, and annunciation.

Response

The intermediate loop pressure to primary loop pressure is maintained at pressures greater than 10 psi. When the pressure on the intermediate loop drops to within 10 psi of the primary loop, the operator is alerted by an alarm. The alarm is on a positive pressure differential and not zero or negative pressure differential.

Each instrument channel includes provisions for insertion of a test signal on the sensor side of the signal conditioning electronics.

The sensor type, locations, setpoints and annunciation are described in PSAR Section 7.5.2.1.1. PSAR Pages 7.5-7, 7.5-8, 7.5-27 have been modified for clarification.

Question 421.42

Section 7.1.2 and 7.2.2 of Chapter 7 of the PSAR reference the use of IEEE standards. Other sections in Chapter 7 make reference to Section 7.1.2 but do not identify specific IEEE standards which were implemented in the system design. Justify why Section 7.3 through 7.7 of the PSAR do not provide enough information to determine whether the IEEE standards are implemented in the design.

Response:

Chapter 7 has been revised to add specific identification of IEEE standards when appropriate as described below. Compliance with IEEE standards for non-safety related systems is not required and therefore use of IEEE standards for those systems is not discussed.

Section 7.2 - This section is amended to clarify the use of IEEE standards.

Section 7.3 - This section is amended to clarify the use of IEEE standards.

Section 7.4 - This section is amended to clarify the use of IEEE standards.

Section 7.5.1 - The Wide Range and Power Range Flux Monitors discussed in this section are safety related, the IEEE standards of Table 7.1-3 are applied to the designs.

Section 7.5.2 - Addresses the types of functions and the sensors used in the plant and does not specifically identify these instruments as safety related or not. Table 7.5-1 identifies the variables which are safety related as does Section 7.2. Paragraph 7.5.2.2 states that the instruments which are a part of the Protection system comply with the requirements of Section 7.1.2 and 7.2.2 which encompasses the IEEE standards listed in Table 7.1-3.

Section 7.5.3 - The sodium level probes discussed in this section are 1E. The remaining instrumentation is non-1E. Section 7.5.3.2 states that the sodium level probes are part of the Reactor Shutdown system and will comply with PPS Design Requirements (Sections 7.1.2 and 7.2.2). The probes, therefore, will comply with IEEE standards identified in these sections as applicable to PPS.

Section 7.5.4 - The Failed Fuel System is not safety related.

Section 7.5.5 - The leak detection systems discussed in this section are not safety related.

Section 7.5.6 - SWRPRS instrumentation and control has two functions. One is to initiate a reactor trip, the other is to isolate the affected loop. The reactor trip function is part of the Plant Protection system and as stated in 7.5.6.2 complies with Sections 7.1.2 and 7.2.2. Isolation of the affected loop is not safety related since it does not compromise the ability to remove decay heat from the unaffected loops.

Sections 7.5.7,  
7.5.8 and  
7.5.9

- The instruments discussed in these sections are safety related, the IEEE standards of Table 7.1-3 are applied to the designs.

Sections 7.6.1,  
7.6.2, 7.6.4 and  
7.6.6

- These Sections have been revised to incorporate applicable IEEE Standards.

Section 7.6.5 - The SGB Flooding Protection System is safety related and section 7.6.5 is amended to clarify the use of IEEE standards.

Sections 7.7  
and 7.8

- No IEEE standards are applied in these sections since the systems described therein are non safety related systems.

Section 7.9 - This section has been amended to clarify the use of IEEE standards.

Question CS421.47

Discuss the design bases for the ventilation systems used for engineered safety feature areas including areas containing systems required for safe shutdown. The discussion should cover redundancy, testability, etc.

Response:

The design bases for the ventilation systems used for engineered safety feature areas are discussed in the PSAR and located in the following sections:

- (1) Sections 6.3.1 and 9.6.1.1 for the Control Building Control Room Habitability System.
- (2) Sections 6.2.5 and 9.6.2.1 for the Reactor Containment Building Annulus Filtration System.
- (3) Sections 6.2.6 and 9.6.3.1 for the Reactor Service Building Filtration System.
- (4) Section 6.2.7 for the Steam Generator Building Aerosol Release Mitigation System.
- (5) Section 9.6.5 for the Diesel Generator Building.

Question CS421.48

Using system schematics, describe the sequence for periodic testing of the:

- a) outlet steam isolation valves
- b) main feedwater control valves
- c) main feedwater isolation valves
- d) auxiliary feedwater system
- e) pressure relief valves at superheater

The discussion should include features used to insure the availability of the safety function during test and measures taken to insure that equipment cannot be left in a bypassed condition after test completion.

Response:

Periodic testing of these components/system will be accomplished as follows:

- a) Outlet Steam Isolation Valves

The test mode of the steam and feedwater isolation gate valves, which are opened hydraulically and closed pneumatically, is as follows:

- o A test mode switch must be activated and held in this position by the operator. This action simultaneously overrides the pressure switch normally maintaining full hydraulic pressure to hold the valve open and de-energize the pneumatic and hydraulic pilot valves, causing the valve to being to close pneumatically.
- o The valve closes until the 10%-closed limit switch is activated. This activation energizes the hydraulic pilot valves which blocks hydraulic flow in the valve actuator and stops the valve stroke.
- o After the operator verifies the valve has stroked to approximately 10% closed, he releases the test mode switch. Upon release of this switch the pressure switch controlling hydraulic pressure in the activator is re-energized and functions to cycle the valve open hydraulically.
- o The operator verifies the valve has returned to full open position, thus completing the verification of valve operability.

The limiting of the valve stroke to approximately 10% closed will permit normal plant operation during valve testing. All safety functions will remain operable, since trip signals will override the valve test mode switch.

b) Main feedwater control valves.

These valves operate at a mid-stroke position which depends on power level and will move whenever power level is changed or whenever there is a system disturbance. Therefore, no additional testing is required to demonstrate valve operability.

c) Main feedwater isolation valves.

These valves will be tested in the same manner as the outlet steam isolation valves.

d) Auxiliary feedwater system.

The following describes the method of periodically testing the SGAHRS system.

This test will be performed once every three months to demonstrate the operability of the SGAHRS Auxiliary Feedwater Subsystem. It will be performed during normal plant operation and under conditions that are as close to design as practical and provides for initiation of the complete sequence that brings the AFW Subsystem into operation for a reactor shutdown following a postulated accident. To ensure the availability of the safety function during the test, the logic design provides for the Plant Protection system initiation signal override of the SGAHRS AFW test switch signal.

The initial conditions for the startup of the SGAHRS for the quarterly test require the plant to be operating at or above 40% power with the SGAHRS filled, the Plant Protection System in operation and SGAHRS Initiation logic in the reset mode. The SGAHRS instrumentation is operable, the controls are in the automatic mode of operation and the valves are in their normal SGAHRS standby position as shown in PSAR Figure 5.1-5a. The protected air cooled condensers (PACC) are on standby with the fans off and louvers closed. All manual interface valves with the Steam Generator System (SGS) are open.

The periodic test procedure is as follows:

- (1) Initiate the Plant Data Handling and Display System (PDH&DS) Procedure for Test Trip Review for recording the following variables:
  - a. PWST level and temperature
  - b. AFW pump inlet and discharge pressure
  - c. AFW pump discharge temperature
  - d. AFW flow
  - e. AFW recirculation flow
  - f. AFW recirculation valve position
  - g. AFW control valve position
  - h. AFW isolation valve position
  - i. AFW turbine isolation valve position
  - j. AFW turbine pressure control valve position

- k. Drive turbine steam inlet pressure
  - l. Drive turbine exhaust pressure
  - m. Drive turbine speed
  - n. Drive motor speed
  - o. Steam drum pressure
  - p. Steam drum level
- (2) Manually start the system for this test with the SGAHRS AFW switch. System startup is entirely automatic upon receipt of the initiation signal. The following automatic actions constitute startup of the SGAHRS in the system test mode and occur as a result of manual operator initiation:
- a. Drive turbine steam supply valves (52AFW118A, B, C) open and steam is supplied to the AFW pump drive turbine (52AFN001) which in turn drives the full-size AFW pump (52AFP001). The drive turbine pressure control valve (52AFV121) opens to modulate steam pressure at 1000 psig at the drive turbine inlet.
  - b. AFW pump drive motors (52AFK001A, B) start and drive the half-size AFW pumps (52AFP002A, B).
  - c. AFW isolation valves (52AFV103A to F) open.
  - d. AFW isolation valves (52AFC104A to F) begin control of AFW flow. In the SGAHRS test mode these valves will close because the steam drum level is being maintained at the normal water level (NWL) by the feedwater system. Since the setpoints for the motor-driven pumps are at 4 in. below NWL, and 18 in. below NWL for the turbine driven pump, no flow from the SGAHRS will be injected into the steam drums.
  - e. AFW pump recirculation valves (52AFV108A, B, C) begin their recirculation flow function. In the SGAHRS test mode these valves will remain open because no flow is being supplied to the steam drums.

The following automatic functions, which normally occur with a SGAHRS initiation, are suppressed during the system test in order to prevent unwanted loss of steam generator system inventory and tripping of the turbine:

- o Opening of the superheater vent control valves (52AV116A, B, C)
- o Open of the steam drum vent control valves (52AFV117A, B, C)
- o Closure of the superheater outlet isolation valves (53SGV012)
- o Closure of the steam drum drain valves (53SGV014 and 015)
- o Opening of the PACC Noncondensable Vent valves (52ACV1-9A to F)
- o Startup of the PACCs

- (3) Observe and confirm the operation of the Auxiliary Feedwater Subsystem after the test initiation. The following status represents the normal operation of the AFW Subsystem under test conditions:
  - a. Motor-driven AFW pumps (52AFP002A, B) running at rated speed.
  - b. Drive turbine steam supply isolation valves (52AFV118A, B, C) are open.
  - c. Drive turbine pressure control valve (52AFV121) is open.
  - d. AFW pump drive turbine (52AFN001) and turbine-driven AFW pump (52AFP001) running at rated speed.
  - e. AFW flow control valves (52AFV104) are closed.
  - f. AFW isolation valves (52AFV103) are open.
  - g. AFW pump recirculation valves (52AFV108) are open.
  - h. Superheater vent control valves (52AFV116) are closed.
  - i. Steam drum vent control valves (52AFV117) are closed.
  - j. Superheater outlet isolation valves (53SGV012A, B, &C) and steam drum drain valves (53SGV014 A, B, C and 105 A, B, C).
- (4) Shut the AFW Subsystem down after 2 minutes and use the plant computer printout to verify all parameters. The subsystem is shut down and returned to standby per Steps (5) to (11) below.
- (5) Shut down the turbine-driven pump as follows:
  - a. Transfer the NORMAL/LONG TERM COOLDOWN switch for the drive turbine steam supply isolation valves (52AFV118A, B, C) to the LONG TERM COOLDOWN mode.
  - b. Close the drive turbine steam supply isolation valves 52AFV118A, B, c.
  - c. Transfer the drive turbine pressure control valve (52AFV121) to the manual control mode. Close the valve and transfer it back to the automatic mode.
- (6) Shut down the motor-driven pump as follows:
  - a. Transfer each NORMAL/LONG TERM COOLDOWN switch for AFW pumps 52AFP002A and B to the LONG TERM COOLDOWN MODE.
  - b. Shutdown AFW pump drive motors 52AFK001A and B.
- (7) Reset the NORMAL/LONG TERM COOLDOWN switches for the AFW pumps to the NORMAL mode.
- (8) Reset SGAHRS test initiation trip logic. When this is done the AFW isolation valves (52AFV103A to F) will automatically close.
- (9) Switch the AFW flow control valves (52AFV104A to F) to the manual control mode and open the valves. Reset the valves back to the automatic control mode.
- (10) Confirm that all SGAHRS controls are in the automatic mode of operation.



- (11) Confirm the final conditions of this procedure are identical to the initial conditions.
- (12) Evaluate the system test results recorded by the PDH&DS and perform corrective maintenance on those components requiring it as demonstrated by the test data and repeat test if necessary.

The following SGAHRS actuated valves also require periodic test:

- o Superheater Vent Control (52AFV116A, B, C)
- o Steam Drum Vent Control (52AFV117A, B, C)

At intervals of three months these valves will be exercised, one at a time, to the position required to fulfill their function. The procedure for the exercising test is as follows:

- (1) Isolate the appropriate isolation valve upstream of the valve to be tested.
- (2) Transfer control switch of the valve to be tested to the manual mode (skip this step if no such switch is provided for the valve).
- (3) Open the valve using the start/stop switch and the manual controller (or open/close switch).
- (4) Confirm the necessary valve movement by exercising the valve while observing the appropriate control room position indicator.
- (5) Close the valve being tested.
- (6) Open the appropriate upstream isolation valve closed in Step (1).
- (7) Transfer control switch for the valve back to automatic mode.
- (8) Repeat Steps (1) through (7) in turn for each valve to be tested.

(e) Pressure relief valves at the superheater

The safety relief valves will be removed and bench tested during plant shutdowns at intervals consistent with ASME code requirements for safety valves. Periodic testing during plant operation is not planned.

Question QCS421.58

Recent review of a plant (Waterford) revealed a situation where heaters are to be used to control temperature and humidity within insulated cabinets housing electrical transmitters that provide input signals to the reactor protection system. These cabinet heaters were found to be unqualified and a concern was raised since possible failure of the heaters could potentially degrade the transmitters, etc.

Please address the above design as it pertains to CRBR. If cabinet heaters are used then describe as a minimum the design criteria used for the heaters.

Response:

The only CRBRP IE equipment which use cabinet heaters are the Sodium Pump Drive System PPS Breakers. The heaters are Class 1E and are qualified to temperature and humidity environments of 125°F and 90% relative humidity.

When heaters are used in IE cabinets, it is a CRBRP requirement to environmentally qualify them according to IEEE 323, if the heaters are required to enable the equipment in the cabinet to perform its safety function.

Question CS721.1

The Atomic Safety and Licensing Appeal Board in ALAB-444 determined that the Safety Evaluation Report for each plant should contain an assessment of each significant unresolved generic safety question. It is the staff's view that the generic issues identified as "Unresolved Safety Issues" (NUREG-0606) are the substantive safety issues referred to by the Appeal Board. Accordingly, we are requesting that you provide your justification for permitting plant operation in consideration of these issues. This should include a description of any measures in terms of design or operating procedures or investigative programs that are being pursued to address these concerns. The justification should provide an overall summary of your position on each issue in addition to a reference to various sections of the PSAR where related information is presented.

There are currently a total of 27 Unresolved Safety Issues. Some of these issues are clearly not applicable to Clinch River and need not be addressed. The remaining issues either clearly apply or the general intent of these issues applies to Clinch River. Those issues that you should address are identified in the following list.

"UNRESOLVED SAFETY ISSUES" (APPLICABLE TASK NOS.)

Waterhammer - (A-1)  
Steam Generator Tube Integrity - (A-3, A-4, A-5)  
Anticipated Transients Without Scram - (A-9) - Resolved\*  
Fracture Toughness of Steam Generator and Reactor Coolant Pump  
Supports - (A-12)  
Systems Interaction in Nuclear Power Plant (A-17)  
Environmental Qualification of Safety-Related Electrical  
Equipment - (A-24) - Resolved\*  
Residual Heat Removal Requirements - (A-31) - Resolved\*  
Control of Heavy Loads Near Spent Fuel - (A-36) - Resolved\*  
Seismic Design Criteria - (A-40)  
Shutdown Decay Heat Removal Requirements - (A-45)  
Seismic Qualification of Equipment in Operating Plants - (A-46)  
Safety Implications of Control Systems - (A-47)  
Hydrogen Control Measures and Effects of Hydrogen Burns on  
Safety Equipment - (A-48)

In responding to this question for each issue you should address the following guidelines: (1) discuss the applicability of the issue to Clinch River; (2) if you consider these issues to be resolved for Clinch River provide the basis for this conclusion; and (3) if you consider this issue unresolved as it applies to Clinch River provide your basis for operation and a description of your relevant programs to resolve the issue.

\*A number of the issues listed above are technically resolved. Your response to this question should address the applicability of the generic resolution to Clinch River.

Response:

CRBRP has considered the "Unresolved Safety Issues" identified in this question and has applied appropriate measures to assure that the plant may be permitted to operate, given due consideration of these issues. Suitable resolutions to the issues which reflect the technology of CRBRP are discussed below.

WATERHAMMER A-1

APPLICABILITY TO CRBRP:

Waterhammer and its equivalent, sodium-hammer, are applicable to the CRBRP plant. Waterhammer events introduce large hydraulic loads, or pressure pulses, into a fluid system, and are the result of rapid condensation of steam pockets, steam-driven slugs of water, pump startup into voided lines, and improper (or sudden) valve closures. Where waterhammer has occurred in water lines, the principal damage has been to pipe hangers and snubbers. In none of the waterhammer incidents reported has there been a release of radioactive material or a disabling of safety systems.

RESOLUTION FOR CRBRP:

Technical resolution for this issue has been effected on CRBRP. The water and steam systems of the CRBRP plant [i.e., the Steam Generator System and the Steam Generator Auxiliary Heat Removal System (SGAHS)] are described in PSAR Sections 5.5 and 5.6.1, respectively. Design resolution of waterhammer will be accomplished by including fill and vent holes in the auxiliary feedwater sparger in the steam drum to preclude waterhammer effects resulting from steam-driven slugs of SGAHS water, and by including hydraulic dampers in the actuators of the water and steam isolation valves to preclude waterhammer effects resulting from the overly rapid closing of a valve. The vent holes are described in revised PSAR Section 5.5.2.3, and the hydraulic dampers are discussed in Section 5.5.3.1.5.2.

Protection against the effects of pipe breaks and waterhammer loads are incorporated in ASME design codes which require consideration of impact loads and dynamic loads in the structural design. The ASME codes are applied to the sodium systems of CRBRP, i.e., the primary heat transport system, the intermediate heat transport system (including the steam generator) and the sodium/water reaction pressure relief system, as well as to the water/steam systems.

The design of the intermediate heat transport system, described in PSAR Section 5.4, has addressed the occurrence of sonic pulses, similar to those produced in waterhammer incidents. Sonic pulses may occur as a result of a large sodium/water reaction caused by a postulated steam generator tube rupture. In addition, the design of the sodium/water reaction pressure relief subsystem, described in PSAR Sections 5.5, 7.5.6 and 15.3.3.3, has considered the effects of accelerated sodium slug flows in the component and piping design.

The absence of sodium isolation valves in the IHTS precludes high decelerations of sodium which could cause waterhammer effects in sodium. The high normal boiling point and high heat of vaporization of sodium make vapor-driven sonic pulses extremely unlikely.

#### STEAM GENERATOR TUBE INTEGRITY (A-3, A-4, A-5)

##### APPLICABILITY TO CRBRP:

This issue is applicable to CRBRP. The design uses steam generators in each of the three heat transport system loops for the transfer of heat from the secondary sodium loop to the water systems. The Issue concerns the capability of steam generator tubes to maintain their integrity under normal operation and accident conditions, should mechanisms exist which can result in tube degradation.

##### RESOLUTION FOR CRBRP:

Technical resolution for this issue has been effected on CRBRP.

The CRBRP Steam Generator design has minimized the potential for corrosion/erosion degradation common to pressurized water reactor steam generators. The tubes in the CRBRP Steam Generator are exposed to the water environment only on their inside surface. The waterside consists of smooth wall tubes terminated in spherical plena. This greatly reduces the potential for tube degradation by corrosion induced wastage, cracking and denting. Preferential corrosion product formation or deposition is minimized since there are no restrictions, crevices, water levels or structure-related concentration-sites present. Water side chemistry is maintained by state-of-the-art, all volatile chemistry control which has been modified from pressurized water reactor practice and which will incorporate fossil plant experience with 2 1/4 Cr-1Mo tube material. Full flow demineralizers, a 2:1 full power recirculation ratio i.e., for each 2 parts water flowing into the steam generator, 1 part is being recirculated and 1 part is fresh feed, and 10% blowdown all contribute to minimizing the potential for waterside corrosion-related problems.

Steam generator tube integrity has been properly addressed in the CRBRP design through specifying that a total of 29% of the 0.109 inch tube wall thickness (Section 5.5.2.3.4 of the PSAR) be allocated for corrosion, cleaning and wear allowances. The reduced thickness is used for all stress and strain calculations while the full thickness is used for weight and seismic calculations. In addition, allowances are provided to compensate for material strength degradation by post weld heat treatment, thermal aging and decarburization. In spite of these reductions in thickness and material strength conservatively based on end-of-life condition, the tube has a 38% margin over the ASME Class 1 criteria for pressure retention.

Erosion of tubes as a result of tube vibration is being addressed in three ways, as discussed in PSAR Section 5.5. First, the design and material selection of the shell (sodium containing) side of the steam generator (SG) provides for acceptable accommodation of tube vibrations; all known flow induced vibration mechanisms have been evaluated. Tube to spacer plate gaps are consistent with guidelines used throughout the heat exchanger industry. Tube spacer plate material (Inconel 718) has been chosen since it has a low

coefficient of friction when coupled with the tube material (2 1/4 Cr-1Mo). Second, to confirm that all flow induced vibration mechanisms are considered, a flow induced vibration program has been implemented using both a full scale model closely representing the prototype unit and a 0.42 scale model. The scale model flow induced vibration tests will assure that mechanisms of unexpected origin in the plant unit design do not exist. Third, CRBRP has developed an ultrasonic tube inspection technique which can detect the tube wear well before the tube wall is thinned beyond that specified for the design, which is discussed in PSAR Appendix G.

#### ANTICIPATED TRANSIENTS WITHOUT SCRAM (A-9)

##### APPLICABILITY TO CRBRP:

This issue is applicable to CRBRP. The issue concerns the potential for a common mode failure to reduce the reliability of protection systems in such a way that the system might not function properly in the event of an anticipated transient.

##### RESOLUTION FOR CRBRP:

Technical resolution of this issue has been achieved for Light Water Reactors through publication of NRC staff position contained in NUREG-0460 Vol. 4. "Anticipated Transients without scram for Light Water Reactors." Specific design features and analyses are prescribed for LWRs. These prescriptions are not appropriate for CRBRP. The issue is resolved on CRBRP as discussed below.

CRBRP incorporates into the design, two independent shutdown systems, either of which has the capability, of itself, to terminate reactor transients and to effect rapid shutdown of the reactor automatically. Strict attention to diversity of the design features and to the separation of the two shutdown systems reduces the likelihood, of the simultaneous prevention of both systems from operating when called upon as a result of a common mode failure, to be incredible. Discussion of the design of the two shutdown systems, and the diversity of their features, is provided in PSAR Sections 4.2.3, 4.3.2., and 7.2.

#### FRACTURE TOUGHNESS OF STEAM GENERATOR SUPPORT (A-12)

##### APPLICABILITY TO CRBRP:

This issue is applicable to CRBRP. This issue concerns the low fracture toughness and potential lamellar tearing in materials used for heat transport system component supports.

##### RESOLUTION FOR CRBRP:

Technical resolution for this issue has been effected on CRBRP.

The design of that portion of the CRBRP Steam Generator Support which is in accordance with the ASME Code requires that impact testing, Charpy V-Notch, of all materials of construction be performed per paragraph NF-2311 of ASME Section III. The acceptance standards of NF-2330 must be met at 50°F maximum. Since the lowest operating temperature of the Steam Generator Support is 125°F, there is adequate margin for protection against non-ductile failures. In addition to the materials fracture toughness requirements, postulated defects are evaluated using the procedure in Appendix G of ASME Section III for all applicable conditions plus shipping, lifting and installation. Therefore, the concern relating to fracture toughness of Steam Generator Supports has been properly and adequately addressed in the CRBRP design.

The building structural steel that supports Steam Generators will be designed in accordance with the AISC Code requirements using ASTM A-36 steel and SA-540 bolting material. Sandia Laboratories' Report SAND78-2348 (Appendix C to NUREG-0577, "Potential for Low Fracture Toughness and Lamellar Tearing on PWR Steam Generator and Reactor Coolant Pump Supports - Resolution of Generic Technical Activity A-12 for Comment") classifies A-36 as falling within Material Group II, i.e., intermediate susceptibility to brittle fracture, and identifies that Group II materials have been judged adequate. SAND78-2348 classifies A540 bolting material as falling within Material Group III, which has also been judged adequate.

The supports for reactor coolant pumps and intermediate heat exchangers are SS304, connected to ASTM A-36 embedded plate with SA-540 bolting material.

CRBRP applies design criteria to the reactor vessel and steam generator supports to preclude conditions leading to lamellar tearing (e.g., material selection, welded joint orientation, and fabrication sequence).

#### SYSTEMS INTERACTION IN NUCLEAR POWER PLANTS (A-17)

##### APPLICABILITY TO CRBRP:

This issue is applicable to CRBRP. This issue concerns the sufficiency of integration of divided responsibilities for design, analysis and installation of systems among teams of engineers with functional specialties such as civil, electrical, mechanical and nuclear, to assure that adverse operational interactions between plant systems are minimized.

##### RESOLUTION FOR CRBRP:

Technical resolution for this issue has been resolved on CRBRP.

CRBRP has implemented a combination of programs and activities directed towards assuring an integrated design which has considered the potential for and provides protection against adverse operational interactions between plant systems. These include the CRBRP quality assurance program, a comprehensive design control program, specialized design reviews, and reliability and probabilistic risk assessment programs.

The plant has been designed to requirements which support a defense in depth philosophy. These requirements assure physical separation and independence of redundant safety systems, diversity of safety features, and protection against hazards such as sodium leaks, sodium/water reactions, line ruptures, missiles, tornadoes, floods, seismic events, fires, human errors, and acts of sabotage. These requirements are described in PSAR Section 1.1.2 and Chapter 3.

To assure that these requirements are properly implemented the CRBRP Quality Assurance Program addresses the design process. This program requires that during the design process emphasis is placed on the control of interfaces between systems. This interfacing is described in PSAR Section 17A.3.1. Independent design reviews, with interdisciplinary memberships and objectives, are required at various stages of the design process. Requirements for these independent design reviews are described in PSAR Chapter 17, Appendix G.

CRBRP conducted extensive Key Systems Reviews (KSRs) cutting across system boundaries. These reviews were conducted by multidisciplined groups of individuals with objectives which included assessments of plant and operator responses during off normal and accident events. Interactions between systems were explicitly considered as part of these reviews. Evaluations of the results of these reviews addressed the potential for adverse systems interactions, including considerations of human, spatial, and functional, coupling effects. A summary report of these reviews (KSRs) was provided in Reference QCS271.1-1.

The CRBRP safety-related reliability program is described in PSAR Appendix C. The results obtained in this program provide additional confidence that systems designs will minimize the potential for adverse operational interactions.

Reference QCS271.1-2 described the CRBRP Probabilistic Risk Assessment (PRA) Program Plan which includes tasks which will demonstrate that the risk of CRBR are acceptably low. The planned methodology will use event trees and fault trees to identify the component failures combinations that could result in a loss of safety function. The PRA activities will specifically evaluate potential adverse interactions between plant systems.

References:

- QCS721.1-1 Letter Longnecker to Check "Summary Report on the conduct of CRBRP Key Systems Reviews," dated Feb. 19, 1982.
- QCS721.1-2 Letter Longnecker to Check "Probabilistic Risk Assessment (PRA) Program Plan," dated June 21, 1982



## ENVIRONMENTAL QUALIFICATION OF SAFETY RELATED ELECTRICAL EQUIPMENT (A-24)

### APPLICABILITY TO CRBRP:

This issue is applicable to CRBRP. CRBRP design include Class 1E Equipment which must be qualified for the environmental conditions in which it may be required to perform.

### RESOLUTION FOR CRBRP:

Technical resolution of this issue has been achieved for Light Water Reactors through publication of NRC staff position contained in NUREG-0588 "Interim Staff Position on Environmental Qualification of Safety-Related Electrical Equipment." The issue is resolved on CRBRP through a program for environmentally qualifying safety-related electrical equipment which is consistent with the objectives and requirements contained in NUREG-0588, Rev. 1 as applied to CRBRP technology. This program is outlined in the response to NRC Question CS270.1, and in PSAR Section 3.11.

## RESIDUAL HEAT REMOVAL REQUIREMENTS (A-31)

### APPLICABILITY TO CRBRP:

This issue is not applicable to CRBRP. The issue concerns the capability of PWRs to go from hot to cold shutdown without the availability of off-site power.

A safe shutdown condition equivalent to a PWR cold shutdown condition is achieved in CRBRP when the plant is brought down from operating temperature to 600°F using the plant shutdown heat removal systems. At the 600°F temperature the plant is in a safe and stable state, and long term cooling is in effect. There is no subsequent requirement to proceed to another mode or state to effect long term shutdown.

The normal decay heat removal path is through the use of the main condenser and feedwater train. However, as the main condenser and feedwater train is not available upon loss of off-site power, the Steam Generator Auxiliary Heat Removal System (SGAHS), which is a safety-related system, is provided for shutdown heat removal and long term decay heat removal, and is independent of the availability of off-site power.

## CONTROL OF HEAVY LOADS NEAR SPENT FUEL (A-36)

### APPLICABILITY TO CRBRP:

This issue is applicable to CRBRP. Although the design of CRBRP does not use spent fuel pools, this concern is applicable to the control of heavy loads over the Ex-Vessel Storage Tank Closure Head and Striker Plate, and over the Fuel Handling Cell.

#### RESOLUTION FOR CRBRP:

Technical resolution for this issue has been achieved through publication of NRC staff position contained in NUREG-0612, "Control of Heavy Loads at Nuclear Power Plants".

The issue is resolved for CRBRP by the application of a single-failure proof crane (in accordance with NUREG-0554, "Single Failure Proof Cranes for Nuclear Power Plants") in both the RSB and RCB for all critical lifts. The Project application of NUREG-0612 is presented in response to NRC Question CS410.3.

#### SEISMIC DESIGN CRITERIA (A-40)

##### APPLICABILITY TO CRBRP:

This issue is applicable to CRBRP. The issue concerns the conservatism of certain aspects of the overall seismic design criteria.

##### RESOLUTION FOR CRBRP:

Technical resolution for this issue has been effected on CRBRP. The seismic design bases and the seismic design of CRBRP conform to the current NRC criteria. CRBRP seismic design criteria are described in PSAR Section 3.7. NRC have not established any other bases which would render conformance to the current criteria inadequate.

#### SHUTDOWN DECAY HEAT REMOVAL REQUIREMENTS (A-45)

##### APPLICABILITY TO CRBRP:

This issue is applicable to CRBRP. This issue concerns the sufficiency of plant capability to remove decay heat. CRBRP must have a highly reliable capability to remove decay heat from the reactor.

##### RESOLUTION FOR CRBRP:

Resolution for CRBRP for this issue has been accomplished by incorporating into the design, multiple, independent, and highly reliable heat transport paths, any one of these paths having sufficient capacity to be able to remove the reactor decay heat by itself. The various heat removal paths and their operating modes embody substantial diversity.

CRBRP Heat Transport System uses three independent loops each of which provides a separate path from the reactor vessel to the ultimate heat sinks. The normal heat removal path includes the main condenser and feedwater train which is used for normal operation and some shutdown heat removal conditions. However, for each path an alternative safety-related path is provided, through the Steam Generator Auxiliary Heat Removal System (SGAHS) which provides its own heat sinks. Thus, it is not necessary to rely upon the main condenser and feedwater train, since SGAHS is available for all anticipated plant events.

The SGAHS system includes the Auxiliary Feedwater Subsystem (AFWS) and Protected Air Cooled Condensers (PACCs) which serve as alternative heat sinks.

The AFWS provides water make-up to the closed loops between the steam generators and the PACCs. The AFWS includes two motor driven and one steam-turbine driven pumps.

The sodium in the Primary and Intermediate Systems of the HTS loops is always at temperatures well below the flash point. Thus, in the unlikely event of a sodium pipe leak in any loop there will not be a loss of heat removal capability due to loss of coolant inventory through flashing. Also, degradation of one loop will not affect heat removal capability in either of the other two loops.

Thus, the plant configuration provides multiple independent paths through the Heat Transport System, which contributes to the high reliability of the plant systems for removing reactor decay heat. These capabilities are discussed in PSAR Section 5.6 and 5.6.1.

CRBRP provides an additional path for decay heat removal, the Direct Heat Removal Service. This system provides a diverse heat removal path to yet another redundant and diverse set of air cooled heat exchangers. This is described in PSAR Section 5.6.2.

#### SEISMIC QUALIFICATION OF EQUIPMENT IN OPERATING PLANTS (A-46)

##### APPLICABILITY TO CRBRP:

This issue is not applicable to CRBRP. The issue is whether operating plants must be reassessed to assure the adequacy of their seismic qualification of equipment. Construction of the Project has not yet commenced and thus, it is not an operating plant. CRBRP resolution of USI A-40 assures the adequacy of Seismic Design Criteria applied to it.

#### SAFETY IMPLICATIONS OF CONTROL SYSTEMS (A-47)

##### APPLICABILITY TO CRBRP:

This issue is applicable to CRBRP. CRBRP is dependent upon the proper functioning of control systems in order to maintain the plant in a safe condition for all normal operations and accidents. This issue concerns the potential for transients or accidents being made more severe as a result of control system failures or malfunctions. These failures or malfunctions may occur independently or as a result of the accident or transient under consideration.

##### RESOLUTION FOR CRBRP:

Technical resolution for this issue has been effected on CRBRP. Design features ensure that control system failures will not prevent automatic or manual initiation and operation of any safety system equipment required to trip the plant or to maintain the plant in a safe shutdown condition following any anticipated operational occurrence or accident. This has been accomplished by providing independence and physical separation between safety system trains and between safety and non-safety systems. For the latter, as a minimum, isolation devices are provided. These devices preclude the propagation of non-safety system equipment faults to the protection systems.

Also, to ensure that the operation of safety system equipment is not impaired, the single-failure criterion has been applied in the plant design. PSAR Section 7.2.2 discusses Plant Protection System (PPS) - Control System interaction. The CRBRP PPS is composed of two independent subsystems, either of which is capable of bringing the plant to a safe shutdown condition.

Further, these two subsystems employ diverse trip functions for PPS activation. Therefore, for any Design Basis transient, there is always more than one trip function provided by these two totally independent subsystems to activate the PPS and terminate the ensuing transient. Details of this design are described in PSAR Section 7.2, and Table 7.2-2.

A wide range of bounding transients and accidents is presently analyzed to ensure that the postulated events would be adequately mitigated by the safety systems. In addition, systematic reviews of safety systems have been performed with the goal of ensuring that the control system failures will not defeat safety system action. The worst conditions for each given type of transient are assumed in the accident analyses. This information is provided in PSAR Chapter 15.

#### HYDROGEN CONTROL MEASURES AND EFFECTS OF HYDROGEN BURNS ON SAFETY EQUIPMENT- A-48

##### APPLICABILITY TO CRBRP

This issue is not applicable to CRBRP. Design basis accidents within the CRBRP containment do not lead to the generation of hydrogen. Accordingly, there is no effect of hydrogen burns which could impact the capability of safety-related equipment to perform its intended safety function. However, accidents beyond the design basis involving hypothetical core disruptive accidents may produce hydrogen as a result of sodium-concrete interactions. The control and burning of the hydrogen from a hypothetical core disruptive accident is addressed in the CRBRP Thermal Margin Beyond Design Basis (CRBRP-3, Vol. 2). In the TMBDB scenario, the hydrogen is ignited in the containment atmosphere by sodium burning with the oxygen in containment. CRBRP-3, Vol. 2 also demonstrates how containment integrity is maintained.

Question CS760.13

Section 15.2.2.2 analyzes a 60c radial movement (stick slip) incident. The analysis does not distinguish between primary or secondary scram. (Only one temperature curve is given). Provide analysis for this transient, listing the appropriate primary and secondary trip functions.

Response

For a 60c step reactivity insertion the power increases in almost step fashion from 100% to over 200% as shown by Figure 15.2.3.3-3. Both the primary and secondary high power trip signals are significantly below the increased power level and thus, both trips would occur simultaneously. The table below summarizes results for the highest cladding temperature hot rod in FA-52 considering both primary and secondary scram (each separately).

SHUTDOWN SYSTEM	REACTOR POWER AT TRIP	MAXIMUM TEMPERATURES (3c)								
		CLADDING			FUEL			COOLANT		
		A	B	C	A	B	C	A	B	C
Primary	115%	1491	0.63	1.6	4576	0.53	1.3	1417	0.63	1.6
Secondary	122%	1544	0.83	2.0	4752	0.63	1.7	1467	0.83	2.1

A - maximum 3c hot spot temperature attained, °F.

B - time to reach maximum temperature, sec.

C - length of time temperature is above initial steady state value, sec.

It should be noted that occurrence of a 60c step reactivity insertion combined with failure of the primary scram would be less probable than an extremely unlikely category event in which case the primary shutdown of a Safe Shutdown Earthquake (Section 15.2.3.3) would envelope the consequential core damage.

Question CS760.28

During the earlier phase of the CRBRP licensing review, it was a regulatory staff position that no credit would be given for shutdown (decay and sensible) heat removal by natural circulation through the heat transport trains of the plant. This position was based on the lack of a data base to support the potential natural circulation capability of the CRBR design. Additionally, there are numerous concerns regarding the adequate simulation/prediction of the thermal/hydraulic characterization of the system operating under natural circulation conditions.

To adequately portray system operation under natural circulation conditions, there are many inter-related factors which must be represented. The overall driving force for the natural circulation flow is a balance between competing pressure losses and gains throughout the reactor vessel and primary system.

To adequately assess the natural circulation capability of CRBRP, appropriate experimental data, both on a component and system-wide basis, must be provided to validate and improve wherever necessary the presently available analytical tools. Table 15.3-1 summarizes the data needs relative to the adequate assessment of natural circulation capability of CRBR. Included in this Table are the key parameters and their importance.

Please provide data, particularly for those items where the availability is noted as "limited" or "none", so that their influence on the natural circulation capability of CRBR can be properly substantiated.

(THIS TABLE IS PART OF NRC'S QUESTION CS760.28.)

TABLE 15.3-1 LMFBR SYSTEM VALIDATION NEEDS RELEVANT TO NATURAL CIRCULATION

COMPONENT	PARAMETER/PHENOMENA	IMPORTANCE	DATA AVAILABILITY
<u>I. REACTOR VESSEL</u>			
1. INLET MODULE	PRESSURE DROP	HIGH	LIMITED
	MIXING DURING PARTIAL FLOW REVERSAL	MEDIUM	NONE
2. OUTLET PLENUM	MIXING AND STRATIFICATION	HIGH	LIMITED
3. ASSEMBLIES	PRESSURE DROP	HIGH	LIMITED/LIMITED SUFFICIENT
	LAMINAR/CRITICAL TRANSITION/TURBULENT		
	HEAT TRANSFER COEFFICIENTS	HIGH	SUFFICIENT
	INTRA-ASSEMBLY REDISTRIBUTION HEAT/FLOW	HIGH	LIMITED
	INTER-ASSEMBLY REDISTRIBUTION HEAT/FLOW	HIGH	LIMITED
	LOW-HEAT FLUX BOILING DRYOUT CORRELATIONS	MEDIUM	LIMITED
	DECAY HEAT	HIGH	?
4. STRUCTURAL MATERIAL	SHUTDOWN HEAT/HEAT LOSSES	MEDIUM	NONE
<u>II. HEAT TRANSPORT SYSTEM</u>			
1. PIPING	PRESSURE DROPS	LOW	SUFFICIENT
	STRATIFICATION	MEDIUM	LIMITED
2. PUMPS	FRICTIONAL TORQUE	HIGH	NONE
	LOCKED ROTOR RESISTANCE	HIGH	LIMITED
3. CHECK VALVE	PRESSURE DROP	HIGH	LIMITED
4. IHX	SHELL SIDE PRESSURE DROP	MEDIUM	LIMITED
	FLOW MALDISTRIBUTION	LOW	NONE

QCS760.28-2

Amend.  
Oct. 19

TABLE 15.3-1 (continued)

COMPONENT	PARAMETER/PHENOMENA	IMPORTANCE	DATA AVAILABILITY
III. STEAM GENERATOR SYSTEM			
1. S.G.	PRESSURE DROPS DRYOUT CORRELATIONS	HIGH MEDIUM	SUFFICIENT SUFFICIENT
2. RECIRC. PUMP	HOMOLOGOUS PUMP CURVES COASTDOWN RATE	HIGH MEDIUM	LIMITED LIMITED
3. HEAT EXCHANGER	LOSS COEFFICIENTS HEAT TRANSFER	MEDIUM HIGH	LIMITED LIMITED FOR EVAPORATOR
4. PACC	PRESSURE LOSSES HEAT TRANSFER	LOW HIGH	LIMITED NONE
5. ISOLATION VALVES	FULL OPEN FLOW AREA	LOW	NONE
6. CHECK VALVE	LOSS COEFFICIENTS	LOW	LIMITED

QCS760.28-3

Amend. 72  
Oct. 1982



## RESPONSE

### I. REACTOR VESSEL

#### 1. Inlet Module

The pressure drop data through the lower inlet modules (LIMs) are given in terms of loss coefficients,  $K$ , and reference areas,  $A$ , as shown in Table 4.4-8 of the PSAR. These values were determined from the experimental data reported in Reference QCS760.28-1, for the blanket orificing test. Full prototype inlet module tests were recently performed at ARD. Preliminary evaluations of these tests indicate the measured pressure drop is within the 20% uncertainty value used in the calculated PSAR values.

No flow reversal is expected in assemblies during natural circulation. Consequently, no such flow condition was contemplated in the LIM experiments.

#### 2. Outlet Plenum - Mixing and Stratification

Contrary to the belief that only limited experimental data are available concerning the reactor vessel upper plenum mixing and stratification phenomena, the problem has been studied quite extensively both experimentally and analytically. The experimental tests include Argonne National Laboratory (ANL) 1/15 scale model water, brine, and sodium tests for both the FFTF and CRBRP upper plenum (References QCS760.28-3, 4), Battelle-Columbus Laboratory (BCL) 0.55 scale FFTF model water and brine tests (Reference QCS760.28-5), and ANL 1/10 scale CRBRP model water tests (References QCS760.28-6 through 10). The experiments performed with the 1/10 scale CRBRP model included studies of: 1) steady state and transient performance of the CRBRP outlet plenum; 2) the effects of thermal oscillation; 3) the suppressor plate and shear web; and 4) the influence of the heterogeneous core geometry upon the outlet plenum mixing. In addition to the studies on steady state and thermal down transient performance, outlet plenum mixing for transient overpower conditions had also been studied and the results are documented in Reference QCS760.28-11. Finally, the influence of scale size and fluid thermal properties in simulating LMFBR outlet plenum behavior was also studied and the results are presented in Reference QCS760.28-12.

In addition to the above experimental studies, several semi-empirical upper plenum mixing codes have been developed based primarily on the scale model water test results. A three region outlet plenum mixing code PLENUM-3 was first proposed by P. A. Howard (Reference QCS760.28-13) of ANL. Based on additional water test data P. A. Howard, et al., later proposed a two region outlet plenum model PLENUM-2 (Reference QCS760.28-14). This two region model was later revised by the same authors into the PLENUM-2A model (see Reference QCS760.28-15).

Aside from these semi-empirical models, the outlet plenum performance had also been studied numerically by the two-dimensional VARR-II (Reference QCS760.28-16) and the three-dimensional TEMPEST (Reference QCS760.28-17) codes.

### 3. Assemblies

#### Pressure Drop

The pressure drop in core assemblies consists of the following components: inlet nozzle, inlet nozzle orifice-shield, shield, rod bundle, and outlet nozzle. There are two forms of pressure drop, i.e., frictional loss and form loss. The former occurs through the rod bundle while the latter covers all other components of the assembly.

The rod bundle frictional loss data for fuel assemblies for the PSAR were obtained from the FFTF Fuel Vibration Tests (References QCS760.28-18a and 18b). Data for inner and radial blanket rod bundles were obtained from the Radial Blanket Heat Transfer Tests and data for similar bundle geometry (Reference QCS760.28-18c) in sodium and water. These data are shown in Figures QCS760.77-1 and -2. (See Question/Response CS760.77.) Both of these figures cover the laminar, transition and turbulent ranges.

Form loss data were obtained from the CRBR fuel assembly inlet/outlet nozzle flow test and CRBR radial blanket flow orificing testing. Tables 4.4-6 and 4.4-7 in the PSAR (Chapter 4) cover the component hydraulic correlations for fuel, inner blanket and radial blanket assemblies.

Additional experimental data for CRBR fuel assemblies have been obtained as shown in Figure QCS760.77-4 (See Question/Response CS760.77). The latest data on fuel assembly friction factor is published in Reference QCS760.28-19. The CRBR control assembly hydraulic tests and blanket assembly flow and vibration tests have been completed and cover a wide range of operating conditions, including natural circulation flow rates. These data is shown in Figure QCS760.77-2 and -3 (See Question/Response CS760.77).

#### Heat Transfer Coefficients

Heat transfer coefficients were selected from a wide range data base and are reported in Reference QCS760.28-20. It should be noted that for natural circulation conditions, the heat flux is low and the film temperature drop generally is negligible, which makes the influence of the heat transfer coefficients relatively unimportant for the natural circulation event.

### Intra-Assembly Heat/Flow Redistribution

Extensive out-of-pile sodium heat transfer test data over the full range of operating conditions on the 61-rod fuel assembly bundle were obtained in the ORNL Thermal-Hydraulic Out-of-Reactor Safety (THORS) facility (Reference QCS760.28-50). Extensive sodium heat transfer test data on a prototypic 61-rod blanket assembly bundle were obtained over a wide range of operating conditions in the WARD GPL facility (References QCS760.28-51 through 60). Both of these data were compared with the COBRA-WC code considering the intra-assembly heat/flow redistribution in Reference QCS760.28-22. In-pile data from the natural circulation experiments conducted in the Experimental Breeder Reactor-II (EBR-II) facility confirmed such intra-assembly redistributions (Reference QCS760.28-21). Specifically, Instrumented Subassembly XX08, Test 7A, was used as a verification of the COBRA-WC code in calculating the sodium temperature at different channel locations and time during the transient. The comparison of code calculated temperatures with the experimental data are presented in Reference QCS760.28-22.

The recent FFTF natural circulation tests also provide confirmatory experimental data on temperatures measured in the instrumented fuel open test assemblies (FOTAs), involving the effect of intra-assembly heat/flow redistribution. These data are also used to verify the COBRA-WC code predictions (Reference QCS760.28-23).

### Inter-Assembly Heat/Flow Redistribution

The EBR-II and FFTF in-pile experimental data listed in the above section also confirm the inter-assembly effects. These factors are also simulated in COBRA-WC code simulation (References QCS760.28-22, 23). The WARD blanket heat transfer test also provides inter-assembly heat transfer data. In addition, further inter-assembly heat/flow redistribution experimental data will be obtained from the instrumented inner blanket assembly WBA-45/46 including during natural circulation. Testing of multi-assemblies in sodium in the THORS out-of-pile facility at ORNL will also provide inter-assembly flow redistribution experimental data.

### Low Heat Flux Boiling Dryout Correlations

Experimental data on low flux boiling is reported in Reference QCS760.28-24, which simulates sodium boiling under low power, low flow conditions. Sodium boiling in a full length 19-pin simulated fuel assembly (THORS Bundle 6A) was tested in the ORNL Thermal-Hydraulic Out-of-Reactor Safety THORS facility (Reference QCS760.28-25). An in-pile test was also performed in the Sodium Loop Safety Facility (SLSF) simulating loss of piping integrity accident (Reference QCS760.28-26). These experiments provide data on sodium boiling under low heat flux and/or dryout conditions. It should be noted that during the CRBR natural circulation event, sodium boiling does not occur. In fact, Reference QCS760.28-2 shows that over 150°F margin exists to boiling for the highest temperature hot rods.

### Decay Heat

Decay heat for an average fuel assembly, average inner blanket assembly and average radial blanket assembly is provided in Table 3.1 of CRBRP-ARD-0308 (Reference QCS760.28-2) for worst case natural circulation analyses. Corresponding decay heat data for the maximum temperature hot rods in FA-52, IBA-99 and RBA-203 are provided in the response to Question CS760.24. The bases for these average region and hot rod decay heat values are given in Reference QCS760.28-2 (Sections 3.2.2.1 and 4.2.2.3) and References QCS760.28-38 through 49.

#### 4. Structural Material

It is assumed that "shutdown heat/heat losses" refers to the inclusion of the reactor vessel and internal sensible heat and reactor vessel heat losses to the atmosphere in natural circulation analyses. The mass used in DEMO analyses is described in CRBRP-ARD-0005. Heat loss from the reactor vessel to the atmosphere, however, has not been included in natural circulation analyses. This is seen as a minor effect and neglecting it would yield conservative results.

## 11. Heat Transport System

### 1. Piping

Pressure Drops - Designated in question as low importance and with sufficient data available.

Stratification - Based on the testing presented in Reference QCS760.28-27, a study of the importance of stratification on natural circulation analyses (Reference QCS760.28-28) concludes that "it can be safely concluded that for flow and temperature transients seen at the entrance to the piping runs (component exit nozzles) during the transition from forced (pumped) flow to natural circulation and operation in that mode, the stratification that would occur in horizontal sections of these piping runs can be ignored. In fact, even under extremely severe stratification assumptions, i.e., stratification to occur at the inlet to a horizontal pipe run and also at the inlet to a vertical riser, the effects of piping stratification on the natural circulation decay heat removal capability are seen to be very small."

### 2. Pumps

Frictional Torque - The CRBRP sodium pump frictional torque correlations used in the most recent DEMO natural circulation analysis (CRBRP-ARD-0308) account for motor windage, bearing losses and friction between the pump shaft and the surrounding fluid. Development of the correlations is based upon experimental data available from prototype pump water test results. A trial-and-error procedure using the pump coastdown speed vs. time data, (see Table QCS760.28-11.1) pumping torque correlation and pump inertia as inputs to the equation of motion for the pump was performed to determine coefficients of the frictional torque correlations.

Locked Rotor Resistance - The CRBRP sodium pump locked rotor resistance correlation used in the most recent DEMO natural circulation analysis (CRBRP-ARD-0308) was developed using experimental data available from prototype pump water test results shown in Figure QCS760.28-11.1.

### 3. Check Valve

Pressure Drop - The pressure drop correlation used in CRBRP natural circulation analyses is based on test data taken on the FFTF 16-inch valve and 6-inch model valve. The detailed testing performed on the FFTF valves and the hydraulic similitude between the FFTF and CRBRP valves negates the need to test the CRBRP check valves further. Scaling and analyses accounting for design differences were used to extrapolate this FFTF data to the CRBRP data (Figure QCS760.28-11.2 and .3).

#### 4. IHX

IHX Shell Side Pressure Drop and Flow Maldistribution - The IHX shell side pressure drops used in the DEMO natural circulation analysis are a combination of vendor experimental data and pressure drop analysis. The IHX pressure drops from upstream of the inlet nozzle to downstream of the outlet nozzle are presented in the following table.

<u>MASS FLOW</u> <u>(%)</u>	<u>ΔP @ 862°F</u> <u>(psl)</u>	<u>ΔP @ 786°F</u> <u>(psl)</u>	<u>ΔP @ 400°F</u> <u>(psl)</u>
100	14.017	13.8586	13.0933
40	2.409	2.38178	2.25025
30	1.46765	1.451	1.37093
10	0.22704	0.22447	0.21208
5	0.07016	0.069367	0.065536
3	0.029877	0.029539	0.027908
1	0.004831	0.004776	0.004512

The flow is based on  $13.82 \times 10^6$  lbm/hr.

Flow maldistribution in the shell side of the IHX, which may be postulated to be induced by buoyancy effects at low primary flows, show insignificant impact on natural circulation transients (Reference QCS760.28-37). The effect of postulated flow maldistribution was analyzed by varying the effective heat transfer area from +33% to -73%. The analysis produced negligible changes in reactor temperatures.

TABLE QCS760.28-11-1

Coastdown Run A

Coastdown Run B

TIME Sec	PUMP SHAFT RPM *	TIME Sec	PUMP SHAFT RPM *	TIME Sec	PUMP SHAFT RPM*	TIME Sec	PUMP SHAFT RPM *
0	1116	30	120	0	1116	52	---
1	855	32	108	1	900	54	---
2	720	34	105	2	738	56	---
3	618	36	96	3	633	58	---
4	540	38	93	4	552	60	51
5	495	40	87	5	492	62	---
6	444	42	75	6	444	64	---
7	405	44	---	7	405	66	---
8	360	46	---	8	366	68	---
9	336	48	---	9	336	70	39
10	312	50	62	10	309	80	30
11	291	55	57	12	270	90	24
12	270	60	48	14	237	100	12
13	255	65	45	16	213	110	6
14	240	70	42	18	195		0
15	228	75	33	20	177		
16	213	80	28	22	---		
17	204	85	24	24	---		
18	195	90	21	26	---		
19	186	95	---	27	---		
20	177	100	18	28	---		
22	159	105	---	30	120		
24	150	120	0	32	---		
26	138			36	---		
28	129			38	---		
				40	87		
				42	---		
				44	---		
				46	---		
				48	---		
				50	66		

\* RPM as Computed From bearing Proximeter Pulses

QCS760.28-11-3

Amend. 72  
Oct. 1982

TABLE QCS760.28-11-2

Coastdown Run C

Coastdown Run D

Coastdown Run E

Coastdown Run F

TIME Sec	PUMP SHAFT RPM *
0	
1	840
2	
3	688
4	522
5	474
6	421
7	390
8	342
9	312
10	297
15	210
20	168
25	138
30	111
35	96
40	81
50	63
60	47
70	35
80	27
90	19
100	13
110	0

TIME Sec	PUMP SHAFT RPM *
0	1129
1	996
2	816
3	684
4	600
5	515
6	450
7	410
8	378
9	342
10	315
12	285
14	258
16	220
18	198
20	185
25	156
30	128
40	101
50	76
60	57
70	45
80	32
90	27
100	17
110	0

TIME Sec	PUMP SHAFT RPM *
0	960
1	---
2	700
3	---
4	540
5	---
6	420
7	---
8	375
9	---
10	310
12	270
14	240
16	215
18	195
20	175
25	140
30	115
35	108
40	85
45	72
50	65
60	50
70	40
80	25
90	21
100	14
110	0

TIME Sec	PUMP SHAFT RPM *
0	795
1	768
2	630
3	540
4	480
5	435
6	390
7	360
8	330
9	312
10	282
12	252
14	222
16	192
18	180
20	162
25	132
30	108
35	90
40	78
50	60
60	45
70	36
80	24
90	15
100	12
110	0

QCS760.28-11-4

\* RPM as Computed From Bearing Proxlmeter Pulses

Amend. 72  
Oct. 1982



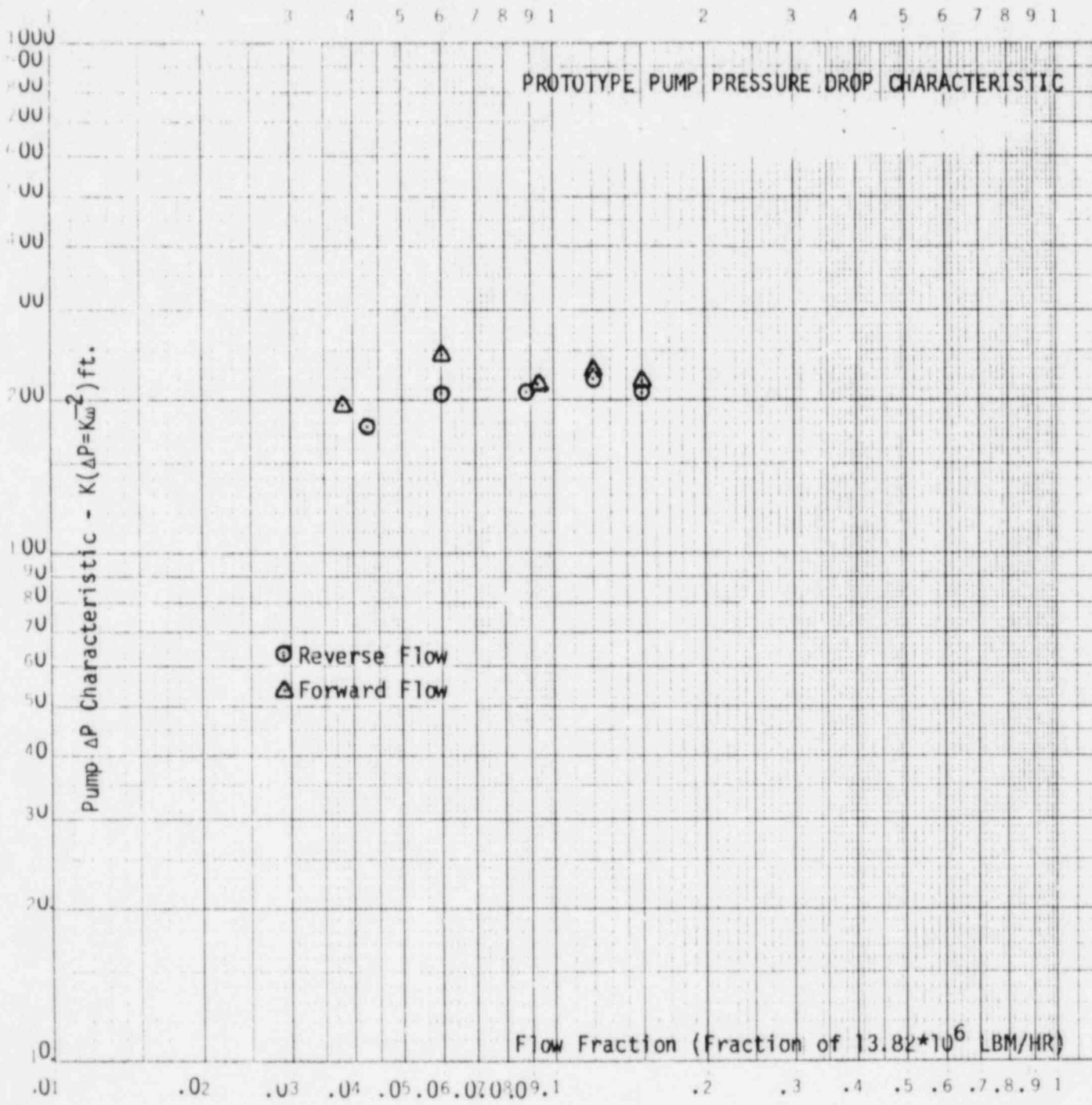


Figure QCS760.28-II.1

QCS760.28-II-5

Amend. 72  
 Oct. 1982

CLCV Pressure Drop

PRESSURE DROP (PSID)\*

.40  
.35  
.30  
.25  
.20  
.15  
.10  
.05  
0

FLOW RATE, % OF DESIGN

0 2 4 6 8 10 12

\*Range shown is from best estimate to +2σ value.

Figure QCS760.28-II.2  
QCS760.28-II-6

Amend. 72  
Oct. 1982

x

I

I

I

I

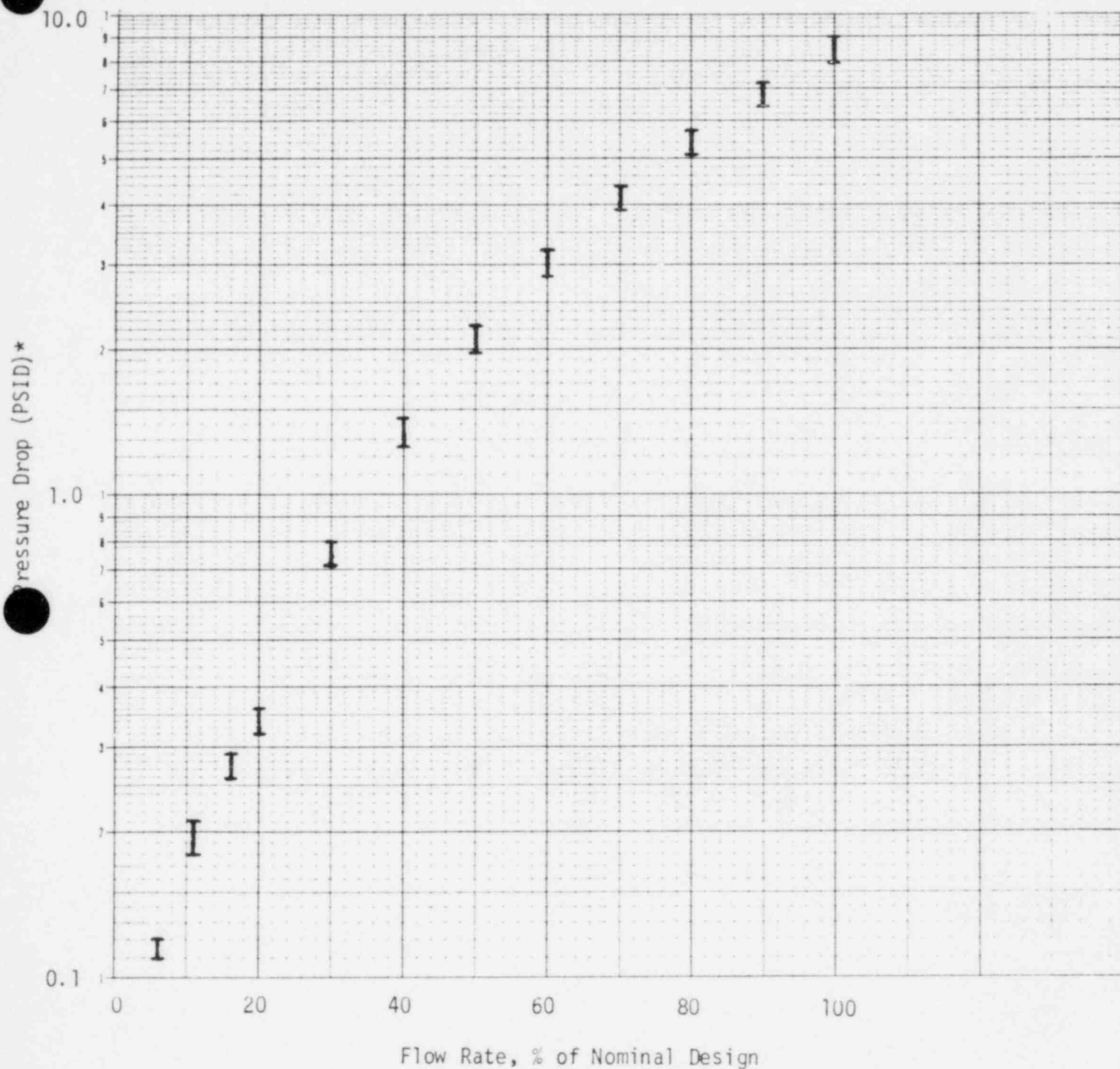
I

I

I

I

# CLCV Pressure Drop



\*Range shown is from best estimate to +2σ value.

Figure QCS760.28-II.3  
QCS760.28-II-7

Amend. 72  
Oct. 1982

### III. Steam Generator System

#### 1. Steam Generator

Pressure Drops - The pressure drops in the shell (sodium) side of the steam generator modules are of minimal importance for natural circulation analysis unless they are high enough to cause the IHTS flow to be less than or equal to the PHTS flow, which would result in a reduction in PHTS flow. The shell side  $\Delta P$  derived analytically and via vendor testing is much lower than that which would adversely impact the PHTS. Therefore, the S.G. shell side pressure drop may be judged to be of moderate importance. The attached module (Figure QCS760.28-III.5) pressure drop test data is from the key Feature and Hydraulic Flow Model (HTM) testing discussed in PSAR Section 5.5. Based on analyses of design differences between the HTM test module and the plant design, the vendor developed the pressure drop correlation used in natural circulation analysis.

As with the shell side, the tube side pressure drop is of minimal importance for natural circulation analyses, unless it impacts the IHTS flow enough to cause a reduction in the PHTS flow. Due to the large differences in density with a phase change in the S.G., relatively large variation in S.G. pressure drops result in only small variations in the recirculation loop conditions during natural circulation conditions. Therefore, the importance of tube side pressure for natural circulation analyses is also small.

Dryout Correlations - Data availability designated as sufficient in question.

#### 2. Recirculation Pump

Homologous Pump Curves - The pump operating characteristics are shown in Figure QCS760.28-III.1. This data was developed by vendor testing. The pump characteristic has an impact on the plant initial conditions, however, the importance of the homologous pump curves to natural circulation is minimal due to the short coastdown.

Coastdown Rate - The minimum pump coastdown rate based on vendor testing at plant conditions is shown in Figure QCS760.28-III.2. There was only minimal scatter in the stop times for the coastdowns performed by the vendor. The DEMO analysis has assumed a linear reduction in pump speed from full speed to 0 in 4 seconds. As the pump is a single speed pump, no steady state testing was performed at reduced speeds. However, vendor experience indicates that the pump will follow the pump affinity laws. As the pump stopped rotor resistance is a major portion of the recirculation loop pressure drop during natural circulation, this data is included as Figure QCS760.28-III.3.

### 3. Heat Exchanger

Loss Coefficients - See discussion presented for III.1 S.G. pressure drop above.

Heat Transfer - The heat transfer correlations used for the steam generators is important to establish the initial conditions and during the coastdown or transition to natural circulation conditions. The units are oversized for the natural circulation condition and, therefore, changes in heat transfer assumptions are overshadowed by the excess heat transfer area.

The two phase flow multiplier and heat transfer correlations used in DEMO are provided in Table QCS760.28-III.1.

### 4. PACC

Pressure Losses & Heat Transfer - Vendor analysis has predicted that the PACC can remove up to 32 percent of its full capacity as a natural draft heat sink. Testing of the PACC unit under natural draft conditions is planned to verify this assumption. The full capacity PACC heat removal capability vs. pressure is presented in Figure QCS760.28-III.4. It should be noted that the PACC capability will have no impact on the IHTS or PHTS flows or on predicted peak core temperatures. Thus, its relative importance on short-term natural circulation behavior of the plant is low.

### 5. Isolation Valves

Full Open Flow Area - The isolation valve design has not been completed. Therefore, per ANS standard B16.34, 1979 which requires a minimum valve ID of at least 90% of the pipe ID, valves will have a full open flow area of at least 81% of the pipe area.

The minimum valve full open flow area is therefore:

$$\begin{aligned} 18'' \text{ Recirculation Pump Inlet} &= 0.9777 \text{ ft}^2 \\ 16'' \text{ Superheater Exit} &= 0.7254 \text{ ft}^2 \\ 12'' \text{ Superheater Inlet} &= 0.4871 \text{ ft}^2 \\ 10'' \text{ Evaporator Inlet} &= 0.3192 \text{ ft}^2 \end{aligned}$$

### 6. Check Valve

Loss Coefficients - The evaporator outlet check valve pressure drop requirement is a maximum of 4 psid at a flow of  $1.1 \times 10^6$  lb/hr. and a quality of 0.50. The low flow requirement is presented in Table QCS760.28-III.2. Note that the port area is equivalent to the pipe flow area.

TABLE QCS760.28-111.1

SUMMARY OF HEAT TRANSFER AND PRESSURE DROP CORRELATIONS

Correlation	Correlations Used in DEMO	
	Correlation	Authors (Ref)
Two Phase Pressure Drop Multiplier	Armand multiplier for liquid condition pressure drop	Armand (QCS760.28-29)
Sodium Side Heat Transfer	$Nu = 17.28 + .0155 (\phi Pe)^{.86}$	Maresca-Dwyer (QCS760.28-30)
Water Side Preheat	$Nu = 0.023 Pr^{.4} Re^{.8}$	Dittus Boelter (QCS760.28-32)
Waterside Subcooled Boiling and Nucleate Boiling	$h = \frac{e^{ps/1260}}{.072} (q'')^{0.5} \left\{ \frac{T_w - T_{sat}}{T_w - T_b} \right\}$	Thom (QCS760.28-32)
Water Side DNB	$x_{dnb} = 1 - \frac{(q) (DEQWS)^{0.1}}{(5.5132 H_{fg})(GS)^{0.51}}$	MacBeth (QCS760.28-33) (Low Flow Rate)
Waterside Transition Boiling	$q = \frac{QDNB - 730 e^{(576/ps)(T_N - T_{W DNB})}}{1 - 730 e^{(576/ps)* RTMI}}$	McDonough, Millich, and King (QCS760.28-34)
Waterside Film Boiling	$Nu = 0.0193 Re^{.8} Pr^{1.23} * (VB/VG)^{.68} (VF/VG)^{.068}$	Bishop, Sandberg and Tong (QCS760.28-35)
Waterside Superheat	$Nu = 0.0133 Re^{0.84} Pr^{0.333}$	Heinemann (QCS760.28-36)

TABLE QCS760.28-III.2

Low Flowrate Pressure Drop

The pressure drop for low flowrates shall not exceed the following limits:

$$P = 1.492 \times 10^{-3} W_{fi} - 0.492 \times 10^{-6} W_{fi}^2$$

for  $W_{fi} < 2500$

$$P = 1.44 \times 10^{-3} W_{fi} - 2.9$$

Where  $W_{fi}$  = flow index  $\frac{W}{A}$

$W$  = flow rate (lb/hr)

$A$  = port area (in<sup>2</sup>)

$v = (1-x) V_f + xV_g$  (ft<sup>3</sup>/lb)

$x$  = quality

$V_f$  = specific volume of saturated liquid  $\frac{(ft)^3}{lb}$

$V_g$  = specific volume of saturated vapor  $\frac{(ft)^3}{lb}$

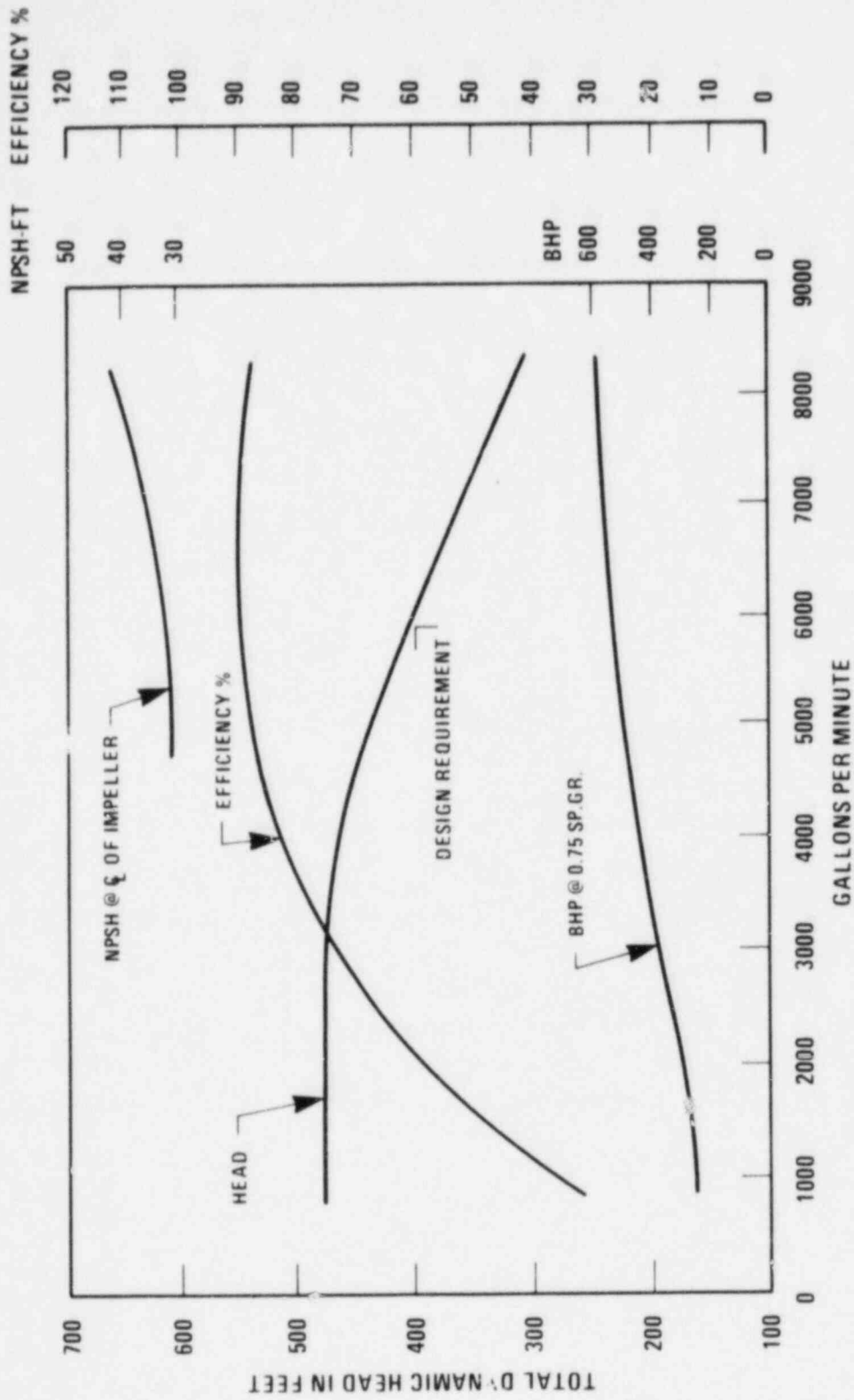


Figure QCS 760.28-III-1. Hot Performance Test Curve for Recirculation Pump

7203-i

QCS760.28-III-5

Amend. 72  
Oct. 1982



7203-3

QCS760.28-III-6

Amend. 72  
Oct. 1982

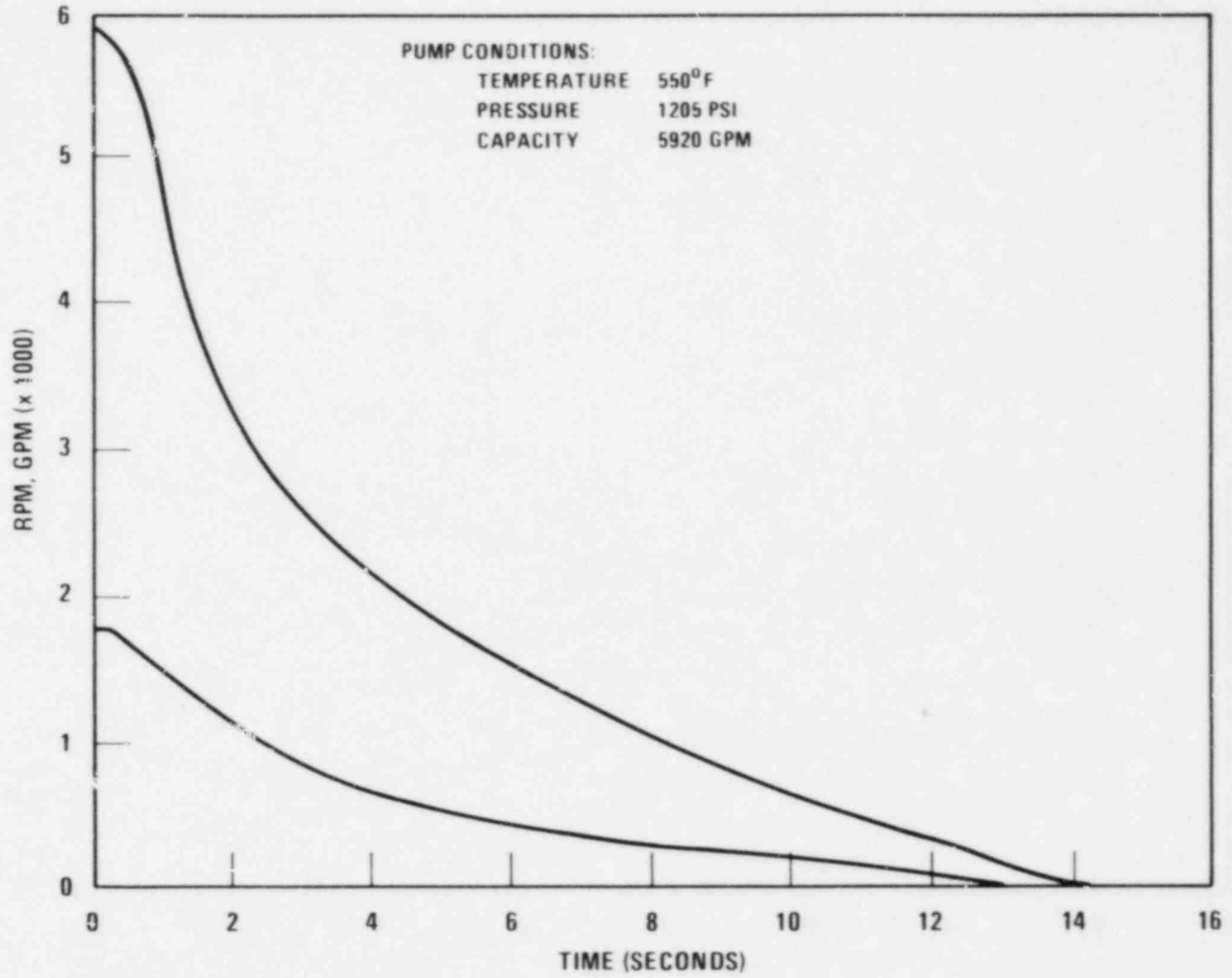


Figure QCS 760.28-III-2. Coast Down Curve for Recirculation Pump

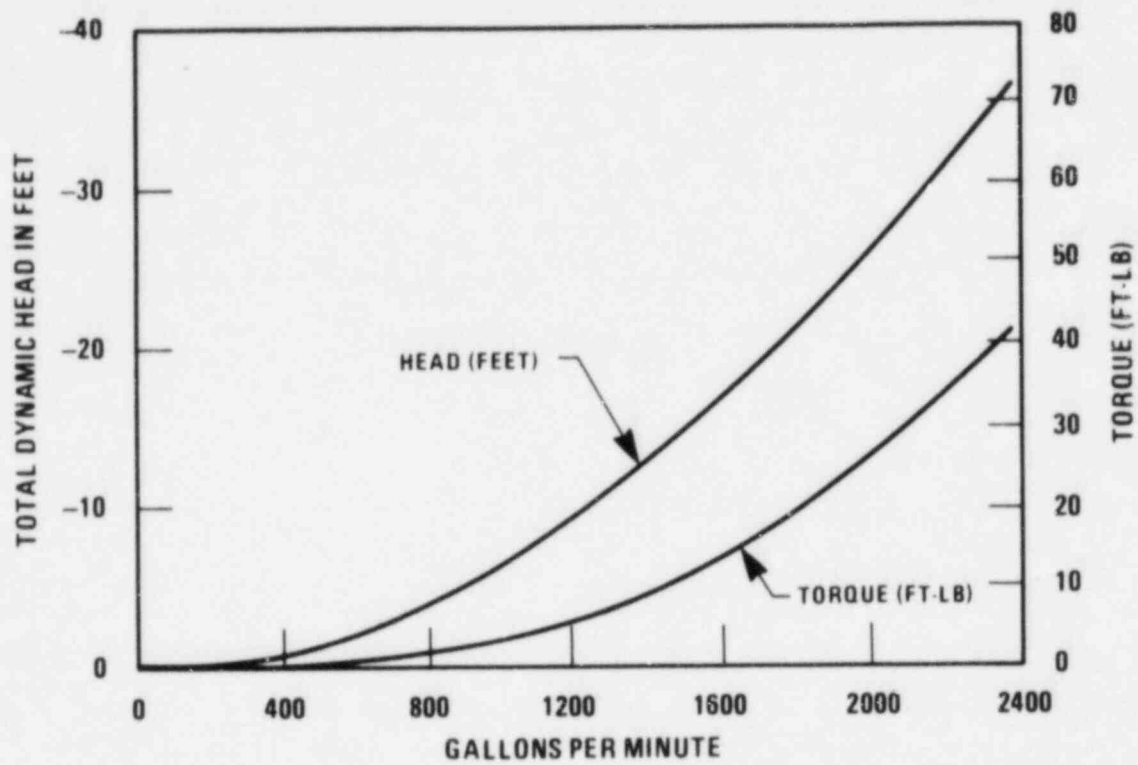


Figure QCS 760.28-III-3. Forward Flow Locked Rotor Flow Impedance Curve

7203-2

QCS760.28-III-7

Amend. 72  
Oct. 1982

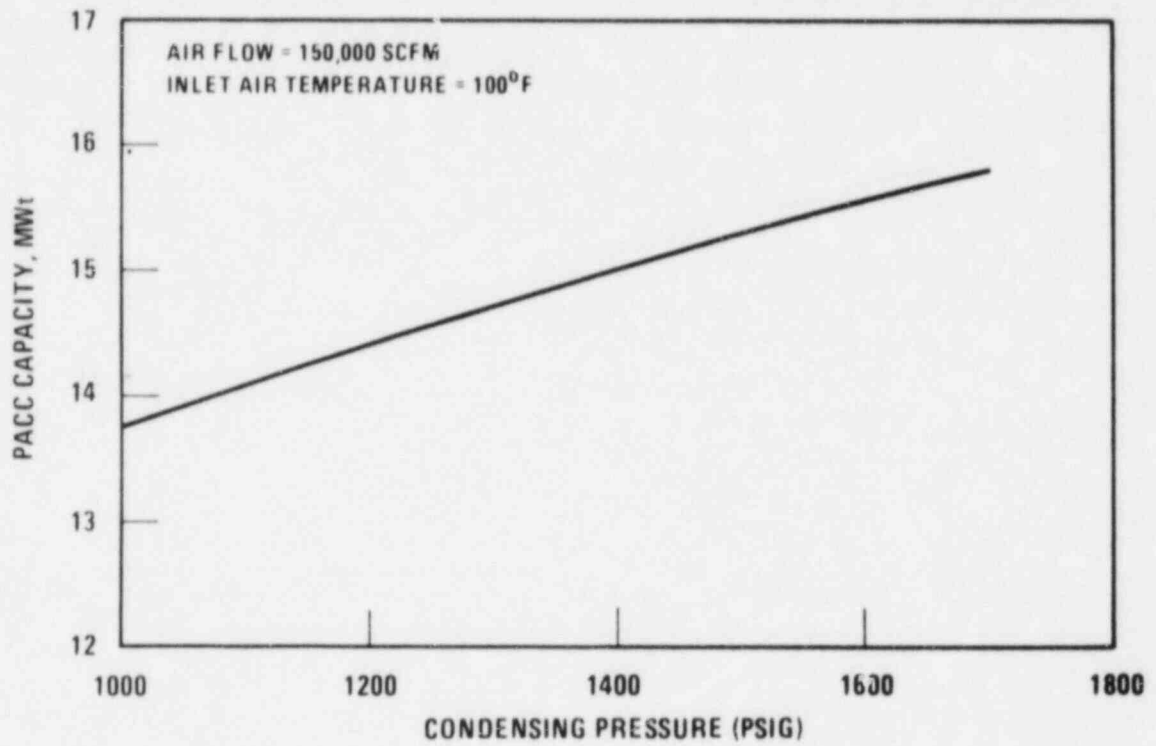


Figure QCS 760.28-III-4. Estimated PACC Capacity Versus Condensing Pressure

7203-4

QCS760.28-III-8

Amend. 72  
Oct. 1982

### HTM Pressure Drop Test Data

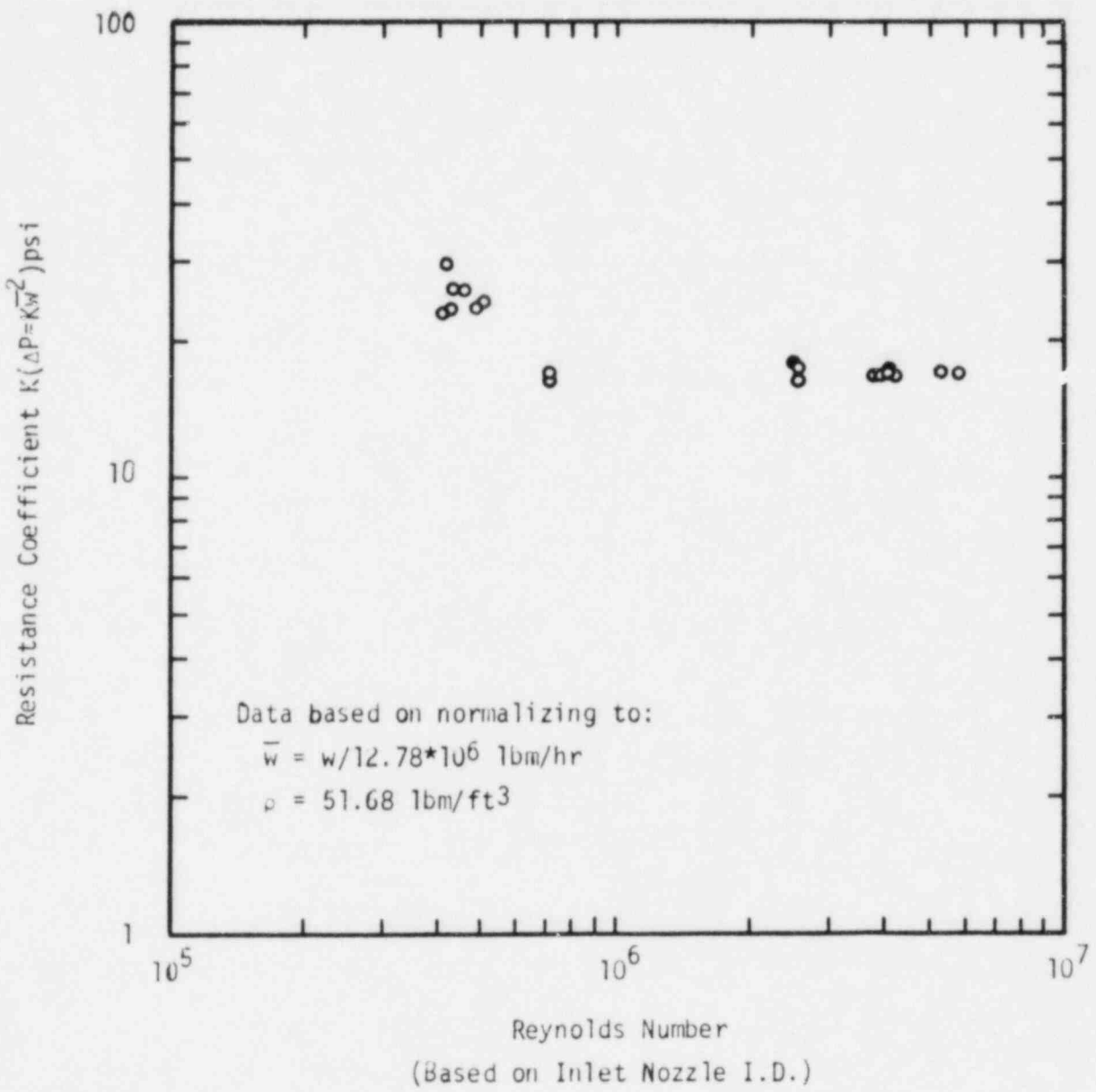


Figure QCS760.28-III.5

REFERENCES:

- QCS760.28-1. WARD-PB-3045-21, "Radial Blanket Design and Development Quarterly Progress Report for Period Ending August 31, 1977", 1977.
- QCS760.28-2. CRBRP-ARD-0308, "Summary Report on the Current Assessment of the Natural Circulation Capability with the Heterogeneous Core", February, 1982.
- QCS760.28-3. J. J. Lorenz, et al., "FFTF Upper Plenum Mixing Studies", ANL-CT-75-45, June, 1975.
- QCS760.28-4. J. J. Lorenz, et al., "An investigation of LMFBR Outlet Plenum Thermal-Hydraulic Behavior During Reactor Scram Transients", ANL-CT-76-18, September, 1975.
- QCS760.28-5. J. A. Carr and L. J. Flanigan, "FFTF Outlet Plenum Buoyancy Effects Study", WARD-2171-64, March, 1975.
- QCS760.28-6. J. J. Lorenz and P. A. Howard, "A Study of CRBR Outlet Plenum Thermal Oscillation During Steady State Conditions", ANL-CT-76-36, July, 1976.
- QCS760.28-7. P. A. Howard and J. J. Lorenz, "CRBR Outlet Plenum Thermal Behavior During Transient Conditions", ANL-CT-76-49, September, 1976.
- QCS760.28-8. P. A. Howard and J. J. Lorenz, "CRBR Outlet Plenum Mixing Studies: Suppressor and Shear Web Tests", ANL-CT-77-7, November, 1976.
- QCS760.28-9. P. A. Howard, "Steady-State CRBR Outlet Plenum Mixing with an AFMS Core", ANL-CT-77-14, April, 1977.
- QCS760.28-10. P. A. Howard, "The Influence of Heterogeneous Core Geometry upon Outlet Plenum Mixing", ANL-CT-78-8, November, 1977.
- QCS760.28-11. P. A. Howard, "Outlet Plenum Mixing for Transient Overpower Conditions of a One Exit Nozzle LMFBR", ANL-CT-78-30, April, 1978.
- QCS760.28-12. J. J. Lorenz, et al., "The Influence of Scale Size and Fluid Thermal Properties in Simulating LMFBR Outlet Plenum Behavior", AIChE Paper 35, National Heat Transfer Conference and AIChE Symposium Series No. 164, Vol. 73, pp. 120-126, 1977.
- QCS760.28-13. P. A. Howard, "Plenum-3: A Lumped Parameter LMFBR Outlet Plenum Mixing Code", ANL-CT-76-32.
- QCS760.28-14. P. A. Howard and J. J. Carbajo, "Plenum-2 - A Two-Region Outlet Plenum Model", ANL-CT-78-16, March, 1978.

- QCS760.28-15. P. A. Howard and J. J. Carbajo, "Plenum-2A - A Program for Transient Analysis of LMFBR Outlet Plenums", ANL-CT-79-17, February, 1979.
- QCS760.28-16. J. L. Cook and P. I. Natiayama, "VARR-II: A Computer Program for Calculating Time Dependent Turbulent Fluid Flows with Slight Density Variation", CRBRP-ARD-0106, Westinghouse Advanced Reactors Division, May, 1975.
- QCS760.28-17. D. S. Trent, "TEMPEST - A Three Dimensional Time Dependent Computer Program for Hydrothermal Analysis", FATE-79-105, Battelle Pacific Northwest Lab., July, 1979.
- QCS760.28-18a. W. L. Thorne, "Pressure Drop Measurements in FFTF Fuel Vibration Tests", HEDL-TC-812, April, 1977.
- QCS760.28-18b. W. L. Thorne, "Pressure Drop Measurements from Fuel Assembly Vibration Test II", HEDL-TC-824, April, 1977.
- QCS760.28-18c. F. C. Engel, R. A. Markley and A. A. Bishop, "Laminar, Transition, and Turbulent Parallel Flow Pressure Drop Across Wire Wrap-Spaced Rod Bundles", Nucl. Sci. and Eng., 69, p. 290, 1979.
- QCS760.28-19. "Friction Factor Correlation for 217-Pin Wire Wrap-Spaced LMFBR Fuel Assemblies", Trans. Amer. Nucl. Soc., 39, p. 1014, 1981.
- QCS760.28-20. M. S. Kozimi and M. D. Carelli, "Heat Transfer Correlation for Analysis of CRBRP Assemblies", CRBRP-ARD-0034, November, 1976.
- QCS760.28-21. J. L. Gillette, et al., "Experimental Study of the Transition from Forced to Natural Circulation in EBR-II at Low Power and Flow", Trans. ASME J. Heat Transfer 102, pp. 525-530, 1980.
- QCS760.28-22. PNL-4128, "A Validation Study of the CØBRA-WC Computer Program for LMFBR Core Thermal-Hydraulic Analysis", Part I - CØBRA-WC Generalized Parameters for Steady State Analysis, 1981.
- QCS760.28-23. PNL-4141, "Pretest Prediction and Post-Test Analysis of the FOTA Temperature Distribution during FFTF Natural Circulation Transients", (to be published in May, 1982).
- QCS760.28-24. A. E. Levin and P. Griffith, "Analytical and Experimental Simulation of Boiling Oscillations in Sodium with a Low Pressure Water System", AIChE Symposium Series No. 208, Vol. 77, p. 78, 1981.
- QCS760.28-25. R. J. Ribando, N. E. Clapp and M. A. Fontana, "Sodium Boiling in a Full Length 19-Pin Simulated Fuel Assembly (THORS Bundle 6A)", ORNL TM-6553, 1979.
- QCS760.28-26. ANL/RAS 77-48, "SLSF In-Reactor Experiment P: A - Interim Post-Test Report", 1977.

- QCS760.28-27. ANL-CT-80-25, "Thermal Transient Induced Pipe Flow Stratification - Phase I", by K. Kasza, et al., June 1980.
- QCS760.28-28. WARD-NC-94000-3, "Fluid Stratification in Piping: An Evaluation of Its Effect on LMFBR Plant System Natural Circulation Analysis", by A. C. Cheung, January, 1982.
- QCS760.28-29. Armond, A. A., "The Resistance During the Movement of a Two-Phase System In Horizontal Pipes", AERE-Trans-828, 1959.
- QCS760.28-30. Maresca, M. W. and Dwyer, D. E., "Heat Transfer to Mercury Flowing In-Line Through a Bundle of Circular Rods", Trans ASME J. Heat Transfer, 86, p. 180, 1964.
- QCS760.28-31. Dittus, F. W., and Boelter, L. M. K., University of California (Berkeley) Pub. Eng., Vol. 2, p. 443, 1930.
- QCS760.28-32. Thom, J. R. s., et al., "Boiling In Sub-Cooled Water During Flow Up Heated Tubes or Annuli", Proceedings of the Institution of Mechanical Engineers, 180 P+3C, pp. 226-246, 1965-66.
- QCS760.28-33. MacBeth, R. V., "Burn-Out Analysis, Part 4: Application of a Local Conditions Hypothesis to World Data for Uniformly Heated Round Tubes and Rectangular Channels", AEEW-R267, 1963.
- QCS760.28-34. McDonough, J. B., Milich, W., and King, E. C., "An Experimental Study of Partial Film Boiling Region with Water at Elevated Pressure in a Round Tube", Chemical Engineering Progress Symposium Series 57, No. 32, pp. 147-208, 1960.
- QCS760.28-35. Bishop, A. A., Sandberg, R. O., and Tong, L. S., "Forced Convection Heat Transfer at High Pressure After Critical Heat Flux", ASME 65-HT-31, 1965.
- QCS760.28-36. Heineman, J. B., "An Experimental Investigation of Heat Transfer to Superheated Steam in Round and Rectangular Channels", ANL-6213, September, 1960.
- QCS760.28-37. WARD-NC-3045-1, "LMFBR Natural Circulation Verification Program (NCVP) Review of Experimental Facilities and Testing Recommendations", by R. D. Coffield and H. P. Planchon, July, 1977.
- QCS760.28-38. Fission Product Decay Library of the Evaluated Nuclear Data File, Version IV (ENDF/B-IV). [Available from, and maintained by, the National Nuclear Data Center (NNDC) at the Brookhaven National Laboratory].
- QCS760.28-39. England, T. R. and Schenter, R. E., "ENDF/B-IV Fission-Product Files: Summary of Major Nuclide Data", LA-6116-MS (ENDF-223), October, 1975.
- QCS760.28-40. Meek, M. E. and Rider, B. F., "Compilation of Fission-Product Yields", NEDO-12154-1, January, 1974.

- QCS760.28-41. Reich, C. W., Helmer, R. G. and Putnam, M. H. "Radioactive-Nuclide Decay Data for ENDF/B", ANCR-1157 (ENDF-120), August, 1974.
- QCS760.28-42. Marr, D. R., "A User's Manual for Computer Code RIBD-II, A Fission-Product Inventory Code", HEDL\_TME-75-76, January, 1975.
- QCS760.28-43. Schmittroth, F., "Uncertainty Analysis of Fission-Product Decay Heat Summation Methods", Nucl. Sci. Eng., 59, p. 117, 1976.
- QCS760.28-44. Schmittroth, F., "Uncertainties in Fission-Product Decay Heat Calculations", Nucl. Sci. Eng., 63, p. 276, 1977.
- QCS760.28-45. England, T. R., Stamatelatos, M. G., Schenter, R. E. and Schmittroth, F., "Fission-Product Source Terms for Reactor Applications", Conference 770708, Proceedings of Topical Meeting on Thermal Reactor Safety, Sun Valley, Idaho (July 31 - August 4, 1977). Also LA-NUREG-6917-MS, August, 1977.
- QCS760.28-46. Schenter, R. E., Schmittroth, F. and England, T. R. "Integral Determination of Fission-Product Inventory and Decay Power", IAEA-213, August, 1977.
- QCS760.28-47. England, T. R., Schenter, R. E. and Schmittroth, F., "Integral Decay Heat Measurements and Comparisons to ENDF/B-IV and V", LA-7422-MS, NUREG-CR-0305, July, 1978.
- QCS760.28-48. Dickens, J. K., Emery, A. F., Love, T. A., McConnell, J. W., Northcutt, K. J., Peelle, R. W. and Weaver, H., "Fission-Product Energy Release for Times Following Thermal-Neutron Fission of Pu<sup>239</sup> Between 2 and 14000 Seconds", ORNL/NUREG-34, April, 1978.
- QCS760.28-49. Yarnell, J. L. and Bendt, P. J., "Calorimetric Fission-Product Decay Heat Measurements for Pu<sup>239</sup>, U<sup>233</sup>, and U<sup>235</sup>", NUREG/CR-0349, LA-7452-MS, September, 1978.
- QCS760.28-50. Morris, R. H., et al., "Single-Phase Sodium Tests In 61-Pin Full-Length Simulated LMFBR Fuel Assembly - Record of Phase I Experimental Data for THORS Bundle 9", ORNL/TM 7315.
- QCS760.28-51. Minushkin, B., Engel, F. C., Atkins, R. J. and Markley, R. A., "Heat Transfer Tests of an Electrically Heated 7-Rod Mockup of an LMFBR Radial Blanket Assembly", ASME-76-WA-HT-80, 1976.
- QCS760.28-52. Engel, F. C., Markley, R. A., and Minushkin, B., "Buoyancy Effects on Sodium Coolant Temperature Profiles Measured in an Electrically Heated Mockup of a 61-Rod Breeder Reactor Blanket Assembly", ASME-78-WA-HT-25, 1978.
- QCS760.28-53. Markley, R. A. and Engel, F. C., "LMFBR Blanket Assembly Heat Transfer and Hydraulic Test Data Evaluation", IWGFR-29, CONF-780296, pp. 229-253, 1979.



- QCS760.28-54. Engel, F. C., Markley, R. A. and Minushkin, B., "Heat Transfer Test Data of a 61-Rod Electrically Heated LMFBR Blanket Assembly Mockup and Their Use for Subchannel Code Calibration", In Fluid Flow and Heat Transfer Over Rod or Tube Bundles, ASME, New York, pp. 223-229, 1979.
- QCS760.28-55. Engel, F. C., Markley, R. A. and Bishop, A. A., "Laminar, Transition and Turbulent Parallel Flow Pressure Drop Across Wire Wrap-Spaced Rod Bundles", Nucl. Sci. and Eng., 69, pp. 290-296, 1979 and 74, p. 226, 1980.
- QCS760.28-56. Engel, F. C., Minushkin, B., Atkins, R. J. and Markley, R. A., "Characterization of Heat Transfer and Temperature Distributions in an Electrically Heated Model of an LMFBR Blanket Assembly", Nucl. Eng. Des., 62, pp. 335-347, 1980.
- QCS760.28-57. Engel, F. C., Markley, R. A. and Minushkin, B., "The Effect of Heat Input Patterns on Temperature Distribution in LMFBR Blanket Assemblies", ANS/ASME International Topical Meeting on Nuclear Reactor Thermal-Hydraulics, Saratoga Springs, NY, October, 1980, NUREG-CP-0014, Vol. 3, pp. 1643-62.
- QCS760.28-58. Engel, F. C., Minushkin, B. and Markley, R. A., "Comparisons of Design Code Predictions with LMFBR Blanket Heat Transfer Test Results", Trans. Am. Nucl. Soc., 35, pp. 665-668, 1980.
- QCS760.28-59. Atkins, R. J., Minushkin, B. and Engel, F. C., "Design, Construction, Characterization and Performance of LMFBR Blanket Assembly Simulator Rods", Proc. International Symposium on Fuel Rod Simulators - Development and Application, Gatlinburg, TN, Conf-801091, pp. 21-31, October, 1980.
- QCS760.28-60. Engel, F. C., Markley, R. A. and Minushkin, B., "Temperature Profiles in Natural and Forced Circulation of Sodium through a Vertical LMFBR Blanket Test Assembly", AIChE Symposium Series No. 208, 77, pp. 265-271, 1981.

Question CS760.30

The natural circulation event has been characterized as an extremely unlikely event justifying cladding temperature limits of 1720°F. Keeping in mind that the worst part of the transient is over in about 2-3 minutes (depending on pump coastdown time):

- a. Provide a clear basis for the frequency estimates for loss of offsite power and failure to start diesels within two minutes.
- b. Estimate the extent of fuel damage if the hot-spot temperature reaches 1720°F during a natural circulation event.

Response

- a. Updated Table 8.2-1 of the PSAR is provided to show that no outages have occurred on the Fort Loudon K-31 line since 1973. CRBRP has recently added a third Class 1E Diesel Generator which will increase the availability of the Diesel Generators. The revised estimates and basis for these estimates for loss of offsite power and failure to start diesels within two minutes will be provided when they are completed and will show further reliability improvement over previous estimates.
- b. The referenced 1720°F criterion is intended to preclude sodium boiling. However, the peak cladding temperatures achieved during a natural circulation event are considerably less than 1720°F.

The methods for evaluating the natural circulation event are outlined in PSAR Section 4.2.1; briefly, the procedure employs transient limit curves which are used in conjunction with conservative estimates of the cladding's in-transient temperature.

The transient limit curves for limiting fuel and blanket pins are summarized in PSAR Figures 4.2-26A, -26B, -28A and -28B. As shown, the cladding temperatures do not exceed their respective limits, even at goal lifetime.

Question CS760.36

Concerning the potential sodium/water reaction, the steam generator design considers only a design basis leak consisting of a single tube, double-ended guillotine rupture of a steam tube followed by two additional single double-ended tube guillotine ruptures, spaced at 1.0 second intervals.

- a. From the very closely packed CRBR steam generator tube arrangement, with one tube surrounded by six adjacent-tubes, if one steam tube was a double-ended rupture, the six adjacent tubes can be involved. Please discuss this case and include your analysis.
- b. In the three tube rupture model, the failures of second and third tube follow at 1.0 second intervals. The effects of this assumption are essentially the same as for a single tube rupture model. Further substantiation as to why adjacent tubes can't rupture at the same time is needed.
- c. What is the response to three simultaneous tube ruptures instead of three staggered ruptures?
- d. The TRANSWRAP results in the PSAR show the initial pressure pulse fails to burst the rupture discs. The peak pressure in the IHX is 331 psia and the design pressure for the IHX tubes is 325 psig. If more than one tube ruptures at the beginning, can the initial pressure pulse burst the rupture discs? What will be the pressure history in the IHX?
- e. The steam generator tube bundle is welded to the tube-sheets. During the Na/H<sub>2</sub>O reaction, the tube sheets suffer the highest pressure pulse impact. Due to hockey-stick shape of the tube bundle, the lower tube sheet will be the most affected. If the lower tube sheet fails, can't the water pour into the shell-side and provide further sodium/water reaction effects?

## Response

### a. Double-Ended Guillotine (DEG)

DEG failure of a steam generator tube is not a credible event. It is rather a convenient and conservative definition on which to base a calculation. Because conditions are not uniform around the initial tube failure, the adjacent 6 tubes will not all be equally affected. Typically, the initial failure will be the consequence of a local effect in the tube wall which results in a directional failure that restricts the reaction zone for potential overheating of adjacent tubes to those tubes that face the initial failure. Statistically, tubes are observed to fail to less than one DEG and to fail asymmetrically so that fewer than six adjacent tubes would be subsequently involved.

The Design Basis Leak (DBL) is derived from analysis of bench scale and large leak test data. Bench-scale tests have led to the understanding of how typical small leak progression occurs in the steam generator tube wall. Figure 15.3.3.3-1 in the PSAR illustrates a typical development of a leak within a steam generator tube. These tests have shown; (1) that a small initial leak progresses, resulting in a leak rate of  $10^{-2}$  lbm  $H_2O$ /sec within two hours, and (2) that a leak of  $10^{-2}$  lbm  $H_2O$ /sec magnitude can produce wastage rates of 0.001 to 0.005 inches/second on target material.

Large Leak Test Reg (LLTR) Series II Test A3 was a leak progression test initiated by exposing a pre-drilled 0.0013 in<sup>2</sup> hole simulating the self-wastage leak indicated in Step 5 in Figure 15.3.3.3-1. This initiator produced a wastage failure in a tube two rows away after sixty seconds. The failure area was less than 0.017 in<sup>2</sup> as compared to the CRBRP SG tube cross-sectional flow area of 0.13 in<sup>2</sup>. Conservative aspects of this result are: (1) the initiator was aimed and spaced to produce the maximum wastage rate on the target tube\*, (2) the sodium was initially static, and (3) the target tube contained initially static water. The leak from the 0.017 in<sup>2</sup> failure produced a wastage/overheating failure in the thin-wall (0.025" compared to 0.109" prototypic) injection tube within 25 to 37 seconds. The failure area in the injection tube was measured post-test as 0.125 in<sup>2</sup>.

---

\*The target distance (two rows away) was previously determined by bench scale experiments to yield the maximum wastage rate on the target tube.

Within 18 to 23 seconds after the injection tube failure, three tubes failed due to a combination of wastage/overheating, undercooling, and overpressure. The latter two effects were conservative in that the initially static, subcooled water in the tubes was vaporized and expelled into the water supply system and the pressure in the tubes rose to 2400-2600 PSI prior to failure. These three failures were determined to be 0.1, 0.20 and 0.17 in<sup>2</sup>.

Japanese large leak tests results have shown that (1) intermediate size leaks produced secondary wastage failures within tens of seconds: failure areas were 0.005 to 0.05 in<sup>2</sup>, and (2) DEG leaks did not produce secondary failure.

Based upon LLTR and foreign data, a plausible leak progression can be developed for the CRBRP steam generator. Taking the representative leak progression sequence illustrated in Figure 15.3.3.3-1 and assuming (1) a leak magnitude equal to or greater than that indicated in Step 1 of the progression depicted, (2) that this leak does not plug, and (3) that this leak and resultant leaks escape operator action, a plausible sequence is as follows:

1. Within two hours the leak has enlarged as shown in Step 5 of the progression depicted.
2. The enlarged leak produces a wastage failure in another tube after more than one minute. The area of this first secondary failure is 0.005-0.05 in<sup>2</sup>.
3. The total water injection rate of about one lbm/sec results in burst of the expansion tank rupture disks (150 PSID) within a few minutes. The event is then terminated by isolation and blowdown of the three steam generators in the affected loop.
4. It is conceivable that additional wastage failures could occur during the few minutes in which system pressure is increasing to the rating of the expansion tank disk. Given (1) that a water leak produces a turbulent diffusion flame which is itself situated in a turbulent flow field of high-conductivity, high-heat capacity liquid sodium, and (2) observed wastage failure areas, the size of these potential additional failures would very likely be comparable to the first secondary failure. These potential secondary failures would simply shorten the time to burst of the expansion tank disk. The sequence described above is considered to represent a conservative, plausible leak progression scenario.

In order to define a clearly conservative DBL (which is not intended to represent either a plausible or mechanistic sequence), it is necessary to include burst of the SWRPRS rupture disks (325 PSID). A rapid Equivalent Double-Ended Guillotine (EDEG) failure serves analytically to burst the SWRPRS disk and also to conservatively bound the failure magnitude. The DBL is defined as follows:

An Equivalent Double-Ended Guillotine (EDEG) failure ( $0.26 \text{ in}^2$ ) of a steam generator tube followed by two additional EDEG tube failures. The two additional EDEG failures occur as follows:

One additional EDEG failure occurs at one second after the initial EDEG failure.

A second initial EDEG failure occurs at two seconds after the initial EDEG failure.

This sequence of three EDEG failures occurs after an intermediate-size leak (less than a DEG) from a steam generator tube has increased local pressures in the IHTS to the threshold of SWRPRS rupture disk burst. The CRBRP DBL is conservative in both the magnitude of and the timing of secondary failures, compared to the conservative plausible leak progression scenario presented above.

- b. A tube failure mechanism already introduced into this discussion is a precursor tube leak, leading to an adjacent tube material wastage/overheating, subsequently leading to pressure rupture of a tube. Figure 760.36-1 shows an array of tubes in cross-section where tube "p" (precursor) is postulated to have an undetected material or manufacturing defect which eventually produces a leak which escapes operator action and causes wastage/overheating on one or more adjacent tubes. The shaded area depicts a potential leak jet, the other surface of which reacts with sodium and thereby develops a high temperature (theoretically as high as  $2700^\circ\text{F}$ , measured as high as  $2200^\circ\text{F}$  in LLTR tests). The source temperature for the overheating is greatest at the reacting interface between the water and the sodium, and less away from the reacting interface.

As the surface of the jet impinges upon the tubes the tube material heats up locally. Fluctuations in the geometry of the jet and the reacting interface during this dynamic event will mitigate the wastage of the adjacent tube but may be insufficient to prevent the metal temperature of an affected tube from rising locally to the point at which the tube wall is too weak to withstand the internal pressure and, therefore, ruptures. Any one of the affected tubes could reach this condition first.

When the pressure rupture occurs, a new, larger water/steam jet is created, with a different profile of tube impingement and localized material wastage/overheating. While the preceding smaller jet and localized material overheating profile may have raised spot temperatures on more than one tube, the pattern of localized overheating is immediately superseded by a new pattern caused by the new, larger water jet. The probability of an additional tube completing its localized wastage/heat-up to a failure temperature before the new overheating profile takes over is considered negligible. (Such an eventuality would be conservatively imposed upon an event which is already extremely unlikely). In any case, two tube failures, both with plausible rupture areas of 20% of an EDEG

tube failure, would still be umbrellaed by the one EDEG tube failure recommended for the design basis event definition. For added conservatism, it may be assumed the larger water jet and resulting material overheating pattern, may, like the precursor jet and associated overheating pattern, be sufficiently stable long enough for rupture temperature to be reached on a nearby tube thereby resulting in an additional tube rupture. On the one hand, the larger jet impinges on more tubes than did the precursor jet, thereby increasing the probability of a failure. On the other hand, the much larger jet is more turbulent and diffuse and less likely to permit the reacting surface of the jet to stay on any particular tube area long enough to overheat it to failure. Of more significance than either of these points is recognition that the new, large jet and resulting sodium/water reaction create a rapidly expanding bubble of hydrogen which drives the sodium rapidly away from the tube rupture location. This rapid movement of the sodium interface substantially reduces the potential for a stable reaction zone on the stationary tube surfaces.

- c. As discussed previously the CRBRP DBL is clearly conservative in both magnitude and timing of secondary failures. As such, the Project considers it inappropriate to evaluate the simultaneous tube ruptures.
- d. Referring to the footnote on Table 5.5-11 of the PSAR, the water injection history input to the TRANSWRAP calculation of the SWR DBL in the evaporator correspond to the following leak sequence:

<u>Time (Sec)</u>	<u>Event</u>
0.0 - 0.3	Water flow rate constant at 2.5 lb/sec (this represents the undetected moderate sized leak which has pressurized the system to just below the disk burst pressure - PSAR page 5.5-24b).
0.3	First Equivalent Double-Ended Guillotine (EDEG) break.
1.3	Second EDEG.
2.3	Third EDEG.

Referring to Figure 5.5-4A and page 5.5-28 of the PSAR, the sharp increase in IHX pressure at 480 milliseconds corresponds to evaporator rupture disk buckling in response to the first EDEG at 300 ms. Predicted peak pressure in the IHX is 331 PSIA as compared to an allowable\* range under emergency conditions of 400 to 760 PSIA.

\*Based on ASME Code Case 1331-8 primary membrane stress criteria.

As discussed previously the CRBRP DBL is clearly conservative in both magnitude and timing of secondary failures. As such, the Project considers it inappropriate to evaluate more than one tube rupture at the beginning.

- e. The results of the analysis of the Na/H<sub>2</sub>O reaction predict that the maximum pressure, 365 PSIA, occurs on the upper tube sheet. The pressure time history at this location is shown in Figure 5.5-4b. The peak pressure at the lower tube sheet during this event is 348 PSIA.

The design pressures on the tubesheets are 325 psig on the sodium side and 1900 to 2400 psig on the water/steam side depending upon the tube sheet location and whether the unit is an evaporator or superheater. Since these Na/H<sub>2</sub>O reaction peak pressures would be enveloped by the design pressure differentials across the tubesheet, these loadings can be accommodated with the same degree of structural reliability as normal operation.



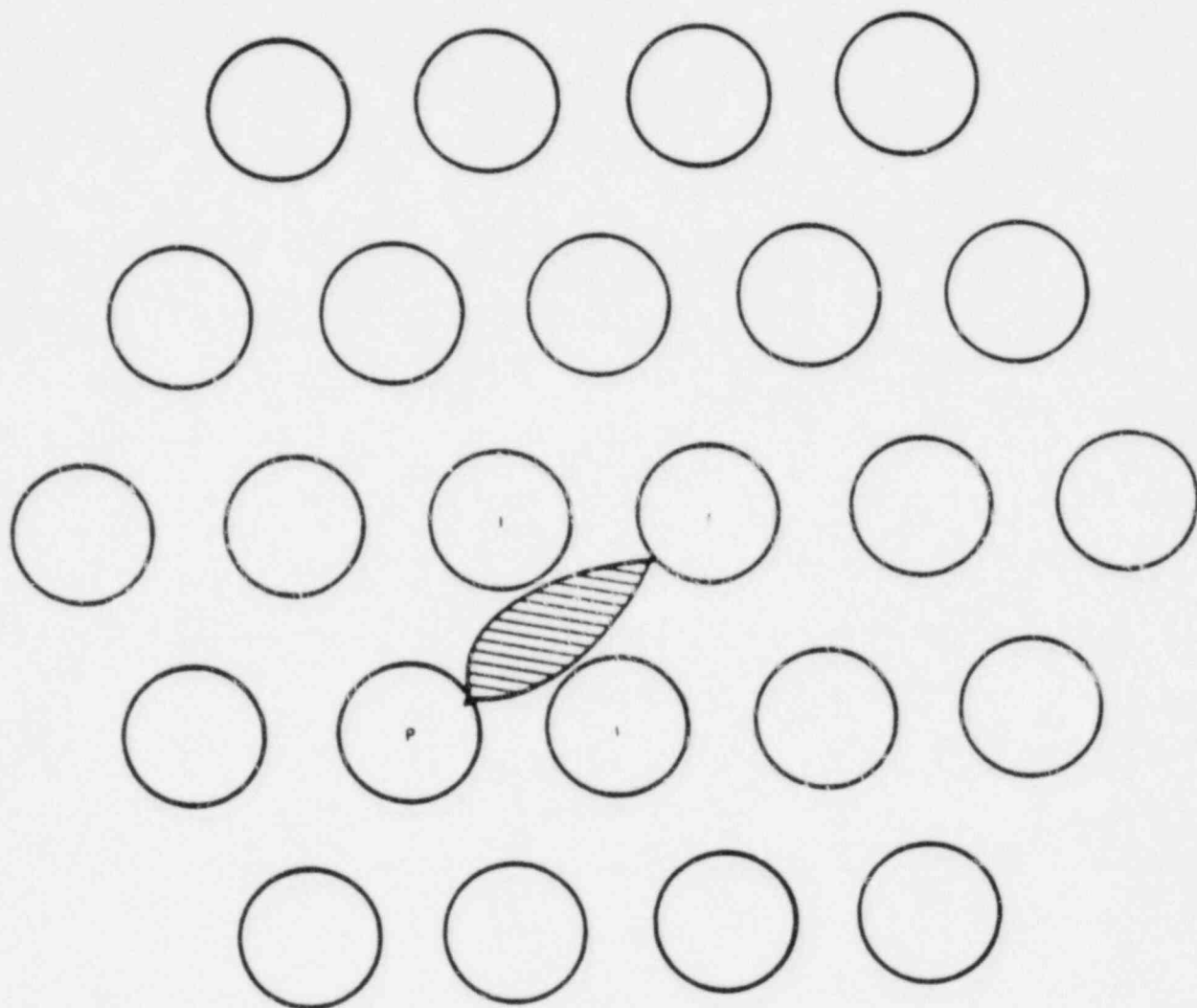


FIGURE 760.36-1

PRECURSOR LEAK "P" PRODUCES JET WHICH HEATS ADJACENT TUBES

Question CS760.105

In Section 5.5.3.6 (Evaluation of Steam Generator Leaks), the design basis leak (DBL) appears to be based on limited operational experience, (with different steam generators) a number of non-prototypical tests and a few prototypical tests. Thus, it appears rather optimistic to conclude that "The conservatism of this postulated DBL will be confirmed through the LLTR test program."

- a. Assuming this test program does not progress as anticipated, and that a larger design basis leak must be considered, identify the largest leak which can be tolerated by the currently proposed design and discuss the feasibility of design changes to accommodate even larger leaks.
- b. Are the systems (particularly the pressure relief system) capable of being modified to accommodate a larger leak if further testing makes it advisable?

Response

- a. The completed LLTR Test Program has confirmed the conservatism in the design basis leak. PSAR Section 5.5.3.1.5.1 has been updated to reflect the results.
- b. The IHTS piping and IHX are adequately protected by the pressure relief system as presently designed. If a change is made to increase the leak size changes may be required in the IHTS piping installation, as well as changes in the pressure relief system.

Question CS760.110

The pump head provided by the various main feedwater and auxiliary feedwater pumps will vary with mass flow rate and pump speed. What are the relationships? Are homologous pump curves available?

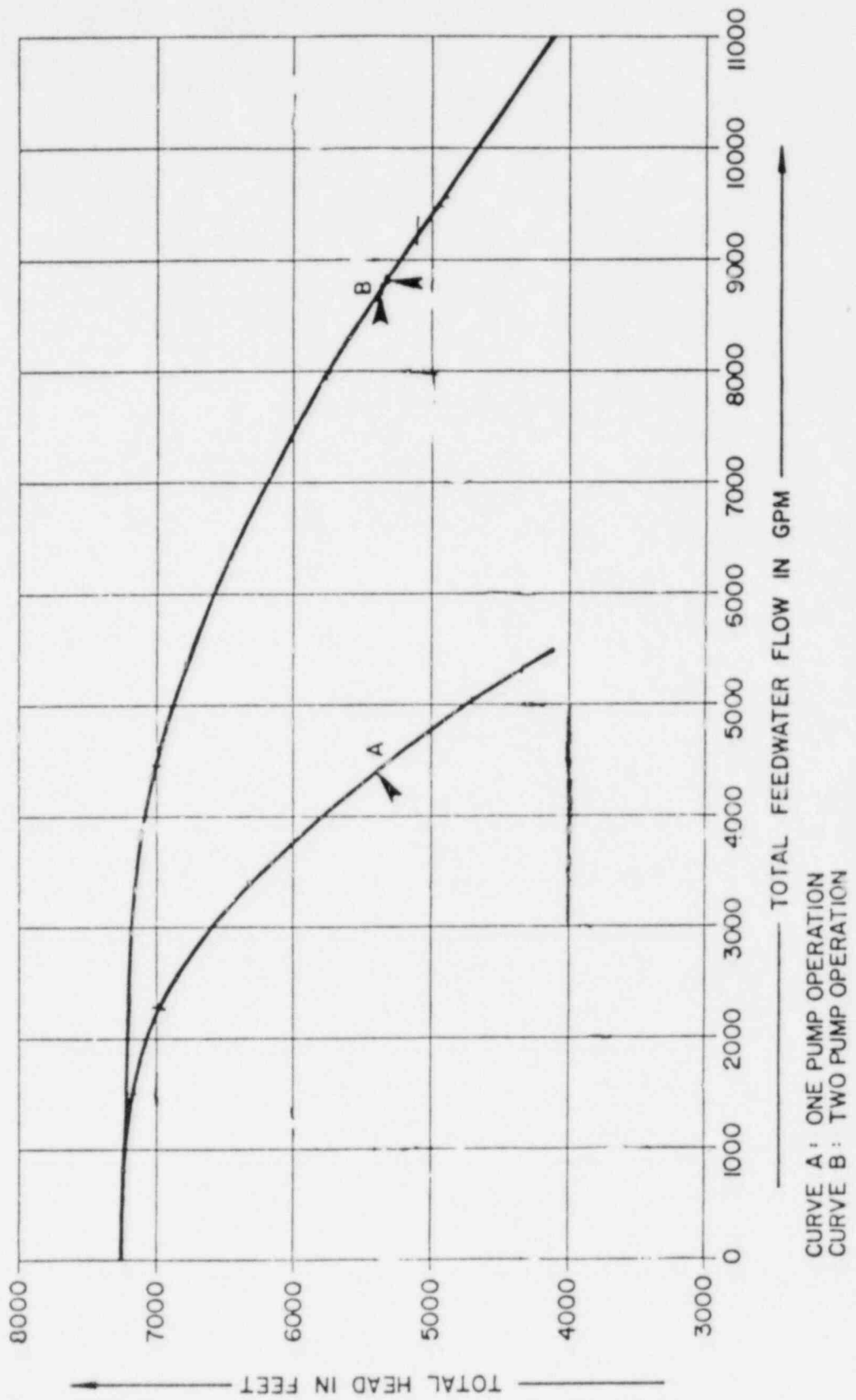
Response

The main (steam generator) feedwater pumps are designed to operate at constant speed. The design speed is 3579 RPM for each of the three 50% capacity motor-driven pumps. The predicted constant speed characteristic curve at the design speed for these pumps is shown in Figure CS760.110-1. These pumps are not safety-related, see Section 10.4.7.1 of the PSAR. As such, the applicant will not specifically update this information if changes are made to this technical information unless requested by the NRC.

The AFW pumps are designed to operate at a constant speed. The design speed is 3560 rpm for the two motor-driven pumps and 4000 rpm for the turbine-driven pump. The predicted constant speed characteristic curves at the design speed for the motor-driven and turbine-driven pumps respectively, are provided in PSAR Figures 5.6-11 and 5.6-12.

Figure CS760.110-1

STEAM GENERATOR FEED PUMP  
HEAD - CAPACITY CURVE



Question CS760.116

The presentation describing the protected air cooled condensers (PACC) needs clarification. Details are needed with respect to tube size and number, tube inner and outer diameter, air volume constraints, estimated natural draft air speed, fan speeds, and so forth. Natural circulation is easily demonstratable if the heat transfer is known. It is essential that the heat removal capability be established for the PACCs under the varying operating conditions.

Response

A description of the PACC heat exchanger tubes is provided in revised PSAR Section 5.6.1.2.3.1, "Protected Air Cooled Condensers (PACC)."

The forced draft air flow for each tube bundle is provided by an axial flow fan which operates at 1200 rpm. At thermal hydraulic design conditions, the air flow is 77600 SCFM with a corresponding fan design power requirement of 53 bhp.

The PACC design will provide air flow control from 10 to 100 percent of rated flow. The PACC design will have natural draft capability. Under natural draft operation an estimated heat removal capability of 32 percent per PACC is available and lead unit tests will be performed at reduced water/steam side pressure to confirm the natural draft heat rejection capability.

Question CS760.131 Transient Effects (5.7.5)

In general, the design transients are not sufficiently described to understand the conditions or the analytical results. The transients are said to be more fully described in Chapter 15 but clarification is needed. In particular, the analysis for the OBE in Chapter 5 quotes a 5 minute manual plant trip whereas the correspondence between Chapter 5 and 15 analyses for the loss of steam generator load is not self-contradictory, but needs to be addressed due to the difference in time scales.

- a. What are the difference between the results presented in 5.7 and those analyzed in Chapter 15. Provide justification for differences.
- b. For the loss of load transient (Section 5.7.3d) provide the steam generator temperature and pressure response and the core temperatures to 2000 seconds.

Response

No inconsistency between Chapters 5.7 and 15 has been identified. It should be noted that the apparent difference in the discussion of the Operating Basis Earthquake (OBE) in these two chapters is due to the differences in application of the OBE to the HTS (Chapter 5.7) and to the Reactor (Chapter 15.2 Reactivity Insertion Design Events). Paragraph 5.7.3.c has been amended to clearly describe the application of the OBE to HTS component analyses.

The steam generator temperature and pressure response and core temperature response is provided in Figures 5.7-6a-k. These data are based on the plant thermal hydraulic design conditions with the hot and cold leg sodium arbitrarily increased 20°F.

It should be noted that inadvertant actuation of the water/steam side of the Sodium/water Reaction Pressure System results in dumping of water/steam sides of both evaporators and the superheater.

Question CS760.166

Please provide a description of how the cell liners and catch pans will be installed in the plant (i.e., construction sequences) to maintain the desired gap for venting between the steel and concrete.

How will it be verified that these spaces were installed correctly after construction?

Response:

Cell Liners:

The cell liner air gap, located between the cell liner plate and the insulating concrete, is prefabricated during the construction of the modular cell liner panels. The CRBRP cell liners for walls and ceilings are installed in prefabricated modular panel sections consisting of the cell liner plate, continuous air gap, liner stud anchors and insulating concrete panel as shown in Figure QCS760.166-1. These modular panels are used as forms for the structural concrete.

The following method summarizes the procedure proposed for use in prefabricating the cell liner air gap. The cell liner plate is precut to size and the stud anchors are installed using the automatic stud welding process. The cell liner panel is placed horizontally with the stud anchors facing upwards and a form for the insulating concrete is placed around its perimeter and around each penetration and embedment location. Over the head of each liner panel stud anchor, 3/8" thick spacer washers are inserted and placed on top of the liner plate. On top of the spacer washers a layer of galvanized expanded metal lath is placed. Slits are cut in the metal lath at the liner stud locations to permit insertion through the stud heads. On top of the expanded metal lath layer, a layer of fine galvanized mesh screening is similarly placed. The fine mesh screen is coated with a combination concrete sealing compound and bond breaker to prevent the insulating concrete from forming laitance on the fine mesh screen and expanded metal lath.

The insulating concrete is then placed on top of the prepared panel and is allowed to cure a minimum of 7 days before the inspection of the air gap. Figure QCS760.166-2 depicts the air gap formation method described.

The air gap formed behind these prefabricated panels will be non-destructively examined prior to installation in the plant to assure continuity of the air gap. The specific examination techniques have not been established but may include direct measurement, use of feeler gages, or optical inspection. During erection and installation the insulating concrete panel joints are sealed. The cell liner panels are welded together and the panels are used as forms for the structural concrete.

Provision for the inspection of the air gap following the liner installation and placement of the structural concrete will be included. Local temporary removable access plates have been located opposite each cell liner vent for the testing of the cell liner vent piping and the in-situ testing of the air

gap. The liner vent piping will be flow tested to assure vent continuity. The proper installation of the air gap will be verified by non-destructive methods or by flow testing. The specific provisions of the vent system testing have not been established.

The proposed method of fabricating the cell liner air gap described in this response will be pretested before final construction and inspection procedures are confirmed. This pretesting program will evaluate alternative methods of air gap formation and alternative non-destructive examination methods of inspecting the air gap behind the liner.

The cell liner floors are constructed in a different sequence than the walls and ceilings. The cell liner floor configuration is shown in Figure QCS760.166-3. The venting of the cell liner floor is provided by a 1/8 inch nominal air gap between the insulating concrete and the liner plate and also by the vent space provided on each side of the embedded beams supporting the cell liner floor plates. This vent space communicates directly with the air gap located in the liner walls.

The elevations of the top of embedded beam steel and top of structural concrete are controlled to result in a 1/8 inch gap when the cell liner plate is placed over the insulating concrete floor panels. These concrete panels are supported on the top of structural concrete and are placed between the embedded beams. They are restrained from lateral movement by angles welded to the web of the embedded beams and extend to the outside projection of the beam flange. These vent spaces will be verified prior to the placement of the cell liner floor panel and the welding of the liner plate to the supporting embedments.

#### Catch Pans:

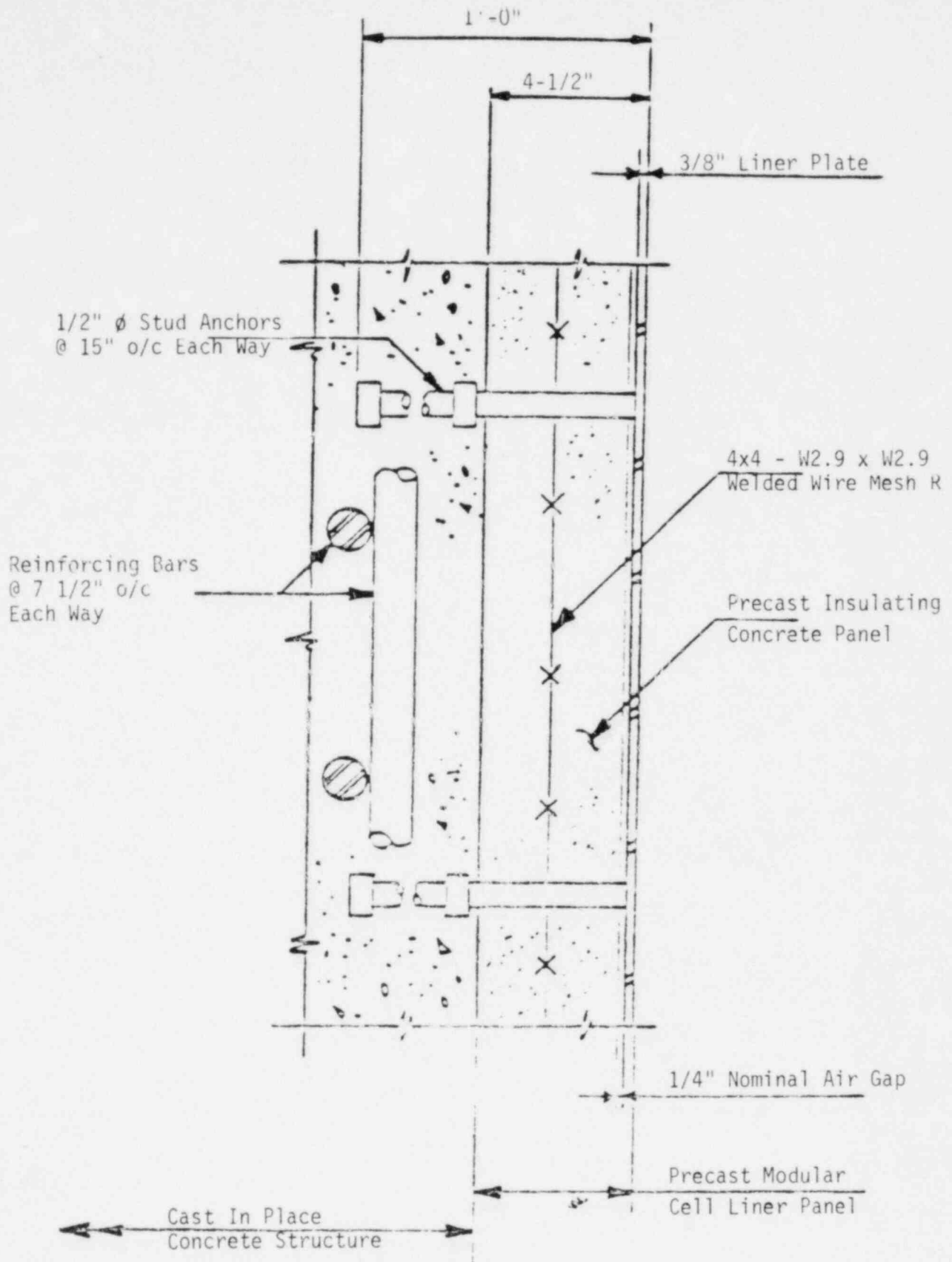
The catch pan system does not have a specially constructed air gap as does the cell liner system.

Because the catch pans are designed to expand freely under thermal loads, there is a space between the catch pan side walls and the building walls to allow for free thermal expansion. This space will provide a minimum entry gap of 1/4 inch under extreme thermal conditions.

Under the catch pan floor, a layer of MgO aggregate is provided to mitigate thermal effects on the supporting reinforced concrete floor. Water vapor released from the concrete will flow through the voids in the MgO aggregate and pass through the space provided around the catch pan side walls. The catch pan system is installed in the equipment cells after the completion of the concrete construction.

Since the catch pans are installed after the completion of the concrete cell structure the gap around the catch pan side walls will be controlled by direct measurement. See Figure QCS760.166-4.

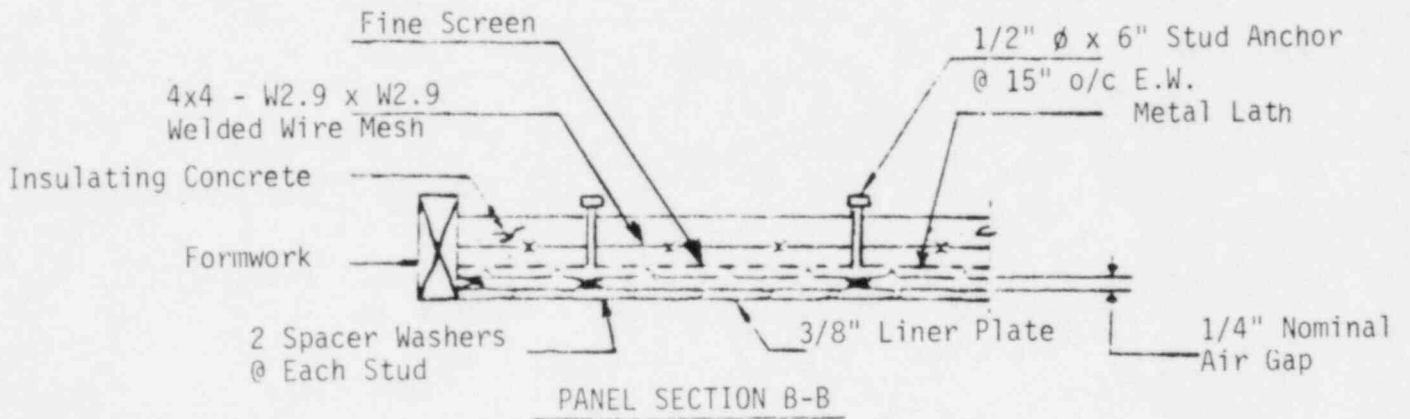
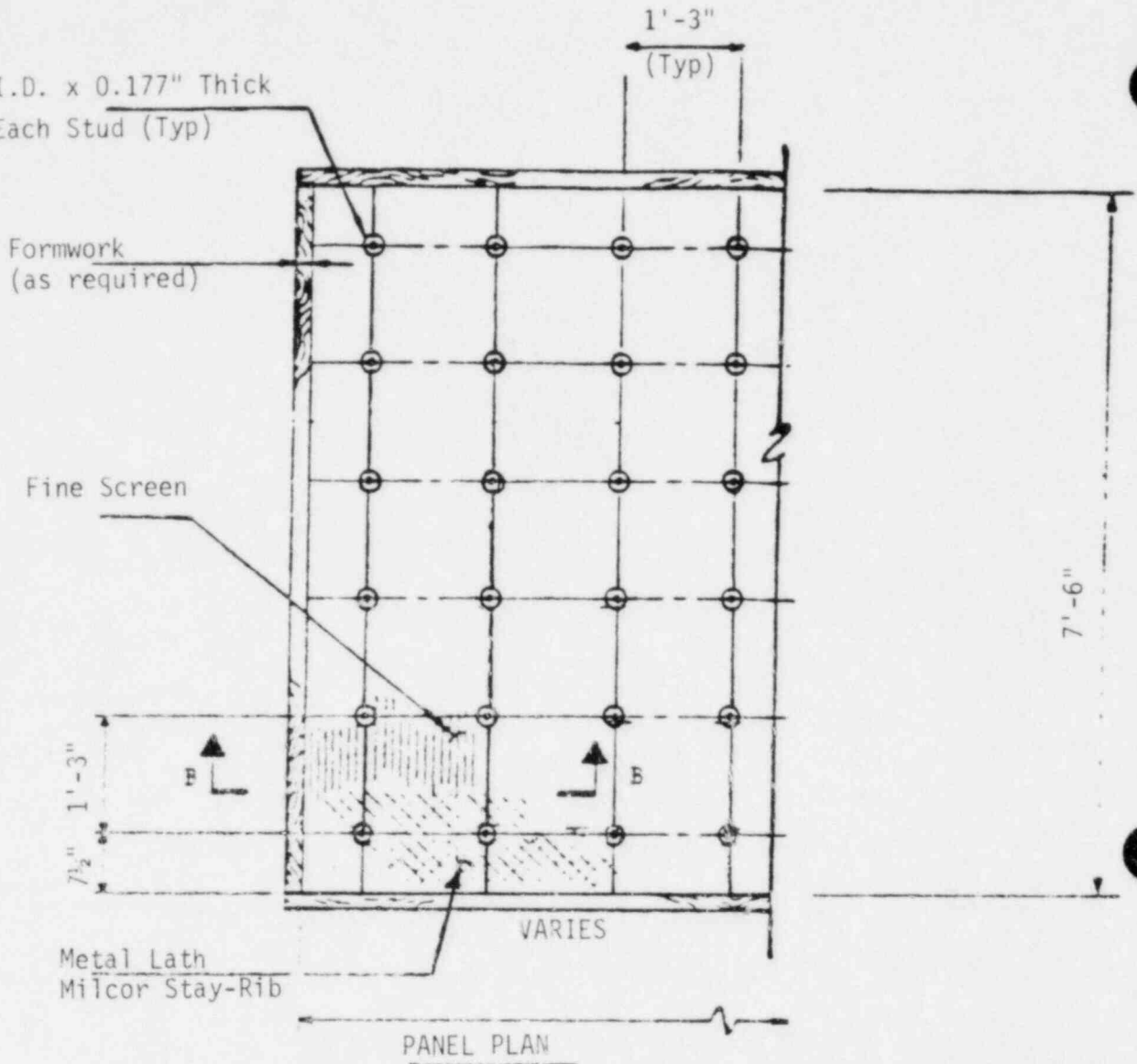




TYPICAL WALL/CEILING LINER PANEL

FIGURE Q760.166-1

2 1-1/16" I.D. x 0.177" Thick Washers @ Each Stud (Typ)

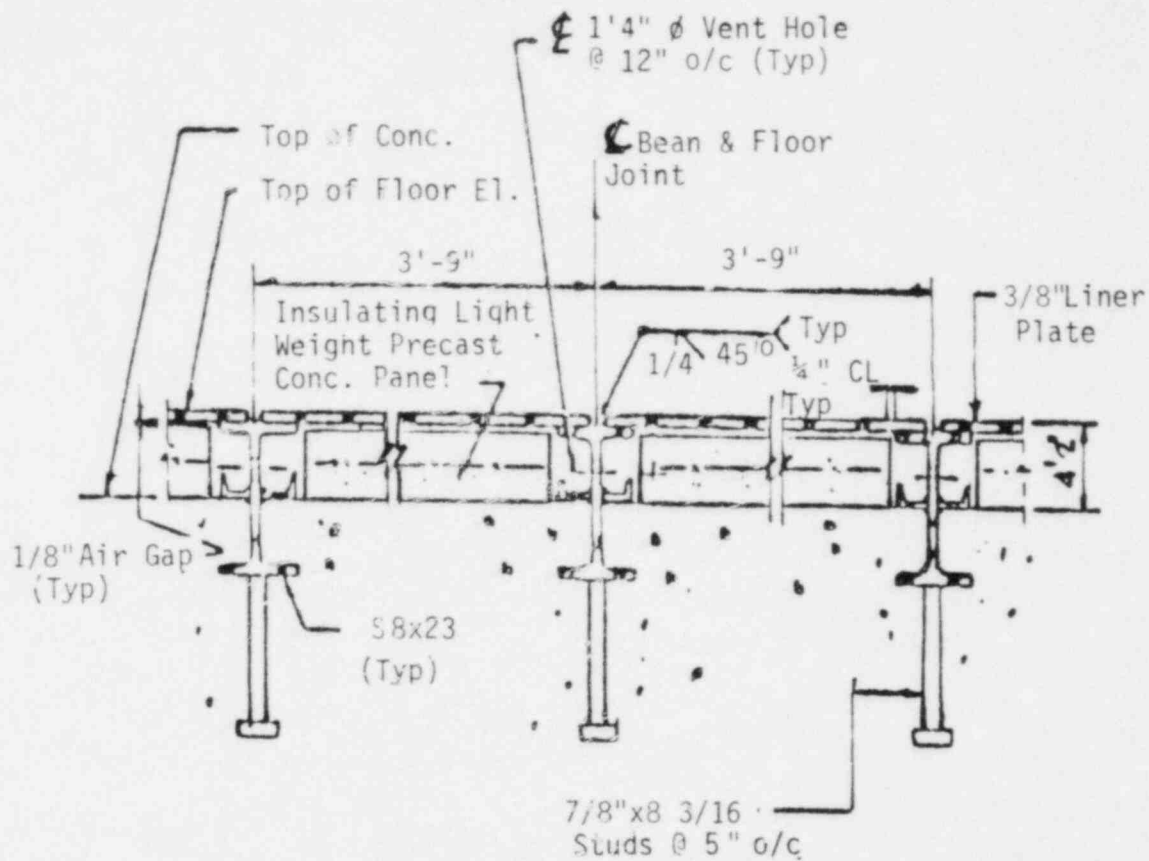


AIR GAP FABRICATION

FIGURE Q760.166-2

QCS760.166-4

Amend. 72  
Oct. 1982

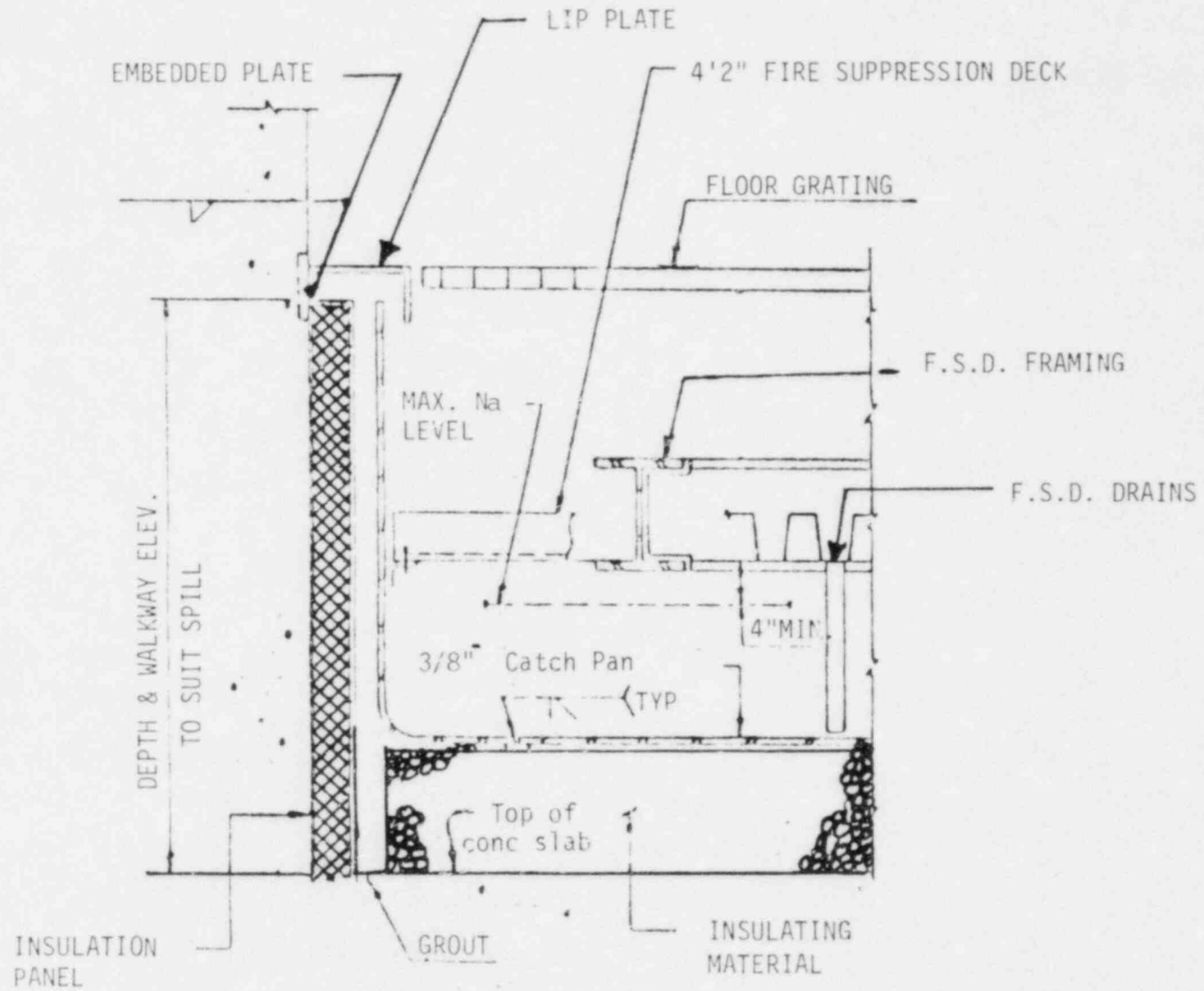


QCS760.166-5

Amend. 72  
 Oct. 1982

TYP FLOOR LINER PLATE DETAIL

FIGURE Q760.166-3



QCS760.166-6

Amend. 72  
Oct. 1982

CATCH PAN WITH FIRE SUPPRESSION DECK

FIGURE QCS760.166-4

Question CS760.172

Please provide simplified sketches of all sodium systems (exclusive of the primary and intermediate HTS) showing the sodium volumes in each major portion of the system and the location (cell number) of each system or portion of the system.

Response:

The simplified sketches and additional information requested are provided in Figures CS760.172-1, 2, and 3. Both sodium and NaK piping and components are included in these figures. Sodium inventories in the components, and cell locations of these components are indicated on these figures. All sodium inventories are referenced to a 400oF coolant temperature, except the primary sodium overflow vessel inventory which is also given for the primary system operating temperature of 850oF.

QCS760.172-2

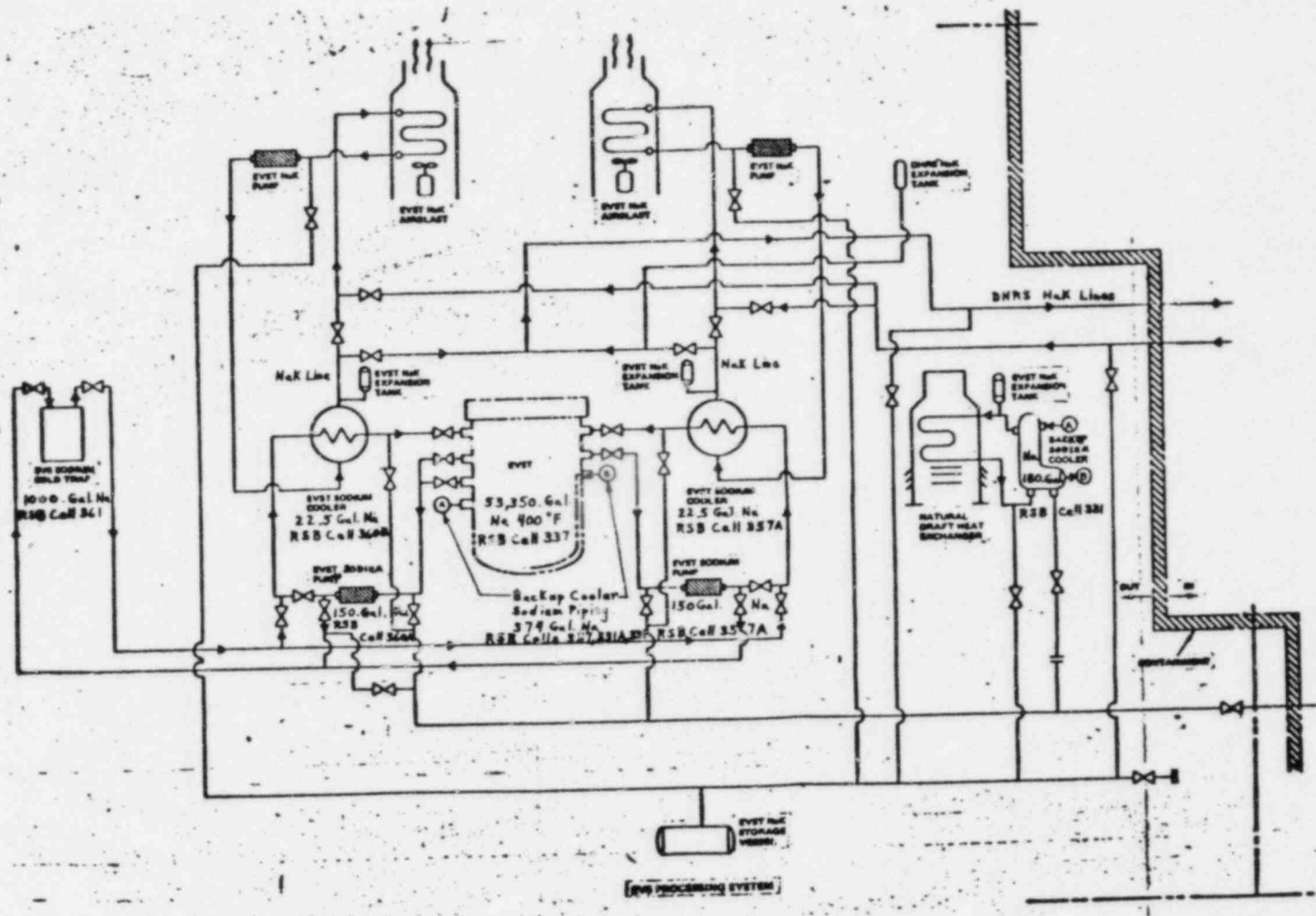


FIGURE CS760.172-1

SODIUM VOLUMES IN THE REACTOR SERVICE BUILDING

Amend. 72  
Oct. 1982



QCS760.172-4

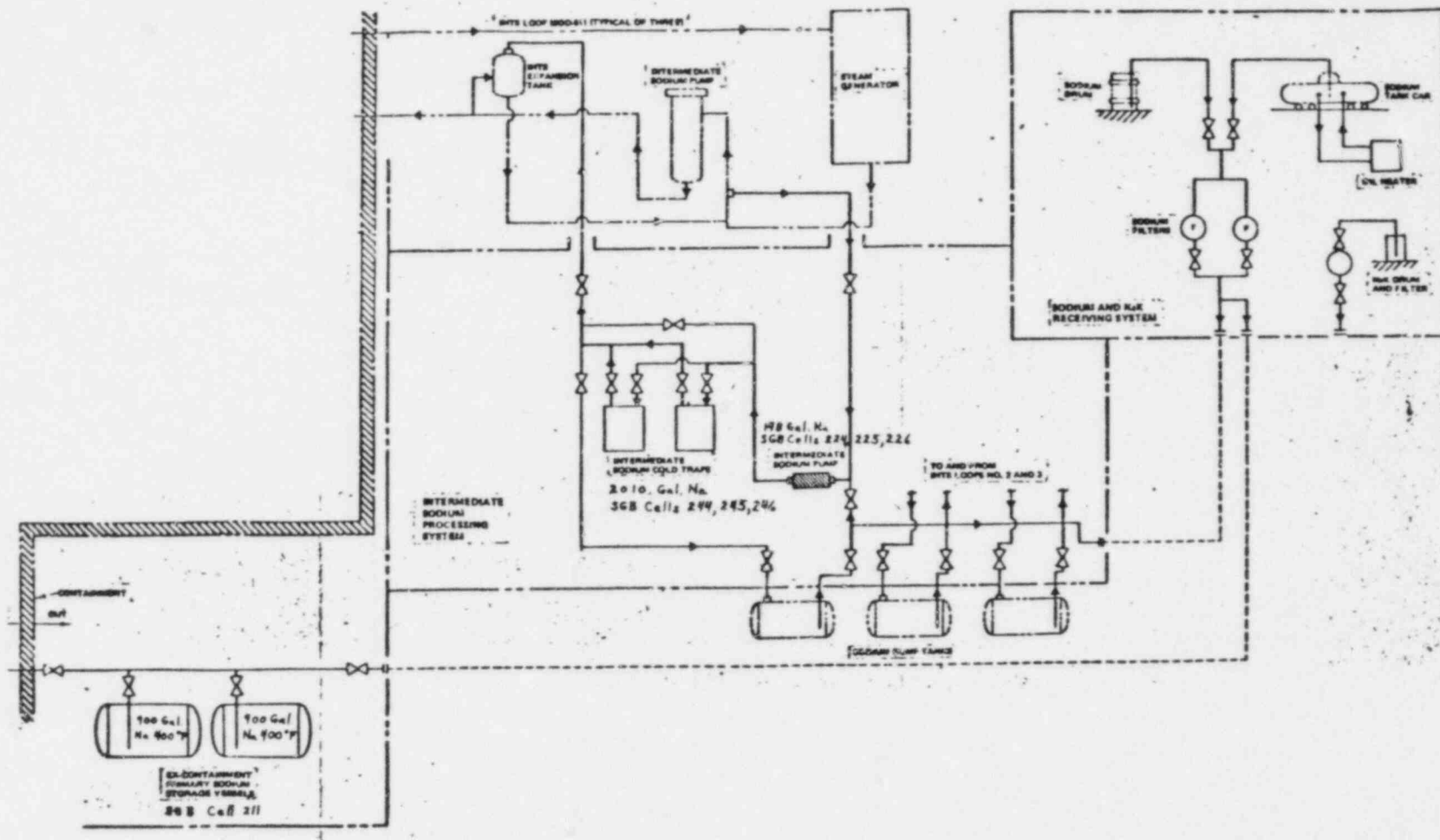


FIGURE CS760.172-3  
SODIUM VOLUMES IN THE STEAM GENERATOR BUILDING

Amend. 72  
Oct. 1982



Question QCS760.175

To enable us to make confirmatory calculations of some key parameters in the nuclear design area the following information is requested:

- a) DOPPLER COEFFICIENT - For BOC 3 conditions please provide the input data (except for the 30-group cross-sections) for each of the steps and codes shown in Fig. 4.3-26 of the PSAR.

Also, please provide the data you used for any biases (derived from critical experiments or SEFOR analysis) applied to your Doppler calculations.

- b) SODIUM VOID COEFFICIENT - For EOC 4 conditions please provide the input data (except for the 30-group cross-sections) for each of the steps and codes shown in Fig. 4.3-28.

Also, please provide the input data for the critical assembly calculations used to determine the sodium void uncertainty.

The above data does not have to be sent as one complete package, but rather should be sent as it becomes available.

Response:

The information requested has been supplied under separate cover in Reference QCS760.175-1.

Reference:

QCS760.175-1 Letter, HQ:S:82:083, J. R. Longenecker to P. S. Check, dated August 20, 1982.

Question QCS760.176

In preparation for writing those sections of the SER dealing with PCRDM, we have found it necessary to secure additional documentation on the D. C. stepper motor used in the system. Specifically, we would like to obtain the following information:

1. Complete description of the motor
2. Equipment specification for the motor, and
3. Test information or data establishing that the specifications are met, including the maximum withdrawal speed in the event an over-speed signal is sent to the controller.

We would also like to know the maximum slew rate of the motor and what power input conditions, however improbable, that would be required to obtain it.

Response:

ITEM 1

Description of PCRD Motor

The PCRD utilizes a collapsible roller nut design which has been successfully used in the past on pressurized water reactors. This type of drive has a non-rotating leadscrew which is driven up or down by a fixed elevation roller nut formed by four ball bearing mounted rollers, equally spaced around the leadscrew. The rollers are inclined from vertical at the leadscrew helix angle and have teeth which engage the leadscrew threads to provide a positive connection to the translating assembly. Two rollers are mounted in each segment arm which are attached by pivot pins to a rotor carried on ball bearings in the motor tube. The complete assembly is shown in PSAR Figure 4.2-101. The motor tube is shown in Figure QCS760.176-1, the segment arms and roller nuts in Figure QCS760.176-2, and the stator in Figure QCS760.176-3.

The roller nut is actuated by a six-phase, four pole stator mounted outside the motor tube. The stator and segment arms together form a reluctance type synchronous stepping motor. The stator windings are energized by direct current which can be switched in a programmed sequence among the six-phase to produce a stepwise rotating magnetic field in the armature region (see Fig. QCS760.176-4). The two segment arms, which make up the motor armature are fabricated from permeable stainless steel and tend to align themselves with the rotor field so as to minimize the magnetic circuit reluctance between adjacent stator poles. The motor armature is, therefore rotated in synchronism with the rotating stator field.

The segment arms pivot in a vertical plane through the leadscrew centerline and are constrained to move through the same angle by means of a synchronizer bearing mounted at the top of the rotor. The armature region of each segment arm is located above the pivot pin, while the rollers are mounted below the pivot pin. When the stator is not energized, the segment arms are held in the collapsed position by springs acting outward below the pivot pin. In this position, the rollers are disengaged from the leadscrew, and the armature section of the segment arms are displaced inward toward the mechanism centerline. When the stator is energized, the armature section of the segment arms are magnetically attracted toward the stator with a force sufficient

to overcome the segment arm spring force and engage the rollers with the leadscrew.

The direction of leadscrew travel is determined by the direction of rotor rotation which, in turn, is determined by the particular switching sequence applied to the stator phase windings. The speed of rotation is controlled by the switching rate, which is adjustable over a wide range by the controller. The rollers remain engaged to the leadscrew during reversal of rotation direction.

If the switching sequence is stopped and the stator is left energized in any of the twelve (12) possible phase combinations, the segment arms continue to be attracted outward and they will hold the leadscrew indefinitely at the elevation achieved when the rotation was stopped. The windings comprising the six phases are so arranged that when energized in a 3 - 2 sequence, the force-pole magnetic pattern formed by the stator rotates in space in 15-degree steps. If the six phases are designated by the letters, A, B, C, D, E and F the sequence for rotation is shown below.

Rotational Degrees	0	15	30	45	60	75	90	105	120	135	150	165
Phases Energized	AB	ABC	BC	BCD	CD	CDE	DE	DEF	EF	EFA	FA	FAB

As shown above, the motor is energized in either a two phase or three phase mode in the hold condition and switches from two phase-to three phase-to two phase while in the run mode. Since the motor is either in a two phase or three phase condition during hold, the two conditions will produce different magnetic field strengths. Theoretically, the three phase condition should produce 1.5 times the magnetic flux of the two phase mode, but in the real motor, it is less than this ratio due to temperature and saturation effects.

For the motor to produce torque, the induced poles in the rotor must lag the stator poles. The torque is roughly a sinusoidal function of the lag angle, and in actual operation, the lag angle adjusts itself to the value just sufficient to balance the applied torque resisting rotation, up to the pull out or pole slip value. The radial moment on the engaged segment arms, called holding moment, is also a function of the rotor lag angle, and in this type of rotor increases somewhat as the lag angle departs from zero.

The radial moment also varies strongly as a function of the collapse angle of the segment arms (as does the peak torque) because of the large change in air gap and the corresponding change in flux linking the arms. Since the segment arms are held in the collapsed position by eight coil springs, the moment required to overcome the springs and bring the rollers into engagement (latch) plots as a straight line, with force increasing toward the fully engaged position. This relationship is shown in Figure QCS760.176-5.

During steady state operation (run or hold mode) the available torque and moment are determined by the available current. The run - hold voltage is specified to be  $175 \pm 5$  volts DC, and will be controlled within this range. Therefore the available current is determined by the resistance of the winding, and the resistance is a function of the stator winding temperature. The temperature of the winding is controlled by a constant flow of nitrogen gas. The specified operating parameters of this stator cooling system are:

Inlet temperature	$55 \pm 5^{\circ}\text{F}$
Outlet temperature	$140^{\circ}\text{F}$ maximum
Pressure at inlet	90 psig minimum 100 psig minimum
Flow	$157 \pm 10$ scfm

During acceptance testing of the PCRDMS at the vendors plant the following typical operating parameters were determined:

Outlet coolant temperature	$= 120 \pm 5^{\circ}\text{F}$
Phase resistance	$= 24.6 \pm 4$ ohms (hot)
Phase current	$= 7.1 \pm .1$ amps

## ITEM 2

The equipment specification for the PCRDM motor is contained in and is a part of the equipment specification for the Primary Control Rod Drive Mechanism. The following are those sections which apply to the motor.

### I. ASME Code Classification

- A. The mechanism motor tube, motor tube holddown ring, and position indicator housing act as part of the reactor primary system boundary, and shall be constructed as a Class 1 vessel meeting requirements of the ASME Boiler and Pressure Vessel Code, Section III.
- B. The design of the CRDM shall be based on the Fast Flux Test Facility (FFTF) CRDM as defined on component drawings.

### II. Environment and Duty Cycle

- A. The external surfaces of the CRDM are exposed to the Head Access Area (HAA) air temperature of 85 °F during normal operation and 140°F maximum for loss of HAA cooling. Normal CRDM internal pressure ranges from 0-20 psig. Design condition for ASME Code evaluation are 500°F and 35 psig.

### B. Neutron Environment

Neutron dose levels above the closure head in the vicinity of the control rod drive mechanisms may range from 100 mr/hr to <2 mr/hr. A shield system/seismic support will shield areas above 100 inches. The corresponding total neutron flux range is approximately  $2 \times 10^4$  r/cm<sup>2</sup>/sec to  $2 \times 10^2 \times 10^2$  n/cm<sup>2</sup> sec.

The above total fluxes correspond to a fast neutron flux  $<2 \times 10^2$  n/cm<sup>2</sup>/sec.

- C. The design life of the CRDM shall be 30 years.

#### D. Duty Cycle

* Total start-stop cycles	$8 \times 10^6$
** Total lifetime scrams	732
***Lifetime travel (0.36 to 9.0 ipm)	17,000 feet

- 
- \* One motor step equals a start-stop cycle
  - \*\* Includes 150 isothermal test scrams
  - \*\*\*Includes start-stop cycles

### III. Loading Conditions

#### A. Stroke

The CRDM shall provide a minimum withdrawal stroke of 36.00 inches as measured from the nominal position (station -351.025) of the top of the control assembly disconnect coupling to the minimum up position of the CRDM rotational stop. The CRDM insertion stroke shall reach and couple with the control assembly at the lowest position with the top of the control assembly disconnect coupling at -351.750. The CRDM maximum withdrawal stroke shall not exceed 37.80 inches as measured from the lowest position (station -351.750) of the top of the control assembly disconnect coupling to the maximum up position of the CRDM rotational stop. The stroke requirements are referenced to a 70°F temperature environment.

The CRDM shall be capable of providing an incremental motion of 0.025 inches (nominal). The nominal selectable in and out CRDM speed range shall be 0.36 to 9.0 inches per minute. The maximum possible withdrawal speed of the CRDM with a failed controller shall be less than 73 inches per minute.

## B. CRDM/CRD Operating Forces

The CRDM shall be designed to exert the following forces:

1. Minimum insertion force on control rod (stuck rod) 1,000 lbs.
2. Minimum withdrawal force sufficient to overcome all worst case forces acting on the control rod assembly is 285 lbs. This force includes control assembly weight (167 lbs), bouyant forces (-30 lbs) and rod friction (148 lbs) acting over the first 8 inches of withdrawal. When the rod is withdrawn above 8 inches and the rod friction force is reduced to 48 pounds and the total force is reduced to 185 lbs.

The CRDM and CRD shall be designed to withstand the following loads. The temperature under which these loads are to be applied is 400°F.

3. Maximum leadscrew driveline tensile load 20,000 lbs
4. Maximum position indicator rod compressive load at refueling temperatures. 1,000 lbs

The CRDM shall resist outward motion of the translating assembly;

5. With the segment arm rollers engaged to the leadscrew (latched), the translating assembly shall not move up when a constant up force of 1800 lbs, or less, is applied to the control rod coupling interface.
6. During a scram operation (stator power interrupt and roller unlatching) the translating assembly outmotion shall be limited when a constant up force of 1800 lbs, or less, is applied to the control rod coupling interface.
7. With the rollers disengaged (unlatched) and the pawl engaged to the leadscrew, the translating assembly outmotion shall be limited when a constant dynamic up force of 1800 lbs, or less, is applied to the control rod coupling interface. Prior to pawl engagement the out-motion velocity is limited (by sodium flow rate) to 25 ips.



8. Since the CRDM employs a pawl design which positively prevents axial outmotion after engagement, the axial outmotion prior to motion arrest shall be limited as follows:

Paragraph (III.B.5) - 0.200 inches  
Paragraph (III.B.6) - 0.600 inches  
Paragraph (III.B.7) - 3.25 inches

The design shall be capable of resisting outward motion in each of the above operating modes a minimum of two times during plant operation.

The up force is not an ASME Code requirement. Structural integrity of the primary pressure boundary to prevent generation of missiles must be maintained under this loading condition.

The CRDM Scram spring shall meet the following:

- |   |   |
|---|---|
| 1. Minimum Spring Force                             | 362 lbs at minimum spring compression with the translating assembly in the "full out" position as limited by the rotational stop. |
| 2. Minimum Spring Stroke                            | 25 inches   |
| 3. **Spring Force at beginning of dashpot operation | 0.00 lbs  |
| 4. Design Temperature                               | 400°F   |

\*\*Defined as elevation (-175.87) where the dashpot piston enters the end of the tapered section of the dashpot cylinder.

#### IV. Scram

##### A. Scram Requirements

The overall Primary control Rod System scram requirements are depicted in PSAR Section 4.2.3 and on PSAR Figure 4.2-93 and include the total time from stator power interrupt to reactivity insertion. The unlatch time is defined as the time from the start of stator current decay to the initial insertion motion of the leadscrew and shall be 90 msec maximum at normal CRDM and stator operating temperatures.

##### B. Dashpot

A dashpot shall be included in the CRD for decelerating the translating driveline and control rod during the last nine inches of a scram insertion. The energy of the scrambled assembly shall be absorbed at a deceleration rate which will limit stresses in the driveline components to an acceptable level. The dashpot shall reduce the velocity of the CRD and Control Rod when scrambled from any position between 0 and 37 inches to less than 14 inches/sec at the time of impact on the hard stop at the end of scram insertion.

#### V. Independence

Each control rod shall be driven and positioned by its own mechanism. Each control rod shall be independent to the extent that protective action is not delayed. The CRDM shall be designed to minimize the probability of simultaneous disability in the scram mode of all CRDMs through systematic, concurrent, undetected failures in the CRDMs resulting from commonality of components or susceptibility to failure due to common environmental conditions, duty cycles, or loads.

#### VI. CRDM Position Indicators

Two independent CRDM position indicator systems shall sense the position of the leadscrew and thus produce two separate signals indicating the relative position of the control rod in the core.

The rotary (relative) position indicating system shall consist of an electromagnetic sensor that counts the revolutions of salient poles of an indicating disc attached to the drive mechanism rotor. The axial resolution of the rotary position indication system shall be 0.10 inches (nominal).

The absolute position indication system shall measure the position of the leadscrew through a sensor located in a housing that projects into the inside diameter of the leadscrew. This system shall not lose its reference position because of mechanism scram. The resolution of the

absolute position indication system shall be 0.50 inches. The system position accuracy over full stroke shall be  $\pm 3.5\%$ , of the full stroke. The accuracy of the position indication sensor over the range of environmental conditions shall be  $\pm 1.62\%$  of the full stroke. the accuracy refers to the ability to measure the true position of the top of the leadscrew.

#### VII. Cooling

A stator cooling system shall be provided. This system shall not act as part of the reactor primary system boundary. The design shall incorporate thermocouples into the stator cooling system and provide the corresponding electrical interface information.

#### VIII. Reactor Refueling

The mechanism design shall permit refueling and fuel transfer operations inside the reactor vessel in the space above the core without disassembly and removal of the mechanism. The design shall permit access to the actuating shaft interlock ring and disconnect actuating shaft so that the disconnect coupling between the driveline and control assembly can be manually operated.

The design shall have provisions for the operation of a manual disconnect tool (not provided as part of this specification) for disconnecting the control rod from the driveline and for holding the leadscrew in a withdrawn position for refueling operations.

IX. Out-Motion Limited Pawl

An OML pawl shall be provided to limit outward motion of the translating assembly. Structural integrity of the pawl system (pawl and mounting brackets and hardware) shall be maintained for a static up force of 4000 lbs acting on the control rod coupling interface. During a scram the pawl shall not produce a drag force on the leadscrew in excess of 19 lbs. (average) based on worst case dimensions with a friction coefficient of 0.8.

X. Internal Seal Requirements

The Seal Requirements listed here are for Internal Seals and not the CRDM pressure boundary.

- (a) Each CRDM shall be equipped with seal arrangements which consist of a Main Bellows Seal, Position Indicator Rod Bellows, Disconnect Actuating Shaft Bellows, and Lower CRDM to Nozzle Extension Conoseal.
- (b) The Seals shall separate the CRDM rotor assembly and leadscrew from the reactor environment.
- (c) All bellows parameters (length of stroke, etc.) shall be compatible with the CRDM parameters.
- (d) The Main Bellows shall collapse upon withdrawal of a control rod and extend upon insertion of a control rod.

- (e) The Disconnect Actuating Shaft Bellows and the Position Indicator Rod Bellows expand and collapse only during operation of the manual disconnect.
- (f) Maximum helium leak rate for each of the four seals listed in (a) above is  $1 \times 10^{-5}$  cm<sup>3</sup>/sec at standard temperature and pressure.
- (g) Bellows seal environment
  - o Temperature - 400°F (maximum)
  - o CRDM - argon gas

The internal fluid in the mechanism above the bellows is normally reactor grade argon gas at 0 to 20 psig. The composition of this gas is as follows:

Argon	-99.996% pure
Oxygen	- 5 ppm maximum (volume)
Hydrogen	- 2 ppm maximum (volume)
Nitrogen	-15 ppm maximum (volume)
Carbonaceous Gases	- 5 ppm maximum (volume)
Water (D.P. -84°F)	- 6 ppm maximum (volume)
Other	- 7 ppm maximum (volume)

An environment of Argon saturated with sodium vapor is to be considered an abnormal condition. The mechanism shall be designed to operate throughout a reactor operating cycle (1 year) when exposed to this abnormal environment. In order to assure that the mechanism continues to operate with a failed bellows, the design shall make provision to prevent sodium from depositing on the rotor assembly parts.

After repair and/or replacement of a failed bellows and cleaning of the CRDM to return it to its normal condition, the mechanism shall continue to function for the remainder of its design life.

- o Reactor cover gas side - Argon gas saturated with sodium vapor (external to bellows).

The environment external to the bellows is reactor grade Argon cover gas saturated with sodium vapor. Normal operating pressure is  $6 \pm 2$  in. w.g. Maximum operating pressure is 7 psig. during shutdown maximum pressure is 11 psig. The composition of the gas is identical to 3.5.2S except as follows:

Oxygen	10 ppm maximum
Hydrogen	50 ppm maximum
Nitrogen	2000 ppm maximum

- o Pressure - Normal operating pressure differential is 0 to +20 psig. Maximum operating pressure differential is -7 to +20 psig. During shutdown, maximum pressure differential is -11 psig. During CRDM fill with Argon gas, maximum over pressure is 35 psig (not an operating condition).

For the leadscrew and position indicator shaft bellows, a positive (+) pressure differential denotes a higher internal bellows pressure with respect to the external pressure and a negative (-) pressure differential denotes a lower internal bellows pressure with respect to the external pressure. For the actuating shaft bellows, a positive (+) pressure differential denotes a lower internal pressure with respect to the external pressure, and a negative (-) pressure differential denotes a higher internal pressure with respect to the external pressure.

- (h) A pressure switch will be provided in the CRDM to sense internal pressure and indicate seal failures.

#### XI. Installation and Removal

The mechanism shall be arranged so that all operations incident to its installation on, and removal from, the reactor can be performed with access only to the head of the reactor vessel. Replacement of the stator assembly shall be possible without penetration of the primary reactor system boundary.

## XII. Electrical

### Stator Design

A redesign of the FFTF stator which meets the requirements of Section III "Loading conditions" and its subsections shall be provided. The design shall be consistent with a mechanism design which is balanced over all parameters, particularly with respect to load capability, scram reliability and stator cooling requirements. The design basis shall be increased margin over worst case loading allowing higher segment arm spring force for improved scram reliability and possible reduction of electrical and cooling power demand.

The stator shall be designed for a 30-year life. Motor lead wire shall conform to MIL-W-8777C and MS-25471. The stator shall have monofilar windings of the double ML type wire. The cooling jacket for the stator shall also be redesigned to be compatible with the cooling requirement of the redesigned stator configuration. The cooling requirements shall not exceed FFTF values:

Cooling Gas	Nitrogen
Supply Pressure	90 to 100 psig
Inlet Gas Temperature	50 to 60°F
Outlet Gas Temperature	130°F maximum
Pressure Drop Across Stator	1.5 ± .5 psi
Heat Load-Each CRDM	12,000 BTU/hr maximum
Flow Rate	157 ± 10 SCFM
Moisture Content	8 ppm by weight maximum

### XIII. Testing Requirements

#### A. Stator Tests

The stator shall be tested at various points during fabrication as indicated below. The results of these tests shall be recorded and maintained in the record book for each particular stator. If thermocouples are required to be incorporated into the stator, these thermocouples shall conform to ASTM E 230.

The individual coil group resistance shall be checked prior to inserting the coils into the stator. Any coil whose resistance varies by more  $\pm 2\%$  from the nominal design value shall be rejected. After all windings have been inserted into the stator and before the lead connections are permanently made, the stator shall be subjected to a DC Insulation Test and an AC Dielectric Strength Test as described below:

The following tests shall be made on the stator upon completion of the lead connections and before varnish impregnation.

##### 1. DC Winding Resistance Test

The resistance of each phase of the stator shall be checked. Resistance which varies by more than  $\pm 2\%$  from the nominal design value, shall be cause for rejection. Also, an unbalance of phase resistance which exceeds  $\pm 1.5\%$  of the average value for all the phases of the stator shall be cause for rejection.

##### 2. DC Insulation Resistance Test

The insulation resistance from all phases and neutral lead to ground shall be checked. The minimum acceptable phase-to-ground resistance at 25°C is 10 megohms.

##### 3. AC Dielectric Strength Test

Apply 1500 volts rms 60 Hz between the stator iron and any one of the stator leads. Voltage shall be applied at a rate of



approximately 100 volts per second, maintained at 1500 volts for 15 seconds, then reduced to zero at approximately 100 volts per second. All of the phases of the stator shall be checked. The stator insulation must not exhibit dielectric breakdown when subjected to the above test voltages. All six phases may be tested simultaneously. In addition, measurements of the maximum compensated current leakage between coils and between windings and the core stack will be recorded for the prototype CRDM stator. From these values an acceptance criteria will be established for the plant unit CRDM stators.

#### 4. Surge Comparison Test

Surge testing shall be conducted using 3000 volts DC and shall check the waveform of power thru the stator phases. Any sharp or jagged indication of a trace, regardless of proximity of comparison between traces, shall be cause for rejection of the stator. Stators which include test instrumentation may be tested at lower voltage subject to Purchaser approval.

After successful completion of these tests, the stator shall be varnish vacuum impregnated and baked. During this processing, the stator leadwires must be protected to prevent the varnish from making them inflexible. Upon completion of this processing the tests described above shall be re-performed and the results recorded.

#### 5. Cooling Jacket Leak and Strength Test

The cooling jacket supplied with the CRDM shall be tested for leakage and strength against pre-defined acceptance criteria.

#### B. Helium Leak Test

A helium leak test shall be performed on the completed CRDM components that serve as part of the primary system environmental boundary. The maximum acceptable leak rate for this test shall be  $1 \times 10^{-4}$  scc/sec/CRDM total for all external leak paths.

If it is determined that a dangerous situation would not exist from pressurization of helium gas, the leak test and strength test, as described below, may be combined. However, if they are not combined, the leak test shall be performed after the strength test.

#### C. Strength Test

A strength test shall be performed on the completed CRDM components that serve as part of the primary system environmental boundary and shall be either pneumatic or hydrostatic.

This test shall be in accordance with NB-6000 of Section III of the ASME Boiler and Pressure Vessel Code. The following general requirements apply to the strength test:

1. Prior to testing, all interior surfaces shall be cleaned. The Supplier shall prepare and submit a detailed cleaning procedure as part of the Fabrication Plan.
2. The component shall be tested at a minimum temperature of 70°F and the test temperature shall be reported in the Fabrication Report.
3. The number of tests above design pressure shall be minimized.
4. Any indication of leakage in the fluid or gas boundary of the components at other than a flanged joint shall be reported. The location and extent of any leak indication and the corrective action taken shall be reported in the Fabrication Report.
5. If a hydrostatic strength test is performed, following this test the mechanism shall be completely drained and internal surfaces shall be completely dried by flushing the still-sealed test assembly with heated dry nitrogen or drawing a vacuum. The pressure component being tested shall be protected from contamination by maintaining the sealed condition and internal environment of dry nitrogen until the helium leak test required by Section XI B is performed.

#### D. CRDM Performance Tests

The prototype CRDM shall be tested to show conformance with the design objectives. This testing will be performed in accordance with detailed requirements designated in this specification. For successful completion of the work, this testing will demonstrate compliance with the design objectives with or without any specified additional equipment attached to the mechanism, as applicable. As a minimum, the following parameters will be investigated and reported:

1. Maximum possible lifting force exerted;
2. Normal lifting force exerted;
3. Maximum possible driving-down force exerted;
4. Normal driving-down force exerted;
5. Maximum torque exerted on the leadscrew;
6. Normal torque exerted on the leadscrew;
7. Total travel during the test for maximum, and normally exerted forces;
8. Stator coil amperage and voltage for maximum and normally exerted, forces and driveline speeds;
9. Stator coil amperage, voltage, and resistance as functions of temperature;
10. Stator coil steady-state temperature variation during operation and holding periods;

11. Stator current decay time and total leadscrew release time as a function of temperature, load, stator power, and misalignment. The unit shall be tested for delay time and release time at four different rotor to motor tube (index) positions and stator to motor tube (index) positions;
12. The CRDM scream characteristics as functions of the stator power, rod speed, and load;
13. Mechanism internal environment parameters including, but not limited to:
  - a. Temperature
  - b. Pressure
  - c. Contained atmosphere
  - d. Lubrication;
14. Dynamic response of the CRDM leadscrew to a single pulse from the controller as well as to travel speeds of 0.36 inches/minute and 9.0 inches/minute;
15. Mechanism cooling system parameters, as applicable;
16. Any other parameters or factors that may have an effect on the mechanism meeting the design objectives.

E. Acceptance Test

1. Acceptance tests shall be performed on each plant unit CRDM/CRD and associated equipment which will establish that the performance of each unit is within acceptable limits established as satisfactory for the CRBRP mechanisms.

2. The translating assembly out-motion requirement shall be verified by testing. Testing shall include the three specified modes of latched, sc̄ram and unlatched.

The test article shall include the Upper CRDM and leadscrew as a minimum. A mass equivalent to the mass of the remaining translating assembly components shall be attached to the leadscrew. The specified up force shall be applied to the bottom of the leadscrew and maintained constant for a stroke of 10 inches at  $10 \pm 1$  inches withdrawn and  $25 \pm 1$  inches withdrawn for the latched and sc̄ram mode. For the unlatched mode the leadscrew shall be a position, with the pawl above the top leadscrew tooth, such that the impact velocity, when the pawl engages the leadscrew top tooth, is equal or greater than 25 ips.

3. The OML pawl maximum drag force requirement shall be verified by test. The system shall meet the requirement during inward motion of the leadscrew with the actual friction coefficient.

ITEM 3 and following request

TEST DATA

- I. One of the specifications for the mechanism is that under the most unusual conditions the withdrawal speed shall not exceed 73 lpm. Conformance to this requirement was demonstrated at the vendors facility as part of the performance test.

The maximum withdrawal speed test was run to determine the axial force which could be exerted by the mechanism as a function of current and withdrawal speed before pole slippage occurs. If the speed is increased or the current decreased beyond the point of pole slippage, the roller nuts will roll out of the leadscrew and the mechanism will scam. The data from this test is shown in Table QCS760.176-1. At the design condition of 175 volts and 7.2 amps, rollout occurs at 43 lpm. The total force required is comprised of the net weight of translating assembly, friction and drag forces, and spring forces from the bellows and scam assist spring. The maximum force at the top of the stroke is 1135 lbs. and the minimum force at the bottom of the stroke is approximately 400 lbs. As the assembly is withdrawn the scam and bellows forces increase. Thus the force in Table QCS760.176-1 is dependent on the axial position of the translating assembly when rollout occurs.

To exceed the design voltage of 175 volts, a series of significant failures must occur in the controller and M-G sets. If all of these failures occurred at the same time, the maximum voltage which could be applied to the stator is 252 volts. As shown in the data in Table QCS760.176-1, at 258 volts, rollout will occur between 60 and 70 lpm if the translating assembly is withdrawn less than 10.5 inches where the spring forces are applied. If the translating assembly is in a normal operating range of 16 inches to 28 inches withdrawn rollout will occur between 50 and 60 lpm. Thus the PCRDM meets the design requirement that it shall never be withdrawn at a speed greater than 73 lpm.

- II. All 18 mechanisms (9 plant units and 9 spares) were acceptance tested. The acceptance test data show that all 18 mechanisms met all test requirements.

III. To determine the response of the PCRDM to loss of stator coolant flow, a series of tests were run a W-ARD. In these tests the stator winding temperature and outlet coolant temperature were measured as a function of time for a variety of coolant flows including complete loss of flow. The results for a complete loss of coolant flow is shown in Figure QCS760.176-6. For this condition, the maximum stator temperature reached an asymptotic value of 660°F in 250 minutes. It should also be noted that the thermocouple measuring the outlet coolant temperature followed the maximum stator temperature heat up rate fairly closely. At 260 minutes, power to the stator was turned off and the stator temperature and outlet coolant temperature were monitored during the cooldown, without the benefit of coolant flow. As shown in Figure QCS760.176-6 the maximum stator temperature and outlet coolant temperature dropped rapidly.

During this test, the assembly was withdrawn to 36.0 inches and placed in 3-phase hold. In this condition the maximum spring force was applied to the driveline, and the maximum heat was generated in the windings. When the maximum stator temperature was obtained, the mechanism was drive down to 25 inches withdrawn and back up to 36 inches five times to demonstrate that the mechanism functioned properly and did not roll out or scam under these abnormal conditions. The mechanism was then scammed and the unlatch time and scam time were measured. The results indicated that the unlatch time was faster than normal and the scam time was normal. When the test was completed and the stator had cooled to ambient temperature, the stator winding resistance and insulation resistance were measured and found to be unchanged. It was concluded that the mechanism and stator has functioned properly during these abnormal conditions and had suffered no degradation or loss of operating life.

In the plant unit mechanisms there is an operating thermocouple and a spare thermocouple which measures the temperature of the outlet cooling nitrogen. These thermocouples will alarm at 200°F to indicate a reduction in stator cooling and an increase in stator temperature. At this time some action may be taken to resolve the problem since the mechanism should not operate indefinitely without coolant flow. This condition is not a safety problem but one of degradation of the mechanism insulation.

TABLE QCS760.176-1

MAXIMUM AXIAL FORCE FOR NO POLE SLIPPAGE IN POUNDS

Withdrawal Speed	6 amps/ 135 V	7 amps/ 170 V	8 amps/ 210 V	9 amps/ 258 V
1	2510	2890	3180	3270
5	2270	2700	2990	3180
10	1980	2420	2610	2890
15	1650	2030	2420	2840
20	1320	1700	2230	2610
30	Rolls out	900	1560	2030
40		Rolls out	980	1510
50			Rolls out	1080
60				600
70				Rolls out



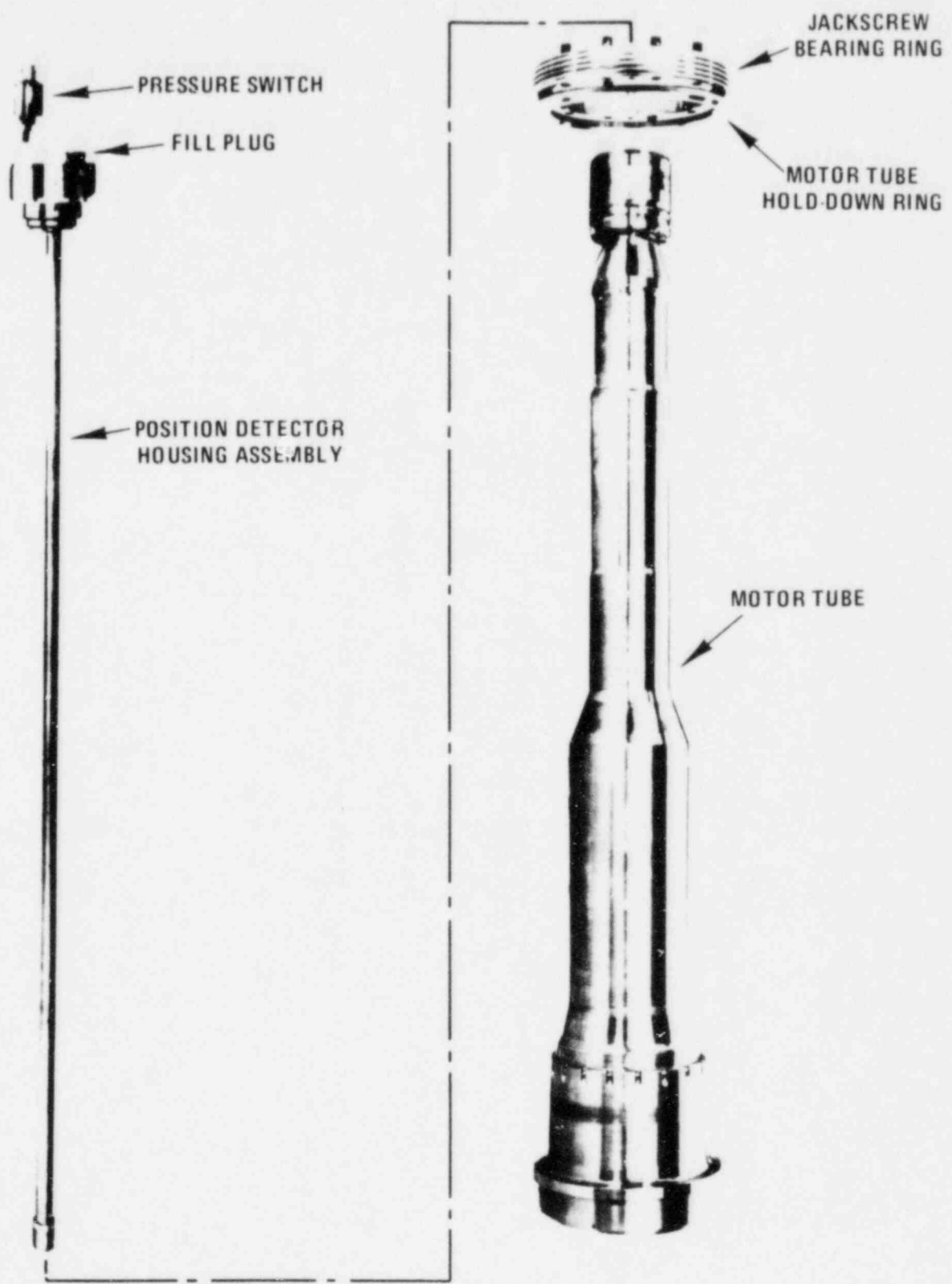


Figure QCS760.176-1. Motor Tube, Hold-Down Ring P.D. Housing, and Pressure Switch

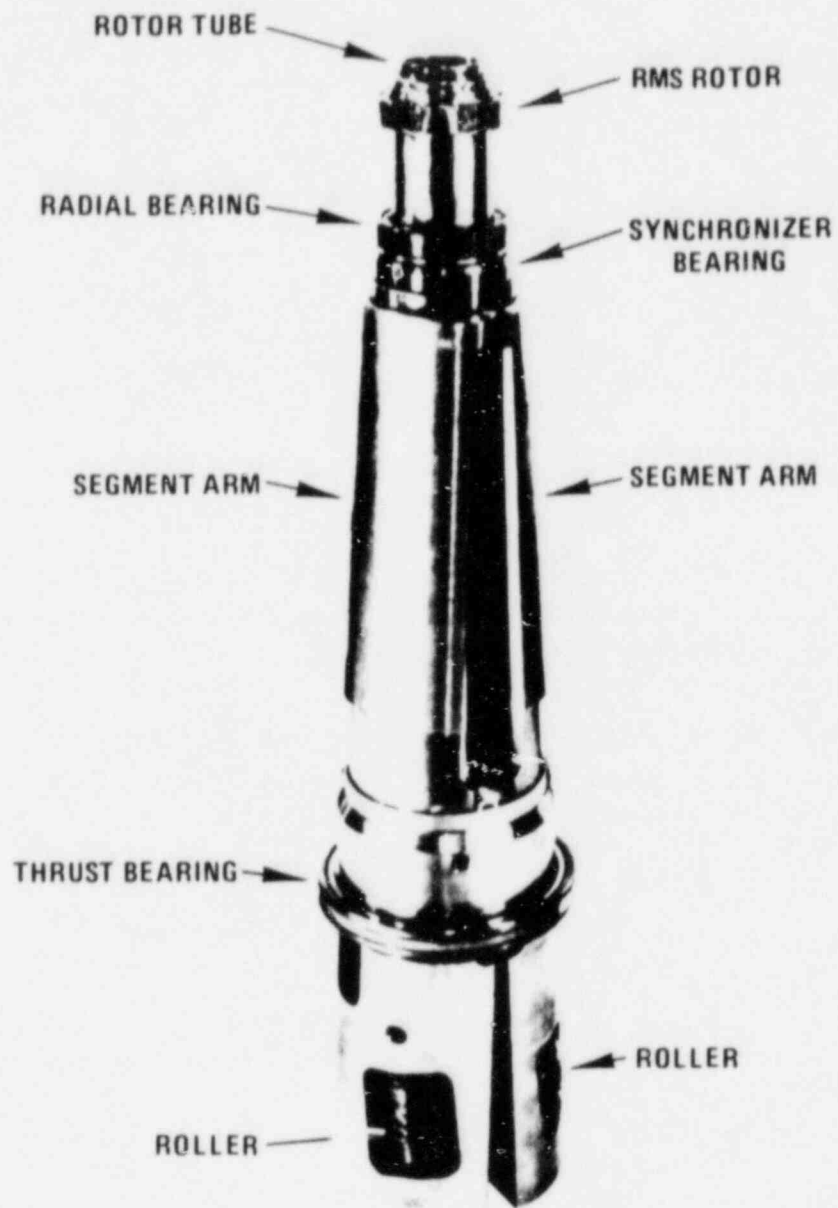


Figure QCS760.176-2. Rotor Assembly

QCS760.176-25

Amend. 72  
Oct. 1982

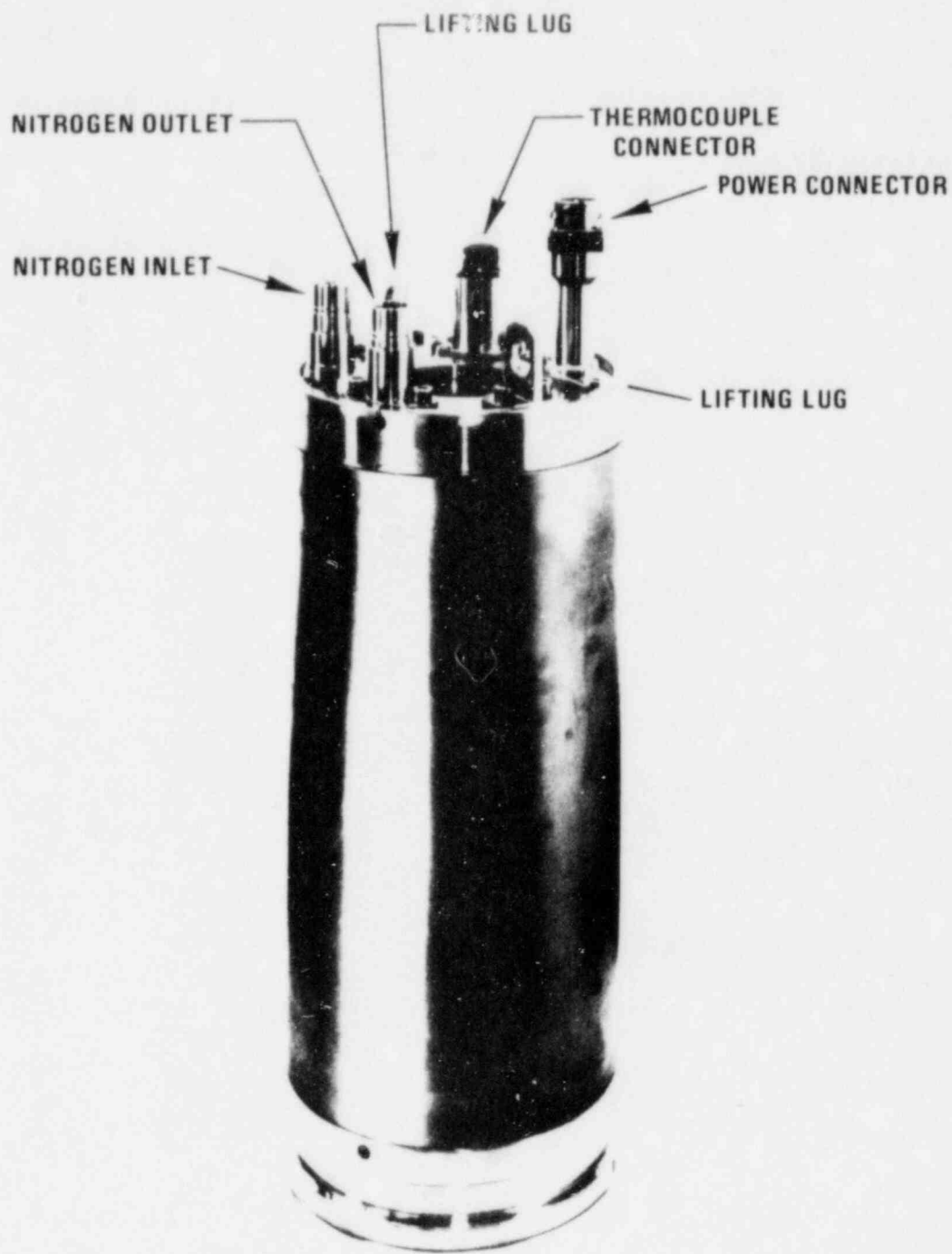


Figure QCS760.176-3. Stator-Jacket Assembly

QCS760.176-26

Amend. 72  
Oct. 1982

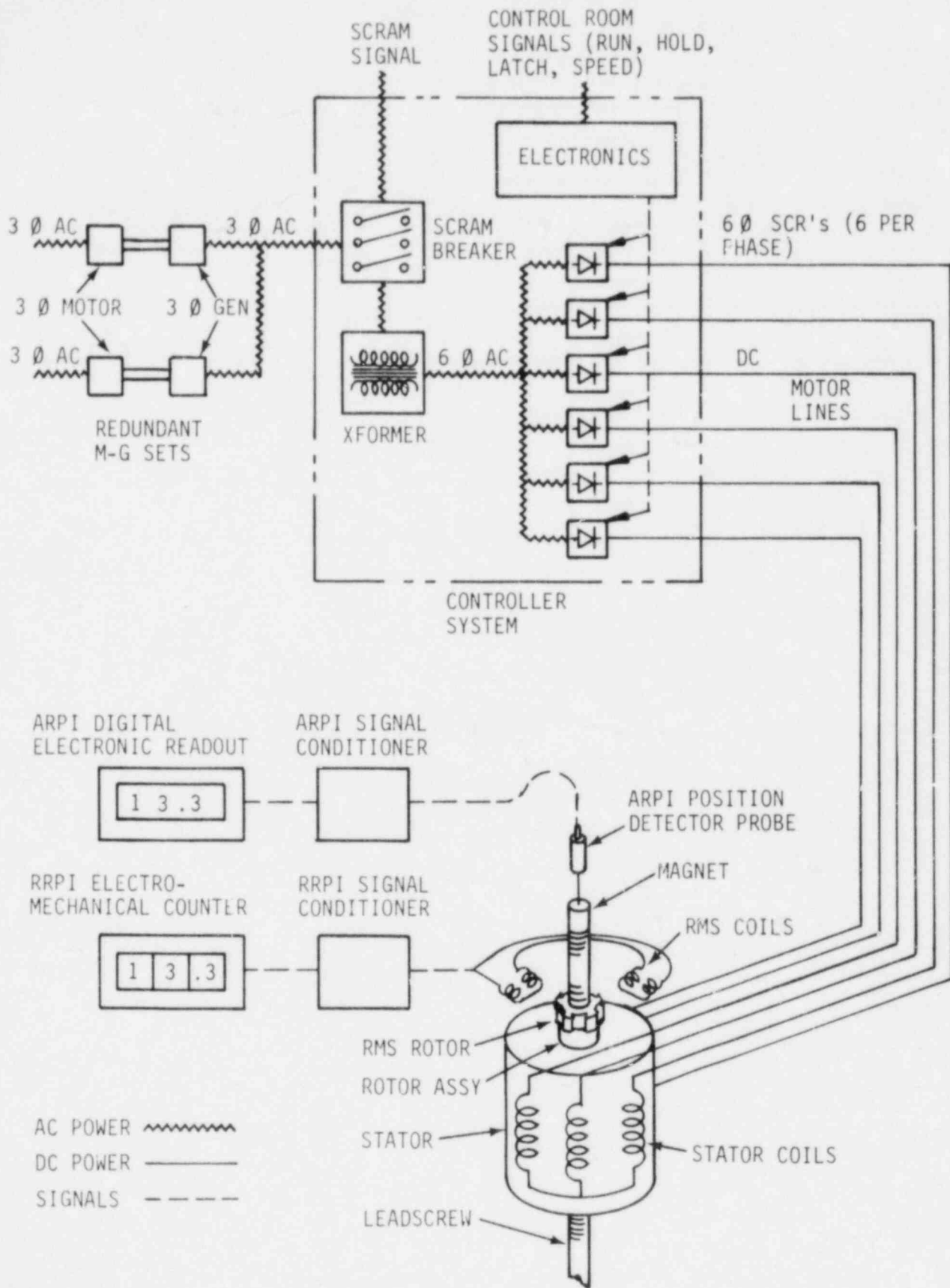


Figure QCS760.176-4. PCRD and Controller System Schematic

Figure QCS760.176-5

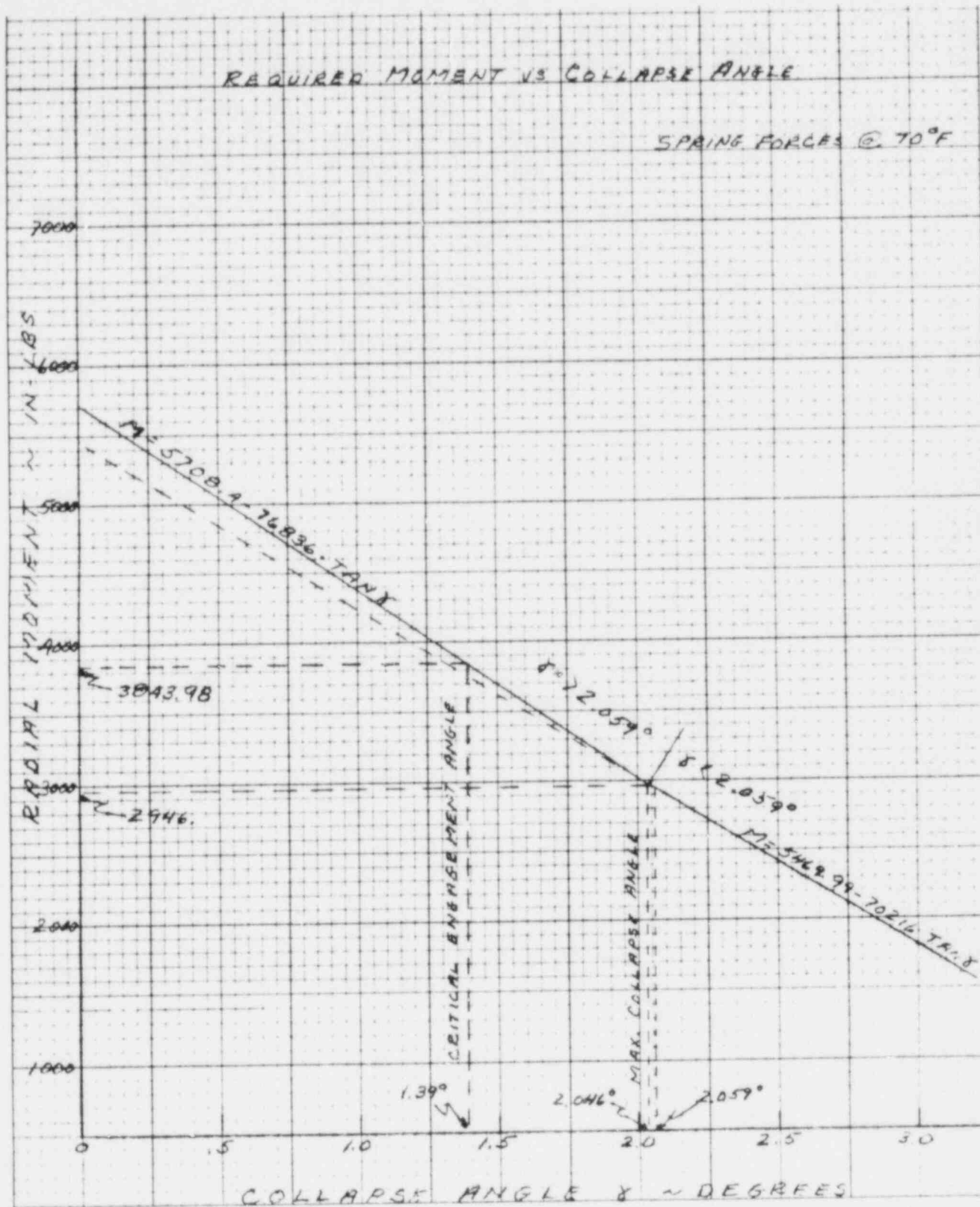
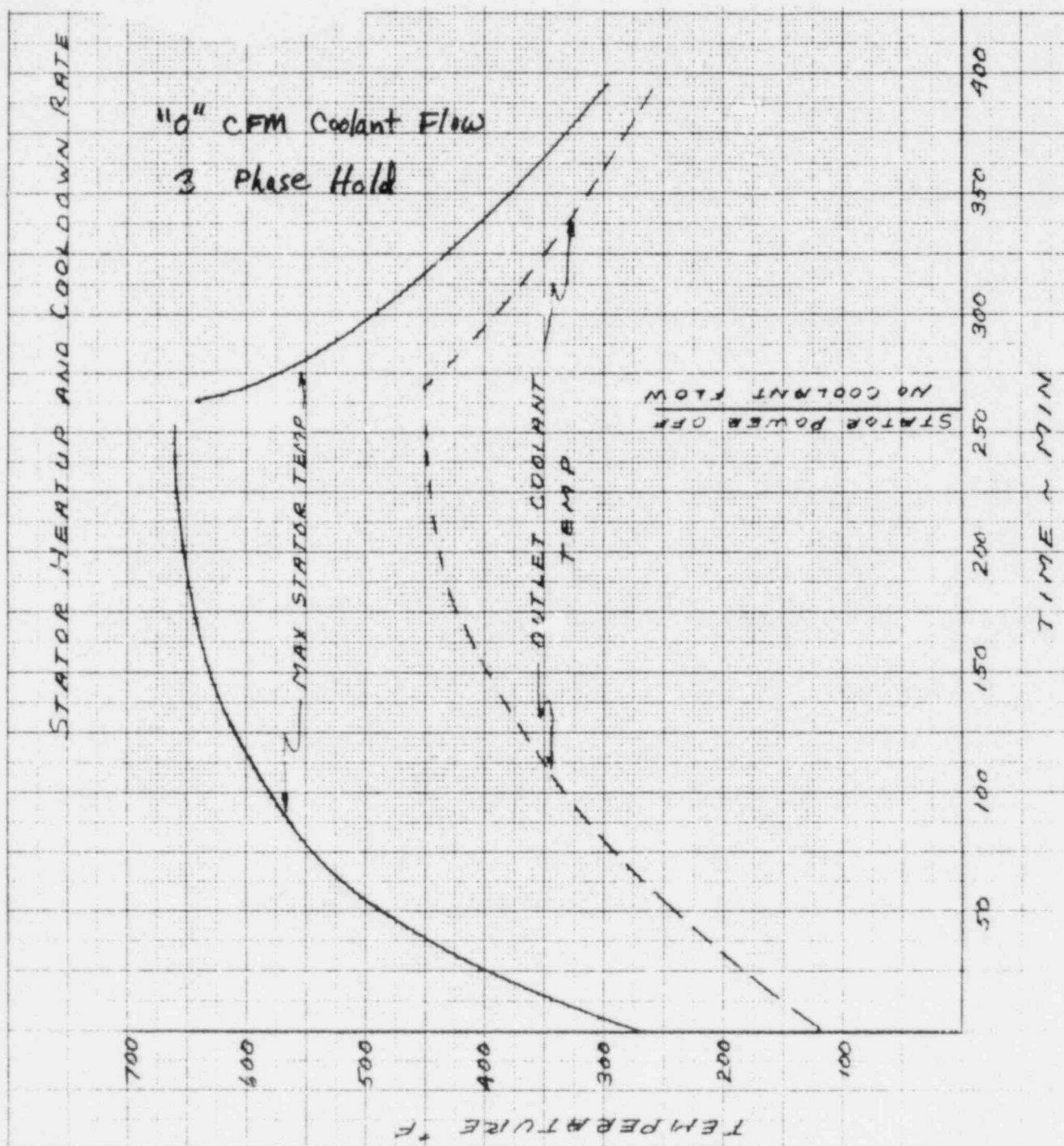


Figure QCS760.176-6 Stator Heatup and Cooldown Rate



Question QCS760.177

Please provide design layout drawings, including dimensions, materials and weldments, for the following:

- 1) containment penetrations, including equipment hatches, personnel-hatches, typical electrical penetrations and typical piping penetrations;
- 2) containment ring stiffeners and overhead crane support;
- 3) structures and components within the containment-confinement annulus, especially those used for filtered venting, including fans and ductwork;
- 4) cell and cell liners, for the reactor cavity, the pipeway cells, an intermediate heat exchanger (IHX) cell, and any other typical piping cells in containment, including seals, vents, the steel plate, its attachment to the concrete, the gaps, the perlite insulating concrete, and the structural concrete; and
- 5) the reactor vessel support ledge.

Response:

The requested layout drawings have been provided under separate cover in Reference QCS760.177-1.

Reference QCS760.177-1: Letter HQ:S:82:077, J. R. Longenecker to P. S. Check, dated August 6, 1982.

### Question CS760.178A1

Can TOP accidents become prompt-critical in such a way that internal fuel motion in lower power channels is the key factor in the energetics determination? Is such an event possible only for midplane failures with low sweepout? How is the degree of sweepout determined? What is the effect of intrasub-assembly incoherence on sweepout?

### Response

The assessment of unprotected TOP events in the CRBRP (Chapter 6 of Ref. QCS760.178A1-1) concluded that a prompt-critical response would not occur for nominal conditions and would be very unlikely even for combinations of pessimistic assumptions on fuel rod failure location (i.e., midplane) and reactivity insertion rates. These conclusions are substantiated by additional considerations of likely reactivity insertion rates, fuel sweepout mechanisms and the effect of intra-assembly incoherence on fuel sweepout.

### Reactivity Insertion Rate

The maximum reactivity insertion rate evaluated for TOP events is an important consideration in determining the potential for energetic consequences. Section 3.3.2 of Ref. QCS760.178A1-2 examined the abnormal reactivity insertion events which could lead to a TOP initiated HCDA. Both anticipated events (Table 15.2-1 of the PSAR) combined with failure of both shutdown systems and events beyond the protection system design bases were considered.

Reactivity insertion rates for the heterogeneous core have subsequently been analyzed. Anticipated events, unlikely events, and extremely unlikely events were considered. Based upon this analysis, there are no identified events that result in reactivity insertions greater than one dollar which occur at rates in excess of 12¢/s.

### Fuel Sweepout Mechanisms and Incoherence Effects

For the nominally predicted upper fuel rod failure locations the initial fuel motion to the failure site results in negative reactivity effects such that the potential for a prompt-critical excursion doesn't exist and the core response is not sensitive to the degree and timing of fuel sweepout from the core. For this case the fuel sweepout response is more directly related to a determination of the potential for damaged core coolability and end state of the transient, as discussed in Sections 6.1.1 and 6.2.2 of Ref. QCS760.178A1-1.

If a fuel rod were assumed to fail at the core midplane (i.e., location of peak axial flux), the initial fuel motion response would result in the maximum positive reactivity feedbacks. This assumption, if coupled with very limited fuel motion in the sodium flow channel, is considered to be the only plausible way in which an unprotected reactivity insertion event in CRBRP could result in a prompt-critical transient.



In recognition of the importance of fuel rod failure location, calculations were performed which assumed coherent, fuel rod midplane failures (Chapter 6, Ref. QCS760.178A1-1). These calculations indicated that prompt-critical conditions did not result from assumed midplane failures in CRBRP. In reaching this conclusion it was recognized that the use of more realistic analytic methods (PLUTO-2) is important in determining the appropriate accident progression. These methods, which are experimentally supported, show that after a brief time interval the net effect of fuel motions (within and outside the fuel rod) lead to negative reactivity consequences, even at relatively high core powers. This is in contrast to the SAS/FCI model which, due to several unrealistic modeling assumptions, predicts incorrect, accelerating positive reactivity at high core powers.

The PLUTO-2 calculations which were performed (Ref. QCS760.178A1-1, Section 6.2 and Appendix E) are conservative in that the larger time-dependent SAS/FCI cavity was used. Although fuel plate-out parameters were not varied, parametric variations in fuel particle size, based on PLUTO-2 applications to TREAT experiments, were used to reduce the predicted amount of fuel sweepout. These calculations still indicated that a prompt-critical transient would not be expected in the CRBRP.

The application of PLUTO-2 to experiments and the phenomenological understanding gained in representing fuel sweepout is summarized in the following. A more detailed discussion of the PLUTO-2 modeling and its bases is provided as an attachment to this response.

Pre- and post-test analyses of TREAT tests E8, H6, and L8 have been performed with PLUTO-2 and its predecessor PLUTO. Although several modeling differences occur between the two computational techniques, reasonable compatibility in predicted conditions exist for the first 20 to 30 milliseconds. This is because none of the significant differences between the codes are physically required on this time frame.

TREAT tests E8 and H6 simulated TOP events in the FFTF at 3 \$/s and 50 c/s, respectively\*. Test E8 conditions were unfavorable for sweepout in that the pump pressure drop and flow through the test section were very low compared to the reactor environment. Nevertheless, there was considerable early fuel sweepout observed by the hodoscope. The observed sweepout was faster than that calculated with PLUTO. This is considered to be due to the assumption of a single fuel particle size in PLUTO. On the whole, the comparison to experiment was very good and on the conservative side; that is slower and less sweepout.

The hydraulic parameters for Test H6 were closer to FFTF and CRBRP hydraulic conditions than Test E8 and had a lower reactivity insertion rate of 50 c/s. The test showed several FCI events separated by more than 100 msec. The first event in the H6 experiment was analyzed with PLUTO (Ref. QCS760.178A1-3). The failure of only one rod was assumed which led to a rapid fuel sweepout of about 10 g above the top of the active fuel. The final hodoscope data, which were available only after the PLUTO analysis, indicate that about 10 g of fuel moved beyond the top of the active fuel within 30 msec and 28 g

---

\* Using 34 cm EBR-II irradiated fuel rods.

within 90 msec. This is an indication that more than one rod may have failed during this time interval.

The main pressure and flow event in test H6 was analyzed with PLUTO-2 (Ref. QCS760.178A1-3). Only a fair agreement with the flow and pressure data could be achieved. This was at least partially due to the limited knowledge about the initial conditions at the beginning of this last event of the experiment. The PLUTO-2 calculation, which assumed the simultaneous failure of three rods, resulted in a rapid upward sweepout of 66 g of fuel. The final hodoscope report (Ref. QCS760.178A1-4) puts the upward dispersal during this event at 78 - 12 g within 30 msec.

The fuel sweepout during this event was relatively massive although the hodoscope data indicate that the rod failures were close to the midplane. Some of the fuel swept upwards may have been fuel which had collected near the midplane due to earlier rod failures. These had led to the failure of the flow tube surrounding the rod bundle which must have caused a low pressure situation near the midplane, reducing the potential for sweepout.

The L8 test simulated the condition in an assembly during a LOF-d-TOP event (Ref. QCS760.178A1-5). At the time of rod failure the sodium velocity had decreased to 1.3 m/sec and the pump pressure was around 0.05 MPa. Although these conditions are not typical for a slow ramp rate TOP accident, this test is nevertheless relevant for the investigation of fuel sweepout. Several features in this test potentially degraded the sweepout: (a) small pump pressure, (b) low initial coolant velocity, and (c) a near-midplane cladding failure location for which the ejected fuel has not much axial momentum; the upward sweepout was nevertheless very rapid. As in the E8 test simulation, the PLUTO-2 calculated sweepout above the top of the active fuel again lagged behind the measured one (see Appendix A).

In Fig. QCS760.178A1-1 normalized fuel reactivity histories of the measured and calculated fuel distributions are shown. These fuel reactivities are obtained by integrating the product of a fuel worth curve and the axial fuel distribution over the length of the pins. It is apparent from the figure that the significant fuel sweepout and dispersal which occurred in this test was well represented by PLUTO-2. According to the hodoscope results the fuel motion reactivity became negative about 20 msec after rod failure in this test (Ref. QCS760.178A1-6). The slight positive reactivity right after pin failure in the test data may be due to a lesser extension of the initial clad rupture above the midplane than assumed in the post-test simulation. However, this may also be due to the disregarding of the fuel self-shielding and can be altogether considered statistically insignificant when compared to earlier variations in the hodoscope reactivity curve.

In summary the available fuel motion data from the TOP in-pile tests in which fuel was injected into liquid sodium show a significant early fuel sweepout. The rapidity of the fuel sweepout does not seem to be strongly affected by the axial cladding failure location or the fraction of pins failing.

The modeling of fuel sweepout just discussed invokes the customary one-dimensional assumptions. This approach does not explicitly account for two-dimensional coolant bypass (incoherence effects) which introduces two

opposing considerations for an assumed midplane failure at a low rate reactivity insertion. In a large rod bundle, coolant bypass effects will be significant in proportion to the time delay between individual intra-assembly fuel failure events. The first consideration is that any time delay between failure events results in a stretch-out of the positive reactivity effect of fuel motion and allows more time for fuel sweepout to occur and reduce reactivity as discussed in Ref. QCS760.178A1-7. The second consideration is the reduced rate of fuel removal. As noted in out-of-pile tests, coherent bundle flow conditions showed more sweepout of simulant fuel than less coherent flow conditions Ref. QCS760.178A1-8. However, it was shown that even under the less coherent test flow conditions neutronically significant sweepout occurred. It is also noted that the TREAT tests used for calibration of the fuel sweepout modeling introduced some degree of incoherence into the calibration process itself.

In considering both effects, the current Project position is that neither the positive effect of delayed failure events nor the retarding effect of coolant bypass on fuel sweepout introduce a significant uncertainty into the reference calculations performed. Again, it is noted that it was possible to simulate the observed fuel sweepout in three experiments fairly well with the PLUTO-2 code (usually the very early sweepout was somewhat underestimated by the code).

The NRC staff review pointed out that the degree of lead assembly failure coherence would be greatest at EOC-3, whereas the Project examined the EOC-4 core configuration in Ref. QCS760.178A1-1. However, initial calculations performed by staff consultants at ANL, which assumed midplane failures and weak fuel sweepout (PLUTO-2 parameters used in these calculations were similar to those used in a successful post-test analysis of the TREAT L8 test except that the parameter controlling fuel plate-out was more conservative), concluded that a sustained prompt-critical condition would not occur for reactivity insertion rates less than 20  $\text{c/s}$  (Ref. QCS760.178A1-9). This conclusion, which is consistent with the Project understanding, will be further confirmed following detailed determination of the EOC-3 neutronics safety parameters.

Hence, for the amount of expected incoherence among fuel assembly failures in response to an unprotected,  $\leq 12 \text{ c/s}$  reactivity ramp insertion, and for the limited positive fuel motion prior to sweepout dominance, a sustained prompt-critical state would not occur in the CRBRP. This nonenergetic response is considered generic to a CRBRP type core driven by a low rate reactivity insertion.

#### References

- QCS760.178A1-1 S. K. Rhow, et al., "An Assessment of HCDA Energetics in the CRBRP Heterogeneous Reactor Core," CRBRP-GEFR-00523, General Electric Company, December 1981.
- QCS760.178A1-2 "Hypothetical Core Disruptive Accident Consideration in CRBRP; Energetics, and Structural Margin Beyond the Design Base," CRBRP-3, Vol. 1.

- QCS760.178A1-3 H. U. Wider and L. A. Semenza, "Analysis of TREAT Transient Overpower Experiments Using the PLUTO Codes," Proc. Specialists Workshop on Predictive Analysis in LMFBR Safety, Los Alamos, New Mexico, LA-7938-C, March 1979.
- QCS760.178A1-4 C. L. Fink, "Final Hodoscope Report for H6," Argonne National Laboratory, ANL/RAS, Report H6.T, May 1980.
- QCS760.178A1-5 C. H. Bowers, et al., "Analysis of TREAT Tests L7 and L8 Using SAS3D, LEVITATE and PLUTO-2," Proc. Specialists Workshop on Predictive Analysis of Material Dynamics in LMFBR Safety, Los Alamos, New Mexico, LA-7938-C, March 1979.
- QCS760.178A1-6 H. U. Wider, et al., "The PLUTO-2 Overpower Excursion Code and a Comparison with EPIC," Proc. Int'l. Mtg. on Fast Reactor Safety, Seattle, Washington, August 1979.
- QCS760.178A1-7 A Padilla, et al., "On the Consequences of Axial Midplane Failures during Hypothetical Transient Overpower Accidents," Proc. Int. Topical Meeting on LMFBR Safety and Related Design and Operational Aspects, July 19-23, 1982, Lyon, France.
- QCS760.178A1-8 B. W. Spencer, et al., "Fuel Motion in the CAMEL TOP-Simulation LMFBR Safety Tests," Proc. Int'l Meeting on Fast Reactor Safety, Seattle, Washington, August 1979.
- QCS760.178A1-9 H. Hummel, P. Pizzica, and P. Garner, Quarterly Report, April-June, 1982, Argonne National Laboratory, ANL-82-24, Vol. II.

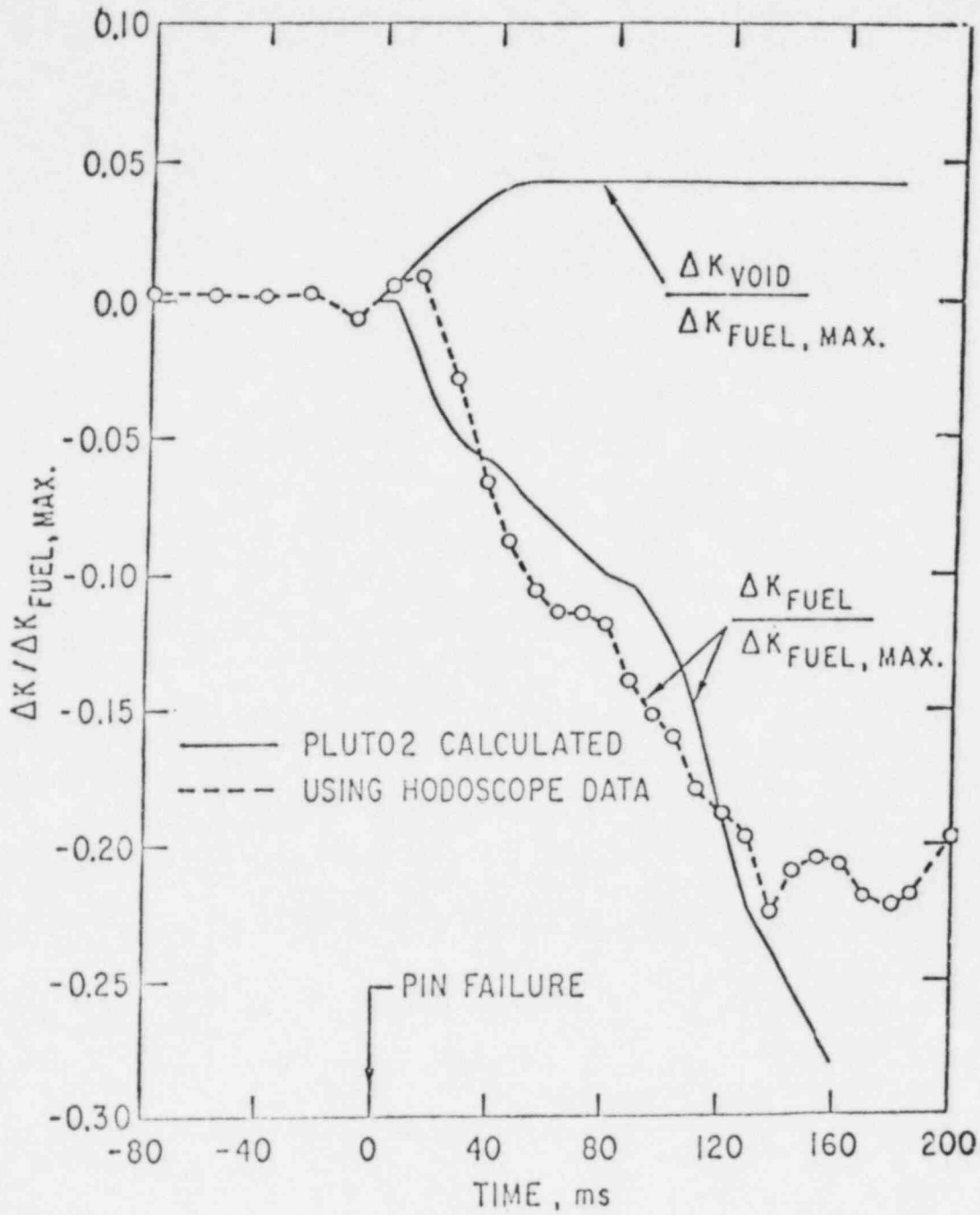


Fig. QCS760.178A1-1 Comparison of PLUTO-2 Calculated Reactivity History for TREAT Test I8.

Fuel Sweepout Modeling in PLUTO-2  
and Its Experimental Bases

This Appendix provides additional detail on the important PLUTO-2 modeling parameters and relevant experimental data used to make judgements on fuel sweepout in the CRBRP during low ramp rate TOP events.

The available fuel motion data from the TOP in-pile tests in which fuel was injected into liquid sodium show a significant early fuel sweepout. The rapidity of the fuel sweepout does not seem to be strongly affected by the axial cladding failure location or the fraction of rods failing.

It is noted that it was possible to simulate the observed fuel sweepout in several experiments fairly well with the PLUTO-2 code (usually the very early sweepout was somewhat underestimated by the code). The important parameters in these post-test simulations are the fraction of rods failing, the axial failure location, and the sodium void fraction below which transition to annular fuel flow is allowed. Somewhat less important are the rod failure pressure, the fuel particle size and fuel plate-out and crust release parameters. One could decrease the calculated negative fuel motion considerably by not allowing the particulate flow regime. However, this would make it impossible to match experimental data.

Two out-of-pile test series to investigate fuel sweepout have been performed. In the ANL-CAMEL experiments (Ref. A-1) about 30% of the injected  $UO_2$ -Mo thermite mixture is typically swept upwards in particulate form and the remaining fuel is plated out near the injection location. In contrast, KFK experiments using electrically heated  $UO_2$  rods (Ref. A-2) show a nearly complete sweepout of the injected fuel. The KFK results, which are in close agreement with the modeling of the early sweepout in PLUTO-2, are more prototypic of the reactor environment in some important respects.

The following sections provide the additional analytic and experimental detail.

In-Rod Fuel Motion and Fuel Ejection Modeling in PLUTO-2

The schematic in Fig. A-1 shows the in-rod and channel fuel motion which are modeled in PLUTO-2. The flow of the molten fuel/fission-gas mixture inside the fuel rods is treated as a homogeneous (i.e., no-slip), compressible, and one-dimensional flow with variable flow cross section.

The assumption of a homogeneous flow inside the rod becomes questionable after an extensive blowdown has led to a sizeable internal void fraction; annular or slug fuel flow may be more appropriate. Homogeneous flow probably exaggerates the in-rod fuel motion towards the clad failure for longer times and for midplane failures is therefore conservative.

The calculation of the ejection through a clad rupture is based on local pressure equilibrium between the fuel rod cell and the adjacent coolant. The

mass ratio of ejected fuel to fission gas is assumed to be the same as that in the ejecting rod mesh cell. A key factor for the ejection rate is the rate of in-rod fuel motion into the ejection cell which is controlled by the small cross section of the molten cavity. The latter is considerably smaller than clad rupture sizes found in the post-test examinations of TREAT tests H5 and R12. For longer times (i.e., tens of milliseconds) a preferential ejection of fission gas may take place based on a PLUTO-2 analysis of the TREAT L8 test (Ref. A-3).

In the context of PLUTO-2 the most conservative assumption is a simultaneous failure of all rods at the midplane. This assumption maximizes the total in-rod fuel motion. The larger fuel masses ejected then promote the transition to an annular fuel flow and subsequent fuel plate-out, and thus, minimize the fuel particle sweepout relative to the fuel mass ejected from the failed rods. This is discussed in more detail in the following sections.

#### Fuel Fragmentation, Transition to Annular Fuel Flow and Fuel Plate-Out

In PLUTO-2 the molten fuel injected into the coolant with a liquid sodium fraction greater than the input value CIBBMN will fragment instantaneously into droplets of one size. These droplets can further fragment into smaller ones after a time delay which is input. Molten fuel ejected into a coolant node with a liquid sodium fraction below CIBBMN will be deposited on the cladding and structure and move as a partially or fully annular film. Molten fuel droplets already existing at a certain elevation will also be deposited on clad and structure if the liquid sodium fraction drops below CIBBMN. Figure A-2 illustrates the possible fuel configurations and flow regimes in an equivalent coolant channel. What fraction of the channel perimeter is wetted by a partially annular flow is determined by a linear interpolation between zero and an input volume fraction CIANIN which defines the volume fraction above which the entire perimeter is wetted. If the bulk temperature of the annular fuel film drops below an input energy EGBBLY and if the outer clad temperature has not yet reached an input temperature TECLMN, which should be at or below the clad solidus, fuel plate-out will be initiated. Additional fuel moving into a node with plated-out fuel may have a higher energy than EGBBLY and may move through this node without plating-out. Existing crusts can remelt due to fission heating and crusts which have completely melted the underlying clad can slide into a neighboring node. For high fuel fractions in the channel the fuel flow regime can also become bubbly in PLUTO-2. However, this flow regime is not relevant for the early sweepout.

The fuel sweepout in PLUTO-2 depends strongly on the flow regimes, and thus, on the parameters controlling the flow regime transitions. For example, if the sodium liquid fraction CIBBMN, below which a transition to annular fuel flow is allowed, is set to a relatively small number, more fuel particles will be generated and swept out. A value of 0.33 was used in the reasonably successful L8 and H6 simulations (Refs. A-3 and A-4). A value of CIBBMN which is below the initial sodium film fraction (usually set to 0.15) can change the calculational results significantly because part of the liquid film has to be evaporated or entrained before the transition to annular fuel flow is possible.

## Fuel-to-Coolant Heat Transfer

In the particulate flow regime the choice of droplet diameter, which is input, is fairly significant. Although the particle drag force changes with the radius, the main effect is on the fuel-to-coolant heat transfer which is assumed to be of the following form in PLUTO-2:

$$h_{f,Na} \cdot A_{f,Na} = \frac{k}{r} \cdot \frac{M_f}{4/3\pi r^3} \cdot 4\pi r^2 \cdot (1 - \alpha_{Na})^{CIA2}$$

$A_{f,Na}$  contact area between fuel and liquid sodium,

$r$  fuel particle or droplet radius,

$k$  fuel thermal conductivity,

$M_f$  total fuel particle mass in a numerical node,

$\alpha_{Na}$  Na void fraction,

CIA2 input constant - a value of 2.0 was used in the H6 and L8 TREAT test analyses.

The fuel particle radii used for successful simulations of TOP experiments were relatively large (0.25-0.17 mm) for tests in which the initial sodium flow velocities and inlet pressures were considerably smaller than expected for realistic TOP conditions. For more prototypical conditions particle radii of 0.1 mm were found to give better agreement. The PLUTO-2 results are not very sensitive to the choice of the above-mentioned input constant CIA2 because the above heat transfer formulation is not used for most nodes in which a high void fraction exists. In nodes containing molten fuel and little liquid sodium the fuel flow regime is partially or fully annular. For this flow regime the fuel-to-sodium heat transfer coefficient is of the form:

$$\frac{1}{h_{f,Na}} = \frac{1}{h_f} + \frac{1}{h_m}$$

where

$$h_f = CIA3 \cdot v_f \cdot C_f \cdot Re_f^{0.8} / D_f$$

and



$$h_m = \begin{cases} \text{HCFFMI} & \text{for } \alpha_{\text{Na}} < 0.5 \\ 2(\text{HCFFMI} \cdot (1 - \alpha_{\text{Na}}) + \text{HCFFMI} \cdot 0.01 \cdot (\alpha_{\text{Na}} - 0.5)) & \text{for } 0.5 < \alpha_{\text{Na}} < 1 \\ (C1 \cdot (D_m \cdot \rho_m \cdot |u_f - u_m|) & \\ (C_m/k_m)^{C2} + C3) k_m/D_m & \text{for } \alpha = 1 \end{cases}$$

where:

subscript f fuel,

subscript m sodium-fission gas mixture,

Re Reynolds number,

$$Re_f = \rho_f |u_f - u_m| D_f / (2v_f)$$

CIA3, C1, C2, C3 input constants,

C specific heat,

k conductivity,

v viscosity,

D hydraulic diameter,

$\alpha$  void fraction

HCFFMI boiling heat transfer coefficient.

The main reason why the heat transfer between fuel and sodium in the annular fuel flow regime is smaller than in the particulate flow regime is however, due to the considerably smaller fuel-to-sodium interaction area in the annular flow regime.

#### PLUTO-2 Applications to In-Pile Tests

Pre- and post-test analyses of TREAT tests E8, H6, and L8 have been performed with PLUTO-2 and its predecessor PLUTO. PLUTO models only a fuel particle flow regime, does not treat fuel plate-out and has a significantly different numerical treatment than PLUTO-2. For TOP conditions the two models nevertheless compare reasonably well up to 20 to 30 milliseconds after rod failure. This is because no extensive fuel flow regime changes and fuel plate-out take place in PLUTO-2 during the early post-failure time in a TOP.

### TREAT Test E8

The E8 test simulated a 3\$/sec TOP accident in FFTF using the MK-II loop. The pressure drop provided by the pump was only about 0.2 MPa and the initial sodium velocity only 3.5 m/sec. Both values are significantly smaller than prototypic ones and have rather certainly decreased the fuel sweepout potential in this test. Nevertheless, there was considerable early fuel sweepout observed by the hodoscope. This is shown in Figs. A-3a and A-3b along with the post-test calculations performed with PLUTO (Ref. A-5). The failure location in this test was probably above the midplane which may have enhanced the sweepout. However, as discussed later, tests such as H6 and L8 with near midplane failures also showed rapid fuel sweepout. From the figures it can be seen that the sweepout in the experiment was faster than in the calculation. This is probably due to the fact that only one particle size is treated in the PLUTO codes. In the experiment there was probably a particle distribution including very small fragments which were swept upwards more rapidly than the average particle. The magnitude of the experimentally observed sweepout is also larger than calculated. This may be partially due to an overestimation by the hodoscope which does not take into account the "un-self-shielding" of fuel which has moved above the active fuel.

A PLUTO pre-test analysis also gave a fair agreement with the early sweepout by assuming simultaneous failure of 3 of the 7 rods. In the test 3 rods probably failed within 15 milliseconds.

### TREAT Tests H6 and L8

Test H6 simulated a 50 cent/sec TOP accident in FFTF using an improved MK-II loop. The pressure drop of 0.76 MPa and the initial flow velocity of 6.7 m/sec were nearly prototypic. The test showed several events which were separated by more than 100 milliseconds. The hodoscope was radially misaligned in this test and covered only half of the rod bundle. Therefore, no attempt was made to compare the calculated and measured fuel distributions in detail. However, the final hodoscope report indicates that most of the fuel motion took place in the half of the bundle which was covered by the hodoscope. This makes the comparison with the calculated sweepout more meaningful.

The L8 test simulated a LOF-d-TOP condition using three GETR-irradiated rods of 86 cm length, and a maximum power of 43 times nominal. The PLUTO-2 calculated sweepout again lagged behind the measured one (see Fig. A-4). For the later times this was probably related to the simplified fuel plate-out and fuel crust release modeling in PLUTO-2. In the pre-test analysis no fuel crust release upon melting of the underlying clad was considered. This led to the discrepancies in the sweepout above the top of the active fuel and modeling changes for the post-test calculation (Ref. A-3).

The relatively good agreement on early fuel sweepout between PLUTO-2 and both TREAT tests H6 and L8 was discussed in the main response to this question.

## Out-of-Pile Phenomenological Evidence on Sweepout

Two series of out-of-pile experiments have been performed to investigate fuel sweepout (Refs. A-1 and A-2). In the CAMEL tests performed at ANL, a  $UO_2$  - molybdenum mixture, generated by a thermite reaction, was injected laterally into flowing sodium in single and seven-pin bundles. Typically about 30% of the injected 25 g of fuel (in 7 rod tests) got swept upwards in particulate form. The remaining fuel plated out near the injection location. X-ray pictures show that the fuel accumulated at least momentarily in the sub-channels, occupying a progressively larger fraction of the channel cross

section as it spread among the rods. Local, small-scale FCI's appear to initiate the fuel dispersal in the form of fuel particles. This is in contrast to the early fuel motion modeling in PLUTO-2 which assumes that all the fuel injected into a liquid sodium stream fragments into droplets.

### References

- A-1 B. W. Spencer, et al., "Fuel Motion in the CAMEL-TOP Simulation LMFBR Safety Tests," Proc. Int'l Meeting on Fast Reactor Safety, August 1979, Seattle, Washington.
- A-2 E. Bojarski, et al., "Results of Out-of-Pile Experiments on Fuel-Sodium Interaction Using X-Ray Technique," Proc. Int'l Meeting on LMFBR Safety, July 1982, Lyon, France.
- A-3 C. H. Bowers, et al., "Analysis of TREAT Tests L7 and L8 Using SAS3D, LEVITATE and PLUTO-2," Proc. Specialists Workshop on Predictive Analysis of Material Dynamics in LMFBR Safety, March 1979, Los Alamos, New Mexico, LA-7938-C.
- A-4 H. U. Wider, et al., "The PLUTO-2 Overpower Excursion Code and a Comparison with EPIC," Proc. Int'l Meeting on Fast Reactor Safety, August 1979, Seattle, Washington.
- A-5 H. U. Wider and L. A. Semenza, "Analysis of TREAT Transient Overpower Experiments Using the PLUTO Codes," Proc. Specialists Workshop on Predictive Analysis in LMFBR Safety, March 1979, Los Alamos, New Mexico, LA-7938-C.

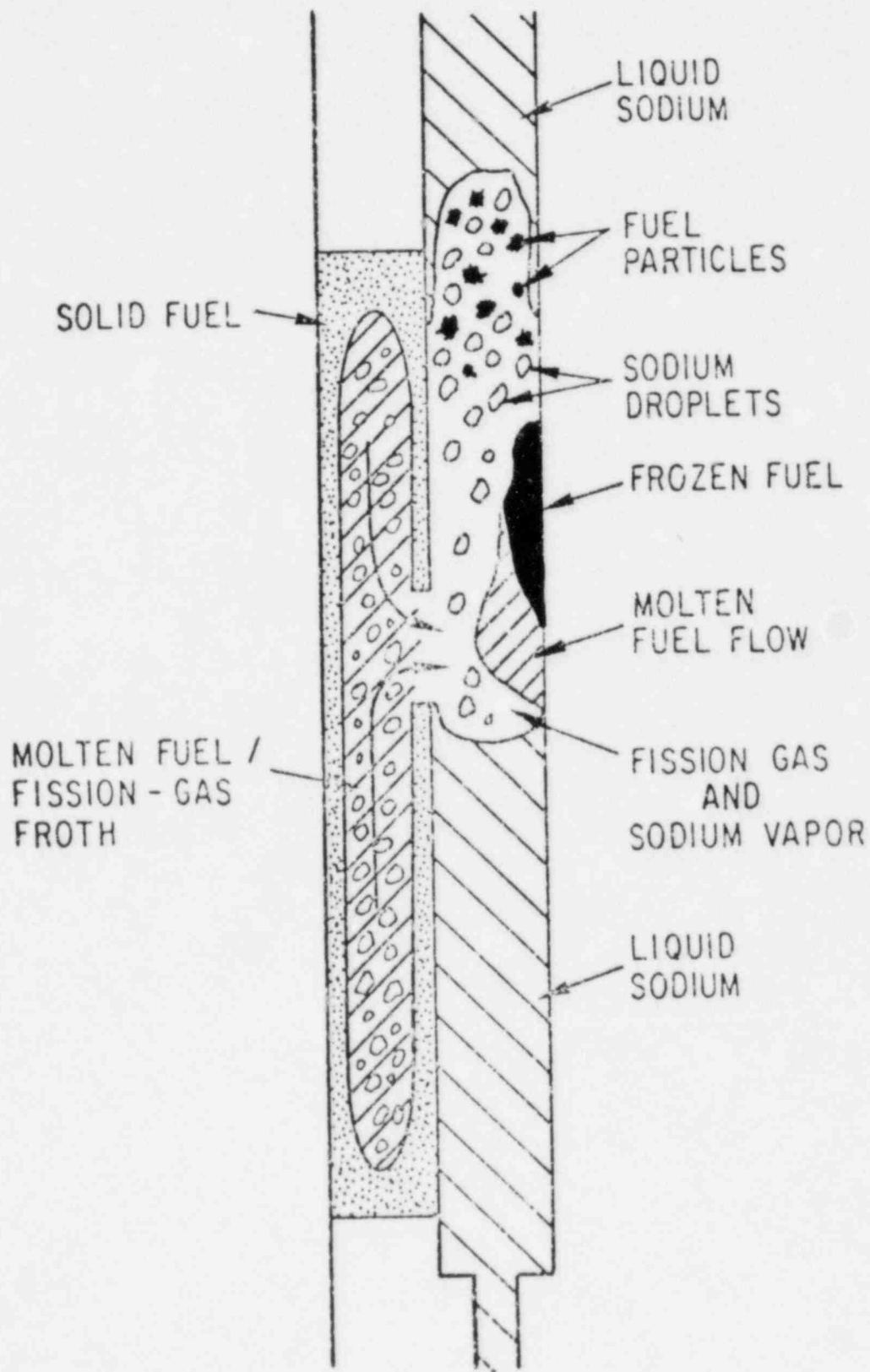


Fig. A-1 Schematic of PLUTO-2.

QCS760.178A1-A7

Amend. 72  
Oct. 1982

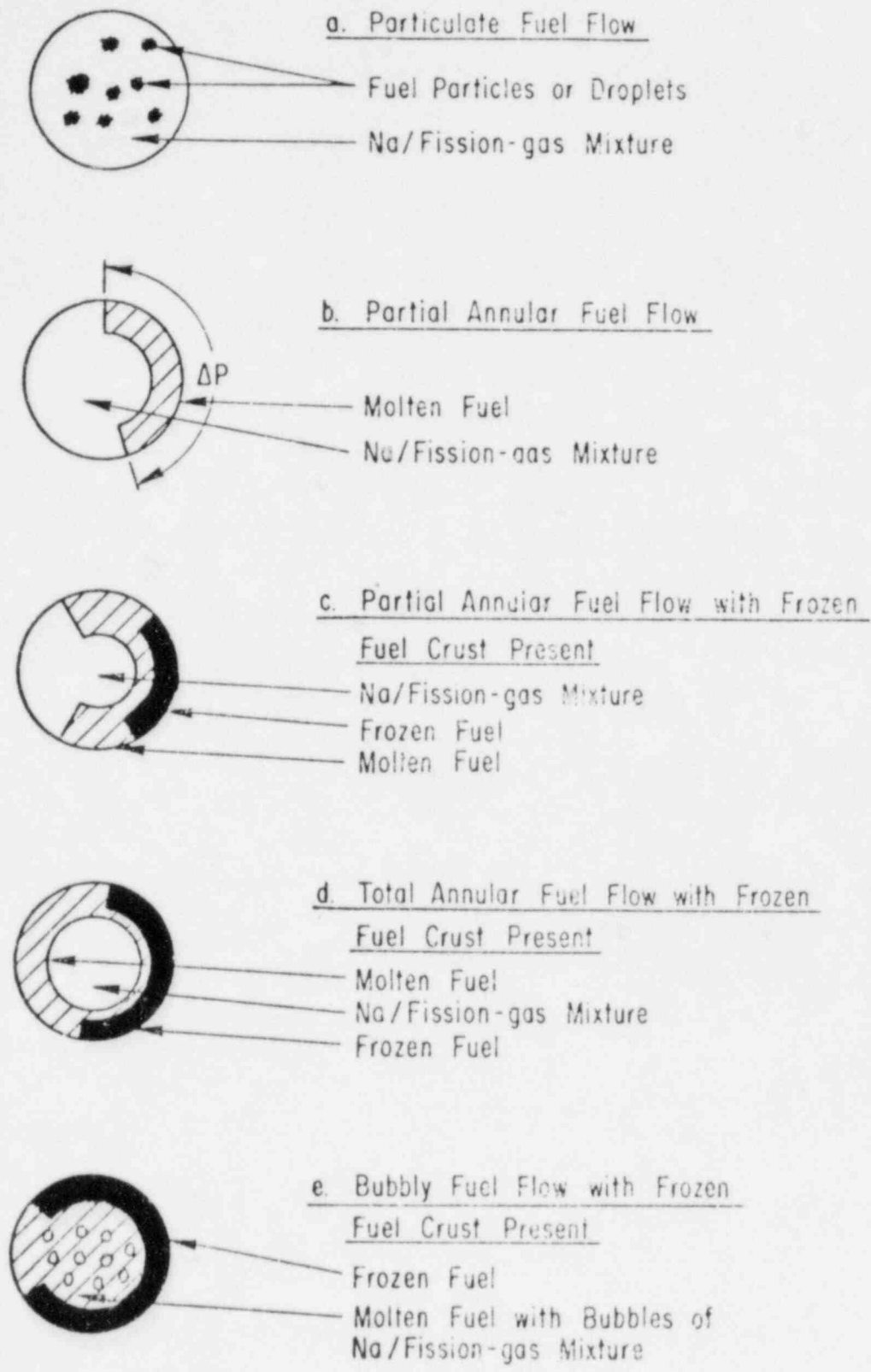


Fig. A-2 Fuel Flow Regimes in PLUTO-2.

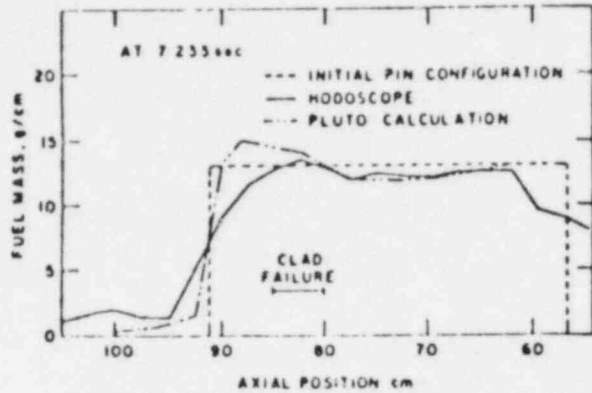


Fig. A-3a Hodoscope-Determined and PLUTO-Calculated Fuel Distributions in E8 at 23 msec after First Fuel Ejection (Top of Initial Fuel at 91 cm).

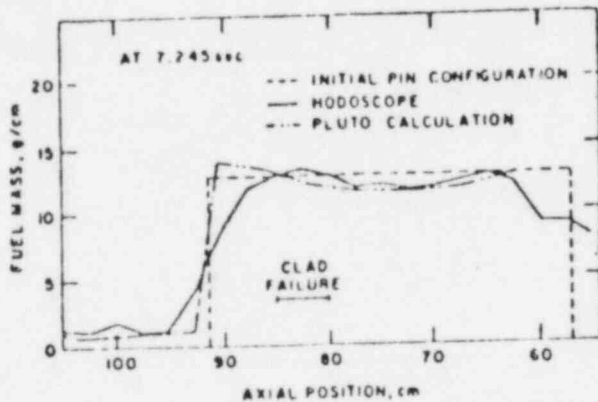


Fig. A-3b Hodoscope-Determined and PLUTO-Calculated Fuel Distributions in E8 at 35 msec after First Fuel Ejection (Top of Initial Fuel at 91 cm).

QCS760.178A1-A10

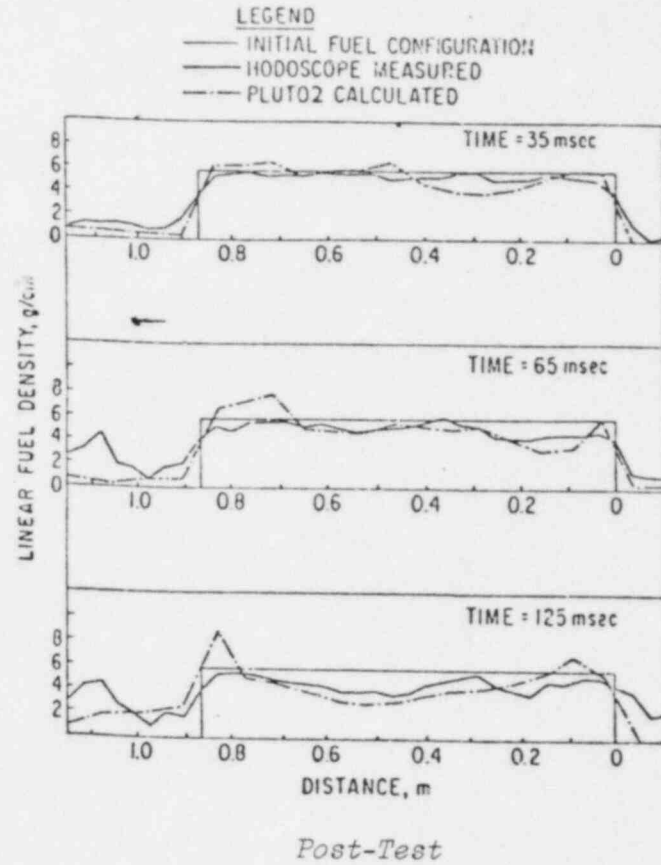
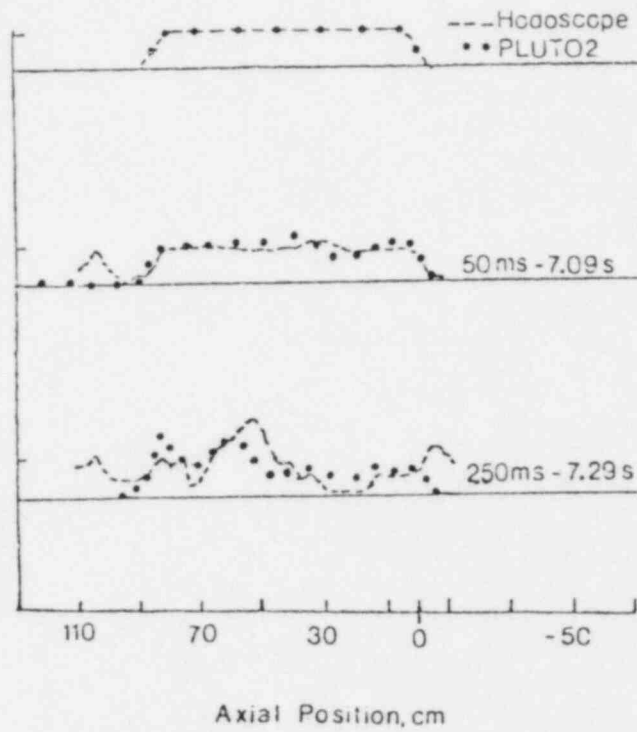


Fig. A-4 Fuel Motion Analysis for L8.

Amend. 72  
Oct. 1982

### Question CS760.178A2

An LOF-d-TOP might still occur if the sodium void worth is 50-60 percent higher and internal fuel motion in TOP type channels can occur. What are the reactivity uncertainties of sodium void, Doppler, axial expansion and lead channel fuel motion? How do you interpret the significance of these uncertainties?

### Response

A detailed review of the reactivity uncertainties used by the Project has been performed. The conservative values previously used (Ref. QCS760.178A2-1) for the Doppler (+ 20%) and fuel expansion (- 40%) are still considered appropriate. The lead channel fuel motion behavior is extensively addressed in the response to QCS760.178A3 and the conclusions on nominal behavior are incorporated herein. The positive sodium void reactivity effect is the most important reactivity insertion mechanism to be considered in the study of loss-of-flow accidents without scram leading to overpower-induced rod failures in unvoided low-power assemblies (LOF-d-TOP). The sodium void has been re-evaluated for the CRBRP BOC-1 and EOC-4 configurations using the same data base and computational methodology as those employed in the analysis of the zero-power experiments at the ZPPR critical facility. The evaluation yields an experimentally-based, best estimate value for the sodium void reactivity and its associated uncertainty.

The impact of the derived coolant void reactivity data on the potential for LOF-d-TOP behavior in CRBRP has been assessed. The EOC-4 core would be the most likely to have LOF-d-TOP potential, due to the occurrence of the maximum positive void reactivity at the end-of-life. Detailed analysis of the loss-of-flow event in the EOC-4 core using the best estimate coolant void reactivity worths upwardly adjusted to very conservatively envelop uncertainties has demonstrated the absence of LOF-d-TOP potential. Recent analysis and results from TREAT test L8 suggest that the autocatalytic reactivity effects previously associated with whole-core LOF-d-TOP events were over-estimated.

The remainder of the response has been divided into two sections dealing first with the sodium void worth and uncertainty determination, followed by a whole-core effect analysis, which supports the absence of LOF-d-TOP.

### Sodium Void Uncertainties

The uncertainties assigned to calculated values of the sodium void reactivity worth are of interest because of their impact on the probability of an LOF-d-TOP. Large uncertainties are often quoted since the sodium void reactivity involves a competition between two large and opposite signed effects; a positive non-leakage component and a negative leakage component. Calculated worths are therefore sensitive to the computational methods, modeling and data which are used. If attempts are made to assess the uncertainties based upon sensitivities to alternative computational models, the results of the study would be quite dependent on the particular methodology. An alternative approach makes use of the available experimental data to deduce a predicted value with associated uncertainties which are independent of the particular methodology. Such an approach has been adopted herein.



During the past decade a large experimental data base has been established on sodium-void reactivity effects in LMFBRs. An assessment of these data has recently been completed at ZPPR and provides the input required to establish an uncertainty for the CRBRP sodium-void reactivity effect (Ref. QCS760.178A2-2). The assessment included analysis of over 100 critical experiments in LMFBR-type assemblies of CRBR size or larger. The same data base (ENDF/B-IV) and methods were used for all of the analyses. Bias factors and uncertainties were obtained as a function of reactor type, size, zone, enrichment, and blanket fissile buildup. By applying such bias factors for CRBR analysis to calculations which use the same methodology as that applied in the critical experiment analysis, a best estimate of physically observable void reactivities can be determined for a specific void configuration. The best estimate value and its uncertainty would be independent of both computational method and differential data base. The results could then be used to assess the accuracy of other analyses such as those used in previous CRBR safety studies. In assigning total uncertainty to the best estimate value, consideration must be given to those effects which are not completely addressed by the critical experiments. Such effects include the impact of fission products, temperature distribution, fuel rod rather than plate geometry, and sequence of voiding.

The reference method used in the analysis of both the critical experiments and the power reactor include exact-perturbation diffusion theory, three-dimensional modeling, twenty or more energy groups, Benoist treatment of neutron streaming, energy and spatial self-shielding corrections, ENDF/B-IV cross section data\* and ENDF/B-V delayed neutron data. Various methods approximations were investigated as part of the assessment study and the only improvements that were found to be significant relative to this reference method were for transport and mesh effects in a few isolated cases.

A comparison of the results of calculation against experiment for different subsets of the ZPPR critical experiment data base is given in Table QCS760.178A2-1. Studies made explicitly for CRBRP during the engineering mockup critical (EMC) experiment program, BOC-1 and EOC-4, are included in the table. The difference between the BOC-1 and EOC-4 results are explained by transport effects that are significant for the clean heterogeneous core, but not for the more homogeneous EOC core.

The approach chosen for biasing the calculated CRBRP sodium coefficients and for assigning uncertainties was to divide the reactor into four zones, and to preserve the integral parameters for those zones. The zones chosen were:

1. Core zones with a positive reactivity signal (central core zones),
2. Core zones with a negative reactivity signal (external core zones),
3. Axial blanket zones,
4. Internal blanket zones.

---

\* Although not relevant for the critical experiment analysis, the power reactor calculations used the ENDF/B-V fission product data.

Table QCS760.178A2-1

## RATIOS OF CALCULATED TO MEASURED REACTIVITIES FOR SODIUM VOIDING

Cases	C/E Before Biasing	% Standard Deviation After Biasing <sup>a</sup>
CRBR-EMC <sup>b</sup> BOC-1, Positive Part of Core	0.98	10
CRBR-EMC EOC-4, Positive Part of Core	1.23	6
101 Mixed Zones <sup>c</sup>	1.08	12
Axial Blankets without Control Rods	0.91	1
Axial Blankets with Control Rods	1.23	2
Core Zones with Negative Reactivity Signals	1.02	9

<sup>a</sup>Separate bias factors applied to positive and negative components of reactivity. For any subset, the average C/E is 1.0 after biasing.

<sup>b</sup>Engineering mockup critical experiments for sodium-void reactivity in CRBR; reactor geometry and composition closely matched.

<sup>c</sup>This and the following entries are LMFBR-type configurations but not CRBRP specific.

Table QCS760.178A2-2 lists the bias factors and the calculational uncertainties assigned to CRBR. In fact, only the central core region of the EOC-4 void reactivity is biased. Because the calculations tend to be more positive than measured reactivities, it is both conservative and easier to use a 1.0 bias factor if the best estimated value is less than unity by an amount significantly smaller than the assigned uncertainty. The uncertainties assigned to external core zones and axial blanket zones are larger than would be indicated by Table QCS760.178A2-1, but these zones were not specifically included in the CRBR-EMC studies.

Table QCS760.178A2-2

BIAS FACTORS AND UNCERTAINTIES FOR  
SODIUM-VOID REACTIVITY IN CRBRP

Zone	Bias Factor <sup>a</sup>		Calculational Uncertainty <sup>b</sup> %	
	BOC-1	EOC-4	BOC-1	EOC-4
Central Core	1.0	0.82	10	6
External Core	1.0	1.0	10	10
Axial Blankets	1.0	1.0	20	20
Internal Blankets	1.0	1.0	20	20

<sup>a</sup>To be multiplied times the calculated value.

<sup>b</sup>To be added in quadrature with uncertainties from other sources (see Table QCS760.178A2-4).

When extrapolating the above zero-power results to a power reactor, additional effects require consideration. Since differences in sodium-void between ZPPR and the CRBR are implicitly accounted for in the calculational models, such effects lead only to additional uncertainties.

The ZPPR assemblies are built of fuel plates whereas the power reactor uses rods. The effects of the different geometry on the calculational uncertainty were investigated by analyzing small zone critical experiments in rod geometry using the reference methods. No significant change in ability to calculate the void worth in the different geometries was noted. As a consequence, no additional uncertainty is required to account for the change in fuel geometry.

The void worth in the power reactor is calculated by assuming that flowing sodium has been voided from all fuel assemblies. The worth tables so derived are used to determine the sodium-void reactivity for the specific reactor configurations throughout the voiding sequence. The uncertainty introduced by this approximation was determined by comparing ZPPR calculation with experiment using both the exact sequence modeling and the more approximate model. An uncertainty of  $\pm 3.5\%$  can be ascribed to this effect.

Although the CRBR-EMC critical experiments matched the nuclide compositions very well, no attempt was made to simulate the build-up of fission products during the fuel cycle. Therefore, an uncertainty arising from the fission product inventory is introduced for the EOC-4 configuration. The fission products increase the non-leakage term in the sodium-void effect through changes in the real and adjoint neutron flux. Calculations were performed to investigate this effect. If an uncertainty of  $\pm 20\%$  is assumed

in the absorption cross section of the fission product data, an uncertainty of  $\pm 4\%$  is introduced in the calculated sodium-void reactivity. There is considerable evidence to suggest that such an uncertainty is very conservative. The reference calculation made use of a lumped fission product derived from the ENDF/B-V data files. A second calculation was run using lumped fission product data from ENDF/B-III which are based on a 20 year old evaluation of Garrison and Roos (Ref. QCS760.178A2-3). The difference in the calculated sodium void reactivity for the two sets of data is less than 0.5%. A recent NEACRP benchmark calculation compared fast reactor spectrum averaged fission product capture data and some of the results are given in Table QCS760.178A2-3. It is of interest to note that the ANL results are  $\sim 9\%$  higher than the mean of all the countries participating in the exercise, and  $\sim 20\%$  higher than the French results which are adjusted to PHENIX operating data. A larger fission product cross section yields a larger sodium-void reactivity since the larger absorption in the middle and low energy regions will reduce the adjoint flux at these energies making the slope more positive and thus increasing the non-leakage component. Hence, a reduction in the ANL fission product capture cross section consistent with the French data would decrease the calculated sodium void reactivity worth. Based upon such results, it seems conservative to assume that the sodium-void reactivity calculated from the reference fission product data has an uncertainty of  $\pm 3\%$ .

Table QCS760.178A2-3

NEACRP BENCHMARK SPECTRUM AVERAGED PSEUDO  
FISSION PRODUCT CAPTURE CROSS SECTION (barns)

Mean of All Participants*	.5002
St. Deviation	.0807
-----	
ANL	.5466
France	.4400
United Kingdom	.5200
Japan	.5613

\* Only four of eight participants are shown in Table QCS760.178A2-3.

The zero-power experiments were performed with fuel temperatures near room temperature whereas the temperature in the CRBR may range from the normal operating conditions to much hotter in an accident scenario. Such variation in temperature is not represented in the sodium-void model. The main impact of raising the fuel temperature in a mixed oxide fueled core is to change the capture rate in  $^{238}\text{U}$  and hence the shape of the adjoint flux and the magnitude of the real flux at resonance energies. The uncertainty in the sodium-void effect at high fuel temperature can be related to the room temperature results through the uncertainty in the Doppler reactivities. It is therefore possible to derive an additional uncertainty in the sodium-void effect at high

temperature relative to room temperature by applying the uncertainties in the Doppler effect. Such an analysis leads to an uncertainty of  $\sim 2.5\%$  (Ref. QCS760.178A2-4).

Table QCS760.178A2-4 lists the percentage uncertainties due to effects other than those inherent in the calculational method. These uncertainties must be added with those given in Table QCS760.178A2-2 to give the total uncertainty.

Table QCS760.178A2-4

ADDITIONAL UNCERTAINTIES IN CRBR SODIUM-VOID REACTIVITY

Source	Uncertainty <sup>a</sup>	
	% of Total Reactivity BOC-1	EOC-4
Fuel Rods Instead of Plates	0	0
Sequence of Voiding	3.5	3.5
Temperature Distribution	2.5	2.5
Fission Products	0	3.0

<sup>a</sup>To be added in quadrature with the values from Table QCS760.178A2-2

Using the reference methods and the appropriate neutronics models, the sodium void reactivity was calculated for the BOC-1 and EOC-4 reactor configurations. Biased region-wise reactivity worths are given in Table QCS760.178A2-5. The data have also been processed in the form of SAS3D channel data to allow a comparison of these best-estimate predictions with earlier values used for CRBR safety analysis. In Table QCS760.178A2-6 the biased worths are compared with the values used in the CRBR analysis as documented in Tables 4-5 and 4-6 of Ref. QCS760.178A2-1. The large discrepancies can be attributed to differences in computational methodology; e.g., ENDF/B-III vs. ENDF-B/IV and First Order Perturbation Theory vs. Exact Perturbation Theory. While the differences may appear large, the new values, even with the uncertainties as discussed below, fall entirely within the uncertainty range documented in Ref. QCS760.A2-1.

Table QCS760.178A2-5

BEST ESTIMATE SODIUM VOID<sup>a</sup> REACTIVITY WORTHS (\$) <sup>b</sup>

	BOC-1	EOC-4
<u>Driver Assemblies</u>		
Core	0.256	1.528
Lower Axial Blanket	-0.225	-0.160
Upper Axial Blanket	-0.177	-0.177
Total	-0.146	1.191
<u>Internal Blanket Assemblies</u>		
Core	1.381	1.593
Lower Axial Extension	0.008	-0.020
Upper Axial Extension	-0.007	-0.006
Total	1.382	1.567

<sup>a</sup>Void flowing sodium, within assemblies (82% of driver and 73% of blanket sodium removal per mesh cell.

<sup>b</sup> $\beta = .0032$

#### Whole-Core Analysis

To provide a measure of the sensitivity of predicted accident energetics to variations in the sodium void reactivity, the SAS3D analysis reported in the response to question QCS760.178A3 was repeated using the higher positive coolant voiding reactivity worths discussed above. The assumptions behind this case are identical to the best estimate EOC-4 case reported in Ref. QCS760.178A2-1, but with TREAT L6/L7 correlated fuel motion modeled as discussed in the response to QCS760.178A3. The EOC-4 core state was chosen because it has the highest positive coolant voiding reactivity effect, and would thus be the most likely to exhibit LOF-d-TOP behavior.

To establish an upper bound for the coolant void worth in the EOC-4 core, the uncertainties contained in Tables QCS760.178A2-2 and -4 were combined quadratically to yield a net uncertainty of 7.9% in the central core (positive reactivity) region, 11.3% in the external core (negative reactivity) region, and 20.7% in the axial and internal blanket regions. In each of the respective regions, an amount of positive reactivity corresponding to twice these uncertainties was then added to the biased, evaluated worth so that positive reactivities in the central core were increased by 15.9%, negative reactivities in the external core were decreased by 22.6% and positive and negative reactivities in the axial and internal blankets were increased and decreased,

Table QCS760.178A2-6 ACTIVE CORE REGION (91 cm) FLOWING SODIUM MATERIAL WORTH, DOLLARS<sup>a</sup>

SAS Channel Number	BOC1				EOC4			
	Assembly Type	Number Assemblies	CEFR <sup>b</sup> 00523	Current Best Estimate	Assembly Type	Number Assemblies	CEFR <sup>b</sup> 00523	Current Best Estimate
1	B	7	.056	.089	B	7	.100	.142
2	F	12	.096	.159	F	21	.386	.454
3	B	15	.152	.229	B	21	.330	.463
4	F	18	.191	.291	F	9	.160	.189
5	B	30	.373	.534	B	36	.559	.735
6	B	6	.068	.101	F	6	.085	.103
7	F	24	.144	.287	F	12	.165	.198
8	B	24	.303	.415	B	12	.125	.158
9	F	18	.090	.183	F	6	.027	.042
10	F	9	.002	.051	F	12	.113	.141
11	F	9	.002	.052	F	24	.366	.425
12	F	12	-.071	-.025	F	12	-.038	-.011
13	F	12	-.072	-.027	F	18	.116	.141
14	F	18	-.454	-.453	F	18	-.200	-.186
15	F	24	-.282	-.263	F	24	-.082	-.059
Total Driver		156	-0.354	0.255		162	1.098	1.438
Total Internal Blankets		82	0.952	1.368		76	1.114	1.498
Total Core		238	0.598	1.623		238	2.212	2.936

<sup>a</sup>  $\beta = .0034$  value used for consistency in comparison with Ref. Q760.178A2-1.

<sup>b</sup> Ref. QCS760.178A2-1.

QCS760.178A2-8

Amend. 72  
Oct. 1982

respectively, by 41.4%. The net results of these changes are summarized in Table QCS760.178A2-7 which shows the maximum positive (i.e., sum of all positive spatial values) coolant voiding reactivity as derived from the SAS3D EOC-4 input deck, the current best estimate biased worths, and the biased worths upwardly adjusted with uncertainties of 15.9%, 22.6%, and 41.4%. The most conservative result shows an effective increase of 31% in the driver sub-assemblies, 84% in the internal blankets, and 52% overall, when compared to the original void worths used in Ref. QCS760.178A2-1.

Table QCS760.178A2-7  
 COMPARISON OF MAXIMUM POSITIVE COOLANT  
 VOIDING REACTIVITIES IN DOLLARS

Region	Ref. QCS760.178A2-1	Current Best Estimate	Current Best Estimate Plus 2 x Uncertainty	Net Increase Over Ref. QCS760.178A2-1
Driver	1.67	1.89	2.19	31%
Internal Blankets	1.12	1.45	2.06	84%
Total	2.79	3.34	4.24	52%

The event sequence predicted by SAS3D using the upwardly adjusted coolant void worths is given in Table QCS760.178A2-8. This event sequence can be directly compared to the event sequence given in Table QCS760.178A3-4 of the response to QCS760.178A3. As the comparison shows, increasing the void worths caused an increase in the maximum power and a shortened time frame for whole core involvement. Coolant boiling begins in every driver assembly before fuel in the hottest assemblies, channel 6, melts and begins to move. The core-wide voiding pattern just prior to the time of fuel motion initiation in channel 6 is shown in Fig. QCS760.178A2-1. As this figure shows, at the time of fuel motion in channel 6, complete core voiding of all the driver assemblies has been achieved in channels 2, 4, 6, 7, 9, 10, and 11. LOF-d-TOP type failures are thus ruled out in these channels. Partial voiding has occurred in channels 12, 13, 14, and 15, and failures into liquid sodium are therefore not ruled out. However, the core power is only a factor of ten above nominal power, and failure conditions are far from being met in these low-power channels. As time progresses, coolant voiding continues until fuel melting in driver channels 2, 4, and 7 at approximately 8.5 P leads to fuel dispersal and initial neutronic shutdown at 17 seconds following loss-of-flow initiation.

At the time of termination of the calculation, the core was subcritical and negative fuel motion reactivity was being added at a rate of -6.9 \$/sec. The core-wide voiding pattern at termination is given in Fig. QCS760.178A2-2. This figure shows that at this point in time, all of the driver assemblies



Table QCS760.178A2-8

## WHOLE CORE ANALYSIS RESULTS WITH ENHANCED COOLANT VOID REACTIVITY WORTHS\*

Time	Event	CHN	P/PO	RHO	RHOD	RHOE	RHOV	RHCF	RHOC
11.9448	Coolant Boiling	6	0.891	-0.059	-0.168	-0.077	0.186	0.0	0.0
13.5350	Coolant Boiling	2	0.936	0.006	-0.193	-0.091	0.289	0.0	0.0
13.8150	Coolant Boiling	4	0.927	-0.011	-0.200	-0.096	0.286	0.0	0.0
14.2150	Coolant Boiling	7	0.920	-0.022	-0.210	-0.103	0.291	0.0	0.0
15.4115	Coolant Boiling	10	1.611	0.367	-0.276	-0.167	0.811	0.0	0.0
15.4365	Coolant Boiling	11	1.656	0.381	-0.280	-0.170	0.831	0.0	0.0
15.7603	Coolant Boiling	9	2.004	0.433	-0.332	-0.221	0.987	0.0	0.0
15.8382	Coolant Boiling	13	2.172	0.466	-0.345	-0.235	1.046	0.0	0.0
16.1720	Coolant Boiling	12	3.610	0.641	-0.406	-0.306	1.353	0.0	0.0
16.2195	Clad Motion	6	4.274	0.686	-0.421	-0.325	1.432	0.0	0.0
16.3095	Peak Reactivity	-	8.711	0.823	-0.476	-0.396	1.648	0.0	0.047
16.3555	Coolant Boiling	15	7.645	0.777	-0.514	-0.439	1.664	0.0	0.067
16.3979	Coolant Boiling	14	6.045	0.702	-0.540	-0.465	1.639	0.0	0.068
16.5470	Fuel Motion	6	9.827	0.788	-0.607	-0.534	1.889	0.0	0.040
16.6258	Peak Power	-	10.877	0.785	-0.656	-0.576	1.977	0.001	0.039
16.6938	Coolant Boiling	5	9.217	0.723	-0.695	-0.605	1.971	0.013	0.039
16.7034	Fuel Motion	7	8.728	0.705	-0.699	-0.607	1.958	0.015	0.038
16.7072	Fuel Motion	2	8.565	0.698	-0.701	-0.608	1.953	0.016	0.038
16.7097	Fuel Motion	4	8.460	0.694	-0.702	-0.608	1.950	0.017	0.037
16.7705	Fuel Motion	10	7.602	0.650	-0.723	-0.613	1.930	-0.051	0.107
16.7805	Fuel Motion	11	8.337	0.679	-0.726	-0.615	1.943	-0.046	0.123
16.7916	Coolant Boiling	3	9.123	0.705	-0.731	-0.616	1.953	-0.038	0.137
16.8286	Fuel Motion	9	6.722	0.590	-0.742	-0.619	1.952	-0.171	0.170
16.8911	Coolant Boiling	1	5.442	0.482	-0.751	-0.623	1.978	-0.348	0.226
16.8911	Coolant Boiling	8	5.442	0.482	-0.751	-0.623	1.978	-0.348	0.226
16.9855	Fuel Motion	13	2.519	-0.109	-0.748	-0.623	2.081	-1.089	0.270
17.0392	Clad Motion	2	1.649	-0.675	-0.735	-0.622	2.292	-1.883	0.271
17.1280	Termination	-	1.393	-0.981	-0.716	-0.620	2.647	-2.510	0.308

\* Nomenclature is as follows: CHN - SAS channel number.  
P/PO - Core power relative to nominal.  
RHO - Net reactivity in dollars.  
RHOX - Reactivity in dollars due to Doppler (D), axial expansion (E), sodium void (V), fuel motion (F), and cladding motion (C).

QCS760.178A2-10

Amend. 72  
Oct. 1982

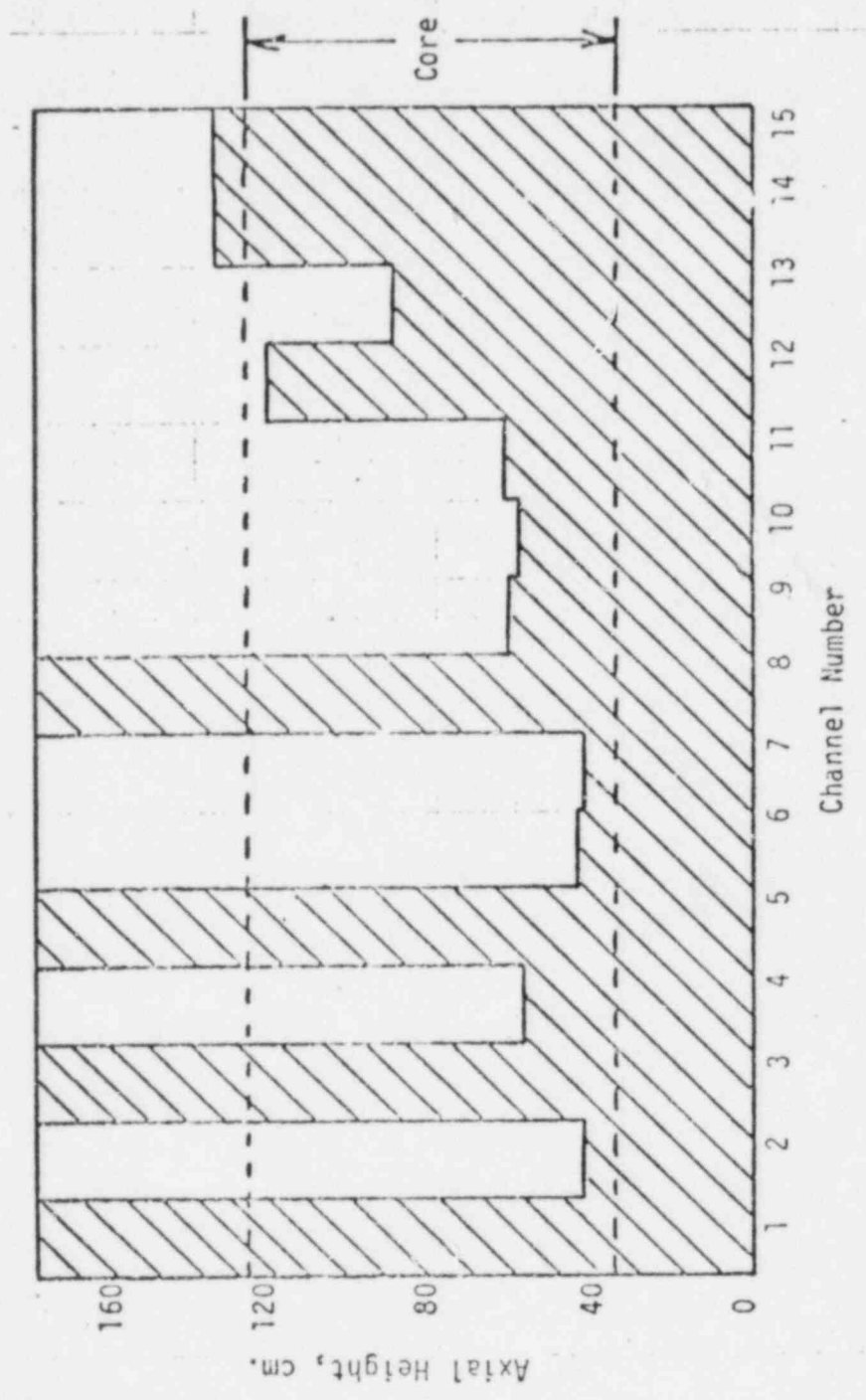


Fig. QCS760.178A2-1 Core Wide Voiding Pattern at Fuel Disruption in Channel 6.

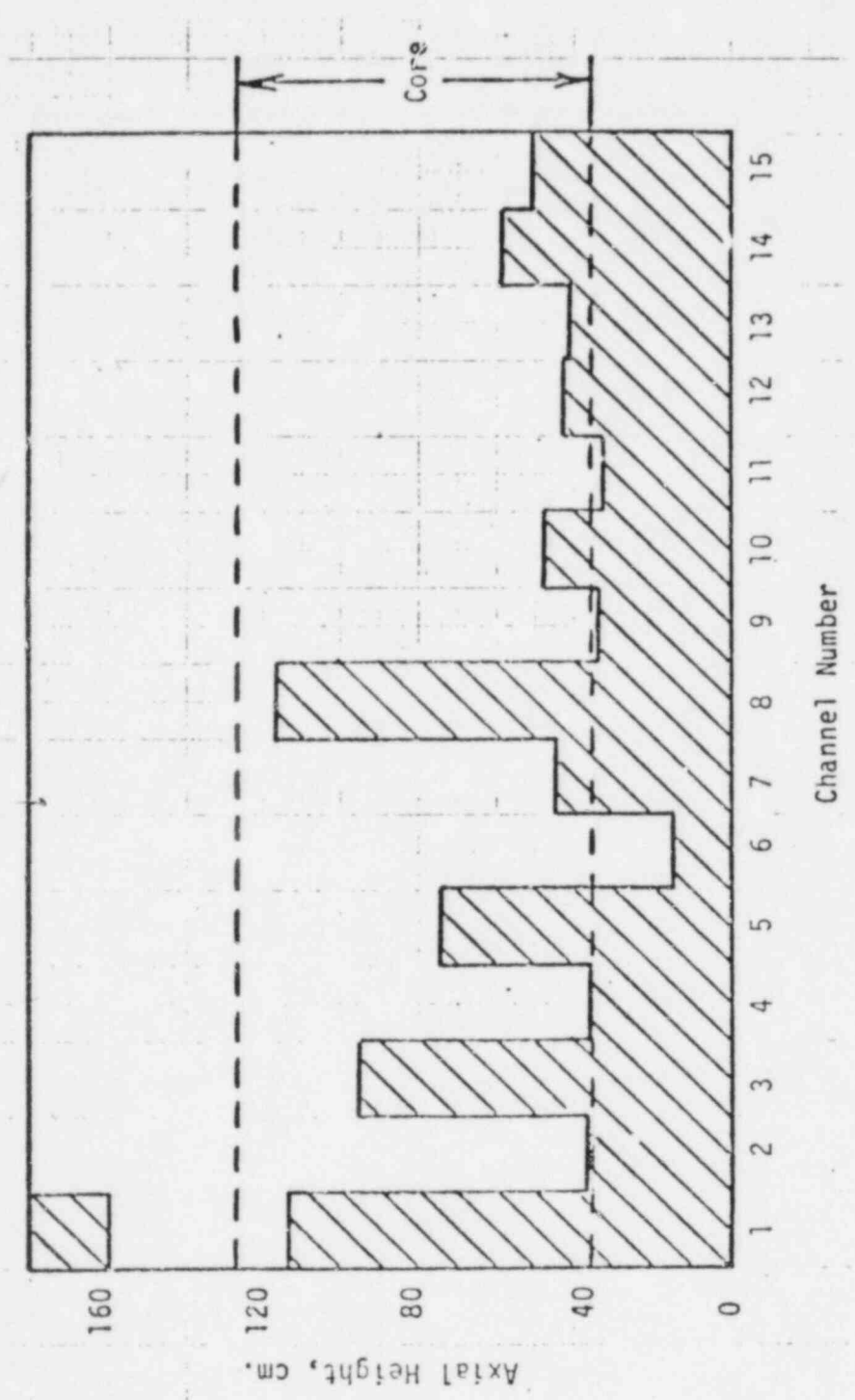


Fig. QCS760.178A2-2 Core Wide Voiding Pattern at Termination.

have completely voided. In addition, internal blanket channels 1, 3, 5, and 8 have begun to void, and given the low power level, no subsequent blanket rod failures would be expected. Rather, continued coolant boiling would be expected, with the positive reactivity addition being offset by the negative fuel dispersal in the disrupted driver assemblies. At termination, the peak fuel temperature was less than 3500°C, and a gradual and benign entry into the melt-out phase would follow.

This analysis demonstrates that when appropriate and experimentally verified fuel motion behavior in voided assemblies is employed, conservative estimates of the uncertainties in the reactivity feedback associated with coolant voiding have little effect on predicted levels of initiating phase energetics. While some details (i.e., transient power levels, time scales, material motions) did change, no threshold for LOF-d-TOP events was found.

#### References

- QCS760.178A2-1 S. K. Rhow, et al., "An Assessment of HCDA Energetics in the CRBRP Heterogeneous Reactor Core," CRBRP-GEFR-00523, General Electric Company, December 1981.
- QCS760.178A2-2 C. L. Beck, et al., "Sodium Void Reactivity in LMFBRs; a Physics Assessment," APR-TM-400, Argonne National Laboratory, September 1981.
- QCS760.178A2-3 J. D. Garrison and B. W. Roos, Nucl. Sci. Eng., 12, p. 115, 1962.
- QCS760.178A2-4 A. T. D. Butland, W. N. Simmons, and J. M. Stevenson, "An Assessment of Methods of Calculating Sodium-Voiding Reactivity in Plutonium-Fueled Fast Reactors," Fast Reactor Physics 1979, Proceedings of an International Symposium on Fast Reactor Physics, Vol. 1, p. 281, Aix-En-Provence, pp. 24-28, September 1979.

Question CS760.178A3

What is the potential for autocatalysis due to plenum fission gas acting on the fuel column to force axial compaction as disruption occurs in the initiating phase of the LOF?

Response

An assessment of this question resulted in the conclusion that the potential for fission gas induced compaction in the CRBRP is negligible, due to the release of the gas into the coolant channel prior to fuel column disruption.

The heterogeneous core design minimizes concern for a range of accidents involving autocatalytic behavior because of the substantial reduction in the sodium void worth in the driver assemblies and the significant incoherence in thermal-hydraulic response at EOC-4 conditions. To provide a resolution to this question, a comprehensive examination of the important physical phenomena and their implication on the assessment of whole core behavior was performed. Included in this examination was a phenomenological review of the response of the plenum fission gas to both cladding failure (depressurization) as well as fuel column compaction during the accident scenario described in Ref. QCS760.178A3-1. In addition, it was recognized that the potential for the plenum gas compaction problem may have been exaggerated by the use of known conservative assumptions in the modeling of fuel dispersal after rod disruption (Ref. QCS760.178A3-1, Section 7.2.1). Thus, a review of relevant experimental information, a detailed examination of critical phenomenology, and a modeling effort to describe fuel motion consistent with the experiments were performed concurrently. With such an assessment providing the justification for fuel dispersal modeling, the whole core dynamic response was re-examined with the SAS3D code.

A preliminary assessment of the physical phenomena associated with potential plenum fission gas effects led to several conclusions. Among the most important of these are: (1) the fission gas plenum pressure is not likely to cause fuel motion to initiate earlier than would be expected based on fuel motion thermal criteria, (2) unless the plenum and upper axial blanket cladding can move far enough upward to clear the blanket fuel pellet stack, such motion will not reduce the plenum pressure sufficiently to preclude influence on fuel motion, (3) the gap between blanket cladding and blanket fuel pellets is expected to remain sufficiently open and free of fission products so that neither gas release through the gap to a cladding failure farther down on the fuel rod nor downward motion of the blanket pellets will be restricted, and (4) the timing of events in the CRBRP best estimate analysis (Ref. QCS760.178A3-1) is such that plenum fission gas influence on fuel motion in some of the later-failing channels (starting with channel 11) might be possible.

The approach taken in this report is to reassess the experimental bases to support a less conservative fuel motion modeling than used in the previous CRBRP analysis. In performing the reassessment, particular attention is paid to the TREAT L6 and L7 LOF experiments which are used to calibrate the SAS 3D/SLUMPY fuel motion model for use in whole-core accident analysis. The SAS3D experiment and whole-core analyses are supplemented with FRAS3 (Refs.

QCS760.178A3-2, -3, -4) calculations to establish the amount of fission gas that is likely to be present in the fuel and available to assist in fuel dispersal following the onset of fuel motion. It is concluded that an experimental-analytic bases can be defined to support more realistic lead fuel channel response to the LOF conditions. When the more realistic modeling is used, it is found that all channels have time to release enough plenum fission gas prior to fuel motion to remove this potential fuel compaction mechanism.

In the remainder of this report, the TREAT LOF tests which have been conducted during the past several years will be briefly characterized. Then the FRAS3 code which provides the basis for estimating the amount of fission gas available to participate in fuel motion will be reviewed. Next, the SAS3D analyses of the L6 and L7 TREAT tests and the CRBR LOF scenario will be described. Finally, some of the sensitivities and uncertainties found in both the test analyses and the whole-core calculations will be identified.

### Experimental Basis

A listing of LOF experiments carried out in the TREAT reactor is made in Table QCS760.178A3-1 (Ref. QCS760.178A3-5). Fuel motion in these experiments was monitored using the fast neutron hodoscope (Ref. QCS760.178A3-6). Although all of these tests are pertinent to the understanding of LOF transients, tests L6 and L7 were selected as the database for calibrating SAS3D/SLUMPY because only tests L6 and L7 were performed using (1) irradiated fuel, (2) nearly meter-length fuel pins, and (3) a 1.2-meter hodoscope collimator viewing height.

From a review of the results of all the tests listed above, it is possible to make some general observations. For the tests that were conducted at nominal power, it was found that fuel which had been irradiated long enough to accumulate a significant gaseous fission-product inventory compacted at a slower rate and to a lesser extent than fresh fuel at the time of melting. When the power levels were at 6 times nominal or higher, the test results indicated dispersive tendencies. It is judged that fission gas was an important contributor to both the slower rate of compaction observed in irradiated fuel at nominal power and the dispersive tendencies observed in the higher power tests.

The L6 and L7 tests were designed to simulate accident conditions that were identified in SAS3D analyses of the CRBRP homogeneous design. The fuel rods used in the tests were irradiated in a thermal-neutron spectrum at a peak linear power of 36 kW/m to a peak burnup of about 3.0 atom percent. The L6 test was designed so that fuel would fail into a voided coolant channel near the time of peak power in a transient in which peak power would be about 10 times nominal. The L7 test had a similar design except that the peak power was to be about 20 times nominal. Both tests achieved their respective objectives.

A description of the tests is given in Ref. QCS760.178A3-7. For the present discussion, the most important instrument is the 1.2-meter fast neutron hodoscope. This device counts collimated fast neutrons produced by fissions in the test fuel to form an image of the fuel. As fuel moves about, the count rate of fast neutrons increases in regions where the fuel density

increases and diminishes in regions where the density decreases thus enabling the hodoscope to form a dynamic image of the fuel relocation.

### FRAS3 Calculations

FRAS3 is the current developmental version of the FRAS code which has been used at Argonne for more than eight years to model transient fission gas behavior in mixed oxide fuels. The FRAS3 code models transient fission gas release as a two-step process. In the first step, gas within the fuel grains is released to the grain boundary. In the second step, gas on the grain boundary is released to the grain edge porosity. Currently, gas that reaches the grain edges is assumed to be released. There is likely to be some time delay between the release of gas to the grain edges and its ultimate release from the fuel; however, it is difficult to quantify this delay since some of the relevant parameters such as the magnitude of the fuel porosity and the permeability are not well known and may actually change during the course of the transient. Neglect of the gas in the grain edge porosity is conservative as far as the whole-core calculations are concerned since a potential contributor to fuel dispersal is not taken into account.

To validate the modeling in the FRAS3 code, predictions of gas release based on FRAS3 calculations have been compared with measured gas releases in a series of FGR tests (Refs. QCS760.178A3-2, -3). In the comparisons, the calculated temperature at a radius of 0.9 times the fuel rod radius was assumed to represent the average temperature of the unrestructured fuel. The FRAS3 calculations actually represent a local release fraction while the measurements represent a release fraction based on the total release from the fuel. A summary of the comparisons is shown in Fig. QCS760.178A3-1, where the solid lines show the measured releases and the dashed lines show the envelope of the FRAS3 calculations for the various test conditions. As a result of these comparisons it was concluded that taking into account the differences that would be expected between a total and local release fraction, and "given the uncertainty in the reported FGR fuel temperatures, FRAS3 can correctly predict the magnitude of the total gas release" (Ref. QCS760.178A3-2).

FRAS3 predictions of the fraction of the initial fission gas concentrations retained near the time of fuel motion initiation for both the L6 and L7 tests and for channel 6 in the EOC-4 SAS3D reactor model are shown in Table QCS760.178A3-2. The initial concentrations are based on SAS3D calculations. The thermal histories used in the calculations for the L6 and L7 tests are based on SAS3D calculations of these tests, and the thermal history used for channel 6 is based on the previous EOC-4 LOF best estimate analysis. Use of these results in the SAS3D analyses will be described later in this report.

### Analysis of the L6 and L7 TREAT Tests

The general approach to the SAS3D analyses of the L6 and L7 experiments is as follows: First, a steady-state calculation was devised to simulate the irradiation history of the fuel elements used in the tests. Following this, a 20-second transient was computed in which the reactor power level, coolant flow rate, and fuel temperatures were brought to the values that prevailed at the beginning of the tests. Finally, the test transient itself was simulated. This procedure was followed not only for each test, but also for the heat balance transients that were conducted prior to each test.

The single-channel representation of the fuel elements and their associated coolant channels is the same as used in the initial SAS3D analysis of the L7 test (Ref. QCS760.178A3-8). However, in the present work, the sodium loop is modeled using the PRIMAR-0 option of the SAS3D code. The pump coastdown is modeled by specifying the coolant inlet pressure as a function of time. The inertial effects of sodium in the test vehicle loop outside the section where the fuel elements were located are modeled by adding 59 centimeters to the effective coolant column inertial length at the channel inlet. Other input assumptions relating to fuel and cladding properties and heat transfer from fuel to cladding and from cladding to coolant are made as nearly like those that would be used in whole-core analyses as feasible. One measure of how well the heat transfer is modeled is provided by comparing calculated boiling times with the apparent boiling time as indicated by test instrumentation. Table QCS760.178A3-3 shows this comparison for the L6 and L7 tests. The calculations utilized a superheat of 10°C for initial bubble formation. The close agreement in the case of L7 is probably fortuitous while better agreement with the L6 result would be desirable. Nevertheless, the comparison is considered satisfactory.

Input for the SAS3D fuel motion model SLUMPY was prepared as follows. Fission gas parameters were evaluated on the basis of the FRAS3 calculations described previously. One of the SLUMPY parameters is the fraction of the initial gas concentration that is present when fuel motion begins. Since the FRAS3 calculations assumed the initial concentration that is computed internally by the SAS3D steady-state calculation, this fraction was set to 0.34 for the L6 test and 0.69 for the L7 test (see Table QCS760.178A3-2). A second parameter specifies the fraction of the gas present at the time of fuel motion initiation that is to be made immediately available. The immediately available gas was assumed to be given by the FRAS3-calculated gas concentrations on the grain boundaries. This fraction was set to 0.28 and 0.07 respectively for L6 and L7. That gas which is not immediately available was released from molten fuel with a time constant of 100 ms and from solid fuel with a time constant of 3 s; these are nominally employed SAS3D values.

Most of the other SLUMPY input parameters were set to default values or to values that had been used in previous homogeneous studies (Ref. QCS760.178A3-9). The number of grams of stainless steel per gram of fuel was set to a small value (0.001) because such a value was needed in the whole core calculations to prevent the flow area available to the SLUMPY compressible zone from becoming excessively large as disrupted fuel was pushed up the coolant channel. Steel vapor, however, was not considered as a potential source for fuel dispersal in either the test analyses or in the whole-core calculations.

To achieve what was regarded as a reasonable match between the SAS3D/SLUMPY calculations and the test data, attention was focused primarily on three parameters. The first of these was the fraction of the gravitational constant used in the equations of motion, the second was a parameter called QSODUM which establishes coupling between the SLUMPY calculation and the coolant dynamics calculation, and the third was the parameter VISFU which permits the viscosity in the compressible zone calculation to be increased when significant amounts of unmelted fuel are present.



Of primary interest in the present analysis is the comparison between the fuel motion as calculated by SAS3D/SLUMPY and that measured in the TREAT tests. A convenient figure of merit to use for this purpose is the reactivity feedback that would be obtained if the observed fuel motion were to occur in an operating LMFBR (Ref. QCS760.178A3-10). Designating this quantity as the relative fuel worth (REF), it is obtained by weighting the computed or measured fuel density changes with a normalized (in this case the homogeneous CRBRP) axial fuel worth distribution and spatially integrating. REF is normalized so that its value is initially zero and is -1.0 if all the fuel is removed. The criterion for choosing values for the SAS3D/SLUMPY parameters was that the slope of the REF obtained from the calculations should be reasonably close to the slope of the experimental REF.

The parameter values which fit L6 and L7 best are 0.2 for the fraction of the gravitational constant, 0.02 for QSODUM, and 10,000 for VISFU. A 50% fuel melt fraction was used as the criterion for initiating the fuel motion calculation. Calculated and experimental REF's obtained using these parameters are plotted as a function of the TREAT reactor energy in Figs. QCS760.178A3-2 and -3. The experimental data were grouped into time bins such that the reactor energy production within each bin was constant. As a result, each of the experimental points has the same statistical significance. The calculated and experimental REF's are plotted in Figs. QCS760.178A3-4 and -5 as a function of time after 14.1 s. The choice of 14.1 s as the origin in these plots was made because this is about the time when thermal hydraulic instrumentation indicated that fuel disruption might have occurred in the L7 test. The 50% melt fraction criterion was reached in the SAS3D calculations at 14.335 s and 14.161 s respectively for the L6 and L7 tests. The agreement between calculation and experiment shown in the figures is regarded as satisfactory and is believed to justify the use of the chosen SLUMPY parameters (other than the fission gas fraction) for the modeling of irradiated fuel motion in whole core calculations. Some discussion of sensitivities observed in the test calculations are given later in this report.

#### Whole-Core Calculations for CRBR EOC-4 LOF

The SAS3D whole-core calculation for the heterogeneous EOC-4 core which is most relevant to the issue addressed herein is summarized below. Input data for this case was essentially the same as was used in the best estimate analysis (Ref. QCS760.178A3-1, Section 7.2.1) except for the following changes. First, all driver fuel channels were set to initiate fuel motion when the fuel melt fraction reaches 50%. Second, integer input variables were set to permit sodium film motion calculations to continue rather than terminate after two seconds of boiling, to also allow slip between fuel particles and fission gas in the lead channel, and to ignore stainless steel vapor pressures in the event of mixing of steel and fuel during the SLUMPY calculation. Third, except for the two variables which specify the amount of fission gas that is present when the fuel motion calculation begins, input variables for SLUMPY were set to the values which were found to provide the best fit for the L6 and L7 tests.

In channel 6, the fraction of the steady-state fission gas concentration assumed to be present when the fuel motion calculation started was set to 0.59, and the fraction of gas present that was made immediately available was set to 0.08. These values are based on the FRAS3 calculations described

earlier. FRAS3 calculations were not performed for the other driver fuel channels, so these same fractions were used for these channels as well. Since the remaining channels have higher burnup than channel 6, it is not clear that use of these fractions is conservative, but these channels are of secondary importance for this case.

An event sequence is shown in Table QCS760.178A3-4. The portion of the transient prior to fuel motion in channel 6 is very similar to that in the earlier CRBRP calculation although the fact that the film motion calculation was allowed to continue in all boiling channels did cause some minor changes in the power level and in the coolant voiding reactivity. Following the initiation of fuel motion in channel 6, the scenario changes. Fuel motion reactivity feedback remains positive in channel 6 for about 146 ms following fuel disruption and the power level continues to rise throughout most of this period reaching a peak of about 4.7 times nominal. Then the fuel motion reactivity becomes more negative and finally drives the reactor subcritical about 406 ms after first fuel motion.

While it is felt that SLUMPY can be calibrated to adequately model fuel motion during the initial disruption, the fact that fuel freezing and plugging is not modeled makes it questionable to continue using the model for much more than a few hundred milliseconds after initial fuel motion. The SAS3D calculation might be terminated at this point. However, to better understand the whole core conditions and, in the belief that negative fuel motion reactivity would continue somewhat beyond the time when SLUMPY encountered time step difficulties, the calculation in channel 6 was stopped and the SAS3D calculation continued. The time when this occurred along with the power level and various reactivity feedbacks is indicated in Table QCS760.178A3-4. Beyond the time indicated, no fuel motion occurred in channel 6, although the fuel was allowed to continue to absorb heat and to transfer heat to its surroundings.

Following termination of the fuel motion calculation in channel 6, the reactor remained subcritical for about 323 ms, and then reached criticality on the strength of coolant voiding and cladding motion. The reactivity remained above critical for about 163 ms during which time the peak reactivity was about 16 cents and the peak power was about 1.8 times nominal. The reactor became subcritical again because of a decline in both the clad motion reactivity and the coolant reactivity. This time the reactor remained subcritical for about 144 ms and then became recritical because of an increase in both the coolant and clad motion reactivities. The reactivity continued to climb until it reached about 26 cents at which time fuel motion was initiated in channel 2. Following fuel disruption in channel 2 the reactivity increased still further partly because of positive fuel motion feedback. Both the power and the reactivity passed through local maxima about the time when fuel motion was initiated in channel 4. About 380 ms after fuel motion started in channel 2, the reactor became subcritical again because of negative fuel motion feedback from channel 2. Reactivity feedbacks from channels 4 and 7 were positive at the end of the calculation and totaled about 28 cents.

To assess the plenum gas release effects on upward steel relocation and the potential for compaction of fuel by the gas remaining in the fission gas plena, it was first estimated that release of this gas could not start until the cladding on the top node of fuel reached a temperature of 1400°C; approximately the melt point. The time between the achievement of this criterion and

the start of clad motion or fuel motion is listed in Table QCS760.178A3-5. Also listed in the table is the approximate gas pressure when the release would start. In those channels where either clad motion or fuel motion or both had not initiated in a channel, the time listed is the time to the end of the calculation. An analysis of the conditions at the time the release should start indicates that the time constant for the release should be about 250 ms. A test calculation for channel 6 using the SAS3D gas release model agreed rather well with this time constant estimate; however, a similar test calculation for channel 9, which had a much higher pressure than in channel 6 indicated that for the higher pressure channels the time constant is somewhat less than 250 ms.

From Table QCS760.178A3-5 it is seen that only two time constants exist for plenum gas release prior to cladding motion for most of the channels. The plenum pressure will be about 4 atm with a continued release (note that this is higher than the sodium inlet plenum pressure) occurring while molten steel is available to move. The gas release would have stopped the sodium vapor flow and an upper cladding blockage would not be anticipated. Instead, a thick lower blockage would form by steel drainage.

Table QCS760.178A3-6 lists the fuel thermal condition in those channels where fuel motion did not occur at the time when the calculation was terminated. The results listed in Tables QCS760.178A3-5 and -6 provide the basis for the conclusion stated at the beginning of this report that the potential for fuel compaction driven by the gas pressures in the fission gas plena is very low. The results in Table QCS760.178A3-5 show that for those channels where fuel motion occurred during the calculation, there is ample time for the pressures in the plena to be relieved prior to fuel motion. Given that the reactor is appreciably subcritical at the end of the calculation, and given the condition of the fuel in those channels that have not yet experienced fuel motion, it seems likely that pressure will be relieved in the plena of those channels long before any fuel motion might start.

#### Sensitivities and Uncertainties

With respect to the experiment analysis, one of the major uncertainties is determining precisely when a given SAS3D-calculated thermal condition (e.g. a 50% fuel melt fraction) actually occurred in the experiment. It was because of this that no attempt was made to try to get the calculated REF to fall directly on the experimental REF for the time interval during which fuel dispersal seemed to be clearly indicated. The systematic trends and scatter in the experimental data also suggested that such an attempt should not be made. In the experiment calculations, the timing of specific thermal events was found to be sensitive, among other things, to the value of the heat transfer coefficient between fuel and cladding, and to the power coupling factor between the TREAT reactor and the fuel in the test vehicle. This latter factor is estimated to have a total uncertainty of  $\pm 10\%$ .

Among the SLUMPY parameters focused on the analyses of the L6 and L7 experiments, it was found that calculations for both tests showed moderate sensitivity to the value chosen for QSODUM. While there did appear to be a preference for a small, non-zero value, the value zero could have been chosen without too much harm to the comparison between calculated and experimental REF's. Calculations for the L6 test were rather strongly sensitive to the

value chosen for the fraction of the gravitational constant, while the calculations for both tests were rather strongly sensitive to the value chosen for the parameter VISFU.

The key to the conclusions reached on the basis of the whole-core analysis is the fuel modeling that was used for channel 6. While the analysis of the L6 and L7 TREAT tests appear to provide strong justification for the modeling used, the most important point seems to be that the fuel in channel 6 was allowed to disperse. A preliminary calculation in the investigation used a value of unity for the fraction of the gravitational constant, values of zero for QSODUM and VISFU, and approximately the same amount of fission gas immediately available. Because of the larger fraction of the gravitational constant, the reactor power reached about 7 times nominal power before fuel motion reactivity feedback from channel 6 began to decrease. SLUMPY was allowed to continue computing fuel motion throughout this case and as a result, late in the transient, partly aided by a rather large decrease in the magnitude of the negative reactivity feedback from channel 6, the reactor became recritical with the reactivity reaching nearly 96 cents. This produced a power burst in which the reactor power reached 42 times nominal. In spite of the differences between this result and the present case, the general conclusions regarding the potential for compaction of fuel by plenum fission gas were very much the same as described in this report.

Termination of the fuel motion calculation in channel 6 introduces some degree of uncertainty into the later portion of the transient. If the fuel motion had been stopped earlier, the negative fuel motion reactivity would have been smaller in magnitude and the reactor would have been less subcritical. The transient would then be changed from about 20.02 s onward. However, the amount of negative fuel motion reactivity computed up to the time of fuel motion cutoff in channel 6 does not appear to be excessive. It is primarily due to the movement of fuel away from the midplane of the reactor core; the total amount of fuel located in the axial blanket at the time of fuel motion cutoff was less than 5 grams per fuel pin. If all this fuel were moved back into the first two nodes in the active core the net reactivity increase would be less than 10 cents and the reactor would still be more than 50 cents subcritical. The time margins between clad failure and fuel motion shown in Table QCS760.178A3-5 appear to be large enough so that this reactivity change would have a negligible effect on conclusions reached herein.

#### Conclusion

The analyses of the whole core response to loss-of-flow (LOF) without scram event have been conducted using methods and a data base which are consistent with the most relevant experimental information. By detailed examination of TREAT LOF experiments L6 and L7 with the SAS3D code and of fission gas release experiments with the FRAS3 code, a technically defensible set of modeling parameters for fuel disruption and dispersal have been identified. When such modeling is utilized in the whole core analysis of the EOC-4 LOF scenario, it has been found that early and significant fuel dispersal takes place and the possibility of autocatalytic behavior leading to energetic hydrodynamic disassembly is highly unlikely. In particular, the mechanism for fuel column compaction by plenum fission gas is generally eliminated by the significant time delay between the initiation of plenum depressurization and fuel rod disruption. This results from the relatively

mild power excursion experienced when experimentally consistent fuel dispersal parameters are used. The sensitivity of the whole core response to fuel motion modeling is relatively weak and, although specific power histories may differ, the general conclusion that plenum fission gas compaction is not a significant concern can be made as long as experimentally consistent fuel motion assumptions are made.

#### References

- QCS760.178A3-1 S. K. Rhow, et.al., "An Assessment of HCDA Energetics in the CRBRP Heterogeneous Reactor Core," CRBRP-GEFR-00523 (December 1981).
- QCS760.178A3-2 T. E. Kraft, "An Evaluation of Recent Transient Fuel Behavior Models Based on Selected Experimental Results," ANL/RAS 80-29 (November 1980).
- QCS760.178A3-3 J. M. Kramer, et.al., "An Analysis of Recent Fuel Disruption Experiments," Intl. Top. Mtg. on LMFBR Safety, Lyon, France (July 1982).
- QCS760.178A3-4 E. E. Gruber and E. H. Randklev, "Comparison of Fission Gas Effects in a Transient Overpower Test (HUT 5-7A) to FRAS3 Code Predictions," Intl. Top. Mtg. on Fast Reactor Safety Technology, Seattle, Washington (August 1979).
- QCS760.178A3-5 R. Simms, et.al., "TREAT Experimental Data Base Regarding Fuel Dispersals in LMFBR Loss-of-Flow Accidents," Proc. of Top. Mtg. on the Reactor Safety Aspects of Fuel Behavior, Sun Valley, Idaho (August 1981).
- QCS760.178A3-6 A. DeVolpi, et.al., "Fast-Neutron Hodoscope at TREAT: Data Processing, Analysis, and Results," Nucl. Tech., Vol. 30, 398 (1976).
- QCS760.178A3-7 R. Simms, et.al., "Loss-of-Flow TREAT Tests L6 and L7 with Irradiated LMFBR-Type Fuel," Nucl. Tech., Vol. 52, 331 (March 1981).
- QCS760.178A3-8 C. H. Bowers, et.al., "Analysis of TREAT Tests L7 and L8 with SAS3D, LEVITATE, and PLUTO-2," Specialists' Workshop on Predictive Analysis of Material Dynamics in LMFBR Safety Experiments, LA-7938-C, Los Alamos Scientific Laboratory (March 13-15, 1979).
- QCS760.178A3-9 W. R. Bohl, et.al., "An Analysis of the Unprotected Loss-of-Flow Accident in the Clinch River Breeder Reactor with an End-of-Cycle Core," ANL/RAS 77-15 (May 1977).
- QCS760.178A3-10 R. Simms, "An Evaluation of Fuel Motion in Recent TREAT Experiments with Liquid-Metal Fast Breeder Reactor Fuel," Nucl. Tech., Vol. 50, 257 (October 1980).

QCS760.178A3-9

Amend. 72  
Oct. 1982

Table QCS760.178A3-1

## TREAT EXPERIMENTS SIMULATING LOSS-OF-FLOW ACCIDENT CONDITIONS

Test Designation	Number of Elements	Fissile Fuel Length, mm	Preirradiation Neutron Spectrum	Hodoscope Collimator Viewing Height m	Peak Transient Power $\div$ Nominal Power <sup>a</sup>
L2	7	340	None	0.5	1
L3	7	340	Fast	0.5	1
L4	7	340	Fast	0.5	1
L5	3	864	Thermal	0.5	6
L6	3	864	Thermal	1.2	10
L7	3	864	Thermal	1.2	20
R3	1	914	None	0.5	1
R4-R6	7	914	None	0.5	1
R7	7	914	None	0.5	15
R8	7	914	None	1.2	1
F1	1	340	Fast	0.5	1
F2	1	340	Fast	0.5	12

<sup>a</sup>Ignoring preheat power phase, if any.

Table QCS760.178A3-2

GAS RETENTION CALCULATED WITH THE FRAS3 CODE NEAR THE  
 TIME OF FUEL DISRUPTION IN TREAT TESTS L6 AND L7 AND  
 FOR CHANNEL 6 IN THE EOC-4 SAS3D CRBR MODEL

Case	Initial Concentration in Unrestructured Fuel, atoms/cc	Percent Retained in Grains	Percent Retained on Grain Boundaries
L6	$1.00 \times 10^{20}$	24	9.5
L7	$1.00 \times 10^{20}$	64	4.7
Ch. 6	$1.34 \times 10^{20}$	54	4.7

Table QCS760.178A3-3

COMPARISON OF MEASURED AND CALCULATED BOILING  
 TIMES FOR THE L6 AND L7 TREAT TESTS

Test	Measured	SAS3D
L6	12.6 s	12.1 s
L7	13.4 s	13.4 s

Table QCS760.178A3-4

## EVENT SEQUENCE FOR EOC-4 LOF SCENARIO

<u>Time</u>	<u>Event</u>	<u>CHN</u>	<u>P/PO</u>	<u>RHO</u>	<u>RHOD</u>	<u>RHOE</u>	<u>RHOV</u>	<u>RHOF</u>	<u>RHOC</u>
12.7655	Coolant Boiling	6	0.821	-0.094	-0.140	-0.050	0.096	0.0	0.0
14.6697	Coolant Boiling	2	0.819	-0.068	-0.156	-0.057	0.145	0.0	0.0
15.0561	Coolant Boiling	4	0.817	-0.069	-0.161	-0.061	0.152	0.0	0.0
15.7772	Coolant Boiling	7	0.851	-0.019	-0.170	-0.068	0.219	0.0	0.0
17.1048	Coolant Boiling	10	1.226	0.234	-0.235	-0.125	0.594	0.0	0.0
17.1998	Coolant Boiling	11	1.269	0.253	-0.242	-0.132	0.627	0.0	0.0
17.5298	Coolant Boiling	9	1.321	0.252	-0.270	-0.159	0.681	0.0	0.0
17.7792	Coolant Boiling	13	1.241	0.190	-0.287	-0.175	0.653	0.0	0.0
17.9242	Clad Motion	6	1.320	0.233	-0.297	-0.186	0.715	0.0	0.0
18.2117	Coolant Boiling	12	2.225	0.514	-0.333	-0.223	0.999	0.0	0.071
18.6442	Coolant Boiling	15	2.570	0.531	-0.397	-0.279	1.130	0.0	0.076
18.8732	Coolant Boiling	14	3.002	0.561	-0.440	-0.315	1.241	0.0	0.075
19.1867	Clad Motion	2	2.889	0.498	-0.495	-0.366	1.282	0.0	0.076
19.3417	Clad Motion	4	3.770	0.594	-0.527	-0.390	1.238	0.0	0.273
19.3617	Fuel Motion	6	3.784	0.590	-0.532	-0.393	1.233	0.0	0.283
19.4129	Coolant Boiling	5	3.695	0.570	-0.544	-0.400	1.200	0.005	0.308
19.4930	Peak Reactivity	0	4.654	0.644	-0.563	-0.411	1.207	0.003	0.408
19.5017	Peak Power	0	4.670	0.643	-0.566	-0.413	1.201	0.002	0.419
19.6092	Clad Motion	7	3.453	0.492	-0.587	-0.426	1.186	-0.110	0.428
19.6163	Coolant Boiling	3	3.437	0.488	-0.588	-0.427	1.186	-0.123	0.441
19.7705	Coolant Boiling	1	1.744	-0.022	-0.594	-0.434	1.145	-0.701	0.560
19.7730	Coolant Boiling	8	1.722	-0.036	-0.594	-0.434	1.145	-0.712	0.559
20.0267	Fuel Motion Off	6	1.049	-0.600	-0.577	-0.433	1.440	-1.523	0.493
20.1267	Clad Motion	10	0.984	-0.651	-0.579	-0.432	1.365	-1.523	0.518
20.1555	Clad Motion	11	1.004	-0.601	-0.578	-0.432	1.389	-1.523	0.543
20.5080	Clad Motion	9	1.514	0.007	-0.588	-0.433	1.565	-1.523	0.987
20.7005	Clad Motion	13	1.506	0.019	-0.597	-0.433	1.586	-1.523	0.986
20.9430	Fuel Motion	2	1.989	0.259	-0.610	-0.431	1.731	-1.523	1.092
21.1105	Fuel Motion	4	2.863	0.470	-0.629	-0.428	1.773	-1.402	1.157
21.1342	Clad Motion	12	2.665	0.425	-0.631	-0.428	1.760	-1.399	1.123
21.5380	Fuel Motion	7	0.681	-1.324	-0.638	-0.425	1.848	-3.711	1.602
21.8117	Clad Motion	15	0.363	-3.377	-0.634	-0.426	1.864	-5.636	1.456
21.8830	Termination	0	0.334	-3.742	-0.633	-0.426	1.837	-5.904	1.385

Nomenclature is as follows:

CHN - SAS channel #.

P/PO - Core power relative to nominal.

RHO - Net reactivity in \$.

RHO(X) - Reactivity in \$ due to Doppler (D), axial expansion (E), sodium void (V), fuel motion (F), cladding motion (C).

Amend. 72  
Oct. 1982



Table QCS760.178A3-5

APPROXIMATE TIMES TO CLADDING AND FUEL MOTION RELATIVE TO  
CLAD FAILURE AND PLENUM-FISSION-GAS PRESSURES AT FAILURE  
(1400°C) OF THE TOP FUEL NODE IN DRIVER ASSEMBLIES AS  
DETERMINED FROM THE SAS3D CALCULATION

Channel	Time to Clad Motion, s	Time to Fuel Motion, s	Pressure at Failure atm
2	0.60	2.36	42
4	0.61	2.38	42
6	1.14	2.58	22
7	0.58	2.51	44
9	0.59	1.96*	39
10	0.55	2.31*	41
11	0.66	2.39*	42
12	0.79	1.54*	34
13	0.70	1.89*	36
14	0.66*	0.66*	26
15	0.79	0.86*	27

\*These are times referred to the end of the calculation since the event in question did not occur.

Table QCS760.178A3-6

FUEL CONDITIONS IN THOSE CHANNELS THAT HAVE NOT INITIATED  
FUEL MOTION BY THE TERMINATION OF THE CALCULATION

Channel	Peak Fuel Melt Fraction or Temperature
9	0.26
10	0.32
11	0.30
12	0.10
13	0.15
14	2656° C
15	0.003

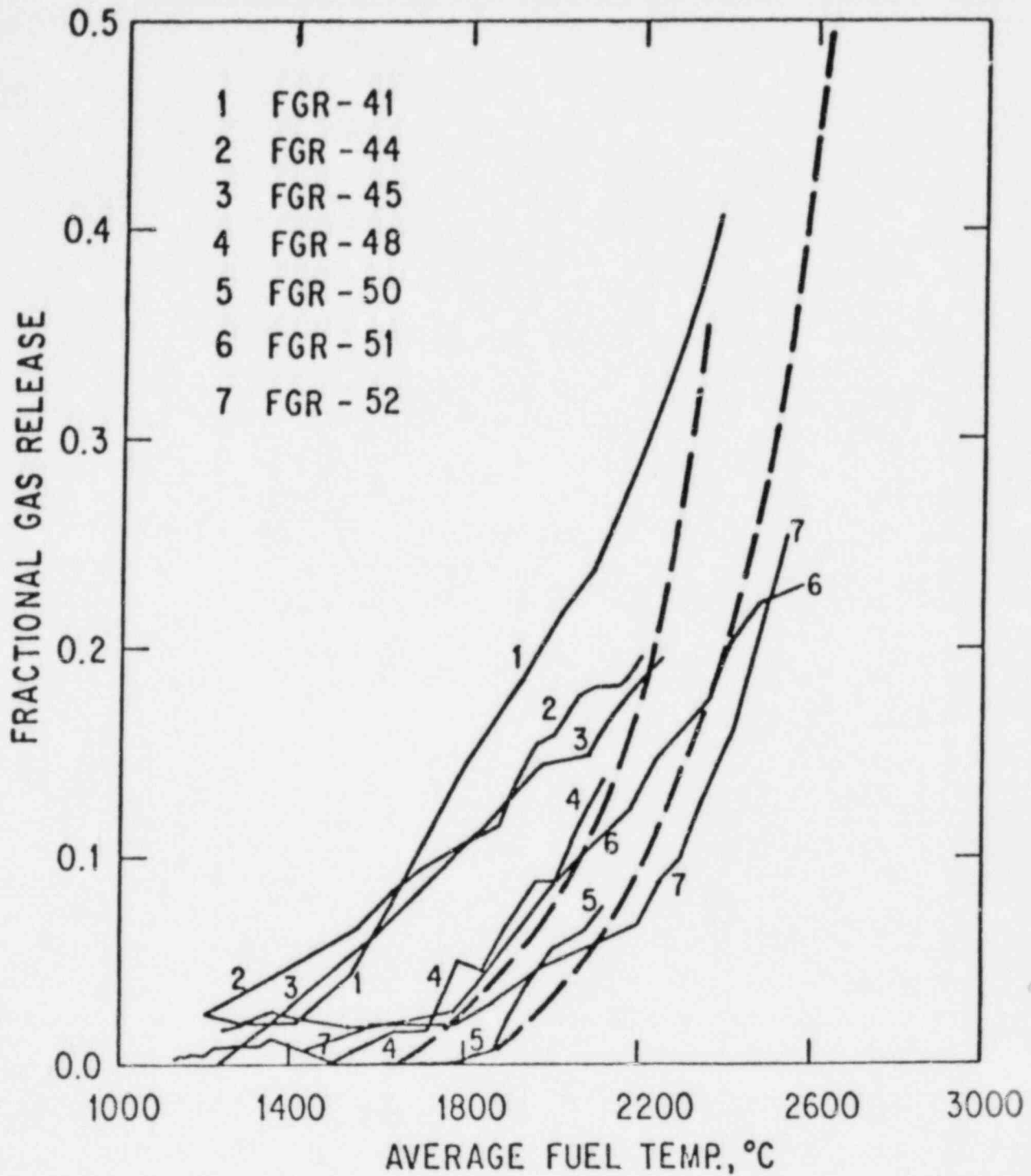


Fig. QCS760.178A3-1 Comparison of Measured (Solid Curves) and Calculated Gas Release Fractions. The Dashed Curves Represent the Envelope of FRAS3 Calculations for the Range of Initial Conditions Corresponding to the Measured Data.

QCS760.178A3-16

Amend. 72  
Oct. 1982

RELATIVE FUEL WORTH

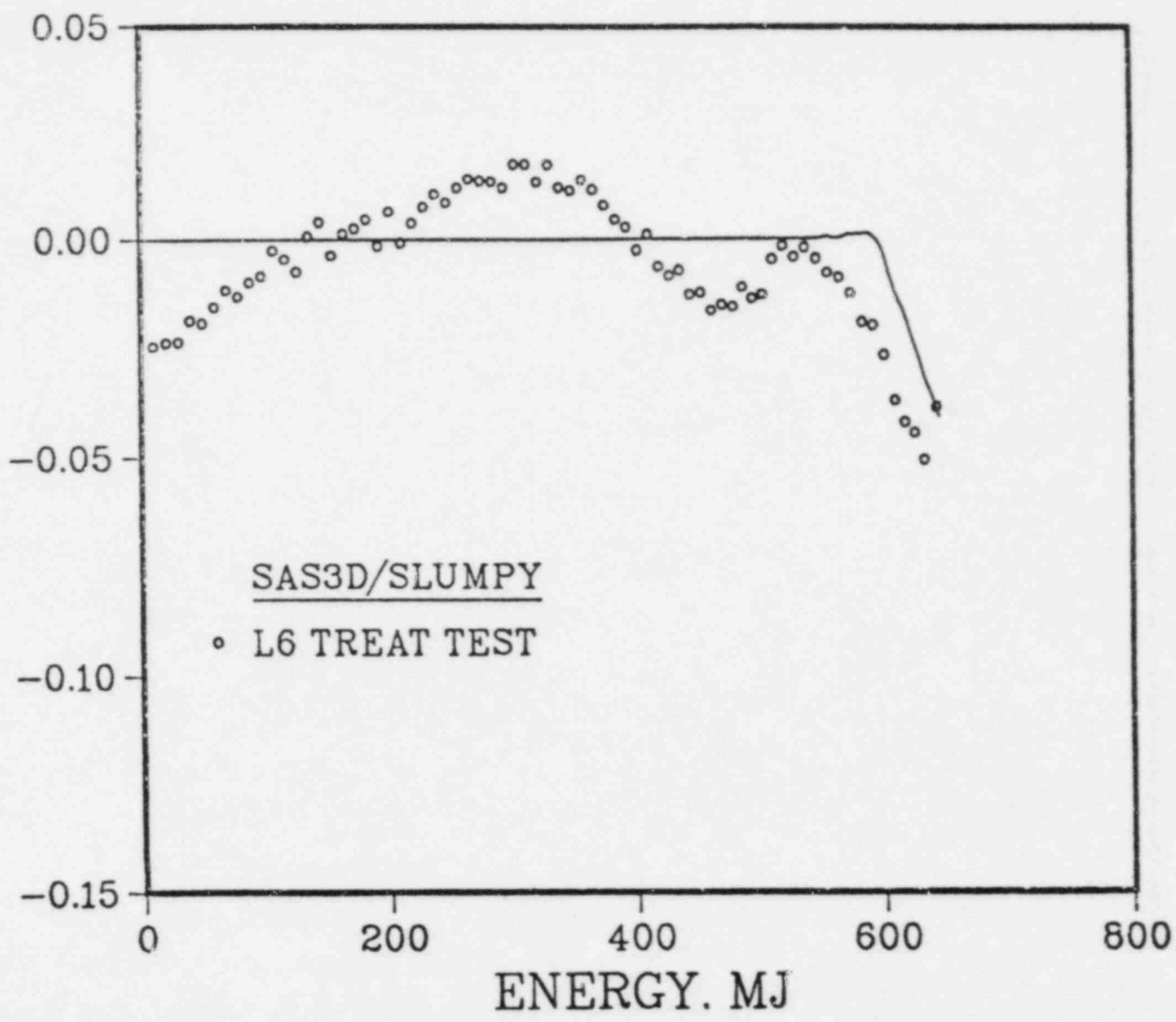


Fig. QCS760.178A3-2 Comparison of Measured and Calculated Relative Fuel Worths as a Function of Reactor Energy for the L6 TREAT Test.

QCS760.178A3-17

Amend. 72  
Oct. 1982

RELATIVE FUEL WORTH

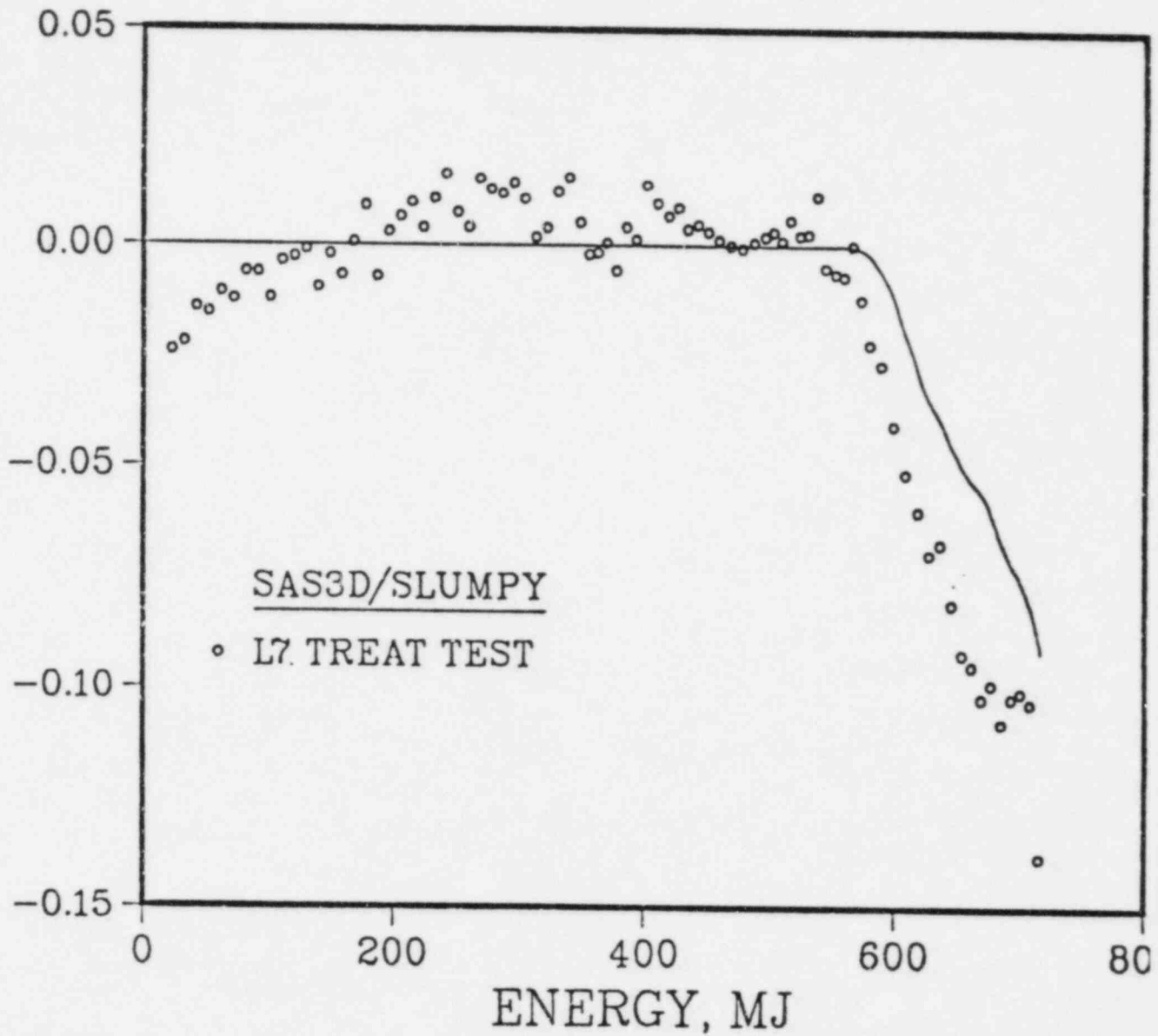


Fig. QCS760.178A3-3 Comparison of Measured and Calculated Relative Fuel Worths as a Function of Reactor Energy for the L7 TREAT Test.

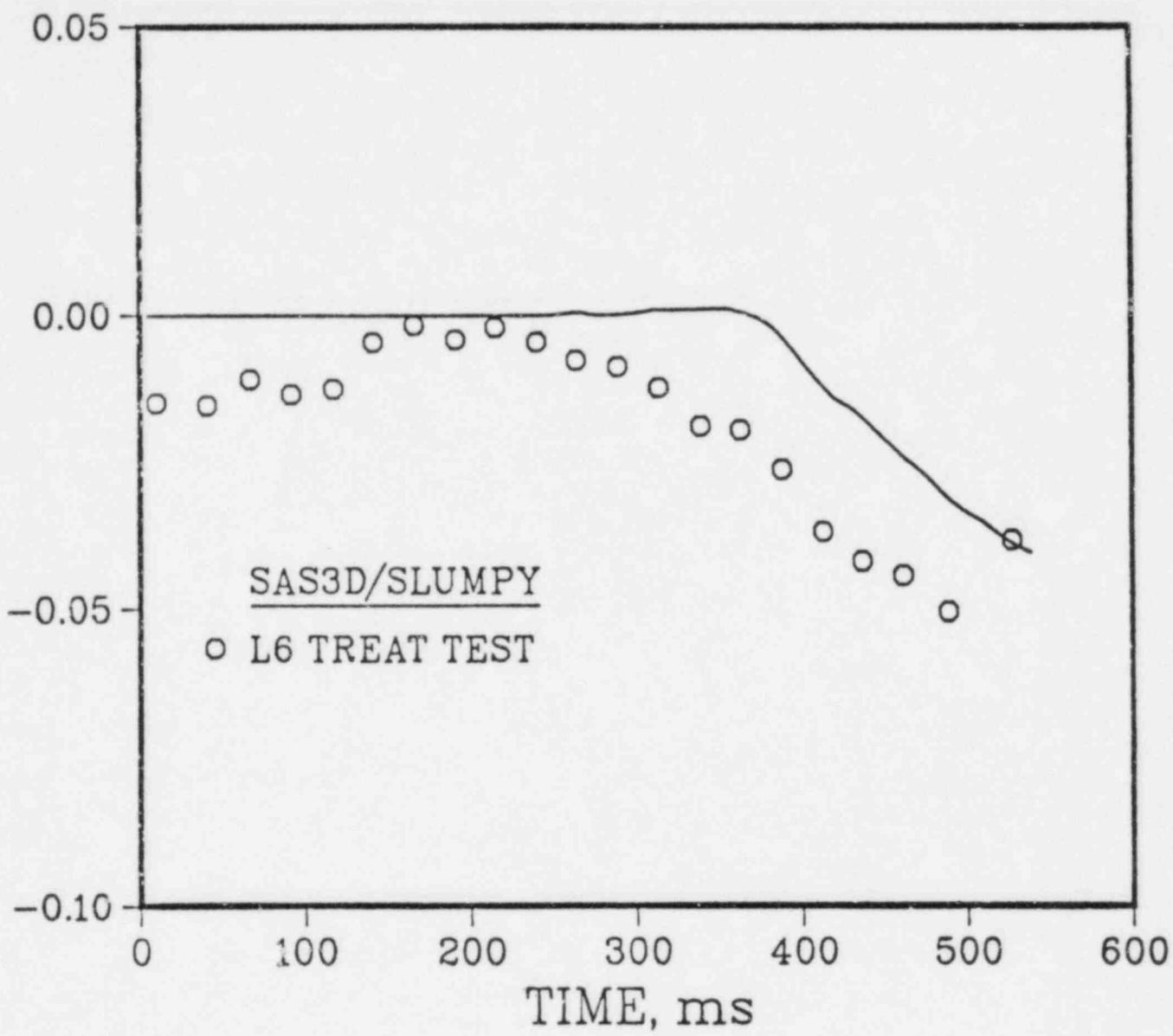


Fig. QCS760.178A3-4 Comparison of Measured and Calculated Relative Fuel Worths as a Function of Time After 14.1 s for the L6 TREAT Test.

QCS760.178A3-19

Amend. 72  
Oct. 1982

RELATIVE FUEL WORTH

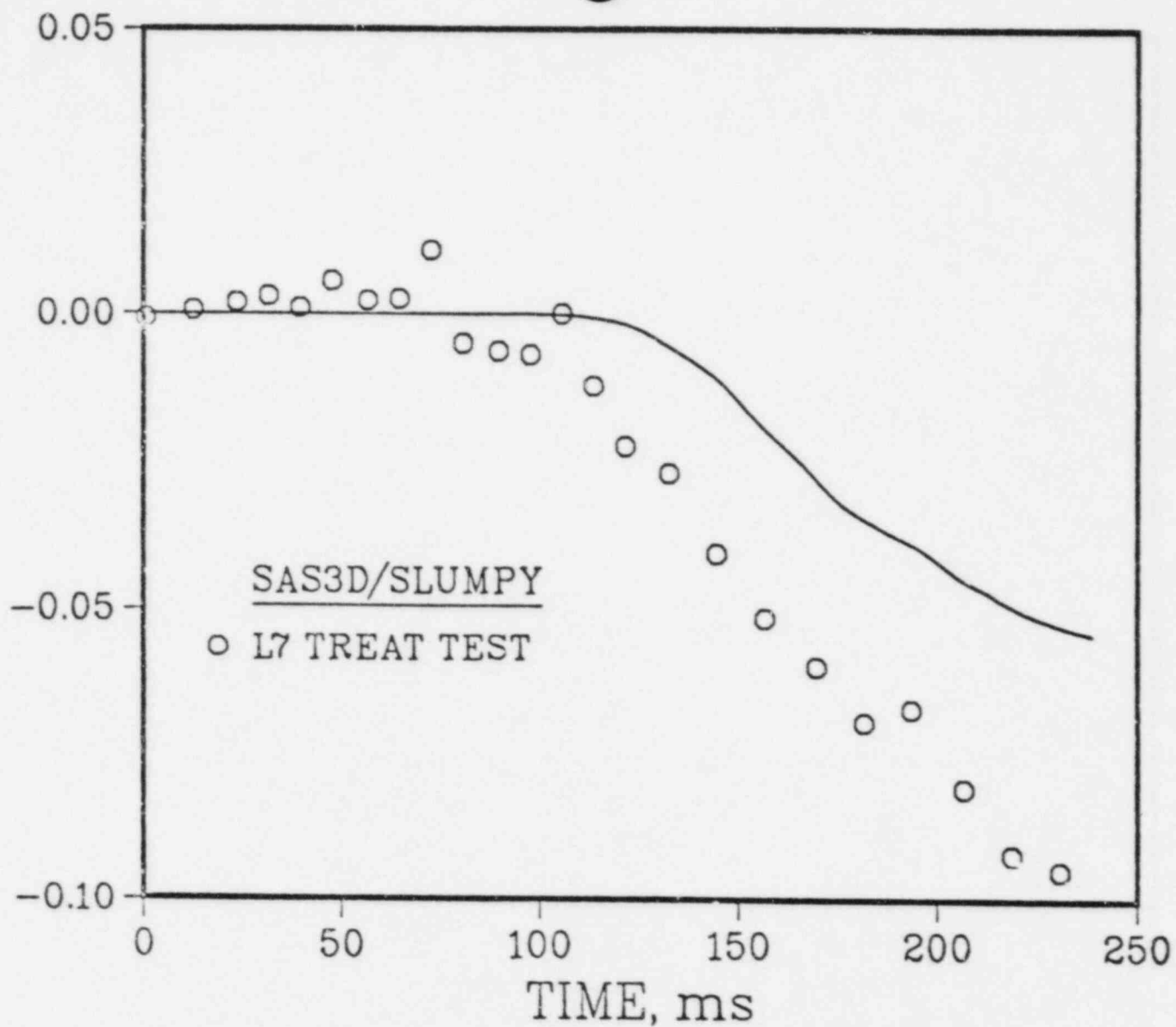


Fig. QCS760.178A3-5 Comparison of Measured and Calculated Relative Fuel Worths as a Function of Time After 14.1 s for the L7 TREAT Test.

Question CS760.178B4

To what extent can steel blockages form throughout the core to prevent fuel removal through normal axial blanket flow channels during the early phase of the LOF? What is the location and character of the steel blockages in these channels?

Response

A significant time interval exists for molten cladding relocation during a loss-of-flow without scram event in the CRBRP. This is true for the entire core burnup cycle (i.e., BOC through EOC) and is principally the result of the very low effective sodium void worth of the heterogeneous design. However, very little upward steel relocation or blockage is expected for the irradiated core condition due to the blowdown of the high pressure plenum fission gas. The gas release opposes the sodium vapor streaming which is the primary mechanism for upward relocation of molten cladding (see response to QCS760.178A-3 for the CRBRP transient analysis). This gas release effect has been experimentally confirmed (Ref. QCS760.178B4-1) and results in only a thick lower steel blockage for irradiated core conditions.

The remaining discussion is therefore primarily focused on the BOC core condition where upper steel blockages are expected to form as shown in Chapter 7 of Ref. QCS760.178B4-2. In response to the first part of the above question, two additional SAS3D calculations were performed for the BOC-1 core to maximize the potential effects on the melt-out phase entrance conditions of the axial location of the blockage as well as uncertainties in core reactivity feedback parameters. The comparative reference for these new calculations is Case 1C, Section 7.1.1 of Ref. QCS760.178B4-1 which presents the best estimate; slow drainage of disrupted fuel comparable to PLUTO-2 calculations.

In order to examine the axial location effect in the first analysis (labeled Case 4) the steel blockage was forced to form upon entering the upper axial blanket, providing the maximum restriction to fuel removal. The core transient response history and extent of steel blockages were found to be quite similar for the reference and modified axial blockage location. Figures QCS760.178B4-1 and -2 depict the core conditions at the onset of fuel motion in each analysis; very little independent steel relocation occurs after this event. Based upon the mechanism of near-fresh fuel melting and drainage, a power burst occurs (comparable to Case 1C) which disperses fuel and leaves the core in a subcritical but higher reactivity state. The peak fuel thermal conditions in the fuel channels which did not disrupt are reasonably similar as shown in Table QCS760.178B4-1. Hence, the CRBRP core dynamic behavior was found to be only weakly affected by the steel blockage axial location. The same extent of steel blockages throughout the core was found to exist upon melt-out phase initiation. In addition to locating the steel blockage at the entrance to the UAB, uncertainties in reactivity parameters were also represented in a manner to slow down the transient response, and thereby allow



additional time for blockage formation. The specific, additional changes made to construct Case 5 (beyond Case 4) were:

1. Local negative sodium voids more negative by 60%\*,
2. Local positive sodium voids more negative by 60%\*,
3. Doppler constant more negative by 20%,
4. Steel worth uniformly reduced by 20%.

Nominal fuel reactivity worths were used for Case 5 since it was a-priori unclear how to bias them; initial fuel drainage has the effect of adding positive reactivity, while subsequent fuel dispersal results in negative reactivity. The expected slowdown in core response was obtained with initial cladding melting and fuel motion occurring approximately 1 and 2.6 seconds later than in the reference case. The slower developing transient and stronger Doppler feedback act to reduce the peak power attained in the fuel drainage induced power burst to 61 P<sub>o</sub>, or about half of the reference case peak value. However, the longer duration of the power burst results in an energy addition comparable to those of the other two calculations. The condition of the core is actually more benign in this case than in the other two as depicted in Fig. QCS760.178B4-3 and Table QCS760.178B4-1. At the onset of fuel disruption, reduced upper steel blockages (Channel 10 blockage is absent) and reduced sodium voiding exist in the core. Concurrently, at the end of the power burst the low power channels contain substantially reduced energy due to the slower, lower power transient and enhanced cooling by diverted sodium flow from the lead channels.

It is concluded that the incorporation of reactivity uncertainties to slow the LOF leads to a more benign transient during the initial part of the LOF. Although the degree of steel blockages is similar to the reference case, there is actually less propensity for upper steel blockages to form in the lower power fuel assemblies of the BOC-1 core during the slower, lower power transient.

Hence, based upon the concept of near fresh fuel drainage upon substantial melting, the maximum extent of steel blockage formation in the UAB is well represented by the best estimate calculations of Ref. QCS760.178B4-1.

In response to the second part of this question, a detailed reassessment of the location and character of the steel blockages was performed. This new examination made use of additional experimental and analytic information which was not included in the understanding represented by Ref. QCS760.178B4-2, see Section 8.2.1. That earlier assessment can be summarized as the following:

- a. In the absence of opposing plenum gas release, gross upward steel relocation will occur due to sodium vapor streaming after cladding melting extends fully across the fuel assembly.

---

\* These reactivity uncertainties were originally stated as approximately two sigma values. Additional, recent information provided in response to QCS760.178A-2 on sodium void worth indicates these values to be substantially more conservative.

- b. The steel blockages which start to form upon entry to the UAB, are thin (millimeters) and vented at the time of fuel disruption.
- c. These blockages will not severely restrict the flow of the hot, pressurized fuel (which results from the predicted core power burst) into the UAB.
- d. Based upon the judgement that pressurized fuel could penetrate the initial steel restriction, the axial location of the steel blockage in the UAB was determined by the SAS calculation. Since SAS3D does not have a fuel freezing calculation, these steel blockages could then be used to restrict, but yet allow the latter fuel penetration into the UAB.
- e. Relative to energetics potential, it is conservative to ignore the effect of plenum fission gases in restricting the formation of an upper steel blockage.

The review focused on the above five points and in particular, an explanation for the differences between the upper blockage formations observed in the TREAT R and SLSF P series experiments and their interpretation for CRBRP. The experiments reviewed were L3, L4, R4 through R8, P3 and P3A. Test R-8 was specifically used to confirm the effect of plenum fission gas release on upper steel blockage formation. The most appropriate analyses in support of experiment interpretation and extrapolation were determined to be those discussed in Ref. QCS760.178B4-3.

The conclusions of the current assessment are in general agreement with the earlier study, but are modified in the areas of blockage thickness and fuel penetration of pre-existing blockages. Further, the differences in the experimentally observed blockage configurations are understandable when examined in light of the different thermal and flow incoherencies which exist between them. Relative to the above listed five points, the current understanding for CRBRP can be summarized as follows:

- a. In the absence of opposing plenum fission gas release, gross upward steel relocation will occur due to sodium vapor streaming once cladding melting extends fully across the fuel assembly.
- b. The steel blockages start to form upon entry to the UAB and become rather thick, especially at the edges, and vented in the CRBRP size fuel assembly. The experimental data (R5, R6, P3A, P3) indicate that the blockage is vented prior to and possibly following fuel disruption. The existence of vents is a natural consequence of the direct relationship between the sodium vapor flow required to relocate steel upward and the flow resistance increase which occurs as the blockage nears completion. The thickness of the blockage is governed by the radial, thermal and flow incoherencies and explained in the following interpretation of the experiments and the CRBRP. The CRBRP fuel assembly has a larger cross-sectional area and contains 217 fuel rods, as compared with the R-series test sections which contain seven fuel rods, and the P3A and P3 test sections which contain 37 fuel rods. This will lead to greater transverse thermal incoherency within a CRBRP fuel assembly. This is

especially true since the LOF tests were designed to produce radial uniformity in the power-to-flow ratio, while a CRBRP fuel assembly is expected to experience larger radial power gradients as well as flow nonuniformities (more coolant area in the outer row of fuel rods). In a LOF, the thermal incoherency leads to varying times of cladding melting initiation among the fuel rods.

The radial incoherency in cladding melting and subsequent motion results in significant differences in the hydraulic resistance across a fuel assembly. This allows sodium vapor to be diverted from a higher resistance flow subchannel where flooding is occurring to a low resistance flow subchannel elsewhere within the assembly. The net effects are: (1) to sustain sodium vapor flow at a relatively high rate for a longer period of time and initiate molten steel sloshing without gross relocation, (2) to enhance molten steel upward motion in the colder outer subchannels of an assembly, thus increasing the upper steel plug thickness at the edges and producing a thinner central region, and (3) to locate the steel at different elevations, thus leading to irregularly shaped vented plugs. The results from the 37-rod P3A test generally support these conclusions, as compared with the results from the 7-rod R-series tests.

The effects of thermal incoherency on molten cladding relocation were studied. Calculations have been performed for tests R4, R5, and P3A, as well as FFTF and CRBRP assemblies. The results were generally in good agreement with the corresponding tests, and supported the trend toward thicker upper blockages for the larger assemblies, (Ref. QCS760.178B4-3).

- c. Based upon preliminary structural calculations, blockage regions which are near melting ( $\sim$  within  $50^{\circ}\text{C}$ ) will not severely restrict the flow of the hot, pressurized fuel into the UAB. Initial interpretation of SLSF test data indicates that the upper blockage in the larger scale, constant power P3 experiment may have been moveable at the time of fuel disruption which would allow pressurized fuel penetration into the UAB.
- d. The experiment which could most likely provide information on this condition was TREAT R7 which represented a power burst to 15 times nominal following steel melting. However, the fuel thermal conditions could not be readily ascertained and it is likely that significant pressurization did not occur. In the CRBRP, the extent of fuel penetration into the UAB will depend upon the relative timing of steel and fuel relocations throughout the core. There is no change in the original judgement that a complete fuel blockage in the UAB, cannot be precluded
- e. For the EOC-4 configuration it appears likely that the plenum fission gas would be released to the sodium flow channel (time constant of 0.25 sec) during the time of gross melting of the cladding. The cladding failure temperature and gas release time constants were estimated to be  $1400^{\circ}\text{C}$  ( $\approx$  melting) and 0.25 seconds,

respectively. TREAT Test R8 shows that under the conditions of simultaneous gas release and steel melting an upper blockage would not be formed (Ref. QCS760.178B4-1). Hence, for the conditions expected in the EOC-4 core (see QCS760.178A3, Table 5) upward steel relocation would not be expected in much of the core.

In summary, there is ample time for steel relocation prior to fuel motion in the CRBRP, primarily due to its low effective sodium void worth. However, since plenum fission gas release from irradiated rods starts almost coincident with steel melting, gross upward steel relocation is not anticipated for irradiated fuel conditions. Upward cladding blockages are however, anticipated for BOC core conditions. In this case they are characterized as forming a short distance into the UAB. The blockage is expected to be relatively thick (cm's) near the bundle edges but irregular and vented to gas flow. The onset of fueled region pressurization could disrupt regions of the steel blockage which are within 50°C of the melting point allowing fuel penetration into the UAB.

The dynamic response of the BOC-1 core and the extent of upper blockage formation throughout the core was found to only be weakly sensitive to large variations in axial blockage location (including the core/UAB boundary) and reactivity feedback parameters. Hence, the initial conditions chosen for analysis of the melt-out phase are appropriate (see response to QCS760.178B5).

#### References

- QCS760.178B4-1 B. W. Spencer, et al., "Interim Report on TREAT Test R8, A Seven-Pin Loss-of-Flow Test with Pressurized Pins," Argonne National Laboratory, ANL/RAS 78-39, September 1978.
- QCS760.178B4-2 S. K. Rhow, et al., "An Assessment of HCDA Energetics in the CRBRP Heterogeneous Reactor Core," CRBRP-GEFR-00523, General Electric Company, December 1981.
- QCS760.178B4-3 M. Ishii, et al., "Multi-Channel Model for Relocation of Molten Cladding in Unprotected Loss-of-Flow Accidents in LMFBR's," Nuc. Sci. & Engr., Vol. 69, p. 297, February 1979.

Table QCS760.178B4-1

FUEL MELT FRACTION (OR MAXIMUM TEMPERATURE)

AT END OF SAS ANALYSIS FOR BOC-1 LOF

SAS Channel Number	Number of Fuel Assemblies	Fuel Melt Fraction or Maximum Temperature (°C)		
		<u>Case 1C</u>	<u>Case 4</u>	<u>Case 5</u>
2	12	0.04	0.08	2679
4	18	0.24	0.28	0.01
14	18	0.07	0.11	2632
15	24	0.30	0.31	2679
Time from Start of LOF (S)		20.4	19.9	23.1
Normalized Energy (FPS) from Initiation of LOF		20.5	20.5	20.5
Energy Produced During Power Burst (FPS)		3.5	3.5	3.5

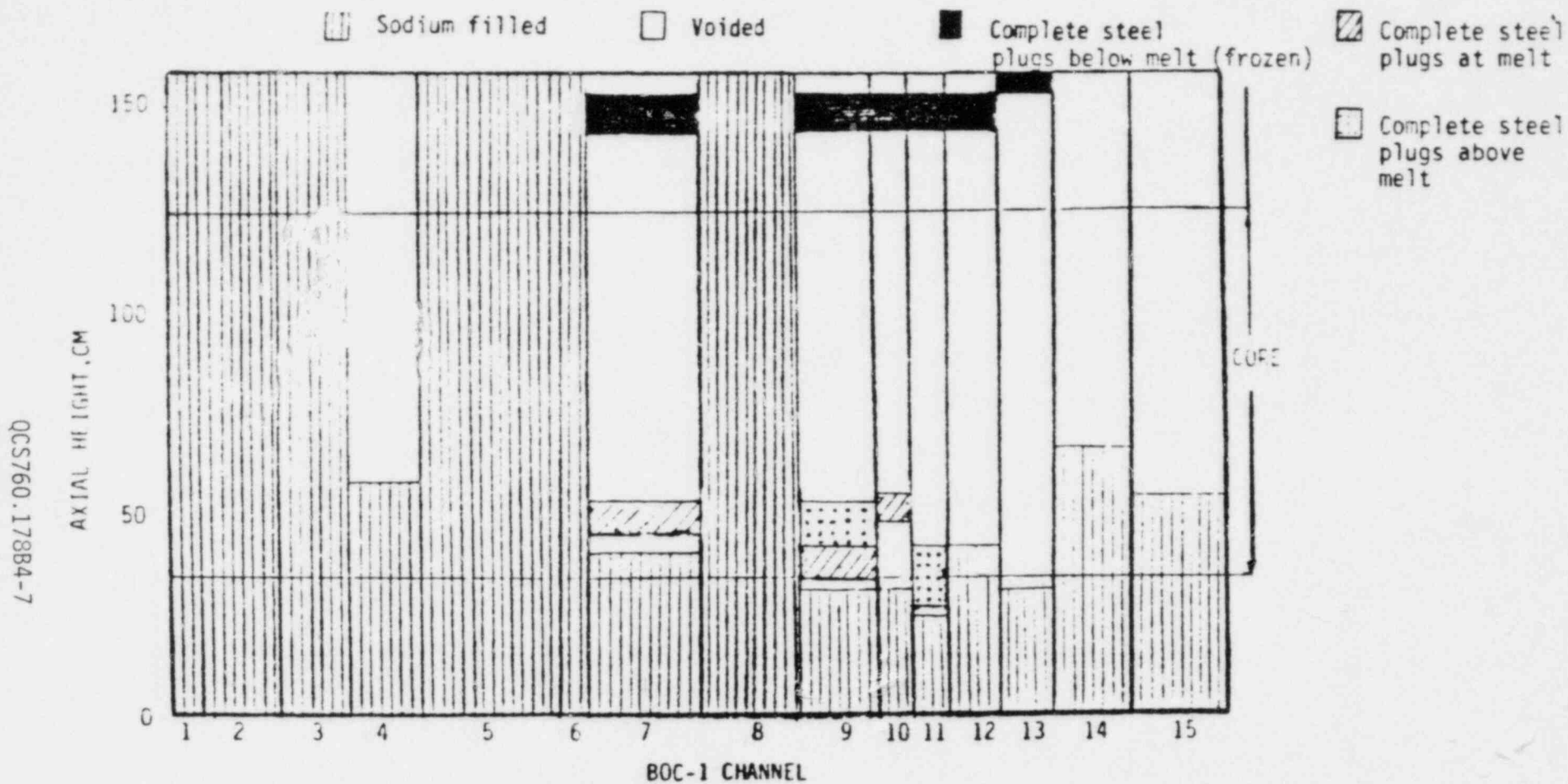
▨ Sodium filled

□ Voided

■ Complete steel  
plugs below melt (frozen)

▨ Complete steel  
plugs at melt

▨ Complete steel  
plugs above  
melt



QCS760.178B4-7

Fig. QCS760.178B4-1 State of Core at Initiation of First Fuel Disruption (Ch. 11) for BOC-1 LOF Case 1C (Doppler =  $-20\phi$ , Axial =  $-38\phi$ , Sodium Void =  $-36\phi$ , Cladding =  $155\phi$ , Net =  $63\phi$ ,  $P = 2.33$  Nominal).

Amend. 72  
Oct. 1982

QCS760.178B4-8

AXIAL HEIGHT, CM

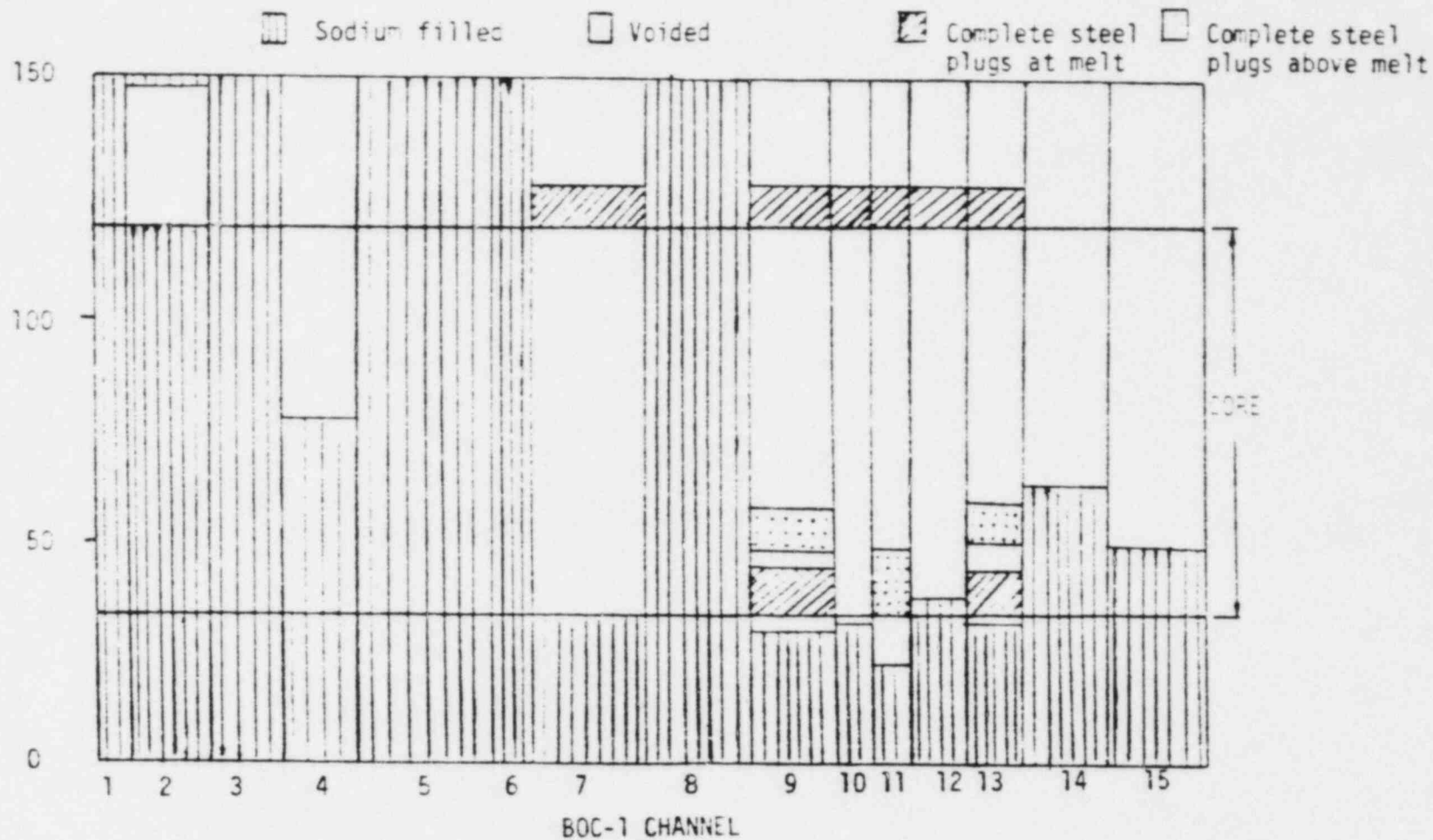


Fig. QCS760.178B4-2 State of Core at Initiation of First Fuel Disruption (Ch. 11) for BOC-1 LOF Case 4 (Doppler =  $-21\phi$ , Axial =  $-38\phi$ , Sodium Void =  $-47\phi$ , Cladding =  $109\phi$ , Net =  $2\phi$ , P = 0.93 Nominal).

Amend. 72  
Oct. 1982





Question CS760.178B5, -C6, -C7

-B5. What is the basis for maintaining continuous subcriticality in the high heat loss environment of early melt-out phase? What are the fuel losses (quantified), taking into account uncertainties in removal path geometries, driving pressures and freezing mechanisms?

-C6. What degree of subcriticality is required to prevent pool recriticality from thermal and fluid dynamics upset conditions? What is your position on the potential for small recriticalities to amplify? What is the justification for your position?

-C7. In assessing benign termination from the boiled-up pool, justify the fuel removal mechanisms and rates. In particular, assess the potential for upper pool sodium entry via rapid condensation of steel vapor pressure.

Response

The key points in the above questions are: (a) basis for continuous subcriticality, (b) fuel removal uncertainties relative to path, driving pressure and freezing mechanism, (c) fuel removal required to prevent recriticality, (d) potential for amplification of recriticality events, (e) termination of boiled-up pool phase including consideration of sodium re-entry. Since these points are all related to the case for achieving a condition of permanent subcriticality following the initiating phase without large energetic reactivity insertions, they are addressed in an integrated manner in this response.

In previous analysis Ref. QCS760.178B5-1 it was shown that early fuel removal through interassembly gaps prevented the large scale pool phase (LSPP). In this reference the LSPP was considered as any contiguous molten mass which is of sufficient size such that its phenomenological behavior will dominate the accident progression relative to energetics potential.

In this response the terminology LSPP refers to the configuration after the melt-out of the internal blanket assemblies. The distinction is made between this more homogeneous configuration and that associated with the merging of molten driver fuel while the inner blanket is intact. The latter is referred to in this response as the melt-out/annular pool phase (MO/APP). This refinement is important in the context of the heterogeneous core design since the phenomenological behavior in the MO/APP introduces additional considerations with significance regarding energetics potential that would not be otherwise discussed in the context of a more homogeneous LSPP.

One of the immediate benefits resulting from the above distinction is to remove the implications that there is an extreme sensitivity to the timing of fuel removal (of the order of 1 to 2 sec) prior to the formation of the LSPP. It can be shown that there are at least several tens of seconds available for fuel removal in the interval from the onset of fuel disruption in driver fuel assemblies until the inner radial blanket fuel assemblies will experience melt-out.

So long as the inner blanket fuel remains intact, there is an effective barrier to coherent dynamic fuel motions which have the potential for

escalating into large ramp rate reactivity insertions. The time required to destroy this barrier is found to be long relative to either (a) the time for fuel removal through several available escape paths such as interassembly gaps and control channels or (b) the time for removal of obstructions to fuel escape in the upper axial blanket (UAB) region.

In this response, consideration has been given to the implications of the extended time scale of the melt-out/annular pool phase (MO/APP) relative to the homogeneous LSPP. Both the potential for recriticality events as well as alternate fuel escape paths have been considered including the potential for sodium re-entry. As a result it is concluded that:

1. Once molten fuel becomes available on an assembly basis, mild recriticality events may be possible but they are limited in amplitude and do not amplify.
2. Multiple paths for fuel removal are available on a short time scale, relative to the melt-out of internal blanket assemblies. Correspondingly, fuel removal is not overly sensitive to fuel penetration model assumptions and fuel escape impedances.
3. There is always time for sufficient fuel removal, i.e., about 40% of the driver fuel, to achieve permanent subcriticality prior to loss of the annular inner blanket barrier.
4. The accident sequence will terminate benignly without the development of a homogeneous large scale confined pool phase as defined in (Ref. QCS760.178B5-1).
5. Sodium re-entry can be ruled out on the basis of excessive sodium vaporization when liquid sodium comes into contact with molten fuel and steel materials.

The details of the response are contained in the following sections. First, the beginning of the melt-out phase is characterized with respect to likely conditions in the driver and blanket fuel assemblies. Then a discussion of the possibility of recriticality events is presented supporting conclusion (1). In the next section fuel removal paths are identified followed by a discussion of the time scale on which these paths are made available. Fuel penetration mechanisms are discussed as well as sensitivity to external constraints, supporting conclusions (2), (3), and (4). Finally a discussion relating to the potential for sodium re-entry is provided to support conclusion (5).

#### Beginning of Melt-Out Phase

The melt-out phase of the accident sequence begins when fuel within individual assemblies in the driver core region starts the process of melting through hexcan wall barriers. For both the BOC-1 and EOC-4 core, this action begins after  $\approx 20$  seconds of initiating phase events (sodium boiling, cladding, and early fuel motion). At this time most of the driver fuel assemblies have experienced fuel disruption ( $\approx 1-2$  s time scale). Internal blanket (IB) assemblies are not voided in the BOC-1 core and have an average fuel temperature  $\approx 1000^\circ\text{C}$  at the core midplane. For the EOC-4 core, IB assemblies may be

partially voided at an average blanket fuel temperature closer to 2000°C at the core midplane. The ratio of blanket fuel to driver fuel specific power level is approximately 1 to 10 for the BOC-1 core and approximately 1 to 3 for the EOC-4 core.

Early in the melt-out phase the driver fuel power level may be about 75 w/g (50% of nominal) tending perhaps to as low as 15 w/g as the merging of assemblies into a continuous annular fuel region becomes more complete. These power levels represent bounds below which, recriticality events cannot be precluded. At higher levels, vapor generation would boilup the pool and largely preclude such events. Recriticality events which do occur would be expected to be very mild and infrequent.

Based on the initiating phase analysis performed so far, cladding blockages are likely to be formed at the bottom of the core. Upper cladding blockages may also be formed, but vented in most of the BOC-1 core. In the EOC-4 core, upper cladding blockages are not expected in view of the effect of plenum fission gas release on cladding movement, as addressed in Response to CS760.178B-4. Therefore, it is concluded that fuel removal into the upper axial blanket region is possible depending on core conditions.

The gaps between hexcan walls which are not adjacent to boiling fuel regions are expected to remain open, not only in the region outside the core, but also in the core region. In the BOC-1 core, the gap sizes are expected to be similar to the fabrication dimensions (0.47 cm) because of negligible swelling of the hexcan steel. In the EOC-4 core driver fuel region, the hexcan steel swelling reduces the gap sizes on the average to about two thirds of the fabrication dimension. Therefore, the interassembly gaps are expected to provide a viable fuel removal path not only in the BOC-1 core but also in the EOC-4 core.

Based on the relative conditions of the driver fuel and the blanket assemblies it is estimated that the time interval between the onset of fuel driver disruption and breakdown of the IB barrier to form a homogeneous pool would be  $\approx$  150 seconds for the BOC-1 core condition and  $\sim$  50 seconds for the EOC-4 core condition based on adiabatic heating. If driver fuel does not flow rapidly from the core region it may also enter and penetrate the IB assemblies causing the IB to melt-out at greater than the adiabatic rate. As shown in Appendix A to this response this effect would reduce the above indicated time intervals by no more than a factor of four for BOC-1 and two for EOC-4 conditions, respectively.

#### Recriticality Events

Recriticality events following the initiating phase have been considered. Such events cannot be generically ruled out in the high heat loss environment at the assembly scale as power decreases to decay heat levels. Fuel compaction is limited by vapor separation and cannot introduce reactivity ramp rates exceeding 20¢/s/assembly which during the early time period would be mitigated by core-wide incoherencies.

Vapor condensation due to influx of cladding steel will be limited since colder steel will be covered by a thermally stable fuel crust. No mechanisms

have been identified which can fragment and rapidly distribute cold steel within the pool.

However, some gradual reduction in vapor flux cannot be precluded with the resultant compaction of fissile material. The response is self-dispersive since an increase in power will very rapidly increase vapor production in the near saturated pool, leading to a reduced fissile density. Reoccurrence and amplification would be possible if the physical event behaved and responded as continuous liquid slug elements bounded by expanding and compressing vapor spaces. However, this is not found to be likely because of vapor-liquid break-up processes resulting from the growth of Taylor type instabilities. These mechanisms and their application to the MO/APP are discussed in Appendix B to this response. It is concluded that the fuel-steel boiling process within a disrupted heterogeneous core should be stable to mild recriticalities at least as long as the annular geometry dominates the fluid dynamic behavior.

#### Fuel Removal Paths

Fuel removal paths important to the termination of the accident sequence include: (a) the upper axial blankets, (b) interassembly gaps, (c) control rod channels, and (d) radial blanket assembly void space.

*Upper Axial Blankets* - The upper axial blanket regions of the driver fuel assemblies provide a fuel escape path on two levels of consideration. On an early time scale, cladding blockage are likely to prevent upward fuel escape for BOC conditions. However, for EOC conditions, downward cladding relocation driven by plenum fission gas escape, will leave an upward escape path for subsequent disrupted fuel. Accounting for coolant channel volume fraction the driver fuel removed upward would be  $\sim 1\%$  per cm of penetration into the UAB (on a assembly basis).

On a larger time scale (several tens of seconds) cladding blockages in the upper axial blanket can be removed as an obstruction to fuel escape by virtue of ablative melting or in EOC conditions by melt-out of the hexcan boundary in the UAB region. The latter can reasonably occur on a time scale of less than 10 sec depending on the fuel penetration.

*Interassembly Gaps* - Figure QCS760.178B5-1 shows the side view of the gaps in the region below the core, and the radial blanket/shield regions. The dimensions shown in this figure are fabrication dimensions at room temperature. Although the gap sizes could be larger in actual cases due to thermal expansion, the fabrication dimensions are used in the present estimation of the gap volume. Furthermore, it is assumed that the gaps in and below the shield block region (.17 cm) will not be available due to fuel plugging as it flows into this constricted region.

Thus, the volume of the gaps available for fuel removal from the core region is estimated, and the results are given in Table QCS760.178B5-1. This table shows that the total gap volume below and outside the core region is much larger than the total liquid volume of the core materials: fuel, cladding, and assembly hexcan walls.

The interassembly gap width in the core region has been calculated using the SAS3D results for the initiating phase at a point in the transient around

the initiation of fuel disruption in the lead assemblies. The hexcan walls in the below-core and radial shield regions have experienced little swelling at both BOC-1 and EOC-4. Therefore, the gap widths in these regions are expected to be approximately 0.48 cm which is a fabrication dimension (0.47 cm) plus thermal expansion. The gap width in the radial blanket regions is taken to be an average between the gap widths in the core and radial shield regions. The gap sizes are summarized in Table QCS760.178B5-2.

*Control Rod Channels* - The fuel removal flow paths in the nine primary and six secondary control assemblies in the reactor core are schematically shown in Figs. QCS760.178B5-2 and -3. The primary control assembly (PCA) has a moveable inner hexcan (attached to the control rods) which partially protrudes into the active core zone. The annular gap which is formed with the outer hexcan has a hydraulic diameter and flow area of approximately 0.75 cm and 5 cm<sup>2</sup>, respectively. The main path for fuel flow is downward into the large open area (empty hexcan) below the moveable control, then through a 3.7 cm diameter hole in the shield region to the orifice zone (8.4 cm diameter). The orifice zone consists of seven one cm thick plates, each of which has six equally spaced and parallel 1.07 cm diameter holes. The plates are separated by open spaces (8.4 cm diameter) 1.27 cm high. After passing through the orifice zone the fuel flows into the inlet nozzle ( $D_H = 6.35$  cm,  $A = 12.47$  cm<sup>2</sup>), then into the large inlet module and ultimately into the reactor inlet plenum.

The secondary control assemblies (SCA) have a different configuration (Fig. QCS760.178B5-3) with the initial path again through an annular region ( $D_H = 0.67$  cm,  $A = 38.5$  cm<sup>2</sup>) past an orifice zone ( $D_H = 0.84$  cm,  $A = 7.4$  cm<sup>2</sup>) into the inlet module. After melting through the guide tube an alternate path is available through a large open area ( $D_H = 10$  cm) and outlet ( $D_H = 3$  cm) into the SCA low pressure plenum (in the inlet module) and then outward to the core barrel region. However, no credit for fuel flow beyond the vent will be taken since an assessment of freezing and plugging potential has not been completed.

Table QCS760.178B5-3 provides the available volumes for fuel removal based on the above geometries.

*Radial Blanket Assembly Void Spaces* - In parallel with melt-through of the inner blanket and control assembly barriers, it is also reasonable to examine the volume available in the outer radial blanket assemblies due to the long time frame available. From geometric considerations the volume readily (sodium flow area) available in the first row of the outer radial blanket represents about 20% of the driver fuel volume.

*Fuel Removal Necessary to Assure Permanent Subcriticality* - Table QCS 760.178B5-4 shows reactivity levels for various disrupted core configurations at BOC-1 (see Appendix C for details of the neutronics modeling). Case 1 represents core conditions after approximately 43% of the total fuel inventory is removed from the core, the remaining fuel in the core annular regions is homogenized and fully compacted, while the internal blanket and control assemblies remain intact. The system is subcritical for this configuration. Case 2 is identical to Case 1 except that the fuel removal is reduced to 33% of the total inventory. The system is substantially above critical for this configuration. In Case 3, about 41% of the total fuel inventory is again

removed from the core. The remaining fuel, internal blanket and control assemblies (without B<sub>4</sub>C) are assumed to be homogenized and fully compacted. This homogeneous pool configuration is substantially subcritical. From these neutronics results, it was concluded that the system will achieve permanent subcriticality as long as about 40% of the total fuel inventory is removed from the core. Based upon preliminary calculations, this also appears to represent a good estimate for EOC conditions.

#### Time Scale to Make Fuel Removal Paths Available Relative to the Annular Pool Phase

Fuel escape paths become available on a short time scale. At EOC conditions the UAB is open at the onset of fuel disruption. Other escape paths become available on a time scale of several seconds following fuel disruption due to melt-through of hexcan boundaries.

The hexcan wall melt-through time was calculated using a finite-difference method. This calculation initiates from the time a molten fuel pool has developed. Initial hexcan wall temperatures for this calculation were determined based on SAS3D calculations. A typical hexcan wall temperature profile just prior to boiling of the assembly molten pool is plotted in Fig. QCS760.178B5-4.

Heat transfer coefficients at the hexcan wall (with stable fuel crusts) were determined from the correlation of internally heated boiling pool test data of Ref. QCS760.178B5-2. Based on this correlation, the heat transfer coefficient for a boiling pool of fuel-steel mixture was calculated to be approximately 2 w/cm<sup>2</sup>-°K. The heat transfer coefficient at the bottom of the pool may be lower than this value because the pool is expected to be more quiescent in this region.<sup>2</sup> The heat transfer coefficient for a quiescent pool is as low as 0.2 w/cm<sup>2</sup>-°K according to Refs. QCS760.178B5-1 and QCS760.178B5-3. This means that the can wall heat transfer coefficient in the bottom region of the pool can be in the range from 0.2 to 2 w/cm<sup>2</sup>-°K. The boiling pool temperature is expected to be 3100°C - 3200°C which is the steel boiling point at an assembly pressure of 3-5 bars.

Based on the above thermal characteristics the hexcan wall melt-through times were calculated using the typical hexcan wall temperature profile (Fig. QCS760.178B5-4) as the initial temperature profile. The results are plotted in Fig. QCS760.178B5-5, which indicates that the major portion of the hexcan wall will melt through within 2 seconds after the boiling pool is formed inside the hexcan.

The flow path through the control assemblies will become available approximately four seconds after being contacted by the boiling (3200°C) fuel-steel pool. This value is based upon a thermal analysis comparable to that just discussed for melting of the fuel assembly hexcan, except that the appropriate internal sodium flow (~ 20% of nominal), geometry and temperatures (~ 400°C) are considered. The estimated melt-through time is approximately proportional to both the driving temperature difference and heat transfer coefficient. Variations in these parameters, which control heat losses from the pool are offsetting in that the pool temperature will increase for reductions in the heat transfer coefficient. Hence, for the expected parameter variations, the control assemblies become available within several seconds

after attack by the pool. A direct calculation of the timing for availability of the radial blankets has not yet been performed. However, based on the high heat fluxes expected, and Ledinegg instability, access to the radial blanket assemblies would be likely and within the time frame of the annular pool phase.

#### Freezing Mechanisms and Limits to Fuel Removal

Once escape paths become available, access to sufficient volume to assure permanent subcriticality can only be limited temporarily by fuel freezing. Experimental results were discussed in Ref. QCS760.178B5-1 which indicated the possibility for fuel penetration into the UAB - fission gas plenum region for distances on the order of 30 to 40 cm. The details of the applicable freezing mechanisms are as yet unresolved. A discussion of mechanisms is found in Appendix D to this response. It is noted that fuel would penetrate much larger distances if the conduction model were used as a basis and somewhat shorter distances than experimental results indicate if the "bulk" freezing model were applied. For UAB penetration, experimental results are presently used as a best estimate for fuel penetration into the UAB in the absence of prior cladding blockages. A pessimistic estimate is provided by the bulk freezing model which would limit fuel penetration to about the extent of the UAB itself ( $\approx 30$  cm).

For interassembly gaps, the conduction theory as discussed in Appendix D is applied as a best estimate (including accounting for sodium flow impedance) while bulk freezing is used as a pessimistic basis. The primary control channel remains unplugged when tested against either conduction or bulk freezing models. On the other hand, plugging cannot be ruled out for the secondary control rod annular gap leading to the inlet orifice.

When either calculations or experimental results are applied to fuel escape paths it is found that (a) the PCA escape path remains unplugged and fuel escape is limited only by hydraulic considerations, (b) fuel penetration into the remaining escape paths, UAB and interassembly gaps, is in some cases individually insufficient to assure subcriticality. However, when collectively coupled with the PCA removal, these paths provide for fuel escape from the core region in sufficient quantity to assure permanent subcriticality.

#### Driving Pressures and Hydraulic Limitations

Once molten fuel moves out of the assemblies, the fuel will flow radially and downward into the open gaps. The gap flow area is small initially as only high power assemblies ( $\sim 20\%$ ) are involved, and then increases as more fuel assemblies are involved. When all the fuel assemblies are involved (i.e., the molten pool reaches the core boundary), the total gap flow area is estimated to be roughly  $3000 \text{ cm}^2$  at BOC-1 and  $2500 \text{ cm}^2$  at EOC-4, assuming that only the gaps between the blanket and control assemblies remain open. The fuel-steel mixture in the assembly is in a dispersive state due to steel boiling. The pressure inside the assembly is expected to be 3-5 bars which is the steel vapor pressure at  $3100 - 3200^\circ\text{C}$ . The pressure in the gaps would be approximately 1.5 bar. Therefore, an initial pressure differential between the assembly and the gaps would be above 1.5 bar.

The effect of sodium impedance to fuel flow in the interassembly gaps is discussed in Appendix D. Based on the conduction model, sodium flow impedance will reduce the gap penetration by no more than 40%. This reduced penetration is still sufficient to accommodate all of the fuel required to assure permanent subcriticality on a time scale that is short (1 to 2 sec) relative to the time scale of the MO/APP.

The fuel temperature was previously estimated to be 3100-3200°C when the fuel assembly hexcan walls melt through. If fuel removal through the interassembly gaps is not sufficient for subcriticality, a molten fuel pool will be formed around the control assemblies, and the power will respond to assure boilup. Therefore, it is reasonable to assume that the molten pool temperature will be about the same as the fuel temperature at melt-through of the hexcan walls, i.e., 3100-3200°C. This temperature corresponds to a steel saturation vapor pressure of 3-5 bar. Since the inlet plenum pressure is approximately 2 bar at this point in the assumed flow coastdown transient, the differential pressure for fuel removal to the inlet module through the control assemblies can be assumed to be approximately 1.5 bar including a static head of 0.5 bar.

The rate of fuel removal from the core (i.e., below the core/LAB interface) is initially rapid until the molten fuel fills a space above the orifice region in the PCA's and the low pressure vent tube outlet of the SCA's. This space will be filled rather quickly after the hexcan walls (and the guide tubes in the case of secondary control assemblies) melt through. The volume of these spaces was estimated to be approximately 79 liters, which corresponds to ~ 11% of the total fuel inventory (6000 kg). After filling the space above the PCA orifice region, the molten fuel will flow through the orifice plates into the inlet module and ultimately into the reactor inlet plenum. In the secondary control assemblies, the molten fuel may flow through the guide tube lower vent (Fig. QCS760.178B5-3) into either or both of the inlet module and out to the core barrel space. However, both of these later SCA paths were assumed to be unavailable because an assessment of the potential for plugging has not yet been performed.

The rate of fuel removal through the PCA orifice region to the inlet module can be estimated by utilizing design information on sodium flow in the PCA (Ref. QCS760.178B5-4). As shown therein, most of the pressure drop occurs through the orifice plates, and a sodium mass flow rate of 5.6 kg/sec per assembly was calculated for a pressure drop of 5.4 bar. Accordingly, based on the pressure drop and density ratios between the sodium flow and fuel flow, the fuel removal rate through the orifice region is calculated to be 9.6 kg/sec per assembly. For the nine PCA's, the total fuel removal rate is 86 kg/sec which corresponds to 1.4% of the total fuel inventory per second.

There are two major effects to be considered in the above estimate: fuel crust formation and two-phase flow (reduced density). The fuel crust reduces the orifice hole diameters, and the "steady-state" reduced hole diameter can be calculated on the basis of energy balance between convection at the crust surface and conduction through the crust. The heat transfer coefficient is calculated to be roughly  $2 \text{ w/cm}^2\text{-}^\circ\text{C}$ , and with the fuel flow at 350°C above its liquidus the hole diameter is reduced from 1.07 cm to 0.94 cm. Using a new loss coefficient, determined for the reduced hole diameter based on design information provided in Ref. QCS760.178B5-4, the fuel removal rate was



recalculated. The total fuel removal rate was reduced from the above estimate by 15% due to the presence of the fuel crust.

Reduction of the flow density reduces the mass flow rate for a given pressure drop. When the flow density is reduced by a factor of 2 (void fraction = 0.5), the mass flow rate is reduced by 30%, i.e., from 1.4%/sec to 1% sec.

In summary, about 11% of the total fuel inventory can be removed into the primary and secondary control assemblies on a short time scale after melt-through of the hexcan walls. In addition, the fuel can be removed through the PCA orifice region into the inlet module and ultimately the reactor inlet plenum, at a rate of about 1% of the total fuel inventory per second even with consideration of the effects of fuel crust and reduced mixture density.

#### Termination of Accident Sequence

The material presented this far along with supporting appendices has developed the basis for (1) fuel removal paths are available, (2) fuel removal is significant even when assessed with either conservative models or experimental results, and (3) significant recriticality events cannot lead to energetic disassembly during the melt-out/annular pool phase.

From this information it follows that the CRBRP hypothetical core disruption accident terminates benignly and that because of the long time scale of the melt-out/annular pool phase the condition of a large scale homogeneous confined pool is not established.

The implications of the preceding discussions can be summarized in Table QCS760.178B5-5. This table shows the multiple paths for fuel removal and the extent of fuel removal that can be accommodated for BOC-1 and EOC-4 core conditions. Early fuel removal is associated with fuel escape dominated by interassembly gap flow as discussed in Ref. QCS760.178B5-1. This would occur on a time scale that is short (1 to 2 sec) relative to the time interval of the annular pool phase. The table also shows that with some reasonably pessimistic estimates relative to early fuel removal, but which at the same time avoid precluding clearly available pathways, permanent subcriticality can be attained on an extended time scale that is still within the time interval of the annular pool phase. Table QCS760.178B5-5 will be discussed by columns.

#### Upper Axial Blanket

The distinction between BOC-1 and EOC-4 core conditions is imbedded in the role of plenum fission gas on cladding blockages. For the BOC-1 core, cladding blockages cannot be precluded but will not be complete throughout the core. However, over the time scale of the MO/APP phase a best estimate would indicate some fuel removal but in quantities insufficient to lead to permanent subcriticality. A pessimistic estimate would take no credit for this removal path during the MO/APP phase. An important consideration of the UAB is introduced because of the extended time required to melt-out the inner blankets. Simple considerations of ablation melting of the UAB would indicate sufficient time is available to erode even rather thick (5 cm) cladding blockages in a time scale shorter than 100 sec. Thus, even if other mechanisms of fuel

removal were denied, the UAB would be open by the time that a large homogeneous pool is established.

For the EOC-4 core plenum, fission gas release during the initiating phase will prevent upper steel blockage as demonstrated in the TREAT R-8 test (see Response to QCS760.178B4). A best estimate consideration would indicate essentially unlimited fuel penetration into the UAB on an assembly basis. While a pessimistic estimate would indicate a more limited penetration perhaps to the end of the blanket section. This is supported by either application of a bulk freezing model or relying solely on thermite injection test results. Again, a key consideration is that the subsequent melt-out of the upper blanket region accounting for fission energy can also occur on a 30 second time scale if fuel melting is used as a basis. The time scale for opening the UAB is much shorter if hexcan melting is visualized as the criterion for separation of blanket region from the fission gas plenum region. Again the above core structure is opened on a time scale less than or equal to the time to melt-through the inner blanket.

#### Interassembly Gaps

The interassembly gaps are also significant pathways for fuel removal. Essentially the total driver fuel inventory can be accommodated by radial flow outward (and downward) if a conduction limited fuel freezing (penetration model) is employed. This will not or need not occur on a one-to-two second time scale. The rate of fuel removal is found to be essentially supply limited. That is, fuel can only be removed as fast as melting occurs. Sodium impedance was evaluated and found at best to reduce unimpeded penetration length by  $\approx 40\%$ . This reduction does not alter the fuel removal inventory. Pessimistic estimates are based on the bulk freezing model and gap sizes for the BOC-1 and EOC-4 core respectively. In the latter cases, the fuel removal may be less than required to achieve permanent subcriticality, but none-the-less when added with other removal paths leads to the same result.

#### Control Rod Assemblies

The control rod assemblies (CRA) play a part in accommodating fuel removal in two ways. First, following melt-through into the voided assembly internals, the process of filling up the CRA from the inlet orifice to the lower axial blanket-core interface removes a fuel inventory of  $\approx 10\%$ . Second, drainage through the lower orifice region of the primary control rod assembly is assumed independent of freezing model. The drainage rate through 9 primary control rod assemblies is conservatively estimated to be within 1 to 2% of the fuel inventory per second. Thus even with the most pessimistic case sufficient fuel inventory is removed prior to inner blanket melt-out to assure permanent subcriticality. It is noted that the inlet orifice region of the secondary control rod assemblies cannot be assured to be free from plugging.

In Table QCS760.178B5-5 only that inventory of fuel associated with the CRA volumes above the inlet orifice is credited. This is to put the role of the CRA on a consistent basis with the best estimate and pessimistic estimate of the time scale for melt-out of the IB assemblies as discussed in the next section.

### Time Scale and Power Level

The overall time scale and power level are interrelated. The best estimate is based on the assumption that driver fuel does not penetrate into the inner blanket region because of rapid removal through the interassembly gaps. The pessimistic time estimate assumes that because of limited fuel removal through the gaps, driver fuel enters the inner blanket fuel region and reduces the melt-out time by a factor of two (EOC-4) and a factor of four (BOC-1).

The average power level in the driver fuel is based on consideration that it is most probably; (1) above decay heat levels (10% of nominal power) because of mild recriticality events, (2) less than 50% of nominal power which should be sufficient to preclude recriticality on an assembly scale because of fuel dispersal, and (3) less than 20% of nominal power after assembly melt-through reduces the surface to volume ratio in the MO/APP. Since assembly merging occurs rapidly after dispersal, a power level of  $\approx 30\%$  of nominal, which is sufficient to assure fuel dispersal, is taken as a basis for the time to melt the IB assemblies.

### Additional Considerations

In the pessimistic consideration above, driver fuel penetration into the inner blanket region, if it should occur, would also be accompanied by an equivalent penetration into the outer radial blanket. This would further reduce or accommodate an inventory of  $\approx 20\%$ .

### Sensitivity

Various sensitivities have been indicated in Table QCS760.178B5-5. An additional sensitivity that is not explicitly presented is that of the details of the power history during the MO/APP. It is felt that the details of the power history are not important so long as large ramp rate recriticalities can be precluded. An increase in power level would shorten the time scale to melt-out the inner blanket regions but would have the off-setting effect of increasing the driving pressure for fuel removal and decreasing the UAB melt-out time.

### Sodium Re-Entry

With multiple fuel escape paths operating in a surrounding liquid sodium environment the question of condensation induced sodium re-entry is natural. By analogy, transient condensation of steam contacting subcooled liquid water can result in sudden depressurization of the steam region and "suction" of the subcooled water toward the steam source. Such rapid condensation has been postulated to explain the occurrence of water hammers during accident transient simulations for pressurized water reactors. The concern has been voiced that, in a process similar to that mentioned above for steam, steel-vapor condensation on upper pool liquid sodium following melt-through of upper core blockages can cause the liquid sodium to be drawn back into the core. This water hammer which is certainly possible with respect to single component systems, is inapplicable to the two-component steel vapor-liquid sodium system because of the volatility of the liquid sodium surface and, therefore, the

participation of sodium vapor during the steel condensation process. A pressure reduction in the steel vapor region due to condensation is immediately compensated for by an equivalent pressure increase due to sodium evaporation.

The thermodynamic arguments are presented in Appendix E. The results of these arguments indicate that for the steel vapor, subcooled sodium liquid system a dual phase conversion process results in a vapor volume increase. For every one cubic cm of steel vapor condensed, 1.3 cubic cm of sodium vapor is produced, which significantly changes the character of the process in comparison with a one-component system such as steam and water. Sodium re-entry caused by rapid steel vapor condensation is not considered applicable to the accident sequence.

#### Response Summary

- While recriticality events cannot be ruled out during the MO/APP phase, these events are inherently mild because of flow regime and geometry considerations. Neither can such events escalate into larger amplitude prompt burst events. As a result of such mild recriticality events, the fuel maintains itself in a highly dispersed state at some low level above decay heat.
- Viable fuel removal paths exist in the UAB (for some core conditions), through interassembly gaps, through control rod assemblies and in some cases by melting into the outer radial blankets.
- In view of the variable and parallel nature of these removal paths the removal of sufficient fuel to assure permanent subcriticality is not overly sensitive to freezing mechanisms, sodium constraint, and viability of individual pathways.
- Removal of ~ 40% of the total driver fuel inventory is sufficient to assure permanent subcriticality.
- Because of the above considerations, removal of sufficient fuel to assure permanent subcriticality can occur prior to melt-out of the inner blanket and formation of a large scale homogeneous pool.
- Even if such events were to occur without losing sufficient inventory, melt-out of the UAB would remove any constraint to the pool and provide another means for termination of the accident sequence.
- During the time when fuel loss is occurring, sodium re-entry is precluded as a source of pressure compaction of the annular pool material.

#### References to Response QCS760.178B5, -C6, -C7

- QCS760.178B5-1      S. K. Rhow, et al., "An Assessment of HCDA Energetics in the CRBRP Heterogeneous Reactor Core," CRBRP-GEFR-00523, General Electric Company, December 1981.

QCS760.178B5-2

G. A. Greene, et al., "Heat Removal Characteristics of Volume Heated Boiling Pools with Inclined Boundaries," BNL-NUREG-51157, Brookhaven National Laboratory, April 1980.

QCS760.178B5-3

E. E. Morris and T. Y. C. Wei, "An Assessment of the Unprotected LOF Accident in the CDS Phase II Heterogeneous Core Design," ANL/RAS 81-1, Argonne National Laboratory, December 1980.

QCS760.178B5-4

D. Y. Nee, "Preliminary Thermal-Hydraulic Performance of CRBRP Preliminary Control Assemblies," CRBRP-ARD--0151, June 1977.

Table Q760.178B5-1

## TOTAL VOLUMES OF CORE MATERIALS AND GAPS BETWEEN ASSEMBLIES

<u>Location</u>	<u>Volume (Liters)</u>
<u>Region Below Core</u>	
Between Core/LAB Interface and Shield Block	110
<u>Radial Blanket Region</u>	
Between Core/LAB Interface and Shield Block	60
Between Core/LAB Interface and ACLP*	110
<u>Radial Shield Region</u>	
Between Core/LAB Interface and Inlet Module	1800
Between Core/LAB Interface and ACLP	250
<u>Region Between Radial Shield Assemblies and Core Barrel</u>	
Below Core/LAB Interface	1300
Between Core/LAB Interface and ACLP	<u>1200</u>
TOTAL	4830**
<u>Total Fuel Assembly Volumes in Core Region (BOC-1)</u>	
Fuel in Liquid State	700
Cladding in Liquid State (including wire wraps)	310
Hexcan in Liquid State	210

\* Above-core load pad at 13 cm into UAB.

\*\* This represents 690% of total core fuel volume..

Table QCS760.178B5-2

WIDTHS OF INTERASSEMBLY GAPS IN CORE REGION  
AND EX-CORE REGIONS

Locations	Gap Width, cm	
	BOC-1	EOC-4
<u>Core Regions</u>		
Between Non-Boiling Assemblies	0.41-0.51	0.22-0.48
Between Non-Boiling Fuel and IB Assemblies	0.42-0.49	0.24-0.49
Between IB Assemblies	0.43-0.48	0.26-0.50
<u>Ex-Core Regions</u>		
Below Core	0.48	0.48
Radial Blanket	0.45-0.48	0.35-0.48
Radial Shield	0.48	0.48

Table QCS760.178B5-3

VOLUMES AVAILABLE TO ACCOMMODATE FUEL IN  
PRIMARY AND SECONDARY CONTROL ASSEMBLIES

---

	<u>Primary</u>	<u>Secondary</u>	<u>Approximate Core Fuel Fraction<sup>1</sup></u>
Number of Assemblies	9	6	-
Volumes Below Core/LAB Inter- face to Flow Restriction <sup>2</sup> (liters)	50	29	0.11
Lower Inlet Modules (liters)	<u>292</u>	<u>-</u>	<u>0.42</u>
Total Volume Available <sup>3</sup> (liters)	342	35	0.53

---

NOTES:

1. Based on 6000 kg of fuel at 8.6 kg/l liquid density.
2. Flow restriction assumed to be orifice plates in PCA and low pressure vent outlet in SCA; see Figs. Q760.178B5-2, -3 for details.
3. Fuel loss through PCA lower inlet module to reactor inlet plenum not indicated here.



Table QCS760.178B5-4

REACTIVITY LEVELS FOR VARIOUS DISRUPTED  
CORE CONFIGURATIONS AT BOC-1

---

<u>Case</u>	<u>Description of Core Configuration</u>	<u>Reactivity (\$)</u>
1	43% of total fuel inventory removed from the core. The remaining fuel in the annular regions is homogenized in the core and fully compacted with IB and CR assemblies intact.	-1.4
2	Same as Case 1 except that only 33% of total fuel inventory is removed.	+10.2
3	41% of total inventory removed from core. The remaining fuel, the IB and CR (except B <sub>4</sub> C) assemblies are homogenized and fully compact.	-10.5

---

Table QCS760.178B5-5 POTENTIAL FOR LOSS OF FUEL INVENTORY PRIOR TO MELT-OUT OF INNER BLANKET ASSEMBLIES

	Location	% Driver Fuel Inventory			Power Level and Time Interval Between Melt-Out/Annular Pool Phase and Homogeneous Pool Phase**
		Upper Axial Blanket and Radial Blanket	Interassembly Gaps	Control Rod Assemblies	
B O C	Early* Fuel Removal	< 10% (1)  Based on Limited Opening in Clad Bkg.	> 40%  Rate of Removal is Fuel Melt Limited	≈ 10%	10 to 5 w/g Bkt. Pwr. Level Initial Temp. 1000°C (avg) Δθ ≈ 150 sec
- 1	Later* Fuel Removal	≈ 20% (1) No fuel Penetration into UAB - RB only	15% Based on BFM <sup>(2)</sup> and BOC Gaps	> 40% (3)	Time Interval Reduced by 1/4 Due to Driver Fuel Penetration into Bkt. Assembly Δθ ≈ 35 sec
E O C	Early* Fuel Removal	> 25%  Based on Exp. Data Limited Clad Bkg.	> 40%  Rate of Removal is Fuel Melt Limited	0% (4)	25 to 10 w/g Bkt. Pwr. Level Initial Temp. 2000°C (avg) Δθ ≈ 46 sec
- 4	Later* Fuel Removal	> 40% Based on BFM <sup>(2)</sup> in UAB (25%) Plus (20%) into RB	> 10% Based on BFM <sup>(2)</sup> and EOC Gaps	> 30% (5)	Time Interval Reduced by 1/2 Due to Driver Fuel Penetration into Bkt. Assembly Δθ ≈ 23 sec

\* Relative to the annular pool phase time interval.

\*\* Defined by loss of inner blanket fuel assemblies structural integrity.

QCS760.178B5-18

Amend. 72  
Oct. 1982

NOTES FOR TABLE QCS760.178B5-5

- (1) Percent removal refers to short time scale following early fuel disruption. UAB is expected to be opened by thermal attack before large homogeneous pool is formed.
- (2) BFM - Bulk freezing model. ORB - Outer Radial Blanket.
- (3) The basis for > 40% is (a) 10% inventory to fill control rod channel, (b) plus draining through control rods at  $\approx 1\%$  1 sec for as long as fuel supply lasts.
- (4) No credit is taken for control channel volumes in the best estimate. Best estimate emphasizes early fuel removal through interassembly gaps.
- (5) The basis for > 30% is (a) above and (b) draining through control rod channels at  $\approx 1\%$  1 sec for  $\sim 20$  secs.

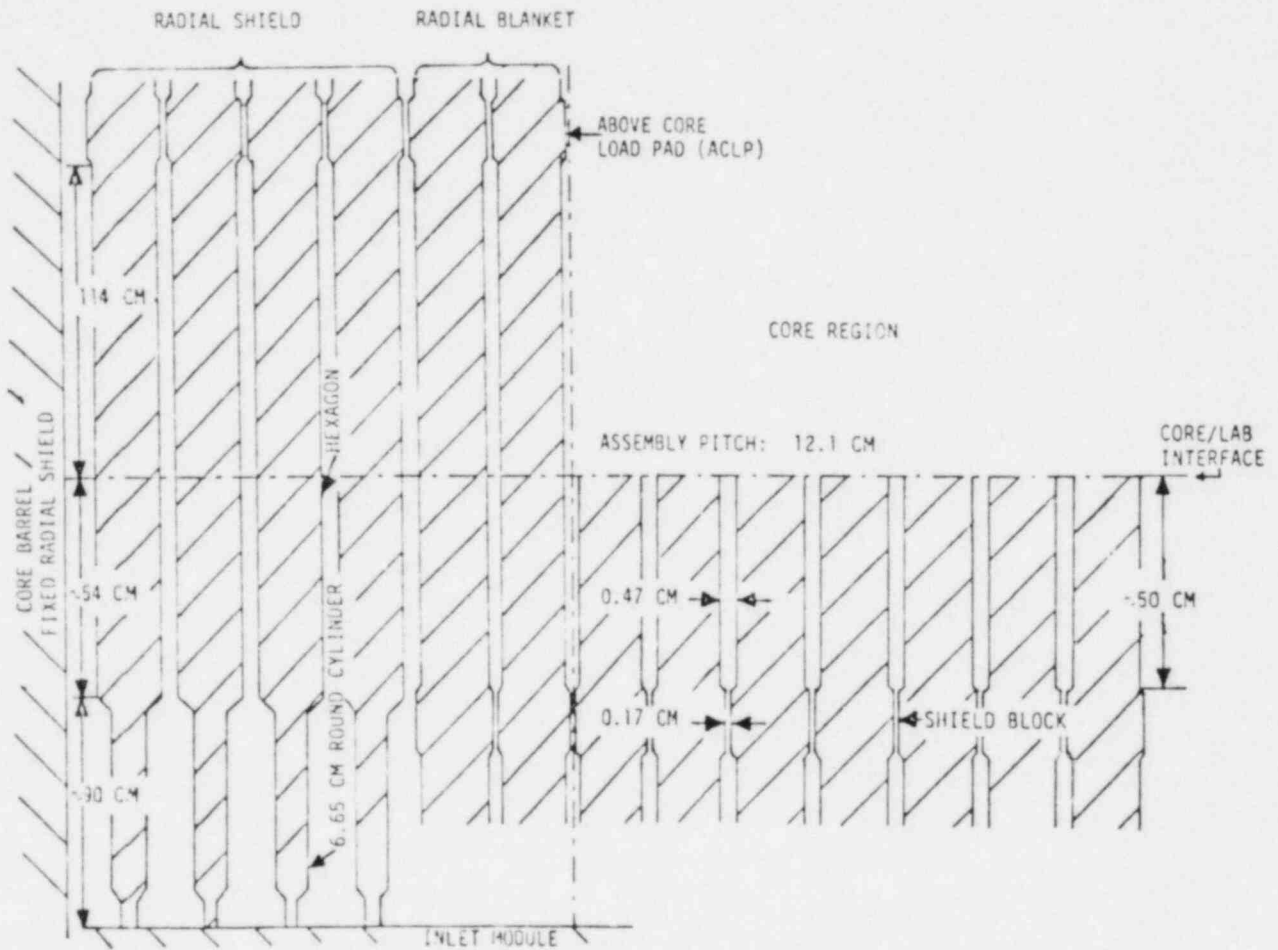


Fig. QCS760.178B5-1 Sketch Showing the Interstitial Gaps Outside and Below the Core Region.

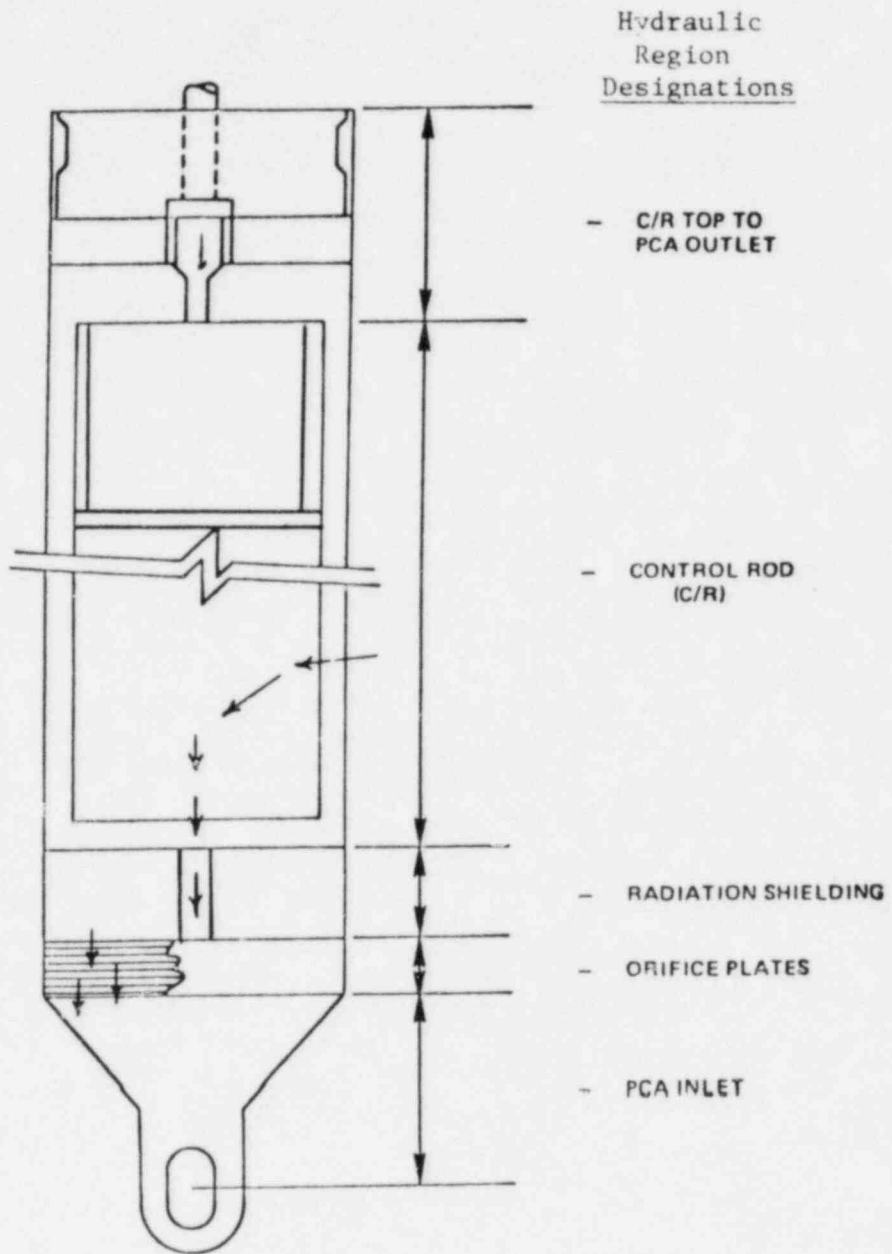


Fig. QCS760.178B5-2 Schematic of Primary Control Assembly.  
 → Indicates Fuel Flow Path.

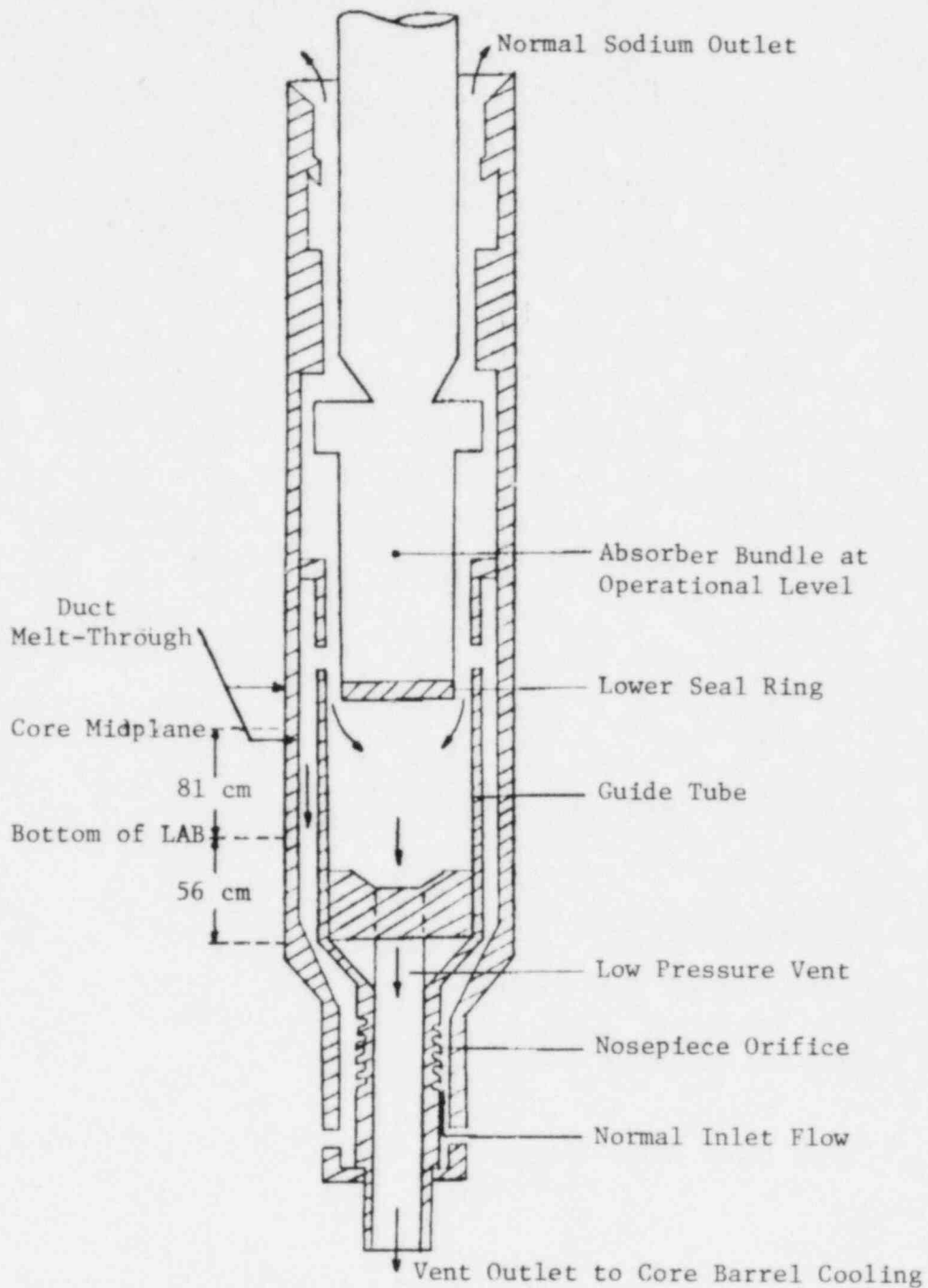
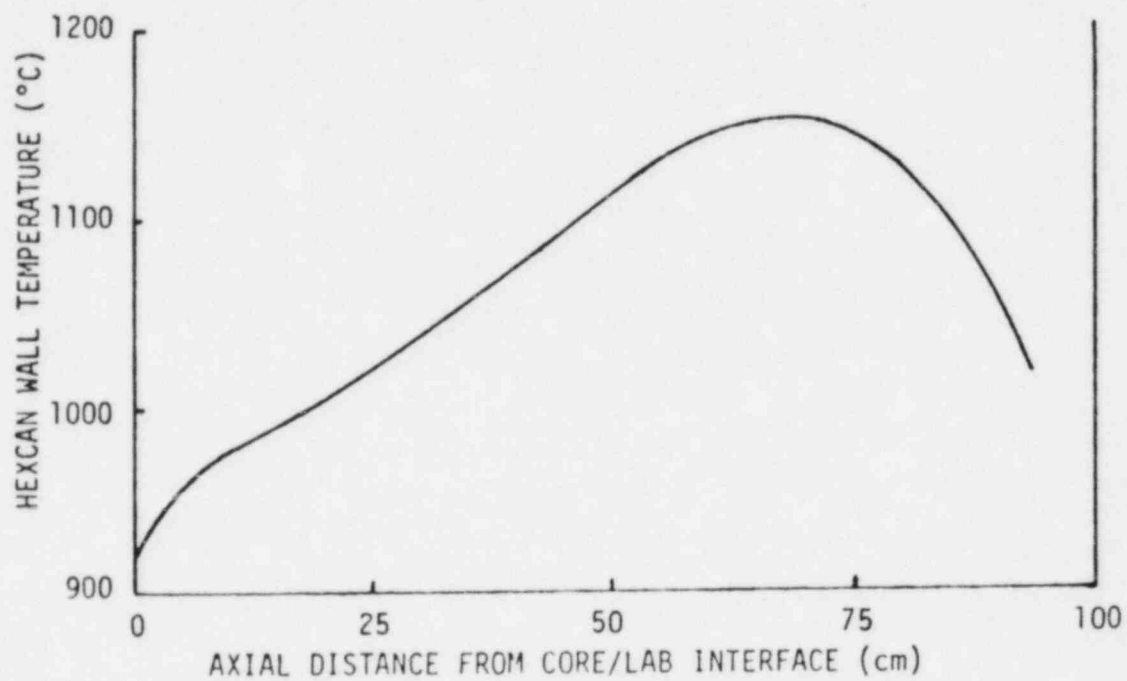


Fig. QCS760.178B5-3 Schematic of SCA Flow Paths for Fuel Removal (not to scale).



*Fig. QCS760.178B5-4 Typical Hexcan Wall Temperature Distribution at Initiation of Pool Boilup.*

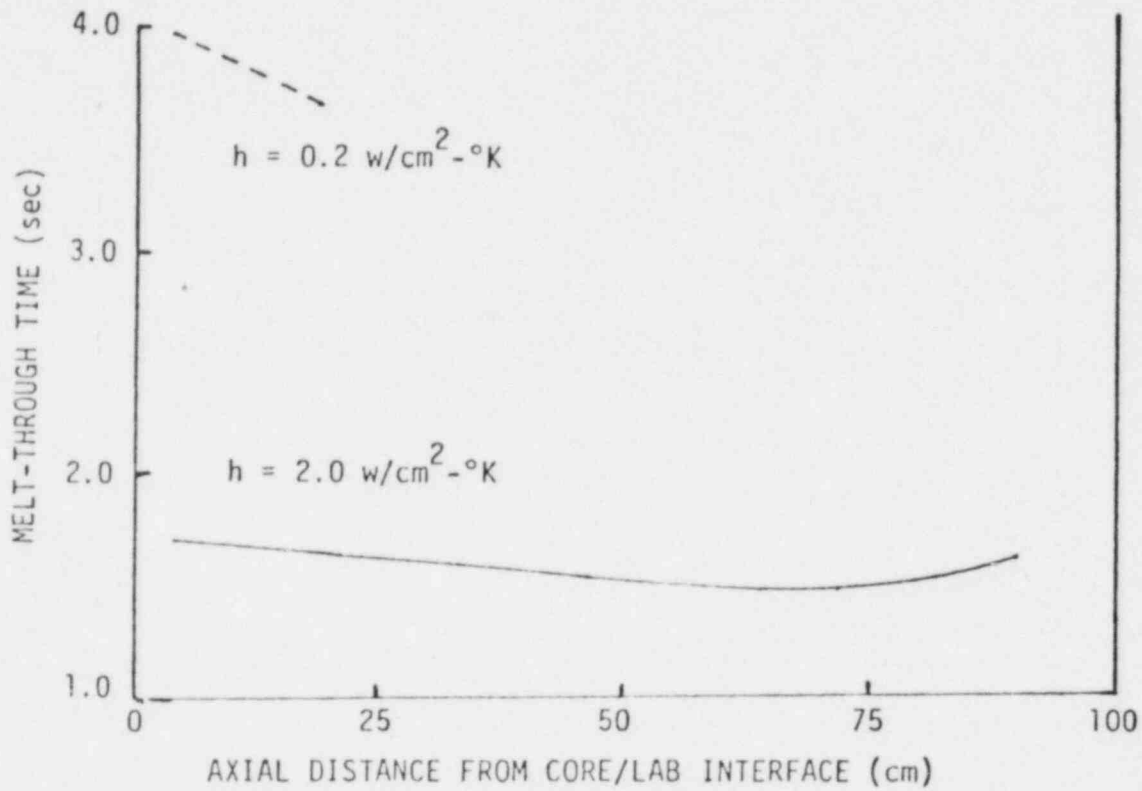


Fig. QCS760.178B5-5 Hexcan Wall Melt-Through Time Since Initiation of Pool Boilup. (Upper Dashed Curve Characteristic of 25 cm Quiescent Region. Lower Solid Curve Characteristic of Fully Boiled Up System).



Melt-Out of Inner Blanket Assemblies

The time required to melt out the inner blanket fuel assemblies is estimated from the following expression derived from an adiabatic energy equation:

$$\Delta\theta = \frac{(2800 - T_i) + \lambda/C}{\frac{FQ}{RC}} \quad (1)$$

where  $\Delta\theta$  is the time to melt in seconds,  $T_i$  is the initial blanket fuel temperature taken as the radial average at centerline or maximum conditions ( $^{\circ}\text{C}$ ),  $\lambda$  is the heat of fusion of fuel (278 j/g),  $C$  is the heat capacity of fuel (0.5 j/g  $^{\circ}\text{C}$ ),  $F$  is the fraction of nominal power for driver fuel,  $Q$  is the nominal power of driver fuel (150 w/g), and  $R$  is the ratio of driver fuel to blanket fuel.

For consideration of the melt-out phase the power level on the average will likely be bounded on the high side by 0.5 times nominal power which may be representative of a level sufficient to prevent recriticality by fuel dispersal in subassembly geometry and by  $\approx .1$  times nominal power representing the short time decay heat level. Thus  $F = .3$  is taken as an average over the MO/APP phase. Utilizing (1) above, the following table indicates the results for:

	<u>EOC-4</u>	<u>BOC-1</u>
F	.3	.3
Q/C	300 $^{\circ}\text{C/s}$	300 $^{\circ}\text{C/s}$
$\lambda/C$	556 $^{\circ}\text{C}$	556 $^{\circ}\text{C}$
$T_i$	2000 $^{\circ}\text{C}$	1000 $^{\circ}\text{C}$
R	3	10
$\Delta\theta$	46 sec	150 sec

Melt-through of the hexcan walls within the core region results in the flow of molten fuel into the gaps; it could also result in the flow of molten fuel into the internal blanket assemblies. Upon entering the blanket assemblies, the molten fuel will fill the voided space between blanket rods. Heat transfer from the molten fuel to the blanket rods will cause the temperature of the blanket material to begin to rise at a rate greater than the adiabatic rate. An estimate of the maximum temperature rise rate  $dT/d\theta$  within the blanket rods surrounded by molten fuel can be obtained by assuming that the

heat generated within the molten fuel is transmitted instantaneously to the blanket rods. This results in the expression

$$\frac{dT}{d\theta} = \frac{1 + \frac{\alpha}{1 - \alpha} R}{\frac{CR}{QF}} \quad (2)$$

where  $\alpha$  is the volume fraction of molten fuel ( $\alpha = 0.24$ ).

In deriving Eq. (2), the transport of the sensible and latent (phase change) energy of the fuel melt to the blanket pins has been neglected. This is permissible since the temperature relaxation time within the blanket rod is approximately 35 sec and there is about four times more blanket rod material than molten fuel by mass. For the EOC-4 core, the ratio  $[\alpha/(1 - \alpha)]R$  is  $\sim 1.0$ . Thus we conclude from Eq. (2) that fuel entering the internal blanket assemblies can decrease the time to involve the internal blankets by no more than a factor of two. For the BOC-1 core the ratio  $[\alpha/(1 - \alpha)]R$  is  $\approx 3$ . Correspondingly, the time to involve the internal blankets can decrease by no more than a factor of four.

Considerations of Recriticality Events in the  
MO/APP of the CRBR Heterogeneous Core

Recriticality events subsequent to the initiating phase can occur. The geometric and the heat sink aspects of the boundary walls of high surface to volume ratio can give rise to fuel density increase. It is noted that motion of cold fuel material can be shown not to initiate large ramp rates. Reactivity insertion from motion of cold fuel are limited to several cents/sub-assembly/sec. The following discussions focus on the hydrodynamic aspects limiting fluid dynamic sources of large ramp rate recriticality events.

Recriticalities may not be precluded, in particular, shortly after termination of the initiating phase. To address this concern, a recriticality scenario is developed for the BOC-1 core by making pessimistic assumptions: (a) dispersed fuel in the high-power fuel assemblies collapses following the initiating phase power burst, (Ref. B-1), and (b) at the same time fuel in the medium-power fuel assemblies experiences a drainage-type collapse. The reactivity insertion rate associated with fuel compaction, which is the main concern in this pessimistic scenario, is estimated below.

In the case of fuel collapse in the high-power assemblies, the dispersed fuel will settle down displacing the vapor. The collapse rate will be controlled by the rate of vapor separation to the region above the pool. Since the flow regime is expected to be liquid continuous toward the end of the collapse, the terminal rise velocity of vapor bubbles can be used as the rate of pool collapse as indicated in Ref. B-2. This terminal velocity in a fuel-dominant pool was calculated to be 23 cm/sec.

The high-power fuel was assumed to be uniformly dispersed prior to collapsing. The reactivity level of the core was first calculated based on these conditions to establish the reference initial reactivity level. Then, the reactivity due to collapse of the pool was calculated by lowering the pool height. It was assumed that the fuel in all the high-power assemblies (channels 9 and 11 in Ref. B-1) is collapsing simultaneously at the same rate. The results of this reactivity calculation produces a ramp rate of about 10\$ /sec.

Fuel in the medium-power assemblies (57) has disrupted and is assumed to be experiencing a drainage-type collapse at termination of the initiating phase analysis. This type of fuel collapse will result in a reactivity insertion at a rate of about 20¢/sec per assembly based on TREAT test data. Thus, the simultaneous fuel motion in the medium-power assemblies is expected to produce a ramp rate of about 10\$ /sec. Therefore, the total ramp rate due to pool collapse in the high-power assemblies and fuel drainage in the medium-power assemblies could be no greater than 20\$ /sec, which is below the range for which hydrodynamic disassembly of the core is expected\*. Thus, it is concluded that fuel compaction would simply expedite the accident progression

\*Less coherent behavior would correspondingly reduce the magnitude relative to these estimates.

by maintaining power between decay heat level and  $\approx .5$  times nominal leading to a permanent subcriticality without an energetic power burst. The response to mild recriticality events is now considered.

Early in time, in response to the power source, the molten fuel flows toward the axial ends of the subassembly in the form of two intact slugs. The liquid slugs are accelerated under the action of the expanding high pressure fuel and/or steel vapors at the center of the subassembly. The occurrence of fluid mechanical instabilities, however, will cause the low-density high pressure vapor region to penetrate and mix with the more dense accelerating slugs. At any location after the lower vapor-liquid fuel interface has passed, the heavier molten fuel is not completely expelled or replaced by the lighter vapor. A thick film of molten fuel will adhere to the subassembly wall while a tongue(s) or finger(s) of the vapor of reduced diameter advances through the center established by the portion of the fuel melt left behind. Moreover, atomization of the fuel film and the wave(s) or spike(s) produced at the lower (unstable) fuel interface will occur by direct action of the expanding vapor region. These processes result in the disintegration of most of the mass of the molten fuel and rapidly transform the postulated fuel slug into a two-phase annular-drop flow. The molten fuel and steel left behind in the form of entrained drops and liquid film in the axial midplane region results in the evaporation of the molten material in this region, the transport of the vapor along the length of the subassembly and the subsequent condensation of the vapor upon relatively cold fuel surface (drops and film) at the axial ends of the subassembly.

If the vapor flux is large enough to maintain the fluid-mechanical balance between interfacial drag and the mass of the fragmented fuel, the dispersed annular flow regime will endure and dominate the boiling process within the disrupted subassembly. On the other hand, suppose we assume that the vapor flux is continuously reduced until it falls below that required to maintain fuel-steel boiling. Clearly, then, the pool will contract and ultimately return to its collapsed configuration, passing successively through the annular drop, churning turbulent and bubbly flow regimes as the vapor flux is reduced. The pool collapse rate will be limited to the bubble rise velocity within the bubbly flow regime. This velocity is less than 30 cm/sec and is too low to produce anything but a mild recriticality. Thus the breakup of the accelerating fuel slugs within a single subassembly eliminates the possibility of severe fuel collapse rates and, therefore, eliminates the amplification of mild recriticalities into super prompt critical bursts.

The physical process that leads to the breakup of the accelerating fuel slugs is the well known Taylor instability (B-3). It has been shown by Taylor that a plane interface between two fluids of different densities in accelerated motion is unstable as long as the acceleration is directed from the lighter to the heavier fluid. The high pressure side of an accelerating fuel slug in a single subassembly is subject to breakup by means of this type of instability, since its motion is largely one dimensional. For simplicity, attention will be focused on a single accelerating fuel slug, as illustrated in Fig. B-1. The theoretical considerations that follow below are necessarily quite imprecise. It is understandable that phenomena so complex as finite-amplitude wave development cannot be analyzed accurately. These simple results constitute order-of-magnitude estimates. Moreover, the analysis does not take into account fuel vaporization or condensation at the liquid fuel

interface or the deposition of molten material on the subassembly walls, which certainly will modify the results quantitatively (see below).

The Taylor instability has been observed under a wide variety of experimental conditions, and the initial phase of the instability has been found to agree well with linearized wave theory. The experimental results may be interpreted roughly as showing that the instability follows the first-order theory during the time

$$\tau = \sqrt{\lambda/a} \quad (1)$$

where  $\lambda$  is the wavelength of the disturbance and "a" is the acceleration of the liquid slug. Typically, under reactor accident conditions,  $\tau = 10$  msec. It therefore appears that the initial development of the instability is of little interest. The succeeding stages of the instability consist of rounded columns of gas or vapor penetrating steadily through the liquid with little change of profile (see Fig. B-1) until the opposite surface of the liquid slug is reached causing the slug to burst. In spite of the presence of these gas columns, the main body of the liquid slug is accelerated as though they did not exist. The gas columns penetrating into the accelerating slug have been found to move relative to the liquid at a constant velocity  $v$  given by

$$v = \sqrt{ad} \quad (2)$$

where  $d$  is the diameter of the penetrating gas column. Thus the penetration distance  $s$  of the column into the slug (Fig. B-1) after time  $t$  is given approximately by

$$s = \sqrt{ad \cdot t} \quad (3)$$

Clearly, the distance  $z$  travelled by the liquid fuel slug during this time is

$$z = \frac{1}{2} at^2 \quad (4)$$

Eliminating  $t$  between Eqs. (3) and (4) yields an expression for the column penetration distance in terms of  $z$ :

$$s = \sqrt{2zd} \quad (5)$$

Equation (5) has a very simple interpretation as a fuel slug breakup criterion. It predicts that only the diameter of the gas columns and the instantaneous location of the accelerating fuel slug influence the breakup of the slug, which should occur when  $s$  equals the axial thickness of the fuel slug. To complete the application of Eq. (5) to an accelerating fuel slug in a reactor subassembly, one need only estimate the diameter of the fuel (or steel) vapor columns. Here we must rely on experimental observations. Photographs of the process indicate a progressive change early in the acceleration transient from a number of surface waves and troughs to a much smaller number of troughs until only one or two round-ended columns of gas remain and penetrate the liquid slug. Thus taking  $d$  to be of the order of the radius of the subassembly duct ( $d \approx 5$  cm) we find from Eq. (5) that columns of core vapor will penetrate approximately 22 cm into the fuel slug after the

slug has traversed one-half of the active core length ( $z \sim 50$  cm), as compared with the slug depth which is typically between 10 and 20 cm.

It should be mentioned that Fig. B-1 falls far short of describing the later stages of development of the Taylor instability. The penetrating gas (vapor) columns compete with one another, the large ones growing at the expense of the small ones. A large quantity of liquid is left adhering to the sides of the channel (subassembly), with the result that the vapor penetrates through the fuel slug at a faster rate than that given by Eq. (2). The vapor-liquid regions on the sides of the spikes (or film) and vapor columns are in relative motion which produces additional surface instability of the Helmholtz type. In particular, the final stage of mixing between liquid fuel and vapor is too complex for detailed description. The important point to be made here, however, is that it is apparent from the preceding discussion that conditions conducive to the breakup of accelerating fuel slugs in subassembly geometry exist following a power burst.

The obvious question of concern is how large can a fuel pool be before its response to a power or pressure source is dominated by radial motion of the liquid fuel rather than one-dimensional expansion as previously discussed. Our focus here is to attempt to identify the threshold pool size above which purely dynamic fuel motion is possible.

Let us consider a spherical cavity of instantaneous radius  $R$  containing fuel or steel vapor at high pressure suddenly formed as a result of a power burst along the axial centerline of a cylindrical pool of molten fuel of diameter  $D$  and instantaneous height  $H$  (see Fig. B-2). The initial height of the pool is designated by  $H_0$ . The constancy of molten fuel volume within the pool requires that

$$\frac{1}{4} D^2 H_0 = \frac{1}{4} D^2 H - \frac{4}{3} R^3 \quad (6)$$

Differentiating this expression twice with respect to time gives the following relation between the instantaneous acceleration of the bubble interface and that of the surface of the pool:

$$\frac{1}{4} D^2 \frac{d^2 H}{dt^2} = 4R \left[ R \frac{d^2 R}{dt^2} + 2 \left( \frac{dR}{dt} \right)^2 \right] \quad (7)$$

The initial phase of the bubble growth and pool expansion is controlled by the inertia of the liquid that completely surrounds the bubble. The bubble is blown up according to the Rayleigh equation for radial motion

$$R \frac{d^2 R}{dt^2} + 2 \left( \frac{dR}{dt} \right)^2 = \frac{P - P_\infty}{\rho} \quad (8)$$

where  $P$  is the pressure within the fuel vapor bubble,  $P_\infty$  is the ambient pressure above the fuel pool and  $\rho$  is the density of the molten fuel. Equation (8) is an approximate form of the Rayleigh equation which gives reasonable solutions for inertia-controlled bubble growth. Strictly speaking, the

coefficient of the second term in Eq. (8) should be 3/2. Eliminating the radial acceleration terms between Eqs. (7) and (8) yields

$$\frac{D^2 \rho}{16R} \frac{d^2 H}{dt^2} \approx P - P_\infty \quad (9)$$

Equation (9) simply expresses the law of motion governing the expansion of the fuel pool when the motion within the pool is three dimensional and little mixing occurs between the expanding vapor cavity and the surrounding molten fuel. While the early expansion is essentially radial, ultimately the growing fuel cavity will "feel" the presence of the vertical wall that contains the pool. The pressure will tend to become uniform across the width of the pool (within the vapor space) and the pool expansion may then be adequately treated as one dimensional. During this period the pool growth is well represented by

$$\rho L \frac{d^2 H}{dt^2} \approx P - P_\infty \quad (10)$$

where L is approximately the initial depth of the bubble center (assumed stationary in time) below the surface of the pool, or, equivalently, the thickness of the fuel slug that is accelerated upward during the one dimensional expansion phase.

For the one dimensional expansion, the appropriate liquid inertia is proportional to the mass of the liquid above the bubble center, or  $\rho L$ . The effective liquid inertia for the early spherical expansion follows from Eq. (9) and is  $D^2 \rho / 16R$ . It is reasonable to suppose that the pool expansion is dominated by one dimensional fuel flow when the "one dimensional inertia" becomes somewhat greater than the "spherical inertia", i.e., when  $\rho L > D^2 \rho / 16R$ , or

$$R > \frac{D^2}{16L} \quad (11)$$

As a numerical example, suppose we consider fuel-pool motion following a power burst at  $L = 25$  cm below the surface of, say, a 50 cm deep pool. The pool is assumed to be about two subassemblies in cross-sectional area, or  $D \approx 20$  cm. Owing to the discrete control subassembly and blanket assembly array within a heterogeneous core, this value of D corresponds to about the largest radially unimpeded region of molten fuel that can form during the MO/APP within the CRBRP. From criterion (11), we calculate that when the radius of the power burst bubble is of the order  $R \approx 2$  cm the pool expansion becomes one dimensional. It is of interest to note that during the spherical growth period we calculate using Eq. (6) that the pool surface rises only 0.1 cm. Thus, for all practical purposes, the pool response to a power burst is one dimensional and subject to the instabilities discussed previously for a single subassembly. The fuel-steel boiling process within a disrupted heterogeneous core should therefore be stable to mild recriticalities.

References for Appendix B to QCS760.178B5-C6, C7

- B-1 S. K. Rhow, et al., "An Assessment of HCDA Energetics in the CRBRP Heterogeneous Reactor Core," CRBRP-GEFR-00523, General Electric Company, December 1981.
- B-2 T. G. Theofanous, "Multiphase Transients with Coolant and Core Materials in LMFBR Core Disruptive Accident Energetics Evaluation," NUREG/CR-0224, Purdue University, July 1978.
- B-3 G. I. Taylor, Proc. Roy. Soc., London, A201, p. 192, 1950.



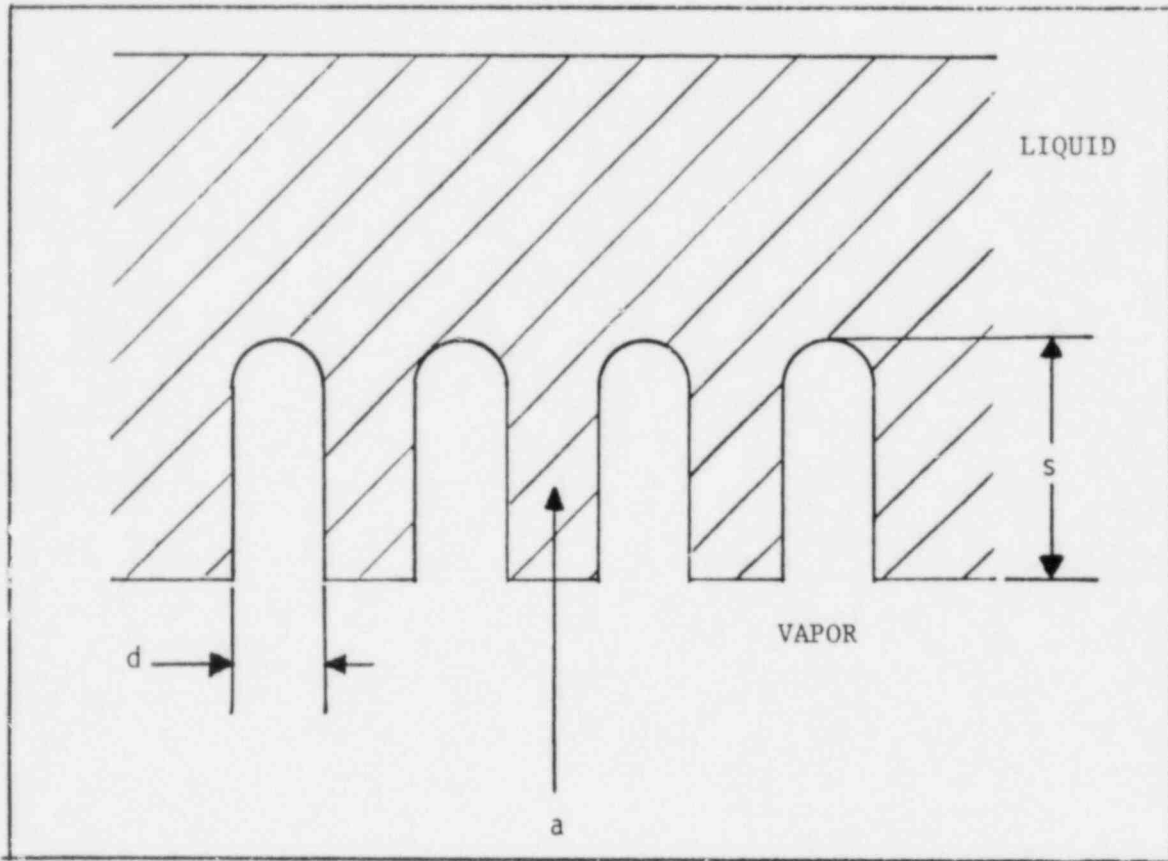


*Fig. B-1 Schematic Illustration of Accelerating Fuel Slug.*

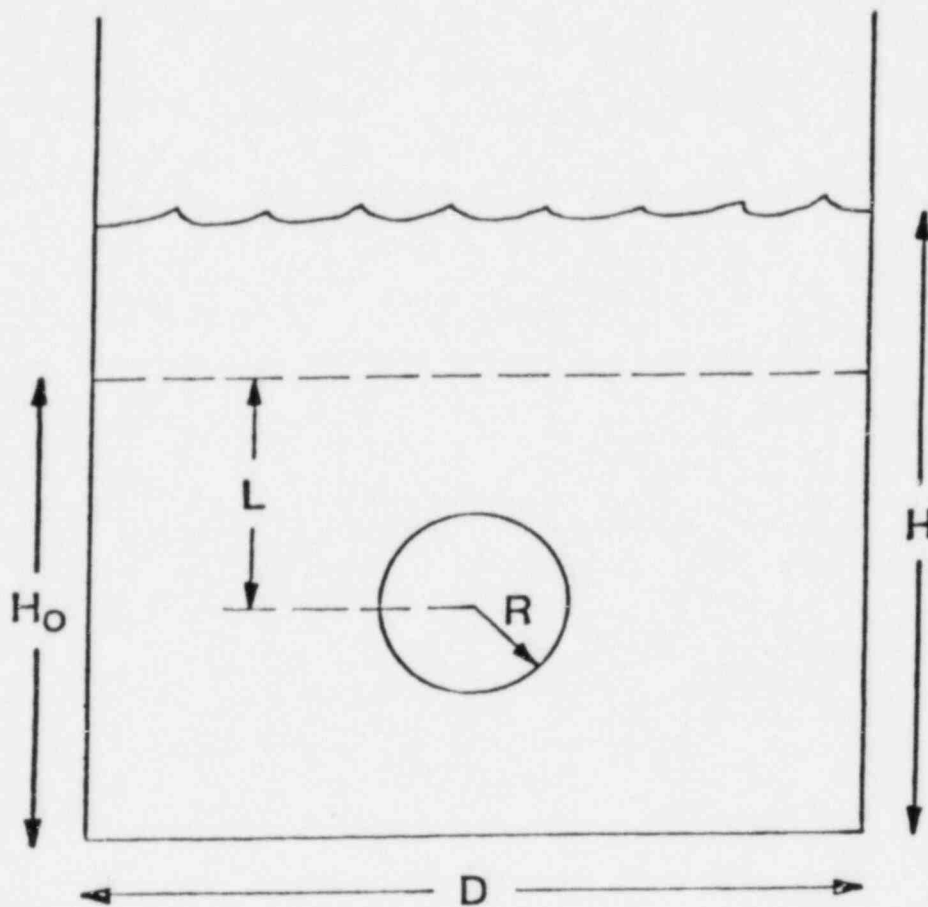


Fig. B-2 Pool Geometry with "Initial Bubble".

APPENDIX C TO: Question CS760.178B5, -C6, -C7

Reactivity Calculations for Various Configurations of Disrupted BOC-1 Core

This appendix documents neutronics calculations which were performed to evaluate reactivity levels for the disrupted core configurations at BOC-1.

The primary objective throughout this neutronics analysis has been to retain as much rigor in the computational modeling as possible while retaining efficient computations. For significantly disrupted core configurations, as are encountered in the melt-out and large-scale pool phase analysis, the presence of large internal voids makes the use of diffusion theory suspect. In order to adequately handle the complex streaming associated with large internal voids S-4 transport theory with isotropic scattering was selected as the computational mode. The use of S-4 transport theory in RZ geometry will adequately handle the isolated blanket islands and control rods while giving the benefit of a rigorous treatment of the internal voids.

The basic cross-section data used for the neutronics<sub>2</sub> analysis were generated from the ENDF/B-IV data files (Ref. C-1). The MC<sup>2</sup>-SDX (Refs. C-2 and C-3) code package was used to process these data. A base library of 171-groups ( $\Delta u = 0.1$ ) was generated using a weighting spectrum from a 2040-group slowing down calculation for an appropriate Pu/U fueled LMFBR core composition (Ref. C-4). Special care was taken in generating <sup>238</sup>U blanket cross-sections. A blanket fine-group library was obtained using the core leakage as an external source for the blanket slowing down problem. Using the combined fine-group base library, broad group libraries were generated with the SDX code. Resonance self-shielding effects were accounted for in voided and non-voided driver, internal blanket, and radial blanket assemblies. An eight group and a twenty group library were obtained for operating conditions (1500°K) and for an elevated temperature (3000°K). Table C-1 shows both group structures. The reference CRBRP design and BOC-1 masses are taken from the CRBRP PSAR and are given in Table C-2. Corresponding to the best-estimate core conditions at termination of initiating phase analysis, a full RZ model for the BOC-1 core was constructed as shown in Fig. C-1. This model represents the base case for disrupted core neutronics calculations.

Three disrupted core configurations were analyzed. In all cases, one-third of the cladding and wire wrap in all fuel assemblies is assumed to relocate into the UAB region. Another one-third of the cladding and wirewrap is relocated into the LAB region. The remaining residual steel including the hexcan walls is assumed to be homogenized with the molten fuel.

Conditions of the core are assumed to be as described in the main text, (Table QCS760.178B5-4) and the fuel removed from the core is assumed to be distributed as follows: 11% in the below-core region, 6% in the radial blanket region, and the remaining fuel removal in the radial shield region. In Case 3 where a core-wide pool is formed with control assemblies available for fuel removal, an additional 8% of the total fuel is assumed to be relocated into the control assemblies.

The results of Cases 1, 2, and 3 appear in Table QCS760.178B5-4 in the main response.

References for Appendix C to QCS760.178B5, -C6, -C7

- C-1 ENDF/B Summary Documentation, BNL-NCS-17541 (ENDF 201), 2nd Edition (ENDF/B-IV), compiled by D. Garber, available from National Nuclear Data Center, Brookhaven National Laboratory, Upton, New York, October 1975.
- C-2 H. Henryson, II, et al., "Mc<sup>2</sup>-2: A Code to Calculate Fast Neutron Spectra and Multigroup Cross Sections," Argonne National Laboratory, ANL-8144, June 1976.
- C-3 B. J. Toppel, et al., "ETEO-2/MC-2/SDX Multigroup Cross Sections, March 14-16, 1978 Radiation Shielding Information Center, Oak Ridge, Tennessee.
- C-4 C. E. Till, et al., "Fast Breeder Reactor Studies," Argonne National Laboratory, ANL-80-40, July 1980.

Table C-1  
 GROUP STRUCTURE FOR 8 AND 20 GROUP  
 CROSS SECTION LIBRARIES

<u>Broad Group Energy, ev</u>	<u>20 Group Library</u>	<u>8 Group Library</u>
$1.0000 \times 10^7$	1	1
$3.6788 \times 10^6$	2	
$2.2313 \times 10^6$	3	
$1.3534 \times 10^6$	4	2
$8.2085 \times 10^5$	5	
$4.9787 \times 10^5$	6	3
$3.0197 \times 10^5$	7	
$1.8316 \times 10^5$	8	4
$1.1109 \times 10^5$	9	
$6.7380 \times 10^4$	10	5
$4.0868 \times 10^4$	11	
$2.4788 \times 10^4$	12	6
$1.5034 \times 10^4$	13	
$9.1188 \times 10^3$	14	7
$5.5309 \times 10^3$	15	
$3.3546 \times 10^3$	16	8
$2.0347 \times 10^3$	17	
$1.2341 \times 10^3$	18	
$4.5400 \times 10^2$	19	
$6.1442 \times 10^1$	20	

Table C-2

## HEAVY METAL\* MASS INVENTORY (kg) FOR CRBRP BOC-1

<u>Fission Produces</u>	<u>Driver</u>	<u>Inner Blankets**</u>	<u>Radial Blanket**</u>	<u>Axial Blankets</u>
239 <sub>Pu</sub>	1468.0			
240 <sub>Pu</sub>	199.7			
241 <sub>Pu</sub>	34.0			
242 <sub>Pu</sub>	3.4			
235 <sub>U</sub>	7.6	16.7	26.9	8.6
238 <sub>U</sub>	3476.0	8253.0	13285.0	4216.0
Fission Products	-	-		
Total Heavy Metal	5188.7	8269.7	13311.9	4224.6

\* Heavy metal excludes oxygen.

\*\* Includes axial extensions.

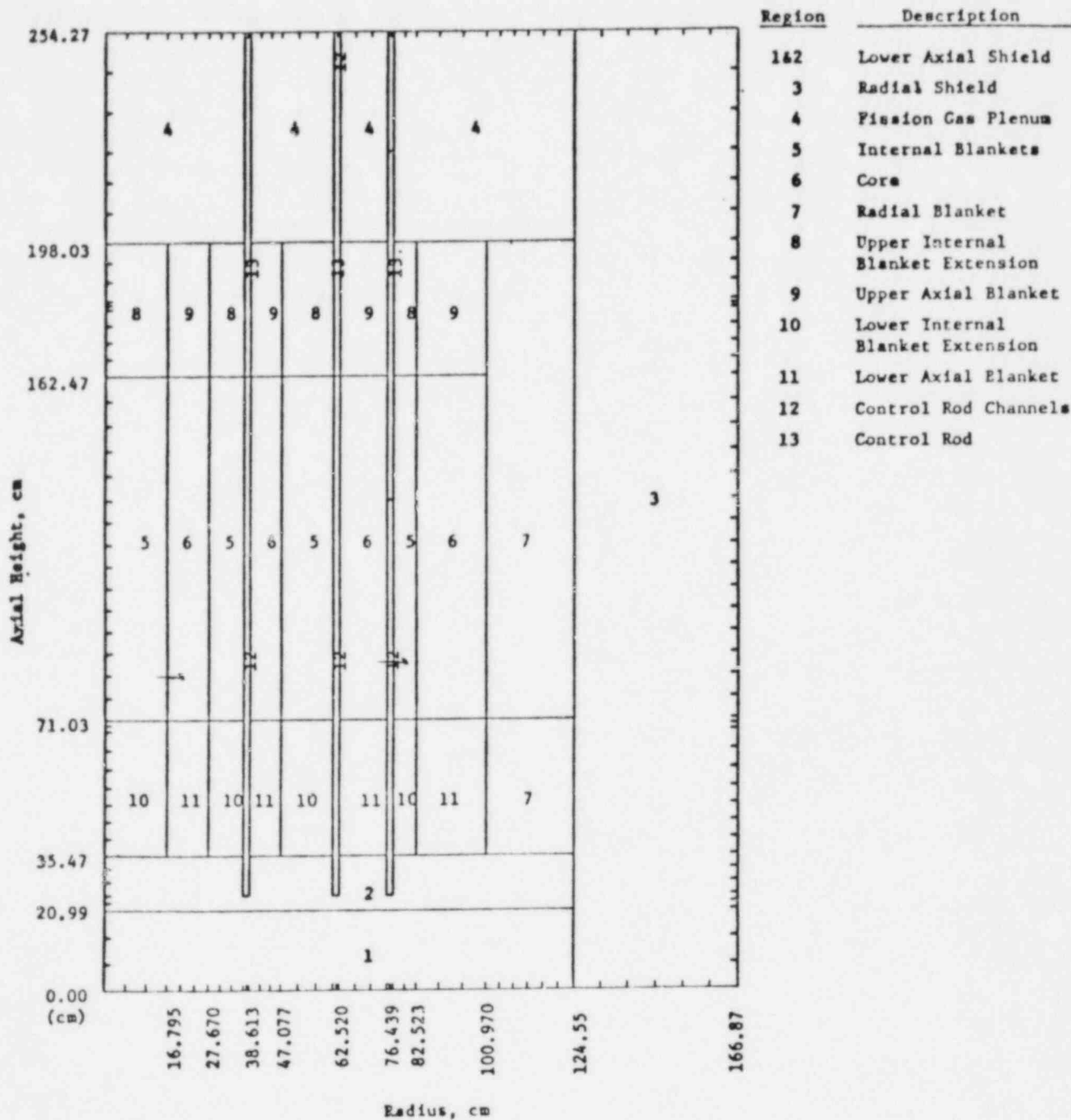


Fig. C-1 CRBRP BOC-1 Melt-Out Phase Base Case.

Freezing Mechanisms

In Ref. D-1, a conduction-limited freezing model was determined to be most appropriate in analyzing fuel flow behavior in gaps or small tubes. Since there has been a concern over applicability of the freezing model in the presence of steel melt layers under fuel crusts and in the case of two-phase mixtures flowing in the gap, this concern is addressed in this Appendix. Again, it is concluded that the conduction-limited freezing model is applicable even when steel melting occurs under the fuel crust, and the gap flow is a two-phase mixture.

Penetration and Freezing of Flow in Melting Channels

When fuel penetration commences between the hottest assembly can walls exceeding  $\sim 800^{\circ}\text{C}$ , the molten fuel-steel hexcan interface temperature will fall between the fusion temperatures for these materials upon contact, resulting in solidification in the molten fuel and melting of the underlying hexcan (gap) wall.<sup>12</sup> Even for sufficiently low initial hexcan temperatures such that melting of the steel hexcan does not begin upon contact with the fuel, steel melting may begin after convective heating from the molten fuel stream raises the fuel crust-solid steel interface temperature to the steel melting temperature. This is likely to occur at locations where the fuel temperature is  $\sim 100^{\circ}\text{C}$  or more above its melting temperature, that is in regions of the core where the fuel first enters the gaps (entrance region).

The concern with the existence of steel melt layers is that they may cause the protective fuel crust to become unstable leading to rapid fuel freezing by bulk solidification (Ref. D-2) or steel freeze plugs as a result of rapid mixing between fuel and steel (Ref. D-3), as have been postulated for thermite fuel penetration into rod bundle geometry\*. It is important to note that the observed behavior of a growing freeze layer on a melting (or fluid) surface does not support the aforementioned mechanisms for rapid freezing in simple flow geometries. The formation of stable, growing freeze layers on the surface of turbulent flows by radiative and convective heat loss to the surrounding atmosphere is quite common. This situation is most prominent in rivers and lava flows. Here stable crust covers are formed under conditions in which the "underlying" fluid is air. In fact, a stream of molten  $\text{UO}_2$  flowing over the lip of a tungsten crucible into a helium atmosphere was observed to form a tube of solid  $\text{UO}_2$  through which the remaining  $\text{UO}_2$  was forced to flow (Ref. D-4). Thus, flowing fuel will ignore the presence of the surrounding steel melt and grow its own channel wall (similar to the lava pipes familiar to the geologist (Ref. D-5). This conclusion also is confirmed by an experimental study in which hot Freon 112A (melting point  $40^{\circ}\text{C}$ ) was injected into a thick-walled ice pipe maintained as its melting temperature throughout (Ref. D-6). While the major emphasis in this study was on the melting attack of the ice pipe wall by very hot turbulent flowing Freon,

\* To date, no experiment has been performed that gives direct evidence of bulk solidification.



Follow-up studies (Ref. D-7) at low Freon injection temperatures show the continuous conduction-limited buildup of a stable Freon layer on the melted ice wall until the pipe is closed to the Freon flow by the solidified layer.

Regarding the problem of mixing between flowing fuel and melted steel in regions where the gap wall may be subject to severe ablation by the fuel flow, it is pertinent to note that ice pipe ablation experiments show no appreciable mixing between the hot pipe flow (Freon) and the melted ice (Refs. D-5, D-7). In some experiments performed at very high Freon flow velocities (Ref. D-6), in the range 7.0 - 17.0 m/s, some of the melted ice in the form of water droplets was entrained by the bulk Freon flow. However, the volume fraction of entrained water was low and the process did not lead to a flow blockage by bulk solidification and/or freezing of the water component. In the ice pipe experiments reported in Ref. D-8, the water film produced along the melting ice pipe wall was found not to be entrained, despite Freon flow Reynolds numbers and velocities as high as 53,000 and 3.0 m/s, respectively. Thus, contrary to the steel-fuel mixing postulated for thermite fuel injected axially into rod bundle configurations, it would appear that very little mixing would take place between fuel and melted steel within the simple gap geometry.

Recently, measurements of the penetration of  $UO_2$  into a thick-walled steel tube have been reported (Refs. D-9, D-10). We present below in some detail a discussion of this so-called TRAN series of in-pile experiments since it represents one of the few series of experiments carried out with pure  $UO_2$  melts (including the conditions of steel wall melting upon contact with fuel) and since there seems to be some confusion in the literature regarding the interpretation of the experiments (Refs. D-9, D-10).

In the TRAN series of in-pile experiments, pure  $UO_2$  is melted using neutronic heating in the Annular Core Research Reactor at Sandia. The  $UO_2$  melt is then accelerated upward into a 130-cm long, steel freezing tube with a 0.32-cm diameter channel by the application of high pressure helium gas to the base of the fuel. Four such experiments have been performed to date, with the injection pressure held approximately constant at 1.0 MPa, the initial steel temperature varied from 400 to 900°C, and the initial fuel temperature varied from 2900 to 3500°C (Ref. D-11). Post-test analysis of cross sections of the tube indicated that melting of the steel wall occurred in the test where the initial steel temperature was 900°C. In all the experiments, the observed final fuel distribution consists of a frozen fuel layer that covers the inside surface of the tube and fuel debris located above the end of the fuel layer (Ref. D-11). The length of the fuel layer varies between 48 and 87 cm, depending on the amount of fuel injected into the tube during any given test (see below). In one experiment, a complete fuel blockage ~ 2 cm long was observed between the fuel debris region and the end of the frozen layer.

A plausible explanation for the existence of the frozen fuel layer, as opposed to a long fuel plug that fills the tube cross section is that when the fuel melt is forced upward into the cold tube the ensuing fuel penetration and freezing process is influenced by the rapid formation of an annular fuel film-helium gas flow. That annular flow is likely due to the limited quantity of fuel material that enters the tube. A possible explanation for the presence of loose fuel debris and, in one test, a short blockage beyond the frozen fuel layer is that in annular flow the gas (helium) core usually

contains a significant number of entrained droplets (fuel) or suspended liquid slugs which can be carried upward by the gas flow to the "clean" tube wall above the fuel layer. While the observed fuel penetration distance is postulated to be due to the limited quantity of fuel material employed, the frozen fuel-layer configuration is demonstrated below to be compatible with the simple conduction-limited freezing mechanism.

In the TRAN tests, about 40 g of  $UO_2$  was rapidly melted; however, only about 20 g of  $UO_2$  entered the freezing tube (Ref. D-11). Vortex motion in the fuel sample may have been responsible for the reduced amount of fuel forced upward into the tube. Whatever the mechanism responsible for the limited quantity of fuel injected into the tube, one could reason as follows: the melt first enters the tube as an all liquid advancing flow, with the only gas-melt interface present being that at the flow front. After the  $\sim 20$  g of fuel melt inventory enters the tube, the flow pattern instantaneously changes into a slug flow in which a single fuel slug (or column) now occupies  $\sim 25$  cm of the tube, followed by the high pressure helium gas. The lower helium gas-fuel interface that must now appear at the tube inlet is highly unstable such that a long finger or bubble of the less dense helium gas penetrates the  $UO_2$  melt slug. That is, at any location after the helium gas-fuel (lower) interface has passed, the heavier molten  $UO_2$  is not completely expelled or replaced by the lighter helium gas. A film of molten  $UO_2$  will adhere to the tube wall while a tongue or finger of the helium gas of reduced diameter advances through the tube core established by the portion of the fuel melt left behind. The helium gas finger should penetrate steadily through the fuel slug with little change in profile until the upper fuel-gas interface or flow front is approached causing the fuel slug, now greatly diminished in size, to burst. The bursting of the slug could result in the "throwing" of some of the melt material above the region occupied by the fuel film, which would explain the presence of loose fuel debris and small blockages beyond the end of the frozen fuel layer. Alternatively, portions of the fuel film may be entrained by the helium gas flow and redeposited on the tube wall downstream of the fuel layer.

There is much direct evidence for the transient slug annular flow transition described in the foregoing. In boiling experiments reported in Ref. D-12, a rapid depressurization technique was used to initiate vapor growth in superheated liquid Freon-113 within a tube. The vapor bubble so formed was observed to act like a piston, pushing the liquid slug out of the tube as it expands, but leaving behind a residual liquid Freon film on the tube wall. In a series of experiments reported in Ref. D-13, air was used to accelerate water or water to accelerate mercury through a tube. Interface displacement measurements clearly indicated that a film of the heavier fluid was left behind after the interface had passed. The explanation for the more dense fluid being left behind is rather straightforward: given an initial tendency for a residual liquid film of the more dense fluid to be left behind in such slug flow processes, this tendency is enhanced by the effect of the pressure gradient acting over the fluids of unequal density (Ref. D-13). The less dense driving fluid is accelerated more rapidly than the more dense displaced fluid. This explanation is the familiar Taylor (Ref. D-14) description of the instability of a bump (or wave) of small amplitude at an interface between a heavy fluid and a light fluid when accelerated in the direction of the heavy fluid. The simple Taylor theory suggests that molten  $UO_2$  fuel and helium gas

in the TRAN tests cannot be separated by a stable interface. The experiments described above (Refs. D-11,D-12) indicate that transient fuel penetration in the Sandia freezing tests is best characterized by a fuel-film annular flow pattern.

With regard to the problem of fuel film survival after the gas source is depleted, we note here that there is more than sufficient time to freeze the film in place by conduction before any significant film drainage can take place. In the TRAN series of experiments the thickness of the frozen fuel layer was observed to be between 0.015 and 0.03 cm. Depending on the film thickness and the initial fuel temperature, which was in the range 2900 - 3500°C, we estimate using conduction-freezing theory (Ref. D-15) that the time required to freeze the film is between  $\sim 10$  ms and  $\sim 100$  ms. Assuming laminar fuel-film flow we calculate a loss of less than 10% of the fuel material due to film drainage before freezing.

In summary, it appears highly likely that the final fuel distribution in the Sandia TRAN freezing tests can be attributed to the limited quantity of fuel employed. The "driving" helium gas displaced and penetrated the fuel melt, causing the rapid formation of an annular fuel film helium gas flow pattern. Furthermore, we expect that the fuel film is frozen in place by conduction-limited solidification; that is, the TRAN tests provided strong evidence for conduction-limited fuel crust growth into an annular two-phase fuel flow in the presence of both solid and melted steel backings. Had an unlimited quantity of fuel been available for injection into the freeze tube, we predict from Ref. D-16 a fuel penetration length of at least 250 cm.

#### Penetration and Freezing of Two-Phase (Fuel-Gas) Mixtures

The flowing core debris during the melt-out phase of the accident sequence is a two-phase gas (or vapor)-fuel melt mixture. Also, the core debris that enters into the gaps between assemblies may contain some amount of molten steel and solid fuel particulate. The presence of molten steel and solid fuel in large quantities will accelerate the freezing rate and increase the frictional resistance that retards the fuel flow, respectively, both of which will tend to reduce the fuel penetration distance into the gaps. Fortunately, only small quantities of these materials are expected to be carried from the disrupted assemblies into the gaps by the escaping fuel.

The source of solid fuel particulate is the unmelted portions of the fuel pellets. The unmelted fuel represents at most about 20% of the total fuel within a disrupted assembly. A large fraction of this solid material ( $\approx 15\%$  volume fraction of total fuel) is located at the bottom of the assembly, away from any potential fuel escape opening in the hexcan wall, and is likely to remain at the bottom owing to its large density compared with that of molten fuel. The remaining unmelted fuel, which is located at the top of the assembly, would be carried with the fuel flow into the gaps. However, since this solid material represents less than approximately 5% volume fraction of fuel and is continuously being eroded by melting, the solid fuel debris that enters the pool from above will not retard the fuel flow in any significant way.

As with solid fuel particulate, very little molten steel is anticipated to be mixed with the molten fuel within a disrupted assembly. The time interval between the complete melting of cladding and that of fuel is such that most of the cladding is moved out of the core region under the influence of both sodium vapor streaming and gravity. Thus, the melting fuel begins to lose its geometry when only a small portion of molten cladding ( $\sim 10\%$ ) is still present in the heated fuel region. Molten steel will also form at the boundaries of the disrupted assemblies. However, unlike the residual cladding films which are "trapped" within the melting rod bundle matrix, the melt films that clings to the hexcan wall are likely to be stable and not entrained by the disrupted fuel. The evidence in support of this conclusion is provided by the observations (mentioned in the foregoing) of stable melt-film behavior in highly turbulent channel flows with an without crust formation (Refs. D-6, D-8).

The molten fuel will move out of the core as a two-phase gas-fuel melt flow. Thus, prediction of the fuel penetration length will depend on our ability to predict (a) the pressure gradient associated with the penetrating flow of the two-phase mixture and (b) the rate of fuel crust buildup in the two-phase mixture. Methods for handling item (a) above are well established and have been reported in numerous papers on two-phase flow. A careful examination of the literature has shown that relatively few papers have dealt with item (b). However, on physical grounds, one would expect the solidification rate of a two-phase mixture to be equal to or less than that of its pure liquid component. In fact, since the rate of deposition of liquid material in a turbulent two-phase flow always exceeds the rate of phase conversion at the channel wall, one would expect the solidification rates to be the same in both cases. Interestingly enough, some experimental work has been reported by Greene, et al., Refs. D-17 through D-20 that appears contrary to this line of reasoning.

In a series of abstracts and government reports, Greene, et al., (Refs. D-17 through D-20) reported the results of an experimental investigation of the transient solidification of a gas-liquid mixture, while flowing downward through a vertical tube with a fixed freeze length. The liquids used in this study were Wood's metal (melting point  $74.6^{\circ}\text{C}$ ) and paraffin wax (melting point  $54^{\circ}\text{C}$ ) and nitrogen gas served as the lighter phase. Experiments were performed over a range of gas injection rates (or void fraction) and at two-phase mixture temperatures equal to and above the solidification temperature. The experiments with liquids at their freezing temperatures are of most interest. Since convection heat exchange at the solid gas-liquid mixture interface is absent in this case, these experiments should permit a clear definition of the effects of the gas phase. The experimental results indicated that as the gas flow rate (or void fraction) increased, the time to completely freeze the test section (plugging time) as well as the mass displaced through the test section decreased. While the observed decreased mass flow rate with increased mass flux could, in a qualitative sense, be attributed to the two-phase friction multiplier, the corresponding decrease in plugging time is difficult to rationalize. In the earlier publications by Greene, et al., (Refs. D-17 through D-19), the authors postulated the entrapment of nitrogen gas bubbles within the solid phase that grows inward from the wall and concluded from their experimental results that the rate of solidification may be several times faster for the two-phase case than for the single-phase case. However,

the solidification of a two-phase structure (solid plus gas) was refuted in a later report (Ref. D-20), as this process was not indicated by post-test observations of the frozen material.

Soon after, Petrie, et al., (Ref. D-21) reported results of an experiment designed to measure directly the growth of an ice layer in a water-nitrogen gas mixture. A planar test section on which ice crusts were grown was vertically suspended in a pool of water contained within a lucite bubble column of square cross section. Nitrogen gas bubbles were formed at a perforated plate located at the bottom of the column. A lateral-traversing thermocouple probe was used to measure the instantaneous ice crust thickness as a function of time. Different water pool temperatures were studied, corresponding to saturated (0°C) and superheated (> 0°C) conditions. The experiments covered a range of void fractions from 0 to 90%. The following conclusions may be made from these experiments. For void fractions up to 90%, the presence of a discontinuous gas phase in a saturated flowing liquid does not affect the freezing of the liquid. The crust surface remains smooth and the void in the two-phase mixture is not trapped in the crust in agreement with the results reports in Ref. D-20. The effect of liquid superheat on the freezing of a flowing two-phase mixture is to enhance the convective heat transfer from the liquid to the crust. The crust surface remains smooth in this case with no evidence of entrapment of the void. In both cases, the crust growth behavior can be modeled by ignoring the presence of gas (except for the effect of the gas flux on the convective heat flux). Obviously, these more direct observations regarding the rate of solidification are not in conformity with the gas-induced decrease in solidification time proposed in Refs. D-17 through D-20.

#### Effect of Liquid Superheat

The fuel temperature is 3100 - 3200°C in the assemblies, and decreases along the flow direction, ultimately to the liquidus point. The heat transfer coefficient,  $h_f$ , can be calculated using the forced convection part of Chen's correlation.

$$h_f = 0.023 \frac{k_f}{D_h} \left( \frac{\rho_f (1 - \alpha) u D_h}{\mu_f} \right)^{0.8} Pr^{0.4} \quad (1)$$

The molten fuel flow velocity is high initially and then decreases with increased penetration distance. Based on typical gap flow conditions with  $\alpha_2 = 0.5$ , the heat transfer coefficient is calculated to be approximately 5 w/cm<sup>2</sup>-°K on the average. Based on the average heat transfer coefficient, 5 w/cm<sup>2</sup>-°K, the thickness of fuel crust on the steel wall initially at 800°C is calculated for various fuel temperatures as shown in Fig. D-1.

It can be seen that the fuel crust thickness is reduced substantially when the fuel temperature is above the liquidus. At above-liquidus fuel temperatures, the crust thickness growth is rapid initially, and then levels off, or even gets reversed before the gaps are plugged (original gap = .47 cm). Namely, the gaps would not be plugged at all if the fuel temperature is as high as shown in Fig. D-1.

The fuel is initially at 3100 - 3200°C when flowing into the gaps and cools down to 2800°C after traveling about 30-40 cm. This indicates that the crust thickness in the 30-40 cm distance would level off at approximately 0.3 mm (see Fig. D-1); the gaps (4. - 5. mm) would remain open in this region. However, the fuel crust will continue to grow beyond this distance where the fuel is at its liquidus. Therefore, an approximate solution for this type of gap flow can be obtained by using a closed-form solution developed in Ref. D-23 for the case where the fuel is at its liquidus temperature. This closed-form solution is applied to the flow beyond the 30-40 cm distance with the pressure drop adjusted for flow inertia and friction loss in the 30-40 cm distance.

Accordingly, the distance of fuel penetration into the gaps before plugging is calculated by

$$\frac{X_p}{D_h} = 0.085 \left( \frac{v_f}{\lambda^2 \alpha_s} \right)^{7/11} \left( \frac{\Delta P D_h^2}{\rho v_f^2} \right)^{4/11} \quad (2)$$

$X_p$  = fuel penetration distance,

$D_h$  = gap initial hydraulic diameter,

$\rho$  = molten fuel density times (1 -  $\alpha$ ),

$C_o$  = total wetted perimeter for outward gap flow,

$v_f$  = kinematic viscosity of molten fuel,

$\lambda$  = growth constant (Ref. D-22),

$\alpha_s$  = thermal diffusivity of frozen fuel,

$\Delta P$  = driving pressure differential.

Using  $D_h = 0.8$  cm (EOC-4 value),  $\rho = 4.3$  g/cm<sup>3</sup>,  $v_f = 0.005$  cm<sup>2</sup>/sec,  $\lambda = 0.93$ ,  $\alpha_s = 0.0064$  cm<sup>2</sup>/sec, and  $\Delta P = 1$  bar. The fuel penetration distance is calculated to be ~ 250 cm (the additional 30-40 cm penetration associated with above-liquidus fuel temperatures is neglected) which is much larger than the gap flow distance between the core boundary and the core barrel (~ 80 cm). Therefore, all the gaps outside the core could be filled with molten fuel without plugging the gap. Since the volume of the gaps in the ex-core region is much larger than the total volume of fuel, all the molten fuel could be removed from the core through the interassembly gaps while the gaps still remain open. Thus, it is concluded that fuel removal through the inter-assembly gaps is limited by the rate of fuel melting in the core, rather than by plugging of the gaps.

#### Bulk Freezing

In the discussion in the foregoing, prediction of fuel penetration into the gaps between assemblies is based on the conduction model, which involves the growth of a stable frozen layer at the channel wall. The results of some

experiments on  $UO_2$  (thermite) fuel flow and freezing in subassembly structure, however, are not consistent with conduction-controlled freezing behavior. The conduction model predicts as much as an order of magnitude longer penetration distance than that observed in many of the thermite freezing tests. It has been concluded from these tests that  $UO_2$  flowing over steel may behave in a manner that prevents the formation of a stable frozen  $UO_2$  layer at the channel wall and, therefore,  $UO_2$  penetration (or freezing) is controlled by turbulent heat transport from the fuel front to the channel wall ("bulk freezing model" D-2). While no direct experimental evidence exists to support this view of freezing, it has gained some popularity in the field of fast reactor safety as it provides a lower (theoretical) bound to the penetration distance of fuel in the channel geometries of interest. Accordingly, the bulk freezing model is utilized here to quantify or bound the effects of uncertainties in freezing mechanisms on fuel escape from the active core region.

According to the bulk freezing concept, the region just behind the leading edge of the penetrating fuel flow, where freezing is expected to occur first, appears as a "slush" and freezing is complete when the latent heat of fusion is "removed" from the slush by further (turbulent) heat loss to the channel wall. Assuming that turbulent heat loss within the complex "tumbling" flow pattern that must exist in the vicinity of the fuel front is well represented by Reynold's analogy, the penetration  $X$  of fuel limited by bulk solidification is readily shown to be given by D-24.

$$X_p = \frac{1}{2} \frac{D_h}{f} \frac{h_{fl}/c + (T_o - T_{mp})}{T_o - T_w} \quad (3)$$

where  $f$  is the dimensionless coefficient of friction ( $f \approx 0.005$ ),  $D_h$  is the hydraulic diameter of the channel,  $h_{fl}$  and  $c$  are the latent heat of fusion and the heat capacity of the flowing fuel respectively,  $T_o$  and  $T_{mp}$  are the fuel temperature at the channel entrance and the fuel melting temperature respectively, and  $T_w$  is the temperature of the channel wall. Within the context of bulk freezing theory, it is assumed that  $T_o$  is equal to the melting temperature of the steel channel wall ( $T_w = 1400^\circ C$ ).

Referring to the process of fuel ejection into the gaps between assemblies, we get from (3)  $X_p = 32$  cm. This result is equivalent to the removal of 15% of the BOC core fuel inventory and 10% of the fuel from the EOC core. The reduced amount of fuel removed from the EOC core simply reflects the smaller gap spacing for this case.

#### Effect of Sodium on Flow of $UO_2$ in Gaps

The gaps between assemblies are interconnected and are filled with liquid sodium during normal operation. A small leakage flow from the inlet module is maintained through the lower assembly support plate structure. The sodium in the interassembly gaps flows to the upper plenum with the most restricted flow paths at the above core load pad (ACLP) locations\*. The pressure in the gaps is approximately 1.5 bar which is the upper plenum pressure plus hydrostatic

\*The frictional resistance to sodium flow in the interassembly gaps is negligible compared with the resistance to sodium flow at the ACLP.

head. The total area of the most restricted flow paths between the interstitial gaps and the upper plenum is roughly  $A_{ACL P} \approx 600 \text{ cm}^2$  with most of the area provided in the radial blanket/shield region.

In the initiating phase analysis, liquid sodium in the gaps is treated as a heat sink by increasing the thermal mass of the hexcan walls. At termination of the initiating phase analysis, the temperature of the fuel assembly hexcan walls with augmented thermal mass is calculated to be 900 to 1200°C in the core region. Therefore, the interassembly gaps are considered to be voided in the core region at initiation of the present melt-out phase analysis. However, the gaps below and outside the core region are not likely to be voided when molten fuel starts to flow in the gaps after melt-through of the fuel assembly. In Ref. D-1, it was concluded that the presence of liquid sodium in the gaps would not introduce significant, sustained fuel-coolant interaction pressurization to retard fuel removal from the core. This conclusion was based on first-principle arguments and supported by applicable experiments. It is shown here that the liquid sodium flow (impedance) to the upper plenum has little effect on fuel penetration into the gaps.

As the fuel flows from the active core region into the gaps, the liquid sodium displaced by the fuel produce a pressure drop at the ACLP locations of magnitude

$$\Delta P_{ACL P} = \frac{C_1}{2} \rho_{Na} u_{ACL P}^2 \quad (4)$$

where  $C_1$  is the effective drag or loss coefficient ( $C_1 \approx 5.0$ ),  $\rho_{Na}$  is the density of liquid sodium, and  $u_{ACL P}$  is the sodium flow velocity through the ACLP. Assuming fuel crusts of instantaneous uniform thickness are left behind on the walls of the interassembly gaps penetrated by the fuel (conduction model), the pressure drop over the instantaneous fuel length  $X$  can be shown to be given by

$$\Delta P_{gap} = \frac{f}{2} \rho_{UO_2} u_{gap}^2 \left(\frac{R_o}{R}\right)^3 \frac{X}{R_o} \quad (5)$$

where  $f$  is the friction factor for turbulent channel flow ( $f = 0.005$ ),  $\rho_{UO_2}$  is the density of molten fuel,  $R_o$  is the gap half width (radius),  $R$  is the instantaneous "radial" location of the fuel crust-melt interface (measured from the channel centerline), and  $u_{gap}$  is the instantaneous fuel flow velocity in the gap.

Since the sodium volumetric displacement rate must equal the volumetric fuel escape rate from the core, we can write the equality

$$u_{gap} A_{core} = u_{ACL P} A_{ACL P} \quad (6)$$

where  $A_{core}$  is the gas cross-sectional area through which the fuel passes as it leaves the active core region. Eliminating  $u_{ACL P}$  in Eq. (4) in favor of  $u_{gap}$  via Eq. (6), adding the result to Eq. (5), and solving for  $u_{gap} = dx/dt$  we get



$$\frac{dX}{dt} = \frac{[2 \Delta P / (f \rho_{UO_2})]^{1/2}}{\left[ \left( \frac{R_o}{R} \right)^3 \frac{X}{R_o} + \frac{C_1 \rho_{Na}}{f \rho_{UO_2}} \left( \frac{A_{core}}{A_{ACLP}} \right)^2 \right]^{1/2}} \quad (7)$$

Since the fuel crust thickness,  $R_o - R$ , is related to time  $t$  through the familiar conduction-theory result

$$R_o - R = 2\lambda(\alpha_{UO_2} t)^{1/2} \quad (8)$$

where  $\alpha_{UO_2}$  is the thermal diffusivity of the fuel and  $\lambda$  is the fuel crust growth constant ( $\lambda = 0.9$ ), Eq. (7) can be transformed to

$$\frac{dX}{dR} = - \frac{B(1 - R/R_o) (R/R_o)^{3/2}}{\left[ \frac{X}{R_o} + \frac{C_1 \rho_{Na}}{f \rho_{UO_2}} \cdot \left( \frac{A_{core}}{A_{ACLP}} \right)^2 \left( \frac{R}{R_o} \right)^3 \right]^{1/2}} \quad (9)$$

where  $B$  is defined as

$$B \equiv \frac{R_o}{2\lambda^2 \alpha_s} \cdot \sqrt{\frac{2\Delta P}{f \rho_{UO_2}}} \quad (10)$$

The final fuel penetration length  $X_p$  is obtained by numerically integrating Eq. (9) in the negative  $R$ -direction from  $R = R_o$  (open gap) when  $X = 0$  to  $R = 0$  (closed gap) when  $X = X_p$ .

In order to explore the effect of the sodium impedance on fuel penetration into the gaps,  $X_p$  has been plotted against the area for fuel escape,  $A_{core}$ , in Fig. D-2. The results shown are based on total fuel driving pressure  $\Delta P = 1$  bar and a channel half-width  $R_o = 0.2$  cm. The dashed curve in the figure corresponds to the fuel penetration length in the absence of liquid sodium. We note from the figure that even for  $A_{core}$  as large as  $4000 \text{ cm}^2$ , which is just about the maximum possible cross-sectional area for fuel escape from the core via the gaps between assemblies, the penetration length is reduced by only 40% by the sodium flow through the ACLP. The reason the fuel penetration length is rather insensitive to the sodium impedance is that in the conduction mode of freezing the penetration length is a weak function of the pressure drop ( $X_p \sim \Delta P^{1/3}$ ). Interestingly enough, since the penetration length based on the bulk freezing model is practically independent of pressure drop (or flow velocity), we can anticipate an even smaller effect of sodium impedance on fuel penetration in this case.

## References

- D-1 S. K. Rhow, et al., "An Assessment of HCDA Energetics in the CRBRP Heterogeneous Reactor Core," CRBRP-GEFR-00523, General Electric Company, December 1981.
- D-2 R. W. Ostensen and J. F. Jackson, "Extended Fuel Motion Study," in Reactor Development Program Progress Report ANL-RDP-18, Argonne National Laboratory, pp. 7.4-7.7, July 1973.
- D-3 M. Epstein, R. E. Henry, M. A. Grolmes, H. K. Fauske, G. T. Goldfuss, D. J. Quinn, and R. L. Roth, "Analytical and Experimental Studies of Transient Fuel Freezing," Proc. Int. Mtg. on Fast Reactor Safety and Related Physics, Vol. IV, USERDA Conf. No. 761001, October 5-8, Chicago, Illinois, pp. 1788-1798, 1976.
- D-4 D. R. Armstrong, "Preliminary Results from 1st UO<sub>2</sub> Dropping Experiment," Private Communication, January 1970; (see also Fig. 3 in M. Epstein, M. A. Grolmes, R. E. Henry, and H. K. Fauske, "Transient Freezing of a Flowing Ceramic Fuel in a Steel Channel," Nucl. Sci. Eng., 61, pp. 310-323, 1976.
- D-5 G. A. MacDonald, Volcanoes, Chapter 5, Prentice-Hall, Inc., Englewood Cliffs, New Jersey, 1972.
- D-6 A. Yim, M. Epstein, S. G. Bankoff, G. A. Lambert, and G. M. Hauser, "Freezing-Melting Heat Transfer in a Tube Flow," Int. J. Heat Mass Transfer, 21, pp. 1185-1198, 1978.
- D-7 D. W. Condiff and G. A. Lambert, Private Communication, 1978.
- D-8 D. O. Lee, S. W. Eisenhower, M. L. Corradini, and R. W. Ostensen, "Forced Convection Melting Heat Transfer in a Tube for a Two-Component System," AIChE Symposium Series, Vol. 75, pp. 55-68, 1979.
- D-9 D. A. McArthur, R. W. Ostensen, and N. Hayden, "In-Core Transition-Phase Fuel-Freezing Experiment TRAN-1," Trans. Am. Nucl. Soc., Vol. 38, pp. 393-394, 1981.
- D-10 D. A. McArthur, S. F. Duliere, and D. J. Sasmor, "Post-Test Analysis of TRAN-1 and TRAN-2 Final Fuel Distributions," Trans. Am. Nucl. Soc., Vol. 39, pp. 676-678, 1981.
- D-11 D. A. McArthur, Private Communication.
- D-12 W. D. Ford, H. K. Fauske, and S. G. Bankoff, "The Slug Expulsion of Freon-113 by Rapid Depressurization of a Vertical Tube," Intl. J. Heat Mass Transfer, Vol. 14, pp. 133-139, 1971.
- D-13 M. A. Grolmes and G. A. Lambert, "Liquid Film Considerations for LMFBR Accident Analysis," Trans. Am. Nucl. Soc., Vol. 35, pp. 353-354, 1980.

- D-14 G. I. Taylor, "The Instability of Liquid Surfaces when Accelerated in a Direction Perpendicular to Their Planes-I," Proc. Royal Soc. of London, Vol. A201, pp. 192-196, 1950.
- D-15 M. Epstein, "Heat Conduction in the  $UO_2$ -Cladding Composite Body with Simultaneous Solidification and Melting," Nucl. Sci. Engng., Vol. 51, pp. 84-87, 1973.
- D-16 M. Epstein, A. Yim, and F. B. Cheung, "Freezing Controlled Penetration of a Saturated Liquid into a Cold Tube," Trans. ASME J. Heat Transfer, Vol. 99, pp. 233-238, 1977.
- D-17 G. A. Greene, D. C. Jones, Jr., and M. S. Kazimi, "Effects of Non-Condensable Void Fraction on Freezing of Flowing Fluids," Trans. Am. Nucl. Soc., Vol. 27, pp. 546-547, 1977.
- D-18 G. A. Greene, D. C. Jones, Jr., M. S. Kazimi, T. Ginsberg, and J. J. Barry, "Analysis and Measurement of Solidification Dynamics of Flowing Two-Phase Non-Condensable Mixtures," Trans. Am. Nucl. Soc., Vol. 28, pp. 465-466, 1978.
- D-19 G. A. Greene, D. C. Jones, Jr., M. S. Kazimi, J. J. Barry, and G. A. Zimmer, "Two-Phase Transient Solidification Dynamics of Flowing Fluids with Non-Condensable Vapors," BNL-NUREG-24486R, 1978.
- D-20 G. A. Greene and J. J. Barry, "Freezing of Multiphase Mixtures Flowing Downward in Circular Tubes," BNL-NUREG-28302, 1980.
- D-21 D. J. Petrie, J. H. Linehan, M. Epstein, G. A. Lambert, and L. J. Stachyra, "Solidification in Two-Phase Flow," J. Heat Transfer, Vol. 102, pp. 784-786, 1980.
- D-22 H. S. Carslaw and J. C. Jaeger, "Conduction of Heat in Solids, 2nd Edition, Clarendon Press, Oxford, 1959.
- D-23 M. Epstein, et al., "Transient Solidification in Flow into a Rod Bundle," J. Heat Transfer, 102, No. 2, May 1980.
- D-24 M. Epstein, M. A. Grolmes, R. E. Henry, and H. K. Fauske, "Transient Freezing of a Flowing Ceramic Fuel in a Steel Channel," Nucl. Sci. Engng., 61, pp. 310-323, 1976.

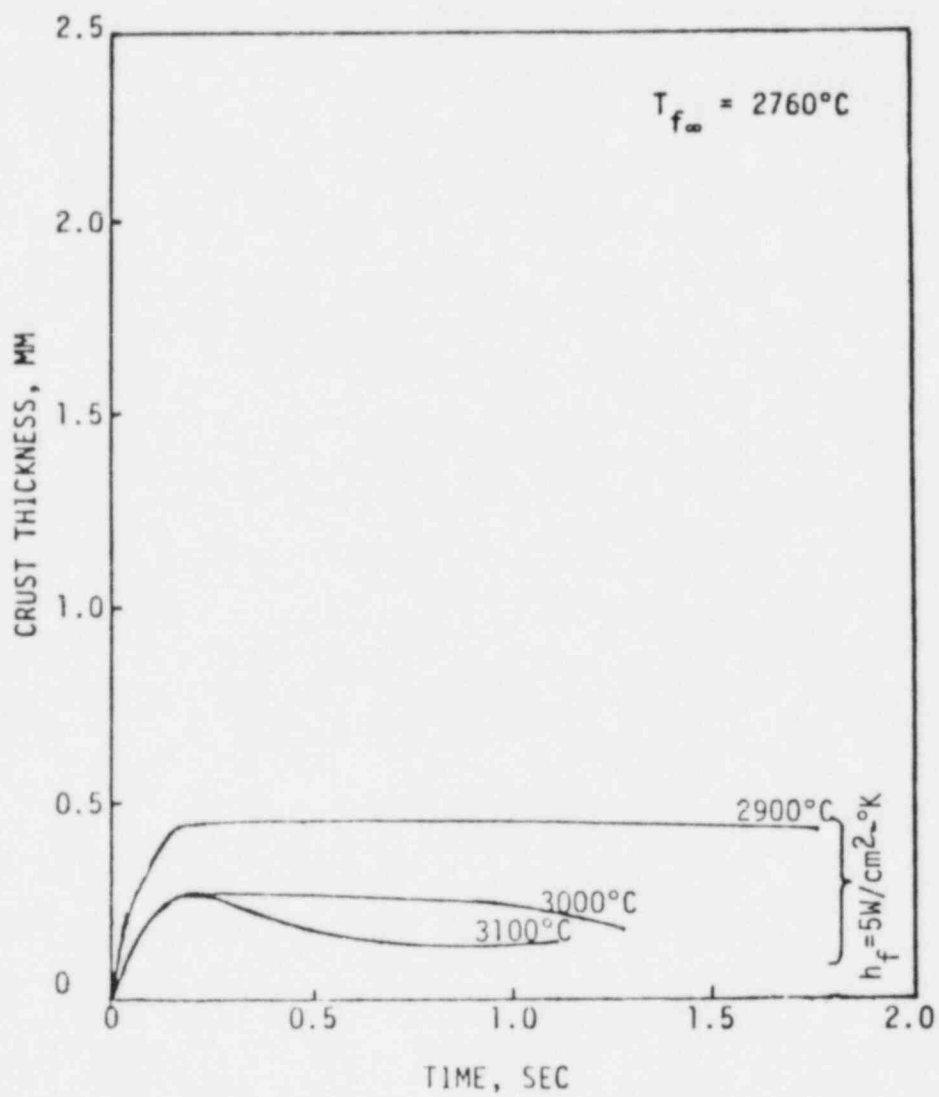


Fig. D-1 Growth of Fuel Crust Thickness on 800°C Steel Wall at Various Fuel Temperatures.

QCS760.178B5-D14

Amend. 72  
Oct. 1982

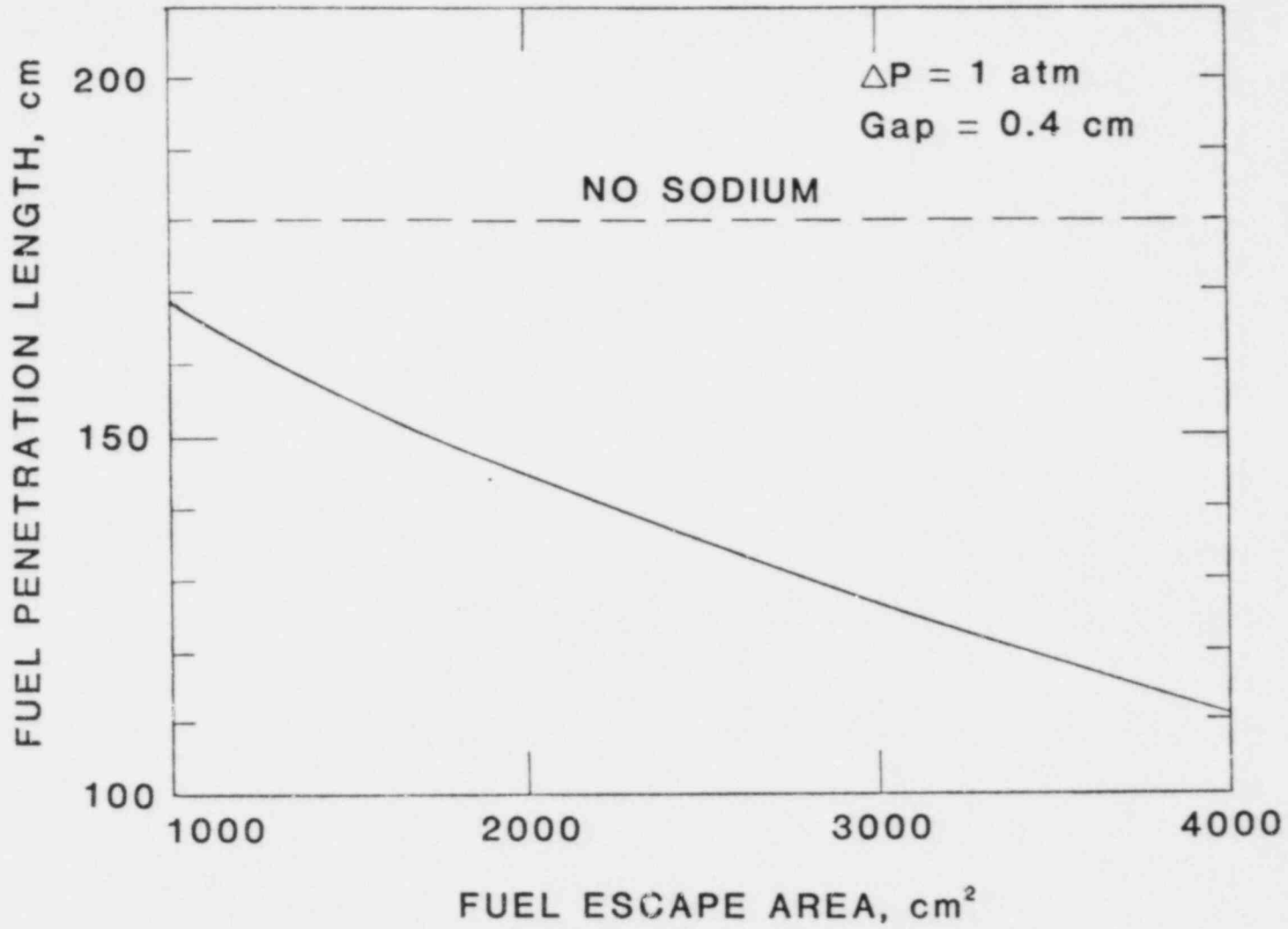


Fig. D-2 Fuel Penetration with Sodium Impedance Considered.

Sodium Re-Entry in the Presence  
of Steel Vapor Condensation

This Appendix considers the processes of vapor condensation in the presence of a second component subcooled volatile liquid in the context of a steel vapor sodium system. The distinctions between this system and a one-component system are drawn out and discussed relative to sodium re-entry in the CRBR safety evaluation.

The volatility of saturated or subcooled liquid sodium subjected to an oncoming stream of pure steel vapor is readily demonstrated by considering the thermal response of the surface of the liquid sodium. Immediately following liquid-vapor contact, the heating of the liquid sodium surface takes place via the kinetic rate of impact and deposition of steel vapor molecules upon the liquid, which form a condensed layer of steel separating the liquid sodium surface from the steel vapor phase. As the condensed steel layer grows, its temperature increases. Heat conduction through the condensed steel and the cold sodium begins to limit the condensation process as the surface temperature of the condensed liquid-steel layer approaches its vapor (boiling) temperature  $T_{bp,ss}$ . This kinetically controlled "preheating period" is estimated to be  $\approx 0.01 \mu\text{sec}$  duration and leaves a steel condensate layer of  $\sim 0.1 \mu$  thick on the liquid sodium surface. During the preheating period, the liquid sodium-condensed steel interface temperature rises from its initial temperature,  $T_i$ , and approaches a constant maximum value,  $T_i$ , when the condensation process becomes conduction limited. If  $T_i$  lies below the boiling temperature of liquid sodium,  $T_{bp,Na}$ , the steel condensation process will continue on the cold liquid sodium surface after the transition from kinetically controlled to conduction controlled condensation is made. This condition would result in the rapid depressurization of the steel vapor region and sodium re-entry into the core. Alternatively, if  $T_i > T_{bp,Na}$ , the liquid sodium just behind the thickening steel condensate layer will reach its boiling point during the preheating period, become slightly superheated and burst the steel layer. At this point in time sodium vaporization will begin and "fill" the void left by the condensing steel (see below).

In order to determine  $T_i$ , we consider the problem in which the region  $x > 0$  initially contains liquid sodium at temperature  $T_o$ . The region  $x < 0$  initially contains steel vapor at its boiling temperature  $T_{bp,ss}$ . Condensation of the steel vapor starts at the plane  $x = 0$  and moves to the left into the steel vapor region. An approximate solution for the interface temperature  $T_i$  can be obtained by neglecting the transient term in solving the conduction equation in the steel condensate layer, so that the temperature distribution  $T_{ss}$  in this region is approximately that corresponding to steady state, that is

$$T_{ss} = T_i + x(T_i - T_{bp,ss})/\delta(t) \quad (1)$$

where  $x = -\delta(t)$  is the surface of separation of the vapor and liquid steel phases.

We impose the energy balance which equates the instantaneous latent heat of steel condensation to the conductive heat loss to the steel condensate layer:

$$\rho_{ss} L_{ss} \frac{d\delta}{dt} = - k_{ss} \left( \frac{\partial T_{ss}}{\partial x} \right)_{x=-\delta} \quad (2)$$

where  $\rho_{ss}$ ,  $L_{ss}$  and  $k_{ss}$  are the liquid density, latent heat of condensation, and liquid thermal conductivity of steel, respectively. Heat flux continuity at  $x = 0$  requires that

$$k_{ss} \left( \frac{\partial T_{ss}}{\partial x} \right)_{x=0} = k_{Na} \left( \frac{\partial T_{Na}}{\partial x} \right)_{x=0} = - \frac{k_{Na} (T_i - T_o)}{\sqrt{\pi \alpha_{Na} t}} \quad (3)$$

where  $\alpha$  is thermal diffusivity,  $t$  is time and the subscript Na refers to the properties of the liquid sodium. The right-hand term in Eq. (3) follows from the fact that the liquid sodium region may be considered to extend to infinity in the positive  $x$ -direction; it is the flux of heat at the surface of a semi-infinite medium. Substituting Eq. (1) into Eqs. (2) and (3), the following system of equations is obtained.

$$\rho_{ss} L_{ss} \frac{d\delta}{dt} = - \frac{k_{ss} (T_i - T_{bp,ss})}{\delta} \quad (4)$$

$$\frac{k_{ss} (T_i - T_{bp,ss})}{\delta} = - \frac{k_{Na} (T_i - T_o)}{\sqrt{\pi \alpha_{Na} t}} \quad (5)$$

Integrating Eq. (4) and substituting the result for  $\delta(t)$  into Eq. (5) gives the steel condensate-liquid sodium interface temperature

$$\frac{T_i - T_o}{T_{bp,ss} - T_o} = \frac{(1 + 4A)^{1/2} - 1}{2A} \quad (6)$$

where

$$A \equiv \frac{2}{\pi} \frac{(k\rho c)_{Na}}{(k\rho c)_{ss}} \cdot \frac{c_{ss} (T_{bp,ss} - T_o)}{L_{ss}} \quad (7)$$

Equation (7) is valid for thick thermal boundary layers in the condensate layer or, equivalently, when  $c_{ss} (T_{bp,ss} - T_o) / L_{ss} \ll 1.0$ . Fortunately, for the steel-sodium system treated here this inequality is always satisfied. Moreover, the parameter  $A$  is also a small quantity for the steel-sodium material pair so the Eq. (4) can be simplified by expanding the square-root term to obtain the final result.

$$\frac{T_i - T_o}{T_{bp,ss} - T_o} = 1 - A \quad (8)$$

Using Eq. (8), it is of interest to calculate the temperature  $T_i$  that would result from the filmwise condensation of steel vapor onto a liquid sodium surface at  $T_o = 500^\circ\text{C}$  (subcooling  $\approx 400^\circ\text{C}$ ). For this system  $A = 0.07$  and from Eq. (8) we estimate  $T_i = 2640^\circ\text{C}$ . Not only does the interface temperature exceed the sodium boiling point ( $\approx 900^\circ\text{C}$ ) but it exceeds its critical temperature ( $\approx 2784^\circ\text{C}$ ) as well. It is clear that under these conditions the foregoing analysis is inapplicable and that steel condensation without sodium vaporization is impossible.

It is interesting to note that sustained sodium vaporization in nearly pure steel vapor is also impossible. To demonstrate this let us suppose that liquid sodium can vaporize into pure hot steel vapor. The sum of the steel vapor partial pressure and the sodium vapor partial pressure at the liquid-vapor interface must equal the total system pressure (the steel vapor pressure far from the interface):

$$P = P_{ss} + P_{sat,Na}(T_i) \quad (9)$$

where  $P$  is the total pressure and is constant,  $P_{ss}$  is the partial pressure of steel vapor and  $P_{sat,Na}(T_i)$  is the equilibrium partial pressure of sodium vapor and is strictly a function of the interface (sodium surface) temperature. We now ask the following question: How low can the liquid sodium surface temperature be before sustained sodium vaporization becomes impossible? This threshold temperature,  $T_i^*$ , should be the dew point temperature for steel vapor at the liquid sodium surface, defined by the condition  $P_{sat,Na}(T_i^*) = P_{ss}$  where subscript  $sat,ss$  refers to the equilibrium partial pressure for steel vapor. If the steel vapor pressure at the sodium surface exceeds  $P_{sat,Na}$  condensation of vapor on the liquid sodium surface will occur and sodium vaporization must terminate. This reasoning leads to an implicit relation between  $T_i^*$ , and the system pressure\*:

$$P_{sat,ss}(T_i^*) + P_{sat,Na}(T_i^*) = P \quad (10)$$

Equation (10) reveals that sustained sodium vaporization is impossible when the liquid sodium-steel vapor interface temperature drops slightly below the sodium boiling point (by much less than  $1^\circ\text{C}$ ) at the system  $P$ . Even accounting for the fact that radiation from "white-hot" steel fog particles will be the predominant form of energy transfer on the steel vapor side of the interface, because of the initial, highly subcooled state of liquid sodium at, say,  $500^\circ\text{C}$ . The energy requirements for maintaining the liquid sodium surface at its boiling temperature cannot be met. Thus, sufficient quantities of steel vapor will reach the liquid sodium surface such that steel condensation

\* The essential difference between a two-component and a one-component system is that there is only one partial pressure interface temperature relation which determines whether the energy exchange leads to condensation or evaporation. Furthermore, in a one-component system phase change in only one direction is permissible.



upon the sodium surface will occur. The condensed steel will probably form "steel frost" on the surface, since the steel vapor temperature must fall below its triple point temperature (sublimation) as it diffuses through sodium vapor toward the vaporizing liquid surface. If the frost layer is sufficiently porous, stable counter-diffusion of steel and sodium vapor at uniform total pressure will occur. Alternatively, the liquid sodium surface may become unstable with respect to vaporization, frequently becoming superheated and shattering any condensed steel layer that tends to form on its surface, resulting in surface temperatures that oscillate about the sodium boiling point.

Regardless of the precise mechanism of energy exchange between hot steel vapor and subcooled sodium, it is clear that sodium evaporation must accompany steel vapor condensation. A simple energy balance reveals that this dual phase conversion process results in a vapor volume increase<sup>3</sup> at constant pressure. For every 1.0 cm<sup>3</sup> of steel vapor condensed, 1.3 cm<sup>3</sup> of sodium vapor is produced from subcooled sodium at  $T = 500^{\circ}\text{C}$ . In summary sodium re-entry into the core by rapid steel vapor depressurization is prevented by sodium vaporization.

Question CS760.178D8

What is your estimate of the force required to produce a mechanically induced relief path via upper internals structures displacement?

Response

Forces of structural significance to the upper internals structure (UIS) can only be produced by an energetic core disassembly, which is a very low probability event in the CRBRP. The Project approach to provide for structural margin beyond the design base (SMBDB) is presented in detail in Ref. QCS760.178D8-1. In summary, an extreme core temperature condition was chosen to both provide a substantial margin for the expected nonenergetic outcome of an HCDA, and to accommodate a large degree of uncertainty and conservatism (including potential work augmentation by sodium) for generic HCDA consequences. Included in the approach was the selection of a fuel isentropic expansion calculation for the thermal-to-mechanical energy conversion process. The UIS has been shown in scale model tests to accommodate the forces which result from the SMBDB specification without major deformation of the support columns, although limited buckling was observed (Ref. 760.178D8-1).

In direct response to the question an assessment of the forces required to significantly displace the UIS has been performed.

Based upon a finite element analysis (ANSYS computer program) of the UIS support columns and a failure mode due to plastic hinging, an estimated static force of  $2.90 \times 10^7$  N ( $6.52 \times 10^6$  lbf) would be required to cause buckling and collapse of all four columns, producing a relief path via significant UIS displacement. The following assumptions were made in obtaining this force: (1) a column temperature of  $538^\circ\text{C}$  ( $1000^\circ\text{F}$ ), (2) average column dimensions of 30.5 cm id and 2.54 cm (1 in.) wall thickness, (3) a typical yield stress of  $1.47 \times 10^8$  N/m<sup>2</sup> (1.25 times the minimum) Ref. QCS760.178D8-2, and (4) the UIS motion limited to the axial direction. The UIS is laterally restrained until key disengagement occurs at a displacement of 18.8 cm.

One way to help characterize the above force required to buckle the UIS columns is to assume that all of the above core structural flow paths are blocked, and that the structure is lifted up against the bottom of the UIS by a uniform core pressure. For this assumed configuration, the required pressure is calculated to be approximately 91 atm.

The ANSYS model utilizes plastic pipe elements for the support columns and elastic shell elements for the UIS structure. The columns are modeled with a slight initial deformation, which in combination with the geometry updating procedure allows column buckling to be analyzed. Figure QCS760.178D8-1 shows the resulting estimate of vertical force on the UIS versus vertical displacement. This result utilized a minimum yield stress of  $1.17 \times 10^8$  N/m<sup>2</sup> and resulted in a maximum axial load of  $2.32 \times 10^7$  N where column buckling occurred. Assuming a maximum value for the yield stress (Ref. QCS760.178D8-3), a maximum axial load of  $5.03 \times 10^7$  N is expected when column buckling would occur. Figure QCS760.178D8-2 provides the bilinear stress-strain relationship used for 316 SS at  $538^\circ\text{C}$  in the ANSYS model. The bilinear curve is very good for strains below 0.05 and within 15% of expected values (Ref. QCS760.178D8-1) for strains below 0.10. Hence, a force of approximately

$2.7 \times 10^7$  N would cause gross upward displacement of the UIS. As stated previously, such large forces would be extremely unlikely in the CRBRP, even under HCDA considerations. The analysis and judgement which support the position that the defined SMBDB core thermal conditions envelope a very large range of uncertainty and conservatism in evaluating core behavior are presented in Ref. QCS760.178D-1. In addition, the choice of a core fuel isentropic expansion process to calculate the resulting structural loads contains further margin relative to real processes. The remainder of the response to this question provides the project basis which support the position that the estimate of the post-disassembly expansion (PDE) structural loads based on the assumption of an isentropic expansion of the fuel is conservative.

Studies, both experimental and analytical, have shown that non-isentropic hydrodynamic and heat transfer processes play a net mitigating role. The combined effect of the non-isentropic processes is to produce a work energy that is substantially lower than the isentropic value. The major non-isentropic processes are:

1. Fuel self-mixing.
2. Non-uniform bubble expansion.
3. Hydrodynamic effects of the UIS.
4. Heat transfer to sodium.
5. Heat transfer to structures.

These processes are discussed below, including a discussion of the supporting experimental and/or analytical evidence. All of these processes have been clearly shown to be mitigating in nature except for heat transfer to sodium which has the potential for work augmentation. The actual sodium work augmentation however, is considered to be negligibly small for expected CRBRP PDE conditions, and in the limit can be bounded via thermodynamic considerations.

1. Fuel Self-Mixing: The pressure gradients in the core and in the expanding bubble cause the higher temperature fuel to accelerate toward the colder fuel. The resulting mixing produces a net heat loss from the hot fuel to the cold fuel, thus reducing the temperature of the hot fuel. Since the fuel vapor pressure is an exponential function of the temperature and steep, local temperature gradients exist in the core, self-mixing has the effect of reducing the core pressurization, and therefore the mechanical loading on the vessel structures. The mitigating consequence of fuel self-mixing for the CRBRP PDE, although clearly based on physical principle and understanding, has not been currently quantified and substantiated for CRBRP. An analytical study did estimate the effect as a 15% to 35% reduction of isentropic potential due to axial or combined axial-radial self-mixing in the homogeneous core (Ref. QCS760.178D8-4).
2. Non-Uniform Expansion: The pressure gradients in the core, and the resultant pressure gradients inside the expanding two-phase bubble, cause the force acting on the sodium pool to be less than if all the fuel vapor was uniformly participating in accelerating the pool. In other words, the relatively low pressure fuel vapor near the

bubble/pool interface dominates the pool acceleration, while the higher pressure fuel vapor farther away from the interface plays a much smaller role in the pool acceleration, and therefore in the subsequent sodium slug impact on the vessel head. Also, vortexing occurs at the bubble/pool interface, which is dissipative.

The mitigating effects of non-uniform expansion were verified experimentally in Purdue University and SRI International nitrogen expansion tests (Refs. QCS760.178D8-5 and -6). These tests employed simple scaled-down models of the CRBRP vessel. The high pressure nitrogen was initially at room temperature. It was released into a water pool containing no structures at the start of the test. Both tests confirmed that the expansion work was substantially less (30%-40%) than the isentropic value. The reduction is attributed primarily to non-uniform expansion of the nitrogen, and to the compression of the cover gas. The non-uniformity in the bubble expansion for the CRBRP would be even greater due to the pressure gradients existing in the core, whereas the nitrogen expansion tests started with a uniform pressure of the nitrogen source.

Analysis of the Purdue tests using straightforward analytical models derived from basic hydrodynamic principles (Ref. QCS760.178D8-5) showed good predictability of the test results, and verified the mitigating role of non-uniform bubble expansion. Analysis of the SRI tests using the more complex SIMMER-II code (Ref. QCS 760.178D8-5) also confirmed the basic effect of non-uniform expansion.

3. Hydrodynamic Effects of UIS: The presence of the UIS alters the expansion of the bubble hydrodynamically by: (a) laterally diverting the flow beneath it, (b) throttling of the flow, and (c) impeding the fluid flow through friction. The lateral diversion of fluid flow (Item a) produces turbulence and vortexing that consumes energy without contributing to the acceleration of the pool and subsequent mechanical loading on the vessel head. This mechanism is very effective in reducing the PDE work energy. Throttling of the flow through the UIS (Items b and c) causes the expansion of the bubble to slow down and to act on a smaller mass of the pool (sodium above the UIS), with approximately the same acceleration as when the UIS is absent, such that the impact loading on the vessel head is reduced.

The hydrodynamic effects of the UIS have been experimentally confirmed via the previously referenced Purdue and SRI programs. Straightforward analyses of the bubble expansion in the presence of the UIS (Ref. QCS760.178D8-8) have verified a correct understanding of the basic flow effects. Again, the more complex analyses of the SRI experiments with SIMMER further substantiate the significant role of the UIS in reducing the isentropic work potential; analytically estimated as a 50% reduction for CRBRP geometries.

4. Heat Transfer to Sodium: This is the only mechanism identified as having a potential for significant augmentation of the PDE work energy relative to the isentropic expansion case. The thermal

interaction between fuel and sodium produces a mitigating factor; the cooling of the fuel due to net heat loss to sodium, and an augmenting factor; the vaporization of liquid sodium which increases the bubble pressure. The trade-off between the two factors is dependent on the relative masses of the sodium and fuel, the fuel temperature, and the compliant space available for component separation. As discussed in Ref. QCS760.178D8-9, Section 8.2.6, the preponderance of experimental evidence supports a benign or mitigating role for the sodium. Two contact modes of importance are the ejection of fuel from rods into sodium within fuel assembly geometry, and the entrainment of sodium into an expanding fuel bubble in the upper vessel sodium pool.

The highest fuel energy tests relevant to the first mode were the TREAT S-11, S-12 and Sandia PBE series, of which PBE-5S and -9S have been reviewed in additional detail. As discussed in the above reference, care must be used when interpreting energy conversion efficiencies in these limited compliance volume autoclave tests. Of the above tests, only PBE-9S reported a significant pressurization event after piston stoppage (i.e., constant volume system), which was interpreted by some as a pressure wave induced fragmentation FCI. However, the interpretation, stated in Ref. QCS760.178D8-9, is that the pressurization resulted from the constant volume enforced mixing and heating.

Some comparisons will help to illustrate this point. The specific sodium mass (defined as the mass of sodium per fuel mass) which is a measure of overall quenching potential has a value of 5 and 0.1 for tests S-11 and PBE-9S. Another comparison is offered by the specific displacement (defined as the compliant volume per fuel mass) which is a measure of the sodium ability to disengage from the hot liquid fuel. The S-11 and PBE-9S values are 1.2 and 0.25 while the corresponding CRBRP value is 3. These comparisons serve to demonstrate that the PBE-9S experiment was, relative to S-11 and CRBRP, an extremely constrained environment which strongly affects the potential for system pressurization. The more compliant S-11 experiment conditions, which are much closer to the CRBRP, resulted in substantially reduced work potential.

Based upon both simulant and real materials experiments wherein thermite produced high temperature fuel was injected into sodium pools (Ref. QCS760.178D8-10) no augmentation of fuel isentropic work potential is expected by sodium entrainment into an expanding fuel bubble. Additionally, the maximum effect of this augmentation process can be limited to a factor of two based on thermodynamic considerations (Ref. QCS760.178D8-11).

Heat Transfer to Structures: The UIS and above-core structure will have a substantial mitigation effect on the core work potential due to the net energy loss from the fuel and its synergistic effect on fuel self-mixing in the core. However, the non-isentropic mitigation role of the heat transfer mechanisms is currently less amenable to quantify and substantiate as compared to the hydrodynamic effects for the CRBRP.

In summary, non-isentropic processes during the post-disassembly expansion will produce a substantial reduction in the work energy from the isentropic value. Although a potential has been indicated for sodium to augment the fuel expansion work, it would be outweighed by the many demonstrated mitigation processes and be enveloped by the Project selection of an isentropic process. The net reduction is conservatively estimated to be at least 35% to 70%, based on only consideration of major contributing processes which can reasonably be quantified by analysis and/or experiments. Hence, the SMBDB specified forces on the UIS and other primary heat transport system components are considered appropriately conservative.

References

- QCS760.178D8-1 "Hypothetical Core Disruptive Accident Consideration in CRBRP; Energetics and Structural Margin Beyond the Design Base," CRBRP-3, Vol. 1.
- QCS760.178D8-2 Nuclear Systems Materials Handbook, Volume 1, Book 1 Property Code 2107 for 304 SS, Rev. 2, 12/74.
- QCS760.178D8-3 Aerospace Structural Metals Handbook, Syracuse University Research Institute, March 1963.
- QCS760.178D8-4 Nuclear Reactor Safety, Quarterly Progress Report, July-September, 1977, Los Alamos Scientific Laboratory, p. 24, LA-7039-PR, January 1978.
- QCS760.178D8-5 J. Simpson, M. Saito, and T. G. Theofanous, "The Termination Phase of Core Disruptive Accidents in LMFBRs, 1980 Annual Report," Purdue University, PNE-81-151, June 1981.
- QCS760.178D8-6 R. J. Tobin and D. J. Cagliostro, "Effects of Vessel Internal Structures on Simulated HCDA Bubble Expansions," SRI International, Technical Report No. 5, November 1978.
- QCS760.178D8-7 T. F. Bott and C. R. Bell, "SIMMER Analysis of SRI Post-Disassembly Expansion Experiments," Los Alamos National Laboratory Report LA-9452-MS, June 1982.
- QCS760.178D8-8 A. M. Christie, "Low Risk Energetics Definition for Design Application," WARD-SR-94000-23, September 1981.
- QCS760.178D8-9 S. K. Rhow, et al., "An Assessment of HCDA Energetics in the CRBRP Heterogeneous Reactor Core," CRRP-GEFR-00523, General Electric Company, December 1981.
- QCS760.178D8-10 R. E. Henry, et al., "Large Scale Vapor Explosions," Proc. Fast Reactor Safety Meeting, p. 922, Beverly Hills, California, April 1974.
- QCS760.178D8-11 D. H. Cho and M. Epstein, "Work Potential from a Mechanical Disassembly at the Voided FFTF Core," Argonne National Laboratory, ANL/RAS 74-17, August 1974.

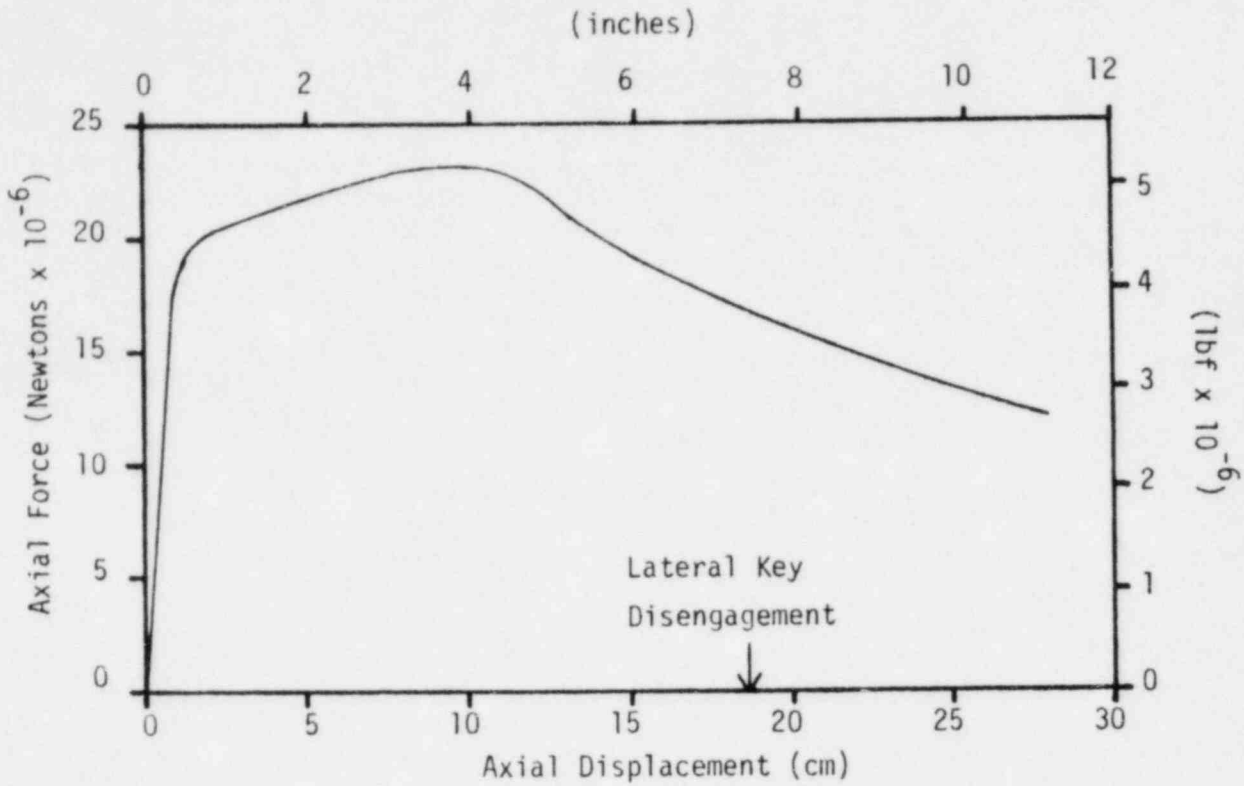


Fig. QCS760.178D8-1 Axial Force vs. UIS Axial Displacement.

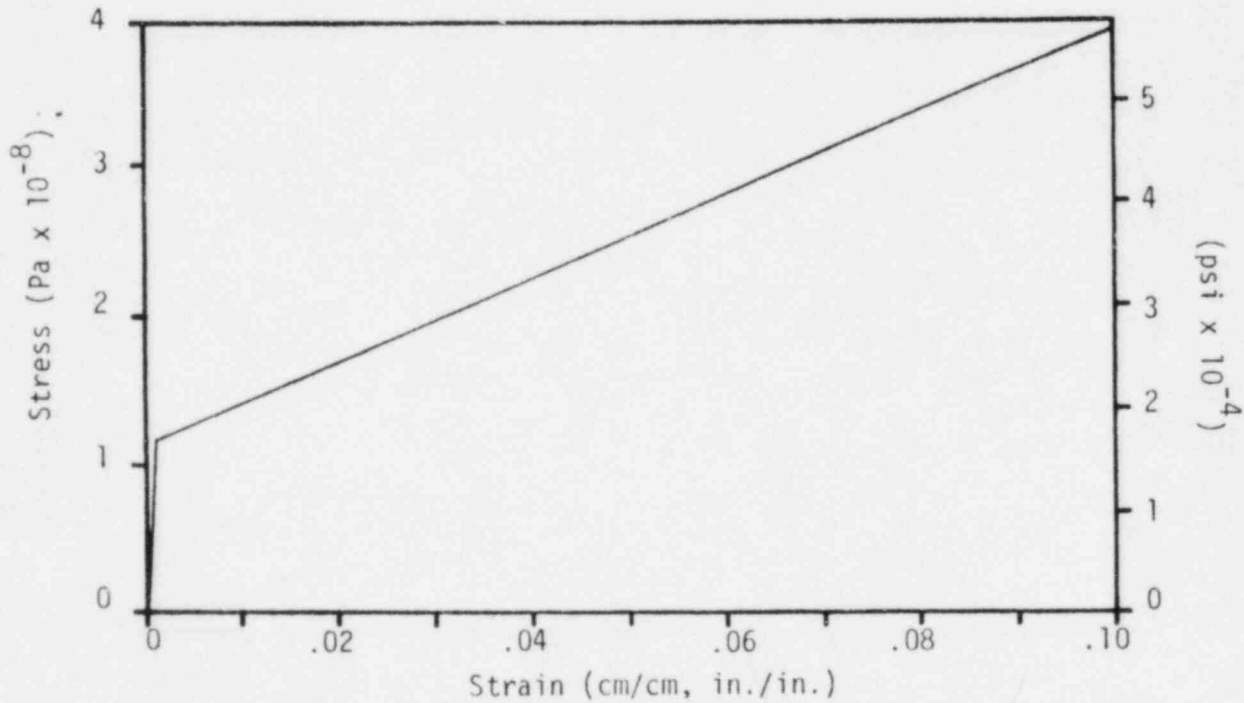


Fig. QCS760.178D8-2 Stress vs. Strain for 316 SS Used in Analysis.